TRANSCRIPTIONAL REGULATION IN ASPERGILLUS NIDULANS DURING NITROGEN SUFFICIENCY

by

DAMIEN J. DOWNES

B.Sc. (Honours), The University of Melbourne, 2009

AN ABSTRACT OF A DISSERTATION

submitted in partial fulfillment of the requirements for the degree

DOCTOR OF PHILOSOPHY

Department of Plant Pathology
College of Agriculture

KANSAS STATE UNIVERSITY
Manhattan, Kansas

2015

Abstract

Fungi can be found living in a range of environments, including soil and the ocean, and as pathogens of plants and animals. The ability of fungi to adapt to diverse and changing environments is dependent on their ability to sense and respond to an array of signals, including the presence or absence of nitrogen nutrients. Fungi can utilize a diverse array of nitrogen nutrients and do so in a regulated and preferential manner. When preferred nitrogen nutrients such as ammonium and glutamine are present (nitrogen sufficiency), genes required for the utilization of alternative nitrogen sources are not expressed. In the absence of a preferred nitrogen source (nitrogen limitation) the genes for utilization of alternative nitrogen sources are transcriptionally derepressed and can be induced by the presence of a particular nitrogen nutrient, such as nitrate or proline. In the absence of any nitrogen nutrient (nitrogen starvation) the expression of some genes is further elevated. In filamentous fungi the expression of genes required for the utilization of nitrogen nutrients is coordinated by the orthologs of the conserved *Aspergillus nidulans* GATA transcription factor AreA, which activates transcription of nitrogen utilization genes. AreA activity is controlled by autogenous transcriptional activation, mRNA transcript stability, regulated nucleo-cytoplasmic distribution, and interactions with NmrA, AreB and TamA. The combined effect of these regulatory mechanisms generally results in AreA being inactive during nitrogen sufficiency and active during nitrogen limitation and nitrogen starvation. However, during nitrogen sufficiency AreA remains active at the promoters of some genes, including *gdhA*, which encodes the key nitrogen assimilation enzyme NADP-dependent glutamate dehydrogenase. In this work we have used both classical genetics and next generation sequencing approaches to examine regulated gene expression and how AreA activity is modulated, primarily during nitrogen sufficiency. We have studied regulation of *gdhA* to characterize how AreA evades nitrogen metabolite repression. We identify leucine biosynthesis as being a key regulatory signal involved in *gdhA* expression and characterize the genes required for leucine biosynthesis. We also show that TamA regulates the *gdhA* promoter by direct DNA binding, which requires interaction with AreA. We have also characterized repression of AreA to identify a potential mode of NmrA corepressor action. Finally, we have characterized the AreA nuclear export signal and explored mechanisms that control regulated nuclear export of AreA.

.

TRANSCRIPTIONAL REGULATION IN ASPERGILLUS NIDULANS DURING NITROGEN SUFFICIENCY

by

DAMIEN J. DOWNES

B.Sc. (Honours), The University of Melbourne, 2009

A DISSERTATION

submitted in partial fulfillment of the requirements for the degree

DOCTOR OF PHILOSOPHY

Department of Plant Pathology
College of Agriculture

KANSAS STATE UNIVERSITY
Manhattan, Kansas

2015

Approved by:

Major Professor
Dr. Richard B. Todd

Abstract

Fungi can be found living in a range of environments, including soil and the ocean, and as pathogens of plants and animals. The ability of fungi to adapt to diverse and changing environments is dependent on their ability to sense and respond to an array of signals, including the presence or absence of nitrogen nutrients. Fungi can utilize a diverse array of nitrogen nutrients and do so in a regulated and preferential manner. When preferred nitrogen nutrients such as ammonium and glutamine are present (nitrogen sufficiency), genes required for the utilization of alternative nitrogen sources are not expressed. In the absence of a preferred nitrogen source (nitrogen limitation) the genes for utilization of alternative nitrogen sources are transcriptionally derepressed and can be induced by the presence of a particular nitrogen nutrient, such as nitrate or proline. In the absence of any nitrogen nutrient (nitrogen starvation) the expression of some genes is further elevated. In filamentous fungi the expression of genes required for the utilization of nitrogen nutrients is coordinated by the orthologs of the conserved *Aspergillus nidulans* GATA transcription factor AreA, which activates transcription of nitrogen utilization genes. AreA activity is controlled by autogenous transcriptional activation, mRNA transcript stability, regulated nucleo-cytoplasmic distribution, and interactions with NmrA, AreB and TamA. The combined effect of these regulatory mechanisms generally results in AreA being inactive during nitrogen sufficiency and active during nitrogen limitation and nitrogen starvation. However, during nitrogen sufficiency AreA remains active at the promoters of some genes, including *gdhA*, which encodes the key nitrogen assimilation enzyme NADP-dependent glutamate dehydrogenase. In this work we have used both classical genetics and next generation sequencing approaches to examine regulated gene expression and how AreA activity is modulated, primarily during nitrogen sufficiency. We have studied regulation of *gdhA* to characterize how AreA evades nitrogen metabolite repression. We identify leucine biosynthesis as being a key regulatory signal involved in *gdhA* expression and characterize the genes required for leucine biosynthesis. We also show that TamA regulates the *gdhA* promoter by direct DNA binding, which requires interaction with AreA. We have also characterized repression of AreA to identify a potential mode of NmrA corepressor action. Finally, we have characterized the AreA nuclear export signal and explored mechanisms that control regulated nuclear export of AreA.

Table of Contents

List of Figures

Chapter 5 – Regulation and mode of action of NmrA

Chapter 6 – The AreA Nuclear Export Signal

List of Tables

Chapter 6 – The AreA Nuclear Export Signal

Chapter 7 – Exploration of protein histidine modification as a mechanism for regulated AreA nuclear export

Appendix C - ValidNESs analysis of GATA factors

[This page has been intentionally, though not entirely, left blank.]

Acknowledgements

Nos esse quasi nanos gigantum humeris insidentes.

– Bernard of Chartres (c.1100)

As Sir Isaac Newton famously professed in a letter to Robert Hooke in 1676, " If I have seen further it is by standing on ye sholders of Giants" [1]. This work too is a result of the many giants in my life: my Mum and Dad, who planted the inquisitive seed and raised me to ask questions, my many inspiring teachers including, Leonie Roberts, Roger McBurney, Mary Nash and Michael Hynes, without whom my passion for research and discovery would not have blossomed, Richard Todd and Meryl Davis who have sculpted me into a better geneticist, and, finally, Brandon Pfannenstiel, Cameron Hunter, and Grethel Busot who made the lab a fun place to be. It is with their support and encouragement that this tome has been written.

I am also grateful to the many friends who made my transition and life in America a less daunting and much more enjoyable experience: the Welch family, the Brohmer family, the Clayton family, the Kokenge family, the Hunter family, Arrow Coffee co, my cryptic crossword brain trust Thomas Preston and Greg Holdridge, the staff and regulars at Rock a Belly Deli, the office ladies Diana, Anita, Jeanna, Stephanie, Danielle, and Jen, all of the students, postdocs and faculty in the Department of Plant Pathology, Carol Shanklin, April Mason, the Frisbee boys, particularly Sean, Kyle, and Pat, and my squash compatriots Tariq, David, Carlos[2] and Dick.

Finally I want to acknowledge the people who contributed time and effort to my experiments, provided unpublished data and formed my examination committee: Anna Brokesh, Trent Woodward, Hubertus Haas, Kendra Siebert, Yanni Lun, Ken Obasa, Tim Todd, Alina Ahkunova, Andrew Princep, Bethany Porter Grabow, Kevin McCluskey, Frank White, John Fellers, Sandy Beeser, Mary-Beth Kirkham, Chris Wong, Chirag Parsania, Miao Zhengqiang.

Thank you all so very much.

[1] The Correspondence of Isaac Newton. Volume 1. (1959) Edited by H.W. Turnbull. University Press p416

"God could not be everywhere, and therefore he made mothers."

–Jewish Proverb

This is dedicated to all the mothers in my life,
who have lifted me up and encouraged me,
have helped me through tough times,
and cheered me through great times.
Thank you.
D.

Chapter 1 - Introduction & Objectives

1.1 Fungi exploit diverse environments by sensing and responding

Fungi inhabit a plethora of environments as free living saprophytes in the soil, as symbionts with plants, in the ocean, and as pathogens of plants and animals. The ability of fungi to adapt to diverse and changing environments is dependent on their ability to sense and respond to an array of signals, including nutrients, stress, temperature, pheromones, light, gases, and in the case of pathogens the host (BAHN *et al.* 2007). One of the many ways in which fungi can respond to signals is through transcriptional regulation. Regulation of large subsets of genes by transcription factors can facilitate broad physiological changes and allow adaptation to a changing or new environment. Infection of plants by fungi represents a dramatic change in environmental conditions. Fungi living in the soil generally have abundant nutrients available, whereas those infecting plant cells have limited access to nutrients (SNOEIJERS *et al.* 2000; BOLTON *et al.* 2006). Therefore, during infection pathogens must drastically reprogram their metabolism for nutrient-limited conditions. In fungi utilization of nitrogen nutrients is coordinated by the orthologs of the conserved *Aspergillus nidulans* GATA transcription factor AreA, which activates transcription of nitrogen utilization genes (WONG *et al.* 2007). In several fungal pathogens AreA orthologs (named AreA, Nit2 and Nut1) are involved in pathogenicity. In *Ustilago maydis,* the *nit2*Δ mutant is compromised for virulence (HORST *et al.* 2012), whereas in *Magnaporthe grisea* the *nut1* mutant is as infectious as wild type though lesion size is reduced (FROELIGER AND CARPENTER 1996). In several other fungal pathogens with extended hemibiotrophic stages, including *Fusarium oxysporum*, *Cladosporium fulvum* and *Colletotrichum lindemuthianum*, deletion of the *areA* ortholog causes reduced or delayed disease (PEREZ-GARCIA *et al.* 2001; PELLIER *et al.* 2003; DIVON AND FLUHR 2007). In addition, *Fusarium verticillioides* AreA is essential for FB_1 mycotoxin production (KIM AND WOLOSHUK 2008), *Fusarium fujikuroi* AreA regulates production of the secondary metabolites gibberellin and bikaverin (TUDZYNSKI AND HOLTER 1998; TUDZYNSKI *et al.* 1998; MIHLAN *et al.* 2003; WIEMANN *et al.* 2009), and *Fusarium graminearum* AreA regulates deoxynivalenol (DON) biosynethsis (XU *et al.* 2015). As fungal plant pathogens pose a major threat to world food supplies, understanding the mechanisms used by fungi to infect plants and scavenge nutrients is critical for global food security.

1.2 Nitrogen metabolite repression

Fungi can utilize a wide array of organic and inorganic compounds as nitrogen sources (Reviewed by MARZLUF 1997; CADDICK 2004; WONG *et al.* 2008). The ability to use a diverse number of compounds requires numerous proteins for both uptake and breakdown of each particular nutrient. To ensure efficient use of the available nitrogen compounds fungi employ a complex regulatory system of induction and repression to control expression of nitrogen metabolic genes (Reviewed by MARZLUF 1997; CADDICK 2004; WONG *et al.* 2008). Under this system genes required for the breakdown of a specific compound are generally only expressed when that compound is present. For example, in *A. nidulans* the presence of nitrate induces the expression of the nitrate transporters *nitA*, *crnA/nrtA* and *crnB/nrtB*, the nitrate reductase *niaD* and the nitrite reductase *niiA* (JOHNSTONE *et al.* 1990; UNKLES *et al.* 1991; NARENDJA *et al.* 2002). Induction of specific sets of genes is often facilitated by a pathway specific transcription factor, many of which fall into the fungal Zn(II)2Cys6 zinc binuclear cluster (or GAL4) family of transcription factors. Examples of such proteins are ArcA (arginine utilization), NirA (nitrate and nitrite utilization), PrnA (proline utilization), and UaY (uric acid utilization) (ANDRIANOPOULOS AND HYNES 1990; BURGER *et al.* 1991a; SUAREZ *et al.* 1995; POKORSKA *et al.* 2000; EMPEL *et al.* 2001). The presence of a high quality nitrogen nutrient that can be easily metabolized, i.e. ammonium or glutamine, is termed nitrogen sufficiency and leads to the repression of genes required for assimilation of alternative nitrogen nutrients, even if the inducing compound is present, a phenomenon known as nitrogen metabolite repression (ARST AND COVE 1973). By this combination of selective repression and induction fungi can utilize the best nitrogen nutrients first and only express genes required for the utilization of the nitrogen compounds that are available. Nitrogen metabolite repression is facilitated via regulation of orthologs of the positive-acting *A. nidulans* GATA transcription factor AreA (ARST AND COVE 1973; HYNES 1975). During nitrogen sufficiency AreA activity is generally repressed due to several mechanisms: regulated *areA* mRNA stablitity, interaction with the corepressor NmrA and the repressor AreB, and regulated nuclear localization (Reviewed by MARZLUF 1997; CADDICK 2004; WONG *et al.* 2008 and discussed in detail below, Section 1.4). Nitrogen limitation leads to derepression and AreA becomes active at the promoters of nitrogen assimilation genes. For many genes the combined action of both AreA (derepression) and a pathway specific transcription factor (induction) are required. However, regulated expression of several genes, including *fmdS*,

which encodes formamidase, is mediated solely via AreA (FRASER *et al.* 2001; TODD *et al.* 2005; WONG *et al.* 2007).

1.3 Regulation by the GATA transcription factor AreA

AreA is a member of the GATA family of transcription factors which are found in all Eukaryotes and control a wide array of important biological processes, including hematopoiesis and cardiac development in mammals (WEISS AND ORKIN 1995; CHARRON AND NEMER 1999), chlorophyll synthesis in plants (BI *et al.* 2005), and iron homeostasis, nitrogen metabolism, and sexual development in fungi (FU AND MARZLUF 1990; KUDLA *et al.* 1990; HAAS *et al.* 1999; HAN *et al.* 2001a). GATA transcription factors have a Cys-X_2-Cys-X_{17-18}-Cys-X_2-Cys DNA-binding domain which co-ordinates a single zinc(II) ion and recognizes a core GATA sequence in DNA (LOWRY AND ATCHLEY 2000). The AreA DNA binding domain recognizes HGATAR sites (where H is a nucleotide other than G and R is a purine) within the promoters of nitrogen utilization genes and is required for transcriptional activation (KUDLA *et al.* 1990; RAVAGNANI *et al.* 1997; STARICH *et al.* 1998). Loss-of-function mutations of *areA* in *A. nidulans*, including mutations which disrupt the DNA binding domain, leads to an inability to utilize alternative nitrogen nutrients (ARST AND COVE 1973; KUDLA *et al.* 1990). AreA is able to bind DNA at specific promoters under both repressing and derepressing nitrogen conditions, and at some promoters AreA leads to chromatin remodeling and nucleosome rearrangement (Figure 1.1) (MURO-PASTOR *et al.* 1999; GOMEZ *et al.* 2003). AreA binding also facilitates an increase in activating chromatin modifications, namely acetylation of histone 3 lysine 9 (H3K9) and lysine 14 (H3K14), by recruiting histone acetyl transferases (BERGER *et al.* 2008; GACEK AND STRAUSS 2012). Finally AreA facilitates activation via interaction with other transcription factors such as NirA and TamA (SMALL *et al.* 1999; SMALL *et al.* 2001; MURO-PASTOR *et al.* 2004).

AreA activates transcription of genes required for utilization of alternative nitrogen nutrients during nitrogen limitation in the absence of the preferred nitrogen sources ammonium or glutamine (ARST AND COVE 1973). Expression of some genes is observed to further increase when no nitrogen sources are present, i.e. during nitrogen starvation (FRASER *et al.* 2001; TODD *et al.* 2005; WONG *et al.* 2007). Although AreA is primarily inactive during nitrogen sufficiency, full expression of nitrogen assimilation genes encoding the ammonium transporter, *meaA*, the NADP-dependent glutamate dehydrogenase, *gdhA*, and glutamine synthase, *glnA*, requires wild type AreA activity under these conditions (MARGELIS *et al.* 2001; MONAHAN *et al.* 2002a; POLOTNIANKA *et al.* 2004; MONAHAN *et al.* 2006). Is has been proposed that promoter-specific elements facilitate the evasion of repression at these genes (POLOTNIANKA *et al.* 2004).

1.4 Post transcriptional regulation of AreA

AreA is regulated transcriptionally, by autogenous activation, post-transcriptionally, by transcript stability and post-translationally by sub-cellular localization and interaction with AreB, NmrA and TamA (LANGDON *et al.* 1995; PLATT *et al.* 1996a,b; ANDRIANOPOULOS *et al.* 1998; SMALL *et al.* 1999; TODD *et al.* 2005; WONG *et al.* 2009). The effect of these mechanisms is a regulated response to nitrogen nutrients (Figure 1.1).

1.4.1 Regulation of areA *mRNA transcript stability.*

Analysis of *areA* mRNA transcript levels on different nitrogen nutrients following inhibition of transcription with proflavin revealed differential transcript stability. It was also shown that deletion of the 3' untranslated region (UTR) leads to increased *areA* mRNA stability and partial derepression of AreA (PLATT *et al.* 1996a,1996b). Conversely, adding the *areA* 3' UTR to an unrelated transcript could reduce its stability during nitrogen sufficiency (MOROZOV *et al.* 2000). The *areA* transcript exhibits instability during nitrogen sufficiency, as well as growth on several other nitrogen sources (e.g asparagine, glutamate, nitrate), with the likely signal being mediated via glutamine abundance, which results in *areA* poly(A) shortening (MOROZOV *et al.* 2000; MOROZOV *et al.* 2001). In eukaryotes mRNA transcript stability is determined by the presence of a 5' cap and a 3' poly(A) tail (MITCHELL AND TOLLERVEY 2000a). Reduced stability is often conferred by shortening of the poly(A) tail, which leads to either decapping or 5'-3' decay (YUE *et al.* 1996) or 3'-5' exosome-dependent decay (MITCHELL AND TOLLERVEY 2000b; BUTLER 2002). Deadenylase activity is generally carried out by either the Ccr4-Caf1-Not complex (ALBERT *et al.* 2000; TUCKER *et al.* 2001; TAKAHASHI *et al.* 2007) or the poly(A)-binding protein-stimulated poly(A) nuclease (BOECK *et al.* 1996; BROWN *et al.* 1996). In *A. nidulans, ccr4*Δ and *caf1*Δ mutations both led to retarded *areA* mRNA degradation in response to high intracellular glutamine levels (MOROZOV *et al.* 2010). An RNA recognition motif protein, RrmA, was identified by pull down analysis of proteins that interact with the *areA* mRNA (KROL *et al.* 2013). RrmA was previously identified as a regulator of arginine metabolism genes (OLSZEWSKA *et al.* 2007). Deletion of *rrmA* showed that RrmA facilitated *areA* mRNA transcript instability (KROL *et al.* 2013). *areA* mRNA degradation was also retarded by deletion of the nucleotidyltransferase encoding *cutA,* which adds a CUCU modification to the 3' of *areA* transcripts (MOROZOV *et al.* 2010). The combined decapping and subsequent

degradation of *areA* mRNA in response to intracellular nitrogen levels provide a mechanism by which levels of the AreA protein is controlled.

1.4.2 Regulation of AreA subcellular localization.

The ability of transcription factors to activate transcription is dependent on interaction with DNA, and for eukaryotes activation requires entry into the nucleus. Therefore cells can regulate transcription factor activity by controlling either entry into, or exit from the nucleus. During nitrogen sufficiency or nitrogen limitation AreA exhibits primarily nucleocytoplasmic localization, however transfer to nitrogen starvation conditions results in gradual nuclear accumulation (TODD *et al.* 2005). AreA nuclear accumulation correlates with an increase in transcription of the AreA-regulated *amdS-lacZ* and *fmdS-lacZ* reporter genes (FRASER *et al.* 2001; TODD *et al.* 2005), as well as with increased binding to the *niaD-niiA* bidirectional promoter (BERGER *et al.* 2008). Regulated nucleocytoplasmic distribution requires the combination of nuclear localization signals (NLS) and nuclear export signals (NES) that mediate nuclear import and export, respectively (NIGG 1997). AreA contains five classical SV40 Large T-antigen NLSs and one non-canonical arginine-based bipartite NLS (HUNTER *et al.* 2014). These six NLSs work co-operatively to facilitate AreA entry into the nucleus, likely by interaction with several of the 17 *A. nidulans* importins (MARKINA-INARRAIRAEGUI 2011; HUNTER *et al.* 2014). Fusion of these NLSs to Green Fluorescent Protein (GFP) showed they were able to enter the nucleus under both nitrogen sufficient and nitrogen starvation conditions, and therefore the AreA NLSs are not regulated by nitrogen nutrient availability (HUNTER *et al.* 2014). Following nitrogen starvation-induced nuclear accumulation of AreA, the addition of any nitrogen nutrient leads to rapid nuclear export (TODD *et al.* 2005). Nuclear export of proteins is primarily facilitated by orthologs of the highly conserved *Schizosaccharomyces pombe* CRM1 exportin (ADACHI AND YANAGIDA 1989; TODA *et al.* 1992), which has been characterized in many systems including *S. cerevisiae, Xenopus* and humans (FORNEROD *et al.* 1997a,b; FUKUDA *et al.* 1997; NEVILLE *et al.* 1997). Several CRM1 proteins, including *S. pombe* CRM1*,* are sensitive to Leptomycin B, which interacts with a specific cysteine residue and blocks nuclear export (KUDO *et al.* 1999). In *Saccharomyces cerevisiae* CRM1 and *A. nidulans* CrmA/KapK, the residue in the equivalent position is a threonine, however substitution to a cysteine confers LMB sensitivity (NEVILLE AND ROSBASH 1999; TODD *et al.* 2005). Using the *crmA*^{T525C} variant it

was shown that LMB prevents AreA nuclear export following nuclear accumulation, indicating that CrmA facilitates regulated AreA nucleocytoplasmic distribution (TODD *et al.* 2005). LMB also blocks NirA nuclear export in the KapK^{T525C} mutant (BERNREITER *et al.* 2007). AreA contains a single predicted CRM1-type NES between residues 703-712 (TODD *et al.* 2005), and deletion of these residues confers AreA nuclear accumulation in the presence of ammonium (D.F. Clarke, M.A. Davis and R.B. Todd, pers. commun.). The slow rate of AreA nuclear accumulation in response to nitrogen starvation, the rapid nuclear export upon the addition of a nitrogen nutrient (TODD *et al.* 2005), and the activity of the AreA NLS signals during both nitrogen sufficiency and nitrogen starvation (HUNTER *et al.* 2014) indicate that nuclear export is the likely regulated step in AreA nuclear accumulation.

1.4.3 Regulation of nitrogen metabolism genes through NmrA

AreA is known to interact directly or indirectly with at least four proteins, AreB, NirA, TamA and NmrA (SMALL *et al.* 1999; SMALL *et al.* 2001; LAMB *et al.* 2004; BERNREITER *et al.* 2007; WONG *et al.* 2009). NirA and TamA are Zn(II)2Cys6 transcriptional activators (BURGER *et al.* 1991a,b; DAVIS *et al.* 1996) whereas AreB and NmrA are both repressors (ANDRIANOPOULOS *et al.* 1998; CONLON *et al.* 2001; WONG *et al.* 2009). *nmrA* was identified and cloned based on sequence similarity to *Neurospora crassa* NMR1 (ANDRIANOPOULOS *et al.* 1998). NmrA and NMR1 primarily act to repress the activity of AreA and its *N. crassa* ortholog NIT2, respectively, during nitrogen sufficiency. Mutation of *nmr-1* leads to derepression of NIT2-dependent gene expression and mutation of *nmrA* leads to partial derepression of AreA activity (FU *et al.* 1988; XIAO *et al.* 1995; ANDRIANOPOULOS *et al.* 1998). When preferred nitrogen sources are absent, NmrA-mediated repression is relieved and AreA can activate its target genes to relieve nitrogen metabolite repression (Figure 1.1). The AreA/NmrA and NIT2/NMR1 interactions are dependent on the AreA and NIT2 C-termini, and mutants lacking the C-terminus show partial or complete derepression (PLATT *et al.* 1996a,b; PAN *et al.* 1997; ANDRIANOPOULOS *et al.* 1998). In *N. crassa* NMR1 also interacts with the NIT2 DNA binding domain and can block DNA binding *in vitro* (XIAO *et al.* 1995; PAN *et al.* 1997); however, despite NmrA interacting with the AreA DNA binding domain (LAMB *et al.* 2003), AreA preferentially binds GATA containing oligonucleotides over NmrA *in vitro* (LAMB *et al.* 2004). Therefore NmrA is unlikely to act by blocking AreA DNA binding.

NmrA is the type member of the NmrA-like structural family whose members include the Human protein HSCARG (ZHENG *et al.* 2007). Proteins in this family have a dinucleotide binding "Rossman fold", similar to that of the short-chain dehydrogenase-reductase (SDR) superfamily (OPPERMANN *et al.* 2003). NmrA, however, lacks the SDR catalytic residue required for dehydrogenase-reductase activity (STAMMERS *et al.* 2001). NmrA-family members may play a role in sensing changes in NAD(P)+ to NAD(P)H ratios to mediate signaling events as NmrA binds both NAD+ and NADP+ with higher affinity than NADH and NADPH (LAMB *et al.* 2003). Despite this, the presence of these molecules does not affect strength of NmrA binding to AreA (LAMB *et al.* 2004). Mutations of residues Asn-12 and Ala-18 within the NmrA NADP+ binding site were shown to prevent *in vitro* NAD+ and NADP+ binding (LAMB *et al.* 2004). In *M. oryzae,* mutation of the NADP+-binding site in NMR1 confers loss of function (WILSON *et al.* 2010). Furthermore, in *A. nidulans,* an *nmrA* loss-of-function mutation selected for derepression in an *areA* 3'UTRΔ background bears a missense mutation in residue T14V (M.A. Davis and R.B. Todd, pers. commun.). Therefore NAD(P)+ binding to the Rossman fold appears to be important for NmrA corepressor function.

Overexpression of *A. nidulans* NmrA inhibits alternative nitrogen source utilization, indicating that NmrA levels are important for repression (WONG *et al.* 2007). This finding is further supported by the regulated proteolysis of NmrA in response to nitrogen starvation by the proteases PnmA, PnmB, and PnmC (ZHAO *et al.* 2010). In wild type strains expression of *nmrA* is regulated by nitrogen source. *nmrA* has higher levels of expression during growth on preferred nitrogen sources than during growth in either nitrogen limitation or starvation conditions (WONG *et al.* 2007; ZHAO *et al.* 2010). Regulated expression of *nmrA* is in part controlled by a positively acting bZip transcription factor, MeaB (WONG *et al.* 2007; WAGNER *et al.* 2010). *meaB* expression is also regulated by nitrogen source, and is expressed highly when preferred nitrogen sources are present (WONG *et al.* 2007). Expression of *meaB* is reduced in the presence of the alternative nitrogen source alanine (SIBTHORP *et al.* 2013), and further reduced during nitrogen starvation (WONG *et al.* 2007). The *meaB* locus also encodes an antisense transcript, which is regulated by AreA via a HGATAR site in the first intron. The *meaB* antisense transcript shows an inverse expression pattern to the *meaB* forward transcript (SIBTHORP *et al.* 2013).

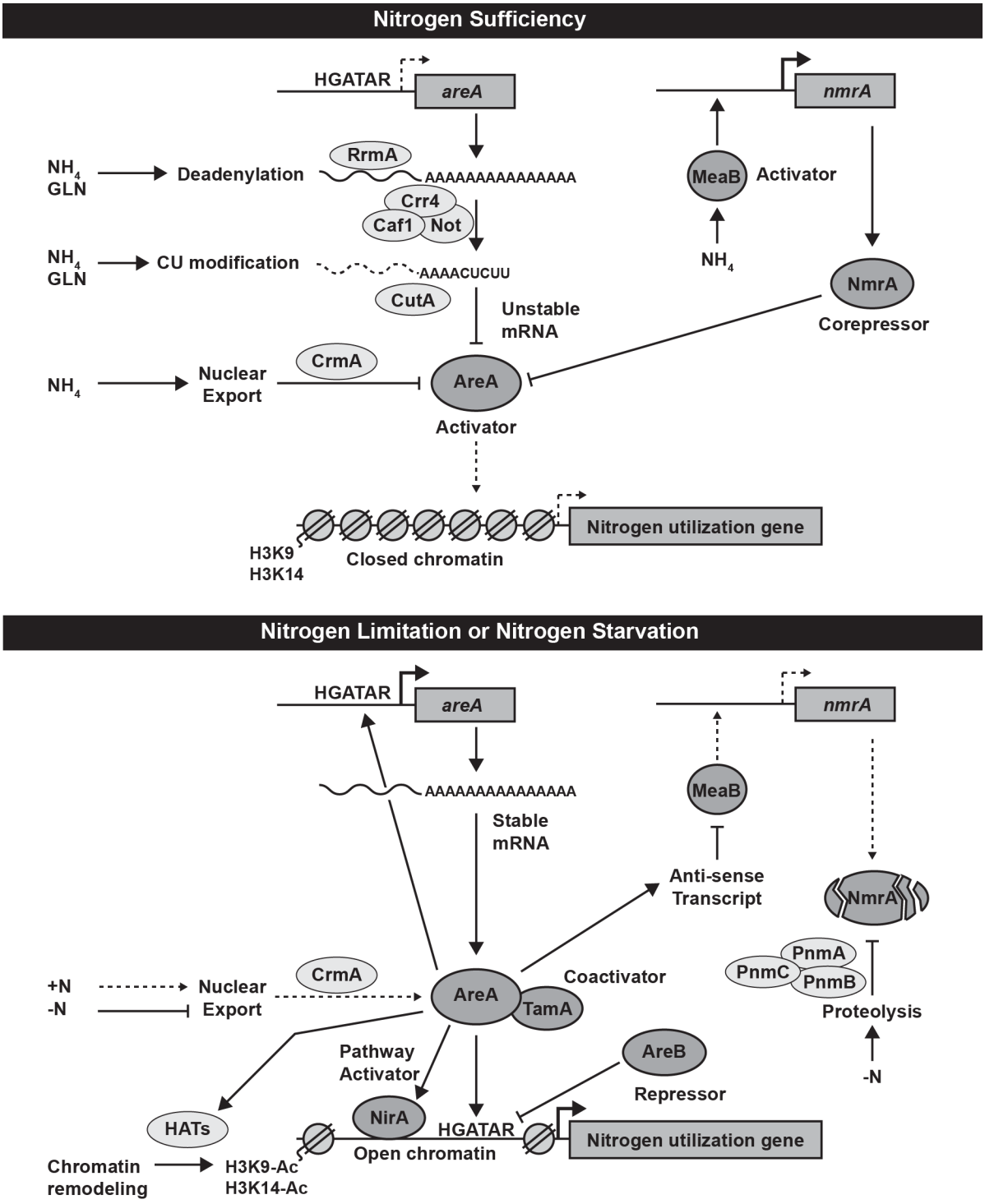

Figure 1.1 Overview of the nitrogen metabolism regulation

Schematic of the regulatory mechanisms involved in nitrogen metabolite repression during nitrogen sufficiency, nitrogen limitation or nitrogen starvation. Adapted from TODD (in press).

1.4.4 Regulation of AreA by interaction with the repressor AreB.

The GATA transcription factor AreB shows nitrogen nutrient regulated expression (CONLON *et al.* 2001). *areB* encodes three protein isoforms which are produced by a combination of different transcription start points, alternative splicing, and different translation start codons, however all three AreB proteins contain a GATA zinc finger DNA-binding motif and a leucine-zipper motif (CONLON *et al.* 2001; WONG *et al.* 2009). In *F. fujikuroi,* the three different protein products of *areB* are conserved and these AreB proteins were shown to interact directly with AreA using bimolecular fluorescence complementation (MICHIELSE *et al.* 2014). Analysis of *areB* mutants in *A. nidulans* shows a role in utilization of a range of nitrogen nutrients including arginine, nitrate and alanine (DZIKOWSKA *et al.* 2003; WONG *et al.* 2009). During nitrogen starvation *areB*Δ mutants showed increased expression of AreA target genes (WONG *et al.* 2009). Conversely, AreB overexpression using *xylP*(p)::*areB* conferred growth inhibition on alternative nitrogen nutrients and loss of AreA-dependent activation of the *fmdS-lacZ* reporter gene during nitrogen limitation or nitrogen starvation (WONG *et al.* 2009). Therefore, it is thought that AreB modulates AreA-dependent gene expression during nitrogen limitation and nitrogen starvation by competitive binding at GATA DNA binding sites, similar to the competition for binding sites observed in *S. cerevisiae* between positive and negative GATA transcription factors. (COFFMAN *et al.* 1997).

1.5 Regulation by the Zn(II)2Cys6 transcription factors TamA and LeuB

In addition to interacting with the repressors NmrA and AreB, AreA also interacts with the Zn(II)2Cys6 zinc-binuclear cluster transcription factor TamA (SMALL *et al.* 1999). TamA was first identified as a regulator of nitrogen metabolic genes through a genetic screen for mutants with simultaneous resistance to multiple toxic nitrogen analogs during nitrogen limitation (KINGHORN AND PATEMAN 1975a). These mutants also had reduced activity of the core nitrogen assimilation enzyme NADP-dependent glutamate dehydrogenase, NADP-GDH encoded by *gdhA* (KINGHORN AND PATEMAN 1975a). The cloning and sequencing of *tamA* revealed that TamA contains a Zn(II)2Cys6 DNA-binding motif, however mutation of this domain did not result in loss-of-function (DAVIS *et al.* 1996). For most transcription factors the DNA-binding domain is considered essential for function, however the closely related *Saccharomyces cerevisiae* transcription factor Dal81p also has a dispensable DNA-binding motif (BRICMONT *et al.* 1991). Expression of *tamA* is regulated by nitrogen source and transcription is induced by nitrate (SCHINKO *et al.* 2010), but unlike AreA, TamA shows constitutive nuclear localization (SMALL *et al.* 2001). Fusion of TamA to the functional Zn(II)2Cys6 DNA-binding domains of AmdR and FacB, which regulate ω-amino acid/lactam and acetate utilization respectively (HYNES 1980; KATZ AND HYNES 1989; ANDRIANOPOULOS AND HYNES 1990; TODD *et al.* 1997), showed that TamA activated transcription in an AreA-dependent manner and could recruit AreA to promoters (SMALL *et al.* 1999). This interaction with AreA was dependent on the AreA C-terminus, which is the same region required for interaction with the NmrA corepressor (ANDRIANOPOULOS *et al.* 1998; SMALL *et al.* 1999). Therefore TamA was thought to primarily function as a co-activator of AreA. Deletion of *tamA* results in both reduced NADP-GDH activity and decreased *gdhA* mRNA levels (POLOTNIANKA *et al.* 2004). Intriguingly, *tamA*Δ had a more severe effect on *gdhA* expression than *areA*Δ, indicating that TamA has roles at the *gdhA* promoter in addition to action as an AreA co-activator (POLOTNIANKA *et al.* 2004). This led to the identification of another Zn(II)2Cys6 transcription factor LeuB from a yeast two-hybrid screen for proteins that interact with TamA (POLOTNIANKA *et al.* 2004). LeuB is the homolog of *S. cerevisiae* Leu3p, which regulates leucine biosynthesis as both an activator and a repressor (FRIDEN AND SCHIMMEL 1988). Leu3p also regulates the *gdhA* homolog in *S. cerevisiae*, *GDH1* (HU *et al.* 1995). Like *leu3* mutants, *leuB*Δ leads to reduced growth in the absence of leucine, i.e.

leaky leucine auxotrophy, and reduced expression of *gdhA* (FRIDEN AND SCHIMMEL 1988; POLOTNIANKA *et al.* 2004). Combination of *leuB*Δ with the *areA217* loss-of-DNA-binding-function mutation was not as severe as *tamA*Δ on levels of NADP-GDH activity, suggesting that TamA may play additional roles in regulating *gdhA* expression (POLOTNIANKA *et al.* 2004).

1.6 Research Objectives

The objectives of this study were: (i) to determine the role of leucine biosynthesis in regulating *gdhA* expression and to identify genes required for leucine biosynthesis, (ii) to characterize regulation of *gdhA* by TamA and to determine the effects of TamA on a whole genome scale, (iii) to identify a mutation responsible for suppression of NmrA-mediated repression, (iv) to characterize the AreA nuclear export signal and carry out a genetic screen to identify genes involved in regulated AreA nuclear export, and (v) to perform analysis of candidate genes which may regulate AreA nuclear export by protein modification of the AreA nuclear export signal.

Chapter 2 - Experimental Procedures

2.1 Strains

2.1.1 Aspergillus nidulans *strains*

A. nidulans strains used in this study that were constructed in the Hynes-Davis lab at The University of Melbourne are listed in Table 2.1 using conventional annotation (CLUTTERBUCK 1973). Strains constructed in the Todd lab at Kansas State University by other lab members or supplied to the Todd lab are listed in Table 2.2, and strains constructed by D.J. Downes are listed in Table 2.3. All strains contain the *veA1* mutation. Detailed descriptions of strain construction are provided in the relevant chapters.

2.1.2 Escherichia coli *strains*

General plasmid manipulation utilized the *E. coli* strain NM522 [F' *proA*$^{+}$*B*$^{+}$ *lacI*^{q} Δ(*lacZ*)*M15*/Δ(*lac-proAB*) *glnV thi*-1 Δ(*hsdS-mcrB*)5] (GOUGH AND MURRAY 1983) or when non-methylated plasmids were required *dcm*$^{-}$ *dam*$^{-}$ SCS110 cells were utilized [*rpsL*(Str^{r}) *thr leu endA thi-1 lacY galK galT ara tonA tsx dam dcm* supE44 Δ(*lac-proAB*) [F´ *traD36 proAB lacI*^{q}ZΔM15]] (Stratagene). Expression of maltose binding protein fusions was carried out in BL21 (DE3) [F^{-} *ompT gal dcm lon hsdS*$_{B}$(r_{B}^{-} m_{B}^{-}) λ(DE3 [*lacI lacUV5-T7 gene 1 ind1 sam7 nin5*])] (WOOD AND MCCRAE 1996). Details of plasmid construction are provided in the relevant chapters.

Table 2.1 "Michael Hynes" *Aspergillus nidulans* strains.

Strain	Genotype
MH1	*biA1*
MH8	*biA1 niiA4 areA102*
MH58	*yA2 AcrA1 galA1 pyroA4 facA303 sB3 nicB3 riboB2*
MH5699	*yA1 areA∆::riboB pyroA4 riboB2 adE20 su(adE20)*
MH8694	*biA1 tamA∆ riboB2*
MH8882	*nmrA∆::Ble*^{R} *amdS-lacZ*
MH9046	*yA1 pabaA1 fmdS-lacZ niiA4*
MH9926	*wA3 pyroA4 gpdA*(p)*areA*^{HA}
MH9949	*biA1 gpdA*(p)*areA*^{HA} *amdS-lacZ*
MH10244	*wA1 yA1 riboB2*
MH10608	*wA3 biA1 gpdA*(p)*areA*$^{HA.H704N.L710I}$
MH10897	*yA1 pabaA1 gpdA*(p)*areA*^{HA} *fmdS-lacZ*
MH10898	*yA1 pabaA1 gpdA*(p)*areA*$^{HA.H704N.L710I}$ *fmdS-lacZ*
MH10967	*yA1 areA∆::riboB riboB2 pyroA4 facB101 fmdS-lacZ*
MH11036	*pyroA4 riboB2 nkuA∆::argB*
MH11050	*yA1 pabaA1 gpdA*(p)*areA*^{HA}(3')*∆::riboB fmdS-lacZ*
MH11091	*yA1 pabaA1 gpdA*(p)*areA*^{HA} *fmdS-lacZ prn309*
MH11131	*yA1 pabaA1 gpdA*(p)*areA*^{HA} *pyroA4 nkuA∆*
MH11132	*yA1 su(adE20) adE20 areA217 riboB2*
MH11167	*nkuA∆ gpdA*(p)*areA*^{HA} *pabaA1 / nkuA∆ gpdA*(p)*areA*^{HA} *pabaA1*
MH11322	*pabaA1 tamA∆ fmdS-lacZ*
MH11324	*biA1 pyroA4 tamA∆ leuB∆::riboB*
MH11457	*gpdA*(p)*areA*$^{HA.\Delta 60\text{-}423}$ *pyroA4 nkuA∆::Bar*
MH11509	*xylP*(p)*nmrA@yA pyroA4 riboB2 fmdS-lacZ nkuA∆*
MH11801	*pabaA1 meaB∆::argB*
MH11808	*pabaA1 tamA*^{C90L}*-A.f.riboB@tamA riboB2*
MH12068	*yA1 pabaA1 pyroA4 gpdA*(p)*areA*$^{HA.\Delta 703\text{-}712}$ *nkuA∆*
MH12101	*niiA4 nkuA∆ pyroA4 A.f.pyroA-gdhA*(-753 bp)*-lacZ@amdS-lacZ*
MH12174	*biA1 niiA4 pyroA4 tamA∆ A.f.pyroA-gdhA*(-753 bp)*-lacZ@amdS-lacZ*
MH12181	*niiA4 pyroA4 leuB∆::riboB A.f.pyroA-gdhA*(-753 bp)*-lacZ@amdS-lacZ*
MH12326	*yA1 pabaA1 fmdS-lacZ pyroA4 riboB2 nkuA∆*
MH12597	*niiA4 tamA*^{C90L}*-A.f.ribo@tamA A.f.pyroA-gdhA*(-753 bp)*-lacZ@amdS-lacZ*
MH12609	*yA1 leuB∆::riboB nkuA∆::Bar niiA4 pyroA4 pabaA1*

Table 2.2 "Richard Todd" *Aspergillus nidulans* strains contructed by others.

Strain[a,b]	Genotype
RT14/A1119	*biA1 chaA1 swoH1*
RT18	*yA1 chaA1 pabaA1 swoH1 gpdA*(p)*areA*^{HA} *fmdS-lacZ*
RT19	*gpdA*(p)*areA*^{HA} *fmdS-lacZ pyroA4*
RT20	*gpdA*(p)*areA*^{HA} *fmdS-lacZ pyroA4 swoH1*
RT21	*yA1 pabaA1 gpdA*(p)*areA*^{HA} *pyroA4 nkuA*Δ::*argB xylP*(p)*swoH*
RT51	*yA1 pabaA1 gpdA*(p)*areA*$^{HA.H704A}$ *pyroA4 nkuA*Δ::*argB*
RT52	*gpdA*(p)*areA*^{HA} *fmdS-lacZ pyroA4 pyrG89 nkuA*Δ::*Bar*
RT54	*gpdA*(p)*areA*^{HA} *fmdS-lacZ pyrG89*
RT59/SS120	*yA1 pyrG89 pyroA4 riboA1 riboB-alcA*(p)*fcp1*
RT60/SS121	*pyrG89 pyroA4 nkuA*Δ::*argB riboB2 riboB-alcA*(p)*bimG*
RT61/SS122	*pyrG89 pyroA4 nkuA*Δ::*argB riboB2 riboB-alcA*(p)*ssu72*
RT62/SS123	*pyrG89 pyroA4 nkuA*Δ::*argB riboB2 riboB-alcA*(p)*pphA*
RT63/SS124	*pyrG89 pyroA4 nkuA*Δ::*argB riboB2 riboB-alcA*(p)*nimT*
RT64/SS87	*pyrG89 pyroA4 nkuA*Δ::*argB riboB2 riboB-alcA*(p)*ppg1*
RT66/SS148	*wA3 pyrG89 argB2 pyroA4 nkuA*Δ::*argB sE15* AN5722Δ::*A.f.pyrG*
RT67/SS150	*wA3 pyrG89 argB2 pyroA4 nkuA*Δ::*argB sE15* AN4544Δ::*A.f.pyrG*
RT68/SS153	*wA3 pyrG89 argB2 pyroA4 nkuA*Δ::*argB sE15 ppg1*Δ::*A.f.pyrG*
RT69/SS154	*wA3 pyrG89 argB2 pyroA4 nkuA*Δ::*argB sE15* AN10077Δ::*A.f.pyrG*
RT70/SS157	*wA3 pyrG89 argB2 pyroA4 nkuA*Δ::*argB sE15* AN10138Δ::*A.f.pyrG*
RT71/SS159	*wA3 pyrG89 argB2 pyroA4 nkuA*Δ::*argB sE15* AN0129Δ::*A.f.pyrG*
RT72/SS160	*wA3 pyrG89 argB2 pyroA4 nkuA*Δ::*argB sE15 ssu72*Δ::*A.f.pyrG*
RT73/SS162	*wA3 pyrG89 argB2 pyroA4 nkuA*Δ::*argB sE15 yvh1*Δ::*A.f.pyrG*
RT74/SS164	*wA3 pyrG89 argB2 pyroA4 nkuA*Δ::*argB sE15* AN0914Δ::*A.f.pyrG*
RT75/SS167	*wA3 pyrG89 argB2 pyroA4 nkuA*Δ::*argB sE15* AN4896Δ::*A.f.pyrG*
RT76/SS125	*pyrG89 pyroA4 nkuA*Δ::*argB riboB2* AN0103Δ::*A.f.pyrG*
RT77/SS129	*pyrG89 pyroA4 nkuA*Δ::*argB riboB2* AN10281Δ::*A.f.pyrG*
RT78/SS130	*pyrG89 pyroA4 nkuA*Δ::*argB riboB2* AN10570Δ::*A.f.pyrG*
RT79/SS132	*pyrG89 pyroA4 nkuA*Δ::*argB riboB2 nem1*Δ::*A.f.pyrG*
RT80/SS133	*pyrG89 pyroA4 nkuA*Δ::*argB riboB2* AN2472Δ::*A.f.pyrG*
RT81/SS135	*pyrG89 pyroA4 nkuA*Δ::*argB riboB2* AN3793Δ::*A.f.pyrG*
RT82/SS137	*pyrG89 pyroA4 nkuA*Δ::*argB riboB2* AN4426Δ::*A.f.pyrG*
RT83/SS140	*pyrG89 pyroA4 nkuA*Δ::*argB riboB2* AN5057Δ::*A.f.pyrG*
RT84/SS141	*pyrG89 pyroA4 nkuA*Δ::*argB riboB2* AN1467Δ::*A.f.pyrG*
RT85/SS143	*pyrG89 pyroA4 nkuA*Δ::*argB riboB2* AN6892Δ::*A.f.pyrG*
RT86/SS145	*pyrG89 pyroA4 nkuA*Δ::*argB riboB2* AN6982Δ::*A.f.pyrG*
RT87/SS170	*pyrG89 pyroA4 nkuA*Δ::*argB riboB2* AN0504Δ::*A.f.pyrG*
RT88/SS147	*pyrG89 pyroA4 nkuA*Δ::*argB riboB2* AN1358Δ::*A.f.pyrG*
RT96	*biA1 gpdA*(p)*areA*^{HA} *pyroA4 fmdS-lacZ crmA*^{T525C}*-A.n.pyrG pyrG89 nkuA*Δ
RT103	*yA1 pabaA1 gpdA*(p)*areA*$^{HA.L710I}$ *pyroA4 nkuA*Δ::*argB*
RT104	*yA1 pabaA1 gpdA*(p)*areA*$^{HA.H704N}$ *fmdS-lacZ pyroA4 nkuA*Δ::*Bar*
RT268	*yA1 pabaA1 gpdA*(p)*areA*$^{HA.H704A}$ *pyroA4 nkuA*Δ::*argB*

[a] A1119 was obtained from The Fungal Genetics Stock Center.

[b] SS# strains provided by Stephen Osmani (Ohio State University).

Table 2.2 "Richard Todd" *Aspergillus nidulans* strains constructed by others (continued).

Strain[a,b]	Genotype
RT315	*yA1 pabaA1 gpdA*(p)*areA*$^{HA.H704E}$ *pyroA4 nkuA*Δ::*argB*
RT316	*yA1 pabaA1 gpdA*(p)*areA*$^{HA.H704F}$ *pyroA4 nkuA*Δ::*argB*
RT317	*yA1 pabaA1 gpdA*(p)*areA*$^{HA.H704D}$ *pyroA4 nkuA*Δ::*argB*
RT411	*pyroA4 pyrG89 nkuA*Δ::*Bar leuD*Δ::*A.f.pyrG*
RT412	*yA1 pyrG89 pabaA1 leuD*Δ::*A.f.pyrG*
RT413	*pyroA4 pyrG89 nkuA*::*Bar leuE*Δ::*A.f.pyrG*
RT414	*yA1 pyrG89 pabaA1 leuE*Δ::*A.f.pyrG*
RT415	*pyroA4 pyrG89 nkuA*::*Bar batA*Δ::*A.f.pyrG*
RT416	*yA1 pyrG89 pabaA1 batA*Δ::*A.f.pyrG*
RT417	*pyroA4 pyrG89 nkuA*Δ::*Bar batE*Δ::*A.f.pyrG*
RT418	*yA1 pyrG89 pabaA1 batE*Δ::*A.f.pyrG*

[a] A1119 was obtained from The Fungal Genetics Stock Center.
[b] SS# strains provided by Stephen Osmani (Ohio State University).

Table 2.3 "Richard Todd" *Aspergillus nidulans* strains constructed by Downes.

Strain	Origin	Genotype
RT116	MH11050 x RT103	*yA1 pabaA1 gpdA*(p)*areA*$^{HA.L710I}$ *pyroA4 fmdS-lacZ nkuA*Δ
RT136	RT20 x MH1208	*yA1 pabaA1 pyroA4 gpdA*(p)*areA*$^{HA.\Delta 703-712}$ *fmdS-lacZ nkuA*Δ
RT139	MH12597 x MH11322	*yA1 tamA*^{C90L}*-A.f.riboB@tamA pyroA4 pabaA1 fmdS-lacZ*
RT153	MH12326 x RT51	*yA1 pabaA1 gpdA*(p)*areA*$^{HA.H704A}$ *fmdS-lacZ*
RT163	MH8694 x MH12326	*biA1 tamA*Δ *riboB2 fmdS-lacZ nkuA*Δ::*Bar*
RT164	MH8694 x MH12326	*yA1 tamA*Δ *riboB2 fmdS-lacZ nkuA*Δ::*Bar*
RT173	MH11808 x RT164	*yA1 tamA*^{C90L}*-A.f.riboB@tamA pabaA1 fmdS-lacZ riboB2 nkuA*Δ
RT174	Transformant of RT52 – Spontaneous diploid	*gpdA*(p)*areA*^{HA} *fmdS-lacZ pyroA4 swoH*$^{+}$ *pyrG89 nkuA*Δ::*Bar* / *gpdA*(p)*areA*^{HA} *fmdS-lacZ pyroA4 swoH*Δ::*A.f.pyrG pyrG89 nkuA*Δ::*Bar*
RT219	MH11036	*pyroA4 riboB2 leuC*Δ::*A.f.pyroA nkuA*Δ::*argB*
RT221	Mutant of MH12399	*xylP*(p)*nmrA@yA pyroA4 pyrG*$^{-}$ *xnrev1-1 niiA4 areA102*
RT244	Transformant of RT96	*biA1 prnA-areA*$^{794-721}$*-gfp-A.f.pyroA@prnA gpdA*(p)*areA*^{HA} *pyroA4 fmdS-lacZ crmA*^{T525C}*-A.n.pyrG pyrG89 nkuA*Δ::*Bar*
RT245	Transformant of RT96	*biA1 prnA-areA*$^{794-721.NES\Delta}$*-gfp-A.f.pyroA@prnA gpdA*(p)*areA*^{HA} *pyroA4 fmdS-lacZ crmA*^{T525C}*-A.n.pyrG pyrG89 nkuA*Δ::*Bar*
RT250	MH11091 x RT54	*yA1 pabaA1 prn-309 pyrG89 gpdA*(p)*areA*^{HA} *fmdS-lacZ*

Table 2.3 "Richard Todd" *Aspergillus nidulans* strains constructed by Downes (continued).

Strain	Origin	Genotype
RT251	Mutant of RT244	*biA1 prnA-areA*$^{794\text{-}721}$*-gfp-A.f.pyroA@prnA gpdA*(p)*areA*^{HA} *pyroA4 fmdS-lacZ crmA*^{T525C}*-A.n.pyrG pyrG89 nkuA*Δ::*Bar ANX1*
RT252	Mutant of RT244	*biA1 prnA-areA*$^{794\text{-}721}$*-gfp-A.f.pyroA@prnA gpdA*(p)*areA*^{HA} *pyroA4 fmdS-lacZ crmA*^{T525C}*-A.n.pyrG pyrG89 nkuA*Δ::*Bar ANX2*
RT253	Mutant of RT244	*biA1 prnA-areA*$^{794\text{-}721}$*-gfp-A.f.pyroA@prnA gpdA*(p)*areA*^{HA} *pyroA4 fmdS-lacZ crmA*^{T525C}*-A.n.pyrG pyrG89 nkuA*Δ::*Bar ANX3*
RT254	Mutant of RT244	*biA1 prnA-areA*$^{794\text{-}721}$*-gfp-A.f.pyroA@prnA gpdA*(p)*areA*^{HA} *pyroA4 fmdS-lacZ crmA*^{T525C}*-A.n.pyrG pyrG89 nkuA*Δ::*Bar ANX4*
RT255	Mutant of RT244	*biA1 prnA-areA*$^{794\text{-}721}$*-gfp-A.f.pyroA@prnA gpdA*(p)*areA*^{HA} *pyroA4 fmdS-lacZ crmA*^{T525C}*-A.n.pyrG pyrG89 nkuA*Δ::*Bar ANX18*
RT256	Mutant of RT244	*biA1 prnA-areA*$^{794\text{-}721}$*-gfp-A.f.pyroA@prnA gpdA*(p)*areA*^{HA} *pyroA4 fmdS-lacZ crmA*^{T525C}*-A.n.pyrG pyrG89 nkuA*Δ::*Bar ANX19*
RT257	Mutant of RT244	*biA1 prnA-areA*$^{794\text{-}721}$*-gfp-A.f.pyroA@prnA gpdA*(p)*areA*^{HA} *pyroA4 fmdS-lacZ crmA*^{T525C}*-A.n.pyrG pyrG89 nkuA*Δ::*Bar ANX20*
RT258	Mutant of RT244	*biA1 prnA-areA*$^{794\text{-}721}$*-gfp-A.f.pyroA@prnA gpdA*(p)*areA*^{HA} *pyroA4 fmdS-lacZ crmA*^{T525C}*-A.n.pyrG pyrG89 nkuA*Δ::*Bar ANX21*
RT259	Mutant of RT244	*biA1 prnA-areA*$^{794\text{-}721}$*-gfp-A.f.pyroA@prnA gpdA*(p)*areA*^{HA} *pyroA4 fmdS-lacZ crmA*^{T525C}*-A.n.pyrG pyrG89 nkuA*Δ::*Bar ANX6*
RT262	Mutant of RT244	*biA1 prnA-areA*$^{794\text{-}721}$*-gfp-A.f.pyroA@prnA gpdA*(p)*areA*^{HA} *pyroA4 fmdS-lacZ crmA*^{T525C}*-A.n.pyrG pyrG89 nkuA*Δ::*Bar ANX25*
RT263	Transformant of RT52	*phmA*Δ*::A.f.pyrG gpdA*(p)*areA*^{HA} *fmdS-lacZ pyroA4 pyrG89 nkuA*Δ
RT280	MH58 / RT259 Diploid	*biA1 prnA-areA*$^{794\text{-}721}$*-gfp-A.f.pyroA@prnA gpdA*(p)*areA*^{HA} *pyroA4 fmdS-lacZ crmA*^{T525C}*-A.n.pyrG pyrG89 nkuA*Δ::*Bar ANX6 / yA2 su(adE20) adE20 AcrA1 galA1 pyroA4 facA303 sB3 nicB8 riboB2*
RT281	MH58 / RT262 Diploid	*biA1 prnA-areA*$^{794\text{-}721}$*-gfp-A.f.pyroA@prnA gpdA*(p)*areA*^{HA} *pyroA4 fmdS-lacZ crmA*^{T525C}*-A.n.pyrG pyrG89 nkuA*Δ::*Bar ANX25 / yA2 su(adE20) adE20 AcrA1 galA1 pyroA4 facA303 sB3 nicB8 riboB2*
RT299	Transformant of MH11036	*pyroA4 riboB2 tamA*^{FLAG}*-A.f.pyro nkuA*Δ::*argB*
RT310	RT299 x MH5699	*yA1 pyroA4 riboB2 tamA*^{FLAG}*-A.f.pyro areA*Δ::*riboB nkuA*Δ

Table 2.3 "Richard Todd" *Aspergillus nidulans* strains constructed by Downes (continued).

Strain	Origin	Genotype
RT311	RT299 x MH11324	*biA1 pyroA4 tamA*^{FLAG}*-A.f.pyro leuB*Δ::*riboB*
RT322	RT310 x RT311	*biA1 pyroA4 riboB2 tamA*^{FLAG}*-A.f.pyro nku*Δ
RT323	RT310 x RT311	*biA1 pyroA4 tamA*^{FLAG}*-A.f.pyro areA*Δ
RT324	RT310 x RT311	*biA1 pyroA4 tamA*^{FLAG}*-A.f.pyro leuB*Δ
RT325	RT310 x RT311	*biA1 pyroA4 tamA*^{FLAG}*-A.f.pyro areA*Δ *leuB*Δ
RT347	Transformant of RT219	*pyroA4 riboB2 leuC*Δ::*A.f.pyro nkuA*Δ::*argB leuC*$^{+}$*@leuC*
RT376	Transformant of RT163	*biA1 tamA*Δ *riboB2 nkuA*Δ::*Bar tamA*$^{C90L.FLAG}$*@fmdS-lacZ*
RT440	Transformant of MH11068	*pyrG89 pyroA4 nkuA*Δ::*Bar batB*Δ::*A.f.pyrG*
RT441	Transformant of MH11068	*pyrG89 pyroA4 nkuA*Δ::*Bar batF*Δ::*A.f.pyrG*
RT444	RT411 x RT414	*pyrG89 pyroA4 leuD*Δ *leuE*Δ
RT453	MH12181 x MH11068	*niiA4 pyroA4 pyrG89 leuB*Δ *A.f.pyroA-gdhA*(-753 bp)-*lacZ@amdS-lacZ*
RT454	RT418 x RT419	*yA1 pyrG89 pabaA1 batE*Δ *batD*Δ
RT457	RT416 x RT440	*pyrG89 pyroA4 batA*Δ *batB*Δ
RT458	RT412 x RT453	*yA1 pabaA1 leuD*Δ *pyrG89 A.f.pyroA-gdhA*(-753 bp)-*lacZ@amdS-lacZ*
RT460	RT412 x RT453	*yA1 pabaA1 leuB*Δ *leuD*Δ *pyrG89 A.f.pyroA-gdhA*(-753 bp)-*lacZ@amdS-lacZ*
RT462	RT412 x RT453	*niiA4 leuB*Δ *leuD*Δ *A.f.pyroA-gdhA*(-753 bp)-*lacZ@amdS-lacZ*
RT465	Transformant of MH11068	*pyrG89* AN4210Δ::*A.f.pyrG pyroA4 nkuA*Δ::*Bar*
RT466	RT441 x RT454	*pabaA1 pyrG89 batE*Δ *batF*Δ
RT472	RT441 x RT454	*yA1 pabaA1 pyrG89 batD*Δ *batE*Δ *batF*Δ
RT473	RT441 x RT454	*yA1 pabaA1 pyrG89 batD*Δ *batF*Δ
RT478	Transformant of MH11068	*pyrG89 pyroA4 nkuA*Δ::*Bar leuR*Δ::*A.f.pyrG*

2.2 Media and Growth Conditions

2.2.1 A. nidulans media and growth conditions

A. nidulans growth conditions and media were as described by COVE (1966), *Aspergillus* Nitrogen-free Minimal media (ANM), adjusted to pH 6.5, was supplemented for auxotrophies (TODD *et al.* 2007a,b). The sole carbon source was either glucose or xylose at 1% (w/v) and nitrogen sources were added to a final concentration of 10 mM, unless otherwise stated.

2.2.2 Bacterial media and growth conditions

Bacteria were grown on Luria broth (LB) supplemented with 50 µg/ml ampicillin to select for ampicillin resistant plasmids, and 0.04 mM IPTG (isopropyl-β-D-thiogalactopyranoside) with 0.005% X-Gal (5-bromo-4-chloro-3-indolyl-β-D-galactoside) for blue-white colony screening as required (SAMBROOK *et al.* 1989).

2.3 Chemical reagents and standard solutions

Binding Buffer (1x)

25 mM HEPES-KOH pH 7.6

40 mM KCl

10 % glycerol

5 mM $ZnCl_2$

MOPS (1x)

20 mM MOPS pH 7.0

5 mM Sodium acetate

1 mM EDTA

Phosphate Buffer (0.2 M)

78 mM Na_2HPO_4
122 mM NaH_2PO_4

Protein extraction buffer

50 mM Tris-HCl pH 8.0

132 mM NaCl

2.7 mM KCl

1.0 mM $ZnCl_2$

1x Amresco protease inhibitor cocktail

Protein denaturing buffer

10 mM Tris-HCl pH 8.0

25 mM Ammonium acetate

1 mM EDTA

10% Trichloroacetic acid

Protein resuspension buffer

100 mM TRIS-HCl pH 11.0

3% Sodium dodecyl sulfate

RNA Extraction buffer

7 M Urea

100 mM Tris-HCl pH 8.0

10 mM EDTA

1 % Sodium dodecyl sulfate

TBE (1x)

89 mM Tris-HCl pH 8.0

89 mM Boric acid

20 mM EDTA

TBS (1x)

25 mM Tris-HCl pH 7.2

150 MM NaCl

2.4 Standard Molecular techniques

2.4.1 DNA manipulation

Plasmid DNA was isolated using Wizard Plus SV Miniprep DNA purification kit (Promega) following the manufacturers instructions and *A. nidulans* genomic DNA isolated according to (LEE AND TAYLOR 1990). PCR products and DNA fragments isolated from agarose gels were cleaned with the Wizard SV Gel and PCR Clean Up System (Promega) following the manufacturer's instructions. Digestion using restriction enzymes (Promega; New England Biolabs), dephosphorylation with Arctic Shrimp alkaline phosphatase (Promega), and ligations using T4 DNA ligase (Promega) were carried out following the manufacturers' instructions. DNA was separated on 1-2% agarose gels by electrophoresis in 1x TAE buffer. DNA was quantified using a Nanodrop 1000. Bacterial cells were rendered competent by treatment with calcium chloride (SAMBROOK *et al.* 1989) and stored at -80ºC. DNA and 100 µl of competent cells were incubated on ice for 10 minutes followed by a 2-minute heat-shock at 37ºC and returned to ice for 1-2 minutes before plating on LB media with 50 µg/ml ampicillin.

2.4.2 RNA preparation

Total RNA was isolated by grinding mycelia under liquid nitrogen and subsequent addition to RNA extraction buffer. Resuspended mycelia were separated by subsequent phenol-chloroform-isoamylalcohol (two) and chloroform purifications. RNA was first precipitated in 3M ammonium acetate and 50% isopropanol then resuspended in DEPC-H_2O and re-precipitated overnight in 4M lithium chloride at -20ºC (SAMBROOK AND RUSSELL 2001). RNA quality was determined by visualization of ribosomal RNA bands after electrophoretic separation in a 1.2% agarose gel containing 1.1% formaldehyde run in 1x MOPS buffer. RNA was treated with RQ1 DNase (Promega) following the manufacturer's instructions. RNA was quantified using a Nanodrop 1000 Spectrophotometer (Thermo Scientific).

2.4.3 Polymerase Chain Reaction

PCR reactions were carried out using Ex-Taq (TaKaRa), Phusion (Finnzymes), or AccuStart II Geltrack PCR SuperMix (Quanta Biosciences) DNA polymerases according to the manufacturers' instructions. Templates were added approximately 1 ng for plasmid DNA and 100 ng *A. nidulans* genomic DNA. All reactions followed the recommended denaturing and annealing conditions with 33-36 amplification cycles. Oligonucleotide primers for PCR (IDT) are described in the relevant chapters.

2.4.4 Southern Blot

DNA samples were resolved in agarose gels and treated with 0.25M HCl for 12 minutes for depurination. DNA was then transferred to either Hybond N+ or XL positively charged membranes (Amersham) using 0.4M NaOH capillary transfer. Probe generatation, hybridization (42ºC overnight), and detection was carried out using the DIG (digoxigenin) High prime DNA labeling and detection starter kit II (Roche) following the manufacturer's instructions. Films exposed to Southern blots were developed in an Ecomax^{TM} X-ray film processor (Protec).

2.4.5 DNA sequencing

DNA sequencing of plasmids and PCR products was carried out by the Kansas State University DNA Sequencing and Genotyping Facility (Kansas, USA). Whole genome sequencing was carried out at the University of Kansas Medical Center Genome Sequencing Facility (Kansas, USA).

2.5 Aspergillus growth and genetic manipulation

2.5.1 Aspergillus nidulans growth and genetic analysis.

A. nidulans growth testing was as described (PONTECORVO *et al.* 1953). *A. nidulans* was crossed and manipulated as described (TODD *et al.* 2007a,b).

2.5.2 A. nidulans transformation

Transformation of *A. nidulans* was carried out as described by ANDRIANOPOULOS AND HYNES (1988) with modifications (DOWNES *et al.* 2013). The *nkuA*Δ strain, which has decreased non-homologous integration, was used for targeted integration (NAYAK *et al.* 2006). Where necessary, heterokaryon rescue to assess lethality was performed as described (OSMANI *et al.* 2006b).

2.5.3 Construction of diploids and determination of ploidy

Construction of diploid strains was as described (TODD *et al.* 2007a). Conidia of potentially diploid strains were suspended in Tween 80 and 20 conidia were measured at 40x magnification. Control haploid conidia from RT52 ranging from ~1500-2000 nm in diameter and control diploid conidia from MH11167 ranging from ~2000-2500 nm in size were used for comparison.

2.5.4 Benlate induced haploidization

Haploidization of diploids was carried out according to TODD *et al.* (2007a) by stab inoculating plates containing 1 μg ml^{-1} of Benlate (Benomyl). Sectors were picked after 10 days.

2.5.5 Growth rate determination

Growth rate is the increase in radius of a single colony per plate over a 5-day period.

2.5.6 4-Nitroquinoline oxide mutagenesis

Mutagenesis was carried out using 4-nitroquinoline 1-oxide (4-NQO; Sigma) primarily as described (BAL *et al.* 1977). ~10^8 conidia were exposed to 4.0 μg ml^{-1} 4-NQO at 37ºC for 30 minutes. 4-NQO was quenched with an equal volume of 0.5 M sodium thiosulfate. A kill curve

was generated and treatments causing 95% death were plated on selective supplemented ANM. Mutated strains were recovered after 2-4 days growth.

2.5.7 5-FOA isolation of uridine and uracil auxotrophs

Uridine and uracil auxotrophs (*pyrG*$^-$) were generated by stab inoculating *pyrG*$^+$ strains onto ANM media containing 5 mM uracil, 10 mM uridine and 1 mg ml^{-1} 5-fluoroorotic acid, 5-FOA (US Biological). Spontaneous *pyrG*$^-$ mutant sectors showing 5-FOA resistance were picked to selective media after two days incubation at 37ºC.

2.6 Characterization of Gene Expression

2.6.1 β-galactosidase and NADP-GDH assays

β-galactosidase and NADP-GDH assays were performed as described (PATEMAN 1969; DAVIS *et al.* 1988) using soluble protein extracts. β-galactosidase specific activity is defined as A_{420} x 10^3 min^{-1} mg^{-1} of soluble protein. NADP-GDH activity is expressed as 1 nmol of NADP reduced min^{-1} mg^{-1} of soluble protein. Protein concentrations were determined using Bio-Rad Assay reagent (Bio-Rad).

2.6.2 Real-time reverse transcriptase-PCR

For Quantitative real-time reverse-transcriptase-PCR (qRT-PCR) cDNA was produced from DNase treated RNA using the Reverse Transcriptase System (Promega) or qScript cDNA SuperMix (Quanta Biosciences). qRT-PCR was carried out in a MyiQ thermocycler (Bio-Rad) with iTAQ™ Universal SYBR® Green Supermix (Bio-Rad) and results analyzed with iQ5 v2.1 (Bio-Rad). Fold change was calculated using the $\Delta\Delta C_T$ efficiency correction method with β-tubulin encoding *benA* as the reference housekeeping gene (MAY *et al.* 1987; PFAFFL 2001; SCHMITTGEN AND LIVAK 2008). Primers (IDT) were designed to specifically amplify cDNA by overlapping a splice junction. Primer efficiencies were calculated from a serial dilution with 3-5 concentrations. Primer sequences, target regions, and efficiencies and are provided in the relevant chapters.

2.7 Microscopy

2.7.1 Immunofluorescence and GFP microscopy

Immunostaining was carried out as described (TODD *et al.* 2005). Microscopy was performed using an Olympus BX51 upright biological reflected fluorescence microscope equipped with Nomarski differential interference contrast (DIC), an EXFO X-Cite 120 Q fluorescence illumination system and a UPlanFLN Plan Semi Apochromat (field number FN26.5) Fluorite 100× oil objective with a numerical aperture of 1.30 as described (HUNTER *et al.* 2014). GFP fluorescence or α-hemagglutinin (α-HA) immunofluorescence was quantified with ImageJ (W. S. Rasband, ImageJ, U.S. National Institutes of Health, Bethesda, Maryland, USA; http://imagej.nih.gov/ij/; 1997 to 2012) using representative raw images using the ratio of fluorescence from adjacent nuclei and cytoplasmic regions.

2.8 Characterization of DNA Binding and protein-protein interaction

2.8.1 Chromatin Immunoprecipitation (ChIP) and ChIP-sequencing (ChIP-seq)

Mycelia were grown for 16 h, fixed in 1% formaldehyde for 20 m then quenched with 0.6 M glycine. Crosslinking was performed for two biological replicates as previously described (SUZUKI *et al.* 2012) using 2 µg of either anti-FLAG (M2, Sigma) or anti-HA (F7, Santa Cruz Biotechnology). Chromatin immunoprecipitation, quantitative real-time PCR, and ChIP-seq were carried out by K.H. Wong (Harvard Medical School, Boston, Massachusetts).

2.8.2 Electrophoretic mobility shift assay (EMSA)

EMSA probes were generated by PCR from MH1 genomic DNA using IR-700 labeled primers (IDT). EMSA was carried out as previously described in 4-6% polyacrylamide gels (TODD *et al.* 1998) run in 1x TBE at 4ºC, with *E. coli* crude extracts, *A. nidulans* crude native and nuclear extracts of immunoprecipitated proteins. Gels were directly visualized using Odyssey Image Studio Software and the Odyssey Fc (LI-COR).

2.9 Protein purification and Western Blot

2.9.1 Bacterial crude extracts

Maltose Binding Protein fusions were purified from *E. coli* cells suspended in 1x Binding Buffer using 0.1 mm silica beads in a FastPrep-24 (MP Bio) at 6.0 m/s 3 times for 40 s with 5 m cooling periods. Cells were then sonicated 16 times for 15 s at 40% with a 15 s rest. Cellular debris was removed by 4ºC centriguation at 18,000 *g* for 10 m. Extracts were concentrated in a Millipore Centrifugal filter Ultracel®.

2.9.2 **A. nidulans** *native whole protein extract*

Native proteins were purified from frozen mycelia by homogenization in 1 ml extraction buffer (50 mM Tris-HCl pH8, 137mM NaCl, 2.7 mM KCl, 1.0 mM $MgCl_2$ and 1x Amresco protease inhibitor cocktail) using FastPrep-24 (MP Bio) at 6.5 m/s 5 times for 20 s with 5 m cooling periods. Mycelial debris was removed by two 4ºC centrifugations at 16,000 *g* for 10 m and 2 m.

2.9.3 **A. nidulans** *denatured whole protein extract*

Denatured proteins were purified from frozen *A. nidulans* mycelia by homogenization in 1 ml denaturing buffer (10 mM Tris-HCl pH8, 25 mM NH_4Acetate, 1mM EDTA, 10% trichloroacetic acid (TCA)) using FastPrep-24 (MP Bio) at 6.5 m/s 5 times for 20 s with 5 m cooling periods. Proteins were pelleted by 4ºC centrifugation at 16,000 g for 10 m. The pellet was washed with Tris-NaOH (pH 11) and resuspended in protein resuspension buffer (0.1 M Tris-HCl pH 11, 3% SDS). Proteins were boiled for 3 minutes and then debris removed by two 4ºC centrifugations at 16,000 *g* for 2 m.

2.9.4 Column Purification of epitope-tagged proteins

FLAG-tagged proteins were purified from native *A. nidulans* protein extracts using the FLAG Immunoprecipitation Kit (Sigma) following the manufacturer's instructions for 3x peptide elution.

2.9.5 SDS-Page electrophoresis and Western Blot

Proteins were separated by 12% SDS-PAGE for either Western blot or Coomassie blue staining. For Western blot, proteins were transferred to PVDF membranes by electroblot, detected using monoclonal 1:15,000 M2 anti-FLAG (Sigma) and 1:10,000 anti-mouse/rabbit-IgG-POD (Roche) antibodies, and development with the BM Chemiluminescence Western blotting kit (Roche). Images were captured using Odyssey Image Studio Software and the Odyssey Fc (LI-COR).

2.10 DNA and RNA Sequencing

2.10.1 Sanger Sequencing of DNA

PCR products and plasmid preps were sequenced on the Applied Biosystems 3730 DNA Analyzer at the DNA Sequencing and Genotyping Facility (Kansas State University) to confirm correct amplification and cloning.

2.10.2 Whole genome sequencing

Genomic DNA was isolated from mycelia grown in 100 ml supplemented ANM with 10 mM ammonium tartrate in shaking flasks for 16 h by grinding in liquid nitrogen as described above (Section 2.4.1). DNA was treated with RNAse A (Sigma), which was subsequently removed by phenol-chloroform isopropanol purification. Additional chloroform purification was carried to remove residual organic reagents. DNA was sent to the Genome Sequencing Facility (Kansas University Medical Center, Kansas City, Kansas) for library generation and sequencing. Genomic libraries were pooled and sequenced in a 50-cycle single end run on the HiSeq2500 Sequencing System (Illumina).

2.10.3 RNA sequencing

Poly A RNA transcriptome libraries from three independent biological replicates were generated using the TruSeq Stranded Total RNA Sample Prep Kit (Illumina). Library insert size and quality was determined by the Integrated Genomics Facility (Kansas State University, Manhattan, Kansas) using the Bioanalyzer 2100 (Agilent) and PicoGreen. Libraries were adjusted to 4 nM for multiplexed sequencing with nine pooled libraries per lane. Pooled libraries

were sequenced in a 50-cycle single end run on the HiSeq2500 Sequencing System (Illumina) at the Genome Sequencing Facility (Kansas University Medical Center, Kansas City, Kansas).

2.11 Bioinformatics & *in silico* analyses

2.11.1 Sequence identification and manipulation.

DNA and protein sequences were downloaded from the *Aspergillus* Genome Database, AspGD (www.aspgd.org; ARNAUD *et al.* 2012), the *Saccharomyces* Genome Database, SGD (www.yeastgenome.com; CHERRY *et al.* 2012) or the Broad Institute genomes database (www.broadinstitute.org). Sequences for animal and plant proteins were identified and downloaded using the NCBI protein database (www.ncbi.nlm.gov/protein) and the EMBL-EBI Pfam database (http://pfam.xfam.org; FINN *et al.* 2014). Protein and sequence similarity was characterized using Blast (www.ncbi.nlm.gov/blast). Sequences mere manipulated and analyzed in Geneious version 5.3.5 created by Biomatters (www.geneious.com). Alignments were created using ClustalW2 (LARKIN *et al.* 2007) or Clustal Omega (SIEVERS *et al.* 2011) on the EMBL-EBI server (http://www.ebi.ac.uk/Tools/msa) and shaded using BoxShade 3.2 (K. Hofmann & M.D.Baron) made available online by ExPASy (www.ch.embnet.org/software/BOX_form.html).

2.11.2 Characterization of regulatory elements.

Putative regulatory elements of groups of genes were identified using SCOPE analysis (www.genie.dartmouth.edu/scope; CARLSON *et al.* 2007) using the 1000 bp upstream *A. nidulans* reference option. Consensus sites were detected across the *A. nidulans* genome using PatMatch (www.aspergillusgenome.org/cgi-bin/PATMATCH/nph-patmatch; YAN *et al.* 2005). Consensus motifs of alignments were generated using WebLogo (www.weblogo.berkley.edu; SCHNEIDER AND STEPHENS 1990; CROOKS *et al.* 2004).

2.11.3 Protein characterization.

Predicted subcellular localization of proteins was determined using PSORTII (NAKAI AND HORTON 1999; NAKAI AND HORTON 2007), WoLF PSORT (HORTON *et al.* 2007) available via the PSORT WWW Server (www.psort.hgc.jp), Predotar 1.03 (https://urgi.versailles.inra.fr/predotar/predotar.html; SMALL *et al.* 2004), MitoProtVII (http://ihg.gsf.de/ihg/mitoprot.html; CLAROS AND VINCENS 1996), and TargetP

(http://www.cbs.dtu.dk/services/TargetP/; NIELSEN *et al.* 2000). Nuclear Export Sequences in proteins were determined using NetNES 1.1 (www.cbs.dtu.dk/services/NetNES; LA COUR *et al.* 2004) and ValidNESs (www.validness.um.edu.tw; FU *et al.* 2013). 9aaTADs were identified using the online prediction tool (http://www.med.muni.cz/9aaTAD/). Protein structure modeling was performed using SWISS-MODEL (http://swissmodel.expasy.org/; ARNOLD *et al.* 2006; GUEX *et al.* 2009; KIEFER *et al.* 2009; BIASINI *et al.* 2014).

2.11.4 Whole genome sequencing.

Analysis of whole genome sequenced was carried out on the Galaxy platform (galaxyproject.org; GIARDINE *et al.* 2005; BLANKENBERG *et al.* 2010b; GOECKS *et al.* 2010). FASTA files were converted to FASTQ format using FASTQ Groomer (BLANKENBERG *et al.* 2010a). Sequence read quality was determined using FastQC (http://www.bioinformatics.babraham.ac.uk/projects/fastqc/). Nucleotides were aligned using BWA for Illumina with default settings (LI AND DURBIN 2009) to the *A. nidulans* FGSC_A4 genome downloaded from AspGD January 8th 2014 (CERQUEIRA *et al.* 2014). Genome coverage was determined using BEDTools (QUINLAN AND HALL 2010). Variants were identified using FreeBayes (GARRISON AND MARTH 2012; BLANKENBERG *et al.* 2014) with default settings except for: report polymorphism probability (-P: 0.01), ploidy (-p: 1), minimum observations (-F: 0.5) and minimum coverage (-!: 4). Variants unique to mutants were identified using the Select Variants tool. High quality SNPs are those that occur only in the mutant with a minimum of four fold coverage and two supporting reads (MCKENNA *et al.* 2010; DEPRISTO *et al.* 2011; VAN DER AUWERA *et al.* 2013).

2.11.5 cDNA sequencing and in silico analyses

cDNA libraries were sequenced on the Illumina Hi-Seq 2500 Sequencing System platform in a 50-cycle single end run by the Genome Sequencing Facility (Kansas University Medical Center, Kansas City, Kansas). Analysis of RNA-seq was carried out on the Galaxy platform (galaxyproject.org; GIARDINE *et al.* 2005; BLANKENBERG *et al.* 2010b; GOECKS *et al.* 2010). FASTA files were converted to FASTQ format using FASTQ Groomer (BLANKENBERG *et al.* 2010a). Sequence quality was determined using FastQC and read trimming was not

required (http://www.bioinformatics.babraham.ac.uk/projects/fastqc/). Nucleotides were aligned to the *A. nidulans* FGSC_A4 genome downloaded from AspGD December 11th 2014 (GALAGAN *et al.* 2005a; CERQUEIRA *et al.* 2014) using TopHat version 2.0.6 (KIM *et al.* 2013) with default settings with the following exceptions: minimum intron length = 10; maximum intron length = 4,000; indel search = NO; maximum alignment number = 40; minimum length of read = 20. Bam files generated from TopHat were downloaded from Galaxy and separated into strand specific Bam files using SAMtools version 1.1 (LI *et al.* 2009). SAMtools was downloaded on 8th December 2014 (www.sourcesforge.net/projects/samtools/files/samtools) with the latest update occurring 23rd September 2014. SAMtools was operated in Bash with the following commands:

> #!/bin/bash

> samtools view -b -F 0x10 INFILE.bam > OUTFILE_F.bam

(For forward reads)

> samtools view -b -f 0x10 INFILE.bam > OUTFILE_R.bam

(For reverse reads)

Seperated Bam files were uploaded to Galaxy and Groomed with FASTQ Groomer (BLANKENBERG *et al.* 2010a). Transcripts were generated using the AspGD annotations (s10_m03_r15) as a template as guide for Cufflinks Version 2.1.1.7 (ARNAUD *et al.* 2012; TRAPNELL *et al.* 2013). Cufflinks was run with default settings with the exception of: max intron length = 4,000; bias correction = yes; multi read correction = yes. Transcripts from all conditions and strains were merged in Cuffmerge with the reverence annotations as a guide. Differential expression was determined using CuffDiff with default settings and maintaining separation of biological replicates to allow for statistical testing (TRAPNELL *et al.* 2013), and analysis carried out in cummeRbund (Version 2.8.2) in R Version 3.1.2 downloaded from http://www.r-project.org/ (The R Core Team; 2012), with the cummeRbund recommended and required plugins (GOFF *et al.* 2013).

2.11.6 ChIP-sequencing analysis

Mycelia of *tamA*^{FLAG} (RT322), *tamA*^{FLAG} *areA*Δ (RT323), *tamA*^{FLAG} *leuB*Δ (RT324) and *tamA*^{FLAG} *areA*Δ *leuB*Δ (RT325) for ChIP-seq were grown in supplemented ANM with 10 mM ammonium or 10 mM glutamine for 16 hours and fixed in 1% formaldehyde for 20 m then quenched with 0.6 M glycine for one minute (SUZUKI *et al.* 2012). Mycelia were rinsed with cold double distilled water and immediately frozen in liquid nitrogen. Two biological replicates were generated for each condition. Samples were stored at -80ºC for less than one month and shipped on dry ice by overnight courier to Boston for further analysis. K. H Wong (Harvard Medical School, Boston, Massachusetts) carried out immunopreciptation, qRT-PCR and ChIP-seq using 2 µg of either anti-FLAG (M2, Sigma). Zhengqiang Miao (University of Macau, Macau SAR, China) identified peak location and fold enrichment using Model-based analysis for ChIP-seq (MACS; ZHANG *et al.* 2008), with a minimum 4-fold enrichment and a p-value of $1x10^{-7}$. Sequences for SCOPE analysis were downloaded from AspGD and submitted to the SCOPE Web interface available at http://genie.dartmouth.edu/scope/ with the *A. nidulans* 1,000 bp fixed upstream region used for comparison (CARLSON *et al.* 2007; CHAKRAVARTY *et al.* 2007a,b).

2.12 Abbreviations used frequently within the text

AH: Aspartate hydroxamate

ANM: *Aspergillus* Nitrogen-free Minimal media

AspGD: *Aspergillus* Genome Database

BAT: Branched chain amino acid aminotransferase

BCAA: Branched chain amino acid

ChIP: Chromatin immunoprecipitation

EMSA: Electrophoretic Mobility Shift Assay

EPSP: 5-enolpyruvylshikimate-3-phosphate synthetase

FGSC: Fungal Genetics Stock Center

GFP: Green Fluorescent Protein

GO: Gene Ontology

GOGAT: NAD-dependent glutamate synthase

GS: Glutamine synthetase

HA: Hemagglutinin

IPM: Isopropylmalate

KIX: Kinase-inducible domain interacting domain

MACl: Methylammonium chloride

MACS: Model-based analysis for ChIP-seq

MBP: Maltose binding protein

NAD-GDH: NAD-dependent glutamate dehydrogenase

NADP-GDH: NADP-dependent glutamate dehydrogenase

NES: Nuclear Export Signal

NLS: Nuclear Import Signal

qRT-PCR; Quantitative real-time reverse-transcriptase PCR

SDR: Short-chain dehydrogenase-reductase

SGD: *Saccharomyces* Genome Database

TU: Thiourea

4-NQO: 4-Nitroquinoline 1-oxide

5-FOA: 5-fluoroorotic acid

9aa TAD: Nine amino acid transactivating domain

Chapter 3 - Branched-chain amino acid biosynthesis

3.1 Abstract

Bacteria, plants, and fungi but not animals synthesize the branched chain amino acids isoleucine, leucine and valine. Mutants of the fungal pathogens *Candida albicans*, *Cryptococcus neoformans*, and *Aspergillus fumigatus* that lack branched chain amino acid biosynthesis have reduced virulence and pathogenicity. Therefore enzymes in the branched chain amino acid biosynthesis pathway are potential targets for antifungal therapy. Branched chain amino acid biosynthesis has been well characterized in the yeast *Saccharomyces cerevisiae* but is less well understood in *Aspergillus* species. In *Aspergillus nidulans* only three of the eight steps in branched chain amino acid biosynthesis have been characterized. In addition the Zn(II)2Cys6 regulator of leucine biosynthesis, LeuB, has been identified, but which genes in the pathways it regulates is not known. We have used gene knockouts to characterize three steps in branched chain amino acid biosynthesis carried out by α-isopropylmalate synthetase, β-isopropylmalate dehydrogenase, and branched chain amino acid aminotransferase. Additionally we have characterized regulated expression of leucine biosynthesis genes using real-time reverse transcriptase PCR. We have also shown that LeuB and leucine biosynthesis regulates expression of *gdhA,* which encodes NADP-dependent glutamate dehydrogenase, a key nitrogen assimilation enzyme. Using promoter analysis we have shown that LeuB regulates *gdhA* through a consensus $CCGN_4CGG$ motif and a non-consensus $CCGN_5CGG$ motif. Finally, we characterized a Zn(II)2Cys6 transcription factor, LeuR, with similarity to LeuB.

3.2 Introduction

The branched chain amino acids (BCAA) leucine, isoleucine, and valine are essential dietary amino acids in mammals. Fungi, however, can synthesize these three amino acids. For this reason, BCAA biosynthesis enzymes have been suggested as possible drug targets for treatment of infections by opportunistic pathogens. Branched chain amino acid auxotrophs in *Cryptococcus neoformans, Candida albicans,* and *Aspergillus fumigatus* show decreased pathogenicity (KINGSBURY *et al.* 2010; OLIVER *et al.* 2012; DO *et al.* 2015). Synthesis of the three BCAAs occurs via a dichotomous biochemical pathway (Figure 3.1) and has been well characterized in the yeast *Saccharomyces cerevisiae* (reviewed by KOHLHAW 2003). Studies of BCAA biosynthesis in *A. fumigatus*, *Aspergillus niger,* and *Aspergillus nidulans* have shown both divergence and similarity with *S. cerevisiae* (MACDONALD *et al.* 1974; WILLIAMS *et al.* 1996; POLOTNIANKA *et al.* 2004; SHIMIZU *et al.* 2010; OLIVER *et al.* 2012). For example, *A. fumigatus* encodes at least two functional dihydroxyacid dehydratases (OLIVER *et al.* 2012) whereas *S. cerevisiae* encodes only one (VELASCO *et al.* 1993), whereas both encode a single α-isopropylmalate isomerase (SKALA *et al.* 1991; POLOTNIANKA *et al.* 2004). Therefore, to fully understand BCAA biosynthesis in the filamentous fungi further studies on the remaining uncharacterized genes were required. The genes encoding α-isopropylmalate synthase, β-isopropylmalate dehydrogenase, and the branched chain amino acid aminotransferase (BAT) in the *A. nidulans* leucine branch of BCAA biosynthesis pathway were not characterized prior to this study (Figure 3.1). The BATs are bidirectional enzymes and, in addition to synthesizing isoleucine, leucine and valine, are required to catalyze the first step in their degradation (DICKINSON AND NORTE 1993).

Leucine biosynthesis in *A. nidulans* is thought to be regulated by the Zn(II)2Cys6 transcription factor, LeuB, as it has similarity to *S. cerevisiae* Leu3p and *leuB*Δ is a leaky leucine auxotroph (POLOTNIANKA *et al.* 2004). LeuB is predicted to act similarly to its yeast homolog Leu3p, which acts as both a repressor and an activator dependent on the level of free leucine in cells (BRISCO AND KOHLHAW 1990). Leu3p acts as a repressor, but is converted to an activator by binding of the leucine biosynthesis pathway intermediate α-isopropylmalate (α-IPM). When leucine is abundant, it interacts with the α-IPM synthetases, Leu4p and Leu9p, to repress their activity and decrease α-IPM production. This decrease in α-IPM results in Leu3p reverting to a

repressor. Thereby cellular leucine levels provide a negative feedback mechanism for regulation of leucine biosynthesis. In addition to regulating specific leucine biosynthesis genes, Leu3p regulates expression of the NADP-dependent glutamate dehydrogenase (NADP-GDH) encoding gene, *GDH1* (HU *et al.* 1995). NADP-GDH acts in the GOGAT cycle to assimilate nitrogen nutrients. Regulation of the *GDH1* ortholog, *gdhA*, by LeuB is conserved in *A. nidulans* (POLOTNIANKA *et al.* 2004). NADP-GDH produces glutamate, which is the final amino donor in leucine biosynthesis, therefore regulation of *gdhA* and *GDH1* by LeuB/Leu3p is thought to ensure sufficient glutamate levels to sustain leucine production. It has been suggested that leucine levels may act as a sensor for amino acids abundance because of the feedback mechanisms provided by leucine abundance, the regulation of NADP-GDH expression by LeuB/Leu3p, and that leucine is one of the most abundant protein-incorporated amino acids and one of the least abundant free cellular amino acids (KOHLHAW 2003). Therefore we were keenly interested in understanding both leucine biosynthesis and regulation by LeuB in *A. nidulans*.

In this chapter we have characterized the genes encoding α-isopropylmalate synthase, β-isopropylmalate dehydrogenase and the branched chain amino acid aminotransferase, resulting in the complete annotation of leucine biosynthesis genes in *A. nidulans*. We have investigated the regulation of these genes by LeuB and the effects of both LeuB and leucine biosynthesis on the regulation of *gdhA*. Parts of this research have been published, and are noted as such at the appropriate sections (DOWNES *et al.* 2013).

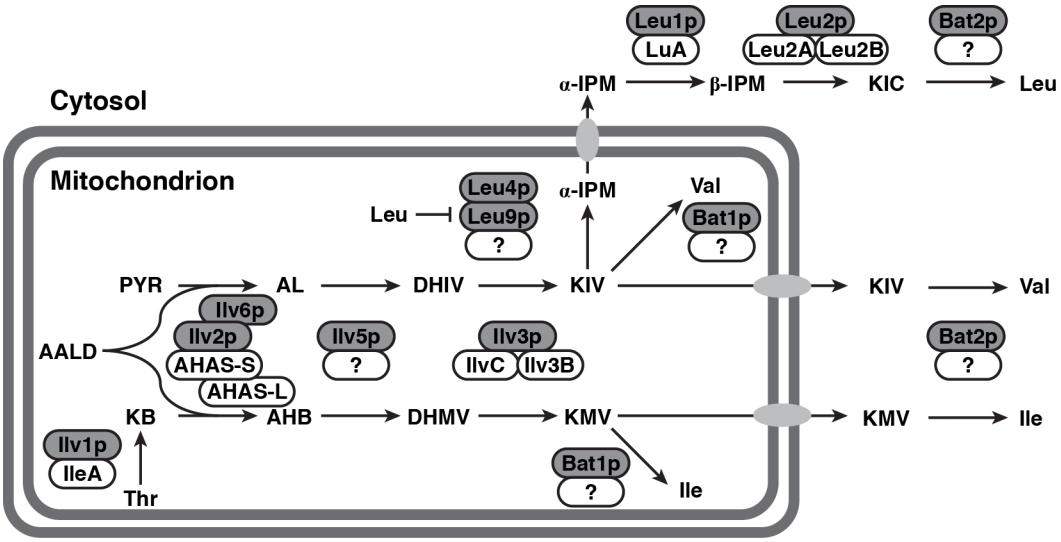

Figure 3.1 Branched chain amino acid biosynthesis in fungi

Subcellular localization and biosynthetic pathway of isoleucine (Ile), leucine (Leu) and valine (Val), with a comparison of *S. cerevisiae* enzymes (grey boxes) and *Aspergillus* enzymes (white boxes), including *A. nidulans* (IleA, AHAS-S, AHAS-L, LuA), *A. fumigatus* (IlvC, Ilv3B) and, *A. niger* (Leu2A, Leu2B). Threonine (Thr); active acetaldehyde (AALD); α-ketobutyrate (KB); pyruvate (PYR); α-aceto-α-hydroxybutyrate (AHB); acetolactate (AL); α,β-dihydroxy-β-methylvalerate (DHMV); α,β-dihydroxyisovalerate (DHIV); α-keto-β-methylvalerate (KMV); α-ketoisovalerate (KIV); α-isopropylmalate (α-IPM); β-isopropylmalate (β-IPM); α-ketoisocaproate (KIC). Adapted from (KOHLHAW 2003).

3.3 Materials & Method

3.3.1 Strain construction

Full genotypes of strains can be found in Tables 2.1-3. Knockout constructs sourced from the FGSC (McCluskey *et al.* 2010) were transformed into MH11059 (*pyroA4 pyrG89 nkuA*Δ) and selected for uracil/uridine prototrophy to generate *leuD*Δ/AN0912 (RT411 Δ -7 to +1,431 bp), *leuE*Δ/AN2793 (RT413; Δ -6 to +1,233 bp), *batA*Δ/AN4323 (RT415; Δ +65 to +1,722 bp), *batB*Δ/AN5957 (RT440; Δ +25 to +1,395 bp), *batD*Δ/AN7876 (RT419; Δ -7 to +1,297 bp), *batE*Δ/AN0385 (RT417; Δ +27 bp to 1,302 bp), *batF*Δ/AN8511 (RT441; Δ -9 to +1,230 bp) and, *leuR*Δ/AN4744 (RT478; Δ +14 to +2,393 bp). All transformants were tested by Southern blot to confirm a single homologous double crossover integration event at the correct locus by probing with the 982 bp *Kpn*I-*Ssp*I fragment of *A.f. pyrG*$^{+}$. Restriction enzymes used for Southern blot analysis and expected band sizes calculated using the reference genome sequence for each gene replacement are listed in Table 3.1. Meiotic crossing was used to generate combinations of the *bat* deletion set and the *leuD*Δ *leuE*Δ double mutant (RT444). RT453, which contains *leuB*Δ and the -753 bp *gdhA-lacZ* reporter, was crossed to *leuD*Δ background to construct RT460 (*leuB*Δ *leuD*Δ -753 bp *gdhA-lacZ*) and RT462 (*leuD*Δ -753 bp *gdhA-lacZ*). RT460 was crossed to RT478 (*leuR*Δ) to generate combinations of *leuB*Δ and *leuD*Δ with *leuR*Δ. The presence of each deletion in the progeny of crosses was confirmed by diagnostic Southern blot; diagnostic digests for each gene deletion are listed in Table 3.1.

Table 3.1 Southern blot analysis of BCAA gene deletion strains.

Gene	Knockout Construct Integration		Meiotic Cross Scoring	
	Restriction Enzyme	Deletion[a] band size(s)	Restriction Enzyme	Deletion[a] band size(s)
leuD	*Eco*RV	4.2 kb	–	–
	*Pst*I	1.5, 4.2 kb		
	*Xho*I	2 kb		
leuE	*Hin*dIII	2.2, 4.3 kb	–	–
	*Eco*RI	4.4, 6.3 kb		
	Sac*I*	1.5, 8.9 kb		
leuR	*Pvu*II	6.8 kb	*Eco*RV	7.8 kb
	*Kpn*I	2.7 kb	*Pvu*II	6.8 kb
	*Apa*I	3.6, 1.8 kb		
batA	*Sac*II	3.3 kb	*Eco*RV	9.3 kb
	*Sna*BI	22 kb	*Cla*I	3.5 kb
			*Nco*I	9.3 kb
batB	*Nco*I	6.1	*Eco*RV	6 kb
	*Sac*II	3.4	*Cla*I	4.5 kb
			*Nco*I	6.1 kb
batC	*Cla*I	8.5 kb	*Eco*RV	7.1 kb
	*Bam*HI	4, 4.7 kb	*Cla*I	8.6 kb
			*Nco*I	9.9 kb
batD	*Hin*dIII	7.1 kb	*Eco*RV	3.9 kb
	*Pst*I	1.7, 2.4 kb	*Cla*I	> 12 kb
	*Bcl*II	3 kb	*Nco*I	13.9 kb
batE	*Bam*HI	1.7, 10 kb	*Eco*RV	11.5 kb
	*Sal*I	0.5, 2.2 kb	*Cla*I	5.1 kb
	*Xho*I	2.5, 7 kb	*Nco*I	7.2 kb
batF	*Cla*I	3.6 kb	*Eco*RV	3.5 kb
	*Xho*I	1.6 kb	*Cla*I	2.7 kb
			*Nco*I	3.1 kb

[a] Using the 982 bp *Kpn*I-*Ssp*I fragment of *A.f. pyrG* as the probe.

3.3.2 Leucine biosynthesis pathway qRT-PCR primers

Primers used for real-time reverse transcriptase PCR (qRT-PCR) are listed in Table 3.2. Primer design and qRT-PCR is described in Chapter 2.6.2

Table 3.2 Leucine biosynthesis real-time reverse transcriptase PCR primers

Target region	Primer Name	Sequence (5' → 3')	Efficiency (54.0ºC)
benA:	benA_RT_F	CCTGCTCCGCTSTCTTCC	87.8 %
	benA_RT_R	GSCTGTTCTTGCTCTGGST	
leuB:	leuB_RT_F	GCTGTTTGACCTTTTCTTC	135.3 %
	leuB_RT_R	AAAGTAAGGGAGAGACAGT	
leuR:	leuR_RT_F	TAGGCTGTTTGACCAATTCT	155.5 %
	leuR_RT_R	ACGAAGGTACTCCTCAGG	
leuC:	leuC_RT_F	TCAAAGATCCCTCTAAGAAATACA	155.4 %
	leuC_RT_R	TTGTTCGCCATCCATAGG	
luA:	luA_RT_F	TCTTGATCTATATCGACAGACA	136.2 %
	luA_RT_R	TGACGAGGTAGGGATGTT	
leuD:	leuD_RT_F	ATTGGTGGCCCAGAATGG	125.15 %
	leuD_RT_R	AATTGCATGGTCGCAAGTTG	
leuE:	leuE_RT_F	AAATCTGAGACCGTGTTC	107.3 %
	leuE_RT_R	ATTCGTCCATTGCATAATC	
batA:	batA_RT_F	GCTTCAGTGCTACTCGTG	137.1 %
	batA_RT_R	TGAACATGTGATCGGTAAAG	
batB:	batB_RT_F	CGAAGTTGTTGAGAAGAC	133.3 %
	batB_RT_R	TGATGAAGAATGCAGTCC	
batC:	batC_RT_F	TCTTTCACTGACCACATC	90.23 %
	batC_RT_R	TTATCGTAGGGAGTGATTTG	
batD:	batD_RT_F	GGGATGAAAGCCTATCGT	Not determined[a]
	batD_RT_R	TAGAAACAGCATCACAAGAAC	
batE:	batE_RT_F	CTCAATCATTCCCTCCTCCTC	98.0 %
	batE_RT_R	CATGGCCGTTAACTTCGC	
batF:	batF_RT_F	AAGTTCGGTAAATGGTCTG	Not determined[a]
	batF_RT_R	CTCCTGTCCGTAGTTGAA	

[a] Expression was undetectable or too low to perform serial dilution analysis.

3.4 Results

3.4.1 Characterization of the A. nidulans α-isopropylmalate synthetase gene leuC.

NOTE: This section on deletion of the leuC gene is a summary of research conducted as part of this thesis that was published in Downes D.J., M.A. Davis, S.D. Kreutzberger, B.L. Taig and R.B Todd (2013) Regulation of the NADP-glutamate dehydrogenase gene *gdhA* in *Aspergillus nidulans* by the Zn(II)2Cys6 transcription factor LeuB. *Microbiology* **159 (12):** 2467-2480. *The full article has been included as Appendix A.*

The production of α-isopropylmalate (α-IPM) in *S. cerevisiae* is carried out by two α-IPM synthetases, encoded by *LEU4* and *LEU9* (BAICHWAL *et al.* 1983; CHANG *et al.* 1984; CHANG *et al.* 1985; CASALONE *et al.* 2000). In *A. nidulans* a single locus, AN0840, had been identified as the *LEU4*/*LEU9* ortholog and named *leuC* (B.L Taig, M.D. Davis, and R.B. Todd, published within this paper). For this work a *leuC*Δ mutant was isolated by homologous double crossover integration of a *leuC::riboB* deletion construct into MH11036 (*nkuA*Δ *riboB2*) and selection for riboflavin prototrophs in the presence of 2 mM leucine. *leuC*Δ conferred leucine auxotrophy and strains containing this mutation can not grow without leucine supplementation (Figure 3.2). The wild type *leuC* gene was PCR-amplified from genomic DNA, cloned, and shown to complement the leucine auxotrophy when transformed into the *leuC*Δ mutant. Therefore, genetic analysis confirms there is a sole α-IPM synthetase in *A. nidulans* (DOWNES *et al.* 2013).

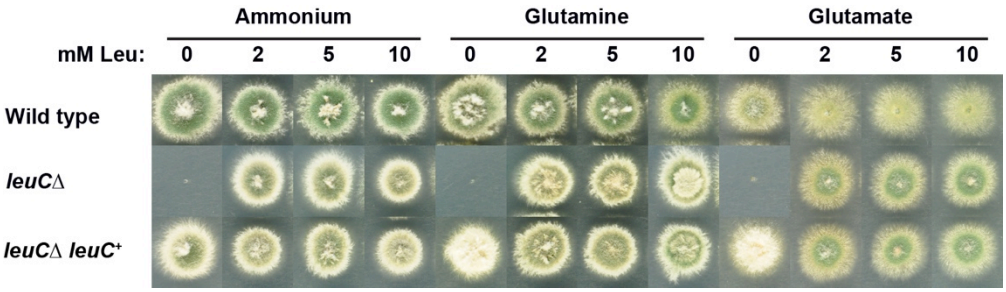

Figure 3.2 *leuC*Δ confers leucine auxotrophy

Wildtype (MH1), *leuC*Δ (RT219) and complemented *leuC*Δ *leuC*$^{+}$ (RT347) were grown at 37ºC for 2 days on supplemented ANM solid media with 10 mM ammonium, glutamate, or glutamine as the nitrogen source with the indicated concentrations of leucine (Leu).

3.4.2 Identification of leucine biosynthesis genes.

To identify the *A. nidulans* genes which encode enzymes required for leucine biosynthesis we performed blastp analysis with known *S. cerevisiae* leucine biosynthesis enzymes. A single gene in yeast, *LEU2*, encodes β-isopropylmalate dehydrogenase (TOH-E *et al.* 1980; ANDREADIS *et al.* 1984), whereas, in *A. niger* two enzymes, Leu2A and Leu2B, encoded by separate genes carry out this role (WILLIAMS *et al.* 1996). To identify the *A. nidulans* β-isopropylmalate dehydrogenase encoding genes we performed blastp analysis with Leu2p as the query and found two proteins with high similarity. These two enzymes, encoded by AN0912 and AN2793, show 64.1% and 50.7% identity with Leu2p respectively and 51.5% identity with each other. AN0912 had 87.9% identity with Leu2A and 52.0% identity with Leu2B, whereas AN2793 had 54.2% and 86.1% identity with these two proteins respectively. Alignment of the five proteins shows strong conservation throughout the entire protein, including in the substrate binding loop and NAD binding motif (Figure 3.3). Consistent with the phylogenetic analysis, *leuD* is found on chromosome VIII in a region of highly conserved gene synteny in all 21 Aspergillus genomes available at AspGD, whereas *leuE* is located on chromosome VI in a region that does not show conserved synteny with the other Aspergilli (data not shown).

S. cerevisiae encodes two branched chain amino acid aminotransferase enzymes, encoded by *BAT1* and *BAT2*, which perform the final step of branched chain amino acid biosynthesis (EDEN *et al.* 1996; KISPAL *et al.* 1996). To identify orthologs of these two genes in *A. nidulans* we performed blastp analysis using either Bat1p or Bat2p as the query. Surprisingly, we found six genes, AN0385, AN4323, AN5957, AN7876, AN7878, and AN8511, predicted to encode BATs with >25% identity to both Bat1p and Bat2p (Table 3.3). Alignment of these eight proteins showed strong conservation of NAD cofactor binding residues and absolute conservation of the catalytic lysine residue (Figure 3.4). The two yeast BATs function in different cellular compartments (Figure 3.1). Bat1p is primarily targeted to mitochondria whereas Bat2p functions in the cytoplasm (KISPAL *et al.* 1996). To predict the subcellular location of the six *A. nidulans* BAT enzymes we used Target P, MitoProtII and Predotar targeting signal prediction software (CLAROS AND VINCENS 1996; NIELSEN *et al.* 1997; EMANUELSSON *et al.* 2000; SMALL *et al.* 2004). For all three algorithms Bat1p, BatA and BatC were predicted to be predominantly mitochondrial and the remaining BAT enzymes were predicted to localize elsewhere in the cell (Table 3.4). Analysis of the alignment of BATs showed Bat1p, BatA and BatC have extended N-

termini containing a predicted mitochondrial targeting signal (Figure 3.4). The identification of the genes encoding α-IPM synthase, β-IPM dehydrogenase and the BCAA aminotransferase completes the annotation of leucine biosynthesis genes in *A. nidulans* (Figure 3.5)

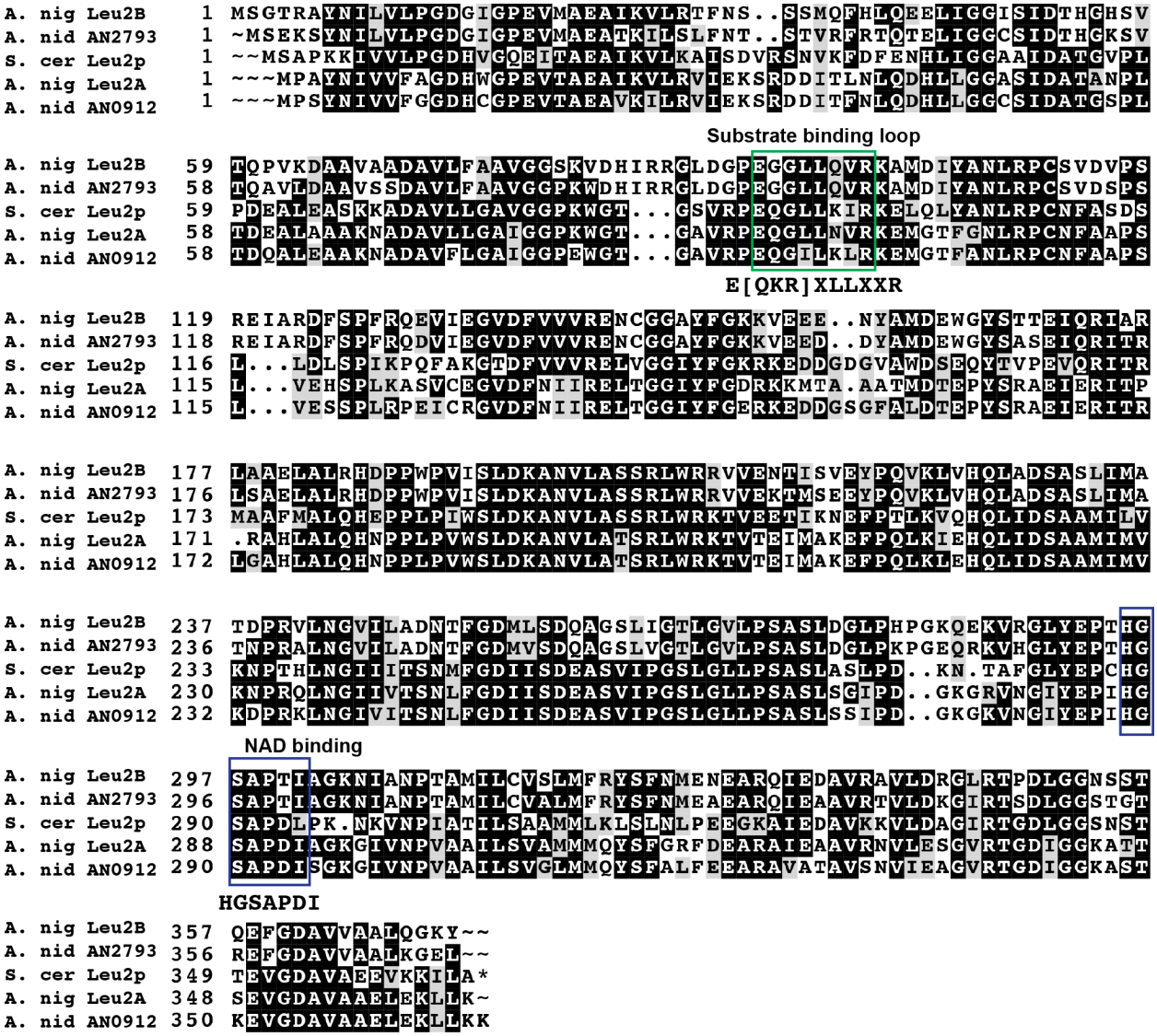

Figure 3.3 Clustal Omega alignment of β-isopropylmalate dehydrogenases

Clustal Omega alignment of Leu2p from *S. cerevisiae* (S. cer) with, AN0912 (LeuD) and AN2793 (LeuE) from *A. nidulans* (A. nid), and Leu2A and Leu2B from *A. niger* (A. nig). The substrate-binding loop (green) and the NAD-binding motif (blue) are boxed (MARCHLER-BAUER *et al.* 2015). Shading was performed with Boxshade with a minimum of 0.6 identity (black) or similarity (gray).

Table 3.3 Identification of BATs.

Locus	New Name	% Protein Identity	
		Bat1p	Bat2p
Sc*BAT1*	–	100.0	77.0
Sc*BAT2*	–	77.0	100.0
AN4323	*batA*	61.2	61.2
AN5957	*batB*	41.2	44.5
AN7878	*batC*	49.1	50.0
AN7876	*batD*	26.5	25.3
AN0385	*batE*	31.1	28.2
AN8511	*batF*	26.7	28.0

Table 3.4 Sub-cellular localization prediction for BATs.

Protein	Target P v1.1[a]				MitoProtII[a]	Predotar V1.03[a]			
	mTP[b]	SP[c]	Other	Loc.[d]		Mito.[b]	ER[e]	Other	Loc.[d]
Bat1p	0.72	0.04	0.27	M	0.83	0.83	0.01	0.17	M
Bat2p	0.12	0.07	0.84	–	0.04	0.00	0.01	0.99	–
BatA	0.52	0.18	0.25	M	0.97	0.56	0.02	0.43	M
BatB	0.13	0.09	0.82	–	0.08	0.00	0.01	0.99	–
BatC	0.96	0.02	0.07	M	0.96	0.90	0.01	0.10	M
BatD	0.09	0.09	0.91	–	0.03	0.00	0.01	0.99	–
BatE	0.10	0.06	0.90	–	0.09	0.00	0.01	0.99	–
BatF	0.05	0.21	0.72	–	0.03	0.00	0.01	0.99	–

[a] Each program predicts probability of targeting to specified subcellular compartments
[b] mTP/Mito.: Mitochondrial
[c] SP: Secreted protein
[d] Loc.: Predicted Location. "M" = Mitochondrial, "–" = Undetermined
[e] ER: Endoplasmic reticulum

Figure 3.4 Clustal Omega alignment of putative BCAA aminotransferases.

Clustal Omega alignment of Bat1p and Bat2p from *S. cerevisiae* with AN4323 (BatA), AN5957 (BatB), AN7878 (BatC), AN7876 (BatD), AN0385 (BatE), and AN8511 (BatF) from *A. nidulans*. The co-factor binding residues (green), and mitochondrial-targeting signals (blue) are highlighted (MARCHLER-BAUER *et al.* 2015). The catalytic lysine is marked with a star above and below. Shading was performed with Boxshade with a minimum of 0.5 identity (black) or similarity (gray).

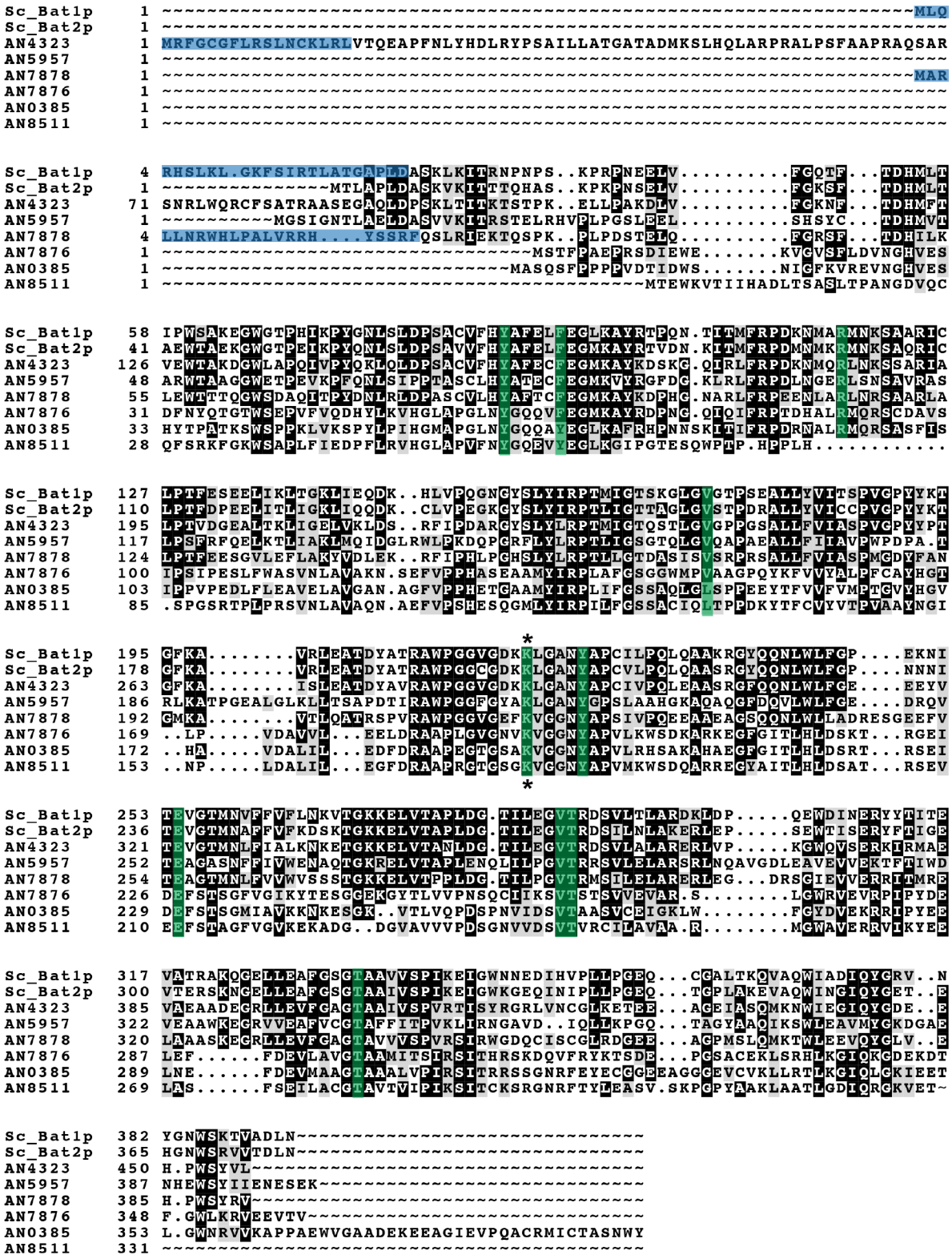

Figure 3.4 Clustal Omega alignment of putative BCAA aminotransferases.

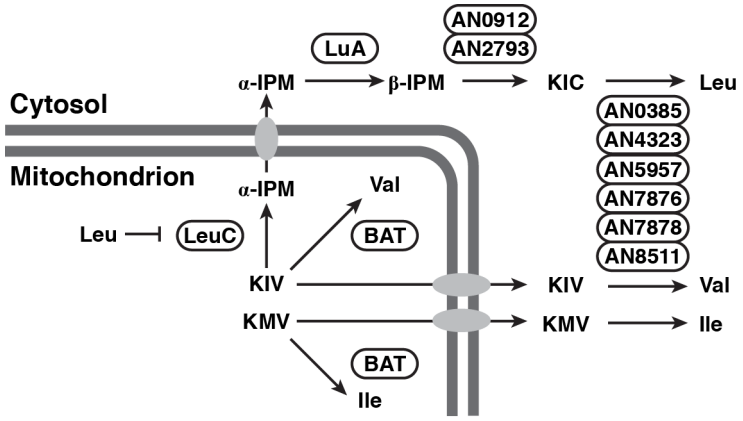

Figure 3.5 Leucine biosynthesis in *A. nidulans.*

Predicted and known enzymes involved in the leucine (Leu) branch of branched chain amino acid biosynthesis. Some or all of the six BATs are also predicted play a role in valine (Val) and isoleucine (Ile) biosynthesis. α-keto-β-methylvalerate (KMV); α-ketoisovalerate (KIV); α-isopropylmalate (α-IPM); β-isopropylmalate (β-IPM); α-ketoisocaproate (KIC). Adapted from (KOHLHAW 2003).

3.4.3 Characterization of the two **A. nidulans** *β-isopropylmalate dehydrogenase genes.*

3.4.3.i Phylogenetic analysis of β-IPM dehydrogenases.

A single gene in *S. cerevisiae*, *LEU2*, encodes β-isopropylmalate dehydrogenase (β-IPM dehydrogenase) (TOH-E *et al.* 1980; ANDREADIS *et al.* 1984). In *A. niger* two enzymes, Leu2A and Leu2B, encoded by separate genes carry out this role (WILLIAMS *et al.* 1996). We identified two putative β-IPM dehydrogenase encoding genes in *A. nidulans*, AN0912 and AN2793, which we named *leuD* and *leuE* respectively. To investigate the origin of the two β-IPM dehydrogenase encoding genes in *A. nidulans* we used the Pfam database (http://pfam.xfam.org/; FINN *et al.* 2014) to identify orthologs in the isocitrate/isopropylmalate dehydrogenase family (PF00180) from 10 Ascomycetes (14 orthologs), three Basidiomycetes (three orthologs), one Planta (two orthologs), four Bacteria (four orthologs) and one Archaea (one ortholog). The 26 proteins were aligned using Clustal Omega. Phylogenies were constructed using the Phylogeny Inference Package (Phylip version 3.696; RETIEF 2000). SEQBOOT was used to generate 100 bootstraped iterations of the original alignment, and phylogenies were constructed using PROML with default settings for multiple datasets. A consensus tree of these 100 phylogenies was generated using CONSENSE and used as the template for a final unrooted Maximum-Likelihood phylogeny of β-IPM dehydrogenases generated in PROML using the original Clustal Omega alignment (Figure 3.6). Interestingly LeuD and LeuE, along with their respective Aspergillus orthologs, formed distinct clades. The LeuD clade is consistent with the positioning of *A. nidulans* in the fungal evolutionary tree (Figure 3.6) (GALAGAN *et al.* 2005b), whereas the LeuE clade is located between the Ascomycota and the Basidiomycota. This additional β-IPM dehydrogenase encoding gene may have arisen by either horizontal gene transfer into an ancestor of the Aspergilli or an ancient duplication in an ascomycete progenitor. The additional copy of the *M. oryzae* β-isopropylmalate dehydrogenase is located in a branch between *Strepotoccous mutans* and the Basidiomycetes, suggesting a separate origin to the LeuE clade.

Figure 3.6 Phylogenetic analysis of β-IPM dehydrogenases.

Unrooted Maximum-Likelihood phylogeny of β-IPM dehydrogenases. Bootstrapping support (100 replicates) greater than 40% is shown. Protein sequences for *A. nidulans* were downloaded from AspGD, sequences for *S. cerevisiae* were downloaded from SGD and all other sequences came from Pfam. **Archaea:** *Sulfobus solfataricus* (Q9UXB2.1); **Bacteria:** *Cornebacteriam ammoniagenes* (D5NZR1.1), *Enterobacter aerogenes* (G0E530.1), *Strepotoccous mutans* (Q8DTG3.1), *Saccharomonospora cyanea* (H5XNC6.1); **Basidiomycota (Basido.):** *Coprinopsis cinerea* (A8NYJ8.1), *Cryptococcus neoformans* (Q5KP37.1), *Ustilago maydis* (Q4P2R4.1); **Ascomycota:** *A. fumigatus* Leu2A (Q4WRM6.1), *A. fumigatus* Leu2B (Q4WLG7.1), *A. nidulans* LeuD, *A. nidulans* LeuE, *A. niger* Leu2A (P87256.1), *A. niger* Leu2B (P87257.1), *A. oryzae* (1: Q2TYA5.1; 2: Q877A9.1), *Botyrotinia fuckeliana* (A6SPE0.1), *Candida albicans* (C4YTB1.1), *Fusarium fujikuroi* (C1L3C2.1), *M. oryzae* (1: G4N5B0.1; 2: G4NIK0.1), *Neurospora crassa* (P34738.2), *S. cerevisiae* Leu2p, *Schizosaccharomyces pombe* (P18869.1); **Planta:** *Chlamydomonas reinhardtii* (1: A8I7N4.1; 2: A8I7N8.1). Evolutionary relationship of fungi is adapted from the Broad Institute Fungal Genome Initiative (http://www.broadinstitute.org/scientific-community/science/projects/fungal-genome-initiative/fungal-genomics). The scale bar corresponds to the branch length for an expected number of 0.2 substitutions per site. The two distinct Aspergillus clades are boxed.

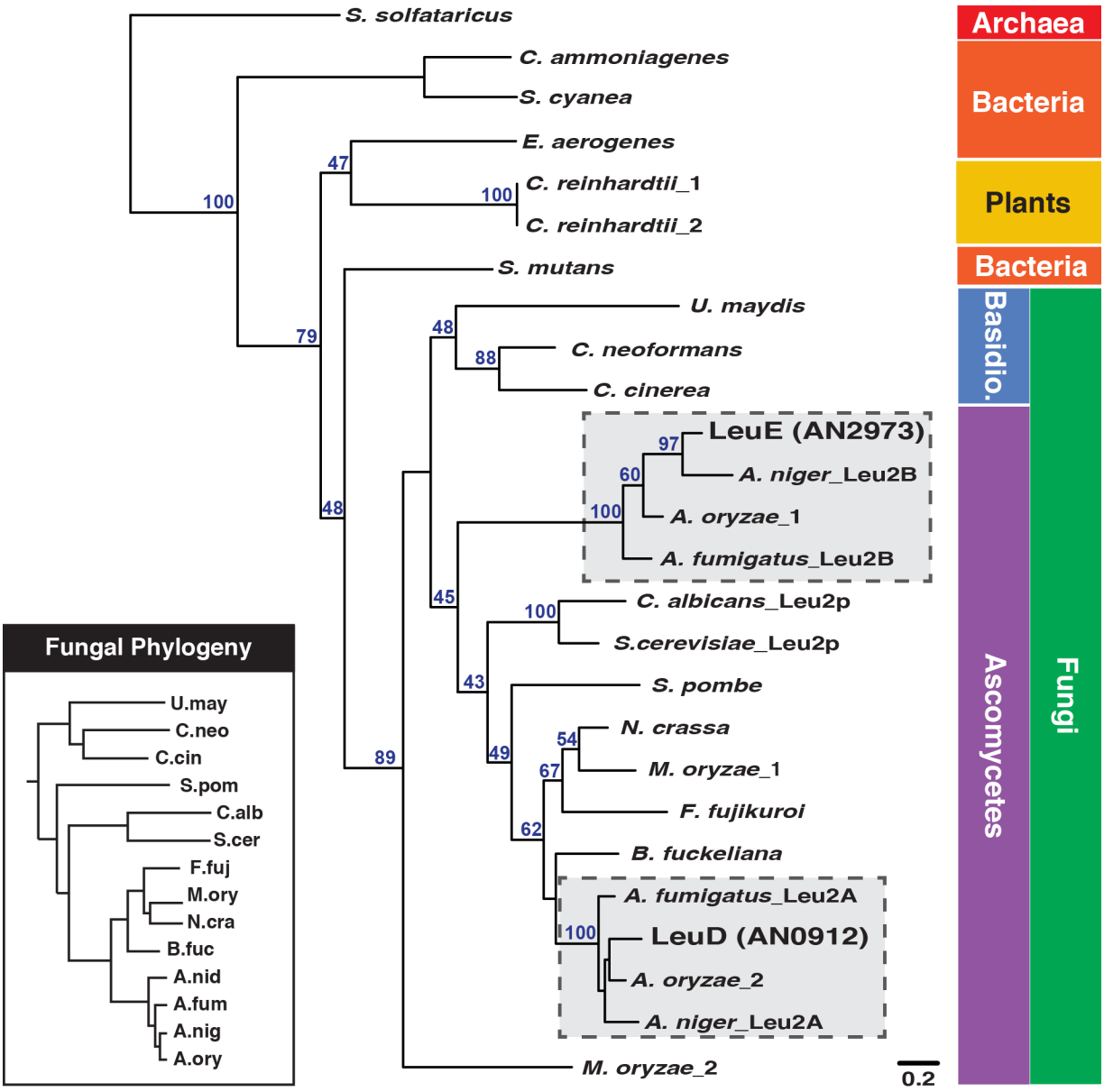

Figure 3.6 Phylogenetic analysis of β-IPM dehydrogenases.

3.4.3.ii leuD *and* leuE *both function in leucine biosynthesis.*

To determine whether both *leuD* and *leuE* are functional genes we generated deletion mutants by gene replacement (Figure 6.7A). The *leuD::A.f. pyrG* and *leuE*::*A.f. pyrG* knockout constructs were transformed into MH11059 (*pyroA4 pyrG89 nkuA*Δ) and transformants selected with leucine supplementation for uridine and uracil (pyrimidine) prototrophy. Integration of knockout constucts by homologous double crossover was confirmed by Southern blot (see Materials and Methods 3.3.1 for details). Deletion of genes required for leucine biosynthesis results in leucine auxotrophy (POLOTNIANKA *et al.* 2004; DOWNES *et al.* 2013). Neither *leuD*Δ nor *leuE*Δ conferred a strict leucine auxotrophy phenotype (Figure 6.4B). However, while *leuE*Δ grew similar to wild type in the presence or absence of leucine, the *leuD*Δ mutant had reduced growth compared with wild type unless supplemented with exogenous leucine. This leaky leucine auxotrophy is similar to that seen in *leuB*Δ strains (POLOTNIANKA *et al.* 2004) and co-segregated with the *A.f. pyrG*$^{+}$ marker in an outcross to a wild type strain (P.A. Migeon and R.B. Todd, pers. commun.). As our bioinformatic analysis only identified two β-IPM dehydrogenase-encoding genes, we predicted the *leuD*Δ *leuE*Δ double mutant would be a strict leucine auxotroph and that the leaky leucine auxotrophy of *leuD*Δ resulted from LeuE activity. Therefore we constructed a double mutant by crossing the *leuD*Δ (*leuD*Δ::*A.f.pyrG pyroA4 pyrG89*) and *leuE*Δ (*leuE*Δ::*A.f.pyrG pabaA1 pyrG89*) mutants. Progeny of the cross showed leucine prototrophy, leaky leucine auxotrophy, and strict leucine auxotrophy in a 2:1:1 ratio (Table 3.5), consistent with *leuD*$^{+}$ *leuE*$^{+}$ and *leuD*$^{+}$ *leuE*Δ being prototrophs, *leuD*Δ *leuE*$^{+}$ being a leaky auxotroph, and *leuD*Δ *leuE*Δ being a strict leucine auxotroph. When both pyrimidine and leucine prototrophy were scored four classes of progeny were observed from this cross:

1. pyrimidine auxotroph, leucine prototroph (*leuD*$^{+}$ *leuE*$^{+}$)
2. pyrimidine prototroph, leucine prototroph (*leuD*$^{+}$ *leuE*Δ)
3. pyrimidine prototroph, leaky leucine auxotroph (*leuD*Δ *leuE*$^{+}$)
4. pyrimidine prototroph, strict leucine auxotroph (*leuD*Δ *leuE*Δ).

The numbers of each class of progeny were seen in a 1:1:1:1 ratio consistent with each *leuD* and *leuE* segregating independently and the *A.f pyrG*$^{+}$ marker co-segregating with both *leuD*Δ and *leuE*Δ (Table 3.5). The other markers in the cross (*pabaA1, pyroA4*) also showed Mendelian segregation. The *leuD*Δ *leuE*Δ strain is a strict leucine auxotroph and only grew when supplemented with exogenous leucine (Figure 3.7B). In *C. neoformans* the *leu1*Δ mutant, which

lacks α-IPM isomerase and is a leucine auxotroph, can be supplemented with leucine on glutamine and asparagine but cannot be repaired with leucine when ammonium is the nitrogen nutrient (DO *et al.* 2015). This effect is thought to result from reduced uptake of leucine on ammonium. We examined growth of the *leuC*Δ mutant, lacking α-IPM isomerase, and the *leuD*Δ *leuE*Δ mutant lacking β-IPM dehydrogenases on a range of nitrogen nutrients. Both the *leuC*Δ and *leuD*Δ *leuE*Δ *A. nidulans* leucine auxotrophic phenotypes could be supplemented with leucine on the preferred nitrogen nutrients ammonium and glutamine and on alternative nutrients (Figures 3.2 & 3.7), indicating that regulation of leucine uptake is not conserved between *C. neoformans* and *A. nidulans*.

We were interested to know the source of the different degrees of effect of *leuD*Δ and *leuE*Δ, and in particular whether *leuD* was simply more highly expressed and/or if the LeuD enzyme was more active. To address the former possibility we examined *leuD* and *leuE* expression by real time RT-PCR. We found that *leuD* had ~42-fold higher expression than *leuE* after 16 hours growth in ANM with 10 mM ammonium. In RNA-seq data generated for the analysis of TamA regulation (Chapter 4) *leuD* showed 12 to 35 fold higher expression than *leuE* when grown on ammonium (35 fold), alanine (12 fold), and glutamine (13 fold) (Figure 3.7C). Higher expression of *leuD* was also seen in publicly available RNA-seq data for the ammonium condition and for alternative nitrogen conditions (SIBTHORP *et al.* 2013), where *leuD* showed between 14 to 46 fold higher expression than *leuE* in wild type cells (Table 3.6). For four other growth conditions available, RNA-seq revealed higher expression for *leuD* than *leuE.* We examined the effect of the *leuD*Δ mutation on *leuE* expression by real-time RT-PCR. In addition we measured the effects of *leuD*Δ on two other leucine biosynthesis genes *luA* and *leuC* by the same method, and *gdhA*, which is co-regulated with leucine biosynthesis, using enzyme activity of LacZ expressed from the *gdhA-lacZ* translational-fusion reporter gene (POLOTNIANKA *et al.* 2004; DOWNES *et al.* 2013). For all three leucine biosynthesis genes and also for *gdhA* we found that *leuD*Δ resulted in increased expression over wild type levels (Figure 6.7D-E). Therefore reduced leucine production as a result of *leuD*Δ results in upregulation of *leuE* and the other leucine biosynthesis genes. As *leuE*Δ had no effect on growth and *leuE* upregulation in the *leuD*Δ deletion mutant is expected to be LeuB dependent we predicted that the *leuB*Δ *leuD*Δ double mutant would be a strict leucine auxotroph. Progeny of the cross of RT412 (*leuD*Δ::*A.f. pyrG pyrG89*) and RT453 (*leuB*Δ::*A.f. ribo pyrG89*) showed leucine prototrophy, leaky leucine

auxotrophy, and strict leucine auxotrophy in a 1:2:1 ratio (Table 3.7), consistent with *leuB*$^+$ *leuD*$^+$ being a prototroph, *leuB*$^+$ *leuD*Δ and *leuB*Δ *leuD*$^+$ being leaky auxotrophs, and *leuB*Δ *leuD*Δ being a strict leucine auxotroph. When both pyrimidine and leucine prototrophy were scored four classes of progeny were observed from this cross:

1. pyrimidine auxotroph, leucine prototroph (*leuB*$^+$ *leuD*$^+$)
2. pyrimidine auxotroph, leaky leucine auxotroph (*leuB*Δ *leuD*$^+$)
3. pyrimidine prototroph, leaky leucine auxotroph (*leuB*$^+$ *leuD*Δ)
4. pyrimidine prototroph, strict leucine auxotroph (*leuB*Δ *leuD*Δ)

The numbers of each class of progeny were seen in a 1:1:1:1 ratio consistent with each gene segregating independently and the *A.f. pyrG*$^+$ marker co-segregating with *leuD*Δ (Table 3.7). The other markers in the cross (*niiA4*, *pabaA1, pyroA4*) also showed Mendelian segregation. The strict leucine auxotrophy of the *leuB*Δ *leuD*Δ double mutant suggests that LeuB regulation of *leuE* is required for leucine biosynthesis in the absence of *leuD*. We assayed the *gdhA-lacZ* reporter gene for expression in the double mutant (Figure 3.7E). Unlike the single *leuD*Δ mutant there was no increase in expression above *leuB*Δ levels in the double mutant, consistent with the *leuD*Δ induced upregulation of leucine biosynthesis genes occuring through LeuB.

Table 3.5 Meiotic cross analysis of *leuD*Δ (RT411) and *leuE*Δ (RT414).

Single phenotype analysis[a]							
Gene						χ^2	**p[b]**
		WT			***pabaA1***		
pabaA	**Obs.**	25			21	0.348	0.555
	Exp.	23			23	(d.f. = 1)	
		WT			***pyroA4***		
pyroA	**Obs.**	22			24	0.087	0.768
	Exp.	23			23	(d.f. = 1)	
		WT	**leu ±**		**leu –**		
leuD, leuE	**Obs.**	22	15		9	1.652	0.437
	Exp.	23	11.5		11.5	(d.f. = 2)	
Paired phenotype analysis[a]							
Gene		***pyr –*** ***leu +***	***pyr +*** ***leu +***	***pyr +*** ***leu ±***	***pyr +*** ***leu –***	χ^2	**p[b]**
pyrG, leuD, leuE	**Obs.**	6	18	13	9	7.043	0.070
	Exp.	11.5	11.5	11.5	11.5	(d.f. = 3)	

[a] Prototrophy (WT/+), leaky auxotrophy (±), strict auxotrophy (–)
[b] Values were calculated using QuickCalcs (http://graphpad.com/quickcalcs/chisquared2/)

Table 3.6 Sibthorp *et al*. (2013) RNA-seq expression levels of BCAA genes.

Enzyme	Locus	Gene	Reads / kbp / Million mapped reads (RPKM)				
			Complete	NH_4	NO_3	4h -N	72h -N
β-IPM dehydrogenase	AN0912	*leuD*	100.40	170.11	212.51	44.80	43.87
	AN2793	*leuE*	2.28	6.07	9.45	0.96	3.10
BCAA aminotransferase	AN0385	*batE*	3.73	7.84	9.33	11.38	18.19
	AN4323	*batA*	72.50	124.48	137.79	23.32	33.58
	AN5957	*batB*	68.01	25.23	29.86	42.15	29.77
	AN7876	*batD*	156.02	28.19	22.35	0.71	0.81
	AN7878	*batC*	103.80	47.45	27.07	8.19	1.19
	AN8511	*batF*	0.00	0.00	0.00	0.00	0.00

Table 3.7 Meiotic cross analysis of *leuB*Δ (RT453) and *leuD*Δ (RT412).

Single phenotype analysis[a]						
Gene(s)					χ^2	**p**[b]
		WT		***niiA4***		
niiA	**Obs.**	23		23	0.000	1.000
	Exp.	23		23	(d.f. = 1)	
		WT		***pabaA1***		
pabaA	**Obs.**	20		26	0.783	0.376
	Exp.	23		23	(d.f. = 1)	
		WT		***pyroA4***		
pyroA	**Obs.**	37		9	0.725	0.394
	Exp.	34.5		11.5	(d.f. = 1)	
		WT	**Leu ±**	**Leu –**		
leuB, leuD	**Obs.**	11	28	7	2.870	0.238
	Exp.	11.5	23	11.5	(d.f. = 2)	

Paired phenotype analysis[a]							
Genes		***pyr –*** ***leu +***	***pyr +*** ***leu +***	***pyr +*** ***leu ±***	***pyr +*** ***leu –***	χ^2	**p**[b]
pyrG, leuB, leuD	**Obs.**	10	18	10	7	5.933	0.114
	Exp.	11.5	11.5	11.5	11.5	(d.f. = 3)	

[a] Prototrophy/utilization (WT/+), leaky auxotropy (±), strict auxotrophy/non-utilization (–)
[b] Values were calculated using QuickCalcs (http://graphpad.com/quickcalcs/chisquared2/)

Figure 3.7 *leuD* encodes the major β-IPM dehydrogenase.

A) Deletions of *leuD* and *leuE* were generated using cassettes provided by the Fungal Genetics Stock Center. **B)** Wild type (MH1), *leuD*Δ (RT411), *leuE*Δ (RT413), *leuD*Δ *leuE*Δ (RT444), *leuB*Δ (MH12181), and *leuB*Δ *leuD*Δ (RT460) strains were grown at 37ºC for 2 days on 1% complete media (1%C) and solid supplemented ANM with or without 2 mM leucine (Leu) and with 10 mM ammonium (NH_4), glutamine (Gln), and nitrate (NO_3) as the nitrogen source. **C)** Reads per kilobase per million mapped reads (RPKM) from RNA-seq of MH1 grown at 37ºC for 16 hours in supplemented liquid ANM with 10 mM ammonium (NH_4), glutamine (Gln) and alanine (Ala). **D)** qRT-PCR quantification of mean fold change in transcript expression in *leuD*Δ (RT411) compared to wild type (MH1) grown at 37ºC for 16 hours in supplemented liquid ANM-10 mM ammonium and 2 mM leucine. Bars indicate the mean fold change of three independent biological replicates (circles) **E)** LacZ specific activity for wild type (MH12101), *leuB*Δ (MH12181), *leuD*Δ (RT458) and, *leuB*Δ *leuD*Δ (RT460) which contain the -753 bp *gdhA-lacZ* reporter construct. Strains were grown at 37ºC for 16 hours in supplemented liquid ANM with 10 mM ammonium and 2 mM leucine. Lower case letters indicate significantly different expression groups $p \leq 0.05$ using two-tailed Student's t-test with unequal distribution. For **C**-**E** Error bars depict SEM (N=3).

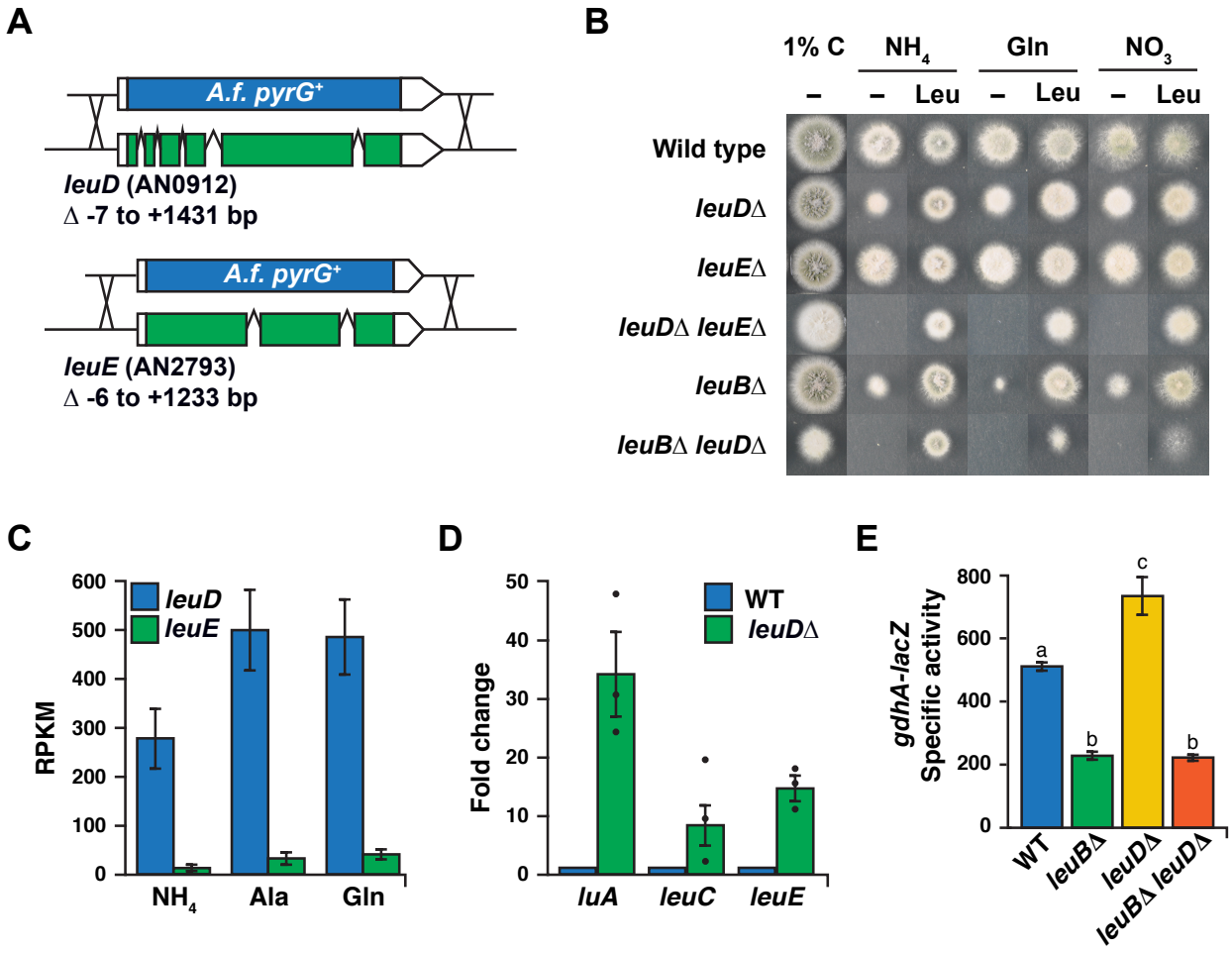

Figure 3.7 *leuD* encodes the major β-IPM dehydrogenase.

3.4.4 Characterization of six branched chain amino acid aminotransferase genes.

3.4.4.i Bioinformatic analyses of BCAA aminotransferases.

To determine the relationship of the six *A. nidulans* BATs we performed phylogenetic analysis (Figure 3.8). In additon to the *A. nidulans* and *S. cerevisiae* proteins we used the Pfam database (FINN *et al.* 2014; http://pfam.xfam.org/) to identify orthologs in the aminotransferase class IV family (PF01063) predicted to be BCAA aminotransferases from eight Ascomycetes (33 proteins), three Basidiomycetes (7 proteins), four Bacteria (5 proteins) and one Archaea (1 protein). An unrooted Maximum-Likelihood consensus phylogeny of BATs was generated in the Phylip package (RETIEF 2000) by the same procedure described above (Section 3.4.3.i) to generate the β-isopropylmalate dehydrogenase phylogeny. The BATs formed two distinct groups within the fungi. Group I, the larger group containing 32/48 of the fungal BATs included BatA (AN4323), BatB (AN5957), BatC (AN7878), and *S. cerevisiae* Bat1p and Bat2p as well as at least one protein from every other fungus examined. Group II was a smaller group, with only 16 proteins, and was almost entirely composed of BAT enzymes from Pezizomycotina genera (*Aspergillus, Penicillium, Fusarium, Neurospora, Magnaporthe*) and lacked any Saccharomycotina genera (*Saccharomyces, Candida*). The only non-Pezizomycete in Group II was the Basidiomycete *Ustilago maydis* Bat2, which formed the base of this clade. Interestingly two of the BAT encoding genes, *batC* and *batD*, are tightly linked physically and are separated by just 2 kbp. The tight linkage of these two genes suggests that they most likely would have arisen from a gene duplication and therefore show high sequence homology. However, the proteins encoded by these genes are highly diverged showing only 28.9% protein sequence identity, and BatC is in Group I and BatD is in Group II of the phylogenetic tree. These two genes are located within a predicted AN7884 secondary metabolism gene cluster (ANDERSEN *et al.* 2013; INGLIS *et al.* 2013; see Chapter 4.4.7.i). *batF* (AN8511) is found adjacent to genes required for terrequinone A biosynthesis (BOUHIRED *et al.* 2007) and may be associated with the secondary metabolism gene cluster. Therefore, based on sequence homology and genomic location, three of the six predicted *A. nidulans* BATs may be involved in secondary metabolism rather than branched chain amino acid biosynthesis. The number of BAT encoding genes was variable amongst the four Aspergilli examined, and we were interested to know which *A. nidulans* BATs were conserved. We therefore examined synteny surrounding of each of the six

A. nidulans BAT encoding genes to identify orthologous genes (Table 3.8). Three of the BAT encoding genes, *batA, batB,* and *batE,* had predicted orthologs in the other three *Aspergillus* species based on high similarity and conserved synteny (AspGD; Table 3.8). *batD* only had orthologs in *A. niger* and *A. oryzae* but not *A. fumigatus* whereas *batC* and *batF* have no predicted ortholog and AspGD cannot therefore generate a ortholog cluster specific to each gene. Surprisingly *A. niger* and *A. oryzae* had additional BAT encoding genes that also lacked clear orthologs (An09g01990, AN05g01100, AO090023000123). Therefore it is likely the putative BAT encoding genes have been repurposed from BCAA biosynthesis in the Aspergilli.

Table 3.8 Orthologous BAT synteny in Aspergilli.

	***A. nidulans* loci in chromosomal order**[a]								
Species	**AN4320**	**AN10545**	**AN10540**	**AN4322**	***batA***	**AN4324**	**AN4325**	**AN10546**	**AN10541**
A. oryzae	–	+	+	+	**Aory1**	+	–	+	–
A. niger	–	+	+	+	**Anig1**	+	–	–	–
A. fumigatus	–	+	+	+	**Afum1**	+	+	+	–
	AN5954	**AN10759**	**AN5955**	**AN5956**	***batB***	**AN10758**	**AN10756**	**AN5959**	**AN5960**
A. oryzae	+	–	–	–	**Aory2**	+	+	+	+
A. niger	–	–	–	–	**Anig2**	+	+	+	+
A. fumigatus	+	–	+	–	**Afum2**	+	+	+	+
	AN7873	**AN7874**	**AN7875**	***batD***	**AN7877**	***batC***	**AN7879**	**AN7880**	**AN7881**
A. oryzae	–	–	–	**Aory4**	–	–	–	+	–
A. niger	+	–	–	**Anig4**	–	–	–	+	–
A. fumigatus	–	–	–	–	–	–	–	+	–
	AN0389	**AN0388**	**AN0387**	**AN0386**	***batE***	**AN0384**	**AN0383**	**AN0382**	**AN0381**
A. oryzae	–	–	–	–	**Aory5**	+	–	–	–
A. niger	–	–	–	–	**Anig5**	+	–	–	+
A. fumigatus	–	–	–	+	**Afum3**	+	–	–	+

[a] Presence of a predicted ortholog in a syntenic region is indicated by a "+" with shading, absence by a "–"

Figure 3.8 Maximum-likelihood phylogeny of BATs.

Unrooted Maximum-Likelihood phylogeny of BCAA aminotransferases. Bootstrapping support (100 replicates) greater than 40% is shown. Protein sequence for Aspergilli were downloaded from AspGD, sequences for *S. cerevisiae* were downloaded from SGD and all other sequences came from Pfam. **Archaea:** *Methanocaldococcis infernus* (D5VSZ6.1); **Bacteria:** *Bacillus subtilis* (1: O31461.1; 2: P39576.5), *Streptomyces clavuligerus* (B5H0M8.1), *S. cyanea* (H5XQS6.1), *Xanthomonas gardneri* (F0C966.1); **Basidiomycota (Basidiomyc.):** *C. cinerea* (1: A8N0B4.2; 2: A8N0V2.2), *C. neoformans* (1: Q5K761.1; 2: Q5KD20.1), *U. maydis* (1: Q4P2X7.1; 2: Q4PAT0.1; 3: Q4PIE8.1); **Ascomycota:** *A. fumigatus* (1: Afu4g06160; 2: Afu2g10420; 3: Afu1g01680), *A. nidulans* (BatA, BatB, BatC, BatD, BatE, BatF), *A. niger* (1: Ani04g00430; 2: An02g06150; 3: An09g01990; 4: An10g00620; 5: An01g06530; 6: An05g01100), *A. oryzae* (1: AO090023000977; 2: AO090011000598; 3: AO090023000123; 4: AO0011000044; 5: AO0005000936), *C. albicans* (1: Q59YS9.1; 2: Q5AHJ9.1; 3: Q5AHX4.1), *Fusarium oxysporum* (1: F9FH16.1; 2: F9FH71.1; 3: F9FL84.1; 4: F9FPH4.1), *M. oryzae* (1: G4MK83.1; 2: G4MNR9.1; 3: G4NDD5.1), *N. crassa* (1: Q9HEB7.2; 2: Q7SFT9.2; 3: Q7S699.1; 4: Q1K779.1), *S. cerevisiae* (Bat1p; Bat2p), *S. pombe* (O14370.2). The scale bar corresponds to the branch length for an expected number of 0.2 substitutions per site. The two distinct fungal BAT clades are boxed.

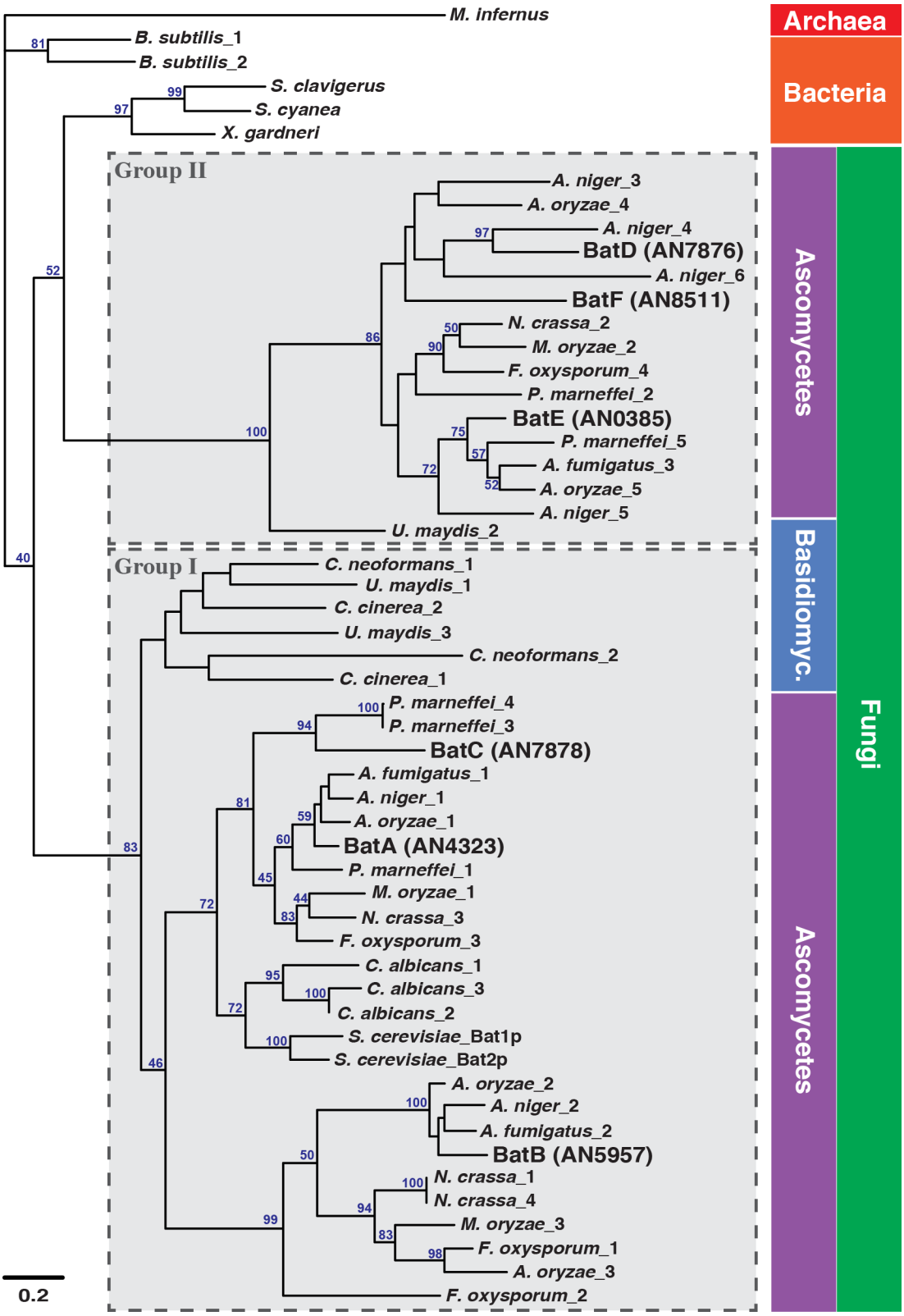

Figure 3.8 Maximum-likelihood phylogeny of BATs.

3.4.4.ii Genetic analysis of six A. nidulans *BATs*

The expansion of the number of BAT encoding genes in *A. nidulans* could indicate specialization for the production of isoleucine, leucine or valine by specific BATs or the evolution of completely new roles. To determine which of the BAT encoding genes were required for branched chain amino acid biosynthesis we attempted to construct individual knockout mutants of each of the six BATs (Figure 3.9A). Deletion constructs from the *A. nidulans* knockout program were transformed into MH11068 (*pyroA4 pyrG89 nkuA*Δ) and transformants were selected for pyrimidine prototrophy in the presence of all three branched chain amino acids. Knockouts for all genes except *batC* were isolated and confirmed by Southern blot (see Materials and Methods 3.3.1 for details). Growth tests of the five individual *bat* knockout mutants showed none were branched chain amino acid auxotrophs (Figure 3.9B). Therefore the *A. nidulans* branched chain amino acid transferases show redundancy.

Analysis of our RNA-seq expression data (Chapter 4) from wild type mycelia grown on ammonium, alanine and glutamine showed that *batA* has the highest expression on all three conditions (Figure 3.9C). *batB* was the next most highly expressed, and showed increased expression on alanine and glutamine compared to ammonium. *batC*, *batD* and *batE* all showed an intermediate level of expression, whereas *batF* was not expressed under any of the three conditions. The pattern of BAT gene expression was similar in publicly available RNA-seq data (SIBTHORP *et al.* 2013), where *batA* showed the highest levels of expression on the sole nitrogen source ammonium, *batB, batC*, *batD* and *batE* had intermediate levels of expression and *batF* was undetectable (Table 3.6). We therefore designed a systematic crossing strategy that would combine the most related and highly expressed genes first (Figure 3.10A). By using this systematic approach we were able to identify a branched chain amino acid auxotroph, *batA*Δ *batB*Δ*,* in the first stages of the crossing regime. Growth tests of the *batA*Δ *batB*Δ double mutant showed no growth after two days in the absence of any of the three branched chain amino acids (Figure 3.10B). However, combination of *batD*Δ*, batE*Δ and *batF*Δ had no effect on BCAA prototrophy. When *batA*Δ *batB*Δ colonies were left for an extended period, 4-5 days, growth was apparent in the absence of leucine but not in the absence of isoleucine or valine (Figure 3.10B). Therefore, while *batA* and *batB* appear to encode the major BAT enzymes, in their absence one or more of the remaining BATs is able to function in leucine biosysnthesis, though much less efficiently than BatA and BatB.

As described earlier (Section 3.4.3.ii), the *C. neoformans leu1*Δ leucine auxotroph is unable to be supplemented during growth on ammonium (Do *et al.* 2015). Although leucine uptake was not repressed by ammonium in *A. nidulans* we were interested to examine whether the *batA*Δ *batB*Δ mutant could be supplemented with isoleucine, leucine and valine on different nitrogen nutrients. We tested growth of the *batA*Δ *batB*Δ mutant on a range of nitrogen nutrients and found it could be supplemented with BCAA on both preferred nitrogen sources (ammonium and glutamine) and alternative nitrogen nutrients (nitrate, glutamate) (Figure 3.10B). Growth of the *batA*Δ *batB*Δ mutant was slower when alanine or glutamine were the sole nitrogen sources and could not be observed until the third day, suggesting alanine may interfere with uptake of one or more branched chain amino acids. As well as functioning in the process of BCAA biosynthesis, BATs also form the first step in degradation of isoleucine, leucine and valine. We therefore assessed whether each of the BAT mutants could utilize each branched chain amino acid as a sole nitrogen source. Only the *batA*Δ *batB*Δ double mutant showed reduced growth on each of the branched chains amino acids as a nitrogen source, the reduction in growth was stronger than on isoleucine and valine than on leucine (Figure 3.11). Therefore BatA and BatB are the predominant BAT enzymes in *A. nidulans* for BCAA biosynthesis and utilization, however one or more of the other BAT enzymes functions in both pathways.

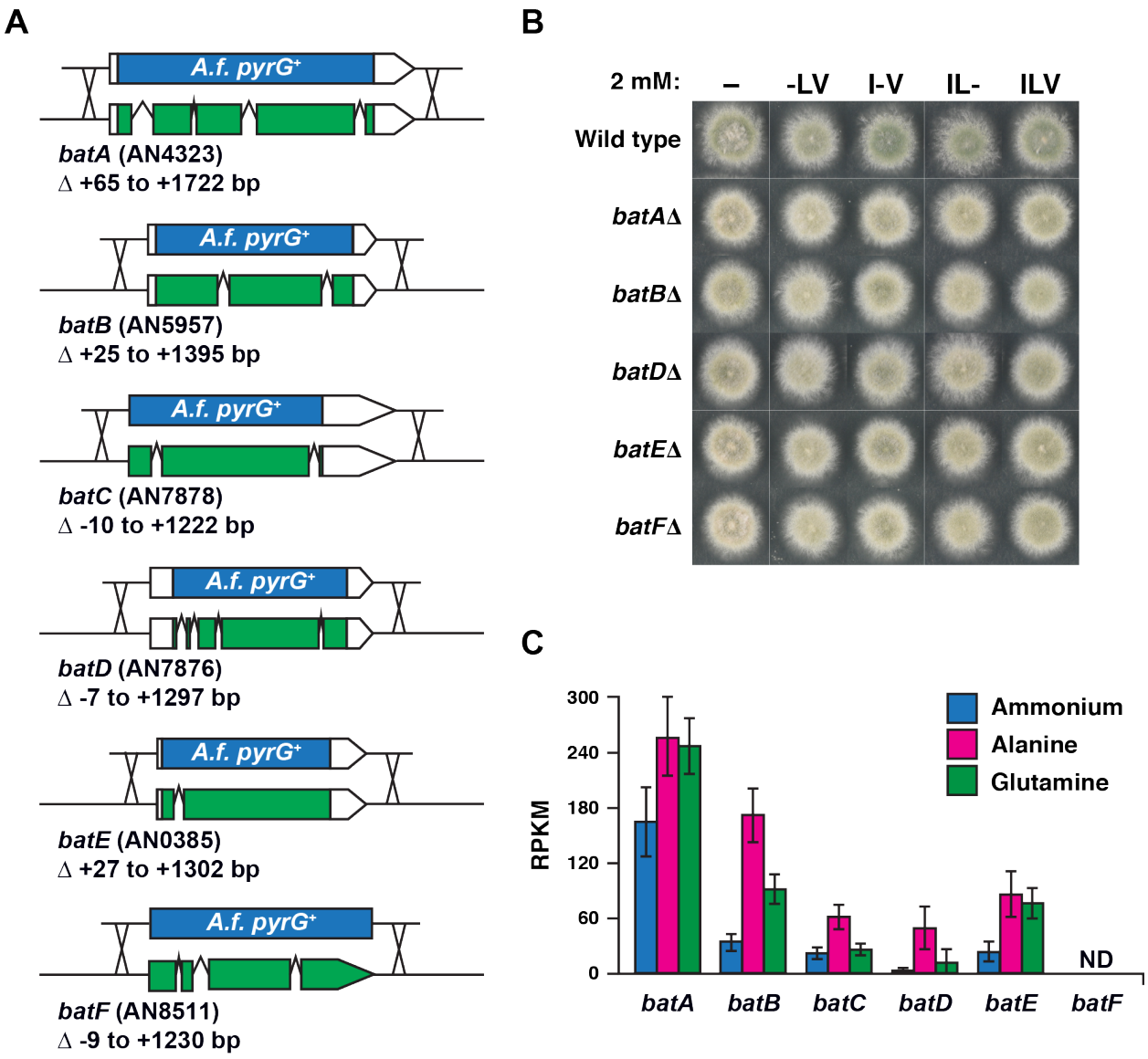

Figure 3.9 Knockout of BATs individually has no effect on growth.

A) Diagrams of the knockouts cassettes from the Fungal Genetics Stock Center **B)** Wild type (MH1), *batA*Δ (RT415), *batB*Δ (RT440), *batD*Δ (RT419), *batE*Δ (RT417) and, *batF*Δ (RT441) strains were grown on supplemented ANM solid media for 2 days with 10 mM nitrate as the predominant nitrogen source and combinations of 2 mM each of isoleucine (I), leucine (L), and valine (V) to supplement potential auxotrophies. – represents an omitted amino acid. **C)** Reads per kilobase per million mapped reads (RPKM) from RNA-seq of MH1 grown at 37ºC for 16 hours in supplemented liquid ANM with 10 mM ammonium, glutamine, and alanine. ND = not detected. Error bars depict SEM

Figure 3.10 Systematic combination of BAT knockouts.

A) Seven crosses were designed to create all possible BAT gene knockout combinations**. B)** Wild type (MH1), *batA*Δ *batB*Δ (RT457), *batD*Δ *batE*Δ (RT454), *batD*Δ *batF*Δ (RT473), *batE*Δ *batF*Δ (RT466), and *batD*Δ *batE*Δ *batF*Δ (RT472) strains were grown on supplemented ANM solid media for 2 days with 10 mM nitrate (NO_3), ammonium (NH_4), glutamine (Gln), alanine (Ala), and glutamate (Glu) as the predominant nitrogen source, and combinations of 2 mM of each of isoleucine (I), leucine (L), and valine (V) to supplement potential auxotrophies. The *batA*Δ *batB*Δ colonies were grown for a further 2 days, 4 days total to test for strict or leaky BCAA auxotrophy.

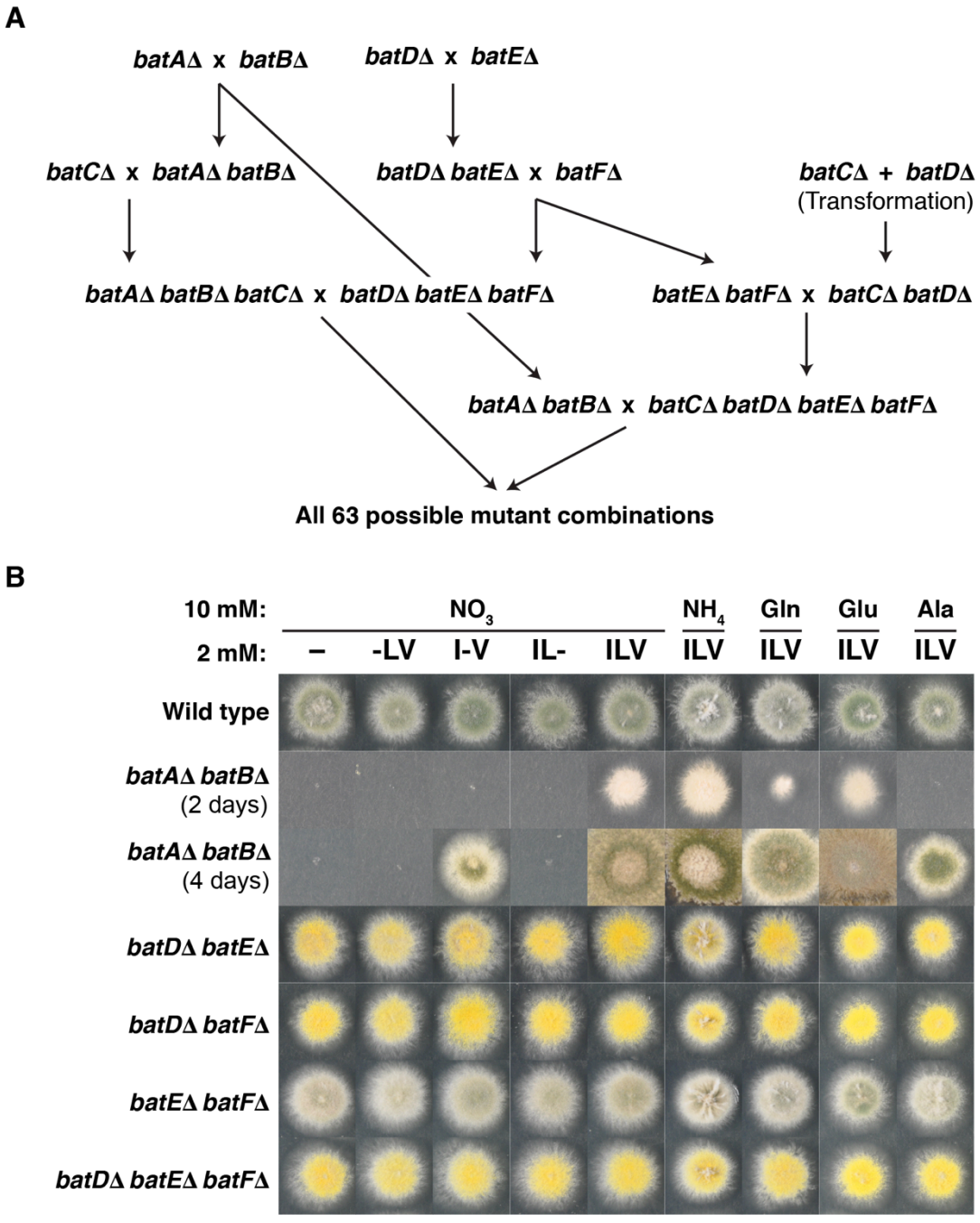

Figure 3.10 Systematic combination of BAT knockouts.

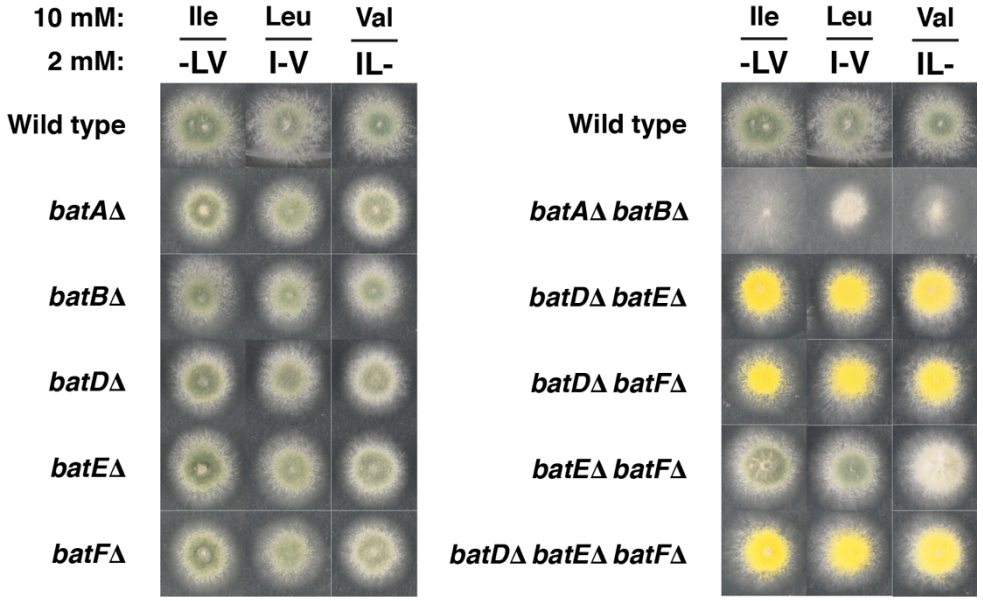

Figure 3.11 Utilization of isoleucine, leucine, and valine by BAT knockout mutants.

Wild type (MH1), *batA*Δ (RT415), *batB*Δ (RT440), *batD*Δ (RT419), *batE*Δ (RT417), *batF*Δ (RT441)**,** *batA*Δ *batB*Δ (RT457), *batD*Δ *batE*Δ (RT454), *batD*Δ *batF*Δ (RT473), *batE*Δ *batF*Δ (RT466), and *batD*Δ *batE*Δ *batF*Δ (RT472) strains were grown on supplemented ANM solid media for 2 days with 10 mM isoleucine (Ile), leucine (Leu), and valine (Val), as the predominant nitrogen source, and combinations of 2 mM of each of isoleucine (I), leucine (L), and valine (V) to supplement auxotrophies.

3.4.5 Regulation of leucine biosynthesis genes

3.4.5.i Leucine biosynthesis regulates the NADP-glutamate dehydrogenase, **gdhA.**

NOTE: This section is a summary of research conducted as part of this dissertation that was published in Downes D.J., M.A. Davis, S.D. Kreutzberger, B.L. Taig and R.B. Todd (2013) Regulation of the NADP-glutamate dehydrogenase gene *gdhA* in *Aspergillus nidulans* by the Zn(II)2Cys6 transcription factor LeuB. *Microbiology* **159 (12):** 2467-2480. *The full article has been included as Appendix A.*

Leucine abundance provides a negative feedback mechanism for regulation of LeuB target genes. As LeuB regulates *gdhA* (POLOTNIANKA *et al.* 2004), we were interested to know whether leucine affects *gdhA* expression. Using exogenous isoleucine, leucine, valine and tyrosine we showed that leucine, but not the other amino acids negatively affected expression of a *gdhA-lacZ* translational fusion reporter gene. Furthermore using leucine biosynthesis mutants predicted to have increased (*luA1*) or decreased (*leuC*Δ) α-IPM levels, we showed that levels of this leucine biosynthesis pathway intermediate positively regulated the level of *gdhA-lacZ* expression, consistent with the regulatory mechanisms affecting Leu3p in *S. cerevisiae*. Using a DNA-binding motif loss-of-function mutant, $leuB^{C69A}$, we showed that LeuB DNA binding is required for regulation of *gdhA*. We therefore used bioinformatics to predict two putative DNA binding motifs in the *gdhA* promoter based upon the Leu3p $CCGN_4CGG$ consensus site. However, while promoter deletion analysis showed LeuB acted via one of these sites, *leuB*Δ affected *gdhA* expression in the absence of both motifs. By further promoter analysis we identified a conserved sequence related to the LeuB/Leu3p motif, $CCGN_5CGG$, through which LeuB acts. We have also shown this motif to be the target of TamA DNA binding in the *gdhA* promoter (DOWNES *et al.* 2014b). LeuB regulation via this novel site may be indirect through the regulation of TamA, or direct via LeuB homodimer binding or by heterodimerization with TamA. We have examined the *tamA* promoter and found a putative LeuB canonical site at -1,391 to -1,382 bp of *tamA* suggesting regulation of the $CCGN_5CGG$ site may be indirect. However, TamA binding at *gdhA* is LeuB dependent (Chapter 4.4.2); therefore we favor the latter theory (Figure 3.12). Finally, using sequence analysis of 44 promoters of *gdhA* orthologs to search for putative LeuB/Leu3p binding motifs we were able to predict conservation of leucine regulation

of these genes for some of the fungi. Notably motifs were absent in *gdhA* promoters of several pathogens, including the phytopathogens *F. fujikuroi, Fusarium graminearum, F. oxysporum,* and *Fusarium verticilioides,* and the animal pathogens *Coccidioides immitis* and *C. albicans*. Interestingly, we found that *leuB*Δ grown in the absence of leucine resulted in a higher concentration of soluble protein in extracts (Figure 3.13). Two possible explanations for this phenomenon are that either the leaky leucine auxotrophy results in a general amino acid starvation response and global up-regulation of protein production, or that the reduced leucine levels modify mycelial cell-wall composition and facilitate enhanced protein extraction. However, these theories remain to be examined.

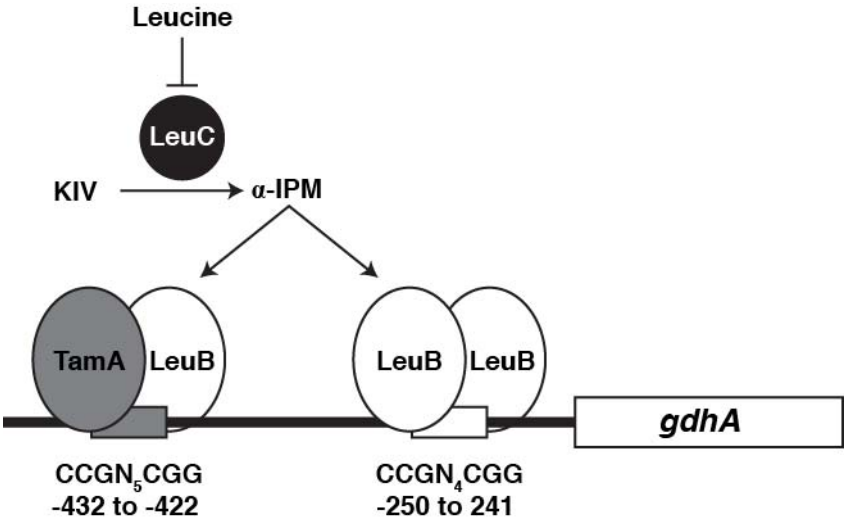

Figure 3.12 Model of LeuB regulation of *gdhA* based upon Downes *et al*., (2013).
LeuB activates *gdhA* expression via a canonical binding site (white box) as a homodimer and at a non-canonical motif (grey box) as a heterodimer with TamA. LeuB is activated by the presence of α-isopropylmalate (α-IPM), which is produced from α-ketoisovalerate (KIV) by the α-IPM synthetase LeuC.

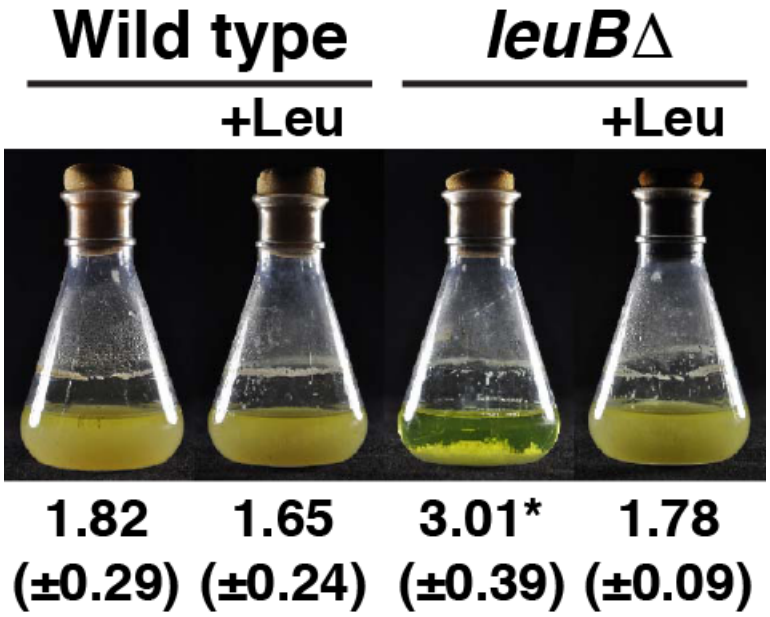

Figure 3.13 Effect of *leuB*Δ on protein extraction.

Mycelia of wild type (MH12101) and *leuB*Δ (MH12181) were grown in supplemented liquid ANM containing 10 mM ammonium with or without 2 mM leucine (Leu) at 37ºC for 16 h with shaking at 120 opm. Soluble proteins were extracted from 0.2 g of mycelia by grinding in 2 ml of 0.2 M phosphate buffer, and protein concentrations (µg/µl) were calculated using Biorad protein reagent. SEM is shown for three replicates. * is $p < 0.05$ using a two-tailed Student's t-test with equal distribution.

3.4.5.ii Identification of a LeuB like transcription factor.

The *Aspergillus* genome is incredibly rich in transcription factors, particularly members of the fungal specific Zn(II)2Cys6 zinc binuclear cluster family (TODD *et al.* 2014). A potential paralog of LeuB, AN4744, is found in the *A. nidulans* genome (H. Haas, pers. commun.). Protein sequence alignment revealed that LeuB and AN4744 show 43.4% identity. We have named AN4744 *leuR* for ***Leu***B like ***R***egulator. Alignment of LeuR with LeuB and Leu3p showed strong conservation of the DNA binding domain, linker and heptad repeats, particularly between LeuB and LeuR. Similarly the Middle Homology Region was also strongly conserved between LeuB and LeuR (Figure 3.14). Conservation of the region directly C-terminal to the DNA binding motif may be significant as it is involved in sequence specific DNA recognition and therefore suggests that these two transcription factors bind similar target sequences (REECE AND PTASHNE 1993). The masking region of Leu3p, involved in feedback regulation by α-IPM, is poorly conserved with LeuB, despite functional conservation of this mechanism. However, this region showed strong conservation between LeuB and LeuR.

Using the AN4744::*A.f.pyrG* knockout cassette from the Fungal Genetics Stock Center we generated a *leuR*Δ mutant by transformation of MH11059 (*pyroA4 pyrG89 nkuA*Δ) and selection for pyrimidine prototrophy (Figure 3.15A). Homologous integration of the knockout construct at *leuR* was confirmed by Southern blot (see Materials and Methods 3.3.1). In contrast to the leaky leucine auxotrophy of the *leuB*Δ mutant (POLOTNIANKA *et al.* 2004), the *leuR*Δ mutant showed no growth defects in the absence of exogenous leucine and was able to utilize each of the three BCAAs as nitrogen nutrients (Figure 3.15B). It will be of interest to determine the effects of *leuR*Δ on expression of leucine biosynthesis genes and to generate a *leuB*Δ *leuR*Δ double mutant to determine if they have any redundant functions.

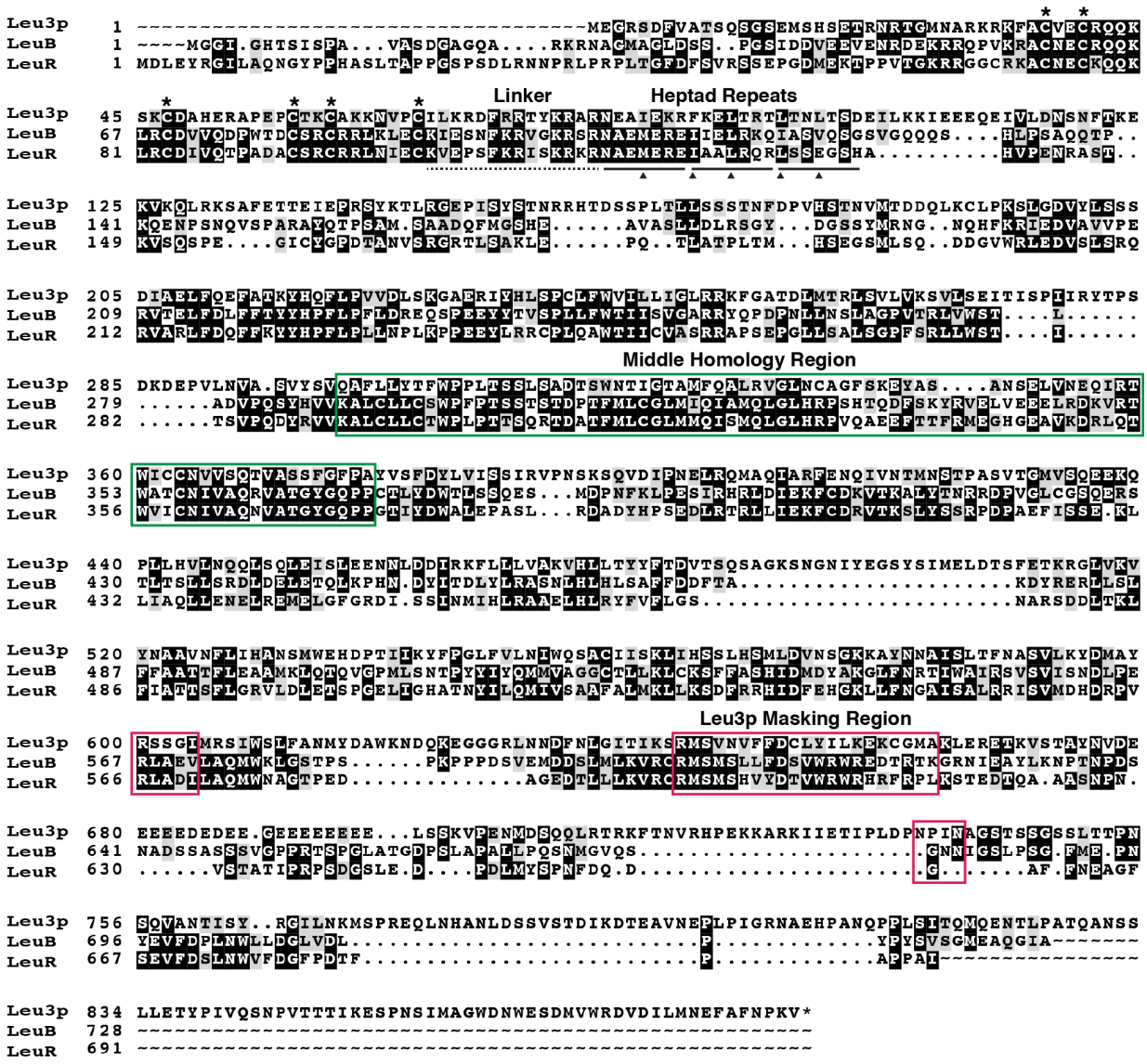

.Figure 3.14 Comparison of the *leuR*, *leuB* and *LEU3* encoded proteins.

Clustal Omega alignment of *A. nidulans* LeuR and LeuB and *S. cerevisiae* Leu3p. The middle homology region is boxed (green), as is the Leu3p α-IPM masking region (red). Cysteines that form the C6 DNA-binding motif are starred; the linker region is underlined (dashed) as are the heptad repeats (solid). Hydrophobic residues in the 1 and 4 positions of the heptad repeats are marked (arrow heads).

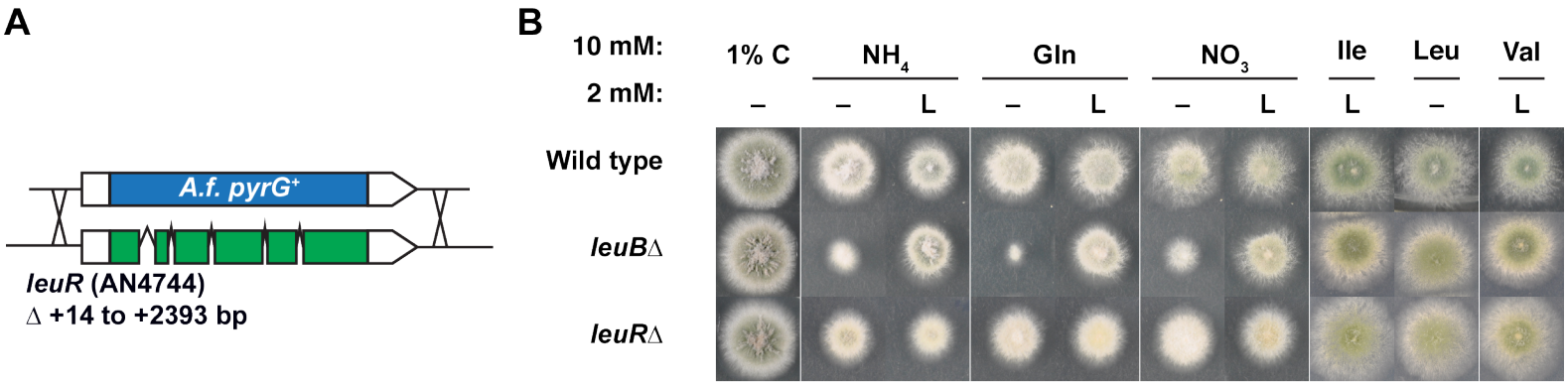

Figure 3.15 Deletion of *leuR* does not affect growth.

A) Diagram of the *leuR*/AN4744 knockout cassette from the Fungal Genetics Stock Center **B)** Wild type (MH1), *leuB*Δ (MH12181), *leuR*Δ (RT478) strains were grown on 1% complete media (1% C) or supplemented ANM solid media for 2 days with 10 mM ammonium (NH_4), glutamine (Gln), nitrate (NO_3) isoleucine (Ile), leucine (Leu), and valine (Val) as the predominant nitrogen source and 2 mM with or without of leucine (L) to supplement auxotrophies.

3.4.5.iii Effect of LeuB on BCAA pathway gene expression

Based on similarity with Leu3p and our analysis of the *gdhA* promoter we expect LeuB to act via canonical $CCGN_4CGG$ binding motifs or the non-canonical $CCGN_5CGG$ motif (DOWNES *et al.* 2013). We identified the canonical motif in the 1 kbp upstream region of 7/12 putative leucine biosynthesis genes (Figure 3.16A); the non-canonical motif was also present in 5/12 promoters. We also used SCOPE computation promoter analysis (CARLSON *et al.* 2007; CHAKRAVARTY *et al.* 2007a,b) to determine any other overrepresented motifs in these 12 promoters when compared with the 1 kbp upstream region of all genes in *A. nidulans*. SCOPE found a motif very similar to the consensus sequence, CGN_4CGS (where S is a C or G nucleotide), was over-represented. This motif includes the predicted LeuB binding site and added six additional putative targets in BCAA biosynthesis gene promoters (Figure 3.16A). When this relaxed motif is taken into account all 12 genes contain a potential LeuB regulatory sequence. Interestingly the non-canonical sites in the *leuB, leuD,* and *leuE* promoters overlap or are adjacent to canonical sites. To determine whether leucine biosynthesis regulates all or any of these genes we performed qRT-PCR on mycelia grown with exogenous leucine, which represses LeuB activation (DOWNES *et al.* 2013) and in a *leuB*Δ strain. Neither *leuB* nor *leuR* had significant changes in expression in response to leucine, however *leuR* expression was decreased in the *leuB*Δ mutant. Seven of the ten leucine biosynthesis genes, *luA, leuC, leuD, leuE, batA, batB,* and *batE,* showed decreased expression in response to exogenous leucine and in the *leuB*Δ mutant compared to wild type (Figure 3.16B). All of the promoters of these leucine biosynthesis genes excepting *batB* contained a canonical $CCGN_4CGG$ LeuB binding site consensus sequence. The *batB* promoter contains the relaxed $CCGN_4CGS$ consensus motif, and therefore LeuB may function through this site at this promoter. We were unable to amplify the *batF* transcript by qRT-PCR, consistent with it being undetectable by RNA-seq (Table 3.6, Figure 3.9C). Interestingly *batC* had increased expression in both the presence of leucine and in the *leuB*Δ mutant, and therefore this may suggest a role in leucine catabolism. To explore other possible regulatory targets of LeuB we performed a PatMatch analysis (YAN *et al.* 2005) searching for the $CCGN_4CGS$ motif in the 1 kbp upstream region of all *A. nidulans* genes. The motif was within 1 kb of 4,408 different genes, over 25% of the genes in the genome, therefore to better understand the breadth of regulation by LeuB more advanced analyses such as ChIP-seq or RNA-seq will need to be performed.

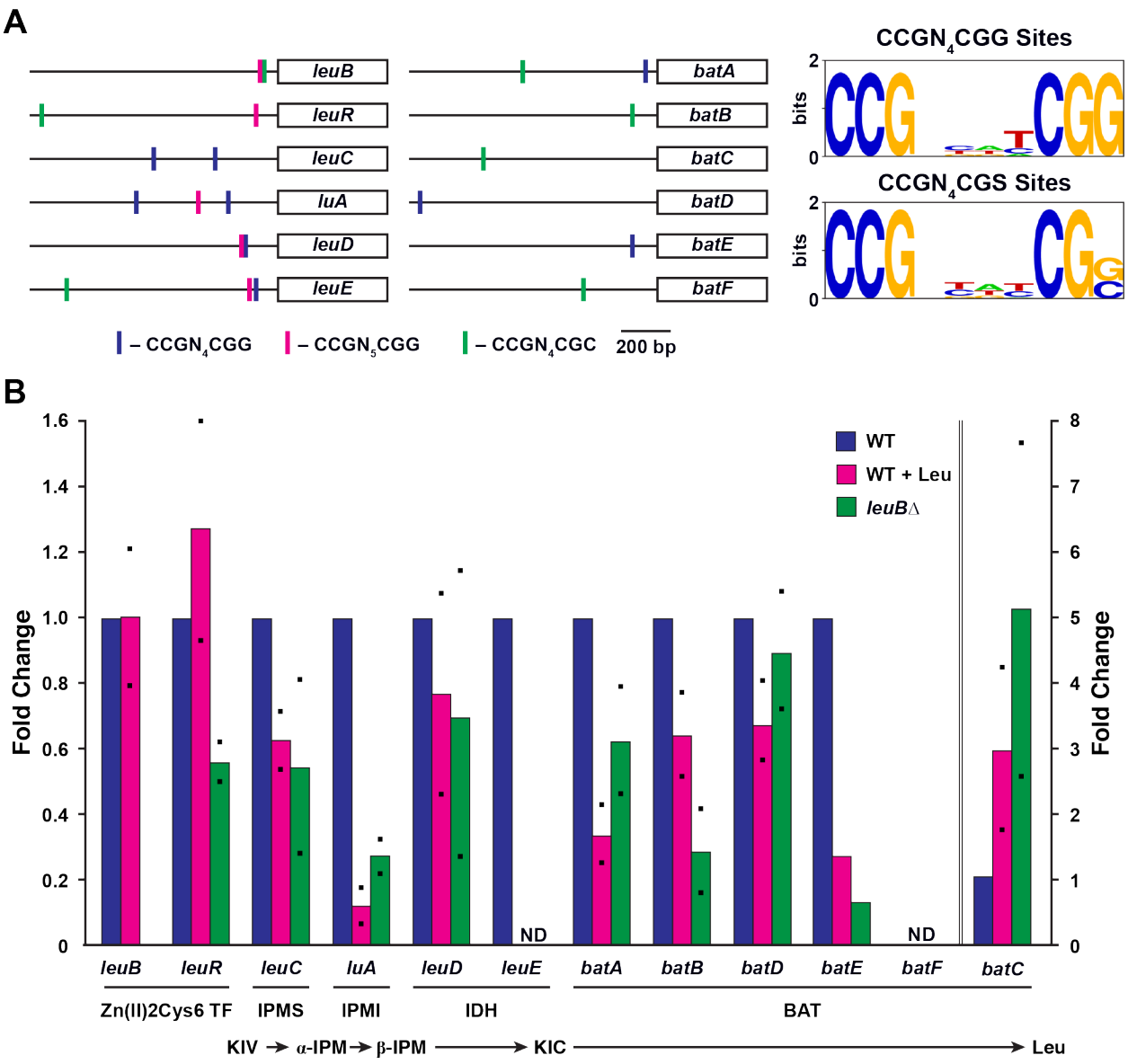

Figure 3.16 LeuB regulation of the leucine biosynthesis genes

A) Location of canonical (blue) and non-canonical (pink) LeuB binding motifs as well as the SCOPE identified relaxed canonical sequences (green) in the promoters of BCAA biosynthesis genes. Motifs were aligned to generate a WebLogo motif of putative binding sites. **B)** Real time reverse transcriptase PCR of BCAA biosynthesis genes from wild type (MH1) and *leuB*Δ (RT12609) grown for 16 hours in supplemented liquid ANM-10 mM ammonium and with or without 2 mM leucine. Expression is relative to wild type; results from two independent replicates are shown (squares), *leuE* and *leuF* were too low to be detectable under several conditions (ND).

3.5 Discussion

Regulation of the core nitrogen assimilation gene *gdhA* by the leucine biosynthesis Zn(II)2Cys6 transcription factor LeuB led to an interest in determining the role of leucine biosynthesis in regulating nitrogen metabolism (POLOTNIANKA *et al.* 2004). Leucine biosynthesis has been well characterized in the model yeast *S. cerevisiae* (reviewed in KOHLHAW 2003) but was less well understood in filamentous fungi, with only one of four steps characterized. In this work we have completed the annotation of the *A. nidulans* leucine biosynthesis pathway and characterized the genes encoding enzymes responsible for the remaining three steps, α-IPM synthetase, β-IPM dehydrogenase and BCAA aminotransferase. Characterization of this pathway has revealed a surprising divergence in the filamentous fungi when compared with yeast, in the number of genes encoding the enzymes for each step. We have also furthered the understanding of how *A. nidulans* regulates leucine biosynthesis by feedback mechanisms and how these mechanisms cross talk with nitrogen assimilation via regulation of the NADP-dependent glutamate dehydrogenase *gdhA*.

3.5.1 From KIV to KIC – making and changing isopropylmalate.

In *S. cerevisiae* ketoisovalerate is converted to α-IPM by two α-IPM synthetases Leu4p and Leu9p. We found a single α-IPM synthetase responsible for leucine biosynthesis in *A. nidulans*. α-IPM is then converted to β-IPM by the isopropylmalate isomerase, which is encoded by a single gene in *S. cerevisiae* (*LEU1*) and *A. nidulans* (*luA*) (SKALA *et al.* 1991; POLOTNIANKA *et al.* 2004). Finally β-IPM is converted to ketoisocaproate by the β-IPM dehydrogenase. *S. cerevisiae* contains a single β-IPM dehydrogenase, Leu2p (TOH-E *et al.* 1980; ANDREADIS *et al.* 1984), but *A. nidulans* contains two, LeuD and LeuE. Therefore, analysis of these three steps of leucine biosynthesis shows pathway conservation and divergence between *A. nidulans* and *S. cerevisiae* for the number of functional genes at each step.

The two functional β-IPM dehydrogenase-encoding genes are conserved in *A. niger* (WILLIAMS *et al.* 1996), and predicted in *A. fumigatus* and *A. oryzae* (AspGD). Our analysis of the LeuD and LeuE phylogeny shows that the two enzymes are conserved amongst the Aspergilli, yet are not closely related to each other. The sequence differences between the two enzymes may indicate ancient gene duplication with divergence and subsequent loss in the

majority of fungal species, or a horizontal gene-transfer event into an *Aspergillus* progenitor species (CHANDRASEKARAN AND BETRÁN 2008; KAESSMANN 2010). The origin of the additional β-IPM dehydrogenase-encoding gene copy remains to be elucidated. The acquisition of additional copies of genes can lead to the evolution of new roles and functions of the encoded protein (WAPINSKI *et al.* 2007), however we found that both *leuD* and *leuE* function in leucine biosynthesis – though *leuE* plays a lesser role based upon its low level of expression and the leaky leucine auxotrophy conferred by *leuD*Δ. It is therefore possible that *leuE* may be in the process of divergence.

3.5.2 BAT gene copy number expansion.

The final step in BCAA biosynthesis is catalyzed by BCAA aminotransferase. *S. cerevisiae* encodes two BATs, one that is predominantly mitochondrial and one that is entirely cytoplasmic (EDEN *et al.* 1996; KISPAL *et al.* 1996). We identified six putative BAT encoding genes in *A. nidulans*, two with products that are predicted to be targeted to the mitochondrion, whereas the remaining four are likely cytoplasmic. Unlike the number of β-IPM dehydrogenase encoding genes, which was conserved among the Aspergilli, there was a high degree of variation in BAT encoding gene number. *A. nidulans* and *A. niger* were the most BAT rich with six copies each, *A. oryzae* has five gene copies and *A. fumigatus* has only three BAT genes. Variation in gene number was also seen amongst the other filamentous fungi in the Pezizomycotina group, including *N. crassa* with three copies, and the phytopathogens *F. oxysporum* and *M. oryzae* with four and three copies respectively. The opportunistic human pathogen *P. marneffei*, which is an AIDS defining pathogen in south-east Asia, is closely related to the Aspergilli and is BAT rich with 5 predicted copies. The number of BAT encoding genes in Ascomycete yeasts and Basidiomycetes was relatively low, with the maximum number of encoded proteins being three (*U. maydis* and *C. albicans*). *S. pombe* has only one BAT encoding gene *eca39*/BCAT, which is required for growth in the absence of valine (EDEN AND BENVENISTY 1998). This high degree of variation in gene number is suggestive of evolution of new roles in the additional gene copies. Our functional analysis of the *A. nidulans* BATs by deletions suggests that only two BAT encoding genes, *batA* and *batB*, are predominantly responsible for BCAA biosynthesis. The dispensability of *batD, batE*, and *batF* for BCAA biosynthesis also suggests of novel roles. The

proteins encoded by these three genes were co-located in a filamentous fungi specific clade in the BAT phylogeny.

Filamentous fungi are particularly rich in clusters of tightly linked genes that encode the production of secondary metabolites (KELLER *et al.* 2005), and BatC, BatD, BatE, and BatF may be associated with evolution of roles in secondary metabolite production. Humans have used secondary metabolites such a tetracycline for their beneficial properties for centuries (BASSETT *et al.* 1980), however the 20th century saw a blossoming of our understanding of both beneficial and harmful secondary metabolites, such as penicillin and aflatoxins respectively (FLEMING 1929; GEORGIANNA AND PAYNE 2009). *batC* and *batD* are located within an uncharacterized secondary metabolite cluster and may play a role in synthesis of the encoded product (INGLIS *et al.* 2013). Similarly, *batF* is adjacent to the terriquinone A biosynthesis cluster. However AN8512, which is the gene between *batF* and the first gene of the cluster *tdiA*, is not required for terriquinone A biosynthesis (BOUHIRED *et al.* 2007). Several genes (AN8509, AN8507, and AN8506) adjacent to the *tdi* cluster have predicted roles in secondary metabolism and there is an uncharacterized cytochrome P450 (AN8510) (KELLY *et al.* 2009). It is possible these genes and *batF* (AN8511) form a second cluster, or are in fact part of the terriquinone A cluster but responsible for producing a related but different metabolite. For example the *mdp* cluster in *A. nidulans* is responsible for the production of monodictyphenone, emodin and emodin derivatives (BOK *et al.* 2009). Similarly, orsellinic acid, lacenoric acid, and the cathepsin K inhibitors F-9775A and F-9775B are produced by the *A. nidulans ors* cluster in response to *Streptomyces rapamycinicus* (SCHROECKH *et al.* 2009). The undetectable expression of AN8511/*batF* under our growth conditions or growth conditions used for RNA-seq by others (SIBTHORP *et al.* 2013) may indicate a requirement for induction of expression and production of the hypothetical secondary metabolite. Many secondary metabolite gene clusters are silent under standard growth conditions and finding the conditions for production of secondary metabolites is a challenging process, which has led to the development of synthetic techniques for induction, such as promoter fusion, and transcription factor overexpression (BRAKHAGE AND SCHROECKH 2011). These techniques may be necessary to determine the role and function of BATs that are not involved in BCAA biosynthesis.

3.5.3 Regulation of leucine biosynthesis

Regulation of leucine biosynthesis is best understood in *S. cerevisiae* where both gene activation and gene repression is mediated by the Zn(II)2Cys6 transcription factor Leu3p (reviewed in KOHLHAW 2003). When cellular leucine is abundant, leucine interacts with the α-IPM synthetase and inhibits its function, this decreases cellular α-IPM levels and leads to Leu3p functioning as a repressor. When leucine levels decrease α-IPM synthetase is not inhibited, α-IPM then interacts with Leu3p causing a conformational change, resulting in Leu3p switching from repressor to activator functions (reviewed in KOHLHAW 2003). We observed repression by exogenous leucine in wild type cells of all six of the genes that function in leucine biosynthesis, *luA, leuC, leuD, leuE, batA*, and *batB,* suggesting this feedback mechanism likely operates in *A. nidulans.* Exogenous leucine also conferred reduced expression of *batD* and *batE* suggesting they may function in leucine biosynthesis. The leaky leucine auxotroph *leuD*Δ mutant results in increased expression of other leucine biosynthesis genes, which is likely a result of reduced cellular levels of the negative feedback mediator leucine, and increased α-IPM inducer levels, due to an increase in β-IPM levels increasing the reverse reaction rate carried out by the bi-directional α-IPM isomerase (EC 4.2.1.33) encoded by *luA*.

The homolog of Leu3p in *A. nidulans* is LeuB. Deletion of *leuB* results in leaky leucine auxotrophy (POLOTNIANKA *et al.* 2004), which we have now shown is due to decreased expression of the six leucine biosynthesis genes. Our analysis of the LeuB DNA-binding domain suggested strong conservation with the Leu3p DNA-binding domain and therefore we predicted binding at the same $CCGN_4CGG$ motif (DOWNES *et al.* 2013). We found this motif in five of the six regulated leucine biosynthesis pathway genes, but it was absent from the 1 kb region upstream of *batB*, which is regulated by LeuB. A similar but relaxed motif $CCGN_4CGS$ was present in all six promoters and, although regulation of *batB* by LeuB could be either direct or indirect, it is possible that LeuB binds at the relaxed motif. Variation in one of the CCG repeats in the Leu3p binding site in the *LEU4* promoter is tolerated (HELLAUER *et al.* 1998). Therefore it is likely that LeuB regulates leucine biosynthesis genes via a motif similar to that known for Leu3p, as was shown for the *gdhA* promoter where a LeuB site of action has been characterized (discussed in Section 3.4.7.i; DOWNES *et al.* 2013). Searches to identify this motif showed it is common throughout the genome and adjacent to thousands of genes. It is unlikely that LeuB

regulates all of these genes, and promoter availability, promoter-specific interactions with other transcription factors, or chromatin remodeling may facilitate binding or regulation at specific sites. In *S. cerevisiae*, genome-wide analysis of Leu3p binding revealed most binding sites occur by chance and that low nucleosome occupancy directs Leu3p to biologically relevant target sites (LIU *et al*. 2006).

3.5.4 Regulatory crosstalk between leucine biosynthesis and nitrogen assimilation.

LeuB was known to activate expression of the NADP-dependent glutamate dehydrogenase *gdhA* (POLOTNIANKA *et al.* 2004). Using mutants in the leucine biosynthesis pathway we showed the expression of *gdhA* was regulated by changes in the cellular α-IPM levels and by exogenous leucine, indicating co-regulation of *gdhA* with the leucine biosynthesis genes. Leucine regulation of *gdhA* can be rationalized in two ways. First, the product of NADP-GDH is glutamate, which acts as the amino group donor for the BAT enzymes in the final step of leucine biosynthesis. Therefore *gdhA* encodes an enzyme that generates a leucine biosynthesis substrate and regulation by LeuB can be a means by controlling leucine biosynthesis. Second, leucine is one of the most abundant protein-incorporated amino acids, but is maintained at very low levels within the cell. In *A. nidulans* leucine represents approximately 2% of the free cellular amino acids (SCHINKO *et al.* 2010). This low level of abundance makes leucine highly sensitive to changes in free amino acids levels as a result of nitrogen assimilation, therefore reduced leucine levels may signal for increased assimilation of nitrogen via regulated expression of *gdhA*. Regulation of *gdhA* by LeuB is carried out via two separate conserved motifs, the first is a $CCGN_4CGG$ consensus site where LeuB is predicted to act as a homodimer. The second related site, $CCGN_5CGG$, is also the target DNA-binding site for TamA and LeuB is required for TamA binding at this site (Chapter 4.4.2). Therefore we predict that LeuB and TamA bind at this site as a heterodimer. The interaction with TamA, which is classically understood to be the coactivator of nitrogen assimilation gene expression (DAVIS *et al.* 1996; SMALL *et al.* 1999), is consistent with free leucine levels regulating nitrogen assimilation. We also identified a second consensus LeuB site in the *gdhA* promoter that acted as a site for a negative regulatory factor. Given that LeuB acts primarily as an activator under the conditions we examined, this site appears to be regulated by a different transcription factor.

3.5.5 Branched chain amino acid enzymes as antifungal targets

Branched chain amino acids are essential for animals, but readily synthesized in bacteria, fungi and plants. The inability of animals to produce BCAA makes the enzymes involved in their synthesis strong candidates for antifungal targets. Indeed, the opportunistic fungal pathogens *A. fumigatus*, *C. neoformans,* and *C. albicans* have reduced virulence and pathogenicity in mouse and zebra fish infection models (KINGSBURY *et al.* 2004; KINGSBURY AND MCCUSKER 2010; OLIVER *et al.* 2012; DO *et al.* 2015). Many commercially available herbicides target amino acid biosynthesis, and herbicides that target essential amino acid biosynthesis have less negative impacts on humans than those which target non-essential amino acid biosynthesis (READE AND COBB 2002). Herbicides targeting essential amino acid biosynthesis are commercially available and can target glutamine biosynthesis via glutamine synthetase (glufosinate), aromatic amino acid biosynthesis via the 5-enolpyruvylshikimate-3-phosphate synthase (EPSP; glyphosphate), and branched chain amino acid biosynthesis via acetohydroxyacid synthetase (AHAS inhibitors, e.g. imidazolinone and sulfonylurea). As with all antimicrobial drugs the emergence of resistant fungal pathogen strains is an ever-present threat (FISHER *et al.* 2012). The glyphosphate resistant EPSP variant from *Agrobacterium* sp. strain CP4, which is used in Roundup Ready® Soybeans (Monsanto), carries a single amino acid substitution which confers resistance (FUNKE *et al.* 2006). Therefore the likelihood of future resistance to herbicides and anti-fungal chemicals means additional antifungal targets should be considered. Our studies of genes required for leucine biosynthesis indicate that chemicals that abolish enzyme activity at any stage of leucine biosynthesis are likely to confer leucine auxotrophy. However, it is important to consider the feedback mechanisms that are present in the Aspergilli. An effective fungicide would need to be highly effective at targeting the leucine biosynthesis enzyme; otherwise increased expression of other leucine biosynthesis pathway genes by LeuB may provide a degree of fungicide tolerance. The strongest target would be α-IPM synthetase (LeuC) as reduced activity of this enzyme leads to decreased α-IPM and leads to repression of leucine biosynthesis genes by LeuB. The benefit of targeting this step would be in cross regulation of nitrogen assimilation by reduced expression of *gdhA* and potentially reduced cellular glutamate and glutamine levels.

3.6 Future Perspectives

Our characterization of the leucine biosynthesis pathway has resulted in a near complete annotation of the genes required for leucine biosynthesis in *Aspergillus nidulans*. However, the *batA*Δ *batB*Δ double mutant grows in the absence of leucine after an extended period. Therefore additional *bat* mutant combinations will be needed to determine which gene(s) provided the residual activity. The selection constraints on the additional BAT and β-IPM dehydrogenase encoding genes are also of interest. Studies of DNA sequence changes may provide evidence for negative, neutral or positive selection at each of these genes. Furthermore the potential roles of *batC, batD* and *batF* in secondary metabolism remain to be determined. Overexpression or deletion of the nearby non-ribosomal peptide synthetases in wild type and mutant backgrounds may lead to identification of the encoded products and whether the aminotransferases play a role in secondary metabolism.

We predict that LeuB and TamA act as a heterodimer at the *gdhA* promoter. We were unable to detect *in vitro* DNA-binding at the *gdhA* promoter of an MBP-TamA fusion protein when expressed in *E. coli* (data not shown). Construction of an MBP-LeuB fusion and mixtures of it with MBP-TamA could be used to show heterodimeric binding. We have also generated ChIP-seq data that shows TamA binding is dependent on LeuB at additional promoters across the genome (Chapter 4.4.6.ii). It will be of interest to generate an epitope tagged LeuB to perform ChIP-seq in both wild type and *tamA*Δ strains to determine the overlap of the TamA and LeuB regulatory networks.

Analysis of a LeuB like transcription factor LeuR, revealed strong similarity to LeuB, particularly in the DNA-binding domain, however deletion of LeuR conferred no obvious growth defects in the absence or presence of leucine in the single mutant. Therefore it will be of interest to determine the effects of *leuR*Δ on expression of leucine biosynthesis genes and to generate a *leuB*Δ *leuR*Δ double mutant to determine if they have any redundant functions. We identified a negative LeuB binding site-like motif in the *gdhA* promoter. The effects of *leuR*Δ on the *gdhA-lacZ* reporter fusions we have generated with and without this site in the promoter, will reveal whether LeuR regulates *gdhA* expression.

Chapter 4 - Dual function transcription factors

4.1 Abstract

Transcription factors can regulate gene expression via either direct DNA binding, or indirect protein-protein interaction with a DNA-binding protein. Transcription factors that contain DNA-binding motifs are generally considered to interact directly with DNA and this domain is usually essential for function. However, for two members of the fungal Zn(II)2Cys6 zinc cluster family of transcription factors, TamA from *Aspergillus nidulans* and Dal81p from *Saccharomyces cerevisiae*, the DNA-binding motif was considered dispensable for function. TamA regulates genes involved in toxic nitrogen analog resistance and *gdhA*, which encodes the key nitrogen assimilation enzyme NADP-dependent glutamate dehydrogenase, and is thought to do so as the coactivator of AreA and/or LeuB. However, *tamA*Δ has a greater effect on *gdhA* expression than the combination of *leuB*Δ and the loss-of-function mutation *areA217*. TamA was therefore expected to play a role beyond that of a coactivator at *gdhA*. We show that the Zn(II)2Cys6 DNA-binding motif of TamA is required for regulation of *gdhA,* and by promoter analysis identify a conserved TamA DNA binding site. By electrophoretic mobility shift assay and chromatin immunoprecipitation (ChIP) we show a FLAG-epitope tagged variant of TamA can interact with this site both *in vitro* and *in vivo*. Therefore TamA acts as a dual-function transcription factor with promoter context dependent DNA-binding and coactivator roles. Using RNA-seq and ChIP-seq and *tamA* deletion and DNA-binding motif mutants we identify the networks of genes regulated by TamA in each regulatory mode, including the GOGAT pathway genes, siderophore biosynthesis genes, secondary metabolite gene clusters and genes involved alcohol metabolism. TamA DNA binding at the *gdhA* promoter is dependent on the presence of AreA and LeuB. However, ChIP-seq in *areA*Δ and *leuB*Δ backgrounds shows that TamA binds independently of these two transcription factors at other locations in the genome. Finally by RNA-seq of *areA*Δ and an *areA* DNA-binding motif mutant we show that the *A. nidulans* GATA DNA binding transcription factor AreA also acts as a dual fuction transcription factor. We conclude that dual-function transcription factors that operate by alternative DNA binding or coactivator mechanisms may be widespread.

4.2 Introduction

NOTE: This introduction is adapted from (DOWNES *et al.* 2014b).

One of the many mechanisms by which organisms respond to environmental stimuli and control growth and development is via transcriptional regulation. Control of gene expression is regulated by DNA-binding transcription factors that bind at sequence specific sites in the promoter (DYNAN AND TJIAN 1985). Transcription factors often are involved in direct protein-protein interactions with DNA-binding domain lacking co-factors that either enhance (co-activators) or reduce (co-repressors) transcription. The classical example of this interactive regulation is the galactose utilization system in *Saccharomyces cerevisiae*. In this system the Zn(II)2Cys6 zinc cluster transcription factor Gal4p binds promoters and the Gal80p non-DNA binding corepressor binds the Gal4p activation domain to repress expression of target genes (reviewed in TRAVEN *et al.* 2006); galactose dependent relief of Gal80p repression is mediated via direct interaction of Gal80p with the co-activator Gal3p (ZENKE *et al.* 1996). This paradigm of DNA-binding transcription factor and non-DNA-binding co-factor is considered intrinsic for the many classes of eukaryotic transcription factors. Fungi encode a range of transcription factors, including numerous Zn(II)2Cys6, C2H2 and GATA zinc coordinating proteins (TODD *et al.* 2014). C2H2 and GATA proteins are present in all eukaryotes, whereas the Zn(II)2Cys6 zinc binuclear cluster family, of which Gal4p is the type protein, is unique to fungi and is the predominant class of transcription factor (MACPHERSON *et al.* 2006; TODD *et al.* 2014).

Many Zn(II)2Cys6 transcription factors are pathway specific regulators (Table 4.1) including for carbon or nitrogen nutrient utilization (e.g. galactose, nitrate) as well as metabolite biosynthesis (e.g. leucine, aflatoxin) and development (BURGER *et al.* 1991a; YU *et al.* 1996; POLOTNIANKA *et al.* 2004; LEE *et al.* 2005; VIENKEN *et al.* 2005; VIENKEN AND FISCHER 2006; CHRISTENSEN *et al.* 2011). The six cysteines of the zinc binuclear cluster coordinate two Zn^{2+} ions, with the first and fourth cysteines acting as bridging ligands coordinating both ions (GARDNER *et al.* COLEMAN 1991; PAN AND COLEMAN 1991). Zn^{2+} binding is required for the correct secondary structure and for DNA binding (PAN AND COLEMAN 1989; PAN AND COLEMAN 1991) and mutation of single cysteine residues within the Zn(II)2Cys6 motif of *S. cerevisiae* Gal4p and Leu3p, *Neurospora crassa* Nit4, and *Aspergillus nidulans* FacB abolishes DNA binding (JOHNSTON AND DOVER 1987; BAI AND KOHLHAW 1991; YUAN *et al.* 1991; TODD *et al.*

1998). Differences in the Zn(II)2Cys6 DNA binding domain and the region carboxy-terminal of the sixth cysteine determine the specificity of Zn(II)2Cys6 transcription factors for sequence-specific DNA binding sites. DNA sequence binding specificity is achieved by recognition of distinct combinations of repeated, inverted or everted CCG trinucleotide repeats (TODD AND ANDRIANOPOULOS 1997; MACPHERSON *et al.* 2006).

In *A. nidulans* nitrogen utilization is regulated by the GATA transcription factor AreA (ARST AND COVE 1973; HYNES 1975). Full wild type expression of the AreA regulated acetamidase encoding *amdS* gene is dependent on the Zn(II)2Cys6 transcription factor TamA (DAVIS *et al.* 1996), which interacts with the C-terminus of AreA (SMALL *et al.* 1999; SMALL *et al.* 2001). *tamA* was first identified as a potential nitrogen utilization regulatory gene in genetic screens for mutants with simultaneous resistance to the toxic nitrogen analogs thiourea, aspartate hydroxamate and methylammonium (KINGHORN AND PATEMAN 1975a). These *tamA* mutants also had reduced activity of the core nitrogen assimilatory enzyme NADP-dependent glutamate dehydrogenase (NADP-GDH), which is encoded by *gdhA* (ARST AND MACDONALD 1973; KINGHORN AND PATEMAN 1973; KINGHORN AND PATEMAN 1975b). Interestingly, mutation of the fourth cysteine of the TamA Zn(II)2Cys6 motif (Cys-90), which is required for DNA binding and/or function in other Zn(II)2Cys6 transcription factors (JOHNSTON AND DOVER 1987; BAI AND KOHLHAW 1991; YUAN *et al.* 1991; TODD *et al.* 1998), did not prevent complementation of the methylammonium resistance phenotype of the *tamA24* loss-of-function mutant (DAVIS *et al.* 1996). Similarly, an in-frame deletion of *tamA* that lacks the DNA-binding motif fully complemented the *tamA*Δ phenotype (SMALL *et al.* 1999; SMALL *et al.* 2001). Therefore, DNA binding was considered dispensable for function. The related *S. cerevisiae* Dal81p protein also contains a dispensable Zn(II)2Cys6 motif (BRICMONT *et al.* 1991; CARDILLO *et al.* 2012). Therefore, despite containing a DNA-binding motif, TamA was considered to act solely as the AreA co-activator. However, *tamA*Δ had a greater effect on *gdhA* expression than *areA*Δ, indicating a role for TamA at *gdhA* in addition to action as a coactivator of AreA (POLOTNIANKA *et al.* 2004). Yeast two-hybrid screening identified a second TamA-interacting transcription factor LeuB. LeuB is required for leucine biosynthesis and *gdhA* expression (POLOTNIANKA *et al.* 2004; Chapter 3), however the effect of *tamA*Δ on *gdhA* expression is greater than *leuB*Δ (POLOTNIANKA *et al.* 2004). Because the effect of *tamA*Δ on *gdhA* expression was greater than the effect of combined *areA* and *leuB* mutants (POLOTNIANKA *et al.* 2004), TamA was expected

to play a greater role than these two proteins. Therefore as part of my undergraduate honours thesis I conducted assays of NADP-GDH activity in *tamA*Δ and *tamA*^{C90L} strains, which showed that the DNA-binding motif was not dispensable for wild type enzyme activity levels. However, the effect of *tamA*Δ was more severe than *tamA*^{C90L}, suggesting that TamA acted as both a DNA-binding activator and a non-DNA binding coactivator at the *gdhA* promoter. Using *gdhA-lacZ* translational fusions with different lengths of the *gdhA* promoter we mapped the TamA non-DNA-binding activity to between -1994 bp and -753 bp upstream of the *gdhA* start codon, and the DNA-binding dependent activity to between -753 bp and -307 bp. Based on sequence analysis of this region we predicted a putative TamA binding-site at -432 bp to -422 bp with conserved characteristic CCG everted repeats (now published as part of DOWNES *et al.* 2014b).

In this chapter we use promoter mutation analysis, electrophoretic mobility shift assays (EMSA) and chromatin immunoprecipitation (ChIP) to identify the TamA DNA-binding site in the *gdhA* promoter and demonstrate DNA binding both *in vitro* and *in vivo*. We also show that binding of TamA at the *gdhA* promoter is dependent on the presence of both AreA and LeuB. As TamA regulates some genes as a non-DNA-binding co-factor and other genes as a DNA-binding transcription factor it represents a rare class of dual-function transcription factors. We use RNA-seq and ChIP-seq to characterize the TamA dual-function regulatory network. Furthermore we use RNA-seq to show that the GATA DNA-binding transcription factor AreA is also a dual function transcription factor.

Table 4.1 Characterized *A. nidulans* Zn(II)2Cys6 transcription factors.

Factor	Function	Reference(s)
AcuK	Gluconeogenesis	HYNES *et al.* (2007)
AcuM	Gluconeogenesis	HYNES *et al.* (2007)
AflR	Aflatoxin biosynthesis	YU *et al.* (1996)
AfoA	Asperfuranone biosynthesis	CHIANG *et al.* (2009a)
ApdR	Aspyridone biosynthesis	BERGMANN *et al.* (2007)
AlcR	Alcohol metabolism	FELENBOK *et al.* (1988)
AmdR	Acetamide, beta-lactam, omega amino acid utilization	ANDRIANOPOULOS & HYNES (1990)
AmyR	Starch metabolism	TANI *et al.* (2001)
ArcA	Arginine catabolism	EMPEL *et al.* (2001)
ClrA	Cellulose degradation	CORADETTI *et al.* (2012)
ClrB	Cellulose degradation	CORADETTI *et al.* (2012)
DbaA	Benzaldehyde derivative biosynthesis	GERKE *et al.* (2012)
FacB	Acetate utilization	KATZ & HYNES (1989), TODD *et al.* (1997)
FarA	Fatty Acid utilization	HYNES *et al.* (2006)
FarB	Fatty acid utilization	HYNES *et al.* (2006)
GalX	Galactose utilization	CHRISTENSEN *et al.* (2011)
GalR	Galactose utilization	CHRISTENSEN *et al.* (2011)
LeuB	Leucine biosynthesis	POLOTNIANKA *et al.* (2004)
LeuR	Leucine biosynthesis?	This work, chapter 3.
NirA	Nitrate utilization	BURGER *et al.* (1991a,b)
NosA	Fruiting body formation	VIENKEN & FISCHER (2006)
MdpE	Monodictyphenone biosynthesis	BOK *et al.* (2009)
OefC	Development	LEE *et al.* (2005)
PbcR	Pimaradiene biosynthesis	BROMANN *et al.* (2012)
PrnA	Proline utilization	CAZELLE *et al.* (1998)
QutA	Quinate utilization	BERI *et al.* (1987)
RhaR	Rhamnose utilization	PARDO & OREJAS (2014)
RosA	Sexual development	VIENKEN *et al.* (2005)
ScfA	Short-chain fatty acid utilization	HYNES *et al.* (2006)
SilA	Light response regulator	DYER & O'GORMAN (2012)
SfgA	Asexual development	SEO *et al.* (2003)
SonC	DNA-damage response	LARSON *et al.* (2014)
TamA	Nitrogen utilization	DAVIS *et al.* (1996)
UaY	Purine degradation	SUAREZ *et al.* (1991)
XlnR	Xylan degradation	TAMAYO *et al.* (2008)

4.3 Materials & Method

4.3.1 RNA-sequencing analysis

4.3.1.i RNA isolation and cDNA library generation

For TamA RNA-seq mycelia of wild type (MH1), *tamA*Δ (MH8694) and *tamA*^{C90L} (MH11808) were grown in supplemented ANM with 10 mM ammonium, glutamine or alanine for 16 hours. For AreA RNA-seq mycelia of wild type (MH10244), *areA*Δ (MH5699) and *areA217* (MH11132) were grown in supplemented ANM with 10 mM ammonium for 16 hours, harvested and rinsed in fresh ANM and transferred to supplemented ANM with 10 mM alanine for a further 4 hours. Mycelia were rinsed with cold double distilled water and frozen in liquid nitrogen immediately. Samples were stored at -80ºC for less than one month before RNA extraction. RNA was isolated by grinding mycelia under liquid nitrogen and subsequent addition to RNA extraction buffer. Resuspended mycelia and RNA were separated by phenol-chloroform-isoamylalcohol (two) and chloroform purifications. RNA was first precipitated in 3M ammonium acetate and 50% isopropanol then resuspended in DEPC-H_2O and re-precipitated overnight in 4M lithium chloride at -20ºC (SAMBROOK AND RUSSELL 2001). RNA quality was determined by visualization of ribosomal RNA bands after electrophoretic separation in a 1.2% agarose gel containing 1.1% formaldehyde run in 1x MOPS buffer. RNA was quantified using a Nanodrop 1000 and stored at -80ºC for less than one month before library preparation. cDNA libraries were generated from 1 µg of total RNA using the TruSeq Stranded Total RNA Library Prep Kit (Illumina) following the manufacturer's instruction. Libraries were quantified using a Nanodrop 1000 and PicoGreen analysis and library quality determined in the Agilent 2100 Bioanalyzer by the Integrated Genomics Facility (Kansas State Univerity, Manhattan, Kansas). Libraries were diluted to 4 nM and pooled with nine samples per multiplex pool.

4.3.1.ii cDNA sequencing and **in silico** *analyses*

cDNA libraries were sequenced on the Illumina Hi-Seq 2500 Sequencing System platform in a 50-cycle single end run by the Genome Sequencing Facility (Kansas University Medical Center, Kansas City, Kansas). Analysis of RNA-seq was carried out on the Galaxy platform (galaxyproject.org; GIARDINE *et al.* 2005; BLANKENBERG *et al.* 2010b; GOECKS *et al.*

2010). FASTA files were converted to FASTQ format using FASTQ Groomer (BLANKENBERG *et al.* 2010a). Sequence quality was determined using FastQC and read trimming was not required (http://www.bioinformatics.babraham.ac.uk/projects/fastqc/). Nucleotides were aligned to the *A. nidulans* FGSC_A4 genome downloaded from AspGD December 11th 2014 (GALAGAN *et al.* 2005a; CERQUEIRA *et al.* 2014) using TopHat version 2.0.6 (KIM *et al.* 2013) with default settings with the following exceptions: minimum intron length = 10; maximum intron length = 4,000; indel search = NO; maximum alignment number = 40; minimum length of read = 20. Bam files generated from TopHat were downloaded from Galaxy and separated into strand specific Bam files using SAMtools version 1.1 (LI *et al.* 2009). SAMtools was downloaded on 8th December 2014 (www.sourcesforge.net/projects/samtools/files/samtools) with the latest update occurring 23rd September 2014. SAMtools was operated in Bash with the following commands:

> #!/bin/bash

> samtools view -b -F 0x10 INFILE.bam > OUTFILE_F.bam

(For forward reads)

> samtools view -b -f 0x10 INFILE.bam > OUTFILE_R.bam

(For reverse reads)

Separated Bam files were uploaded to Galaxy and Groomed with FASTQ Groomer (BLANKENBERG *et al.* 2010a). Transcripts were generated using the AspGD annotations (s10_m03_r15) as a template as guide for Cufflinks Version 2.1.1.7 (ARNAUD *et al.* 2012; TRAPNELL *et al.* 2013). Cufflinks was run with default settings with the exception of: max intron length = 4,000; bias correction = yes; multi read correction = yes. Transcripts from all conditions and strains were merged in Cuffmerge with the reference annotation as a guide. Differential expression was determined using CuffDiff with default settings and maintaining separation of BAM alignments for biological replicates to allow for statistical testing (TRAPNELL *et al.* 2013), and analysis carried out in cummeRbund (Version 2.8.2) in R Version 3.1.2 downloaded from http://www.r-project.org/ (The R Core Team; 2012), with the cummeRbund recommended and required plugins (GOFF *et al.* 2013). Differential expression is based on Cuffdiff analysis of significantly different expression with $p \leq 0.05$ and $q \leq 0.05$ with no minimum fold change.

4.3.1.iii GO enrichment and GO network analyses

GO enrichment analysis was carried out on the FetGOat server (NITSCHE *et al.* 2011) for overrepresented terms from the biological processes and biological functions with a minimum of two terms and Benjamani and Hochberg correction with q-value ≤ 0.05 (http://www.broadinstitute.org/fetgoat/). Chirag Parsania (University of Macau, Macau SAR, China) generated GO enriched networks from identified differentially expressed genes using CytoScape (YEUNG *et al.* 2008).

4.3.2 ChIP-sequencing analysis

Mycelia of *tamA*^{FLAG} (RT322), *tamA*^{FLAG} *areA*Δ (RT323), *tamA*^{FLAG} *leuB*Δ (RT324) and *tamA*^{FLAG} *areA*Δ *leuB*Δ (RT325) for ChIP-seq were grown in supplemented ANM with 10 mM ammonium or 10 mM glutamine for 16 hours and fixed in 1% formaldehyde for 20 m then quenched with 0.6 M glycine for one minute (SUZUKI *et al.* 2012). Mycelia were rinsed with cold double distilled water and immediately frozen in liquid nitrogen. Two biological replicates were generated for each condition. Samples were stored at -80ºC for less than one month and shipped on dry ice by overnight courier to Boston for further analysis. K. H Wong (Harvard Medical School, Boston, Massachusetts) carried out immunopreciptation, quantitative real-time PCR, and ChIP-seq using 2 µg of either anti-FLAG (M2, Sigma). Zhengqiang Miao (University of Macau, Macau SAR, China) identified peak location and fold enrichment using Model-based analysis for ChIP-seq (MACS; ZHANG *et al.* 2008), with a minimum 4-fold enrichment and a p-value of $1x10^{-7}$. For peaks between convergent and divergent genes, both genes are reported. For peaks upstream of one gene and downstream of a second gene only the gene with upstream promoter binding is reported. Sequences for SCOPE analysis were downloaded from AspGD and submitted to the SCOPE Web interface available at http://genie.dartmouth.edu/scope/ with the *A. nidulans* 1,000 bp fixed upstream region used for comparison (CARLSON *et al.* 2007; CHAKRAVARTY *et al.* 2007a,b).

4.3.3 Primers for qRT-PCR

Primers used for real-time reverse transcriptase PCR (qRT-PCR) are listed in Table 4.2. Primer design and qRT-PCR is described in Chapter 2.6.2.

Table 4.2 Real-time reverse-transcriptase PCR primers.

Primer	Sequence (5' → 3')	Target region	Efficiency (55.9ºC)
benA_RT_F	CCTCGCTCCGCTATCTTCC	*benA*: +1,354 to +1,486 bp	100.7 %
benA_RT_R	GACTGGTTCTTGCTGTGGAT		
gltA_RT_F	GGAGTCCATCAAGCAGTT	*gltA*: +542 to +636 bp	109.5 %
gltA_RT_R	GACCGAGAATGGTTGAATC		

4.4 Results

4.4.1 TamA is a dual function transcription factor

NOTE: This is a partial summary of research conducted as part of this dissertation that was published as Downes D.J., M.A. Davis, K.H. Wong, S.D Kreutzberger, M.J. Hynes, & R.B. Todd (2014b) Dual DNA-binding and coactivator functions of *Aspergillus nidulans* TamA, a Zn(II)2Cys6 transcription factor. *Molecular Microbiology* **92(6):** 1198-1211. *The full article and supplementary data has been included as Appendix B.*

As part of my undergraduate honours thesis I determined that TamA regulated *gdhA* in a DNA-binding motif dependent manner between -753 bp and -307 bp. Based on sequence analysis of this region I identified a putative TamA binding-site at -432 bp to -422 bp with conserved characteristic CCG everted repeats. For this work I confirmed that TamA regulates the native *gdhA* in a DNA-binding-dependent manner by real-time RT-PCR. I constructed and gene-targeted a *gdhA-lacZ* reporter lacking base pairs -431 to -422, and showed that this site was required for TamA activation of *gdhA* expression. We FLAG epitope tagged both wild type TamA and the Zn(II)2Cys6 DNA binding motif C90L mutant TamA and using chromatin immunoprecipitation (ChIP) we were able to detect binding of $TamA^{FLAG}$ but not $TamA^{C90L.FLAG}$ at the *gdhA* promoter during growth on various nitrogen nutrients. Therefore TamA is a *bona fide* DNA-binding transcription factor. Interestingly the strength of TamA binding, measured as fold enrichment, differed for different nitrogen sources and correlated with the level of *gdhA-lacZ* expression. Using immunoprecipitated $TamA^{FLAG}$ and $TamA^{C90L.FLAG}$ for EMSA we showed *in vitro* binding to a *gdhA* promoter DNA probe by wild type but not the mutant protein. Finally, as TamA interacts with AreA, we determined the effects this interaction played on DNA binding at the *gdhA* promoter *in vivo*. We found using ChIP that levels of $TamA^{FLAG}$ binding were reduced in an *areA*Δ mutant, and $AreA^{HA}$ binding levels were reduced in a *tamA*Δ mutant. Furthermore, regulation of the *gdhA-lacZ* reporter gene by AreA was dependent on the presence of the TamA binding site. Therefore AreA and TamA act cooperatively to bind to and regulate the *gdhA* promoter.

4.4.2 TamA binding is LeuB dependent.

In addition to interaction with AreA, TamA also interacts with the Zn(II)2Cys6 transcription factor LeuB (POLOTNIANKA *et al.* 2004). We have shown that LeuB regulates *gdhA* expression through the TamA DNA-binding site (DOWNES *et al.* 2013), although it is unclear whether this regulation is direct or indirect. To determine if LeuB was required for TamA DNA binding at this site, we performed ChIP of TamA^{FLAG} in a *leuB*Δ mutant and observed reduced binding compared to the wild type strain (Figure 4.1). Therefore, both LeuB and AreA are required for efficient TamA binding at the *gdhA* promoter.

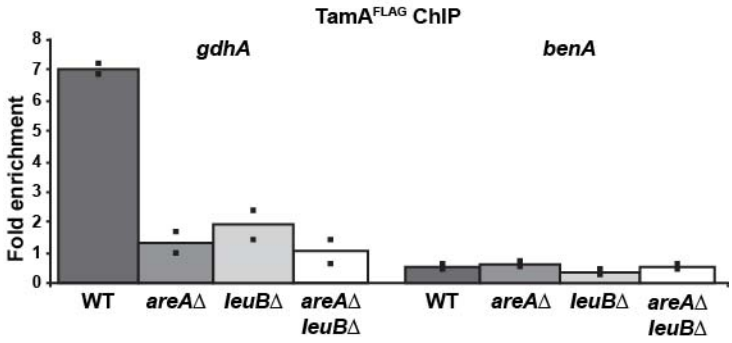

Figure 4.1 LeuB is required for TamA DNA-binding at *gdhA*.

ChIP of TamA^{FLAG} was performed on wild type (RT322), *areA*Δ (RT323), *leuB*Δ (RT324) and *areA*Δ *leuB*Δ (RT325) after 16 hours growth on ammonium. Fold enrichment of *gdhA* (-531 to -382 bp) and the *β*-tubulin encoding *benA* (-224 bp to -125 bp) is over the *gdhA* coding region (+310 to +407 bp). The mean fold enrichment (bars) of two independent biological replicates (squares) is shown. Results for wild type and *areA*Δ were published in Downes (2014).

4.4.3 TamA may interact with additional proteins.

To ensure that TamA^{FLAG} and TamA$^{C90L\text{-}FLAG}$ were expressed as stable proteins we performed column immuno-purification followed by Western blot (Appendix B). Coomassie Brilliant Blue staining of eluates showed a large number of bands co-purified with both tagged TamA proteins (Figure 4.2). Several of these co-purified protein bands were consistently observed across multiple purifications and from purification of both wild type and mutant TamA. The presence of additional proteins in TamA purifications may indicate additional proteins with which TamA interacts.

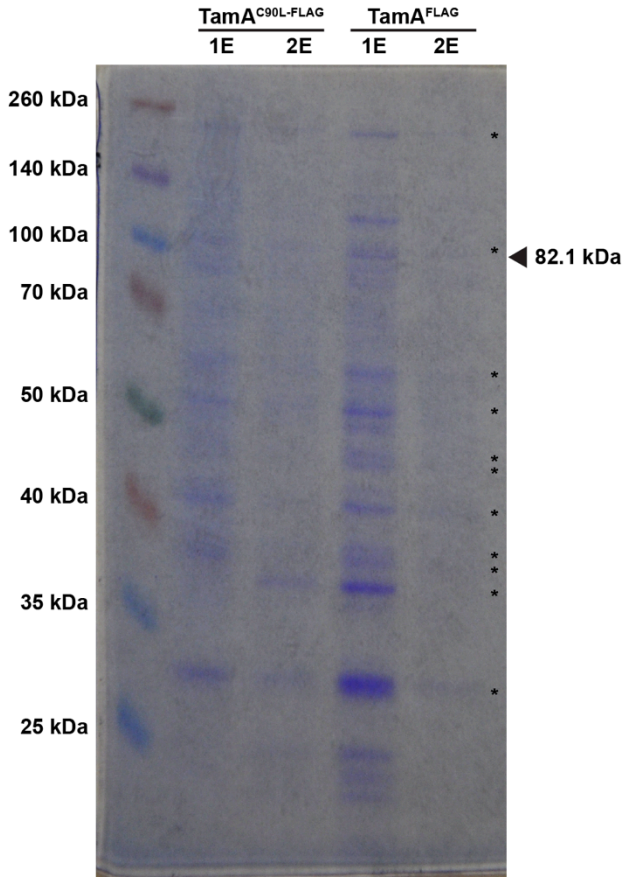

Figure 4.2 Immuno-precipitated TamA. *tamA*^{FLAG} (RT322) and *tamA*$^{C90L.FLAG}$ (RT376) were grown for 16 hours in supplemented liquid ANM with 10 mM ammonium. Proteins were purified and immuno-precipitated in an anti-FLAG column with two elutions (1E and 2E). Proteins were separated on a 6% polyacrylamide gel by electrophoresis and stained with Coomassie Brilliant Blue. TamA^{FLAG} and TamA$^{C90L.FLAG}$ are predicted to be approximately 82.1 kDa in size. Bands common between each pulldown are marked with stars.

4.4.4 Characterization of the TamA regulatory network

Our analysis of TamA function at *gdhA, fmdS,* and *amdS* revealed promoter context-specific DNA binding or non-DNA binding coactivator mechanisms of action for TamA (DOWNES *et al.* 2014b). To determine the extent of TamA regulation via both the co-activator and DNA-binding modes of action across the genome, and to identify novel regulatory target genes we performed RNA-seq. To distinguish each mode of action we sequenced cDNA libraries from wild type, *tamA*Δ, and the *tamA*^{C90L} DNA binding motif mutant strains grown with glucose as the carbon source on ammonium, glutamine or alanine. Stranded cDNA libraries from three independent biological replicates were barcoded and pooled for multiplex sequencing with nine samples per lane. Multiplexed libraries were sequenced on the Illumina Hi-Seq 2500 platform and generated an average of 22.7 million reads per library with a minimum of 14.1 million reads and a maximum of 37.7 million reads (Figure 4.3A). Reads were mapped to the *A. nidulans* FGSC_A4 genome (Version S10) using TopHat (TRAPNELL *et al.* 2013) with an average of 91.90% of reads mapping to the genome. Bam files containing mapped forward or reverse reads were separated using SAMtools (Li 2009) and transcripts were generated using the AspGD annotations (s10_m03_r15) as a template for Cufflinks (TRAPNELL *et al.* 2013). Transcripts from all conditions and strains were merged in Cuffmerge to provide a basis for differential gene expression using CuffDiff (TRAPNELL *et al.* 2013). For all three conditions reads mapped equally across the genome in each of the strains (Figure 4.3B-D). Expression of the housekeeping genes *actA* (ɣ-actin; FIDEL *et al.* 1988), *benA* (*β*-tubulin; MAY *et al.* 1987) and AN2316 a putative cytochrome-c oxidase was consistent in wild type, *tamA*Δ, and *tamA*^{C90L} in all three growth conditions (Figure 4.3E). Therefore the libraries were of sufficient quality for differential gene expression analysis.

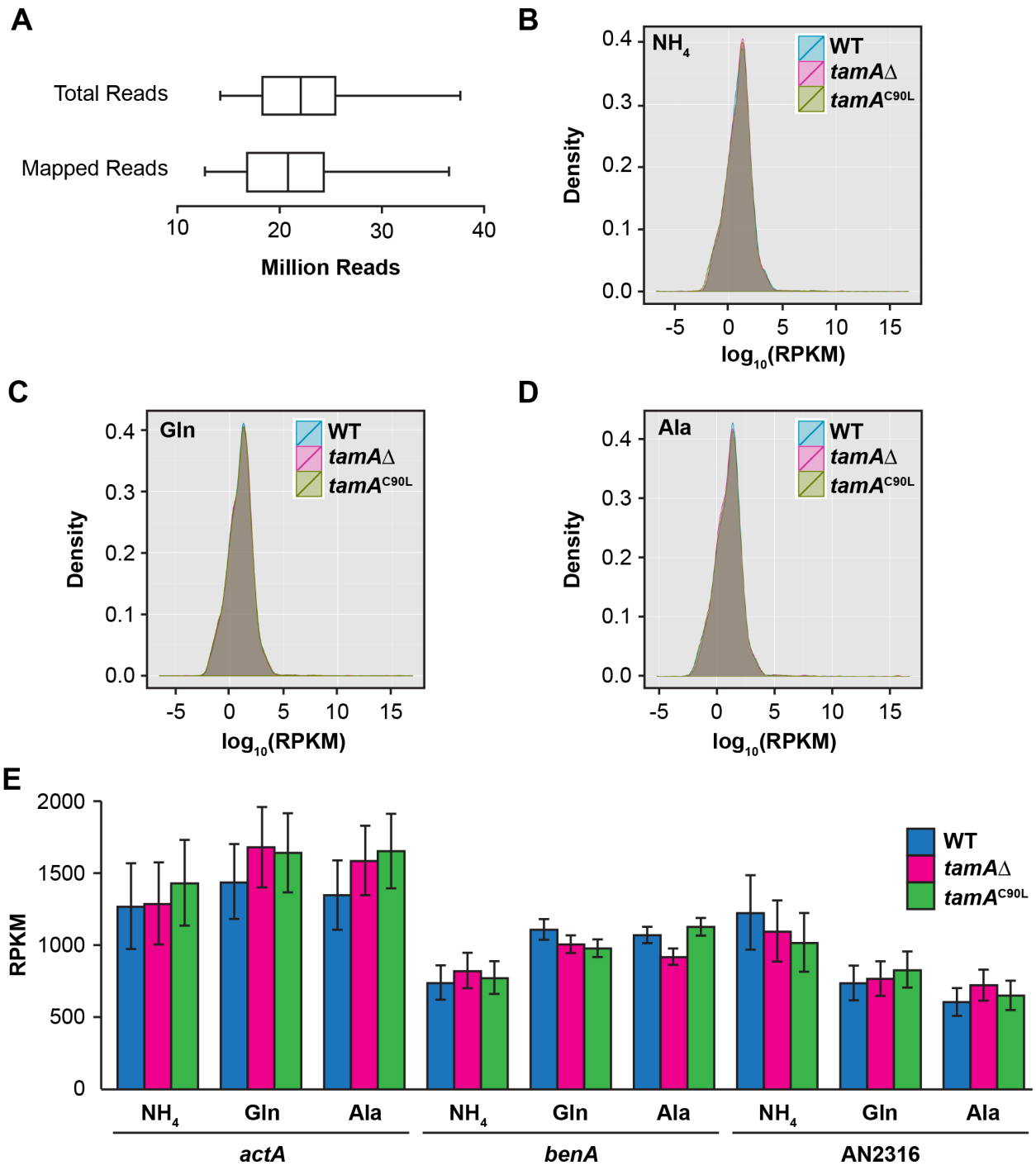

Figure 4.3 RNA-seq read mapping and quality control.

A) RNA-seq reads from wild type (MH1), *tamA*Δ (MH8694) and *tamA*^{C90L} (MH11808) after 16 hours growth in supplemented ANM with 10 mM ammonium (NH_4), glutamine (Gln) or alanine (Ala) were mapped using Bowtie. **B-D.** Density of mapped reads shows proportion of loci with a given number of reads per kilobase per million mapped reads (RPKM) **E.** Expression of house keeping genes was determined with cummeRbund. Errror bars depict SEM (N= 3).

4.4.4.i TamA regulates distinct sets of genes dependent on growth condition.

Cuffdiff analysis for each of the three growth conditions identified a total of 2,132 genes with differential expression in *tamA*Δ compared to wild type. Differential expression of 7.5% of these genes (161) was observed in all three conditions, 25.4% (541) on two conditions, while the majority of genes, 67.1% (1,430), were only differentially expressed on one condition (Figure 4.4A). TamA is known to act as a transcription activator as *tamA*Δ causes decreased expression of genes where it is thought to or known to act directly at the promoter (DAVIS *et al.* 1996; SMALL *et al.* 1999; SMALL *et al.* 2001; POLOTNIANKA *et al.* 2004; DOWNES *et al.* 2014b). Interestingly the number of genes with increased expression in *tamA*Δ (1,233 genes) was greater than those with decreased expression (1,073 genes) suggesting that TamA may have both positive and negative roles in regulating gene expression (Figure 4.4B). For 174 genes, expression increased on one nitrogen source and decreased on another nitrogen condition (Figure 4.4C). We compared genes with increased expression in *tamA*Δ with those with decreased expression for each condition. In each pairwise comparison between ammonium, glutamine and alanine genes that were regulated positively under one condition and negatively on another were observed, indicating that TamA can regulate the same gene as an activator or a repressor, and that TamA can act as an activator or repressor under all three conditions (Figure 4.4D)

Figure 4.4 Differentially expressed genes in *tamA*Δ compared with wild type.

Genes with differential expression in *tamA*Δ (MH8694) versus wild type (MH1) after 16 hours growth in supplemented ANM with 10 mM ammonium (NH_4; green), glutamine (Gln) or alanine (Ala; red) were identified using CuffDiff. **A)** Differentially expressed genes from growth on glutamine (blue), ammonium (green) or alanine (red) were compared for regulation on multiple conditions. **B)** Genes were separated into increased or decreased expression to compare genes with the same direction of expression change on each nitrogen condition. **C)** Genes showing increased or decreased expression on any nitrogen source were compared to identify genes that are activated and repressed by TamA. **D)** Comparison of genes with increased expression versus genes with decreased expression on each nitrogen nutrient. Gene sets with increased expression (↑) and decreased expression (↓) in *tamA*Δ compared to wild type are marked.

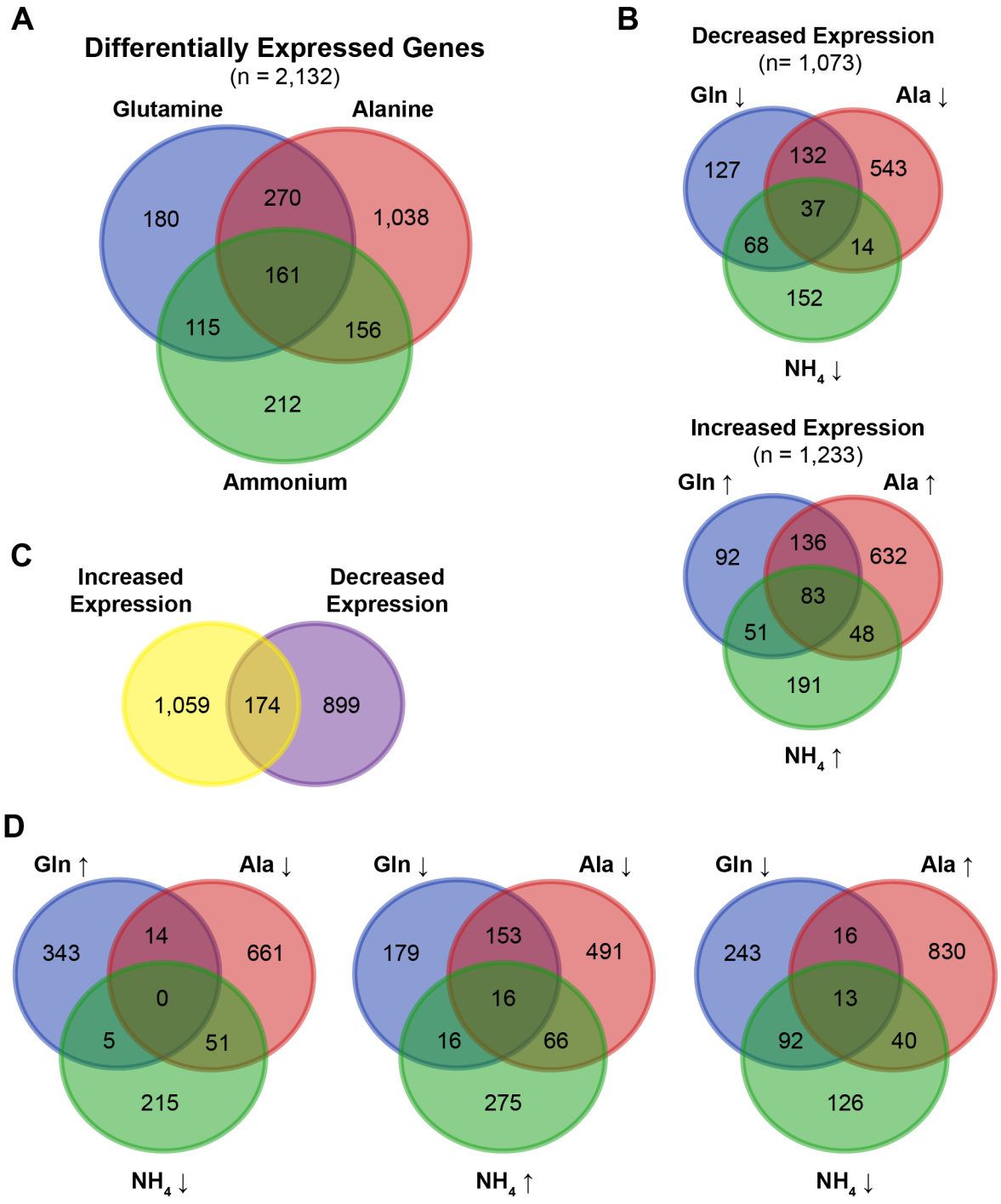

Figure 4.4 Differentially expressed genes in *tamA*Δ compared with wild type.

4.4.4.ii TamA acts across the genome by non-DNA-binding and DNA-binding.

As TamA functions as both a DNA-binding transcription factor and a non-DNA-binding co-factor we wanted to determine the extent of each specific mode of action amongst the differentially expressed genes. Therefore we compared expression of genes in wild type versus *tamA*^{C90L} and *tamA*Δ versus *tamA*^{C90L}. Genes that are regulated (directly as primary targets or indirectly as secondary targets) by DNA-binding will show significantly different expression in wildtype versus *tamA*^{C90L} but not in *tamA*Δ versus *tamA*^{C90L} (Figure 4.5A). Genes that are directly or indirectly regulated by the non-DNA-binding mechanism will significantly differ in expression in *tamA*Δ versus *tamA*^{C90L} but not wild type versus *tamA*^{C90L}. Finally, some genes, including *gdhA*, are regulated by both mechanisms under the same growth condition and are dual mode of action targets. These genes will have differential expression in both comparisons (Figure 4.5A). Most dual function targets will show the same direction of expression change in both *tamA*Δ and *tamA*^{C90L}, and can be considered unidirectional dual mode of action targets where TamA acts as an activator and coactivator, or as a repressor and corepressor. However, dual mode of action targets may also show a decrease in expression in *tamA*Δ but an increase in expression in *tamA*^{C90L} or *vice versa*, and are bidirectional targets (Figure 4.5A). This can be explained by either of two mechanisms. The first is via direct regulation of the target gene promoter where TamA may function as a co-activator of a strong activating complex, and as a DNA-binding repressor in a weak repressor manner (Figure 4.5B). In *tamA*Δ both the strong activator effect and the weak repressor effect are lost resulting in a net decrease in activation. In *tamA*^{C90L} only the weak repressor is lost resulting in a net increase in activation. This same phenomenon can also be achieved at secondary targets by co-activator regulation of a positively acting transcription factor and DNA-binding dependent activation of a weak repressor (Figure 4.5C). Combinations of direct and indirect modes of action are possible at some genes.

By analysis of the changes of expression in *tamA*Δ and *tamA*^{C90L} we were able to determine the TamA mode of activity for ~70% of differentially expressed genes, where the relationship between wild type, *tamA*Δ and *tamA*^{C90L} was clearly delineated. For the remaining ~30% of differentially expressed genes in the *tamA*Δ mutant compared with wild type, expression in the *tamA*^{C90L} mutant was intermediate between but not significantly different from wild type or *tamA*Δ, and therefore the mode of positive or negative action could not be distinguished. In all three conditions the proportion of DNA-binding targets was approximately

equivalent to the proportion of non-DNA binding targets, though there were a greater percentage of DNA-binding targets on ammonium and fewer on alanine (Figure 4.6A) suggesting nitrogen source may influence TamA mode of action. On each condition dual mode of action targets represented 8-15% of differentially expressed genes with roughly equivalent numbers of unidirectional and bidirectional targets. To determine if genes are regulated specifically by one mode of action under all conditions or by different modes depending on the nitrogen nutrient source we performed Venn analysis (Figure 4.6B). We found 45% of genes (965/2,132) were regulated by a single mode of action, either the DNA-binding or non-DNA-binding mechanism, in all three growth conditions. Additionally, 78 genes (3.6%) were regulated by both DNA-binding and non-DNA binding modes of action on different nitrogen nutrients but were not dual mode of action targets on the same condition. Almost half of the dual mode of action targets (165/335) showed regulation by specific DNA-binding or non-DNA-binding mechanisms on different conditions. When genes were separated by direction of the expression change caused by *tamA*Δ, the relative number of DNA-binding targets to co-activator targets was greater for genes with decreased expression than for the relative number of DNA-binding targets to corepressor targets for genes with increased expression (compare Figure 4.6C and 4.6D). This is consistent with TamA DNA-binding regulation being more frequently associated with direct targets and TamA being an activator at most direct target genes, but affecting indirect target genes in either a positive or negative manner, rather than TamA acting directly as a repressor/corepressor.

Figure 4.5 Expected modes of TamA regulation.

A) Theoretical expression patterns of different classes of regulatory target of TamA activation. Letters (a,b,c) indicate significantly different expression levels. Dual mode of action is simultaneous action by both DNA-binding dependent and DNA-binding independent regulatory mechanisms. Undetermined activator (positive regulation) and undetermined repressor (negative regulation) results when expression levels in $tamA^{C90L}$ are not significantly different from either wild type or *tamA*Δ (a,b). **B-C)** Bidirectional positive or negative dual mode of action action may occur via direct regulation of a single promoter **(B)** or multiple promoters **(C)**. Numbers indicate strength of activation (+) or repression (–) of transcription.

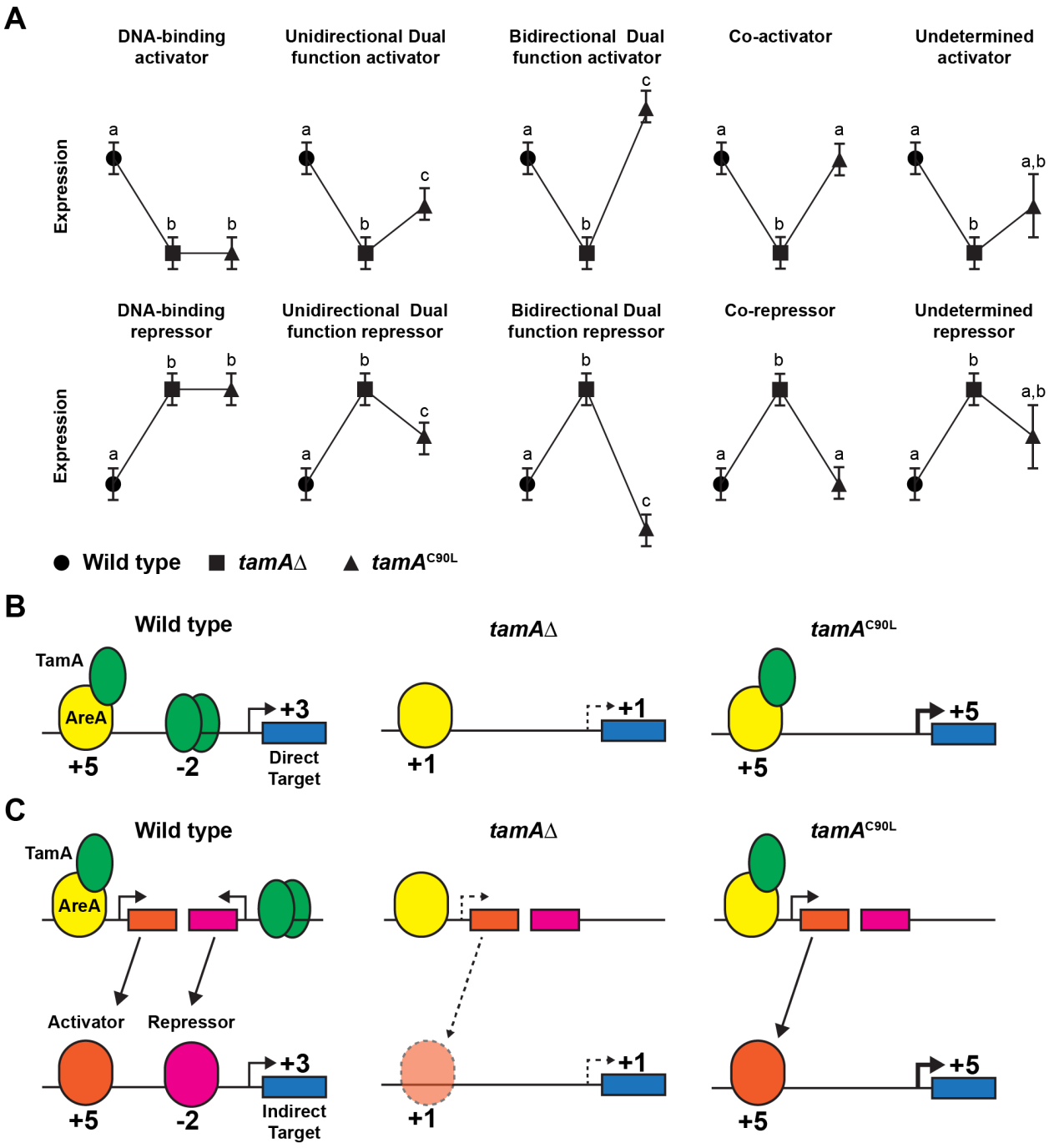

Figure 4.5 Expected modes of TamA regulation.

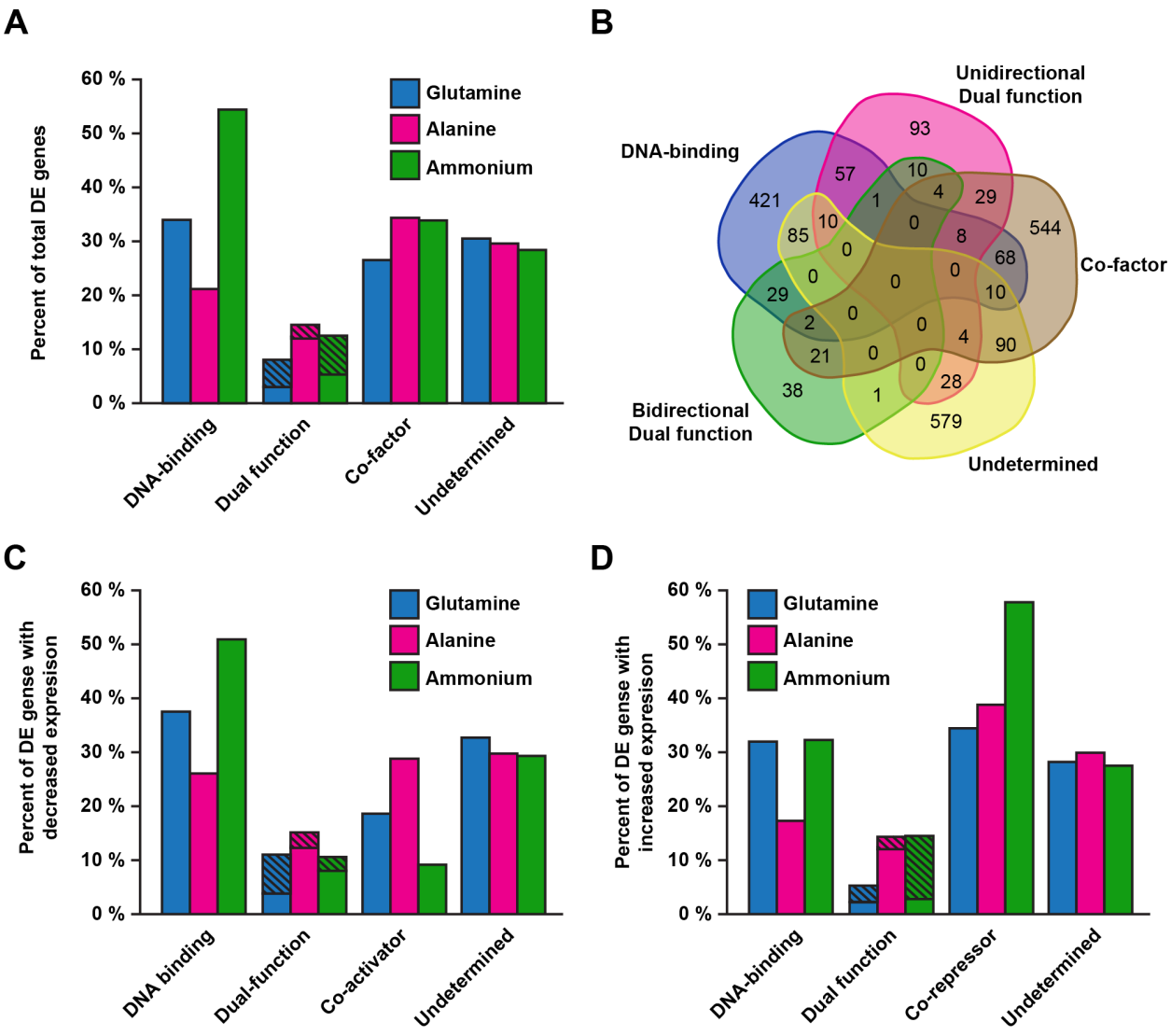

Figure 4.6 Mode of action of TamA in regulating differentially expressed genes.

A) Genes that are regulated by different TamA mechanisms of action after growth for 16 h in supplemented ANM with 10 mM ammonium, glutamine, and alanine were compared by percent of differentially expressed (DE) genes. Percent of dual mode of action regulated genes that show opposite effects of *tamA*Δ and *tamA*^{C90L} (bidirectional dual mode of action targets) are marked with diagonal lines. **(B)** Venn diagram analyses. **C-D)** TamA modes of action were compared amongst genes with decreased **(C)** and increased **(D)** expression in *tamA*Δ by percent of differentially expressed genes within each subgroup.

4.4.4.iii Gene Ontology Enrichment analysis of tamA∆ differentially expressed genes.

To determine whether TamA regulates specific sets of genes, we performed Gene Ontology (GO) enrichment analysis using the Fisher's exact test GO analysis tool, FetGOat (NITSCHE *et al.* 2011). Analysis for biological process and molecular function was carried out for each condition on total differentially expressed genes as well as separately for genes with increased or decreased expression in *tamA*∆ compared with wild type (Table 4.3 and Table 4.4). Differentially expressed genes on all three nitrogen nutrients showed GO enrichment for acetate metabolism, carboxylic acid metabolism, cellular ketone metabolism, organic acid metabolism, oxoacid metabolism, primary alcohol metabolism and small molecule metabolism from the biological processes GO terms (Table 4.3). Therefore TamA regulates genes in pathways other than nitrogen metabolism. The only enriched molecular function in all three conditions was oxidoreductase activity (Table 4.4). While the differentially expressed genes on ammonium and glutamine with increased expression in the *tamA*∆ mutant compared with wild type were enriched for numerous GO terms, only one term (ammonium transport) was enriched in the genes with decreased expression. Therefore on the preferred nitrogen sources TamA activates transcription of ammonium transporters and a diverse set of genes that do not fall into specific GO clusters. On the alternative nitrogen source alanine, an array of GO terms were enriched both in genes with increased expression and genes with decreased expression, including cellular nitrogen compound biosynthesis, nitrogen utilization, nitrogen compound transport, and regulation of nitrogen utilization consistent with the known functions of TamA and its interaction with the global nitrogen regulator, AreA.

Table 4.3 Biological process GO enrichment analysis.

Process	NH_4 All	NH_4 Up/Down[a]	Gln All	Gln Up/Down[a]	Ala All	Ala Up/Down[a]
acetaldehyde catabolic process	3	3	3	3		
acetaldehyde metabolic process	3	3	3	3		
acetate catabolic process	4	4				
acetate metabolic process	7	7	6	5	8	8
alcohol catabolic process	8	7				11
alcohol metabolic process						26
aldehyde catabolic process		3				
amide biosynthetic process					11	6
amide biosynthetic process						5
amine metabolic process					63	37
amine transport						10
amino acid transport		7				
ammonium transport			3	3		
antibiotic biosynthetic process					8	5
antibiotic metabolic process					10	6
aspartate family amino acid biosynthetic process			5			
aspartate family amino acid catabolic process		3	4	4		
aspartate family amino acid metabolic process		6	12	9	13	
beta-lactam antibiotic biosynthetic process					8	5
beta-lactam antibiotic metabolic process					10	6
biotin biosynthetic process						3
biotin metabolic process						3
branched chain family amino acid metabolic process					9	6
carbohydrate catabolic process						20
carbohydrate metabolic process						38
carboxylic acid biosynthetic process			21		38	19
carboxylic acid catabolic process	11	10	13	11	18	
carboxylic acid metabolic process	44	33	48	27	86	41
carboxylic acid transport	12	9				
cellular aldehyde metabolic process	6	6				
cellular amide metabolic process					17	9
cellular amine metabolic process			28		58	36
cellular amino acid metabolic process			27		51	31
cellular iron ion homeostasis		5				
cellular ketone metabolic process	44	33	48	27	86	41
cellular lactam biosynthetic process					8	5
cellular lactam biosynthetic process					10	6
cellular lipid catabolic process		5				
cellular nitrogen compound biosynthetic process			24		50	26
dicarboxylic acid metabolic process	9	8				
drug metabolic process					10	6
ethanol catabolic process	5	4	5	4		
ethanol metabolic process	6	5	6	5	6	6
fatty acid metabolic process		8				
galactonate metabolic process	4	3				
generation of precursor metabolites and energy						20

[a] Number of genes with significantly enriched GO terms, Fisher's exact test $p \leq 0.05$; false discovery rate $q \leq 0.05$

[b] Enrichment of genes with increased (yellow) or decreased (blue) expression in *tamA*Δ.

Table 4.3 Biological process GO enrichment analysis (continued).

Function	NH_4[a] All	NH_4[a] Up/Down[b]	Gln[a] All	Gln[a] Function	Ala[a] All	Ala[a] Up/Down[b]
glutamine family amino acid biosynthetic process						4
glycine metabolic process					4	4
glycolysis						15
heterocycle biosynthetic process					28	
ion transport					23	
iron assimilation	3	3				
iron assimilation by chelation and transport	3	3				
iron chelate transport	3	3				
iron ion homeostasis		5				
iron ion transport	5	4			7	
lipid catabolic process		5				23
monocarboxylic acid catabolic process		6				3
monocarboxylic acid metabolic process	20	18	20			14
negative regulation of transport					4	5
nitrogen compound transport		9				4
nitrogen utilization			6		6	19
nucleobase transport					4	
organic acid biosynthetic process			21		38	46
organic acid catabolic process	11	10	13	11	18	42
organic acid metabolic process	45	33	49	27	88	
organic acid metabolic process						
organic acid transport	12	9				
organic anion transport	4					
organic cation transport			4			41
organic substance transport	15	11				5
oxoacid metabolic process	44	33	48	27	86	6
penicillin biosynthetic process					8	4
penicillin metabolic process					10	8
positive regulation of conidium formation						5
positive regulation of developmental process					10	7
positive regulation of reproductive process						
positive regulation of sporulation					9	6
primary alcohol catabolic process	5	4	5	4		11
primary alcohol metabolic process	6	5	6	5	6	5
protein folding						3
protein refolding						9
pyrimidine base transport					3	9
pyruvate metabolic process						8
regulation of anatomical structure morphogenesis						4
regulation of asexual sporulation						8
regulation of cellular amine metabolic process					5	10
regulation of conidium formation						3
regulation of developmental process						6
regulation of nitrogen utilization					4	9
regulation of reproductive process						12
regulation of sporulation						12

[a] Number of genes with significantly enriched GO terms, Fisher's exact test $p \leq 0.05$; false discovery rate $q \leq 0.05$

[b] Enrichment of genes with increased (yellow) or decreased (blue) expression in *tamA*Δ.

Table 4.3 Biological process GO enrichment analysis (continued).

Function	All	NH_4[a] Up/Down[b]	All	Gln[a] Function	All	Ala[a] Up/Down[b]
response to external stimulus						12
response to extracellular stimulus						17
response to nutrient levels						11
response to oxidative stress						
response to starvation						
secondary metabolic process		9			20	
serine family amino acid metabolic process			7			28
siderophore transport	3	3				24
small molecule biosynthetic process			29		61	58
small molecule catabolic process	19	16	22	15	33	
small molecule metabolic process	57	40	65	39	126	
sulfur compound biosynthetic process					13	
threonine catabolic process		3	4	4		
threonine metabolic process	4	3	5	4		
transition metal ion transport	6				11	

[a] Number of genes with significantly enriched GO terms, Fisher's exact test $p \leq 0.05$; false discovery rate $q \leq 0.05$
[b] Enrichment of genes with increased (yellow) or decreased (blue) expression in *tamA*Δ.

Table 4.4 Biological function GO enrichment analysis.

Function	All	NH_4[a] Up/Down[b]	All	Gln[a] Up/Down[b]	All	Ala[a] Up/Down[b]
amino acid transmembrane transporter activity	9	7				
ammonium transmembrane transporter activity			3	3		
antioxidant activity			6			
carboxylic acid transmembrane transporter activity	12	9				
glycine dehydrogenase (decarboxylating) activity						3
lyase activity			15			
nucleic acid binding transcription factor activity						12
nucleobase transmembrane transporter activity						4
organic acid transmembrane transporter activity	12	9				
oxidoreductase activity	37	25	52	27	84	49
oxidoreductase activity				25		35
- acting on CH-OH group of donors	16	13	16			
- acting on peroxide as acceptor			6			
- acting on the CH-NH2 group of donors			5	4	7	5
- acting on the CH-NH2 group of donors, disulfide as acceptor						3
- acting on the CH-NH2 group of donors, NAD or NADP as acceptor			3			
- acting on the CH-OH group of donors, NAD or NADP as acceptor	13	10				
peroxidase activity			6			
sequence-specific DNA binding transcription factor activity						12
substrate-specific transmembrane transporter activity		16				26
substrate-specific transporter activity						26
transmembrane transporter activity						26
transporter activity						28

[a] Number of genes with significantly enriched GO terms, Fisher's exact test $p \leq 0.05$; false discovery rate $q \leq 0.05$
[b] Enrichment of genes with increased (yellow) or decreased (blue) expression in *tamA*Δ.

4.4.4.iv Network analysis of TamA regulated genes.

To better understand the relationships between genes in each of the different GO enriched terms we generated networks of the differentially expressed genes using CytoScape (YEUNG *et al.* 2008). CytoScape identifies enriched GO terms that form a network of overlapping terms. For example enrichment of genes with both of the GO associated terms "glutamate metabolism" and "amine metabolism" would lead to a node for each term and a line connecting the nodes, indicating the genes are shared between the two terms. The larger a node the more genes that have that term, and the more shared terms between two nodes the thicker the connecting line. We generated a network of total differentially expressed genes in *tamA*Δ compared with wild type during growth on ammonium, glutamine and alanine. The network had four clusters of GO enriched terms (Figure 4.7A). The largest cluster contained six terms involved in general cellular metabolism (i.e. cellular amine metabolism, carboxylic acid metabolism, cellular ketone metabolism, monocarboxylic acid metabolism, organic acid metabolism, and oxoacid metabolism), and each node was connected to the other five nodes. The other three clusters all consisted of a single node and represented oxidation-reduction, transmembrane transport, and secondary metabolism. We also wanted to determine if the DNA-binding targets and cofactor targets shared similar or distinct networks. Therefore we generated four networks:

1. DNA-binding targets that had decreased expression in *tamA*Δ (Figure 4.7B)
2. DNA-binding targets that had increased expression in *tamA*Δ (Figure 4.7C)
3. Co-activator targets (Figure 4.7D)
4. Co-repressor targets (Figure 4.7E).

For both DNA binding and DNA binding-independent modes of action there was a unique node in genes with increased expression representing oxidation-reduction, otherwise all other clusters were distinct to the specific network (Figure 4.7C,E). DNA-binding activator targets included a five-node cluster associated with siderophore biosynthesis and iron homeostasis (e.g. ferricrocin biosynthesis, nonribosomal peptide synthesis) and a two-node cluster for syncytium formation (Figure 4.7B). TamA co-activator targets had GO terms associated primarily with nitrogen metabolism (e.g. glutamate metabolism, nucleobase metabolism) and transport (e.g. ion transport, nitrate transport, amino acid transport) (Figure 4.7C). Therefore TamA activates and represses distinct networks of genes by different regulatory modes of action.

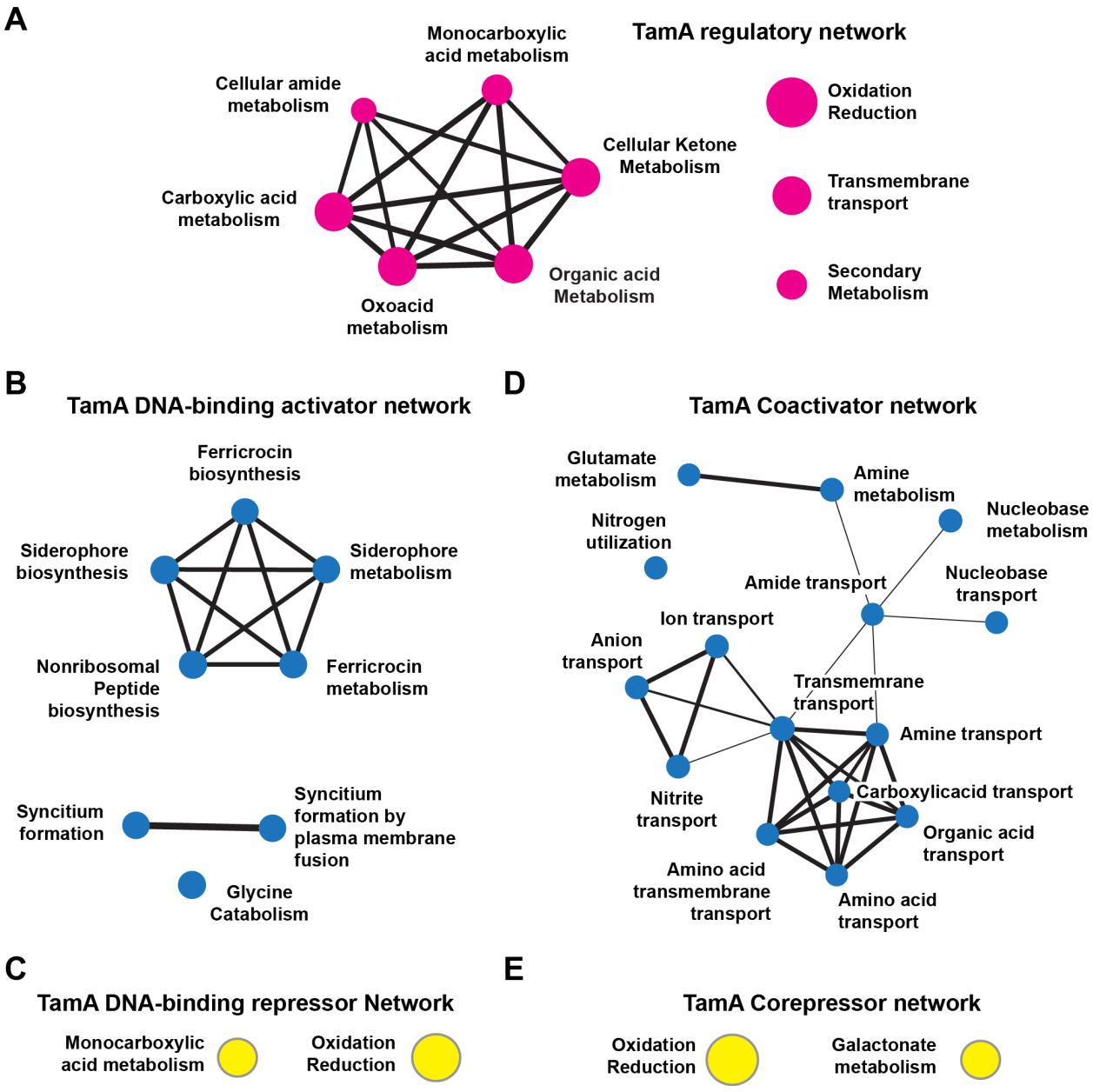

Figure 4.7 GO Network analysis of TamA regulated genes.

GO enriched networks were generated from total differentially expressed genes **(A),** from genes that are regulated by TamA DNA-binding dependent activation **(B)** or repression **(C)**, and from genes that are regulated by TamA as a non-DNA-binding co-activator **(D)** or co-repressor **(E)** Node size indicates relative number of terms, and lines between nodes indicate number of shared members between nodes.

4.4.5 Pathway and cluster analysis of differentially expressed genes.

While GO enrichment and network analysis give a general overall picture of TamA regulation, we were interested to see the specific effects of TamA at a gene and pathway level. Therefore we examined genes which may be responsible for toxic nitrogen analog resistance, the GOGAT cycle genes, nitrogen regulation transcription factors, carbon metabolism, acetate and alcohol metabolism, proline utilization, siderophore biosynthesis and iron regulation, regulation of secondary metabolism, and specific secondary metabolism clusters including the clusters encoding penicillin and terriquinone. Our analysis, outlined below, shows condition specific and mode of action specific regulation by TamA at a diverse set of genes.

4.4.5.i Toxic nitrogen analog resistance

TamA was initially identified as a nitrogen regulatory protein encoding gene in a genetic screen selecting for simultaneous resistance to the toxic nitrogen analogs thiourea (TU), aspartate hydroxamate (AH) and methylammonium chloride (MACl) during growth on alternative nitrogen nutrients such as alanine; the first letters of each compound giving rise to the name *tamA* (KINGHORN AND PATEMAN 1975a). The *tamA* mutants isolated were resistant to each compound and to chlorate (ClO_3). Resistance to these toxic nitrogen analogs is seen in the *tamA*Δ mutant but is TamA DNA-binding motif independent (Figure 4.8A) (DAVIS *et al.* 1996), however with the exception of MACl (MONAHAN *et al.* 2006), the exact genes responsible for resistance of *tamA* mutants to toxic analogs have not previously been identified. Therefore we examined possible genes responsible for these resistance phenotypes by examining differential expression in *tamA*Δ compared to wild type during growth on alanine as the nitrogen source.

Resistance to Thiourea

Thiourea is an analog of urea; urea is imported into cells by the high-affinity urea/H^+ symporter, encoded by *ureA* (ABREU *et al.* 2010), and then broken down by a urease, encoded by *ureB* (MACKAY AND PATEMAN 1982). Characterization of *ureA* shows that *ureA*Δ and *ureA* loss-of-function mutations confer resistance to TU (SANGUINETTI *et al.* 2014). Expression of both *ureA* and *ureB* was decreased in the *tamA*Δ mutant but not in *tamA*^{C90L} during growth on alanine (Figure 4.8B,C). *ureD,* which is involved in urea utilization (MACKAY AND PATEMAN 1982), and AN2598, the predicted homolog of the DUR3 urea transporter from *S. cerevisiae* (ELBERRY *et al.* 1993), did not show altered expression in either *tam*AΔ or *tamA*^{C90L} (data not shown).

Therefore thiourea resistance in the *tamA*Δ mutant may arise from the combined effects of decreased expression of *ureA* and *ureB*.

Resistance to Aspartate hydroxamate

Aspartate hydroxamate is an analog of asparagine and reduced asparaginase activity is associated with AH resistance (DRAINAS AND PATEMAN 1977). Amongst the differentially expressed genes in *tamA*Δ were two genes predicted to encode enzymes with asparaginase activity, *ahtA* (AN0300) and *apnA* (ARST AND BAILEY 1980), and a predicted asparagine transporter (AN3888). Expression of *ahtA* and AN3888 was reduced in *tamA*Δ, whereas *apnA* had increased expression (Figure 4.8D-F). Two other aspargine transporters, AN1766 and AN5198, and the serine racemase AN2525, the predicted homolog of *S. cerevisiae* SRY1 and a putative AH target (WADA *et al.* 2003), had no change of expression in *tamA*Δ (data not shown). Therefore the combined effect of reduced AH uptake via AN3888 and reduced *ahtA* expression is likely to be the source of resistance.

Resistance to Methylammonium

Methylammonium is an analog of ammonium, which is taken up by the ammonium transporters encoded by *meaA*, *mepA*, *mepB* and *mepC* (MONAHAN *et al.* 2002a,b; MONAHAN *et al.* 2006). During growth on alanine the most highly expressed of these genes are *meaA* and *mepA* and the *tamA*Δ mutant has reduced expression of both genes, which results in reduced MACl uptake (MONAHAN *et al.* 2006). Our data for *tamA*Δ were consistent with previous findings, however we also saw a decrease in *mepB* expression (Figure 4.8G-I). We also identified an antisense transcript for *mepB* (Figure 4.9A). The anti-sense transcript begins at +1581 bp, within the fifth exon, and extends to -682 bp relative to the *mepB* ATG. This novel transcript showed low levels of expression without significant difference between conditions or in the mutants (Figure 4.9B).

Resistance to Chlorate

Chlorate is a toxic analog of nitrate (COVE 1976). Nitrate transporters, encoded by *crnA/nrtA*, *crnB/nrtB* and *nitA* (BROWNLEE AND ARST 1983; UNKLES *et al.* 2001; WANG *et al.* 2008), take up nitrate and it is subsequently broken down by the *niaD* encoded nitrate reductase, and the *niiA* encoded nitrite reductase (JOHNSTONE *et al.* 1990). Five genes, *cnxABC, cnxE, cnxF,*

cnxG, and, *cnxH*, which encode enzymes for the production of the nitrate reductase molybdopterin cofactor, are also required for nitrate utilization (PATEMAN *et al.* 1976; UNKLES *et al.* 1997; APPLEYARD *et al.* 1998; HECK *et al.* 2002). It has been suggested that chlorate toxicity may occur through both nitrate reductase and the nitrate pathway-specific transcription factor NirA (COVE 1976). Expression of *nrtB*, *nitA,* and *niaD* was reduced in *tamA*Δ (Figure 4.8J-L), but none of the other genes, including *nirA*, showed altered expression (data not shown). Therefore resistance to ClO_3 in the *tamA*Δ mutant could be conferred by reduced uptake, reduced breakdown or a combination of both.

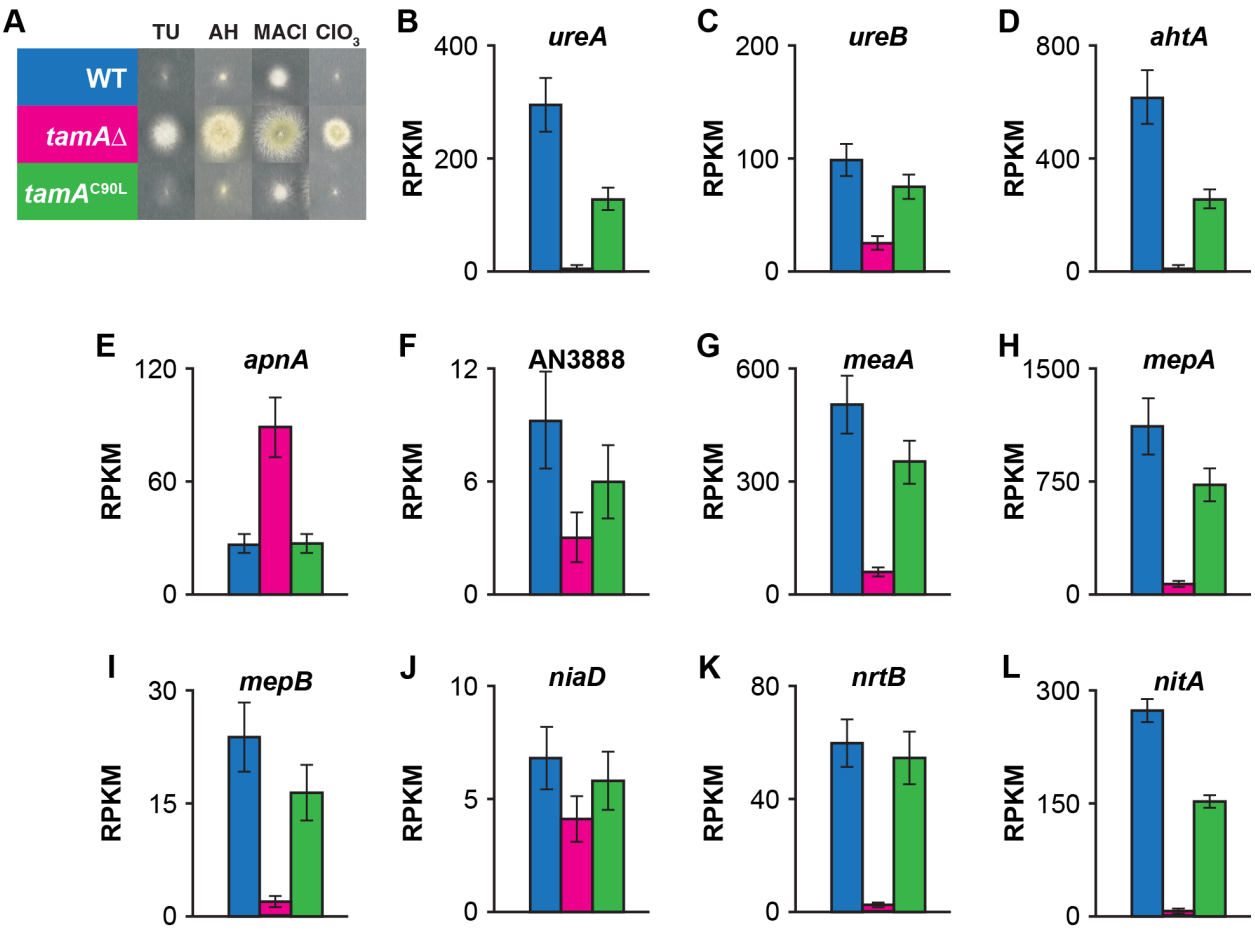

Figure 4.8 Regulation of genes responsible for toxic nitrogen analog resistance.

A) Growth of wild type (MH1), *tamA*Δ (MH8694), and *tamA*^{C90L} (MH11808) on supplemented ANM with 10 mM alanine and the toxic nitrogen analogs 10 mM thio urea (TU), 0.3 mM aspartate hydroxamate (AH), 200 mM methylamonium chloride (MACl), and 5 mM chlorate (ClO_3). **B-L)** Expression of genes with predicted roles involved in the *tamA*Δ resistance to toxic nitrogen analogs expressed as reads per kilobase per million mapped reads (RPKM) after 16 h growth in supplemented ANM with 10 mM alanine as the nitrogen source. Error bars depict SEM (N=3). Wild type (blue), *tam*Δ (pink) and *tamA*^{C90L} (green) are indicated in panel A.

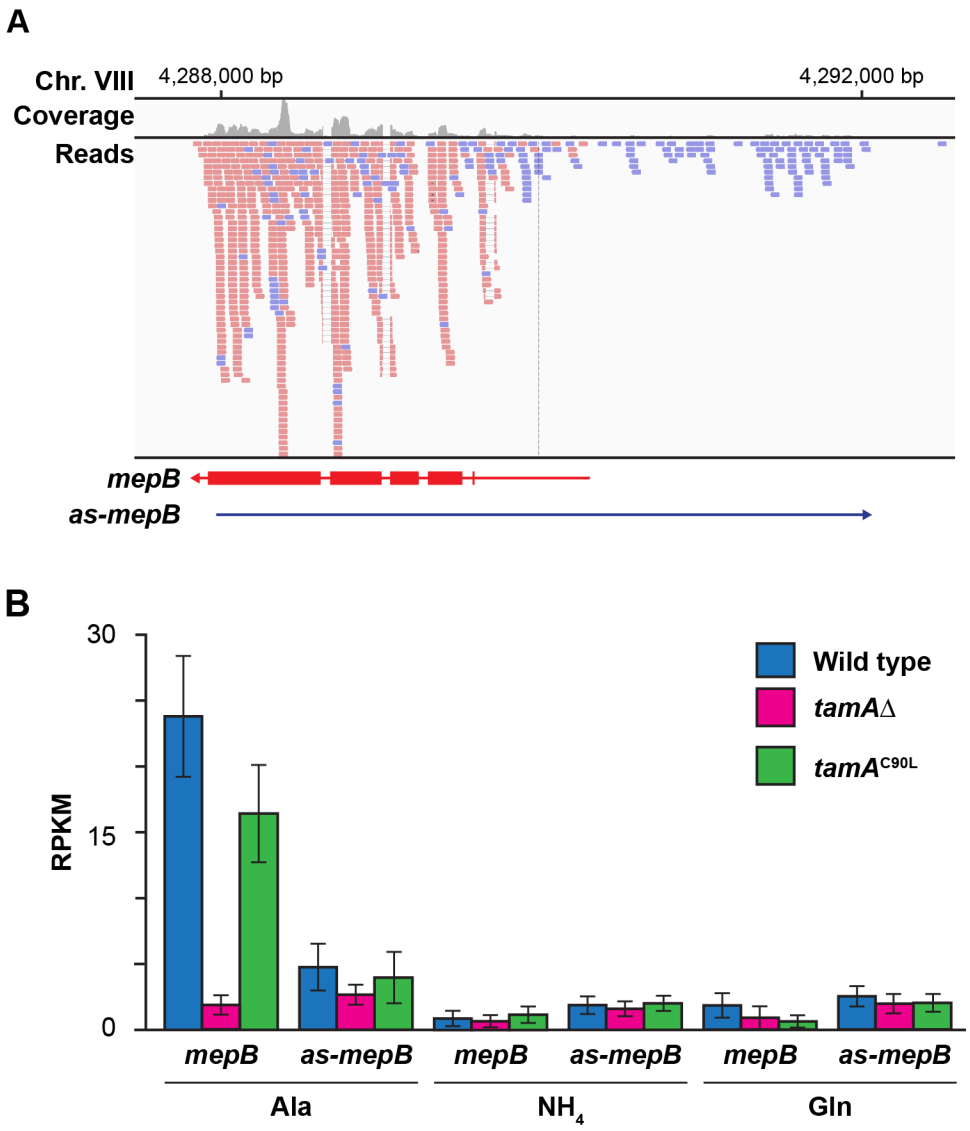

Figure 4.9 Identification of an anti-sense *mepB* transcript.

A) TopHat mapped reads of forward (blue) and reverse (red) transcripts from the *mepB* locus on chromosome VIII (Chr. VIII) from wild type (MH1) grown on 10 mM alanine. **B)** Expression of *mepB* and *as-mepB* in wild type (blue), *tam*Δ (MH8694; pink) and $tamA^{C90L}$ (MH11808; green) after 16 h growth on supplemented ANM with 10 mM alanine (Ala), ammonium (NH_4), and glutamine (Gln) expressed as reads per kilobase per million mapped reads (RPKM). Error bars depict SEM (N=3).

4.4.5.ii GOGAT Pathway

TamA regulates the core nitrogen assimilation gene *gdhA* (POLOTNIANKA *et al.* 2004) and we have shown that this is by both co-activator and direct TamA DNA-binding mechanisms (This work; DOWNES *et al.* 2014b). *gdhA* is one of four enzymes that form the GOGAT cycle which interconverts 2-oxoglutarate, glutamate and glutamine (KINGHORN AND PATEMAN 1973). The *gdhA* encoded NADP-dependent glutamate dehydrogenase (NADP-GDH) converts 2-oxoglutarate from the TCA cycle to glutamate (Figure 4.10A), which is converted to glutamine by a glutamine synthetase (GS), encoded by *glnA* (MARGELIS *et al.* 2001). The pathway can operate in the reverse direction whereby NAD-dependent glutamate synthase (GOGAT), encoded by *gltA* (MACHEDA *et al.* 1999), converts glutamine to glutamate, which is converted to 2-oxoglutarate by NAD-glutamate dehydrogenase (NAD-GDH) encoded by *gdhB* (KINGHORN AND PATEMAN 1973). Expression of *gdhA* in the RNA-seq data was consistent with our previous findings of reduced expression in *tamA* mutants, with *tamA*Δ having a greater effect than $tamA^{C90L}$, consistent with TamA having DNA-binding and coactivator roles at *gdhA* (Figure 4.10A). We had previously performed real-time RT-PCR on *gltA* during growth on glutamine and identified an effect of *tamA*Δ (Figure 4.10B). We were therefore interested to know whether TamA regulates the other three GOGAT cycle genes. We found *glnA* showed reduced expression in *tamA*Δ but not in the $tamA^{C90L}$ mutant under all three nitrogen conditions, indicating regulation by the co-activator mode of action (Figure 4.10A). Interestingly *gltA* showed reduced expression in *tamA*Δ during growth on glutamine and increased expression only in *tamA*Δ during growth on alanine but no effect of $tamA^{C90L}$ suggesting nitrogen nutrient dependent regulation via both TamA co-activation and co-repression. Finally *gdhB* showed increased expression under all three conditions, consistent with the abundance of nitrogen nutrients repressing the production of 2-oxoglutarate for the TCA cycle. During growth on glutamine TamA promotes production of NADP-GDH, GS and GOGAT and represses NAD-GDH suggesting that TamA promotes conversion of nitrogen compounds towards the production of glutamate (Figure 4.10C). During growth on ammonium and alanine TamA activates NADP-GDH and GS expression and represses or is inactive in regulating GOGAT and NAD-GDH production, suggesting TamA promotes the production of both glutamine and glutamate (Figure 4.10D). The different effects of TamA on these genes on the different nitrogen nutrients suggest that TamA is required for regulating via transcriptional control the flux of nutrients through the GOGAT cycle.

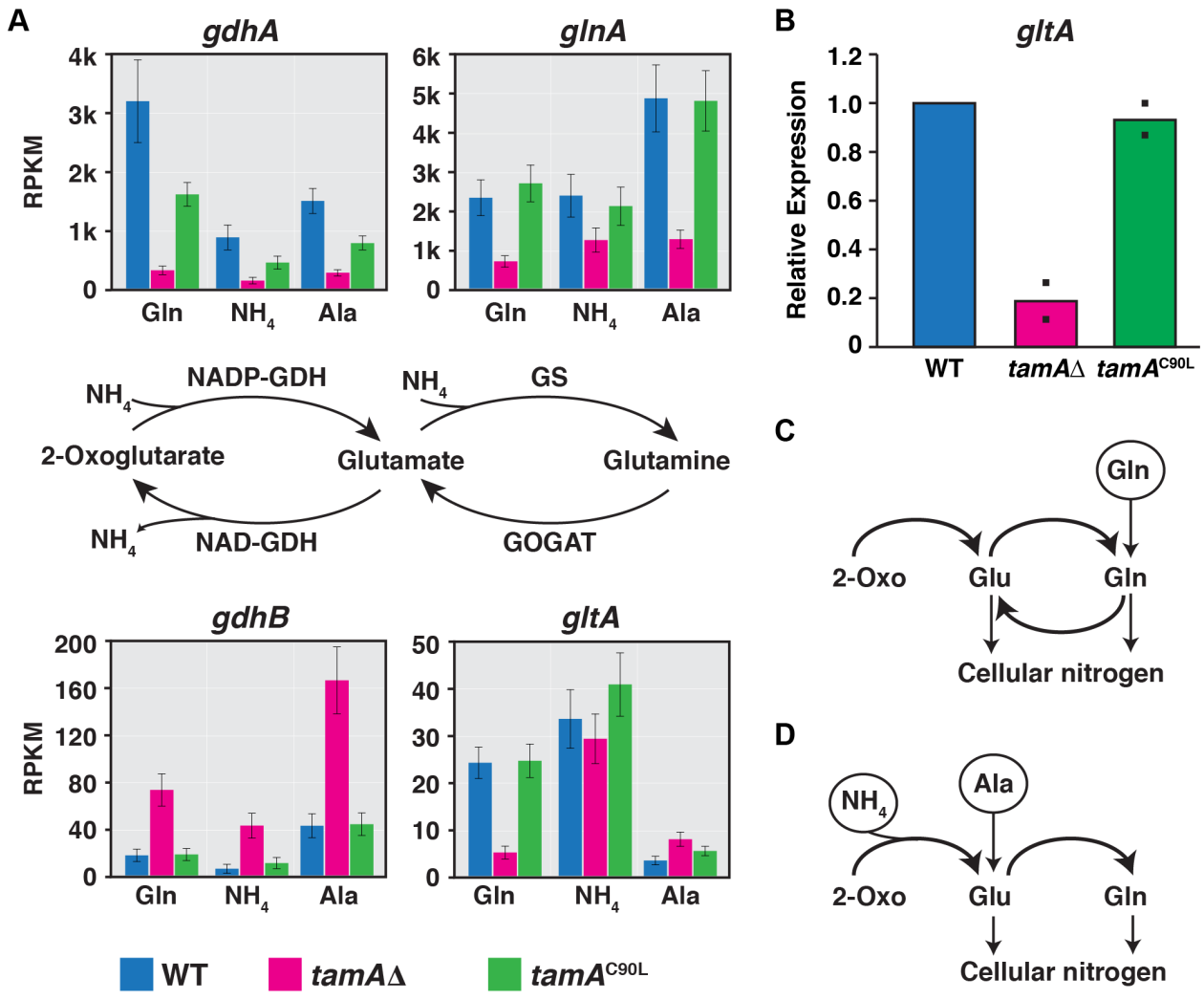

Figure 4.10 TamA regulation of the GOGAT pathway

A) Expression of genes that are involved in nitrogen assimilation via the GOGAT pathway expressed as reads per kilobase per million mapped reads (RPKM). Expression data was generated from RNA-seq of wild type (WT; MH1), *tamA*Δ (MH8694), and *tamA*^{C90L} (MH11808) strains grown in supplemented ANM with 10 mM glutamine (Gln), ammonium (NH_4) or alanine (Ala). Error bars depict SEM (N=3). **B)** qRT-PCR of *gltA* (+542 bp to +636 bp) from wild type (WT; MH12101), *tamA*Δ (MH12174) and *tamA*^{C90L} (MH12597) strains grown in supplemented ANM with 10 mM glutamine (Gln) for 16 h. Bars show the mean relative expression to wild type from two biological replicates (squares). **C-D)** Regulation of flux through the GOGAT cycle by TamA when glutamine **(C)** and ammonium or alanine **(D)** are provided as exogenous nitrogen nutrients (circles).

4.4.5.iii Nitrogen regulatory genes

Nitrogen metabolite repression is regulated by the combined action of the positive factors AreA, TamA and MeaB, and the repressive factors AreB, and NmrA, (reviewed in Chapter 1.4). Expression of *areA*, *nmrA,* and *areB* (Figure 4.11A), but not *meaB* (data not shown), was altered in the *tamA* mutants though each gene showed its own regulation pattern. *nmrA* expression was increased on all three conditions in *tamA*Δ but not *tamA*^{C90L} (Figure 4.11A) indicating TamA negatively regulates *nmrA* in a co-factor mode. *areB* showed decreased expression only on the alternative nitrogen source alanine and only in the *tamA*Δ (Figure 4.11B). Therefore, TamA regulates *areB* as coactivator only on alanine. Finally, *areA* showed decreased expression in both *tamA*Δ and *tamA*^{C90L} during growth on alanine and glutamine, however expression was unchanged on ammonium (Figure 4.11C). Therefore TamA acts via DNA binding to regulate *areA* expression on glutamine and alanine but not ammonium.

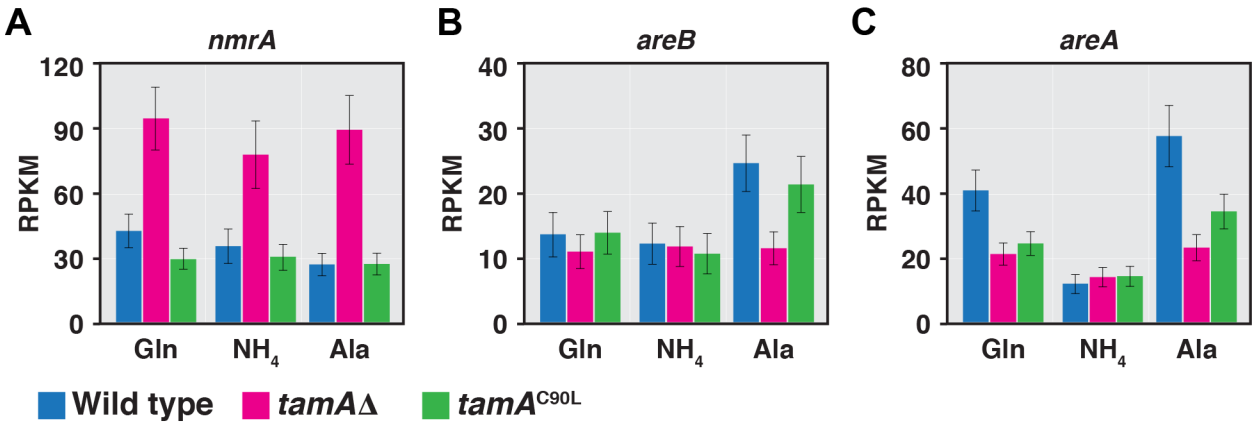

Figure 4.11 Regulation of nitrogen utilization transcription factors.

Expression of the nitrogen regulatory genes *nmrA* **(A)**, *areB* **(B)**, and *areA* **(C)** expressed as reads per kilobase per million mapped reads (RPKM). Expression data was generated from RNA-seq of wild type (MH1), *tamA*Δ (MH8694) and *tamA*^{C90L} (MH11808) strains grown in supplemented ANM with 10 mM glutamine (Gln), ammonium (NH_4) or alanine (Ala). Error bars depict SEM (N=3).

4.4.5.iv Proline utilization gene cluster

A. nidulans can utilize proline as either a carbon or a nitrogen nutrient (CUBERO *et al.* 2000). The genes required for proline utilization are encoded in a gene cluster (JONES *et al.* 1981; HULL *et al.* 1989) which contains genes for the regulatory Zn(II)2Cys6 transcription factor, *prnA* (CAZELLE *et al.* 1998), a proline transporter, *prnB* (SOPHIANOPOULOU AND SCAZZOCCHIO 1989), a proline dehydrogenase, *prnD* (GARCIA *et al.* 2004), a delta-1-pyrroline-5-carboxylate dehydrogenase (JONES *et al.* 1981) and a proline inducible gene of unknown function *prnX* (GOMEZ *et al.* 2003) (Figure 4.12A). The bi-directional promoter between *prnB* and *prnD* is repressed by the presence of glucose, via a C2H2 transcription repressor CreA, and by the presence of preferred nitrogen sources, which is relieved via AreA (SOPHIANOPOULOU AND SCAZZOCCHIO 1989; GOMEZ *et al.* 2003; GARCIA *et al.* 2004). The *prn* cluster expression is induced by proline via PrnA (CAZELLE *et al.* 1998). We examined the expression of these five genes in our glucose-repressing and nitrogen-repressing or nitrogen-derepressing RNA-seq growth conditions. We found that *prnD, prnB,* and *prnC* were expressed in wild type at low levels on glutamine or ammonium and elevated under nitrogen derepressing (alanine) conditions, consistent with previous work (CUBERO *et al.* 2000). There was no effect of the *tamA* mutants on *prnD, prnB,* or *prnC* expression on glutamine or ammonium, but the derepressed levels of expression on alanine were reduced in *tamA*Δ and $tamA^{C90L}$. Therefore TamA activated all three genes in a DNA-binding motif-dependent manner during growth on alanine (Figure 4.12B). *prnX* was expressed on glutamine, ammonium and alanine. TamA regulated *prnX* positively on alanine but in a DNA-binding independent manner. TamA did not regulate expression of the transcription factor *prnA* under any of our tested conditions. Furthermore, none of the genes in the *prn* cluster showed differential expression in the *tamA* mutants on glucose-ammonium or glucose-glutamine suggesting that TamA is not involved in glucose repression of these genes.

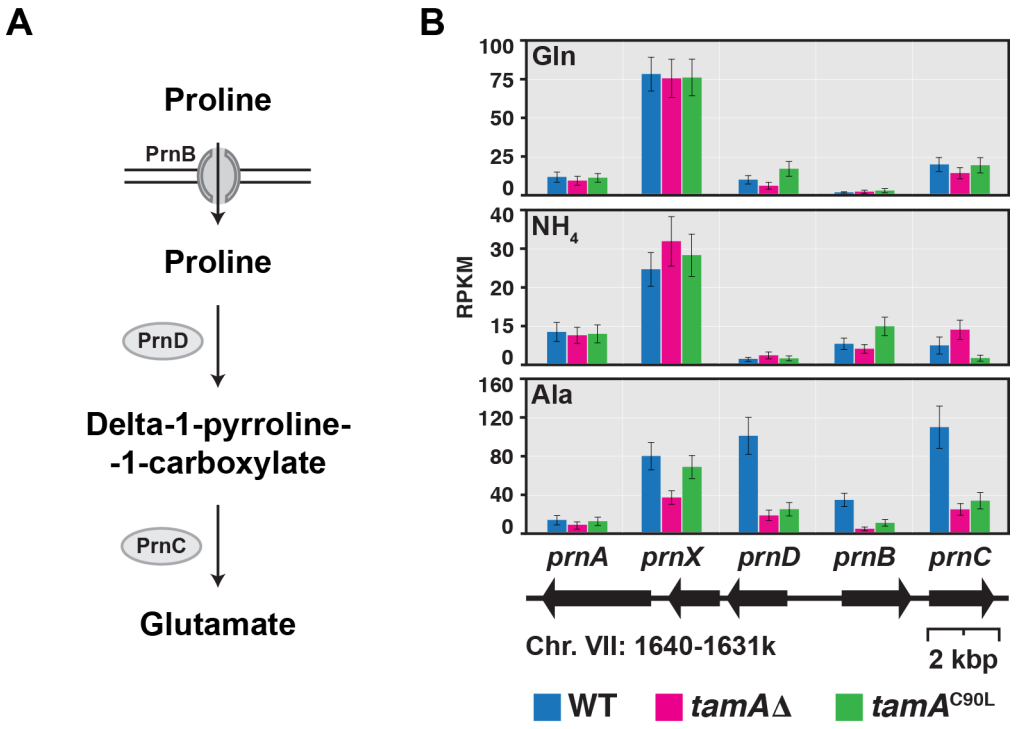

Figure 4.12 DNA-binding dependent regulation of proline utilization.

A) Extracellular proline is taken into the cell by the transporter PrnB and then broken down by the subsequent actions of PrnD and PrnC. **B)** Expression of the genes within the *prn* cluster expressed as reads per kilobase per million mapped reads (RPKM). Expression data was generated from RNA-seq of wild type (MH1), *tamA*Δ (MH8694) and $tamA^{C90L}$ (MH11808) strains grown in supplemented ANM with 10 mM glutamine (Gln), ammonium (NH_4) or alanine (Ala). Error bars depict SEM (N=3).

4.4.5.v Global carbon metabolism network

CreA regulates the expression of genes required for carbon metabolism (HYNES AND KELLY 1977; DOWZER AND KELLY 1991). CreA represses expression of genes required for the utilization of alternative carbon nutrients such as acetamide and alcohol when glucose is present. Glucose was used as the carbon source in our RNA-seq experiments and we would expect carbon metabolism genes to be under carbon catabolite repression. Our analysis of RNA-seq data highlighted several genes involved in core carbon metabolism that were differentially expressed in the *tamA* mutants. These genes included several glycolysis/gluconeogenesis genes (e.g *acuD, acuE, acuF, acuG, acuK, acuL, acuN*, *ipdA*, *facA*, *pfkA, pgkA*), and starch utilization genes (*glaB*, *amy*G). The majority of these genes showed differential expression on alanine and some were differentially expressed on ammonium or glutamine. Due to the widespread effects of *tamA* on carbon metabolism we mapped differentially expressed genes to a metabolism network (Figures 4.13). The majority of genes we examined showed increased expression in *tamA*Δ, including genes in the glycolysis (e.g. *pfkA, pgkA*) and gluconeogenesis (e.g *acuD, acuF*) pathways. Genes in pathways that feed into glycolysis and gluconeogenesis (e.g. *alcA*, *alcC, ladB,* and *adgB*) also showed increased expression in *tamA*Δ and *tamA*^{C90L} compared to wild type. Therefore in wild type mycelia TamA appears to repress glycolytic and gluconeogenic genes by a DNA-binding dependent mode of action.

Figure 4.13 Regulation of carbon metabolism on alanine.

Pathway analysis of differentially expressed genes in core and peripheral carbon metabolism pathways after growth on supplemented ANM (1% glucose) with 10 mM alanine. Genes with increased expression (green arrows) or decreased expression (blue arrows) in the *tamA*Δ mutant compared with wild type are shown in red text. Expression of genes in *tamA*^{C90L} was used to determine regulation by DNA-binding dependent (solid arrows) and non-DNA-binding or undetermined (broken arrows) modes of TamA action. Genes that are not differentially expressed in *tamA*Δ compared with wild type are gray.

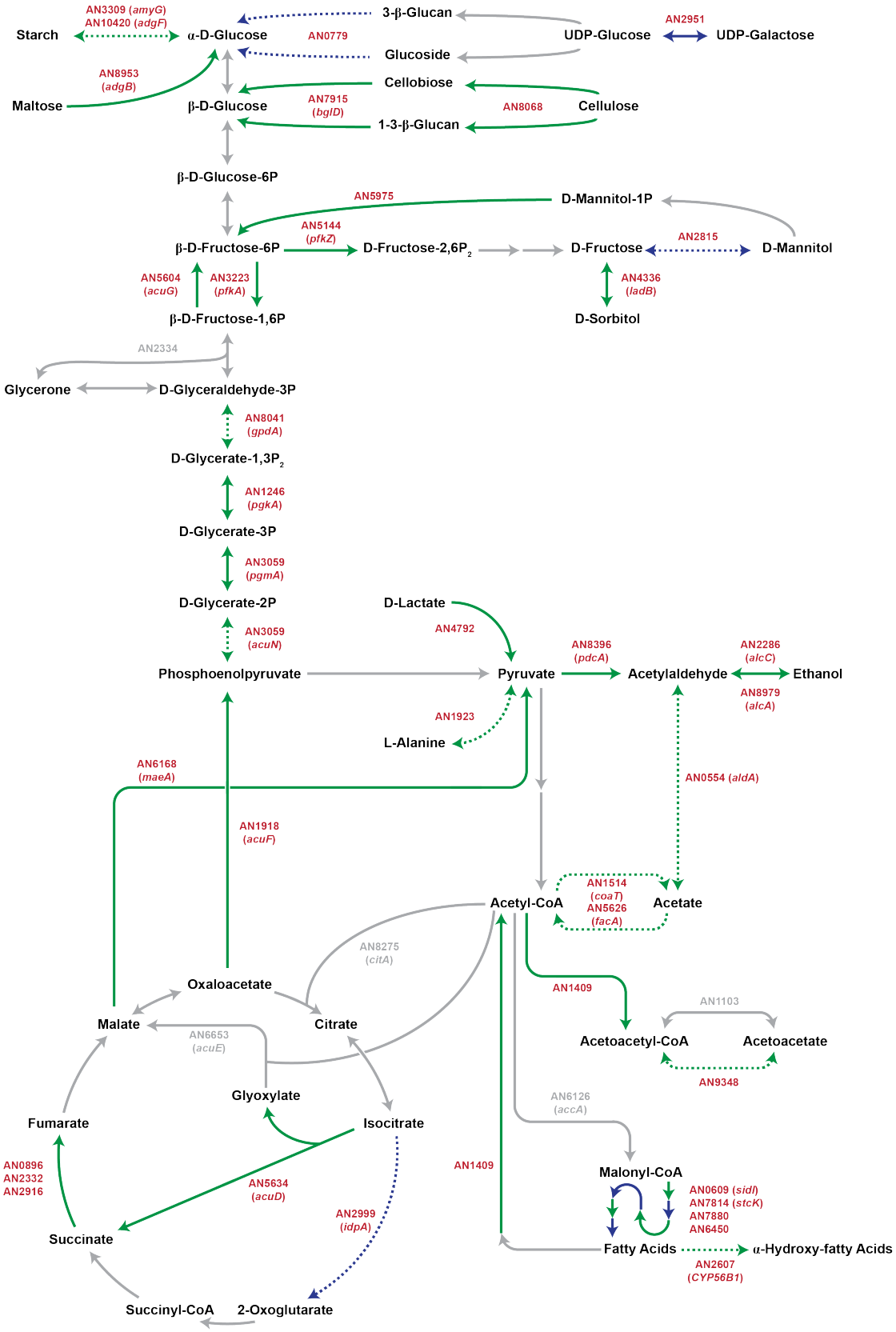

Figure 4.13 TamA regulation of carbon metabolism on glucose and alanine.

4.4.5.vi Alcohol metabolism

GO process enrichment and network analysis highlighted alcohol metabolism as being enriched amongst differentially expressed genes on all three nitrogen conditions (Table 4.3). The genes identified as enriched are *acpA, alcA, alcC, alcM, alcR, alcS, aldA* and *pdcA*. Two other members of the *alc* gene cluster, *alcU* and *alcP,* which are not GO annotated as alcohol metabolic genes, were also differentially expressed. We examined the expression of all ten genes and the final gene within the cluster, *alcB,* in each of the three nitrogen conditions. The most significant change in expression was observed during growth on the preferred nitrogen nutrient glutamine, where expression of 8/11 genes was increased in the *tamA*Δ mutant (Table 4.5). Four genes also showed increased expression in *tamA*^{C90L}, though to a lesser extent than *tamA*Δ. The only gene with decreased expression in *tamA*Δ was *acpA* and this was observed on both of the preferred nitrogen sources. On alanine, five genes showed decreased expression, however the ethanol utilization pathway transcription regulator, *alcR*, was not differentially expressed indicating TamA acts at these promoters with AlcR or via a separate signaling pathway. Therefore TamA represses ethanol utilization genes mostly independently of its DNA binding motif.

Table 4.5 Derepression of ethanol utilization genes.

		Fold Change vs wild type[a]					
		Gln		NH_4		Ala	
Gene	Function	*tamA*Δ	*tamA*^{C90L}	*tamA*Δ	*tamA*^{C90L}	*tamA*Δ	*tamA*^{C90L}
acpA	Acetate permease	0.53	0.62	0.55	0.71	0.88	0.93
alcA	Alcohol dehydrogenase	4.72	1.45	10.13	0.55	3.12	1.96
alcB	Alcohol dehydrogenase II	1.37	1.13	1.25	1.02	0.84	0.86
alcC	Alcohol dehydrogenase III	1.44	1.47	0.39	2.60	5.78	5.90
alcM	Unknown function	3.08	1.06	18.11	0.81	3.44	1.49
alcP	Gluconolactonase	2.22	1.55	1.51	0.71	1.17	1.18
alcR	Zn(II)2Cys6 regulator	1.69	1.09	3.16	0.91	0.86	0.99
alcS	Unknown function	3.17	0.80	14.51	0.56	4.43	1.77
alcU	Unknown function	8.12	1.18	7.32	0.89	1.27	1.87
aldA	Aldehyde dehydrogenase	2.40	1.66	3.60	0.81	1.45	1.27
pdcA	Pyruvate decarboxylase	1.34	1.26	0.95	1.00	1.84	1.37

[a] Genes with significantly increased (yellow) or decreased (blue) expression are highlighted. ($p \leq 0.05$, $q \leq 0.05$)

4.4.5.vii Siderophore biosynthesis and iron homeostasis.

Iron is an essential co-factor for numerous cellular enzymes. Fungi actively source iron from the environment through the production of siderophores (MIETHKE AND MARAHIEL 2007). Siderophores are made from the nitrogenous compound ornithine (BARRY AND CHALLIS 2009). Because iron is a redox-active metal, high levels can cause oxidative stress (LIN *et al.* 2011), and iron levels are therefore maintained in homeostasis (KOSMAN 2003). The GATA factor SreA represses iron uptake genes when iron is abundant (HAAS *et al.* 1999). When iron becomes depleted the Janus transcription factor HapX interacts with the CCAAT-binding complex to promote expression of iron uptake genes (HORTSCHANSKY *et al.* 2007). During growth on ammonium and alanine, genes for iron assimilation, iron chelate transport, iron homeostasis, iron ion transport, and siderophore transport were significantly enriched in genes with increased expression in *tamA*Δ in the GO process analysis (Table 4.3). In addition to these genes we identified siderophore biosynthesis genes, heme-binding protein genes, a metalloreductase involved in iron homeostasis (*freA;* OBEREGGER *et al.* 2002), the iron metabolism transcription factor genes *hapX* and *sreA,* and genes regulated by HapX in the differentially expressed genes list (Table. 4.6). Twenty-five genes were differentially expressed in *tamA*Δ during growth on alanine, while 8 genes were differentially expressed on glutamine and 14 genes showed differential expression in *tamA*Δ on ammonium. During growth on ammonium *hapX* and 8/10 siderophore biosynthesis genes showed increased expression; whereas, during growth on alanine *hapX* showed decreased expression and *sreA* showed increased expression. Therefore we might expect SreA and HapX target genes to have decreased expression as an indirect effect of *tamA*Δ. Consistent with this, four genes involved in siderophore biosynthesis showed reduced expression in *tamA*Δ grown on alanine. Furthermore, four HapX regulated genes showed the same trend as protein level changes, observed using 2D-chromotography and mass-spectroscopy (MS), in *hapX*Δ (HORTSCHANSKY *et al.* 2007). Surprisingly, four genes that encode proteins with reduced abundance in *hapX*Δ (HORTSCHANSKY *et al.* 2007) showed increased expression in *tam*Δ grown on alanine, suggesting TamA regulation of these genes is not solely through *hapX* regulation. Genes encoding proteins involved in heme binding generally showed increased expression in *tamA*Δ grown on alanine suggesting a possible nitrogen signal repressing these genes via TamA.

Table 4.6 Differentially expressed genes involved in iron homeostasis.

Gene	Fold Change vs wild type[a]					
	Gln		NH_4		Ala	
	*tamA*Δ	*tamA*^{C90L}	*tamA*Δ	*tamA*^{C90L}	*tamA*Δ	*tamA*^{C90L}
Regulators						
hapX	0.80	0.56	2.01	1.22	0.59	0.55
sreA	1.21	0.93	1.22	1.12	2.21	1.00
Siderophore biosynthesis and transport						
mirB	0.93	0.71	6.78	1.19	0.87	0.73
sidC	0.54	0.59	1.59	1.20	0.89	0.73
sidD	1.08	0.72	2.73	1.92	1.17	0.76
sidF	0.99	0.76	2.14	1.06	0.64	0.70
sidH	1.20	0.95	1.54	1.23	0.70	0.86
sidI	0.83	0.66	2.64	1.39	0.57	0.61
sidL	0.75	0.76	1.24	1.35	0.90	0.56
AN5378	1.18	0.78	2.32	1.43	1.81	0.84
AN6400	0.84	0.84	1.76	1.52	0.58	0.82
AN7884	0.77	0.71	1.89	2.52	0.80	0.37
Iron Ion Homeostasis						
AN3690	1.18	0.96	1.14	1.38	0.58	0.89
AN7518	3.79	3.21	2.84	2.34	2.59	1.00
AN8683	0.85	0.62	2.54	0.96	0.39	0.57
AN10893	0.08	0.14	0.18	0.45	2.62	1.51
Heme binding and biosynthesis						
freA[b]	0.98	1.12	1.20	1.06	0.58	0.99
AN1915	1.22	1.41	0.81	1.07	1.54	1.09
AN2778	1.32	0.78	3.11	0.31	0.52	0.42
AN4051	0.57	0.67	0.62	0.62	1.40	0.66
AN4424	1.37	1.07	1.91	1.25	0.95	1.05
AN5130	1.40	1.40	1.11	1.48	2.41	1.44
AN7752	1.40	1.14	1.07	1.15	1.59	1.23
AN9108	1.12	0.96	3.25	0.87	4.11	1.14
HapX regulated[c]						
AN0443 (↓)	1.84	2.06	1.21	1.37	1.72	1.70
AN3161 (↓)	0.62	0.56	0.44	0.66	0.70	0.64
AN3206 (↓)	1.79	1.13	1.92	1.68	5.35	2.40
AN4288 (↓)	1.20	1.18	0.93	1.00	1.50	1.26
AN5652 (↓)	1.11	1.53	0.98	1.37	0.59	1.02
AN6004 (↑)	0.78	0.91	0.52	0.63	1.46	1.20
AN8406 (↓)	0.96	0.97	0.84	0.51	1.58	1.13
AN10139 (↑)	1.12	0.97	0.87	0.84	1.74	1.24

[a] Genes with significantly increased (yellow) or decreased (blue) expression are highlighted.
[b] *freA* is upregulated during iron limitation (Obregger 2002)
[c] Altered protein levels in *hapX*Δ mutant indicated after the gene (Horchansky 2007)

4.4.5.viii Secondary metabolism regulators

Fungi produce a wide array of biologically active secondary metabolites including penicillin, which was discovered in the early 20th century (FLEMING 1929) and harmful toxins such as aflatoxin (reviewed in GEORGIANNA AND PAYNE 2009). Production of many secondary metabolites is regulated by nitrogen availability, and in *Fusarium* species, nitrogen regulation of gibberellin, beauvericin, fumonisin, fusarielin H, bikaverin, and trichothecenes (DON) biosynthesis is controlled by the AreA ortholog (reviewed in TUDZYNSKI 2014). In *A. nidulans,* nitrogen metabolism has been implicated in regulation of sterigmatacystin production (FENG AND LEONARD 1998) and spiroanthrones production is induced by nitrogen starvation (SCHERLACH *et al.* 2011). Genes encoding secondary metabolites are often arranged in clusters and are regulated by cluster specific transcription factors and master secondary metabolism regulatory proteins. In *A. nidulans,* the master regulatory proteins include members of the velvet family VeA, VelB, VosA, and VelC, and the methyltransferase-domain protein LaeA (reviewed by BAYRAM AND BRAUS 2012), which is thought to bring about changes in gene expression by chromatin modification (REYES-DOMINGUEZ *et al.* 2008; GACEK AND STRAUSS 2012). There are eight LaeA like methyltransferases in *A. nidulans* that may function in secondary metabolism (PALMER *et al.* 2013). We examined expression of these genes and a further 66 transcription factors that lie within secondary metabolite clusters (INGLIS *et al.* 2013). We found differential expression of 18 secondary metabolism pathway-specific regulatory genes, as well as *veA*, *velB, llmD, llmJ,* and the master regulator *laeA* (Table 4.7). Most of the regulatory genes that were differentially expressed in *tamA*Δ showed reduced expression and were regulated primarily during growth on alanine. Notably *scpR,* which regulates asperfuranone biosynthesis (BERGMANN *et al.* 2010), showed decreased expression on all three conditions and in both *tamA*Δ and $tamA^{C90L}$.

Table 4.7 Differential expression of secondary metabolism regulators.

Gene	Cluster or Function	Fold Change vs wild type[a]					
		Gln		NH_4		Ala	
		*tamA*Δ	*tamA*^{C90L}	*tamA*Δ	*tamA*^{C90L}	*tamA*Δ	*tamA*^{C90L}
apdR	Aspyridone	0.79	0.75	0.89	0.75	2.06	1.78
dbaA	Benzaldehyde derivative	0.55	0.31	1.71	0.14	0.69	0.20
dbaG	Benzaldehyde derivative	0.38	0.34	4.08	0.97	0.90	0.15
hapX	Siderophores	0.80	0.56	2.01	1.22	0.59	0.55
mtfA	Regulates multiple clusters	0.41	0.39	0.86	0.38	0.34	0.45
laeA	Methyltransferase	0.79	0.78	0.91	0.93	0.41	0.67
llmD	Methyltransferase	0.84	0.74	0.63	0.82	1.32	1.40
llmJ	Methyltransferase	0.78	0.93	1.72	0.73	0.45	0.90
scpR	Asperfuranone	0.29	0.30	0.46	0.28	0.47	0.38
veA	Global SM regulator	0.80	0.76	1.05	0.86	0.63	0.68
velB	Global SM regulator	0.70	0.77	0.96	0.68	0.31	0.51
AN10600	NPRS AN4827	0.54	0.94	1.76	0.87	0.62	0.70
AN1686	–	1.04	0.93	2.06	1.82	0.84	1.04
AN2036	–	0.25	0.39	0.67	0.52	1.03	0.55
AN2392	–	0.26	0.58	1.78	1.89	0.18	0.82
AN2553	–	0.62	0.67	0.58	0.52	0.65	0.70
AN3269	–	0.48	0.68	1.06	0.75	0.62	0.64
AN3280	–	1.45	1.04	2.22	1.02	1.83	1.14
AN3385	PKS AN3386	0.69	1.44	1.90	1.83	0.55	0.80
AN3911	NRPS AN10486	0.84	1.47	0.94	1.48	0.56	1.19
AN6430	PKS AN6431	1.05	1.34	0.85	0.91	3.06	1.34
AN7921	–	0.82	1.00	1.43	1.30	0.53	0.69
AN8103	NRPS AN8105	1.24	1.03	1.08	0.76	0.52	1.00
AN8377	Austinol, dehydroaustinol	1.30	0.98	3.18	3.82	2.38	1.01

[a] Genes with significantly increased (yellow) or decreased (blue) expression are highlighted.

4.4.5.ix Characterized secondary metabolite biosynthesis clusters.

A. nidulans has several well-characterized secondary metabolite clusters, including those which synthesize aspyridone, asperfuranone, penicillin, terrequinone, microperfuranone and sterigmatocystin. Amongst the genes differentially expressed in our data set were genes from each of these six secondary metabolism pathways. Expression of some genes required for aspyridone biosynthesis, including the pathway regulator *apdR*, showed increased expression in *tamA*Δ during growth on alanine (Table 4.8) but were mostly unchanged on the preferred nitrogen sources or by $tamA^{C90L}$. The terrequinone cluster contains five genes (BOUHIRED *et al.* 2007), however only *tdiB* was differentially expressed in the *tamA* mutants. The pattern of *tdiB* expression was the same as seen for aspyridone genes, showing a 3.08 fold increase in expression in *tamA*Δ during growth on alanine (Table 4.8). Therefore TamA may repress biosynsthesis of both aspyridone and terriquinone on alanine.

Penicillin biosynthesis requires the *acvA, ipnA,* and *aatA* genes (RAMON *et al.* 1987; MACCABE *et al.* 1990; TOBIN *et al.* 1990; MACCABE *et al.* 1991). In *Pencillium chrysogenum* expression of *acnA* and *ipnA* is regulated by the AreA homolog NRE and is repressed by ammonium (KOLAR *et al.* 1991; HAAS AND MARZLUF 1995). All three genes in *A. nidulans* showed strong induction of expression during growth on alanine compared with glutamine and ammonium (Figure 4.14). Expression of these genes was decreased in both *tamA*Δ and $tamA^{C90L}$ during growth on alanine (Figure 4.14; Table 4.8). A fourth gene*, hdaA,* which encodes a histone deacetylase that represses penicillin biosynthesis (TRIBUS *et al.* 2005; SHAABAN *et al.* 2010), showed decreased expression in both *tamA*Δ and $tamA^{C90L}$ during growth on alanine (Table 4.8). Therefore, TamA appears to be involved in nitrogen regulation of penicillin biosynthesis by DNA-dependent activation. Genes within the microperfuranone cluster were regulated similarly to penicillin genes showing reduced expression in both *tamA*Δ and $tamA^{C90L}$ on alanine (Table 4.8). AN3394, which encodes a cytochrome P450, and is generally co-regulated with *micA* (KELLY *et al.* 2009; ANDERSEN *et al.* 2013) also showed decreased expression on both of the preferred nitrogen sources. Therefore, as with penicillin biosynthesis, TamA appears to positively regulate microperfuranone biosynthesis during growth on alanine. Finally four of the genes in the sterigmatocystin cluster showed differential expression; *stcA* and *stcK* showed increased expression in *tamA*Δ during drowth on alanine, whereas *stcU* and *stcV* showed

increased expression on ammonium. Therefore TamA may repress sterigmatocystin biosynthesis on multiple nitrogen nutrients.

The asperfuranone gene cluster is regulated by the C2H2 transcription factor ScpR (BERGMANN *et al.* 2010), which had at least a two-fold reduction of expression in both *tamA* mutants on all three nitrogen nutrients (Table 4.7). Examination of the genes involved in asperfuranone biosynthesis showed that only *afoE,* which encodes a putative polyketide synthase (PKS; CHIANG *et al.* 2009b), had altered expression and only on glutamine in *tamA*Δ (1.74 fold increase, Table 4.8). The lack of altered expression of other genes in the cluster may be due to the fact they are not induced by the cluster activator AfoA or that TamA regulates asperfuanone biosynthesis via regulated expression of *scpR* and the PKS backbone encoding gene *afoE* (CHIANG *et al.* 2009b). Although TamA regulates six secondary metabolite biosynthetic pathway gene clusters the effects of TamA action between gene clusters differs. The difference likely comes about through the regulation of different transcription factors or interaction with different regulators at each gene cluster.

Table 4.8 Regulation of well characterized secondary metabolite clusters.

	Fold Change vs wild type[a]					
	Gln		NH_4		Ala	
Gene	*tamA*Δ	*tamA*^{C90L}	*tamA*Δ	*tamA*^{C90L}	*tamA*Δ	*tamA*^{C90L}
Aspyridone						
apdA	1.27	1.28	0.85	1.00	1.96	1.58
apdB	2.75	0.94	1.12	2.70	4.69	0.72
apdC	1.00	1.00	0.01	1.21	8.75	2.40
apdD	0.24	0.01	1.91	0.01	7.21	1.59
apdE	1.44	1.18	2.79	2.71	3.98	1.66
apdF	0.80	0.79	0.60	0.47	1.76	0.83
apdG	0.95	1.08	1.23	0.71	0.80	0.97
apdR	0.79	0.75	0.89	0.75	2.06	0.89
Terrequinone						
tdiA	1.62	0.22	1.52	0.95	3.92	1.35
tdiB	1.09	0.95	0.79	0.64	3.08	1.48
tdiC, tdiD	2.73	0.96	1.11	8.53	0.93	1.24
tdiE	1.38	0.51	0.79	0.24	1.23	0.59
Penicillin						
aatA	0.59	0.60	0.96	0.74	0.12	0.40
acvA	0.48	0.76	0.66	0.70	0.25	0.37
ipnA	1.48	1.01	1.06	1.25	0.16	0.44
hdaA[b]	0.91	1.12	0.82	1.00	1.58	1.35
Microperfuranone						
micA, AN3395[c]	0.67	0.73	0.71	0.70	0.95	0.62
AN3394	0.41	0.53	0.31	0.33	0.48	0.47
Sterigmatocystin						
stcA	1.55	1.21	2.03	2.07	2.41	1.03
stcK	0.98	0.90	1.73	1.14	2.67	1.30
stcU, stcV[c]	1.38	1.17	1.92	1.17	1.48	1.29
Asperfuranone						
afoA	1.00	0.79	0.74	0.43	0.45	0.65
afoB	0.92	1.03	0.36	0.54	2.13	2.26
afoC	0.92	1.03	0.90	0.43	0.99	0.90
afoD	0.83	0.72	0.63	0.38	0.85	0.75
afoE	1.74	1.59	2.67	2.28	5.75	3.19
afoF	1.35	0.85	1.35	0.37	3.22	1.19
afoG	0.81	2.16	1.00	1.00	3.88	0.50

[a] Genes with significantly increased (yellow) or decreased (blue) expression are highlighted.

[b] *hdaA*Δ results in increased penicillin production (Shaaban et al 2010)

[c] *tdiC* with *tdiD, micA* with AN3395, and *stcU* with *stcV*, were recognized as single genes by Cufflinks.

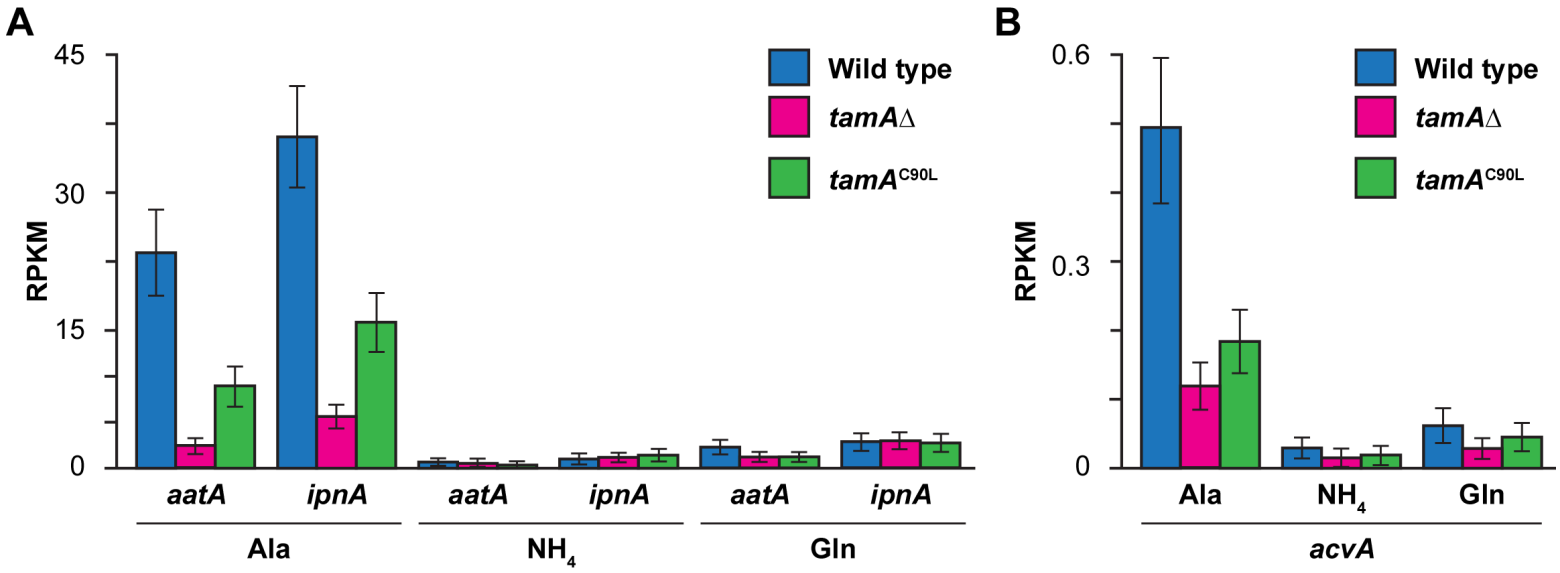

Figure 4.14 Nitrogen metabolite repression of penicillin biosynthesis genes.

Expression of the penicillin biosynthesis genes *aatA*, *ipnA*, **(A)** and *acvA* **(B)** expressed as reads per kilobase per million mapped reads (RPKM). Expression data was generated from RNA-seq of wild type (MH1), *tamA*Δ (MH8694) and *tamA*^{C90L} (MH11808) strains grown in supplemented ANM with 10 mM glutamine (Gln), ammonium (NH_4) or alanine (Ala). Error bars depict SEM (N=3).

4.4.6 TamA shows condition specific binding at a diverse set of genes.

Our RNA-seq analysis highlighted the important role TamA plays in regulating a diverse set of genes, however we were unable to identify directly regulated target genes using this approach. To identify direct TamA targets we performed ChIP-seq on wild type $TamA^{FLAG}$ strains grown in the presence of ammonium or glutamine. Sequence reads were aligned to the *A. nidulans* genome reference sequence and peaks called using Model-based analysis for ChIP-seq (MACS; ZHANG *et al.* 2008), with a minimum 4-fold enrichment and a p-value $\leq 1x10^{-7}$. Using this analysis we identified 46 TamA binding peaks adjacent to 71 genes (Table 4.9). For 19 peaks, binding was observed on both ammonium and glutamine, one binding event was ammonium specific (*gelA*) and 26 were glutamine specific. Binding was observed upstream of 50 genes (31 peaks) and downstream of 21 genes (15 peaks). For binding in gene promoters the distance of a peak to the ATG of the nearest gene ranged from 90 to 2,768 bp, with the median distance being 415 bp (Figure 4.15A). Most of the TamA binding peaks were adjacent to uncharacterized genes (Table 4.9). Promoter binding was observed in the *gdhA* promoter (Figure 4.15B), consistent with the TamA sites of action and DNA binding site we established (see above 4.4.1; DOWNES *et al.* 2014b). Binding was also observed at the *tamA* promoter suggesting auto-regulation (Figure 4.15C) and at several other genes involved in nitrogen nutrient assimilation including the uric acid permease *uapC* (Figure 4.15D), the nitrate assimilation regulator *nirA* (Figure 4.15E), glutamine synthase *glnA*, and putative amino acid transporters (AN0856, AN8785). Among the other genes adjacent to TamA binding peaks were several carbon metabolism genes were represented including a glucose transporter (*mstE*), and glucan and starch degrading enzymes (*agsB*, *amyD*, *gelA*). Binding was also seen near a number of secondary metabolism genes, including the regulator *veA*, two cytochrome-P450 genes (AN3349, AN7131), a cluster of siderophore genes (*sidC*, *sidI*, AN0608), and in the bidirectional promoters of six genes in a predicted secondary metabolite cluster with an unknown product (AN7873, AN7874, AN7889, AN7880, AN7883, AN7884). During growth on ammonium TamA acts as co-repressor of *fmdS* (Figure 4.15F) and a co-activator upstream of the -753 bp region of *gdhA* (DAVIS *et al.* 1996; DOWNES *et al.* 2014b). To ensure we were observing actual TamA-DNA binding events in our data we examined the *fmdS* promoter and the upstream *gdhA* region and detected no binding. In the RNA-seq analysis *tamA*Δ but not $tamA^{C90L}$ conferred

reduced expression of *glnA* (Figure 4.10); therefore, TamA regulates *glnA* expression as a co-activator. However, we identified a $TamA^{FLAG}$ ChIP-seq peak 2.2 kb upstream of *glnA*. As TamA binding was seen upstream of 1/3 of our examined co-factor mode of action targets we can expect most of the ChIP-seq peaks result from direct TamA-DNA binding though some may result from cofactor binding.

Table 4.9 Genes adjacent to TamA^{FLAG} ChIP-seq peaks.

Gene	Name	*S. cerevisiae* Ortholog	Description
AN0098	*nirA*		Putative Gal4-type zinc finger protein that regulates expression of genes involved in nitrate assimilation
AN0607	*sidC*		Non-ribosomal peptide synthetase; similar to ferrichrome peptide synthetases; involved in ferricrocin (FC) siderophore biosynthesis
AN0608			Ortholog(s) have role in N',N'',N'''-triacetylfusarinine C biosynthetic process, ergosterol biosynthetic process, siderophore biosynthetic process and peroxisome localization
AN0609	*sidI*		Triacetylfusarinine C (TAFC) biosynthetic enoyl-CoA hydratase; siderophore biosynthetic enzyme
AN0610			Ortholog(s) have cytosol, nucleus localization
AN0844			Protein required for actin cytoskeleton organization and cell cycle progression; ortholog of S. cerevisiae Sda1p;
AN0845			Ortholog of A. oryzae RIB40 : AO090003000396, Aspergillus wentii : Aspwe1_0118965, Aspergillus versicolor : Aspve1_0024021 and Aspergillus niger ATCC 1015 : 182627-mRNA
AN0856			Putative amino acid transporter; expression reduced after exposure to farnesol
AN0857			Ortholog of A. nidulans FGSC A4 : AN6924, AN5943, AN8512, AN8548, AN8661, AN4642 and A. fumigatus Af293 : Afu1g15290, Afu3g00850, Afu4g08850, Afu7g00920
AN10160			Ortholog of A. nidulans FGSC A4 : AN2370, AN0323, A. fumigatus Af293 : Afu1g02440, Afu4g02760, A. niger CBS 513.88 : An01g05750, An12g09350, An13g03290 and A. oryzae RIB40 : AO090020000719, AO090005000852
AN10329			Predicted mariner transposon-related ORF
AN1038		TRS130	Ortholog(s) have Rab guanyl-nucleotide exchange factor activity and role in CVT pathway, early endosome to Golgi transport, intra-Golgi vesicle-mediated transport, macroautophagy, regulation of Rab GTPase activity
AN10392			Has domain(s) with predicted UDP-N-acetylmuramate dehydrogenase activity, flavin adenine dinucleotide binding, oxidoreductase activity, acting on CH-OH group of donors activity and role in oxidation-reduction process
AN10459			Ortholog(s) have cytosol localization
AN1052	*veA*		Protein involved in light-sensitive control of differentiation and secondary metabolism; localizes to the nucleus in dark and to both nucleus and cytoplasm in the light; induced by light; AspGD sequence represents the veA1 mutant allele
AN10900			Has domain(s) with predicted serine-type peptidase activity and role in proteolysis
AN11288			Protein of unknown function
AN1148		PPN1	Ortholog(s) have endopolyphosphatase activity, exopolyphosphatase activity, role in polyphosphate catabolic process and fungal-type vacuole membrane, nucleus localization
AN11623			Protein of unknown function
AN11670			Protein of unknown function
AN11748			Protein of unknown function
AN11749			Protein of unknown function
AN11844			Protein of unknown function
AN11921			Ortholog(s) have role in response to amino acid
AN12030			Protein of unknown function
AN12077			Protein of unknown function
AN12232			Protein of unknown function
AN12359			Protein of unknown function
AN12414			Protein of unknown function
AN2498			Ortholog of A. fumigatus Af293 : Afu3g14090, A. oryzae RIB40 : AO090012000646, Aspergillus wentii : Aspwe1_0407854, Aspergillus sydowii : Aspsy1_0148141 and Aspergillus terreus NIH2624 : ATET_04020
AN2499			Ortholog(s) have role in cellular response to cadmium ion, detoxification of cadmium ion and cytosol, nucleus localization
AN2616			Has domain(s) with predicted RNA binding, RNA-directed DNA polymerase activity, nucleic acid binding activity and role in DNA integration, RNA-dependent DNA replication

Table 4.9 Genes adjacent to TamA^{FLAG} ChIP-seq peaks (continued).

Gene	Name	*S.cerevisiae* Ortholog	Description
AN2626			Ortholog of A. nidulans FGSC A4 : AN1620, A. fumigatus Af293 : Afu8g02040/och3, A. niger CBS 513.88 : An03g01090/hocA, An05g02320 and A. oryzae RIB40 : AO090010000615
AN2628			Predicted mariner transposon-related ORF
AN2944	*tamA*	*DAL81*	Transcriptional co-activator of the major nitrogen regulatory protein AreA; binds and activates gdhA promoter; transcript is induced by nitrate
AN2953			Ortholog of A. fumigatus Af293 : Afu3g07890, A. niger CBS 513.88 : An02g11360, A. oryzae RIB40 : AO090005001486, Aspergillus wentii : Aspwe1_0041944 and Aspergillus sydowii : Aspsy1_0056308
AN2954			Ortholog of A. fumigatus Af293 : Afu3g07870, A. niger CBS 513.88 : An02g11390, A. oryzae RIB40 : AO090005001484, Aspergillus wentii : Aspwe1_0029219 and Aspergillus sydowii : Aspsy1_0042610
AN2955			Has domain(s) with predicted role in biosynthetic process
AN3245			Protein of unknown function
AN3246			Ortholog of Aspergillus aculeatus ATCC16872 : Aacu16872_057585
AN3307	*agsB*		Catalytic subunit of the major alpha-1,3 glucan synthase complex; mutants grow as dispersed hyphae in liquid culture
AN3308	*amyD*		Putative alpha-amylase with a predicted role in starch metabolism; predicted glycosyl phosphatidylinositol (GPI)-anchor
AN3349	*CYP659A1*		Putative cytochrome P450
AN4159	*glnA*	*GLN1*	Putative glutamate-ammonia ligase with a predicted role in glutamate and glutamine metabolism; intracellular; transcript upregulated by nitrate limitation; protein abundance decreased by menadione stress and induced by farnesol
AN4375			Ortholog of A. nidulans FGSC A4 : AN2913, A. fumigatus Af293 : Afu3g07740, Afu4g06610, A. niger CBS 513.88 : An04g00930 and A. oryzae RIB40 : AO090023000927, AO090020000420
AN4376	*gdhA*	*GDH1*	Putative NADP-linked glutamate dehydrogenase; predicted role in glutamate/glutamine metabolism; involved in nitrogen catabolite repression; induced by low nitrate; intracellular, menadione stress-induced protein; protein induced by farnesol
AN5245			Protein of unknown function
AN5860	*mstE*		Low affinity glucose transporter of the major facilitator superfamily (MFS); transcriptionally repressed by growth on xylose
AN6230	*medA*		Protein involved in regulation of conidiophore development; required for normal temporal expression of brlA; mutation causes aberrant conidiophores
AN6473			Ortholog of A. fumigatus Af293 : Afu1g16430, Neosartorya fischeri NRRL 181 : NFIA_009010, Aspergillus versicolor : Aspve1_0315435 and Aspergillus fumigatus A1163 : AFUB_015770
AN6730	*uapC*		Low-to-moderate capacity, broad specificity purine permease; putative paralog of UapA; localized to the cell periphery, relocalizes to vacuoles in the presence of ammonium
AN6731	*sdeA*		Putative delta-9-stearic acid desaturase; converts palmitic acid and stearic acid to palmitoleic acid and oleic acid; null mutant has increased fatty acid content; synthetically lethal with sdeB mutation; expression reduced by farnesol
AN7130			Ortholog of A. nidulans FGSC A4 : AN2942, AN10320 and A. fumigatus Af293 : Afu3g15110, Afu4g08715
AN7131	CYP52H1		Putative cytochrome P450
AN7133			Protein of unknown function
AN7873			Putative multifunctional enzyme with a predicted role in cytosolic fatty acid formation; predicted secondary metabolism gene cluster member
AN7874			Protein of unknown function; predicted secondary metabolism gene cluster member
AN7879			Predicted ABC transporter; predicted secondary metabolism gene cluster member
AN7880			Putative fatty-acyl-CoA synthase with a predicted role in cytosolic fatty acid formation; predicted secondary metabolism gene cluster member
AN7883			Protein of unknown function; predicted secondary metabolism gene cluster member
AN7884			Putative nonribosomal peptide synthase (NRPS) similar to ferrichrome peptide synthetases involved in siderophore biosynthesis; predicted backbone enzyme of a secondary metabolism gene cluster member

Table 4.9 Genes adjacent to TamA^{FLAG} ChIP-seq peaks (continued).

Gene	Name	*S. cerevisiae* Ortholog	Description
AN8505			Ortholog of Aspergillus brasiliensis : Aspbr1_0111846, Aspergillus fumigatus A1163 : AFUB_075260, Aspergillus niger ATCC 1015 : 199457-mRNA and Aspergillus aculeatus ATCC16872 : Aacu16872_050877
AN8576			Has domain(s) with predicted RNA binding, RNA-directed DNA polymerase activity, nucleic acid binding activity and role in RNA-dependent DNA replication
AN8664			Ortholog(s) have cytosol, nucleus localization
AN8739			Protein of unknown function
AN8740			Protein of unknown function
AN8785		*AGC1*	Ortholog(s) have L-aspartate transmembrane transporter activity, L-glutamate transmembrane transporter activity, antiporter activity, uniporter activity
AN8950			Protein of unknown function
AN9523			Ortholog of A. fumigatus Af293 : Afu5g12040, A. niger CBS 513.88 : An18g02305, A. oryzae RIB40 : AO090120000321, Aspergillus wentii : Aspwe1_0445614 and Aspergillus sydowii : Aspsy1_0054923
tF(GAA)4	*tF*(GAA)4		tRNA-Phe, predicted by tRNAscan-SE; GAA anticodon

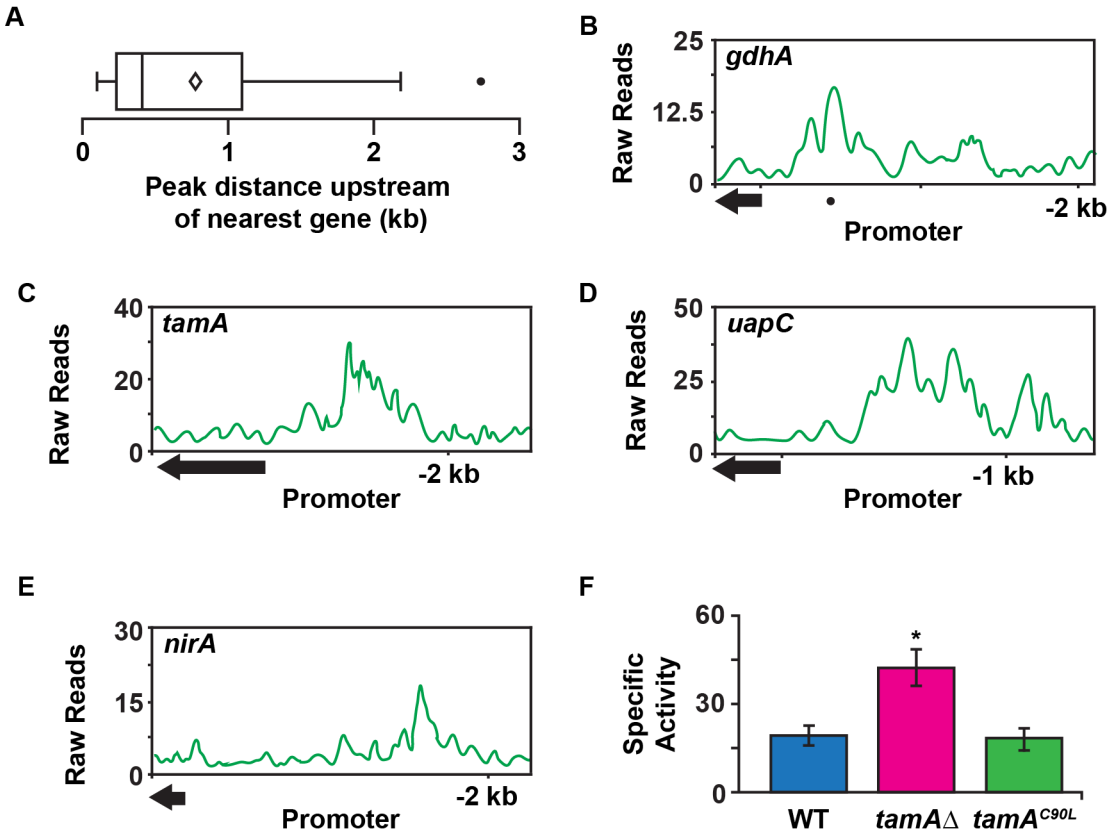

Figure 4.15 TamA^{FLAG} ChIP-seq identified binding peaks.

A) Box plot of distance of peaks upstream of the ATG. The mean is shown as a diamond and outliers (≥ Q3 + 1.5 x Interquartile range) are circles **B-E)** Sequence coverage from ChIP-seq of *tamA*^{FLAG} *tamA*^{FLAG} (WT; RT322) grown in supplemented-ANM with 10 mM glutamine for 16 hours. The beginning of the coding region is shown as a black arrow. The known TamA binding site at -432 to -422 bp in the *gdhA* promoter (B) is shown as a black circle. **F)** Expression of the *fmdS-lacZ* reporter in wild type (WT; MH9046), *tamA*Δ (MH11322) and *tamA*^{C90L} (RT139) after growth in supplemented ANM with 10 mM ammonium. Error bars depict SEM (n=4). * for $p \leq 0.05$ using a two tailed unequal distribution Student's t-test.

4.4.6.i Promoter analysis

PatMATCH allows identification of specific motifs in the *A. nidulans* genome and can be used to identify motifs in gene promoters (YAN *et al.* 2005). PatMATCH analysis of *A. nidulans* promoters using the known TamA DNA-binding motif at *gdhA,* CCGAACTTCGG, failed to identify any of the genes where binding was observed by ChIP-seq. This approach identified only two other *A. nidulans* genes, *mdpF* and AN1403, with an exact match to this sequence in their promoters. The sites were not conserved in *Aspergillus oryzae, Aspergillus niger* or *Aspergillus fumigatus* (DOWNES *et al.* 2014b) and neither site was associated with $TamA^{FLAG}$ binding peaks. The absence of this motif in the $TamA^{FLAG}$ bound promoters of genes identified by ChIP-seq may arise from variation in the AACTT spacer sequence, or TamA may bind at additional motifs as a heterodimer with unknown proteins. To identify putative TamA binding motifs we performed a SCOPE analysis of the regions under each peak (CARLSON *et al.* 2007). SCOPE combines three algorithms, BEAM – for non-degenerate motifs, PRISM – for degenerate motifs, and SPACER – for bipartite motifs, typical of those seen in Zn(II)2Cys6 transcription factors (CHAKRAVARTY *et al.* 2007a,b). SPACER functions by searching for overrepresented sequences and motifs in a given set of gene promoters in comparison to the 1,000 bp upstream region of all genes with in genome (CHAKRAVARTY *et al.* 2007a,b). The sequences under 22 peaks that were within 1,000 kb upstream of a gene start codon were downloaded from AspGD and used for SPACER analysis. SPACER identified ten motifs that were overrepresented in these 22 regions (Table 4.10). However, no motif was present in all 22 promoters, nor was the known TamA binding site in the *gdhA* promoter represented in any of the ten motifs. The lack of a single consensus sequence under all of the 22 peaks suggests TamA may be able to recognize multiple sequences by interacting with different DNA-binding partners at each promoter.

Table 4.10 SPACER analysis of TamA binding peaks within 1 kb of a gene start codon.

Consensus Motif[a]	Sig Value[b]	Coverage[c]	Downstream Genes
 GTAHBDWHYGTAW	27.8	22.7%	AN0607, AN0608/*sidC,* AN2953, AN3307, AN3308, AN7873, AN7874 AN7879, AN7880
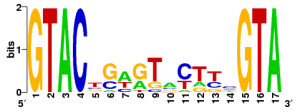 GTACNVHDBNHDBNGTA	17.5	31.8%	AN0607, AN0608/*sidC,* AN11921, AN2953, AN3307, AN3308, AN3349, AN10392, AN7883, AN7884, AN7879, AN7880
 CWAGNHHNDNACTA	15.7	22.7%	AN11921, AN2953, AN6473, AN7133, AN7131, AN8664, AN12030
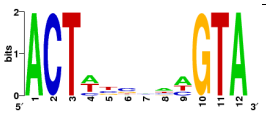 ACTHNNNNHGTA	15.1	40.9%	AN0856, AN0857, AN4375, AN4376/*gdhA*, AN6473, AN7133, AN7131, AN7884, AN7873, AN7879, AN7880, AN8505, AN8664, AN102030, AN8785
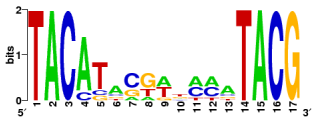 TACMBNVDDNHHNTACG	15.0	18.2%	AN3307, AN3308, AN7878, AN7880, AN8664, AN12030, AN8785
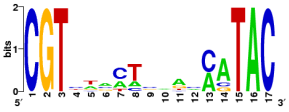 CGTNNNHHNNNNMVTAC	14.1	31.8%	AN2944/*tamA*, AN2953, AN3307, AN3308, AN3349, AN10392, AN4375, AN7883, AN4376/*gdhA*, AN7884, AN8785
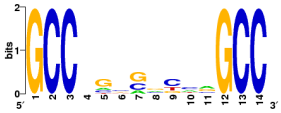 GCCNNNVNNNNGCC	12.8	40.9%	AN0607/*sidC*, AN0608, AN11921, AN2626, AN4375 AN10329, AN2953, AN4376/*gdhA*, AN6730/*uapC*, AN6731/*sdeA*, AN8576, AN11623, AN8664, AN12030
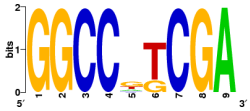 GGCCNKCGA	12.5	18.2%	AN11921, AN2953, AN4375, AN8664, AN4376/*gdhA*, AN12030
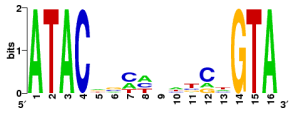 ATACNNHHNNNVNGTA	12.3	31.8%	AN3307, AN3308, AN6473, AN7883, AN7884, AN7879, AN7880, AN8505, AN8785
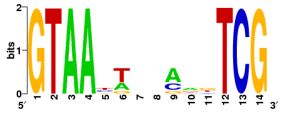 GTAANDNNVNNTCG	10.9	31.8%	AN2626, AN10329, AN3307, AN12030, AN6730/*uapC*, AN7131, AN7133, AN6731/*sdeA*, AN7879, AN7880, AN8576, AN11623, AN8664, AN3308

[a] Units measure bits of information proportional to sequence conservation.
[b] Sig score measures over-representation of a given motif as the -$\log_2$ of the expected number of motifs of the given length and degeneracy. A higher score is representative of greater overrepresentation.
[c] Percent of the 22 peaks this consensus sequence is present underneath.

4.4.6.ii TamA binds independently of AreA and LeuB at some promoters.

As TamA binding at *gdhA* is dependent on both AreA and LeuB (DOWNES *et al.* 2014b; see section 4.4.2) we were interested to know whether all TamA binding events require these two transcription factors. TamA was bound at 46 sites adjacent to 71 genes on ammonium in the wild type strain. We therefore determined whether AreA and LeuB are required for TamA DNA-binding at each of these sites. Of the 71 genes six lacked $TamA^{FLAG}$ binding in the *areA*Δ, *leuB*Δ, and *areA*Δ *leuB*Δ mutants, including *gdhA,* whereas 11 genes were bound in all three mutants (Figure 4.16). Therefore TamA shows binding at some sites that is dependent on both AreA and LeuB and binding at other promoters that is independent of AreA and LeuB. Binding at three genes was dependent on wild type *leuB* but not on *areA,* whereas only one binding event (at *tamA*) was *areA*-dependent but not *leuB*-dependent. Therefore TamA shows a combinatorial array of binding with AreA and LeuB. The different binding patterns are likely due to promoter specific elements. The remaining 14 genes showed an unusual binding pattern, where binding was lost in *leuB*Δ but maintained in *areA*Δ *leuB*Δ. It is possible that at these genes TamA binding is dependent on LeuB only when AreA is present, suggesting interaction between the three proteins modulates TamA binding. We also identifed 35 binding events that were only observed in the *areA*Δ and/or *leuB*Δ mutants and not in wild type (Figure 4.16). These binding events were upstream of genes of related function (Table 4.11), for example *sidA* and AN4041 (siderophore biosynthesis/heme binding), *exgC*, *fksA*, *gelC* and AN6786 (glucan metabolism), *dbaA* and *mtfA* (regulation of secondary metabolism), AN6787 (cytochrome-P450). These additional binding events observed in the *areA*Δ, *leuB*Δ, and/or *areA*Δ *leuB*Δ mutants may represent true TamA binding sites used under other growth conditions. The ability to observe these binding events in the mutants may be facilitated by TamA no longer being sequestered at promoters such as *gdhA* by AreA and LeuB, i.e. loss of titration through interactions with AreA or LeuB and/or loss of binding at AreA/LeuB dependent DNA binding sites.

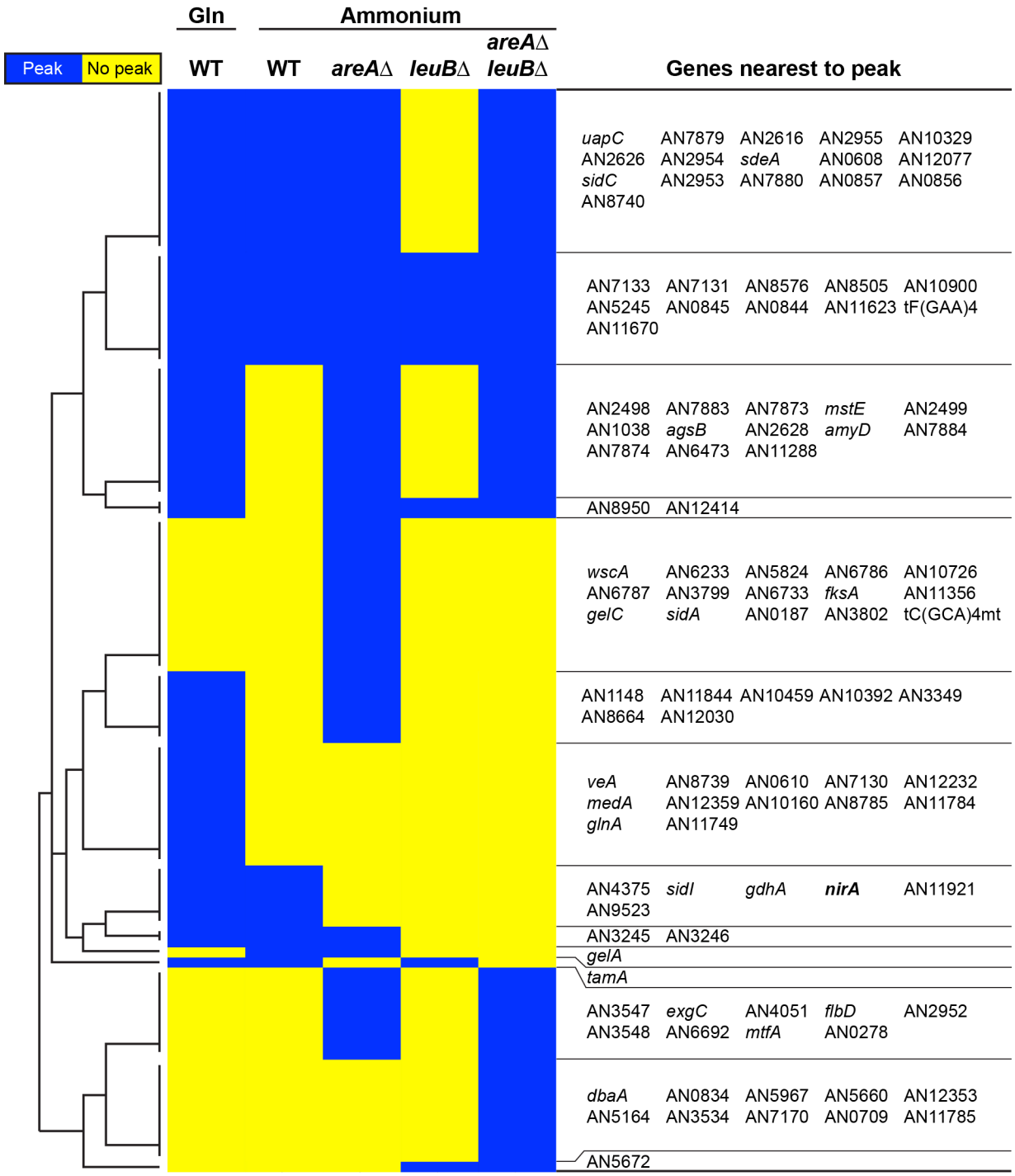

Figure 4.16 TamA binds with and without the aid of AreA and LeuB

Heatmap of TamA^{FLAG} binding peak presence (blue) and absence (yellow) adjacent to genes after ChIP-seq of *tamA*^{FLAG} (WT; RT322), *tamA*^{FLAG} *areA*Δ (RT323), *tamA*^{FLAG} *leuB*Δ (RT324) and *tamA*^{FLAG} *areA*Δ *leuB*Δ (RT325) after 16 hours growth in supplemented liquid ANM with 10 mM glutamine (Gln) and ammonium.

Table 4.11 Genes adjacent to TamA^{FLAG} peaks only observed in *areA*Δ and *leuB*Δ mutants.

Gene	Name	*S. cerevisiae* Ortholog	Description
AN0187			Protein of unknown function
AN0278		*RPL29*	Ortholog(s) have structural constituent of ribosome activity, role in cytoplasmic translation and cytosolic large ribosomal subunit, nucleolus localization
AN0279	*flbD*		Putative transcription factor involved in regulation of asexual and sexual development and in response to nitrogen starvation; contains a myb-like DNA-binding domain
AN0709			Putative zinc-finger protein; expression upregulated after exposure to farnesol
AN0834			Putative ER protein-translocation complex subunit; transcript levels increase during the unfolded-protein response (UPR); ortholog of S. cerevisiae Sec63p
AN10726			Protein of unknown function
AN11356			Protein of unknown function
AN11785			Protein of unknown function
AN12353			Protein of unknown function
AN2952			Ortholog of A. nidulans FGSC A4 : AN8368, A. fumigatus Af293 : Afu3g07900, Afu4g14080, Afu8g00900, A. niger CBS 513.88 : An02g11330, An03g05560 and A. oryzae RIB40 : AO090120000471
AN3534			Protein of unknown function
AN3547			Has domain(s) with predicted ADP binding, catalytic activity, microtubule motor activity, role in nucleoside metabolic process and kinesin complex localization
AN3548			Ortholog of Aspergillus glaucus : Aspgl1_0026445
AN3729	*fksA*	*FKS1*	Putative 1,3-beta-glucan synthase with a predicted role in glucan biosynthesis
AN3730	*gelC*	*GAS1*	Putative 1,3-beta-transglycosidase with a predicted role in glucan processing
AN3799		*ZRT2*	Ortholog(s) have low-affinity zinc ion transmembrane transporter activity, role in low-affinity zinc ion transport, response to zinc ion and plasma membrane localization
AN3802			Protein of unknown function; PalA-dependent expression independent of pH
AN4051			Has domain(s) with predicted heme binding, iron ion binding, oxygen binding activity and role in oxygen transport
AN4052	*exgC*	*EXG1*	Putative glucan 1,3-beta-glucosidase with a predicted role in glucan metabolism
AN4170	*creD*		Arrestin domains and PY motif-containing protein with homology to Saccharomyces cerevisiae Rod1p and Rog3p proteins; expression reduced after exposure to farnesol
AN5164		*NAM9*	Ortholog(s) have structural constituent of ribosome activity and mitochondrial small ribosomal subunit localization
AN5660	*wscA*		Putative plasma membrane sensor-transducer; N- and O- glycosylated and localized in the cell wall and membrane; mutants display a high frequency of swollen hyphae under hypo-osmotic conditions; required for conidiation
AN5672			Has domain(s) with predicted catalytic activity and role in metabolic process
AN5823	*sidA*		L-ornithine N5-monooxygenase; involved in siderophore biosynthesis; null mutant inviable unless medium is supplemented with siderophores
AN5824		*AKR1*	Ortholog(s) have palmitoyltransferase activity and role in protein palmitoylation, protein targeting to membrane, regulation of endocytosis, regulation of pheromone-dependent signal transduction involved in conjugation with cellular fusion
AN5967			Protein of unknown function
AN6233			Ortholog(s) have nucleolus localization
AN6692			Protein of unknown function
AN6733			Ortholog(s) have sequence-specific DNA binding activity and cytoplasm, nucleus, spindle localization
AN6786			Putative beta-1,4-endoglucanase
AN6787	CYP682C1		Putative cytochrome P450
AN7170			Protein of unknown function; transcript upregulated in response to camptothecin
AN7657	*gelA*	*GAS5*	Putative 1,3-beta-transglycosidase with a predicted role in glucan processing; predicted glycosyl phosphatidylinositol (GPI)-anchor; palA-dependent expression independent of pH
AN7896	*dbaA*		Zn(II)2Cys6 transcription factor with a role in secondary metabolite biosynthesis; member of the dba gene cluster; overexpression upregulates dba gene cluster expression; dba cluster expression is coregulated
AN8741	*mtfA*		Putative C2H2 transcription factor involved in regulation of secondary metabolism and morphogenesis
tC(GCA)4mt			Mitochondrial tRNA-Cys, predicted by tRNAscan-SE; GCA anticodon

4.4.7 Integration of TamA^{FLAG} ChIP-seq and tamA mutant RNA-seq data.

We were interested to know which differentially expressed genes in our RNA-seq data set were direct targets of TamA. To determine this we compared differentially expressed genes in the *tamA*Δ and/or *tamA*^{C90L} mutants with genes with proximal TamA^{FLAG} binding in wild type in ChIP-seq analysis. Overall 40 of the 71 genes with nearby TamA binding on glutamine or ammonium showed differential expression under one of the three nitrogen conditions (Figure 4.17), 18 of these genes had DNA-binding and differential expression under the same condition and 6 of the genes were bound and regulated on both ammonium and glutamine (Table 4.12). We observed a large difference in number of genes with differential expression on glutamine and ammonium (1,094) compared with the number of peaks under the same conditions (46). This difference may be due to the higher sensitivity of RNA-seq than ChIP-seq and the identification of indirect TamA targets by RNA-seq. It is likely that TamA binds at additional locations in the genome that were not detected by ChIP-seq. The majority of TamA targets that were differentially expressed and adjacent to a TamA binding site were uncharacterized genes, the characterized genes encode two GOGAT pathway enzymes, two siderophore biosynthesis enzymes and a sugar transporter (Table 4.12). ChIP-seq peaks were primarily associated with either TamA DNA-binding dependent regulation or TamA dual-function regulation, however co-factor regulation was associated with several peaks, suggesting ChIP may be sensitive enough to detect indirect interaction with DNA for non-DNA-binding transcription factors at some promoters. Interestingly, binding was observed at AN0845 and AN5245 on both ammonium and glutamine but TamA showed nitrogen source-dependent modes of regulation, with TamA acting as an activator on ammonium and coactivator on glutamine. Similarly TamA bound in the *sidC* promoter on both ammonium and glutamine but functioned as a co-repressor and a DNA-binding activator under these conditions respectively. *gdhA* was the only proximally TamA^{FLAG}-bound gene regulated by both DNA binding and cofactor functions on the same condition (dual mode of action), as previously shown by ChIP, real-time RT-PCR and reporter gene assays (DOWNES *et al.* 2014a). Consistent with TamA generally acting as a transcription activator, all but three of the 24 binding events observed on glutamine or ammonium were associated with activator/coactivator roles, and at all three repressed genes TamA functioned as a co-factor. Analysis of the distance of binding for each role showed both co-activator and binding roles were associated with both binding close to <500 bp and far from >1 kb the start codon.

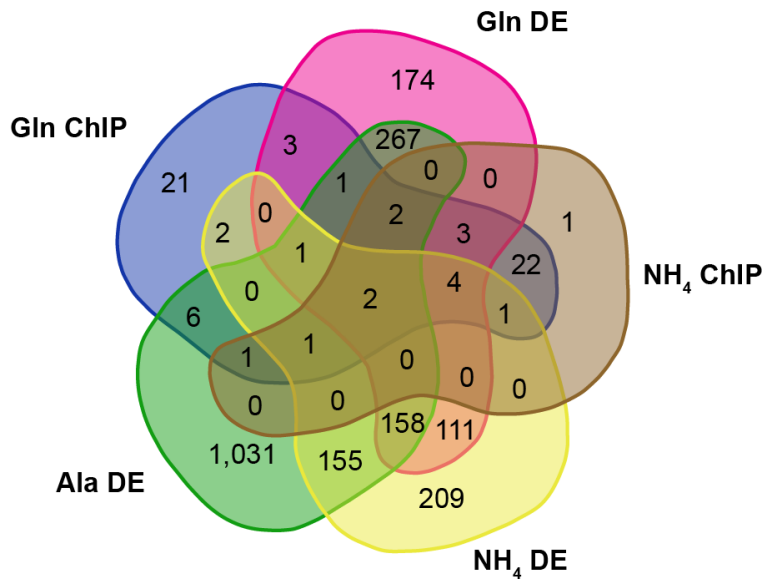

Figure 4.17 Comparison of RNA-seq and ChIP-seq targets

Venn diagram comparison of genes with differential expression on glutamine (Gln DE), ammonium (NH_4 DE) and alanine (Ala DE) with those adjectent to $TamA^{FLAG}$ binding sites from ChIP-seq on glutamine (Gln ChIP) and ammonium (NH_4 ChIP).

Table 4.12 Regulation of direct TamA targets.

	RNA-seq determined TamA function		ChIP-seq binding		Dependent upon (NH_4)		Distance to peak from ATG
Gene	**Gln**	**NH_4**	**Gln**	**NH_4**	**AreA**	**LeuB**	
AN4376 (*gdhA*)	Dual-activator	Dual-activator	+	+	Yes	Yes	-341 bp
AN0845	Co-activator	Activator	+	+	No	No	+954 bp
AN5245	Co-activator	Activator	+	+	No	No	+819 bp
AN2954	Activator	Activator	+	+	No	Yes	-707 bp
AN0607 (*sidC*)	Activator	Co-repressor	+	+	No	Yes	-460 bp
AN2953	Activator	Activator	+	+	No	Yes	-844 bp
AN4159 (*glnA*)	Co-activator		+	–	–	–	-2,245 bp
AN7880	Activator		+	+	No	Yes	-373 bp
AN7879	Activator		+	+	No	Yes	-470 bp
AN3246	Activator		+	+	No	Yes	+2,530 bp
AN2955	Activator		+	+	No	Yes	-1,267 bp
AN4375	Activator		+	+	Yes	Yes	-4,985 bp
AN10392	Undetermined		+	–	–	–	-4,707 bp
AN7883	Activator		+	+	No	Yes	-410 bp
AN7873	Co-activator		+	+	No	Yes	-324 bp
AN5860 (*mstE*)	Co-activator		+	–	–	–	-1,721 bp
AN0609 (*sidI*)		Co-repressor	+	+	Yes	Yes	-1,185 bp
AN9523		Co-repressor	+	+	Yes	Yes	-233 bp

4.4.7.i AN7884 secondary metabolism cluster

Although TamA was observed to regulate several predicted and characterized secondary metabolism genes, we were particularly interested in regulation of the AN7884 cluster as it showed promoter binding in our ChIP-seq experiments and differential expression in our RNA-seq experiments. TamA binding peaks were observed in the bidirectional promoters of AN7873-AN7874, AN7879-AN7880, and AN7883-AN7884 on glutamine (Figure 4.18A). In wild type mycelia the genes within this cluster showed low levels of expression on ammonium and alanine but and were increased on glutamine (data not shown). When we examined expression of the 13 predicted members of the gene cluster we found no effects of either *tamA*Δ or *tamA*^{C90L} during growth on either alanine or ammonium, but nine genes had reduced expression in both *tamA*Δ and *tamA*^{C90L} during growth on glutamine, suggesting TamA-dependent activation as a DNA-binding activator (Figure 4.18B). AN7874 and AN7876 also showed reduced expression in both *tamA*Δ and *tamA*^{C90L}, however this change was significant in only one of the two cuffdiff statistical analyses. In addition, AN7873 showed reduced expression only in *tamA*Δ indicating activation by TamA as a coactivator. Therefore 12 of the 13 genes in this cluster are likely to be regulated by TamA. SCOPE analysis of the sequences under the three peaks in this cluster identified five motifs that were present in all three regions (Table 4.13). However, none of the five consensus sites was consistent with the typical CGG repeats associated with most Zn(II)2Cys6 transcription factor binding sites (TODD AND ANDRIANOPOULOS 1997). Notably regulation of several genes in this cluster was TamA DNA-binding motif dependent, however no TamA promoter binding was detected in the adjacent intergeneic region by ChIP-seq analysis. Transcripts from this region come from both strands and showed clear delineation, excluding the possibility of the genes being transcribed from a single mRNA "operon". The observation of "distant activation" could be due to lower sensitivity of our TamA^{FLAG} ChIP-seq analysis than the RNA-seq in detecting targets. Alternatively, TamA may be able to regulate genes at a distance from the DNA binding sites in promoters of nearby genes. While activation at a distance through enhancers is common for animal transcription factors it is not common for fungal transcription factor binding sites to act at as enhancers.

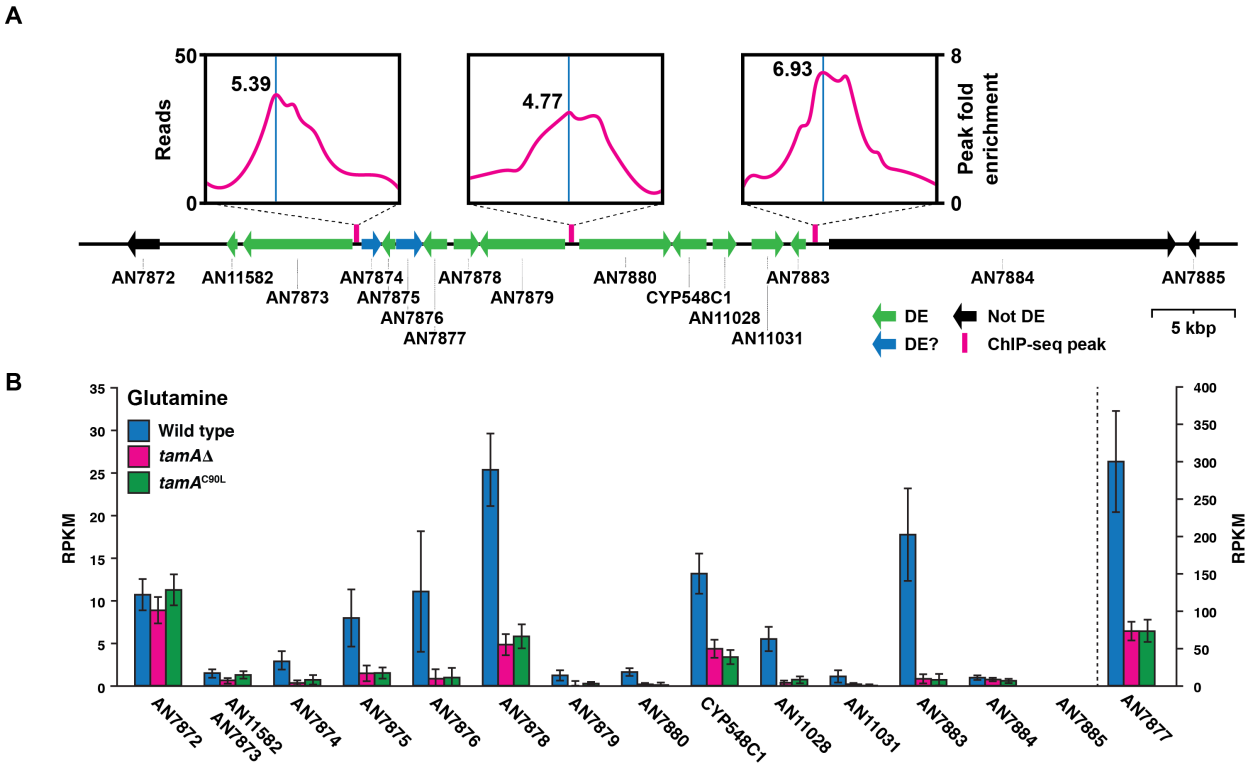

Figure 4.18 Binding at and regulation of the AN7884 secondary metabolite cluster.

A) Gene structure of the AN7884 secondary metabolite cluster showing the location of ChIP-seq identified TamA^{FLAG} binding peaks in two biological replicates of RT322 after 16 hours growth in supplemented ANM with 10 mM glutamine. Peak profiles are shown with number of aligned reads and fold enrichment at the apex (blue line) noted. Cuffdiff identified differentially expressed (DE) genes with $p \leq 0.05$ and $q \leq 0.05$ are green whereas those with $p \leq 0.05$ and $0.20 \leq q \leq 0.05$ are blue. **B)** Expression of genes in the AN7874 secondary metabolite cluster in wild type (MH1), *tamA*Δ (MH8694) and *tamA*^{C90L} (MH11808) strains grown in supplemented ANM with 10 mM glutamine. Error bars depict SEM (N=3). Expression is in reads per kilobase per million aligned reads (RPKM). Note the different scale for AN7877.

Table 4.13 Regulation of the uncharacterized AN7884 secondary metabolite cluster.

Consensus Motif [a]	Sig Value[b]	Number of times present			Program
		AN7873 AN7874	AN7879 AN7880	AN7883 AN7884	
 ACRDWHVDTAC	39.2	2	8	1	SPACER
 ATACG	21.0	2	9	1	BEAM
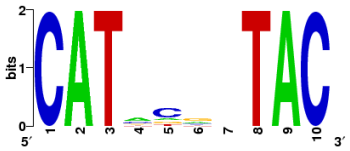 CATNNNNTAC	8.2	1	5	1	SPACER
 KNRGCB	5.3	20	19	24	PRISM
 ATTAC	2.7	4	2	1	PRISM

[a] Units measure bits of information proportional to sequence conservation.
[b] Sig score measures over-representation of a given motif as the -$\log_2$ of the expected number of motifs of the given length and degeneracy. A higher score is representative of greater overrepresentation.

4.4.8 RNA-seq characterization of AreA modes of action

Reports of dual mode of action transcription factors are extremely rare. In addition to TamA, dual modes of action have been reported for the basic Helix-Loop-Helix Hairy repressor in *Drosophilia*, *Xenopus*, and zebrafish (KAGEYAMA *et al.* 2007; NICHANE *et al.* 2008), as well as the mouse SCL/TAL-1 transcription factor (KASSOUF *et al.* 2008). However unlike TamA, which acts as a coactivator or DNA-binding factor dependent on promoter context in a single cell type, dual function of the SCL/TAL-1 proteins is cell type dependent. With a collaborator we are working to characterize the DNA-binding and regulatory network of the AreA GATA transcription factor in response to different nitrogen conditions using ChIP-seq of $AreA^{HA}$ and RNA-polymerase II, and RNA-seq of wild type, *areA*Δ and *areA217* (K.H. Wong, D.J. Downes, G.Y. Busot, and R.B. Todd unpublished). The *areA217* mutant phenotype is caused by an amino acid substitution in the DNA-binding domain that abolishes DNA-binding (KUDLA *et al.* 1990; PLATT *et al.* 1996b). However, this loss-of-DNA binding-function mutant is able to activate gene expression when recruited to a promoter by a FacB-TamA fusion protein (SMALL *et al.* 1999). Therefore AreA acts as a co-activator in this synthetic situation. We were keen to know if, like TamA, AreA regulates genes as both a coactivator and a DNA-binding activator. To distinguish each mode of action we prepared RNA from wild type, *areA*Δ, and *areA217* strains grown on ammonium for 16 hours and transferred to alanine for 4 hours. Stranded cDNA libraries from three independent biological replicates were barcoded and pooled for multiplex sequencing with nine samples per lane. Multiplexed libraries were sequenced on the Hi-Seq 2500 platform and generated an average of 22.4 million reads per library with a minimum of 16.6 million reads and a maximum of 29.5 million reads. Reads were mapped to the *A. nidulans* FGSC_A4 genome sequence (Version S10) with an average of 94.46% of reads mapping to the genome following the same protocol described earlier for *tamA* RNA-seq (Section 4.4.4). For all three conditions reads mapped equally across the genome in each of the strains and housekeeping genes were not differentially expressed (data not shown).

4.4.8.i AreA acts as a cofactor

We identified 3,795 genes with differential expression in *areA*Δ compared to wild type. This is a remarkable ~35% of the genome and demonstrates the importance of nitrogen metabolism on all aspects of organismal physiology. We compared the differentially expressed genes in *areA*Δ and *areA217* for different modes of action using the model expression profiles described earlier (Section 4.4.4; Figure 4.19). We were able to distinguish mode of action at 89% of the genes; the majority (37.1%) of genes were regulated by a DNA-binding dependent mechanism and AreA regulated 568 genes (15%) by the co-factor mode of action. AreA also regulated a large number of genes (33.7%) simultaneously by both DNA binding and DNA binding-independent mechanisms. Interestingly, dual mode of action was less common than either co-factor or DNA-binding dependent modes of activity for TamA, but for AreA dual mode of action was as common as DNA-binding dependent regulation. When loci were separated by increased and decreased expression in *areA*Δ compared to wild type, DNA binding was comparatively richer in genes with decreased expression (43%), i.e activator targets, than for those with increased expression (37%), i.e repressed targets. This difference is consistent with AreA acting primarily as a transcription activator at direct targets.

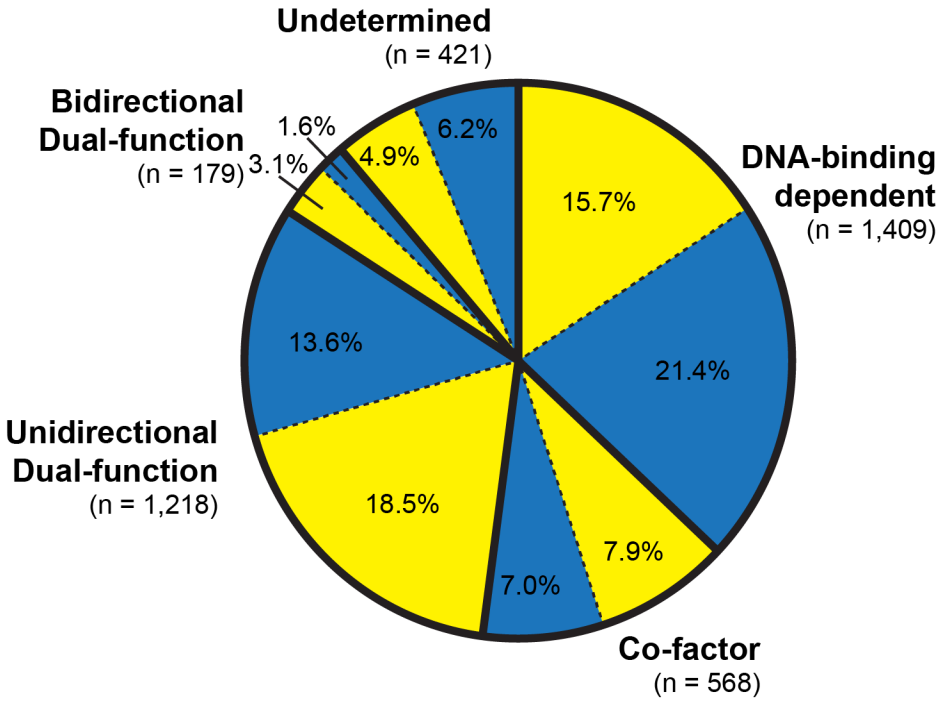

Figure 4.19 AreA is a dual function transcription factor.

Differentially expressed genes as determined by RNA-seq analysis of wild type (MH10244), *areA*Δ (MH5699) and *areA217* (MH11132) strains grown for 16 hours in supplemented ANM with 10 mM ammonium and transferred to alanine for a further 4 hours. Genes were classified into AreA regulatory function based on expression profiles compared to wild type as outlined in Figure 4.5A. Solid lines separate different functions. Broken lines separate genes in each funcion with increased (yellow) and decreased (blue) expression in *areA*Δ compared to wild type.

4.5 Discussion

4.5.1 TamA regulation of gdhA by DNA binding.

Transcription factors have been studied for decades since the discovery that SV40 interacted with sequence specific regions of DNA (TJIAN 1978). The paradigm for understanding gene regulation by transcription factors has been that the DNA-binding domain is required for function. Fungi have a kingdom specific family of Zn(II)2Cys6 binuclear cluster transcription factors of which Gal4p from *S. cerevisiae* is the prototype. However, two proteins in this family have been identified as having dispensable DNA binding motifs: *S. cerevisiae* Dal81p and *A. nidulans* TamA (BRICMONT *et al.* 1991; DAVIS *et al.* 1996). The presence of a conserved but dispensable DNA binding motif has long puzzled researchers. The strong effect of *tamA*Δ at the *gdhA* promoter relative to the effects of *areA*Δ and *leuB*Δ (POLOTNIANKA *et al.* 2004) suggested that TamA may directly bind DNA at this promoter. We have now shown, using both assays of NADP-GDH activity and of *gdhA* expression by means of real-time reverse-transcriptase PCR and reporter gene fusions, that the DNA-binding domain of TamA is not dispensable for function at this promoter (DOWNES *et al.* 2014b). This contrasts with TamA action at the promoters of the nitrogen utilization genes *amdS* and *fmdS,* and genes required for sensitivity to toxic nitrogen analogs. This dichotomy in function is a novel means by which fungal transcription factors can regulate gene expression by DNA-binding dependent or DNA-binding independent mechanisms. Dual DNA binding and non-DNA binding functions have also been described for the basic Helix-Loop-Helix (bHLH) Hairy-Enhancer of Split repressors in *Drosophilia*, *Xenopus,* and zebrafish and the bHLH SCL/TAL-1 transcription factor in mouse (KAGEYAMA *et al.* 2007; KASSOUF *et al.* 2008; NICHANE *et al.* 2008). However, unlike TamA where dual function is observed in a single cell type, dual function in these proteins is cell type dependent.

The regulation of genes by these separate TamA DNA-binding and protein-binding mechanisms is likely promoter context dependent and controlled by the presence of specific DNA-binding sites in the promoter and interaction with other proteins that bind to the promoter. We have shown that TamA binds the *gdhA* promoter *in vitro* and *in vivo*, and that binding *in vivo* is dependent on both the GATA transcription factor AreA and the Zn(II)2Cys6 transcription factor LeuB. AreA also shows co-operative binding with another Zn(II)2Cys6 transcription factor, NirA, at the bidirectional *niiA-niaD* promoter (NARENDJA *et al.* 2002; BERGER *et al.*

2006), a phenomenom also observed for the *N. crassa* orthologs Nit2 and Nit4 (FENG AND MARZLUF 1998). TamA occupancy at the *gdhA* promoter was also dependent on the available nitrogen nutrient, with a greater presence on nitrate and glutamine and lesser presence on glutamate. Several yeast transcription factors are regulated by direct interaction with metabolites and act as nutrient sensors, such as Put3p with proline, Prp1p with orotic acid, and War1p with benzoic acid (reviewed in SELLICK AND REECE 2005). Furthermore, arginine promotes DNA binding of the *S. cerevisiae* arginine biosynthesis Arg81p-Mcm1p complex (AMAR *et al.* 2000). The differences seen in TamA binding at *gdhA* may result from interaction with a nitrogen metabolite and direct nutrient sensing could act as a mechanism to modulate regulation by TamA.

4.5.2 Genome wide regulation by TamA.

Prior to this study TamA was known to act at the promoters of *amdS* and *gdhA* and a handful of unidentified genes that confer sensitivity to toxic nitrogen analogs (KINGHORN AND PATEMAN 1975a; DAVIS *et al.* 1996; POLOTNIANKA *et al.* 2004). *tamA* mutants show very few observable phenotypic growth changes, notably resistance to thiourea, chlorate, methylammonium, and aspartate hydroxamate, and slightly reduced growth on ammonium (KINGHORN AND PATEMAN 1975a; DAVIS *et al.* 1996). RNA-seq showed that TamA regulates an extraordinary number of genes across the genome, including those for nitrogen metabolism, carbon metabolism, secondary metabolism and iron homeostasis. Network analysis of TamA DNA-binding dependent and DNA-binding independent targets demarcated different enriched GO terms for each function. TamA regulation by DNA binding was enriched for siderophore biosynthesis whereas DNA-binding independent regulation was enriched for nitrogen metabolism. The DNA-binding independent or co-activator role of TamA at nitrogen utilization genes is consistent with known interaction with AreA (SMALL *et al.* 1999) and observed DNA-binding independent resistance to toxic nitrogen analogs (DAVIS *et al.* 1996). Using a comparison of gene expression in wild type, *tamA*Δ, and $tamA^{C90L}$ we were able to identify several genes that may confer toxic nitrogen analog sensitivity. For each toxic nitrogen analog TamA regulated two or more candidate genes, and these represented both transport protein genes and enzyme encoding genes, the only exception being methylammonium where three transport

encoding genes were identified as regulated by TamA. TamA also regulates expression of *glnA* and *gdhA*, both of which encode enzymes that directly assimilate ammonium, and both genes have lower expression in *tamA*Δ than *tamA*^{C90L}. Therefore reduced expression of *gdhA* and *glnA* could contribute to *tamA*Δ conferred methylammonium resistance.

TamA showed widespread effects on gene expression across the genome, with ~20% of genes differentially expressed on at least one condition and a third of these genes being regulated by the DNA-binding mode of action. In comparison there were relatively few TamA binding events detected by ChIP-seq. We have yet to perform ChIP-seq on alanine, however, the likely total number of TamA binding targets is unlikely to increase significantly. The low number of binding events may be a result of either technical or biological factors. For ChIP-seq we used a single C-terminal FLAG-epitope tag on TamA, although a 3xFLAG tag is commonly used for this technique (FUREY 2012). The affinity of the M2 anti-FLAG antibody to a single tag is likely lower than to the 3x tag and therefore the identified peaks may only be the ones with greatest TamA occupancy. Surrounding chromatin, interacting proteins, and the location of the tag on the protein (KIDDER *et al.* 2011) could also affect antibody affinity and these factors may play a role in the number of identified TamA peaks. We also performed ChIP-seq using multiplexing, which reduces total coverage generated for each sequenced library and lowers the overall sensitivity for each sample. Therefore, the peaks observed in our experiments may represent only the subset of strongest binding events. Furthermore, we used a high stringency cut-off in MACS peak-calling for our ChIP-seq, $p \leq 1x10^{-7}$ compared with the default $p \leq 1x10^{-5}$ (ZHANG *et al.* 2008), which may have excluded a set of weakly bound genuine targets, and a comparatively relaxed stringency in analysis of our RNA-Seq data. Alternatively, the relatively low number of bound genes compared with differentially expressed genes could be a true reflection of TamA binding. The two genes regulated by TamA and with upstream binding on all tested conditions were *gdhA* and the uncharacterized AN2954. *gdhA* encodes a core metabolism enzyme which is at the interface of carbon metabolism via the TCA cycle, and nitrogen metabolism via the GOGAT cycle.

4.5.3 Is TamA involved in carbon catabolite repression?

In addition to nitrogen assimilation gene regulation we observed in the *tamA* mutants an increase in expression of many carbon metabolism genes, particularly during growth on alanine as the nitrogen source. The primary carbon source during our experiments was glucose, and therefore we expect genes for gluconeogenesis (e.g. *acuD, acuF, acuG*) and utilization of alternative carbon nutrients (e.g. *alcA, alcC*) to be repressed by the CreA carbon catabolite repressor (HYNES AND KELLY 1977; DOWZER AND KELLY 1991). We saw increased expression of these genes in a TamA DNA-binding dependent manner. This increase in expression could be mediated by several mechanisms. One possibility is that TamA is involved directly in carbon catabolite repression and acts as a minor regulator of these genes. Alternatively, reduced expression of the NADP-dependent glutamate dehydrogenase *gdhA*, and increased expression of the NAD-dependent glutamate dehydrogenase *gdhB* likely leads to a net increase in the TCA cycle intermediate 2-oxoglutarate. Increased 2-oxoglutarate levels may result in a signal to relieve carbon catabolite repression and produce glucose for storage. 2-oxoglutarate and 2-oxoglutarate producing carbon nutrients, such as proline and glutamate, induce expression of *acuF* in a GOGAT cycle dependent manner, possibly by increasing the levels of the TCA cycle intermediates succinate and malate (HYNES *et al.* 2002). It will be of interest to determine whether repression by TamA of these carbon metabolic genes is CreA-dependent or via an independent mechanism.

4.5.4 TamA regulation of iron homeostasis and secondary metabolism.

The TamA DNA-binding dependent regulation of *hapX* and siderophore biosynthesis genes was unexpected. TamA appears to repress siderophore biosynthesis genes as a non-DNA binding co-factor during growth on ammonium, but during growth on alanine TamA activates these genes as a DNA-binding protein. $TamA^{FLAG}$ ChIP-seq revealed binding upstream of several siderophore biosynthesis genes, including *sidC* and *sidI*. In addition to regulating the iron metabolism pathway genes, TamA also regulated the pathway regulators SreA and HapX. The control of these two genes by TamA may be a means by which nitrogen signals are integrated into regulation of iron homeostasis (Figure 4.20). Siderophore biosynthesis requires the expression of the non-ribososmal peptide synthase encoded by *sidD* (VON DOHREN 2009;

GRUNDLINGER *et al.* 2013), a class of protein commonly involved in secondary metabolite production. In addition to regulating siderophore genes TamA also regulated several secondary metabolite clusters, including activating penicillin and microperfuranone biosynthesis and activating expression of an uncharacterized secondary metabolite cluster. Nitrogen metabolism regulates secondary metabolism in both an AreA dependent manner, e.g. fumonisin in *F. verticillioidies* (KIM AND WOLOSHUK 2008), and an AreA independent manner, e.g. Apicidin F and Fusaric acid in *F. fujikuroi* (NIEHAUS *et al.* 2014; NIEHAUS *et al.* 2014). Regulation of some AreA independent secondary metabolites, is AreB dependent (reviewed in TUDZYNSKI 2014), however Fusarin C production in *F. fujikuroi* is regulated by nitrogen in an AreA and AreB independent manner (DIAZ-SANCHEZ *et al.* 2012; NIEHAUS *et al.* 2013). Regulation of the penicillin, microperfuranone and AN7874 cluster by TamA was DNA-binding domain dependent and may be the means by which secondary metabolite production is regulated by nitrogen metabolism in an AreA and AreB independent manner.

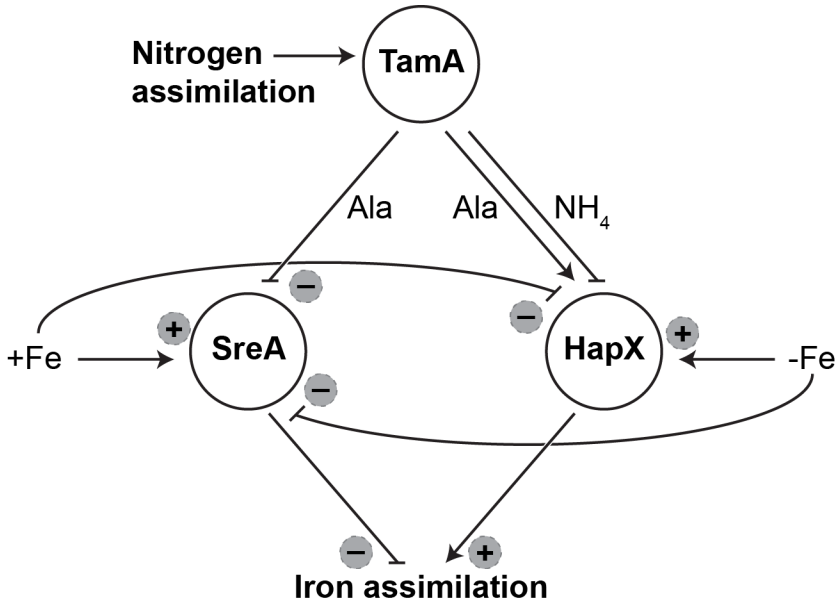

Figure 4.20 TamA regulation of iron homeostatsis.

During growth on ammonium (NH_4) TamA represses *hapX* expression whereas during growth on alanine (Ala) TamA activates *hapX* expression and represses *sreA* expression.

4.5.5 TamA regulation involving additional transcription factors.

Our ChIP-seq analysis of $TamA^{FLAG}$ showed that TamA binds at some genes independently of AreA and LeuB, at some genes with either AreA or LeuB, and at other genes with both AreA and LeuB. We also observed a number of proteins that co-purified with both $TamA^{FLAG}$ and $TamA^{C90L\text{-}FLAG}$. Given the distinct heterogeneity in TamA requiring AreA and/or LeuB to bind at different sites throughout the genome it is possible that TamA interacts with a range of transcription factors to achieve genome wide regulation. Zn(II)2Cys6 transcription factors can function as either homodimers, as with Gal4p (REECE AND PTASHNE 1993), or as heterodimers, for example *A. nidulans* AcuK and AcuM (SUZUKI *et al.* 2012) or *S. cerevisiae* Pdr1p and Pdr3p (WOLFGER *et al.* 1997; MAMNUN *et al.* 2002). Certain transcription factors are also known to form both heterodimers and homodimers. *S. cerevisiae* Oaf1p can form either a homodimer (TRZCINSKA-DANIELEWICZ *et al.* 2008), or a heterodimer with Pip2p (ROTTENSTEINER *et al.* 1997; BAUMGARTNER *et al.* 1999). Similarly the human transcription factor Jun forms both homodimers and heterodimers with Fos (KERPPOLA AND CURRAN 1991). The ability of transcription factors to form different multimers allows them to target a greater number of genes by binding at different DNA target sites, allow integration of responses to different signals, and provides a means through which regulatory networks can be rewired. The lack of a consistent Zn(II)2Cys6 CCG repeat motif under the TamA ChIP-seq peaks may indicate TamA is binding at multiple recognition sites in complex with one or more unknown transcription factors.

4.5.6 Dual mode of action may be a common mechanism for transcription factors.

TamA was first classified as having a dispensable DNA-binding domain for known functions (DAVIS *et al.* 1996). By studing the regulation of the core nitrogen assimilation gene we have shown the DNA-binding motif is not dispensable for TamA function and shown TamA is a dual function transcription factor (DOWNES *et al.* 2014b). This was the first such report for a Zn(II)2Cys6 fungal transcription factor. Using RNA-seq of the *tamA*Δ deletion mutant and *tamA*^{C90L} loss-of-DNA-binding mutant we showed that TamA regulates a large proportion of the genome through its DNA-binding dependent and DNA-binding independent modes of action. Using a similar approach with two *areA* mutants, *areA*Δ and *areA217*, we have also shown that the GATA family of transcription factors can also function simultaneously by DNA binding dependent and DNA binding independent mechanisms. The bHLH transcription factor family also shows dual function for mammalian TAL1 and the Hairy-Enhancer of Split repressors in Xenopus, zebrafish and Drosophila (KAGEYAMA *et al.* 2007; KASSOUF *et al.* 2008; NICHANE *et al.* 2008). Therefore three classes of transcription factor across a wide variety of organisms now share dual DNA binding and non-DNA binding modes of action. The prevalence of dual modes of action remains unclear. Only one other genome-wide study of this type of dual function regulator has been performed. ChIP-seq analysis of wild type and the DNA-binding motif mutant was performed for TAL1 (KASSOUF *et al.* 2010). Kassouf and colleagues analyzed the TAL1 dual function regulatory network using ChIP-seq and microarray analysis of wild type TAL1$^{WT/WT}$ and TAL1$^{RER/RER}$ DNA-binding motif mutant in erythroid cells. Using ChIP-seq they were able to detect 2,994 peaks, 594 of which remained in the Tal1$^{RER/RER}$ mutant indicating they could detect non-DNA-binding target genes. As with our TamA^{FLAG} ChIP seq not all TAL1 binding events were associated with changes in regulation. When they compared expression analysis from the wild type and mutant cells they were able to identify 83 direct DNA-binding targets, ~16% of the differentially expressed genes in the TAL1$^{RER/RER}$ mutant, including genes for several transcription factors and structural proteins involved in erythropoiesis (KASSOUF *et al.* 2010). Our RNA-seq experiments show that this technique provides a powerful tool for identifying the DNA binding and DNA-binding-independent regulatory networks of a dual function transcription factor. Therefore this strategy can be exploited to determine the prevalence of dual modes of action for other transcription factors with a range of functions in a variety of organisms.

4.5.7 Dual functions may promote regulatory network plasticity.

Transcription factor networks are extremely plastic and changes in DNA binding sites in orthologous gene promoters are observed in closely related species (TSONG *et al.* 2006). Often changes in DNA binding sites and *trans* acting transcription factors do not lead to overall changes in the network out-put (TSONG *et al.* 2006). For example, mating type in *S. cerevisiae* is determined by repression of the **a** mating type specific genes in **α** cells by the α2 homeodomain protein. In the related yeast *C. albicans* **a** specific genes are not regulated by α2 in the **α** cells, but instead are activated in the **a** cells by the HMG-domain transcription factor a2. In *Kluyveromyces lactis* both mechanisms are observed (TSONG *et al.* 2006). The regulatory mechanisms in this network are different but the net outcome is the same. Changes in regulatory networks can also result from gene duplications and novel protein-protein interactions which lead to increased regulatory complexity (BAKER *et al.* 2013). Dual function transcription factors may facilitate changes in regulatory circuitry by providing an evolutionary or fitness advantage to cells with sequence changes in their promoter that lead to DNA binding (Figure 4.21). Changes in regulatory network would evolve whereby a bound transcription factor interacts with a non-DNA-binding transcription factor. Over time the promoter would develop mutations and evolve a DNA-binding site for the second transcription factor, this transcription factor is no longer dependent on the primary transcription factor for promoter interaction and both proteins can work co-operatively or independently. Further changes may the lead to loss of interaction between the two transcription factors. Promoter plasticity changes following this evolutionary scheme may lead to net stability in the regulatory network or the addition of novel signals (Figure 4.21).

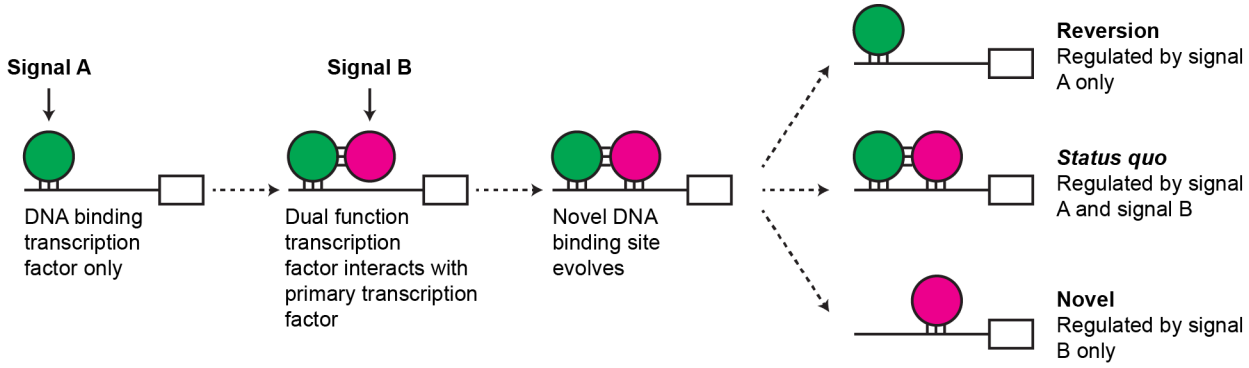

Figure 4.21 Dual function facilitates regulatory network plasticity.

Model of how protein-protein interactions and protein-DNA interactions by dual function transcription factors can bring genes under the control of novel regulatory signals and lead to gradual evolution of regulatory networks.

4.6 Future Directions

We have now shown that, in addition to bHLH transcription factors, Zn(II)2Cys6 transcription factors and GATA transcription factors can operate by two distinct DNA binding and DNA binding-independent modes of action. These distinct functions have now been observed in *Aspergillus*, mouse, *Xenopus*, zebrafish and *Drosophila.* Therefore three classes of transcription factor across a wide variety of organisms now share dual DNA binding dependent and independent modes of action. The prevalence of dual modes of action remains unclear. We have now shown that RNA-seq experiments provide a powerful tool for identifying the DNA binding and DNA-binding-independent regulatory networks of a dual function transcription factor. Therefore this strategy can be exploited to determine the prevalence of dual modes of action for other transcription factors with a range of functions in a variety of organisms. The prevalence of dual function Zn(II)2Cys6 factors in yeast could readily by examined by RNA-seq of knockout and DNA-binding domain mutants of *DAL81* and *GAL4* that already exist. Mutants in other families of transcription factor could also be used, for example the *C. elegans* genes *lin-1* and *lin-31*, which encode members of the winged-helix and ETS domain familes respectively, have both knockout and point mutation alleles with loss-of-DNA-binding (MILLER, HESS, DOROQUEZ AND ANDREWS 2000; MILEY *et al.* 2004).

Our TamA^{FLAG} ChIP-seq analysis in the *areA*Δ and *leuB*Δ backgrounds showed that TamA binds at other promoters independently of these two proteins. We also observed a number of additional proteins that co-purified with TamA^{FLAG} and TamA$^{C90L.FLAG}$. These bands may represent different transcription factors that TamA interacts with. The analysis of regions under TamA ChIP-seq peaks failed to identify a strong consensus motif. The co-purified bands should be examined by Mass Spectroscopy (MS) to identify candidate TamA interacting transcription factors. Novel candidate TamA interacting proteins could then be confirmed by yeast-two hybrid analysis, co-immunoprecipitation or bimolecular fluorescence complementation. Identifying other proteins that TamA can bind with may help in dissecting promoters to identify TamA binding sites. The combined TamA ChIP-seq/RNA-seq analyses also highlighted a role for TamA in regulation of secondary metabolite clusters, including the uncharacterized AN7874 cluster. Deletion of the nonribosomal peptide synthase in this cluster (AN7884) could be used to identify a missing metabolite by MS of mycelial extracts grown on glutamine.

[This page is not blank.]

Chapter 5 - Regulation and mode of action of NmrA

5.1 Abstract

Regulation of the GATA transcription activator AreA in response to different nitrogen nutrients is mediated by an array of mechanisms, including protein-protein interactions with the co-repressor NmrA. However, the exact mode of action of NmrA remains to be determined. It is known that the level of *nmrA* expression is important for function. The bZIP transcription activator MeaB facilitates regulated expression of *nmrA*. Both *meaB* and *nmrA* show high levels of expression during nitrogen sufficiency when AreA is least active. During nitrogen limitation or nitrogen starvation, when AreA is most active, *meaB* and *nmrA* show reduced expression. The extent of MeaB function at the *nmrA* promoter is perceived in the literature as controversial. Using quantitative real-time reverse transcriptase PCR we have characterized *meaB* and *nmrA* expression and we show that MeaB is required for the wild type pattern of *nmrA* expression. To further understand the role of NmrA we have characterized a novel mutant isolated as an extragenic suppressor of the effects of *nmrA* overexpression. By whole genome sequencing we identified mutations unique to the mutant in two candidate genes, AN4102 and AN4210. The mutation in AN4102 is a conservative missense mutation, whereas the mutation in AN4210 is a frame shift truncation. This mutation is most likely to confer suppression of *nmrA* overexpression. AN4210 is predicted to encode a protein containing a MED15/GAL11 domain found in a transcription mediator complex component. This suggests NmrA represses AreA though either direct or indirect interaction with the RNA polymerase II mediator complex.

5.2 Introduction

Coordinate gene expression by the *Aspergillus nidulans* GATA factor AreA in response to nitrogen nutrients is an intricately regulated process, as outlined in Chapter 1. One of the mechanisms that regulate AreA activity is a protein-protein interaction with NmrA, a co-repressor. *nmrA* was identified and cloned based on sequence similarity to *Neurospora crassa* NMR1 (ANDRIANOPOULOS *et al.* 1998). NmrA represses the activity of AreA during nitrogen sufficiency as deletion of *nmrA* leads to partial derepression of AreA (ANDRIANOPOULOS *et al.* 1998). In *N. crassa,* NMR1 represses activitiy of the AreA ortholog NIT2 and mutation of *nmr-1* leads to derepression (FU *et al.* 1988; XIAO *et al.* 1995). When preferred nitrogen sources are absent, NmrA/NMR1-mediated repression is relaxed and AreA/NIT2 activates its target genes to relieve nitrogen metabolite repression (Figure 5.1). The C-terminal region of AreA/NIT2 is required for repression by NmrA and Nmr1, as mutants lacking the C-terminus show partial derepression (PLATT *et al.* 1996a,b; PAN *et al.* 1997; ANDRIANOPOULOS *et al.* 1998). In *N. crassa,* NMR1 also interacts with the NIT2 DNA binding domain and can block DNA binding *in vitro* (XIAO *et al.* 1995; PAN *et al.* 1997). In *A. nidulans*, despite NmrA interacting with the AreA DNA binding domain (LAMB *et al.* 2003), AreA preferentially binds GATA containing oligonucleotides over NmrA *in vitro* (LAMB *et al.* 2004). Therefore NmrA is thought to act by means other than blocking AreA DNA binding.

NmrA is the type member of the NmrA-like structural family whose members include the Human protein HSCARG (ZHENG *et al.* 2007). Proteins in this family have a Rossman fold, similar to that of the short-chain dehydrogenase-reductase (SDR) superfamily. In *Magnaporthe oryzae nmr1*^{T13V}, which encodes a single residue substitution in the NADP-binding site of NMR1, is unable to complement the *nmr1*Δ mutant (WILSON *et al.* 2010). However, *A. nidulans* NmrA lacks the SDR catalytic motif required for dehydrogenase-reductase activity (STAMMERS *et al.* 2001), suggesting NADP binding but not NADP reduction is required for NmrA function. NmrA-family members may play a role in sensing changes in NAD(P)+ to NAD(P)H ratios to bring about signaling events as NmrA binds both NAD+ and NADP+ with higher affinity than NADH and NADPH (LAMB *et al.* 2003). Despite this, the presence of these molecules does not affect strength of NmrA binding to AreA (LAMB *et al.* 2003) so the role of the Rossman fold, if any, in repression remains to be established.

Overexpression of NmrA inhibits *A. nidulans* from utilizing alternative nitrogen sources, indicating that NmrA levels are important for repression (WONG *et al.* 2007). This finding is further supported by the regulated proteolysis of NmrA in response to alternative nitrogen sources (ZHAO *et al.* 2010). In wild type strains expression of *nmrA* mRNA is regulated by nitrogen source. *nmrA* has higher levels of expression during growth on preferred nitrogen sources than during growth in either nitrogen limitation or nitrogen starvation conditions (WONG *et al.* 2007; ZHAO *et al.* 2010). Regulated expression of *nmrA* is in part controlled by a positively acting bZip transcription factor, MeaB (Figure 5.1) (WONG *et al.* 2007; WAGNER *et al.* 2010). *meaB* expression is also regulated by nitrogen source, and is expressed highly when preferred nitrogen sources are present (WONG *et al.* 2007). Expression of *meaB* is reduced in the presence of the alternative nitrogen source alanine (SIBTHORP *et al.* 2013), and further reduced during nitrogen starvation (WONG *et al.* 2007). The *meaB* locus also encodes an antisense transcript (Figures 3.1 & 5.2), which is regulated by AreA via a HGATAR site in the first intron. The *meaB* antisense transcript shows an inverse expression pattern to the forward *meaB* transcript (SIBTHORP *et al.* 2013) and is thought to control the MeaB-NmrA-AreA regulatory circuit by an unknown mechanism (Figure 5.1).

It was shown by WONG *et al.* (2007) that the bZip transcription factor MeaB is required for wild-type levels of *nmrA* expression during nitrogen sufficiency. In their paper they stated: "*regulated expression of* nmrA *is dependent on MeaB*". This conclusion was disputed in subsequent work by WAGNER *et al.* (2010), as they found using quantitative Northern that *nmrA* is expressed, though at a lower level, in the *meaB*Δ mutant. Wong *et al*. also observed low levels of *nmrA* expression in the *meaB*Δ mutant. In this chapter we have used quantitative reverse transcriptase PCR to investigate the regulated expression of both *nmrA* and *meaB* and show that the wild type expression pattern of *nmrA* is dependent on the presence of MeaB.

To further understand the mechanism of NmrA action, spontaneous suppressors of *nmrA* overexpression with restored growth on nitrate were isolated (M.A. Davis, unpublished data). Several mutations occurred in *nmrA,* one mapped to *areA,* one mapped to *xylR,* and one was not linked to these loci. The novel unlinked mutant showed a fluffy (aconidial) growth phenotype with few reduced conidiophores (R.B. Todd and M.A. Davis, unpublished data). We have used next generation sequencing to identify the likely causative mutation in the novel mutant.

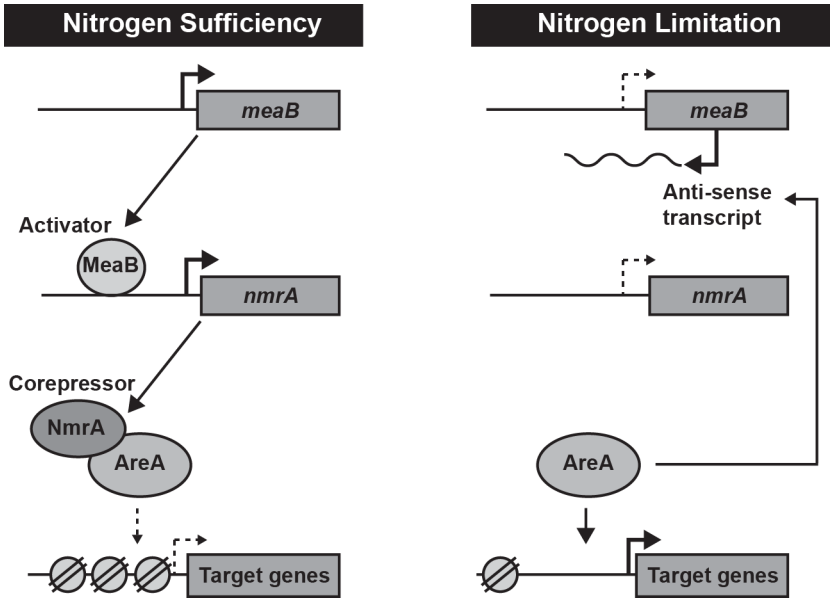

Figure 5.1 MeaB, NmrA and AreA form a regulatory feedback loop

meaB encodes a bZIP transcription activator, which promotes transcription of the *nmrA* co-repressor during nitrogen sufficient conditions (glutamine and ammonium). NmrA interacts with the DNA-binding domain and C-terminus of AreA to repress target gene expression by an unknown mechanism. During nitrogen limitation and nitrogen starvation AreA upregulates an antisense transcript of *meaB* via a HGATAR site in the first intron. Increased antisense transcript expression correlates with reduced *meaB* and *nmrA* expression and derepression of AreA.

5.3 Materials & Method

5.3.1 Plasmid construction

To reconstruct AN4210$^{A1707\Delta}$ the +256 to +3,124 bp coding region of AN4210 excluding the first ATG codon but containing the A1707Δ mutation was amplified from MH12399 with AN4210_f (5'-GCACTCCTTGTCTGTCACTAAGCAC-3') and AN4210_r (5'-CCTCTGGGGCATTCTTGCCG-3'). The resultant fragment was digested with *Bam*HI/*Sac*I leaving the +962 to +2,582 bp region of AN4210, which was ligated into *Bam*HI/*Sac*I cut pSM6392, containing the *A.f. riboB*$^{+}$ selectable marker, to produce pDD234. Wild type AN4210 (-879 to +5,460 bp) was amplified from MH1 using primers supplied by the FGSC (5'-GTAACGCCAGGGTTTTCCCAGTCACGACGCCTCTCCTCTCCTCTCTCTT-3' and 5'-GCGGATAACAATTTCACACAGGAAACAGCGGCTCTCACCTGGTACTTAT-3') and ligated into pGEM-T-easy to generate pAB236.

5.3.2 Whole genome sequencing

Genomic DNA was isolated from MH8, MH11509 and MH12399 after overnight growth in supplemented liquid ANM with 10 mM ammonium. DNA extraction, sequencing and analysis are described in detail in Chapter 2.10 and 2.11.

5.3.3 Strain construction

A *pyrG*$^{-}$ uracil and uridine auxotroph of MH12399 (*xylP*(p)::*nmrA-A.f.pyroA-yA xnrev1-1 niiA4 areA102 nkuA*Δ *pyroA4*) was isolated by treatment with 1 mg ml^{-1} 5-FOA on supplemented ANM-ammonium media (see Chapter 2.5.7) making RT221 (*xylP*(p)::*nmrA-A.f.pyro-yA xnrev1-1 niiA4 areA102 nkuA*Δ *pyroA4 pyrG*$^{-}$). Deletion of AN4102 and AN4210, confirmation, and analysis of the AN4012Δ and AN4210Δ mutants was performed by CC Hunter, AM Brokesh, and RB Todd. pDD234 was transformed into MH11509 (*xylP*(p)::*nmrA-A.f.pyroA-yA pyroA4 riboB2 fmdS-lacZ nkuA*Δ) and plated on media lacking riboflavin. pAB236 was co-transformed with pAB4626 (BORNEMAN *et al.* 2001), which contains *A.n. pyrG* in pBluescript SK+, into RT221 and protoplasts were plated on uridine and uracil lacking media.

5.3.4 Primers for qRT-PCR

Primers used for real-time reverse transcriptase PCR (qRT-PCR) are listed in Table 5.1. Primer design and qRT-PCR is described in Chapter 2.6.2.

Table 5.1 *benA*, *meaA*, *meaB* and *nmrA* qRT-PCR primers

Primer	Sequence (5' → 3')	Target region	Efficiency (55.9ºC)
benA_RT_F	CCTCGCTCCGCTATCTTCC	*benA*: +1354 to +1486 bp	100.7 %
benA_RT_R	GACTGGTTCTTGCTGTGGAT		
meaA_RT_F	TTCGGTCTGATGAAGGTT	*meaA*: +477 to +609 bp	101.4 %
meaA_RT_R	ATCTGGTAGAAGGCGTAG		
meaB_RT_F	CCTTCTGCGTACTATCCAT	*meaB*: +1235 to +1386 bp	108.4 %
meaB_RT_R	ATTCGTGCTCGTCATCAA		
nmrA_RT_F	AAGGTCGAGATCAAAGTCA	*nmrA*: +807 to +918 bp	111.2 %
nmrA_RT_F	GGGAGAATTCGGGTAGAG		

5.3.5 Protein domain identification

SWISS-MODEL was used to generate prediction of partial protein structure of AN4210. The entire protein sequence of AN4210 was used to identify templates. Modeling was carried out on AN4210 residues 50-120 and residues 53-123 with CBP and Gal11p respectively using default settings for modeling (BIASINI *et al.* 2014). 9aaTADs were identified using an online prediction tool (http://www.med.muni.cz/9aaTAD/) (PISKACEK *et al.* 2007) with the entire protein sequence of AreA and NmrA with the moderately stringent pattern, which is recommended as generally best for mammalian and yeast transcription factors.

5.4 Results

5.4.1 Regulated expression of meaB and nmrA

Previous studies of *nmrA* and *meaB* expression have used either semi-quantitative reverse transcriptase PCR (RT-PCR) (WONG *et al.* 2007) or quantitative Northern blot analysis (WAGNER *et al.* 2010; SIBTHORP *et al.* 2013). Though useful techniques when fold change is large, neither is precise for small changes and can be affected by factors such as anti-sense transcripts. The region amplified to quantify *meaB* expression in the Wong *et al.* study overlaps an antisense transcript (SIBTHORP *et al.* 2013) (Figure 5.2). To properly investigate the relationship between *nmrA* and *meaB* expression we performed quantitative real-time reverse-transcriptase PCR (qRT-PCR) of mRNAs of both genes and the ammonium permease *meaA*. In wild type strains *meaB* expression was highest on ammonium and alanine and decreased during nitrogen starvation (Figure 5.3A). We did not see a significant decrease in *meaB* expression on alanine when compared with ammonium that has been described (SIBTHORP *et al.* 2013). During growth on alanine and during nitrogen starvation *meaB* expression was unaffected by *nmrA*Δ, however there was a slight reduction (26%) of expression in the *nmrA*Δ mutant during growth on ammonium. Analysis of *nmrA* expression in wild type showed high levels of expression during growth on ammonium with reduced expression when preferred nitrogen sources were absent (Figure 5.3B). *nmrA* transcript expression was reduced during growth on ammonium by 82% in the *meaB*Δ mutant. During nitrogen limitation and nitrogen starvation there was no effect of *meaB*Δ on *nmrA* expression (Figure 5.3B). Quantitative RT-PCR of *meaA* in wild type showed increased expression when preferred nitrogen sources are absent compared to during growth in the presence of ammonium (Figure 5.3C), consistent with it being a target of AreA activation (MONAHAN *et al.* 2002a). Furthermore, *nmrA*Δ also led to an increase in expression during growth on ammonium but not on alanine or during nitrogen starvation when NmrA activity is reduced. Interestingly *meaB*Δ had no effect on *meaA* expression during growth on ammonium despite causing significantly reduced *nmrA* transcript levels. However, *meaB*Δ led to a strong reduction of *meaA* expression during growth on alanine suggesting a nitrogen regulatory role independent of *nmrA*. The decrease we observed in *meaB* expression in the *nmrA*Δ mutant during growth on ammonium was not observed in the previous studies, however expression profiles on alanine and during nitrogen starvation were consistent in the three data sets (WONG *et*

al. 2007; WAGNER *et al.* 2010) and shows NmrA does not regulate *meaB* under these condtions. Expression of *nmrA,* which was the source of interpretational differences between the two published articles, was similar in all three data sets. The greatest effect of *meaB*Δ on *nmrA* expression was during growth on ammonium. As reported by Wong and colleagues the expression pattern of *nmrA* is clearly dependent on MeaB regulation, however *nmrA* expression is not entirely dependent on MeaB, consistent with the findings of both WONG *et al.* (2007) and WAGNER *et al.* (2010).

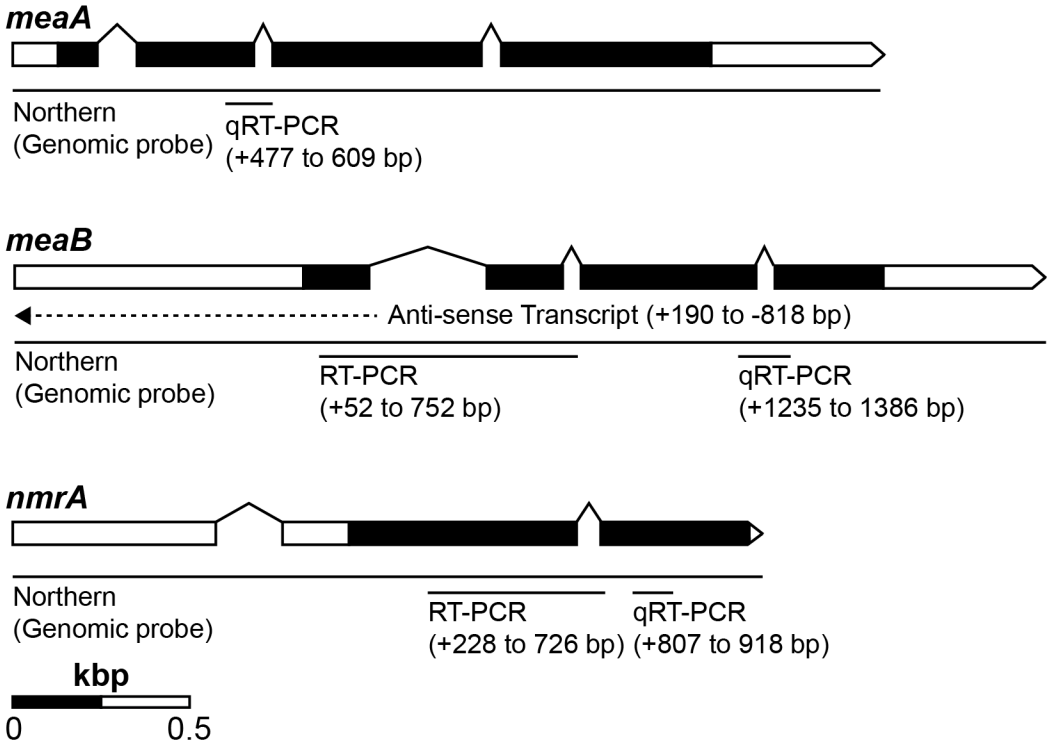

Figure 5.2 Methods for measuring expression of *meaA, meaB* and *nmrA*.

Regulated expression of the ammonium permease gene *meaA* and the transcription factor genes *meaB* and *nmrA* were measured using quantitative Northern blot, semi-quantitative reverse-transcription PCR (RT-PCR) and quantitative real-time reverse-transcription PCR (qRT-PCR). Probes indicated for Northern (WAGNER *et al.* 2010), RT-PCR (WONG *et al.* 2007) and, qRT-PCR (this study) are indicated with nucleotide co-ordinates relative to the +1 ATG. Probes for *meaB* used by Wong *et al*. and Wagner *et al.* overlapped with the *meaB* antisense transcript that was discovered later (SIBTHORP *et al.* 2013).

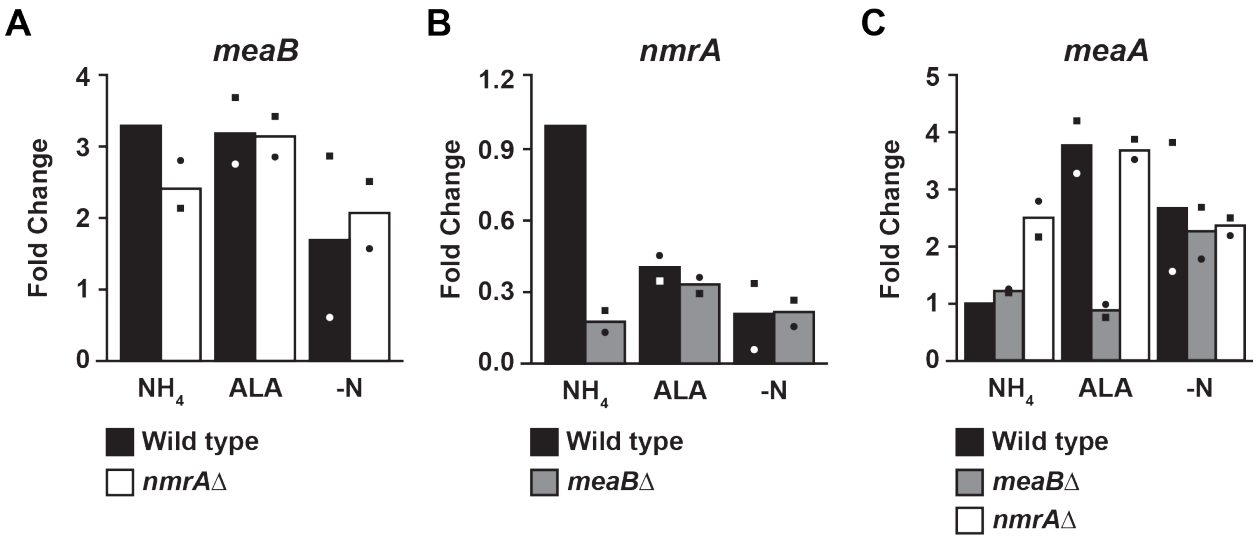

Figure 5.3 Regulated expression of *meaB*, *nmrA* and *meaA*.

qRT-PCR of *meaB* (A), *nmrA* (B) and *meaA* (C) from wild type (MH1), *nmrA*Δ (MH8882), and *meaB*Δ (MH11801) after growth in supplemented-ANM with 10 mM ammonium (NH_4) and 10 mM alanine (ALA) at 37ºC for 16 h or after growth with ammonium for 16 h and transfer to nitrogen starvation (-N) for 4 h. Two biological replicates are presented (squares and circles) bars represent mean relative expression to WT growth on NH_4 (bars).

5.4.2 Characterization of a suppressor of **nmrA** *overexpression.*

5.4.2.i Phenotypic effects of XNREV1-1.

AreA activation of target genes can be modulated by ectopic overexpression of the co-repressor NmrA (WONG *et al.* 2007). When *nmrA* is overexpressed using the xylose-inducible *xylP* promoter *A. nidulans* grows poorly on alternative nitrogen sources (Fig 5.4A). A spontaneous suppressor mutant able to utilize nitrate during NmrA overexpression was isolated and designated XNREV1-1 for ***x****ylP*(p)*::****n****mrA* **rev**ertant (M.A. Davis, unpublished data). XNREV1-1 was determined to be unlinked to either *areA* or *nmrA* in crosses (M.A. Davis, unpublished data). Unfortunately the original XNREV1-1 mutant was lost, however a single progeny MH12399 from the cross of XNREV1-1 to MH8 (*biA1 areA102 niiA4*) was recovered. Genotyping of this strain by growth testing showed it had inherited the *niiA4* nitrite reductase loss-of-function mutation (PATEMAN *et al.* 1967) from the MH8 parent, thus suppression of *nmrA* overexpression on nitrate could not be confirmed. However, this progeny showed suppression of *nmrA* overexpression on glutamate, alanine and ɣ-aminobutyric acid (GABA) (Figure 5.4A). As well as suppressing *nmrA* overexpression, the XNREV1-1 mutant has a fluffy, aconidial colony morphology with a slower growth rate than wild type (Figure 5.4B,C). The fluffy colony morphology is due to reduced conidiophores that produce few condia (Figure 5.4B), reminiscent of mutations in the chromatin-remodeling SAGA complex genes *adaB* and *gcnE* (REYES-DOMINGUEZ *et al.* 2008; CANOVAS *et al.* 2014). Sequencing of the coding region of the SAGA complex genes, *adaB, adaC,* and *gcnE* from XNREV1-1 showed all three genes were wild type in MH12399 (K.S. Siebert and R.B. Todd, unpublished data).

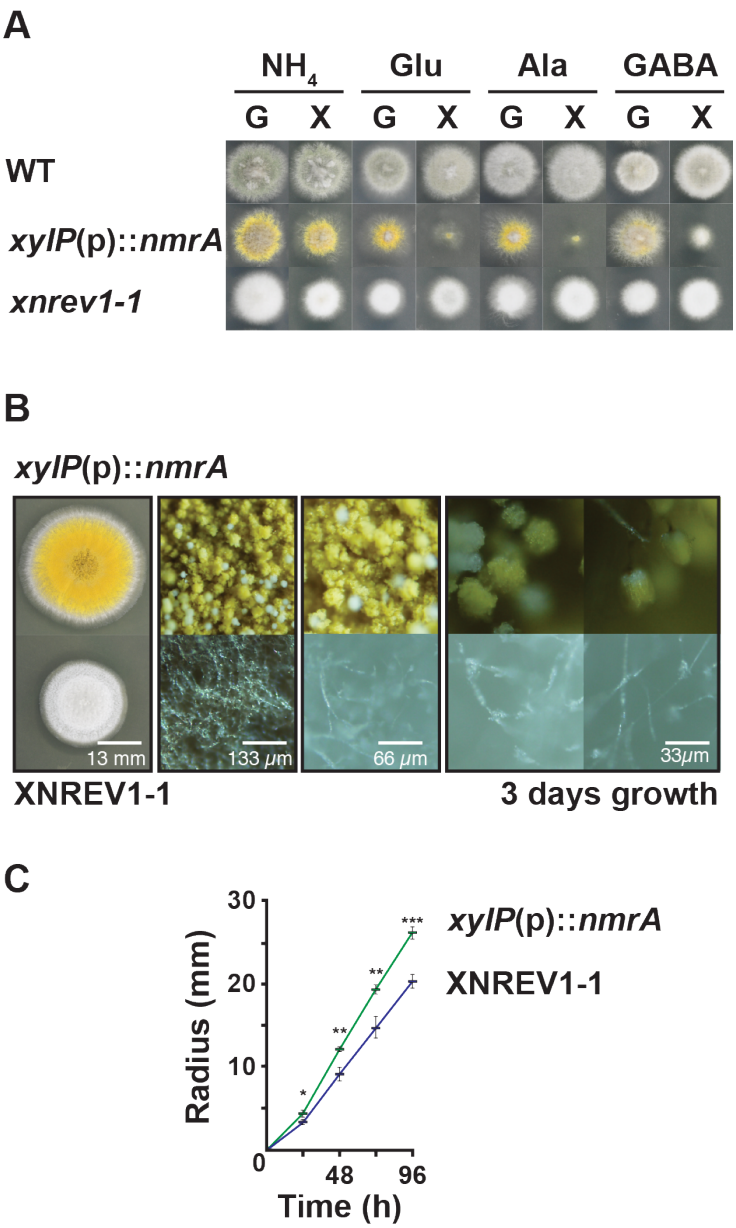

Figure 5.4 XNREV1-1 suppresses *nmrA* overexpression.

A) Wild type (MH1; WT), an *nmrA* overexpressing strain (MH11509; *xylP*(p)::*nmrA*) and XNREV1-1 (MH12399) grown on supplemented carbon free media containing either 1% glucose (G) or 1% xylose (X) and 10 mM ammonium tartrate (NH_4), glutamate (Glu), alanine (Ala), or ɣ-aminobutyric acid (GABA). **B)** Microscopy of MH11509 and XNREV1-1 colonies and conidiophores after three days growth on 1% complete media. **C)** Growth rate of MH11509 and XNREV1-1 on 1% complete media. Significant difference (* = $p < 0.05$, ** = $p < 0.01$ and *** = $p < 0.005$) was calculated using the two-tailed Student's t-test with unequal distribution for three biological replicates.

5.4.2.ii Identification of putative XNREV1-1 causative mutations.

To identify the gene associated with the causative mutation in XNREV1-1 a cloning by complementation approach was adopted. A spontaneous uridine and uracil auxotroph of MH12399 was isolated by selection for 5-FOA resistance. The resultant *pyrG*$^{-}$ strain was transformed with the AMA-*niaD* genomic library, containing the *A. fumigatus pyrG*$^{+}$ selectable marker (OSHEROV *et al.* 2000), and plated on both non-selective media (containing uracil and uridine) and selective media (lacking uracil and uridine). Protoplasts germinating on non-selective media were visually screened for restored conidiation, however no conidiating transformants were apparent after three separate transformations. Thirteen *pyrG*$^{+}$ transformants were isolated from selective media after two transformations, all of which maintained the fluffy phenotype. Growth tests of these strains on xylose media showed they were able to utilize alternative nitrogen sources glutamate and alanine during *nmrA* overexpression, i.e. were not complemented for suppression of NmrA overexpression (data not shown). As the poor conidiation phenotype negatively impacted the number of protoplasts able to be generated for each transformation it was apparent a large number of transformations would be required to identify XNREV1-1 by complementation. Recent studies in several filamentous fungi have highlighted the ease of identifying causative mutations from outcrossed progeny of genetic screens by whole genome sequencing (MCCLUSKEY *et al.* 2011; POMRANING *et al.* 2012; BIELSKA *et al.* 2014; DOWNES *et al.* 2014a; TAN *et al.* 2014; YAO *et al.* 2014; also see Chapter 6.4.4.i). Therefore a whole genome sequencing approach was taken to identify the causative mutation in XNREV1-1.

Genomic DNA isolated from the XNREV1-1 outcrossed progeny MH12399, the outcross parent MH8, and the original parent of the spontaneous sector MH11509 was sequenced using the Illumina HiSeq-2500 Platform. The sequence reads generated from the three strains were aligned to the *A. nidulans* reference genome (Version S10) using a Burrows-Wheeler Alignment (LI AND DURBIN 2009) with an average of 20-fold to 50-fold coverage across the genome (Figure 5.5A). Only 2.3% of the genome had less than 4-fold coverage required for confident variant calling. Variants present in each of the three strains were identified using Free Bayes (GARRISON AND MARTH 2012). In total 1,864 sequence variants were identified by comparison to the FGSC_A4 reference genome, only two of which were unique to XNREV1-1 (Figure 5.5B). The two unique mutations in XNREV1-1 were in the coding regions of AN4102 (*bglA*) and AN4210,

which were 337 kbp apart on chromosome II. *bglA* is predicted to encode a beta-glucosidase (SALAZAR *et al.* 2009). The mutation within *bglA* is a guanine to adenine transition (G914A) resulting in an alanine to threonine substitution at residue 206 (Figure 5.5C). This alanine residue is conserved in 18 of the 19 species in the *Aspergillus* genome database, the exception being *Aspergillus aculeatus,* which has a serine at this position (Figure 5.6). Additionally, Ala-206 from BglA is not conserved in orthologs from *Candida albicans* (BGL22: tryptophan), *N. crassa* (Gh3-2: serine) or *Schizosaccharomyces pombe* (SPBC1683.04.1: arginine), nor is it conserved in the other 15 *A. nidulans* beta-glucosidases (data not shown). The mutation within AN4210 is a single nucleotide deletion (A1707Δ) in a methionine codon resulting in a frame shift that adds 27 amino acids before truncating the protein (Figure 5.5D). Computational Gene Ontology (GO) analysis predicts that AN4210 encodes a RNA Polymerase II mediator complex cofactor. Blastp of *S. cerevisiae* with AN4210 identified MCM1 as having the highest similarity (Table 5.2). MCM1 is involved in the formation of both activator and repressor holoenzyme complexes of RNA polymerase II (ELBLE AND TYE 1991). In addition to MCM1, 4 other blastp-identified proteins (DEF1, IXR1, GAL11 and CYC8) are involved in transcriptional regulation (NOGI AND FUKASAWA 1980; ZHOU AND ELLEDGE 1992; BROWN *et al.* 1993; WOUDSTRA *et al.* 2002). However, blastp of *A. nidulans* with each of the top 10 identified proteins failed to identify AN4210 suggesting there may not be a direct *S. cerevisiae* ortholog. Comparison of the regions of similarity of the 10 yeast proteins showed that each had a region of similarity to the 500-600 residue region of AN4210 (Figure 5.7A). VPR1, DEF1, IXR1, GAL11 and CYC8 had a second region of similarity between 800-1,050 of AN4210. DEF1, PIN4, IXR1, and GAL11 also had a region of similarity between 250-400 of AN4210. Finally we used Interprot (www.ebi.ac.uk/interpro) to identify putative functional domains in AN4210. The AN4210 protein (Q5B5H0) is predicted to contain a MED15/GAL11 domain located between residues 962 and 1,078 and a C2H2-like zinc finger between residues 1,209-1,237. Protein sequence alignment AN4210 with its orthologs from *A. oryzae, A. fumigatus* and *A. niger* showed that both domains were conserved (Figure 5.7B,C). Proteins with the MED15 domain form a component of the Mediator complex, which integrates gene specific transcriptional regulatory signals to control the core RNA polymerase II machinery (reviewed in ALLEN AND TAATJES 2015). C2H2 zinc fingers may bind to DNA, RNA, proteins or lipids (MATTHEWS AND SUNDE 2002; GAMSJAEGER *et al.* 2007). As both of these putative functional domains of AN4210 are absent in

the XNREV1-1 mutant due to truncation, and the mutation in *bglA* is a conservative substitution in a non-conserved residue, the mutation in AN4210 is most likely to be the causative mutation.

Table 5.2 Top 10 hits from blastp analysis of AN4210 against *S. cerevisiae* proteins

Hit	Protein	Score (bits)	E value	Function	blastp of *A. nidulans*
1	MCM1	41.0	0.96 x10^{-4}	Transcription factor; plays a central role in the formation of both repressor and activator holoenzyme complexes	McmA[a] RlmA AN1325
2	VRP1	31.8	0.71 x10^{-2}	Proline-rich actin-associated protein; involved in cytoskeletal organization and cytokinesis	AN1120 AN3152 AN4270[a]
3	DEF1	37.1	0.17 x10^{-1}	RNA Pol II degradation factor; complexes with Rad26p and enables ubiquitination and proteolysis of RNA Pol II	McnC[a] AN0995 An4557
4	PIN4	36.4	0.11	Protein involved in G2/M phase progression and response to DNA damage	AN8038[a] AN6681 AN1517
5	YBR016W	31.1	0.16	Tail-anchored plasma membrane protein	FksA AN11757 AN6779
6	NAB2	32.2	0.24	Nuclear polyadenylated RNA-binding protein	AN3919[a] AN0736 AN12197
7	IXR1	31.5	0.32	Transcriptional repressor that regulates hypoxic genes	HmbA HmbC AN1962
8	GAL11	25.8	0.38	Subunit of the RNA Pol II mediator complex, acting as target of activators and repressors	AN1660 AN2073
9	CYC8	33.6	0.42	General transcriptional co-repressor	SsnF[a] AN3014 AN3547
10	NAB3	32.2	0.98	RNA-binding protein, subunit of Nrd1 complex	AN5009[a] AN4978 AN1517

[a] AspGD predicted ortholog or best hit.

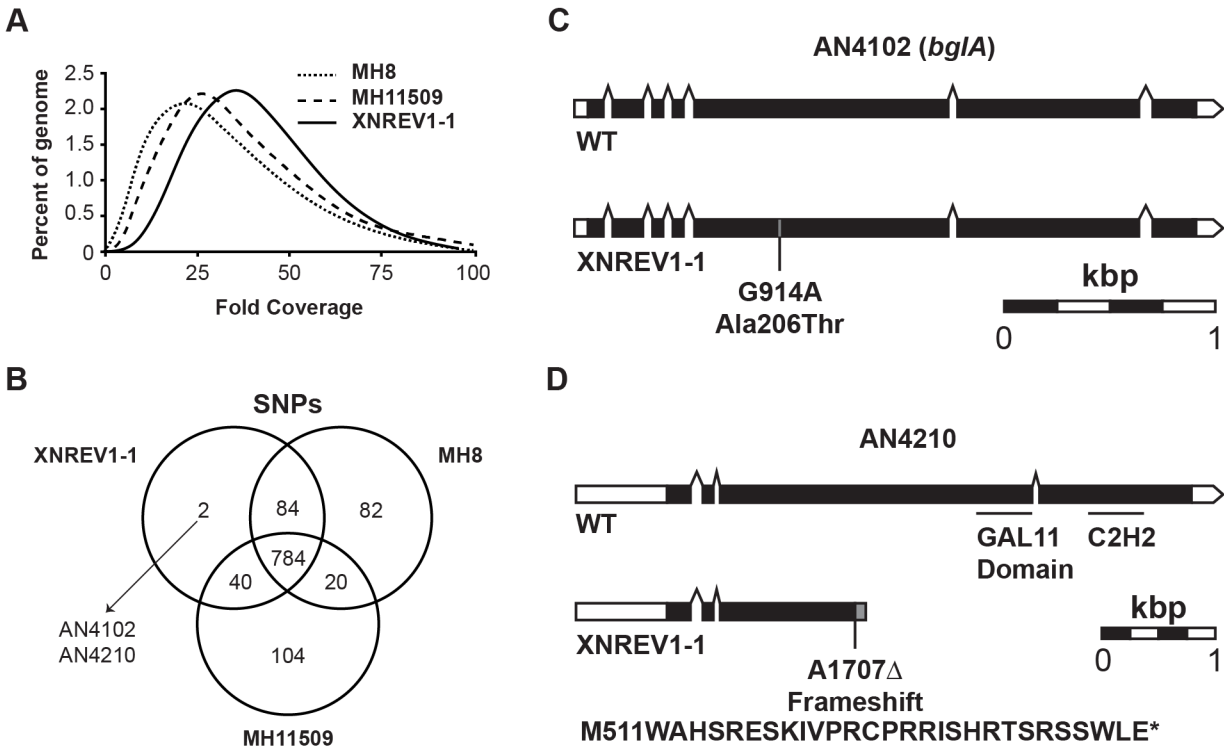

Figure 5.5 Whole genome sequencing of XNREV1-1.

A) Percent coverage of reads across the genomes following BWA alignment of reads from MH8, MH11509 and XNREV1-1 (MH12399) to the FGSC_A4 reference genome. **B)** Sequence variants identified using FreeBayes from XNREV1-1, MH8 and MH11509 were compared for presence in each strain. Transcripts of AN4102 (*bglA*) **(C)** and AN4210 **(D)** predicted to be produced in both wild type (WT) and XNREV1-1 strains. A GAL11/MED15 domain and a C2H2-zinc finger domain were identified in AN4210 by Uniprot analysis.

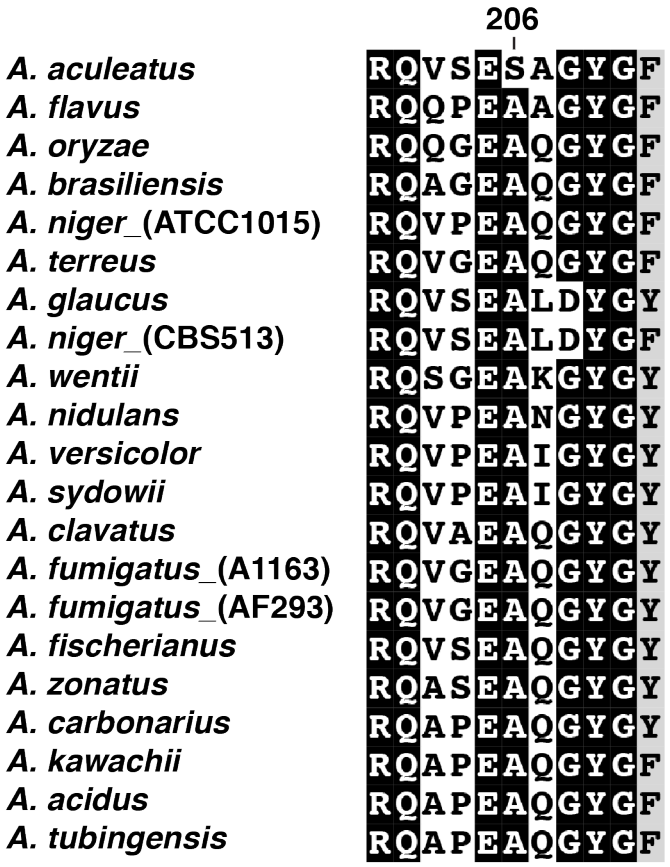

Figure 5.6 Alignment of AN4201/BglA orthologs

Clustal Omega alignment of the residues flanking Alanine 206 from *A. nidulans* AN4201/BglA, which is substituted to threonine in XNREV1-1, with the equivalent region from *Aspergillus* orthologs as identified from AspGD. Residues with ≥90% identity (black) and ≥90% similarity (gray) are shown.

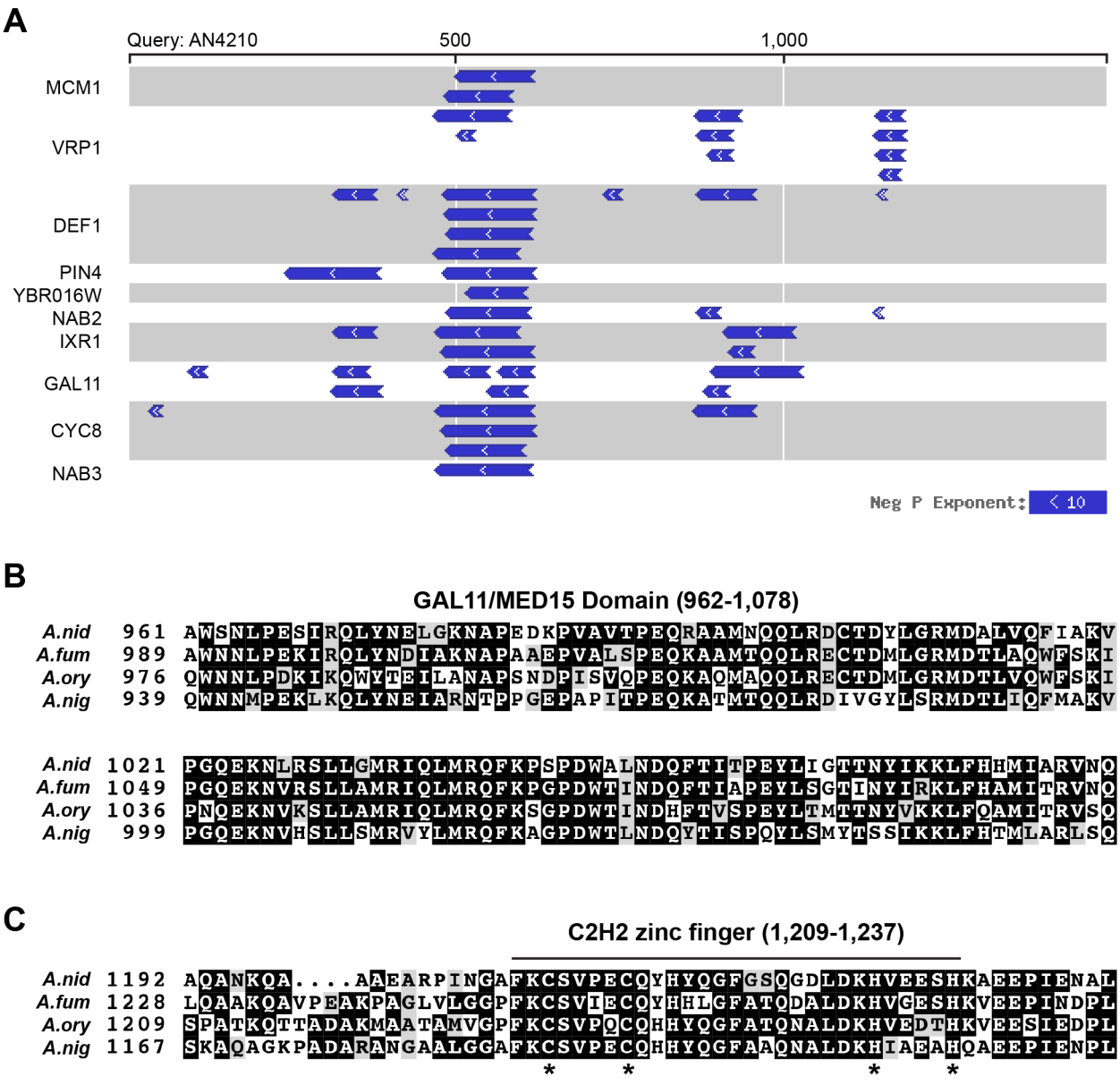

Figure 5.7 Identification of putative functional domains in AN4210

A) Regions of similarity (blue arrows) for *S. cerevisiae* proteins identified by blastp with the AN4210 protein sequence. Shading is used to distinguish genes. **B and C)** Sections of a Clustal Omega alignment of the full *A. nidulans* AN4210 (A.nid) sequence with orthologs from *A.fumigatus* (A.fum: Afu1g06060), *A. oryzae* (A.ory:AO090009000478), and *A. niger* (A.nig: An18g04690) showing the putative GAL11/MED15 **(B)** and C2H2-like zinc finger **(C)** domains. Cysteine and Histidine residues that would co-ordinate the zinc ion are marked with stars.

5.4.2.iii A frameshift truncation in AN4210 is the likely XNREV1-1 causative mutation.

To determine whether the mutation in AN4210 was responsible for conferring suppression of *nmrA* overexpression, we attempted to reconstruct the AN4210$^{A1707\Delta}$ mutation in a wild type strain. A plasmid containing the +962 to +2,582 bp region of AN4210$^{A1707\Delta}$ and the *A.f.riboB* selectable marker was transformed into MH11036 (*pyroA4 riboB2 nkuA*Δ) with selection for riboflavin prototrophy (Figure 5.8). 22 Ribo^{+} transformants with a sectoring morphology consistent with heterokaryon growth were recovered. Heterokaryon rescue for 10 of these transformants on selective media failed to isolate a haploid strain.

An alternative strategy to mutant reconstruction is complementation of the mutant phenotype with the wild type gene. The wild type AN4210 gene was cloned for complementation of the XNREV1-1 phenotype (C.C. Hunter, A.M. Brokesh, and R.B Todd, unpublished data). AN4210 cloned in the pGEM-T-EASY vector was cotransformed with the *A.n.pyrG* selectable marker in pAB4626 (BORNEMAN *et al.* 2001) into RT221 (XNREV1-1 *nkuA*Δ *pyrG*$^{-}$) and selected for pyrimidine prototrophy. Unfortunately no transformants were recovered and we have not yet reconstructed or complemented the AN4210$^{A1707\Delta}$ mutation. Complementary work generated deletion mutants of both AN4210 and *bglA* using constructs from the Fungal Genetics Stock Center as part of an undergraduate research project (C.C. Hunter, A.M. Brokesh, and R.B. Todd, unpublished data). *bglA*Δ had no effect on colony morphology and did not suppress *nmrA* overexpression. Deletion of AN4210 conferred both a fluffy aconidial morphology and partial suppression of *nmrA* overexpression (A.M. Brokesh, C.C Hunter and R.B Todd, pers. commun.). Therefore NmrA-mediated repression of AreA is in part facilitated through the likely mediator complex component AN4210.

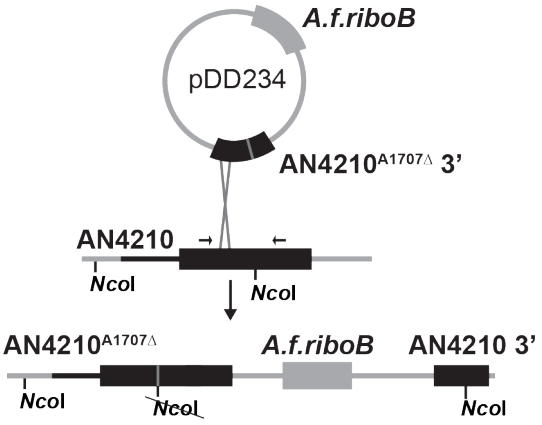

Figure 5.8 Reconstruction of AN4210$^{A1707\Delta}$

Strategy for reconstruction of AN4210$^{A1707\Delta}$ in MH11509 by single crossover upstream of the A1707Δ lesion.

5.4.3 Protein Domain analysis of AN4210, and AreA, NmrA

5.4.3.i Identification of a KIX domain within AN4210.

Eukaryotic mediator complexes contain a single homolog of MED15, which all contain the MED15 domain and MED15 is poorly conserved. For example, the *Drosophila melanogaster* and *Homo sapiens* MED15 proteins share only 41% similarity (POSS *et al.* 2013). Therefore the presence of the MED15 domain in AN4210 suggests that it is the functional ortholog despite considerable sequence divergence (25% similarity between AN4210 and *S. cerevisiae* Gal11p). Both MED15 (*H. sapiens*) and Gal11p (*S. cerevisiae*) have been shown to contain a kinase-inducible domain interacting (KIX) domain in their N-terminus (YANG *et al.* 2006; THAKUR *et al.* 2008; THAKUR *et al.* 2009). KIX domains were first identified in cAMP-responsive element-binding protein (CREB)-binding protein (CBP) from mouse (PARKER *et al.* 1996). We sought to determine whether AN4210 also contains a KIX domain. Alignment of the KIX domains from MED15 and Gal11p with AN4210 showed similarity to the N-terminal region though not strong conservation (Figure 5.9A), consistent with the poor sequence conservation between the MED15 and CBP KIX domains (YANG *et al.* 2006). Three-helix bundles characterize KIX domains; therefore we used protein-structure modeling with SWISS-MODEL to search for a KIX domain in AN4210 (BIASINI *et al.* 2014). The full AN4210 protein sequence was submitted and modeling templates identified. Suggested templates included CBP (AN4210 residues 50-120), Gal11p (residues 53-123 and 661-728), Chromosome Structural Maintenance of Chromosome Protein 1A (residues 1,026-1,075), and Kruppel-Like Factor 4 (residues 1,208-1,246). The CBP and N-terminal Gal11p templates were used to generate predicted structures of the AN4210 KIX domain. These models show a strong match to the three-helix bundle structure despite low sequence identity with CBP (20.9%) and Gal11p (21.1%). The model-to-template match is strongest within the helices and weakest in the first turn (Figure 5.9B,C). Therefore the N-terminal region of AN4210 is likely to contain a KIX domain.

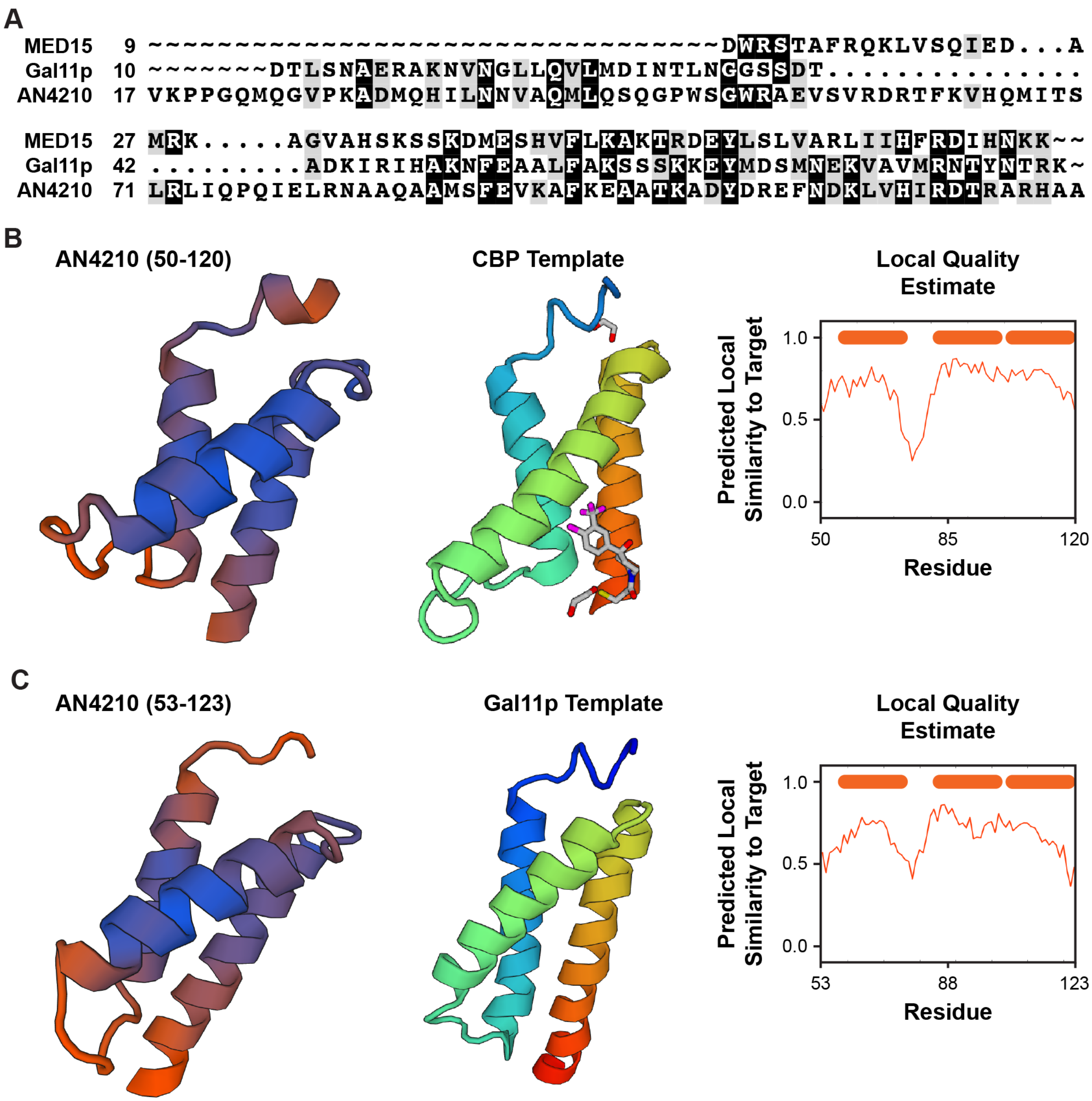

Figure 5.9 Predicted structure of the AN4210 KIX domain.

A) Clustal Omega alignment of the MED15 and Gal11p KIX domains with AN4210. **B-C)** Modeled structure of the AN4210 KIX domain constructed from the CBP (2LXS.1) and Gal11p (2K0N.1.A) templates. Model structure is colored from poor match (orange) to good match (blue). Templates are rainbow colored from N-terminus (blue) to C-terminus (red). Quality estimate plots are as generated during Swiss-Model modeling. Helices are marked on the plots with orange boxes.

5.4.3.ii Prediction of 9amino acid transactivating domains in AreA and NmrA.

The KIX domain of Gal11p is required for interaction with several transcription factors including Gal4p (HIDALGO *et al.* 2001), Gcn4p (JEDIDI *et al.* 2010), Pdr1p and Pdr3p (THAKUR *et al.* 2008), and Oaf1p (THAKUR *et al.* 2009). These proteins interact with the KIX domain via a 9 amino acid transactivation domain (9aa TAD) (PISKACEK *et al.* 2007). As AN4210 is likely to contain a KIX domain and also facilitates NmrA repression of AreA, we considered it likely either one or both these proteins would have a 9aa TAD to mediate protein-protein interactions. 9aa TADs are composed of alternating hydrophobic and hydrophilic stretches of amino acids (PISKACEK *et al.* 2007). We analyzed NmrA and AreA for the presence of 9aa TADs using the online prediction tool (PISKACEK *et al.* 2007; http://www.med.muni.cz/9aaTAD/). NmrA and AreA each returned three putative 9aa TAD sequences with between a 67% and a 92% match to the model (Table 5.3). For comparison the confirmed 9aa TAD of Pip2p returns a 75% match (PISKACEK *et al.* 2015). We compared the hydrophobicity plots for each of the predicted NmrA and AreA 9aa TADs with those from Gal11p, Leu3p and Pip2p (PISKACEK *et al.* 2015). The NmrA1 TAD motif had three peaks, however the NmrA2 and NmrA3 TAD motifs both showed a similar profile to the Gal11p 9aa TAD. As the structure of NmrA has been determined (STAMMERS *et al.* 2001), we investigated the location of each of the three predicted NmrA 9aa TADs. All three had residues at the surface of the protein suggesting that they would be able to interact with the KIX domain of AN4210 (Figure 5.10). The AreA1 TAD motif was similar in hydrophobicity to the Leu3p KIX motif, and the AreA3 TAD motif showed a similar hydrophobicity plot to the Pip2p KIX motif, however the AreA2 TAD motif lacked hydrophobicity pattern similarity to any of these three confirmed motifs as it contained three hydrophobic peaks (Figure 5.10). The presence of putative 9aa TADs within both NmrA and AreA suggest that either protein may interact with AN4210 to facilitate nitrogen nutrient regulation.

Table 5.3 9aa TAD prediction.

Motif	Sequence	Start	Stop	Match
AreA				
AreA1	ENLTWRMMA	123	131	92 %
AreA2	DTVSDAMNL	179	187	83 %
AreA3	SDMNSNMAW	539	547	67 %
NmrA				
NmrA1	GLIAEELQA	41	49	83 %
NmrA2	GTIQHYIYS	103	111	83 %
NmrA3	GVISQRVTD	311	319	75 %

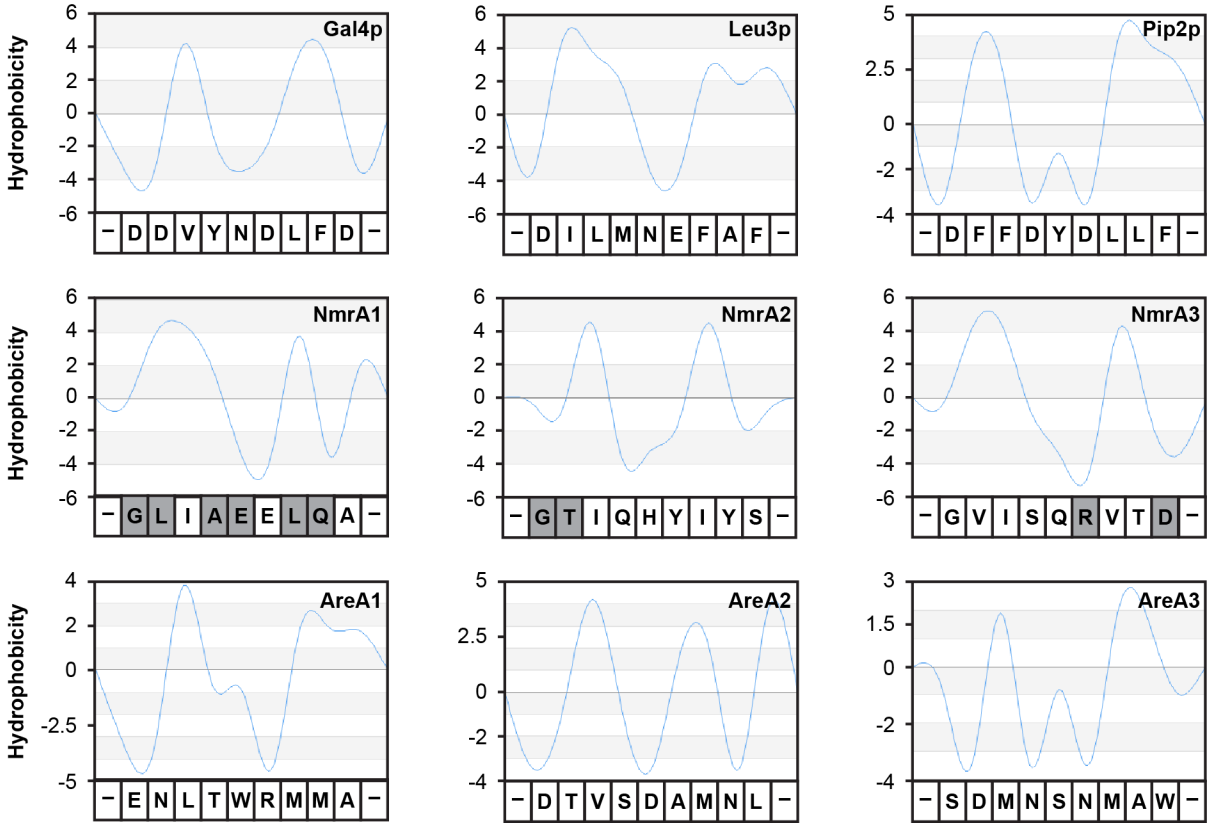

Figure 5.10 Hydrophobic profiles of NmrA and AreA 9aa transactivation domains.

Hydrophobisicty plots of three characterized 9aa TADs (PISKACEK *et al.* 2007; PISKACEK *et al.* 2015) and the six predicted domains from AreA and NmrA. Residues on the surface of NmrA are shaded gray.

5.5 Discussion

5.5.1 Expression and regulation of meaB and nmrA.

Fungi are able to fine tune gene expression in response to different nitrogen nutrients and efficiently use the preferred nitrogen nutrients ammonium and glutamine first (ARST AND COVE 1973). In filamentous fungi regulation of nitrogen metabolite repression is mediated through the action of orthologs of the *A. nidulans* GATA factor AreA, the co-repressor NmrA and the bZip transcription activator MeaB (reviewed in WONG *et al.* 2008). AreA activates the expression of genes required for assimilation of alternative nitrogen nutrients when preferred nitrogen nutrients are absent, whereas NmrA and MeaB (via activation of NmrA) act to repress transcription of these genes during nitrogen sufficiency. The expression of *areA, nmrA,* and *meaB* is responsive to different nitrogen nutrients. Using real-time reverse transcription RT-PCR we demonstrated that *nmrA* and *meaB* show highest expression during nitrogen sufficiency and reduced expression during nitrogen limitation and nitrogen starvation. This was consistent with findings from Northern blot (WAGNER *et al.* 2010) and RT-PCR (WONG *et al.* 2007). We also showed reduced expression of *nmrA* in a *meaB*Δ mutant during nitrogen sufficiency but no effect of this mutation during growth on alanine (nitrogen limitation) or during nitrogen starvation. The expression of *nmrA* in *meaB*Δ was roughly 20% of that seen in wild type during growth on ammonium, showing that wild type levels of *nmrA* mRNA are MeaB dependent. Expression of *nmrA* in the *meaB*Δ mutant during growth on ammonium was also lower than *nmrA* expression in wild type strains during either nitrogen limitation or starvation, suggesting the predominate transcriptional activation of *nmrA* comes from MeaB and that the nitrogen nutrient dependent pattern of *nmrA* is MeaB dependent. By comparing our results with published data we found consistent results between quantitative Northern blot, reverse transcriptase PCR, and quantitative real time reverse transcriptase PCR despite previous perceived disagreement in interpretation (WONG *et al.* 2007; WAGNER *et al.* 2010).

5.5.2 The Mediator complex as a target of NmrA repression.

In *N. crassa* the NmrA homolog, NMR1, blocks NIT2 binding DNA during nitrogen sufficiency by interaction with the NIT2 DNA-binding domain (XIAO *et al.* 1995; PAN *et al.* 1997). In *A. nidulans* NmrA also interacts with the AreA DNA-binding domain but does not block DNA-binding *in vitro* (LAMB *et al.* 2003; LAMB *et al.* 2004). Furthermore, AreA binds at the *niiA-niaD* bidirectional promoter during nitrogen sufficiency (MURO-PASTOR *et al.* 1999). Therefore, while NmrA may function to block AreA DNA binding at some promoters, repression is also likely to be mediated by a second mechanism. A previous genetic screen isolated a strain, XNREV1-1, which carried a spontaneous mutation conferring suppression of the negative effect of NmrA overexpression. We have used whole genome sequencing to identify the likely XNREV1-1 causative mutation in the MED15 mediator complex gene AN4210. Only two mutations unique to the mutant were observed, indicating that whole genome sequencing of spontaneous mutant genomes can be used to readily identify causative mutations. The mediator complex is made up of 30 proteins and is involved in formation of the transcription pre-initiation complex, which integrates multiple regulatory signals through each of the protein components (MALIK AND ROEDER 2010). The MED15 component of mediator was first identified as Gal11p in *S. cerevisiae* and was required for galactose utilization (NOGI AND FUKASAWA 1980). MED15 is located in the tail of the mediator complex (GUGLIELMI *et al.* 2004) and is associated with sterol regulation (YANG *et al.* 2006) as well as pancreatic and breast cancer in humans (ROSENBAUM *et al.* 2005; ZHAO *et al.* 2013). As well as the conserved MED15 domain, MED15 proteins also contain a KIX domain required for interaction with regulatory transcription factors (YANG *et al.* 2006; THAKUR *et al.* 2008; THAKUR *et al.* 2009). We were able to identify a putative KIX domain in AN4210 by protein structure modeling with strong predicted similarity to both the prototypical CBP KIX domain and the Gal11p KIX domain (PARKER *et al.* 1996). Deletion of AN4210 suppressed the NmrA overexpression phenotype suggesting it may be the target of NmrA repression (C.C. Hunter, A.M. Brokesh, and R.B. Todd, pers. commun.). Analysis of AN4210Δ shows that AreA is derepressed as the mutant is sensitive to toxic nitrogen analogs during nitrogen sufficiency in the absence of *nmrA* overexpression (C.C. Hunter, A.M. Brokesh, and R.B. Todd, pers. commun.), suggesting that NmrA repression and not *xylP* regulation is the affected step. Therefore, we have identified the mediator complex as a target through which NmrA mediates nitrogen metabolite repression.

5.5.3 Regulation of AreA through the MED15 subunit.

MED15 subunits of the mediator complex interact with activating proteins such as Gal4p and Gcn4p via a 9 amino acid transactivation domain (HIDALGO *et al.* 2001; PISKACEK *et al.* 2007; JEDIDI *et al.* 2010). While many subunits of the mediator complex are targets of either an activator or a repressor, MED15 is the only subunit to be identified from genetic screens for activators and for repressors (reviewed CARLSON 1997). Using prediction software we identified three putative 9aaTADs in each of AreA and NmrA. Gcn4p also contains three activating domains and these act additively in interaction with MED15 (JEDIDI *et al.* 2010; PISKACEK *et al.* 2015). Therefore either or both of AreA and NmrA may interact with AN4210 through one or more 9aaTAD. Mutation of one of the NmrA 9aaTADs in *nmrA*^{S111I} results in derepression (T. Woodward and M.A. Davis, pers. commun.). This mutation changes a hydrophilic residue for a hydrophobic residue and would alter the hydrophobic-hydrophilic-hydrophobic profile characteristic of 9aa TADs (PISKACEK *et al.* 2007). Therefore this domain may interact with AN4210 and mediate repression. The interaction between AreA, NmrA, and AN4210 may be similar to that for *S. cerevisiae* Tup1p, Gcn4p, and Gall1p. In this system the activator Gcn4p and the repressor Tup1p interact with an overlapping region of Gall1p and compete for binding (HAN *et al.* 2001b). Under this model during amino acid sufficiency the general transcription corepressor Tup1p has a stronger interaction with Gal11p and transcription is repressed, whereas during amino acid starvation Gcn4p interacts more strongly with Gal11p and transcription is activated (CONLAN *et al.* 1999; HAN *et al.* 2001b; HINNEBUSCH AND NATARAJAN 2002). In *A. nidulans* NmrA is highly expressed during nitrogen sufficiency, and in response to high intracellular glutamine levels NmrA may interact with AN4210 leading to transcriptional repression by inhibition of the Mediator complex. During nitrogen limitation and nitrogen starvation, decreased expression and proteolysis of NmrA, and removal of the repression signal would lead to loss of interaction between NmrA and AN4210, allowing interaction of AreA with the Mediator activation complex (Figure 5.11).

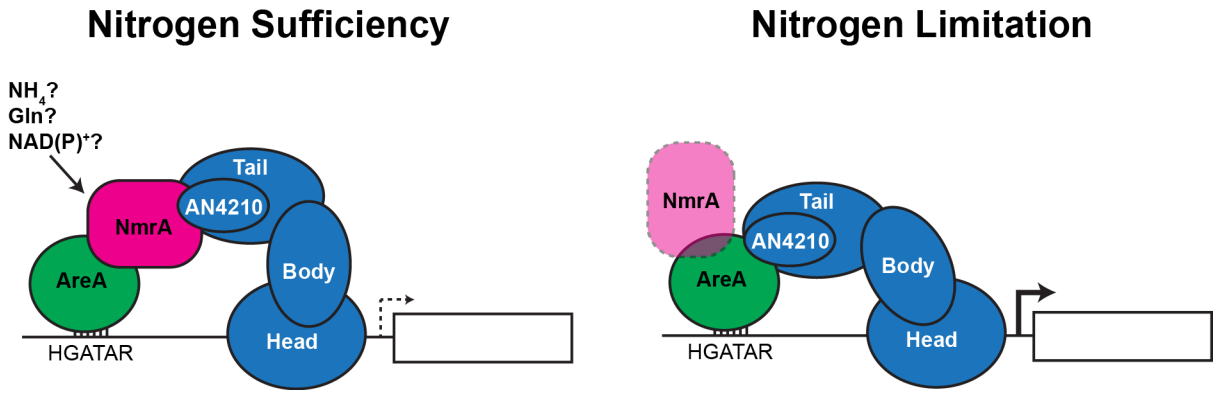

Figure 5.11 Model of NmrA repression of AreA via AN4210/MED15

NmrA and AreA compete for interaction with *A. nidulans* mediator complex in a nitrogen condition dependent manner. Either expression levels of NmrA or a signal molecule may determine the outcome of this competition.

5.6 Future Directions

A clear understanding of the mechanism underlying regulation of AreA by the co-repressor NmrA has proved elusive. The identification of AN4210 via a genetic suppressor screen has provided a new clue in understanding how NmrA functions to repress AreA activity. Several lines of investigations are opened up by this research. The AN4210$^{A1707\Delta}$ mutation leads to the predicted loss of both the MED15 and C2H2-zinc finger motifs. It will be important to distinguish which of these domains is required for NmrA-dependent repression. In-frame deletions of each domain or point mutations of the C2H2-zinc finger motif will help to determine their function. These mutants should be created in a *xylP*(p)::*nmrA* background to determine if they confer suppression of *nmrA* overexpression phenotypes. Interestingly the C2H2-zinc finger motif is not present in Gal11p suggesting that AN4210 may have evolved additional roles. C2H2-zinc fingers are able to bind DNA, RNA, proteins and lipids (MATTHEWS AND SUNDE 2002; GAMSJAEGER *et al.* 2007), and therefore this domain may play a role in protein-protein interaction or nutrient sensing. Mutation of this domain may provide clues to its role. The divergence of AN4210 from Gall11p may indicate a greater divergence of the *A. nidulans* mediator complex. Currently there are no characterized mediator genes in *A. nidulans*, so studies to determine the similarity with yeast will be interesting. For example, determining whether GAL11 complements AN4210Δ. Characterization of the other components of the Mediator Complex by generation of knock-outs will reveal whether other subunits are required for NmrA repression of AreA. In addition to the two C-terminal domains of AN4210 we have identified putative KIX domains that may interact with putative 9aa TADs in NmrA and/or AreA. Characterization of the requirement of the KIX domain and each of the NmrA 9aa TADs for NmrA repression will be important for understanding how NmrA functions. This will be best demonstrated by mutational analysis and demonstration of protein-protein interaction(s).

Previous mutations have failed to identify the specific AreA activation domain (S.D. Kreutzberger, L.S. Lee, M.A. Davis, R.B. Todd, unpublished data). Deletion of the AreA1 and AreA2 TAD motifs in combination (Δ60-423) and deletion of AreA3 TAD (Δ424-599) does not lead to derepression or have a significant effect on activation of *fmdS-lacZ* reporter gene expression (HUNTER *et al.* 2014; S.D. Kreutzberger, L.S. Lee, M.A. Davis, and R.B. Todd, pers. commun.). Mutating these three motifs in combination may be necessary to determine whether these 9aa TAD motifs are involved in AreA transcriptional activation.

[Otherwise, just a blank page.]

Chapter 6 - The AreA Nuclear Export Signal

6.1 Abstract

The *Aspergillus nidulans* GATA transcription factor AreA is regulated by a combination of transcriptional, post-transcriptional and post-translational mechanisms. One such mechanism is regulated nucleocytoplasmic distribution. During nitrogen sufficiency AreA cycles between the nucleus and the cytoplasm. However, during nitrogen starvation AreA slowly accumulates in the nucleus over several hours. Nuclear accumulated AreA is rapidly exported to the cytoplasm when nitrogen nutrients are added to nitrogen-starved cells. Relative nuclear and cytoplasmic protein levels are determined by the interplay of nuclear import and nuclear export. AreA contains six characterized nuclear import signals and one major predicted leucine-rich CRM1-type nuclear export signal. Our analysis of animal, fungal and plant GATA factors finds that hydrophobic CRM1-type nuclear export signals are common among this class of proteins in all eukaryotes and are frequently associated with a GATA zinc finger DNA-binding domain. The dynamics of slow nuclear accumulation and rapid nuclear export of AreA indicate that nuclear export is the key regulated step in AreA nucleocytoplasmic distribution. Using protein fusions and mutational analysis we have determined that the AreA nuclear export signal at residues 703-712 is both sufficient and necessary for nuclear export. To further understand AreA nuclear export we analyzed the effects of missense substitutions of two leucine residues in the nuclear export signal, which correspond to residues critical for nuclear export of some other CRM1-dependent nuclear export signals, but found they were not required for nuclear export. However, mutation of the conserved histidine-704 does disrupt nuclear export. We have carried out a genetic screen for mutants with disrupted nuclear export of a fusion protein containing the AreA nuclear export signal to identify novel proteins involved in regulated AreA localization. Using whole genome sequencing we have identified mutations in one of the mutants arising from this screen. This mutant contains 70 sequence differences compared with the unmutagenized parent, however the likely causative mutation confers substitution of a conserved proline in an essential nuclear pore protein AN2808/*nup159* .

6.2 Introduction

For transcription factors to regulate gene expression it is necessary for them to be localized to the nucleus. For many transcription factors, import into the nucleus via a nuclear localization signal results in constitutive nuclear localization. For example, the *Aspergillus nidulans* transcription factor PrnA contains a tripartite nuclear localization signal (NLS) and is constitutively nuclear (POKORSKA *et al.* 2000), as is TamA (SMALL *et al.* 2001). Some transcription factors are also exported from the nucleus as a result of a nuclear export signal (NES) and the control of nucleocytoplasmic distribution of transcription factors can therefore be used to regulate transcription factor activity and therefore gene expression (NIGG 1997). For example, the Zn(II)2Cys6 transcription factor NirA, which regulates nitrate utilization, is primarily cytoplasmic in the absence of nitrate but in the presence of nitrate NirA shows nuclear accumulation (BERNREITER *et al.* 2007). Similarly AmyR, which regulates amylolytic genes in *A. nidulans*, only accumulates in the nucleus in response to the inducer isomaltose (MAKITA *et al.* 2009). Another protein with regulated subcellular distribution is the *Aspergillus nidulans* GATA transcription factor AreA (TODD *et al.* 2005). AreA localization has been visualized using a hemagglutinin (HA) epitope tagged variant $AreA^{HA}$. During nitrogen sufficiency $AreA^{HA}$ is present in both the nucleus and the cytoplasm. During nitrogen starvation, the complete absence of exogenous nitrogen nutrients, $AreA^{HA}$ progressively accumulates in the nucleus over several hours resulting in predominantly nuclear localization (Figure 6.1), however the addition of a nitrogen nutrient leads to rapid nuclear export within minutes (TODD *et al.* 2005). Nuclear accumulation is correlated with increased expression of the AreA-regulated genes *fmdS* and *amdS* (FRASER *et al.* 2001; TODD *et al.* 2005). Regulated nucleocytoplasmic distribution is observed in the AreA ortholog Gln3p in *S. cerevisiae* (BECK AND HALL 1999; BERTRAM *et al.* 2000). During nitrogen sufficiency Ure2p sequesters phosphorylated Gln3p in the cytoplasm. Nuclear import of Gln3p can be signaled by nitrogen limitation or rapamycin (BECK AND HALL 1999; BERTRAM *et al.* 2000). Regulated nuclear accumulation is also observed for the AreA homolog in *Fusarium fujikuroi* (MICHIELSE *et al.* 2014), but not in *Gibberella zeae* where AreA accumulates in the nucleus during nitrogen starvation and in the presence of nitrate (MIN *et al.* 2012). However, some regulation of nuclear distribution likely exists in *G. zeae,* as there are lower levels of AreA in the nucleus during growth on nitrogen rich complete media (MIN *et al.*

2012). Nuclear accumulation has also been reported for the mammalian AreA orthologs GATA4 and GATA6 (MORISCO *et al.* 2012).

To achieve regulated nucleocytoplasmic distribution often requires the combination of nuclear import signals (NLS) and nuclear export signals (NES). AreA contains five classical SV40 Large T-antigen NLSs and one non-canonical arginine-based bipartite NLS (HUNTER *et al.* 2014). These six NLSs work cooperatively to facilitate AreA entry into the nucleus, likely by interaction with several of the 17 *A. nidulans* importins (MARKINA-INARRAIRAEGUI *et al.* 2011; HUNTER *et al.* 2014). Fusion of these NLSs to GFP showed they were able to direct nuclear import under both nitrogen sufficient and nitrogen starvation conditions (HUNTER *et al.* 2014). AreA contains a putative CRM1 exportin-type nuclear export signal at residues 703-712 adjacent to the DNA-binding domain (TODD *et al.* 2005). CRM1-type NESs have been now been characterized in more than 200 eukaryotic proteins including the AreA homolog Gln3p (CARVALHO *et al.* 2001; CARVALHO AND ZHENG 2003), and several medically important proteins, such as Huntingtin (XIA *et al.* 2003; MAIURI *et al.* 2013), p53 (STOMMEL *et al.* 1999) and N-WASP (SUETSUGU AND TAKENAWA 2003). The CRM1-type NES was originally identified as leucine rich (FISCHER *et al.* 1995; FORNEROD *et al.* 1997b), however the consensus sequence for this type of nuclear export signal has now been expanded and is characterized by spaced hydrophobic residues, such as leucine, that interact with the five hydrophobic binding pockets which form the CRM1 cargo-binding site (GUTTLER *et al.* 2010). Many CRM1 exportins are sensitive to the drug Leptomycin B (LMB) and in *Schizosaccharomyces pombe* LMB targets a specific cysteine residue (C529) to block function (KUDO *et al.* 1999). In *Saccharomyces cerevisiae* CRM1 and *A. nidulans* CrmA/KapK a threonine residue is found at the equivalent position to this cysteine, and these fungi are LMB resistant (NEVILLE AND ROSBASH 1999; TODD *et al.* 2005). However, engineered substitution of the resistant threonine to a cysteine in CRM1 and CrmA/KapK confers LMB sensitivity (NEVILLE AND ROSBASH 1999; TODD *et al.* 2005). Using the *crmA*^{T525C} variant of *A. nidulans* it was shown that LMB prevents nuclear export of nuclear accumulated AreA^{HA} following exogenous addition of ammonium, indicating that CrmA facilitates regulated AreA nucleocytoplasmic distribution (TODD *et al.* 2005). As AreA^{HA} accumulates slowly in the nucleus in response to nitrogen starvation, but is rapidly exported upon the addition of many nitrogen sources (TODD *et al.* 2005; R.B. Todd unpublished), and that the AreA NLSs fused to GFP enter the nucleus during both nitrogen sufficiency and nitrogen

starvation (HUNTER *et al.* 2014) it is likely that nuclear export is the regulated step in AreA nuclear accumulation. We therefore sought to characterize the predicted AreA nuclear export signal and performed bioinformatics analyses to determine whether regulated nucleocytoplasmic distribution may be a common feature of GATA factors.

Using predictive software we determined that putative CRM1-type NESs are extremely common in fungal, plant, and animal GATA factors, and in animals these signals tend to be adjacent to the GATA-zinc finger motif as in AreA. By fusing green fluorescent protein (GFP) to the AreA NES and to the constitutively nuclear proline utilization transcription factor PrnA (CAZELLE *et al.* 1998; POKORSKA *et al.* 2000) we have shown that the AreA NES is sufficient to confer nuclear export and loss-of-function on PrnA. Furthermore deletion of the NES from $AreA^{HA}$ confers nuclear accumulation. Interestingly mutation of two conserved leucines within the AreA NES did not disrupt $AreA^{HA}$ nuclear export, however a serendipitously identified mutation in histidine-704 conferred increased AreA nuclear localization. Finally, using the selectable proline non-utilization phenotype conferred by *prnA-areA*^{NES}*-gfp* we carried out a genetic screen to identify mutants deficient in nuclear export via the AreA NES. We have used whole genome sequencing to identify one of the likely causative mutations in an essential nuclear pore protein AN2808/*nup159* (DE SOUZA *et al.* 2004; OSMANI *et al.* 2006a).

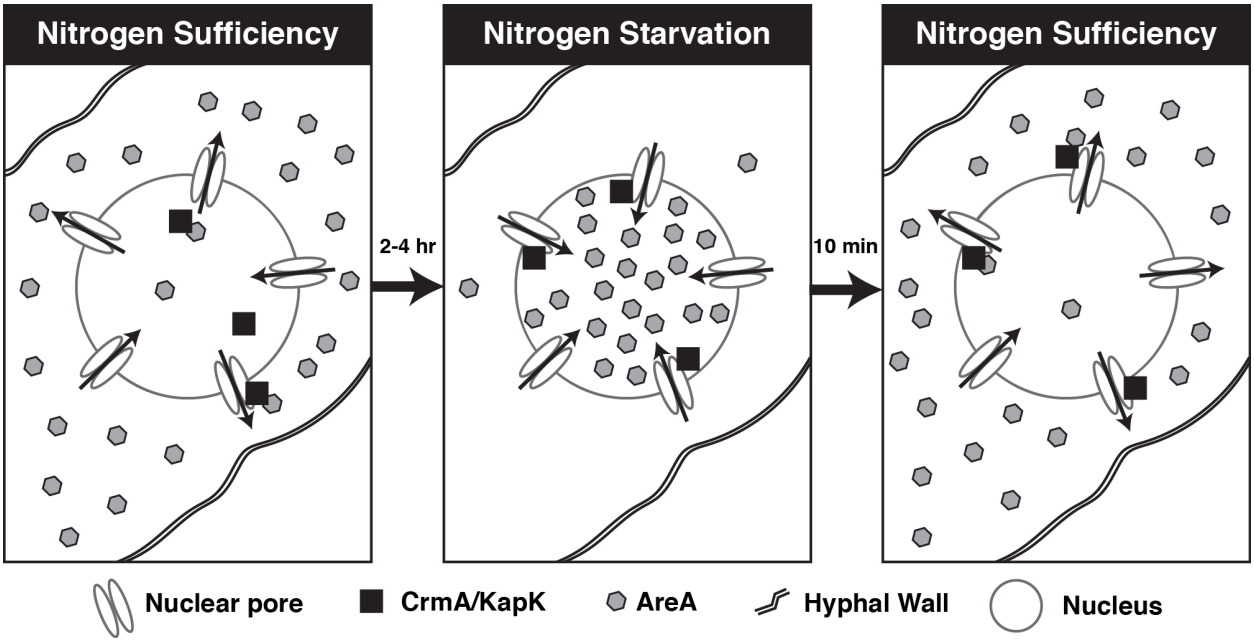

Figure 6.1 Regulated AreA nucleo-cytoplasmic distribution

During nitrogen sufficiency AreA cycles between the nucleus and the cytoplasm. Transfer to nitrogen starvation conditions results in progressive nuclear accumulation of AreA over several hours, and this nuclear accumulation is rapidly lost when nitrogen nutrients are added to the media.

6.3 Materials & Method

6.3.1 Plasmid construction

The *prnA* 3' sequence (+1,736 to +2,825 bp) had been previously fused to *areA*$^{694\text{-}721}$ (+2,136 to +2,231 bp) and *areA*$^{694\text{-}721.NES\Delta}$ (+2,136 to +2,165 bp, +2,202 to +2,231 bp) sequences by Kendra Siebert (Kansas State University) using fusion PCR and ligated into pGEM T-easy to generate pKS124 and pKS127 respectively. The *are*A$^{694\text{-}721}$ sequence had also been fused to *gfp-trpC* and ligated into pGEM T-easy to generate pKS118 (K.S. Siebert and R.B. Todd unpublished). The wild type and NESΔ *areA* sequences in all three constructs have a *Bcl*I site at +2,209 to +2,214 bp. The *prnA-areA*$^{694\text{-}721}$, *prnA-areA*$^{694\text{-}721.NES\Delta}$, and *areA*$^{694\text{-}721}$*-gfp-trpC* fragments were excised from pKS124, pKS127, and pKS118 by digestion with *Spe*I/*Bcl*I and ligated into *Spe*I cut p6363 to generate pDD163 (*prnA-areA*$^{694\text{-}721}$*-gfp-trpC*) and pDD164 (*prnA-areA*$^{694\text{-}721.NES\Delta}$*-gfp-trpC*). The *prnA-areA*$^{694\text{-}721./NES\Delta}$*-gfp* region of these plasmids was then amplified using the T7 universal primer (5'-TAATACGACTCACTATAGGG-3') and gfpBglII_rev (5'-TTTTAGAT**CTA**CTTGTACAGCTCGTCC-3'), which contains a stop codon (bold) and a *Bgl*II restriction site (underlined), to remove the *trpC* sequence. PCR fragments were digested with *Bgl*II and ligated into *Bam*HI digested pSM6363, containing the *A.f. pyroA* selectable marker, to generate pDD166 (*prnA-areA*$^{694\text{-}721}$*-gfp*) and pDD167 (*prnA-areA*$^{694\text{-}721.NES\Delta}$*-gfp*).

6.3.2 Strain construction

The full list of strains used in this chapter and their complete genotypes can be found in Tables 2.1-3. Relevant genotypes are provided throughout the chapter. pDD166 and pDD167 were transformed into RT96 (*pyroA4 nkuA*Δ*::Bar*) and selected for pyridoxine prototrophy. Single homologous integration of pDD166 and pDD167 at the *prnA* locus was confirmed by Southern blot in RT244 (*prnA-areA*$^{694\text{-}721}$*-gfp*) and RT245 (*prnA-areA*$^{694\text{-}721.NES\Delta}$*-gfp*) respectively using the entire *prnA-areA*$^{694\text{-}721}$*-gfp* sequence amplified from pDD166 with T7 and T3 (5'-ATTAACCCTCACTAAAGGGA-3') as probe. Genomic DNA was digested with *Eco*RV (Bands: wild type: 2.5, 4.0 kb, fusion genes: 1.0, 2.5, 4.0, 4.5) and *Xho*I (Bands: wild type: 6.0 kb, fusion genes: 3.5, 9.4 kb). Multicopy integration resulted in a 6.5 kb band in the *Xho*I digest. Hemagglutinin (HA) tagged variants of the *areA* NES encoding region were previously

generated by two-step gene replacement (C.C Hunter, K.S. Siebert, D.F. Clarke, K.H. Wong, M.A. Davis and R.B. Todd unpublished). *gpdA*(p)::*areA*$^{HA.\Delta 703\text{-}712}$ *fmdS-lacZ* (RT116) was generated by crossing RT20 (*gpdA*(p)::*areA*^{HA} *fmdS-lacZ*) with MH12068 (*gpdA*(p)::*areA*$^{HA.\Delta 703\text{-}712}$). *gpdA*(p)::*areA*$^{HA.H704A}$ *fmdS-lacZ* (RT153) was generated by crossing MH12326 (*fmdS-lacZ*) with RT51 (*gpdA*(p)::*areA*$^{HA.H704A}$). *gpdA*(p)::*areA*$^{HA.L70I}$ *fmdS-lacZ* (RT116) was generated by crossing MH11050 (*areA*Δ *fmdS-lacZ*) with RT103 (*gpdA*(p)::*areA*$^{HA.L710I}$).

6.3.3 ANX mutant characterization

In conjunction with B.T. Pfannenstiel ANX mutants were mapped by crossing to RT250 (*prn-309 pyrG89*) and the mutations in ANX1 (RT251), ANX2 (RT252), ANX3 (RT253), ANX4 (RT254), ANX18 (RT255), ANX19 (RT256), ANX20 (RT257), and ANX21 (RT258) were identifed by PCR and sequencing. Genomic DNA was isolated from strains in which the ANX mutation mapped to the *prnA*^{NLS}-*areA*$^{693\text{-}721}$-*gfp* fusion gene and the +2718 bp (in *prnA*) to +2,998 bp (in *gfp*) region amplified with prn3'_fwd (5'-TCACGGCTATTCCGTGCTTTGA-3') and gfp_rev (5'-ACGCTGAACTTGTGGCCGTTTA-3'). The PCR product was then sequenced using the gfp_rev primer. The +1,521 to +4,921 bp region of AN2808/*nup159* was amplified from ANX25 genomic using nup_fwd (5'CGCAGTCAACACAACCGCAGC-3') and nup_rev (5'-CCGCCCGAGACCTGCAAGT-3').

6.4 Results

6.4.1 Bioinformatic survey of CRM1-type Nuclear Export Signals

6.4.1.i The CRM1-type Nuclear Export Signal is conserved in AreA orthologs.

Todd and colleagues (2005) identified a single predicted CRM1-type leucine-rich nuclear export signal (NES) located at residues 703 to 712 (LHGVVRPLSL) of AreA, overlapping the C-terminal sequence of the GATA DNA-binding domain. The CRM1-type nuclear export signal is characterized by spaced hydrophobic residues that interact with five hydrophobic binding pockets in the CRM1 cargo-binding site (GUTTLER *et al.* 2010). Recent studies have expanded the possible NES consensus to multiple classes (KOSUGI *et al.* 2008; FUNG AND CHOOK 2014). We analyzed the putative AreA NES and determined that it fits both Class 1a and Class 1d (Figure 6.2A). Class 1a contains the PKI NES with an additional fifth hydrophobic residue, ϕ^0 (GUTTLER *et al.* 2010). The AreA NES also has a hydrophobic residue in the ϕ^0 position (Figure 6.2A). To determine the extent of conservation of the NES in AreA homologs we aligned the *A. nidulans* AreA zinc finger and NES with the equivalent region from Gln3p and Gat1p (*S. cerevisiae* and *Candida albicans*), NIT2 (*Neurospora crassa*), Gaf1p (*S. pombe*), Nut1 (*Magnaporthe oryzae*) and AreA (*Penicillium marneffei, Histoplasma capsulatum* and *F. fujikuroi*). The NES residues are almost completely conserved, contrasting with the downstream residues and those upstream of the adjacent DNA binding domain, which show poor conservation (Figure 6.2B). We also performed a ValidNESs computational analysis of the sequences of these proteins. ValidNESs predicts NES motifs based on the NESsential prediction model, which incorporates both primary sequence and sequence meta-features (e.g. predicted disorder), to report the ϕ^2-$X_{2\text{-}3}$-ϕ^3-X_1-ϕ^4 sequence with associated probabilities of function (FU *et al.* 2011; FU *et al.* 2013). Homologs from all eight species have a predicted NES similar to the one identified in AreA (Table 6.1). Of the 10 proteins investigated only Gln3p from *C. albicans* lacked the predicted motif adjacent to the GATA zinc finger motif (Figure 6.3). Therefore nuclear export of AreA homologs may be conserved throughout most of the fungal kingdom. ValidNESs analysis also identified a putative NES in AreA at residues 129 to 134 with similar probability of function to the one predicted at 706-712 (Table 6.1), however this motif was poorly conserved in AreA homologs (Figure 6.3).

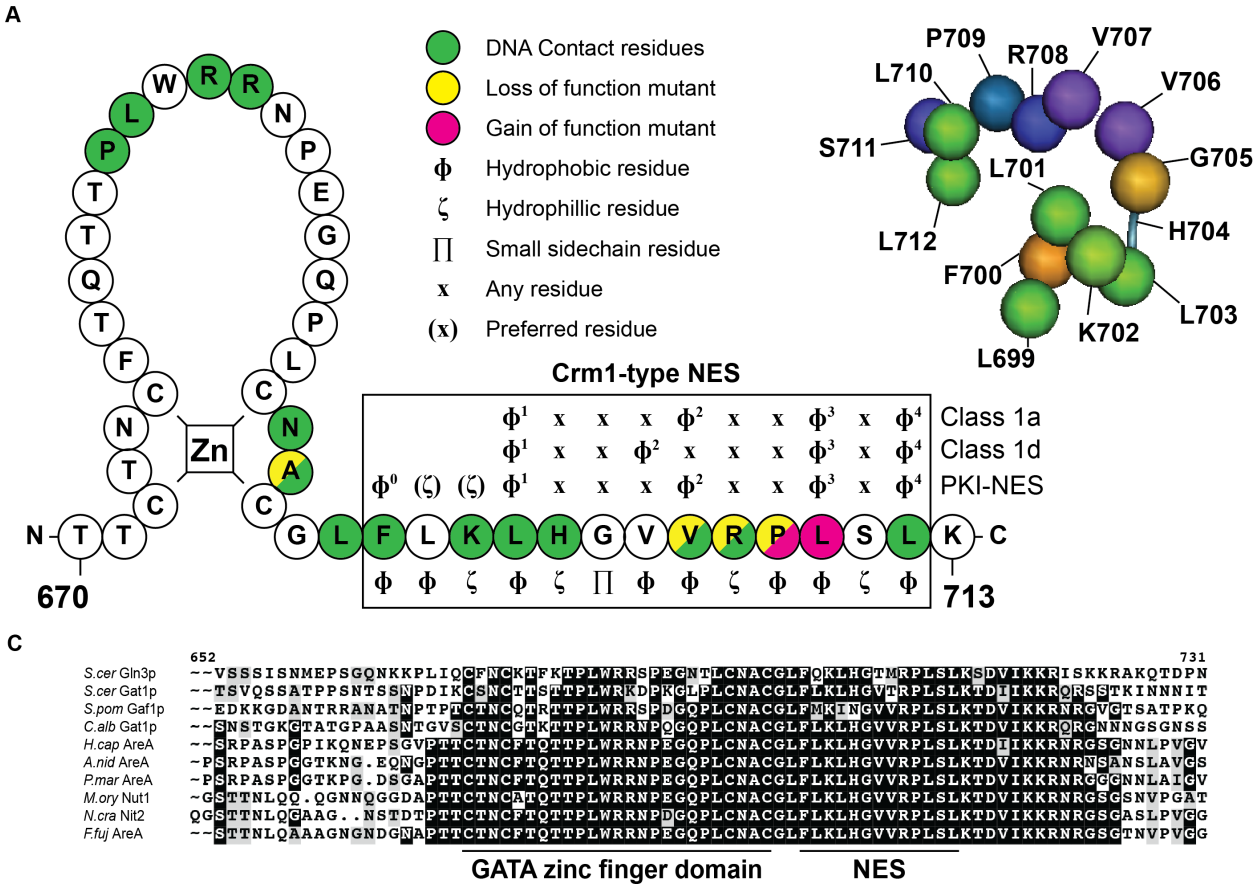

Figure 6.2 Structure and conservation of the AreA Nuclear Export Signal.

A) Schematic of the AreA GATA motif and NES adapted from STARICH *et al.* (1998). Loss-of-function mutations are based on reduced growth on nitrate and gain-of-function for derepression of nitrate reductase during growth on ammonium (PLATT *et al.* 1996a). Hydrophobic residues were compared with reported NES consensus sequences and the Protein Kinase A Inhibitor (PKI) NES, which is a member of Class 1a (KOSUGI *et al.* 2008; GUTTLER *et al.* 2010; FUNG AND CHOOK 2014). The structure of the hydrophobic NES residues is a portion of the crystal structure of the AreA DNA-binding domain PDB ID: 4GAT (KOTAKA *et al.* 2008) **B)** Clustal Omega alignment of the *A. nidulans* AreA $CX_2CX_{17}CX_2C$ GATA motif with homologs from *S. cerevisiae* (*S.cer*), *C. albicans* (*C.alb*), *N. crassa* (*N.cra*), *S. pombe* (*S.pom*), *M. oryzae* (*M.ory*), *P. marneffei* (*P.mar*), *H. capsulatum* (*H.cap*) and, *F. fujikuroi* (*F.fuj*).

Table 6.1 ValidNESs analysis of AreA homologs

Species	Protein & Accession Number	Protein Level Probability[1]	Coordinates	Motif	Motif Probability[2]
A. nidulans	AreA	0.56	706 to 712	VVRPLSL	0.66
	XP_681936		129 to 134	MMALSL	0.63
			707 to 712	VRPLSL	0.46
			338 to 343	LDTFNL	0.30
			187 to 192	LDDFII	0.18
S. cerevisiae	Gat1p	0.40	343 to 349	VTRPLSL	0.43
	P43574		503 to 508	LDWLNL	0.24
			135 to 140	LSDMNL	0.17
			447 to 453	FRPDMNM	0.15
			22 to 28	IYIDIYI	0.15
	Gln3p	0.94	723 to 728	LDWLKF	0.76
	AAA34645		340 to 345	MRPLSL	0.48
			433 to 439	VPSPVLM	0.21
			14 to 20	LNSHLDV	0.16
			139 to 144	VDQFNM	0.16
C. albicans	Gat1p	0.44	471 to 477	VVRPLSL	0.57
	EAK97535		472 to 477	VRPLSL	0.38
			368 to 374	FNTSLSV	0.34
			283 to 289	LNSTVSI	0.28
			187 to 192	LDPLAF	0.28
			165 to 171	VNHHMEI	0.26
	Gln3p	0.46	93 to 99	LLSPLSI	0.67
	EAL03205		94 to 99	LSPLSI	0.49
			34 to 39	IDNLHL	0.37
			586 to 591	LEAIDM	0.37
			14 to 20	VPSIVDL	0.22
			675 to 680	LDWLKF	0.17
N. crassa	Nit-2	0.49	776 to 782	VVRPLSL	0.59
	AAB03891		393 to 398	LDTVGL	0.57
			777 to 782	VRPLSL	0.46
S. pombe	Gaf1p	0.45	489 to 495	VGTAMGV	0.74
	EIW10745		65 to 70	LMSINL	0.57
			668 to 674	VVRPLSL	0.41
			820 to 826	FDTDLGM	0.38
			669 to 674	VRPLSL	0.23
P. marneffei	AreA	0.47	652 to 658	VVRPLSL	0.65
	XP_002148896		85 to 90	MMAMSL	0.54
			653 to 658	VPRLSL	0.51
M. oryzae	Nut1	0.49	696 to 702	VVRPLSL	0.58
	XP_003720998		697 to 702	VRPLSL	0.45
			111 to 116	MMHVNL	0.36
F. fujikuroi	AreA	0.41	727 to 733	VVRPLSL	0.53
	P78688		728 to 733	VRPLSL	0.52
			138 to 143	MMALNI	0.18
H. capsulatum	AreA	0.44	175 to 180	MMAMNL	0.60
	EER43822		755 to 761	VVRPLSL	0.41
			756 to 761	VRPLSL	0.35
			550 to 556	VVNMFTF	0.16

[1] NESsential score at the protein level indicates how likely the given protein contains a NES.

[2] NESsential score of each putative site indicates the probability to be a functional NES.

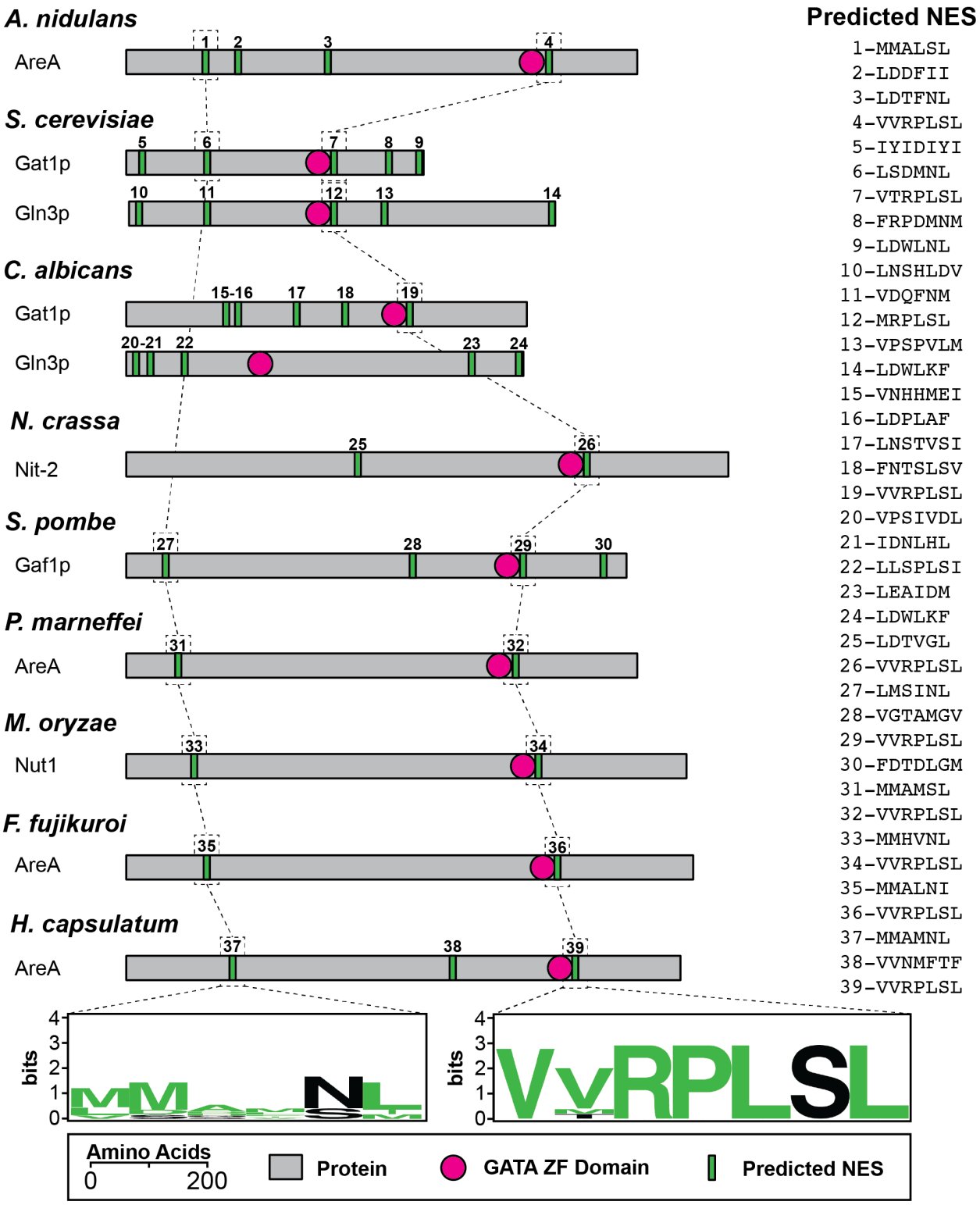

Figure 6.3 Distribution of ValidNESs predicted NES motifs in AreA homologs

ValidNESs predicted NES motifs with similar sequence and location were used to generate consensus motifs. Units are bits of information proportional to sequence conservation.

6.4.1.ii CRM1-type Nuclear Export Signals are abundant in GATA factors.

In addition to *A. nidulans* AreA, regulated nucleocytoplasmic distribution has been observed for the *F. fujikuroi* AreA ortholog (MICHIELSE *et al.* 2014) and the human GATA transcription factors, GATA4 and GATA6 (MORISCO *et al.* 2001; USHIJIMA AND MAEDA 2012). Therefore we determined whether CRM1-type Nuclear Export Signals are common in other GATA transcription factors. We performed ValidNESs analysis of an additional 31 animal, 29 plant and 45 fungal GATA factors, including all five AreA paralogs from *A. nidulans* (Appendix C, Table C.1). Of the 116 GATA factors analyzed 102 (87.1%) had putative CRM1-type NES motifs, 38 of which (32.7%) had more than two predicted NESs. When analyzed for distribution within the proteins there was no clear trend in either plant or fungal GATA factors (Appendix C, Figures C.1-2). However, like AreA, 22 animal GATA factors had a putative NES C-terminal of the second zinc finger domain (Figure 6.4). A consensus motif of this site shows a high degree of similarity to the predicted AreA NES consensus (compare motifs in Figure 6.3 & Figure 6.4). Furthermore, alignment of this region showed conservation between the putative animal NESs and AreA for both the hydrophobic residues and flanking amino acids (Figure 6.5). The high prevalence of CRM1-type NESs in GATA factors suggests that nuclear export may be a common mechanism for controlling the activity of this family of proteins throughout the Eukaryota.

Figure 6.4 Distribution of ValidNESs predicted NES motifs in animal GATA factors

ValidNESs predicted NES motifs for animal GATA factors were mapped onto the respective protein. Motifs adjacent to a DNA binding motif (bolded) were used to generate consensus motifs. Units are bits of information proportional to sequence conservation.

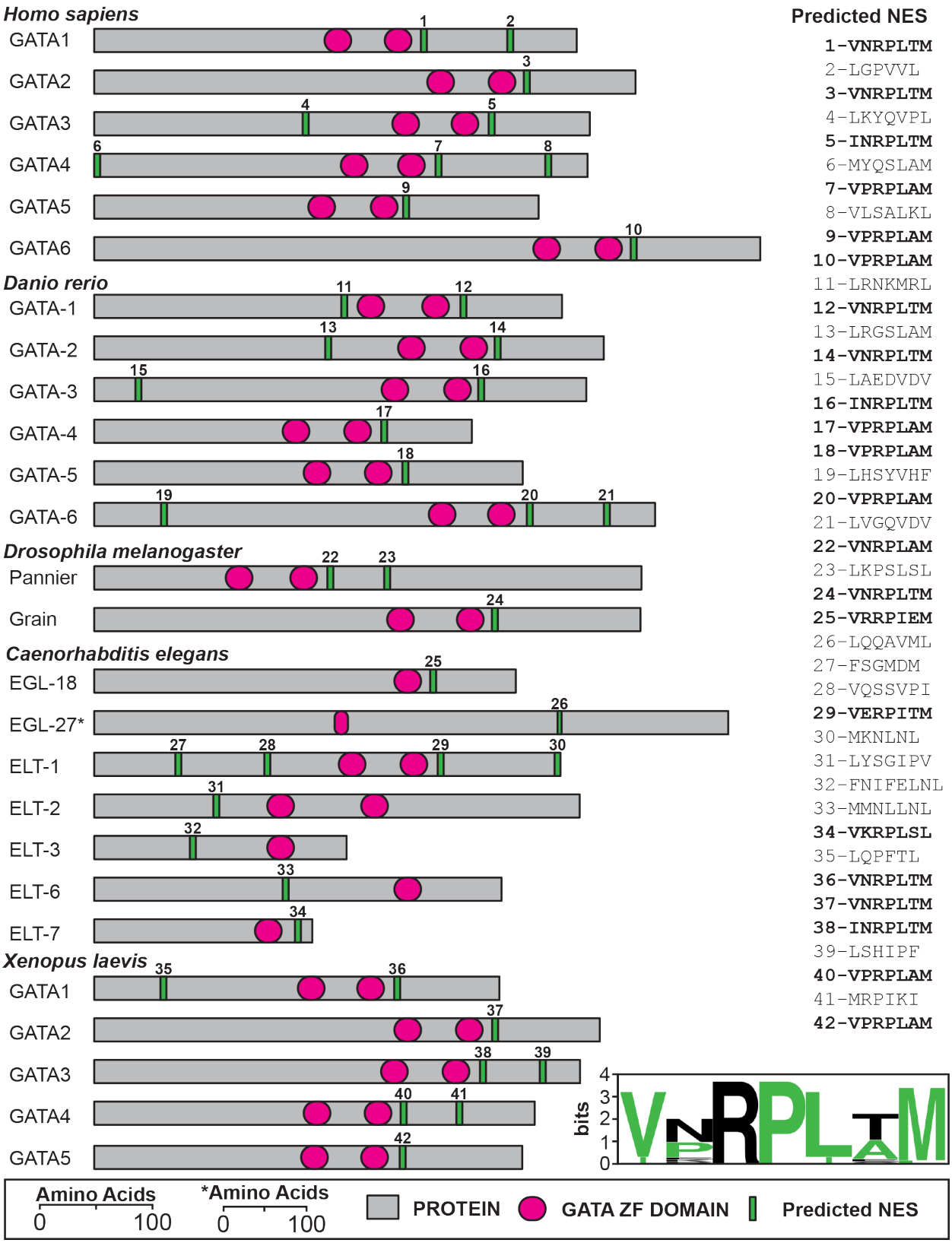

Figure 6.4 Distribution of ValidNESs predicted NES motifs animal GATA factors

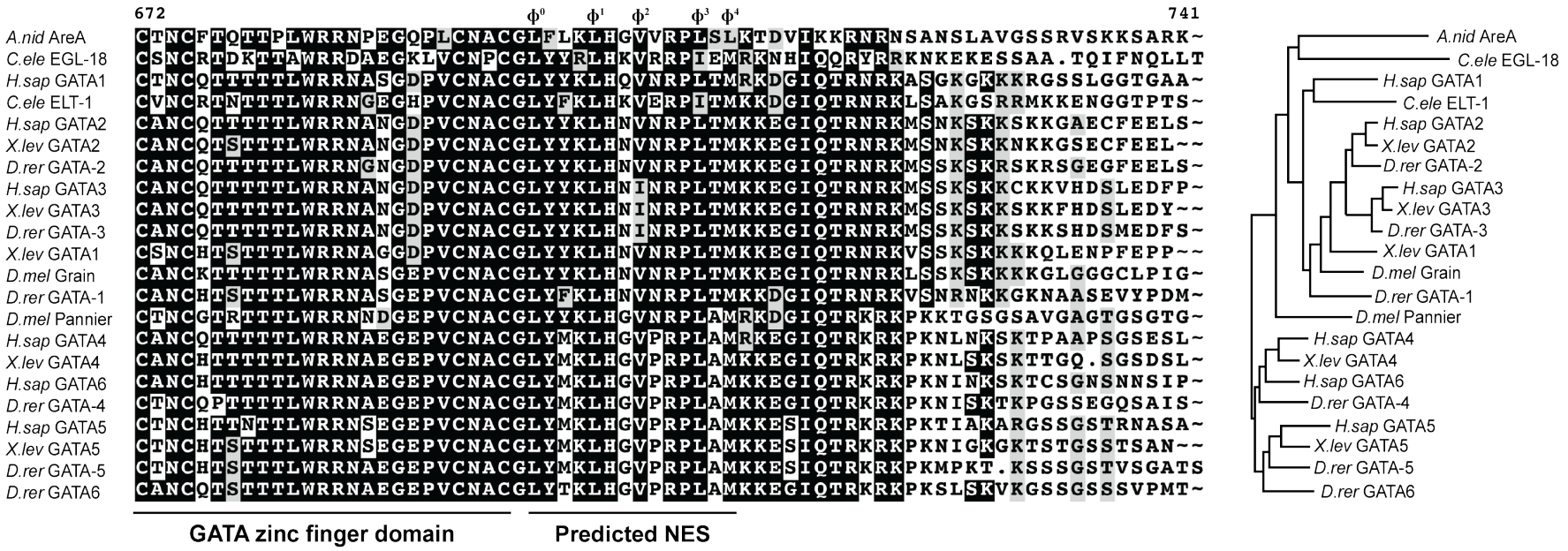

Figure 6.5 Nuclear Export Signal motifs are prevalent in eukaryotic GATA factors

Clustal Omega alignment of the DNA binding domain and predicted NES sequences of GATA factors from *A. nidulans* (*A. nid*), *C. elegans* (*C.ele*), *Homo sapiens* (*H.sap*), *Xenopus levis* (*X.lev*), *Danio rerio* (*D.rer*) and *Drosophila melanogaster* (*D.mel*) with a Clustal Omega generated un-rooted neighbor-joining tree of aligned sequences. Hydrophobic residues 0-4 are marked (ϕ^X).

6.4.2 Functional characterization of the AreA Nuclear Export Signal.

6.4.2.i The AreA Nuclear Export Signal is sufficient for nuclear export.

To determine if the predicted NES at residues 703-712 in AreA was functional we tested whether it was sufficient to confer nuclear export when fused to a nuclear localized GFP reporter protein. *A. nidulans* PrnA is a constitutively nuclear transcription factor, which is required for proline utilization (CAZELLE *et al.* 1998; POKORSKA *et al.* 2000). We fused sequences encoding the predicted AreA NES (residues 694 to 721) and GFP in-frame to the 3' end of the *prnA* gene in a plasmid containing the *A.f.pyroA* selectable marker. This fusion gene plasmid was transformed into RT96 (*pyroA4 nkuA*Δ) and pyridoxine prototrophs were selected (Figure 6.6A). Southern blot analysis (data not shown) confirmed that the construct was integrated at *prnA* by single homologous crossover to generate a full-length fusion gene replacing the wild type *prnA* gene and encoding $PrnA^{NLS}$-$AreA^{694\text{-}721}$-GFP (Figure 6.6B). Constitutive nuclear localization of the PrnA-GFP fusion protein is observed as localization to distinct foci within the nuclei (Pokorska et al., 2000). Fusion of the $AreA^{694\text{-}721}$-GFP to PrnA conferred loss of nuclear localization (Figure 6.7A) and the *prnA*^{NLS}-*areA*$^{694\text{-}721}$-*gfp* strain was unable to utilize proline as either a carbon or nitrogen source (Figure 6.7B). We also constructed using a similar strategy a strain lacking AreA residues 703-712 in the fusion protein (Figure 6.6B). The protein lacking the ten NES residues, $PrnA^{NLS}$-$AreA^{694\text{-}721.NES\Delta}$-GFP, localized within nuclear foci (Figure 6.7A), as observed for PrnA-GFP by Pokorska et al. (2000). This strain retained the ability to utilize proline as a nitrogen source though with reduced growth (Figure 6.7B). Therefore the predicted AreA NES is sufficient to direct nuclear export, and furthermore, cytoplasmic sequestration by the AreA NES confers a *prnA* loss-of-function phenotype.

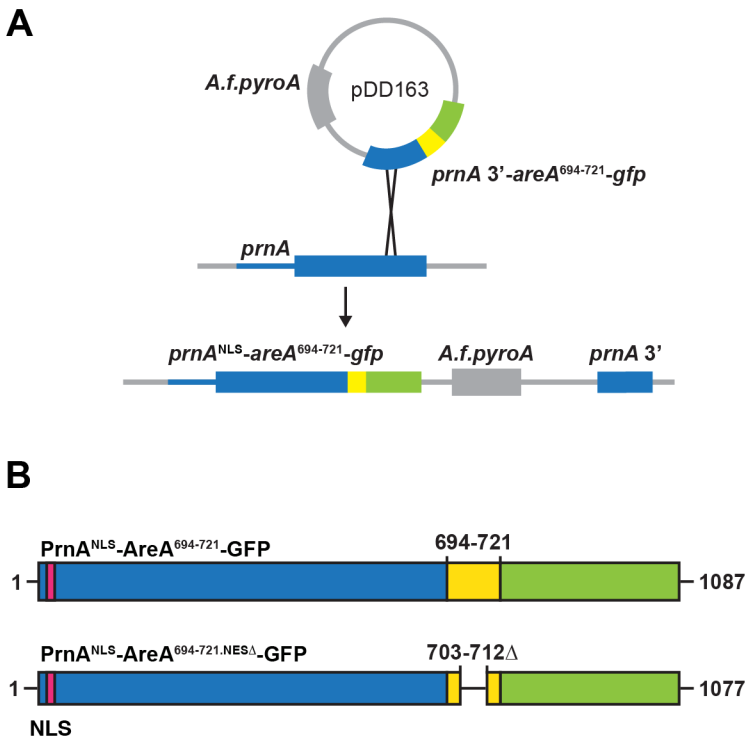

Figure 6.6 Construction of the *prnA*^{NLS}-*areA*^{NES}-*gfp* fusion gene

A) A gene fusion of the *prnA* 3'-*areA*$^{694-721}$-*gfp* in pDD163, which contains the *A.f. pyroA* selectable marker, was integrated by single crossover into the *prnA* locus to generate a full copy of *prnA* fused to *areA*^{NES}-*gfp*. **B)** Proteins expressed from the fusion genes created by integration of pDD163 and pDD164, which lacked the coding region for AreA residues 703-712.

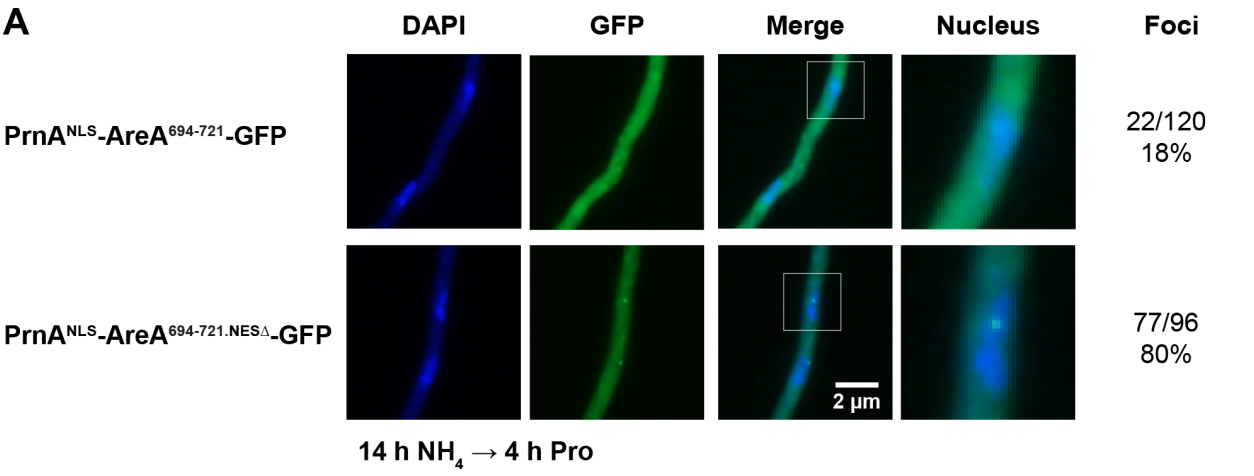

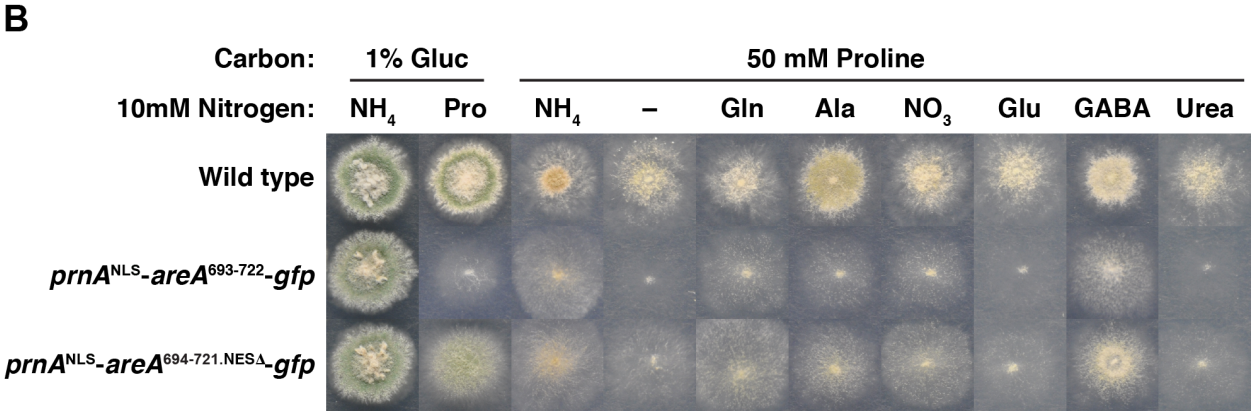

Figure 6.7 The AreA NES is sufficient for export of PrnA from the nucleus

A) Localization of PrnA^{NLS}-AreA$^{694-721}$-GFP or a fusion lacking the AreA residues 703-712 (NESΔ) after growth at 25ºC in supplemented-ANM containing 10 mM ammonium for 14 hours and then transferred to supplemented-ANM containing 10 mM proline for a further 4 hours. DAPI stains the nuclei. GFP was detected by direct UV fluorescence microscopy. **B)** Growth of wild type (MH1), *prnA*^{NLS}-*areA*$^{693-721}$-*gfp* (RT244), and *prnA*^{NLS}-*areA*$^{693-721.NESΔ}$-*gfp* (RT245) on supplemented-ANM with either 1% w/v glucose (Gluc) or 50 mM proline as the carbon source and 10 mM ammonium tartrate (NH_4), proline (Pro), glutamine (Gln), alanine (Ala), nitrate (NO_3), glutamate (Glu), ɣ-aminobutyric acid (GABA), or urea as the nitrogen source at 37ºC for 2 days.

6.4.2.ii AreA residues 703-712 are required for efficient nuclear export.

To determine if the predicted AreA NES was required for regulated nuclear export an HA-epitope tagged *gpdA*(p)*areA* gene replacement variant lacking residues 703-712 (AreA$^{HA.\Delta 703\text{-}712}$) was constructed (D.F. Clarke, M.A. Davis, and R.B. Todd, unpublished). Strains expressing AreA$^{HA.\Delta 703\text{-}712}$ grew like wild type on the preferred nitrogen sources ammonium and glutamine but, like *areA*Δ, had reduced growth on the alternative nitrogen sources alanine, glutamate and proline, and nitrate (Figure 6.8A). To measure the effects of the NES deletion on AreA-dependent gene expression we assayed the *fmdS-lacZ* reporter gene (FRASER *et al.* 2001) and found reduced expression in the *gpdA*(p)*areA*$^{HA.\Delta 703\text{-}712}$ mutant compared with wild type (Figure 6.8B). Therefore residues 703-712 are required for AreA activation capacity. This is likely to be unrelated to the nuclear export role of these residues but instead may be due to loss of DNA binding as the NES contains several residues that directly contact the DNA (STARICH *et al.* 1998). To determine the nucleocytoplasmic distribution of AreA$^{HA.\Delta 703\text{-}712}$ we performed indirect immunofluorescence microscopy on germlings grown in the presence of the preferred nitrogen source ammonium and during nitrogen starvation. The wild type AreA^{HA} protein showed a lower level of nuclear fluorescence than cytoplasmic fluorescence when grown on ammonium, but during nitrogen starvation AreA^{HA} accumulated in the nucleus (Figure 6.8C). Under both conditions the AreA$^{HA.\Delta 703\text{-}712}$ protein showed nuclear accumulation (Figure 6.8C). AreA nuclear export can be triggered by ammonium or by the alternative nitrogen sources alanine and proline (TODD *et al.* 2005). During growth on either alanine or proline as nitrogen sources AreA$^{HA.\Delta 703\text{-}712}$ accumulated in the nucleus (Figure 6.9). Carbon starvation is another known nuclear export signal for AreA, and AreA^{HA} does not accumulate in the nucleus during carbon starvation (TODD *et al.* 2005). Notably when mycelia are starved for both carbon and nitrogen the carbon export signal overrides the nitrogen nuclear accumulation signal (TODD *et al.* 2005). Fluorescence microscopy after carbon starvation with either ammonium as the nitrogen source or with simultaneous nitrogen starvation revealed nuclear accumulation of AreA$^{HA.\Delta 703\text{-}712}$ (Figure 6.9). Therefore under all tested conditions AreA^{HA} is able to enter the nucleus and the NES is required to maintain wild type nucleocytoplasmic distribution. Interestingly, during growth on ammonium and on ammonium during carbon starvation there is a significant level of AreA$^{HA.\Delta 703\text{-}712}$ fluorescence in the cytoplasm (Figures 6.8C & 6.9), whereas during nitrogen starvation and during growth on

alanine and proline AreA$^{HA.\Delta 703-712}$ is almost entirely nuclear. Given that AreA$^{HA.\Delta 703-712}$ lacking a nuclear export signal should accumulate for the entire growth period (rather than only following transfer to nitrogen starvation conditions as for wild type) it is surprising that complete nuclear localization is not seen when four hours is sufficient time for wild type AreA^{HA} to completely accumulate during nitrogen starvation. The lack of cell cycle arrest in the presence of nitrogen nutrients may allow dispersal of AreA to the cytoplasm during mitotic division, as observed for other *A. nidulans* nuclear proteins (DE SOUZA *et al.* 2004; DE SOUZA *et al.* 2006), and this may impede the rate of nuclear accumulation of AreA$^{HA.\Delta 703-712}$ under these conditions, however we did not see strong accumulation during carbon starvation, which also likely induces cell cycle arrest, when ammonium was present. It is possible therefore that a second nuclear export signal functions under these conditions or that nuclear import is regulated and slower on ammonium. The ValidNES software predicted three additional CRM1-type NESs at residues 129 to 134 (MMALSL), 187 to 192 (LDDFII), and 338 to 343 (LDTFNL) (Table 6.1). During analysis of AreA nuclear localization signals a mutant lacking residues 60 to 423, *areA*$^{HA.\Delta 60-423}$, was generated (HUNTER *et al.* 2014). This mutant lacks three of the five classical NLSs, but importantly also lacks all three of the predicted additional NES signals. The protein encoded by *areA*$^{HA.\Delta 60-423}$ activates *fmdS-lacZ* reporter gene expression and permits the use of alternative nitrogen sources similar to wild type, as the three remaining NLSs are sufficient for nuclear import (HUNTER *et al.* 2014). Immunofluorescence microscopy of this strain showed that deletion of these three putative NES motifs does not confer AreA nuclear accumulation during growth on ammonium (Figure 6.8C) (HUNTER *et al.* 2014). Therefore these three putative NES sequences do not play a major role in AreA nuclear export when the primary NES at residues 703-712 is present. However, analysis of nucleocytoplasmic fluorescence ratios shows a significant increase in nuclear levels of AreA$^{HA.\Delta 60-423}$ compared to wild type germlings grown on ammonium. Therefore one or more of these three sequences may function as a nuclear export sequence, albeit relatively weakly to the NES at residues 703-712.

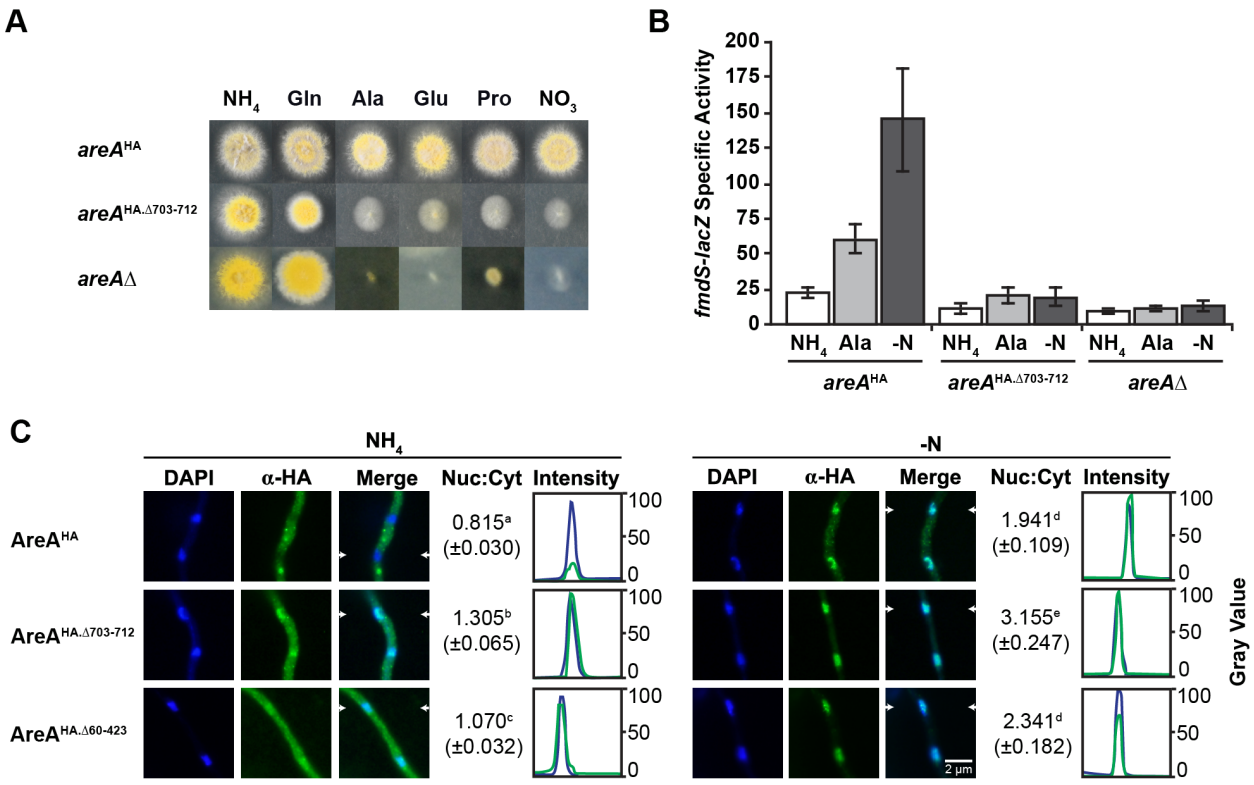

Figure 6.8 The AreA NES is required for export of AreA^{HA} from the nucleus

A) Growth of *gpdA*(p)*areA*^{HA} (MH10897), *gpdA*(p)*areA*$^{HA.\Delta 703\text{-}712}$ (MH12068) and *areA*Δ (RT10967) on solid supplemented-ANM with 10 mM ammonium (NH_4), glutamine (Gln), glutamate (Glu), alanine (Ala), proline (Pro), or nitrate (NO_3) at 37ºC for 2 days. **B)** Expression of the *fmdS-lacZ* reporter in *areA*^{HA} (MH10897), *areA*$^{HA.\Delta 703\text{-}712}$ (RT136) and *areA*Δ (MH10967) after 16 hours growth in supplemented-ANM with 10 mM ammonium tartrate before transfer to 10 mM ammonium (NH_4), alanine (Ala) or nitrogen starvation (-N) at 37ºC for 4 hours. **C)** The subcellular distribution of AreA^{HA} (MH9949), AreA$^{HA.\Delta 703\text{-}712}$ (MH12068), and AreA$^{HA.\Delta 60\text{-}423}$ (MH11457) after growth at 25ºC in supplemented liquid-ANM containing 10 mM ammonium for 14 hours and transferred to supplemented-ANM containing 10 mM ammonium (NH_4) or no nitrogen source (-N) for 4 hours. DAPI stains the nuclei. AreA^{HA} (α-HA) was visualized by UV fluorescence microscopy following immunostaining with α-HA (3F10) and Alexa Fluor-488-conjugated goat anti-rat antibodies. Nuclear to Cytoplasmic fluorescence ratio (Nuc : Cyt) was calculated from the mean α-HA fluorescence ratio of 13 nuclei and adjacent cytoplasm. SEM is shown. Superscript lowercase letters indicate significantly different groups using the two-tailed Student's t-test ($p < 0.05$). Arrowheads show transects used to generate a fluorescence intensity plots for DAPI (blue) and α-HA (green).

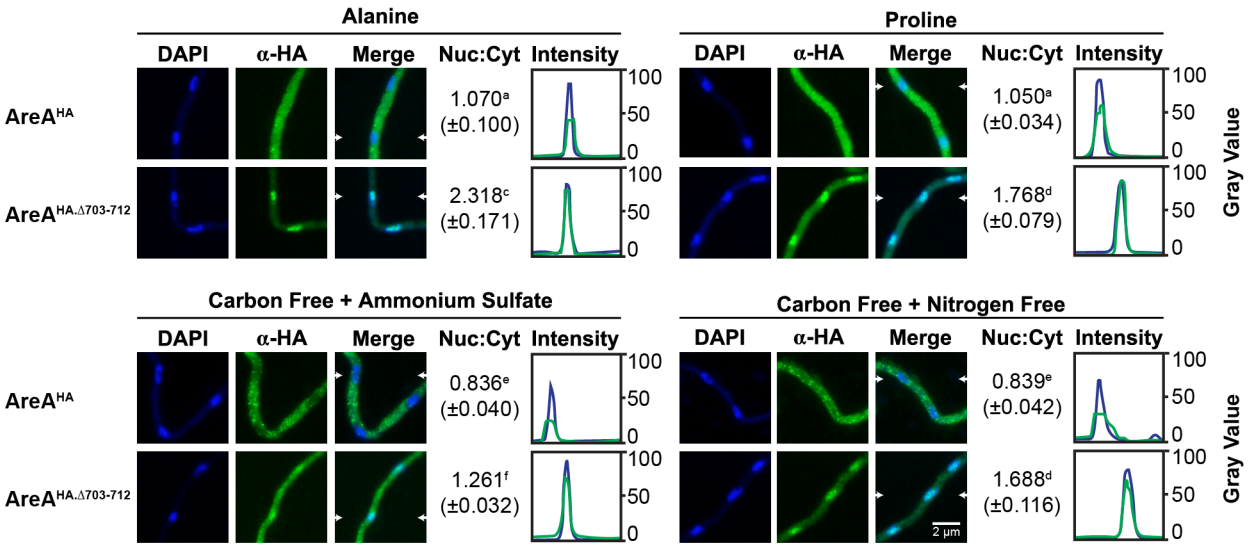

Figure 6.9 AreA$^{HA.\Delta 703\text{-}712}$ accumulates under all tested conditions

Localization of of AreA^{HA} (MH9949) and AreA$^{HA.\Delta 703\text{-}712}$ (MH12068) after growth at 25ºC in supplemented liquid ANM with 10 mM ammonium for 14hours and transferred to supplemented liquid ANM with 10 mM alanine or proline, to supplemented carbon starvation media with 10 mM ammonium sulfate, or supplemented carbon starvation media lacking a nitrogen source for four hours. DAPI stains the nuclei. AreA^{HA} (α-HA) was visualized by UV fluorescence microscopy following immunostaining with α-HA (3F10) and Alexa Fluor-488-conjugated goat anti-rat antibodies. Nuclear to Cytoplasmic fluorescence ratio (Nuc : Cyt) was calculated from the mean α-HA fluorescence ratio of 13 nuclei and adjacent cytoplasm. SEM is shown. Superscript lowercase letters indicate significantly different groups using the two-tailed Student's t-test ($p < 0.05$). Arrowheads show transects used to generate a fluorescence intensity plots for DAPI (blue) and α-HA (green).

6.4.3 Mutational analysis of the strong AreA nuclear export signal

6.4.3.i AreA Histidine 704 is required for regulated nuclear export.

The CRM1 nuclear export signal was identified as being "leucine rich" (FORNEROD *et al.* 1997a), however it is now known that hydrophobic residues are required for interaction with the five hydrophobic pockets of the CRM1-cargo binding site (GUTTLER *et al.* 2010). Mutation of hydrophobic residues within the NESs of some proteins results in loss of nuclear export (e.g. FISCHER *et al.* 1995; WEN *et al.* 1995; STOMMEL *et al.* 1999; HENDERSON AND ELEFTHERIOU 2000). NES hydrophobic residues equivalent to AreA Leu-710 and Leu-712 are the key residues for most NESs, and mutation of either or both is often, though not always, sufficient to disrupt NES function (WEN *et al.* 1995; MAIURI *et al.* 2013). The importance of Leu-710 and Leu-712 within the AreA NES was previously tested with strains where each leucine was mutated to alanine, as well as a double Leu-710-Ala/Leu-712-Ala mutant, however all three mutants showed wild type AreA nuclear localization (R.B. Todd unpublished). A mutation substituting Leu-710 for isoleucine (Leu-710-Ile) has been previously reported to confer derepression of the AreA-regulated nitrate reductase gene *niaD* (PLATT *et al.* 1996a). To analyze the effects of Leu-710-Ile on AreA subcellular distribution a HA-epitope tagged version of $AreA^{L710I}$ was required. During the construction of the Leu-710-Ile mutant an additional mutation in the NES was serendipitously introduced to generate a His-704-Asn/Leu-710-Ile double mutant (Figure 6.10A) (M.A. Davis, and R.B. Todd, unpublished). This double mutant was able to utilize alternative nitrogen sources (Figure 6.10B) and had expression levels of *fmdS-lacZ* similar to wild type (Figure 6.10C). Immunofluorescence microscopy showed that nuclear localization of $AreA^{HA.H704N.L710I}$ was increased compared with the wild type $AreA^{HA}$ control during growth on ammonium (Figure 6.10D). To determine if a single mutation or both mutations together were responsible for this phenotype, separate His-704-Asn and Leu-710-Ile mutants were generated (K.S. Siebert and R.B. Todd, unpublished). Consistent with the double mutant, both strains had wild type AreA function (Figure 6.10B-C). Immunofluorescence microscopy revealed that $AreA^{HA.H704N}$ but not $AreA^{HA.L710I}$ showed increased nuclear localization compared with wild type $AreA^{HA}$ on ammonium (Figure 6.10D). Therefore His-704 of the AreA NES is required for wild type AreA nucleocytoplasmic distribution. The histidine residue is conserved in almost all fungal AreA homologs (Figure 6.2B) and in all animal orthologs (Figure 6.5), suggesting

functional importance. The consensus motif for the CRM1-type NES motifs indicates a preference for hydrophilic residues prior to ϕ^1 (AreA Leu-703), but no bias afterwards (Figure 6.2A; GUTTLER *et al.* 2010), however there is a general preference for small charged residues between the hydrophobic residues of the NES (KOSUGI *et al.* 2008; FUNG AND CHOOK 2014). Mutation of His-704 to Asn represents replacement of a positively charged residue with a non-charged polar residue. This change may therefore disturb the interaction of adjacent hydrophobic leucine in the AreA NES with the CrmA binding pocket. Alternatively, protein modification is a means by which nuclear export is regulated (e.g. PAPP *et al.* 2006; USHIJIMA AND MAEDA 2012) and His-704 may be modified by a regulatory protein to facilitate export; mutation of His-704 may remove the target residue of a regulatory protein and block regulated nuclear export of AreA. Protein histidines may be modified by phosphorylation or methylation (BOYER *et al.* 1962; ASATOOR AND ARMSTRONG 1967; JOHNSON *et al.* 1967), suggesting His-704 may be the target of a possible regulatory modification; this possibility is explored in Chapter 7.

Figure 6.10 AreA Histidine 704 is required for export from the nucleus.

A) Substitutions made in the AreA NES **B)** Growth of *areA*^{HA} (MH10897), *areA*$^{HA.H704N.L710I}$ (MH10898), *areA*$^{HA.H704N}$ (RT104), and *areA*$^{HA.L710I}$ (RT116) on 1% complete media and supplemented solid-ANM with 10 mM ammonium (NH_4), glutamine (Gln), glutamate (Glu), alanine (Ala), proline (Pro), nitrate (NO_3), and without nitrogen (-N) at 37ºC for 2 days. **C)** Expression of the *fmdS-lacZ* reporter in *areA*^{HA} (MH10897), *areA*$^{HA.H704N.L710I}$ (MH10898), *areA*$^{HA.H704N}$ (RT104), *areA*$^{HA.L710I}$ (RT116), and *areA*Δ (MH10967) after 16 hours growth in supplemented liquid-ANM with 10 mM ammonium tartrate before transfer to supplemented liquid-ANM with 10 mM ammonium (NH_4), alanine (Ala) or without nitrogen (-N) at 37ºC for a further 4 hours. **D)** Localization of AreA^{HA} (MH9949), AreA$^{HA.H704N.L710I}$ (MH10608), AreA$^{HA.H704N}$ (RT104), and AreA$^{HA.L710I}$ (RT103) after growth at 25ºC in supplemented liquid-ANM with 10 mM ammonium for 14 hours and transferred to 10 mM ammonium (NH_4) or nitrogen starvation (-N) for 4 hours. DAPI stains DNA and marks the location of nuclei. AreA^{HA} (α-HA) was visualized by UV fluorescence microscopy following immunostaining with α-HA (3F10) and Alexa Fluor-488-conjugated goat anti-rat antibodies. Nuclear to Cytoplasmic fluorescence ratio (Nuc : Cyt) was calculated from the mean α-HA fluorescence ratio of 13 nuclei and adjacent cytoplasm. SEM is shown. Superscript lowercase letters indicate significantly different groups using the two-tailed Student's t-test ($p < 0.05$). Arrowheads show transects used to generate a fluorescence intensity plots for DAPI (blue) and α-HA (green).

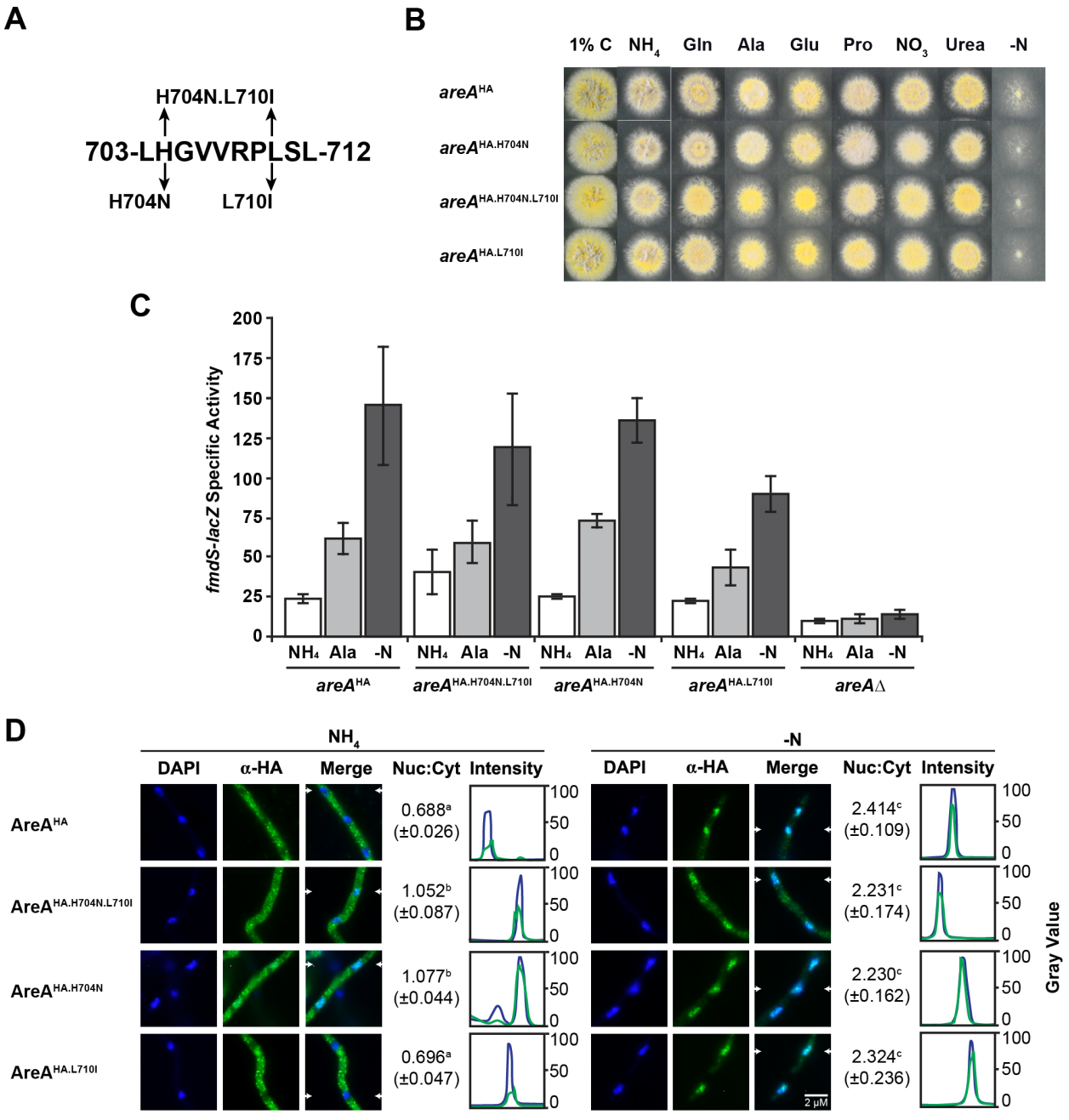

Figure 6.10 Histidine-704 is required for efficient nuclear export.

6.4.4 A genetic screen for loss of regulated AreA nuclear export

6.4.4.i Characterization of 4-nitroquinoline 1-oxide as a mutagen.

NOTE: This is a summary of research conducted as part of this dissertation that was published in Downes D.J., M. Chonofsky, K. Tan, B.T. Pfannenstiel, S. L. Reck-Peterson & R.B. Todd (2014a) Characterization of the Mutagenic Spectrum of 4-Nitroquinoline 1-Oxide (4-NQO) in *Aspergillus nidulans* by Whole Genome Sequencing. *G3 (Bethseda)* **4 (12):** 2483-2492. *The full article has been included as Appendix B.*

Many mutagens are available to *A. nidulans* researchers for mutagenesis. We prefer to use 4-nitroquinoline 1-oxide (4-NQO) because it can generate both loss-of-function and altered function mutations by single base pair substitution, and it can be inactivated, making it safer than some other mutagens. 4-NQO has been used to generate mutants in *A. nidulans* for several decades (BAL *et al.* 1977), however its molecular effects as a mutagen have never been characterized in this species. Studies in *Escherichia coli, Salmonella typhimurium, Saccharomyces cerevisiae,* and *Schizosaccharomyces pomb*e showed that 4-NQO specifically targets guanine residues to generate substitution mutations (PRAKASH *et al.* 1974; JANNER *et al.* 1979; ROSENKRANZ AND POIRIER 1979). However, these experiments were carried out using reversion tester strains which although useful cannot distinguish multiple mutations, extragenic suppressors or G:C to C:G transversions (PRAKASH AND SHERMAN 1973). To determine the mutagenic spectrum of 4-NQO in *A. nidulans* we collaborated with Samara Reck-Peterson (Harvard Medical School) who had generated and sequenced the genomes of dozens of 4-NQO induced mutants. Using the called variants identified by the Reck-Peterson lab we mapped and characterized each lesion. Overall nearly 4000 mutations were analyzed. These mutations were almost entirely single nucleotide substitutions, were evenly distributed across the genome and were not influenced by flanking sequence. The total number of mutations per strain was between 23 and 240 mutations, with the average number of lesions being 100. Interestingly different doses of 4-NQO did not confer a significant difference in the number of lesions in recovered strains. Mutations of guanine-cytosine base pairs occurred 19 times as frequently as mutation of adenine-thymine base pairs (Figure 6.11), however each possible substitution type was observed. Therefore 4-NQO is able to target all possible bases and generate all possible mutations. Using

our data we developed a probability based equation to predict the 4-NQO dose required per number of treated conidia to generate a saturation screen.

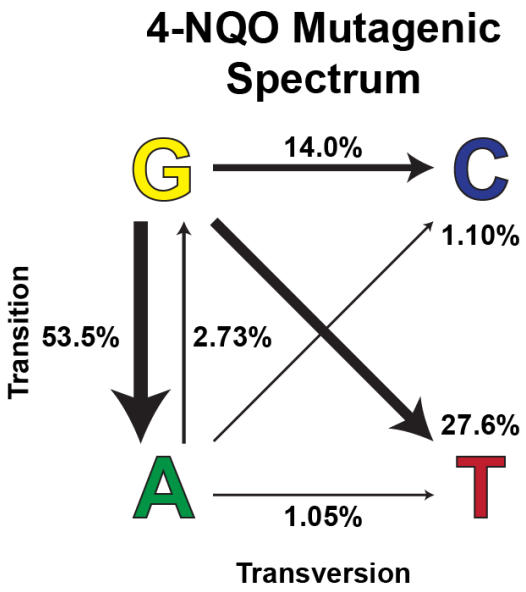

Figure 6.11 Mutagenic spectrum of 4-NQO

4-NQO forms adducts of both adenine and guanine, leading to all possible transitions and transversions (Adapted from DOWNES *et al.* 2014a).

6.4.4.ii Generation and classification of nuclear export mutants.

Fusion of the *areA* NES to *prnA* resulted in a proline non-utilizing phenotype (Figure 6.7B). We took advantage of this phenotype to carry out a genetic screen for novel mutants deficient in AreA NES nuclear export (Figure 6.12A). This screen was designed to readily identify mutations in the *areA* NES encoded in the *prnA*^{NLS}-*areA*$^{694\text{-}621}$-*gfp* construct (Class 1), the *crmA* exportin (Class 2) or novel regulatory protein or export machinery protein encoding genes required for nuclear export via the AreA NES (Class 3) by a single cross (Figure 6.12B). Mutants of RT244 (*prnA*^{NLS}-*areA*$^{694\text{-}621}$-*gfp crmA*^{T525C}-*pyrG*) were generated by treatment with the toxic mutagen 4-NQO, and mutated conidia were selected for utilization of proline as a nitrogen source. 34 putative mutants were recovered from the initial screen and designated ANX1-34 for **A**reA **N**uclear e**X**port deficient. 24 ANX mutants were pyridoxine auxotrophs due to loss of the *A.f.pyroA*$^{+}$ selectable marker in the construct by recombination. The remaining ten mutants were outcrossed to RT250 (*prn-309 pyrG89*) to map the mutations. ANX causative mutations within the fusion gene are predicted to segregate with the fusion gene as a single gene with two alleles from this cross (*prnA*^{NLS}-*areA*$^{694\text{-}621.ANX}$-*gfp* and *prn-309*) and generate 50% proline utilizing progeny. ANX causative mutations unlinked to the fusion gene are predicted to segregate independently of the fusion gene, i.e. two genes with two alleles (ANX^{+} with ANX^{-} and *prnA*^{NLS}-*areA*$^{694\text{-}621}$-*gfp* with *prn-309*), and generate 25% proline utilizing progeny. In conjunction with B.T Pfannenstiel nine of the ten ANX mutants were mapped. Eight mutants (ANX1-4 and ANX18-21) were mapped as *prnA*^{NLS}-*areA*$^{694\text{-}621.ANX}$-*gfp* alleles (Table 6.2). The *prnA 3'* and *areA* region of the fusion gene was PCR-amplified from these mutants and sequenced. All eight mutations resulted in nonsense substitutions upstream of the NES (Table 6.3). Of the two remaining mutants only one, ANX6, was able to be analyzed by meiotic cross, and was determined as unlinked to the *prnA* locus (Table 6.2). As *crmA*^{T525C} was generated with the *pyrG*$^{+}$ marker ANX mutations within *crmA* can be determined by cosegregation of proline utilization and pyrimidine prototrophy. Mutations that are in neither the *prnA* or *crmA* loci will generate a 1:1 ratio of proline-utilizating pyrimidine-prototroph progeny to proline-utilizating pyrimidine-auxotroph progeny. We isolated 17 proline utilizing progeny from the ANX6 cross and nine of these were pyrimidine-prototrophs. Therefore ANX6 segregates independently of *crmA*^{T525C}-*pyrG* (χ^2 = 0.06, d.f. = 1, p = 0.81). The final mutant, ANX25, rapidly loses the proline utilization phenotype when removed from selective media, however they maintain the

A.f. pyroA selectable marker associated with the construct. When crossed, the ANX25 proline utilization phenotype was not present in progeny, however all other markers segregated at the expected frequency. Because of these observations it was concluded this mutant also likely fell into Class 3.

ANX6 and ANX25 were both able to grow on proline or other alternative nitrogen sources (Figure 6.13A); when grown on proline for an extended period ANX25 secreted a bright red pigment into the media (Figure 6.13B). Both strains showed delayed spore germination when grown in liquid media (Figure 6.13C). To confirm that proline utilization in these mutants is as a result of altered nuclear export, fluorescence microscopy was used to visualize $PrnA^{NLS}$-$AreA^{694-621}$-GFP. The fusion protein had an increased number of nuclear foci in the mutant compared with wild type in the two mutants when grown on proline (Figure 6.14A), indicating that both ANX6 and ANX25 are true nuclear export deficient mutants. We expected that the Class 2 and 3 mutants identified in our screen would also affect $AreA^{HA}$ nuclear export. Immunofluorescnece microscopy showed increased nuclear localization of $AreA^{HA}$ in the ANX6 and ANX25 mutants compared with wild type when grown on ammonium (Fig 6.14B). Therefore the ANX6 and ANX25 mutants affect nuclear export of both $PrnA^{NLS}$-$AreA^{694-621}$-GFP and $AreA^{HA}$. Haploidization of diploids is a useful technique for mapping new mutations to one of the eight *A. nidulans* chromosomes (TODD *et al.* 2007a). Therefore diploids were generated of ANX6 and ANX25 with the mapping strain MSF (*yA1 AcrA1 galA1 pyroA4 facA303 sB3 nicB3 riboB2*), which carries a marker on each chromosome (MCCULLY AND FORBES 1965). During haploidization of the ANX/MSF diploid one copy of each homologous chromosome will be lost to generate haploid individuals, and the ANX mutation will segregate among the haploids in repulsion to the marker on the homologous chromosome. As the ANX phenotype of suppression of proline non-utilization could only be scored in the presence of the *prnA*^{NLS}-*areA*$^{694-621}$-*gfp* fusion gene on chromosome VII, only pyridoxine prototroph colonies containing the *A.f.pyroA* selectable marker associated with integration of the fusion gene construct were analyzed. Furthermore, there is no mapping marker on chromosome IV as the *pyroA4* mutation is homozygous in the diploid. Mutations on chromosome VII will co-segregate with *A.f. pyroA,* whereas mutations on chromosome IV can be distinguished by, lack of co-segregation with *A.f. pyroA,* and lack of segregation in repulsion for any of the other six chromsomes. Haploidization of the ANX6/MSF diploid mapped the putative ANX6 causative mutation to chromosome III

(Table 6.4). The ANX6 mutant has not yet been further characterized. Proline utilization was absent in pyridoxine prototroph haploids generated from ANX25/MSF, despite other markers segregating and therefore this mutation could not be mapped.

Table 6.2 Crossing analysis of ANX genetic screen mutants and RT250.

Mutant		$H_0$1: One gene with two alleles (*prn-309/prnA*^{NLS}*-AreA*$^{694\text{-}621.ANX}$*-gfp)* – Expect 50% Prn$^+$			$H_0$2: Two genes with two alleles (*ANX*$^{+/-}$ *& prn-309/prnA*^{NLS}*-AreA*$^{694\text{-}621}$*-gfp)* – Expect 25% Prn$^+$		
	Prn$^+$ progeny	χ^2 (d.f = 1)	P	Reject or Retain $H_0$1	χ^2 (d.f = 1)	P	Reject or Retain $H_0$2
WT	0/46	46.00	< 0.01	Reject	15.33	< 0.01	Reject
ANX1	26/46	0.783	0.37	Retain	8.377	< 0.01	Reject
ANX2	25/46	0.348	0.55	Retain	21.13	< 0.01	Reject
ANX3	26/46	0.783	0.37	Retain	8.377	< 0.01	Reject
ANX4	24/46	0.087	0.76	Retain	18.11	< 0.01	Reject
ANX6	17/64	14.06	< 0.01	Reject	0.083	0.77	Retain
ANX18	22/46	0.087	0.76	Retain	12.78	< 0.01	Reject
ANX19	25/46	0.348	0.55	Retain	21.13	< 0.01	Reject
ANX20	26/46	0.783	0.37	Retain	8.377	< 0.01	Reject
ANX21	24/46	0.087	0.76	Retain	18.11	< 0.01	Reject
ANX25[a]	0/46	46.00	< 0.01	Reject	15.33	< 0.01	Reject
NESΔ	28/46	2.174	0.14	Retain	31.56	< 0.01	Reject

[a] *prn*$^+$ did not segregate in this cross but all other markers did.

Table 6.3 Sequence changes in the *prnA*^{NLS}*-areA*$^{694\text{-}621}$*-gfp* fusion gene mutants.

Mutant	Change	Protein sequence	Effect
WT	Nil	GQTGPSSGAGPGLPGELDMKEGWMTFCNACGLFLK**LHGVVRPLSL**KTD	Wild type
ANX1	Δ bp	GQTGPSSGAGRVSQESWI*	Frameshift
ANX2	G → T	GQTGPSSGAGPGLPGELDMK*	Nonsense
ANX3	G → T	GQT*	Nonsense
ANX4	C → A	GQTGPS*	Nonsense
ANX18	C → A	GQTGPSSGAGPGLPGELDMKEGWMTFCNA*	Nonsense
ANX19	G → T	GQTGPSSGAGPGLP*	Nonsense
ANX20	Δ bp	GQTGPSSGAGPGLVSQESWI*	Frameshift
ANX21	G → T	GQTGPSSGAGPGLP*	Nonsense

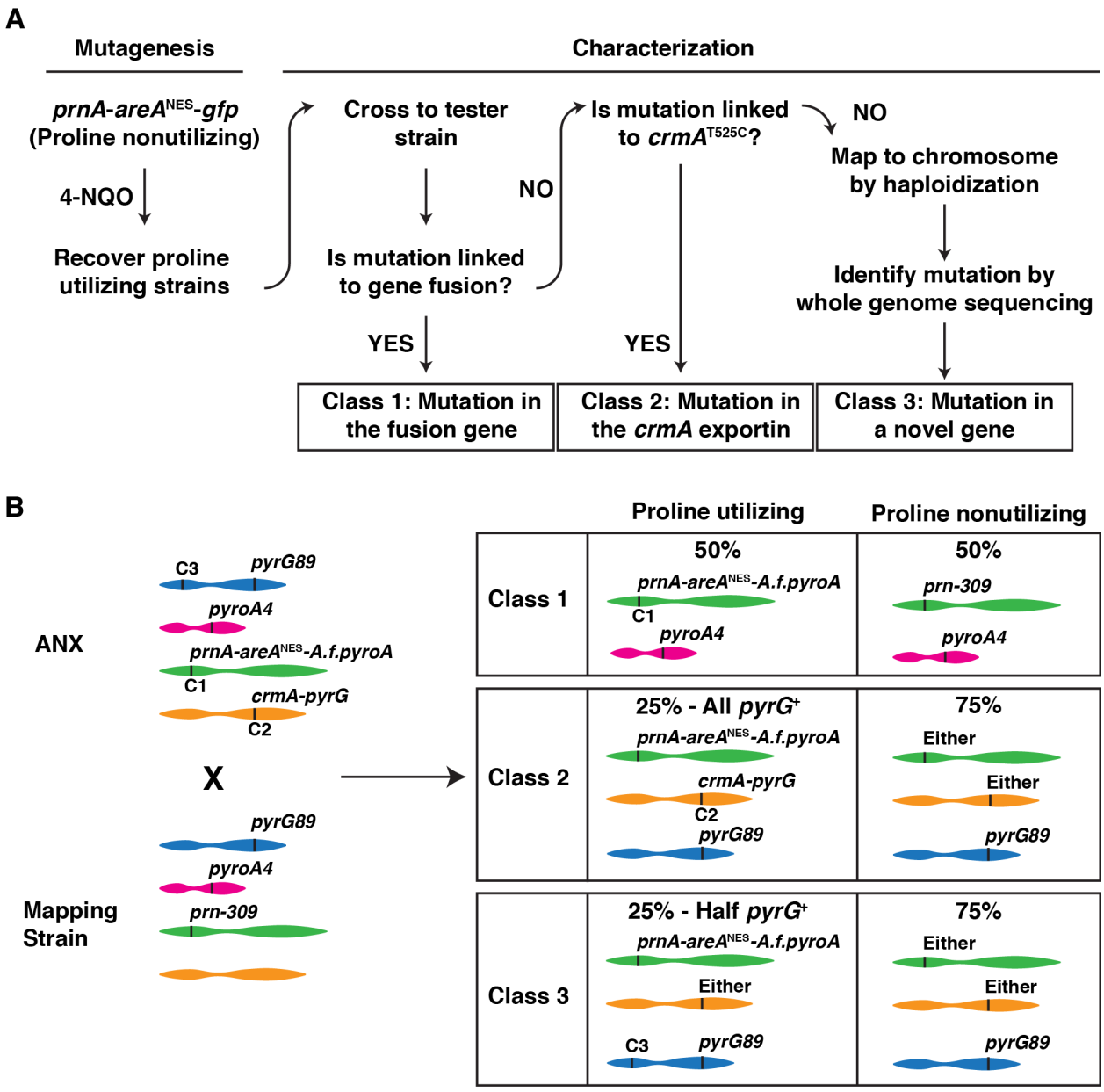

Figure 6.12 Design of the AreA^{NES} nuclear export genetic screen.

Strategy for the generation of mutants defective in regulated AreA nuclear export **(A)** and a method to quickly classify the causative mutation as affecting the *prnA*^{NLS}-*areA*$^{694\text{-}621}$-*gfp* construct (Class 1), the CrmA exportin (Class 2) or a novel gene (Class 3) by meiotic crossing **(B)**. As mutations in Class 2 and 3 both represent mutations unlinked to the fusion gene both classes will have one quarter of proline utilizing progeny. Because *crmA* from the mutagenesis strain is tagged with *pyrG*$^{+}$ mutants at this locus can be tracked, all proline utilizing progeny will be uridine and uracil prototrophs and thus the two classes can be distinguished.

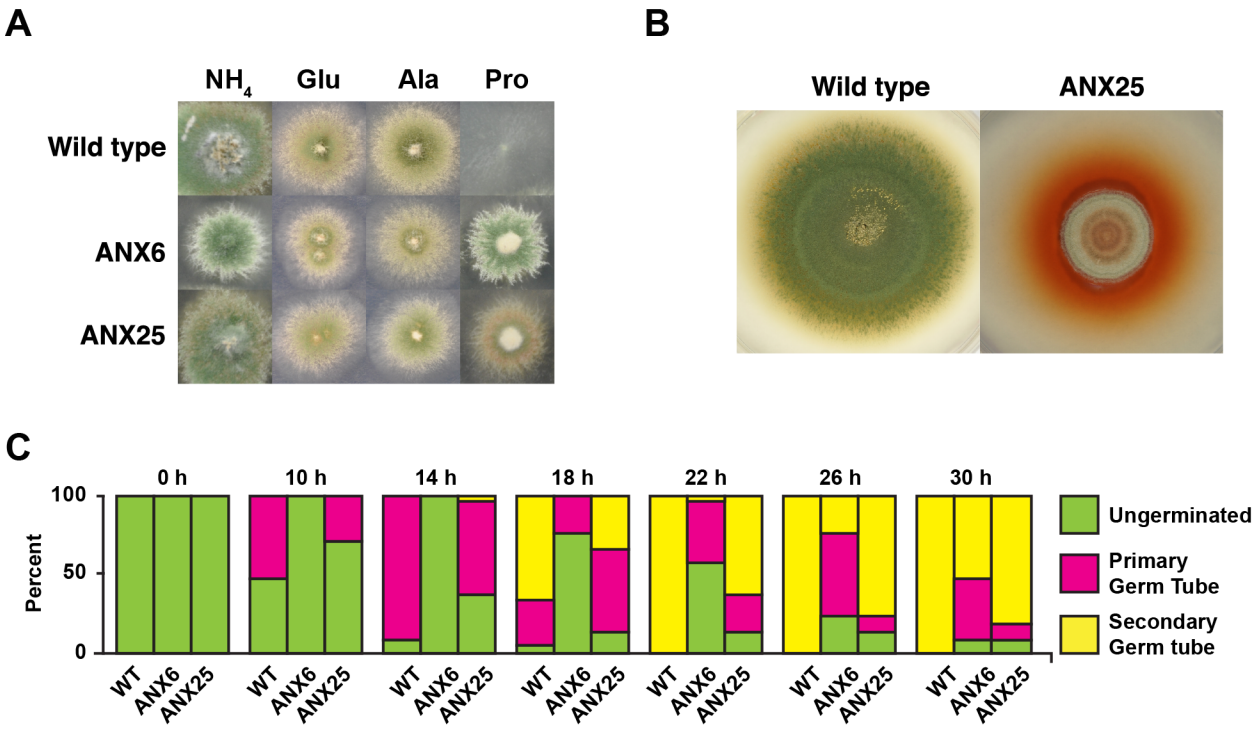

Figure 6.13 Effects of ANX6 and ANX25 on growth.

A) Growth of *prnA*^{NLS}-*areA*$^{694-621}$-*gfp* (RT244), ANX6 (RT259), and ANX25 (RT262) after 2 days at 37ºC on supplemented solid-ANM containing 10 mM ammonium (NH_4), glutamine (Glu), alanine (Ala), or proline (Pro). **B)** Growth of wild type (MH1) and ANX25 (RT262) after 5 days at 37ºC on solid supplemented-ANM containing 10 mM proline **C)** Germination of wild type (MH1), ANX6 (RT259) and ANX25 (RT262) in supplemented liquid-ANM containing 10 mM ammonium. At each timepoint 50 conidia were assessed for the presence of one germ tube (primary) or two germ tubes (secondary).

Figure 6.14 Effects of ANX6 and ANX25 on nuclear export.

A) Localization of $PrnA^{NLS}$-$AreA^{694-721}$-GFP in wildtype (RT244), ANX6 (RT259) and ANX25 (RT262) after growth at 25ºC in supplemented-ANM containing 10 mM ammonium for 14 hours and then transferred to supplemented-ANM containing 10 mM proline for a further 4 hours. DAPI stains the nuclei. GFP was detected by direct UV fluorescence microscopy. **B)** Localization of $AreA^{HA}$ in wildtype (RT244), ANX6 (RT259) and ANX25 (RT262) after growth at 25ºC in supplemented liquid-ANM with 10 mM ammonium for 18 hours. DAPI stains DNA and marks the location of nuclei. $AreA^{HA}$ (α-HA) was visualized by UV fluorescence microscopy following immunostaining with α-HA (3F10) and Alexa Fluor-488-conjugated goat anti-rat antibodies. Nuclear to Cytoplasmic fluorescence ratio (Nuc : Cyt) was calculated from the mean α-HA fluorescence ratio of 13 nuclei and adjacent cytoplasm. SEM is shown. Superscript lowercase letters indicate significantly different groups using the two-tailed Student's t-test ($p < 0.05$). Arrowheads show transects used to generate a fluorescence intensity plots for DAPI (blue) and α-HA (green).

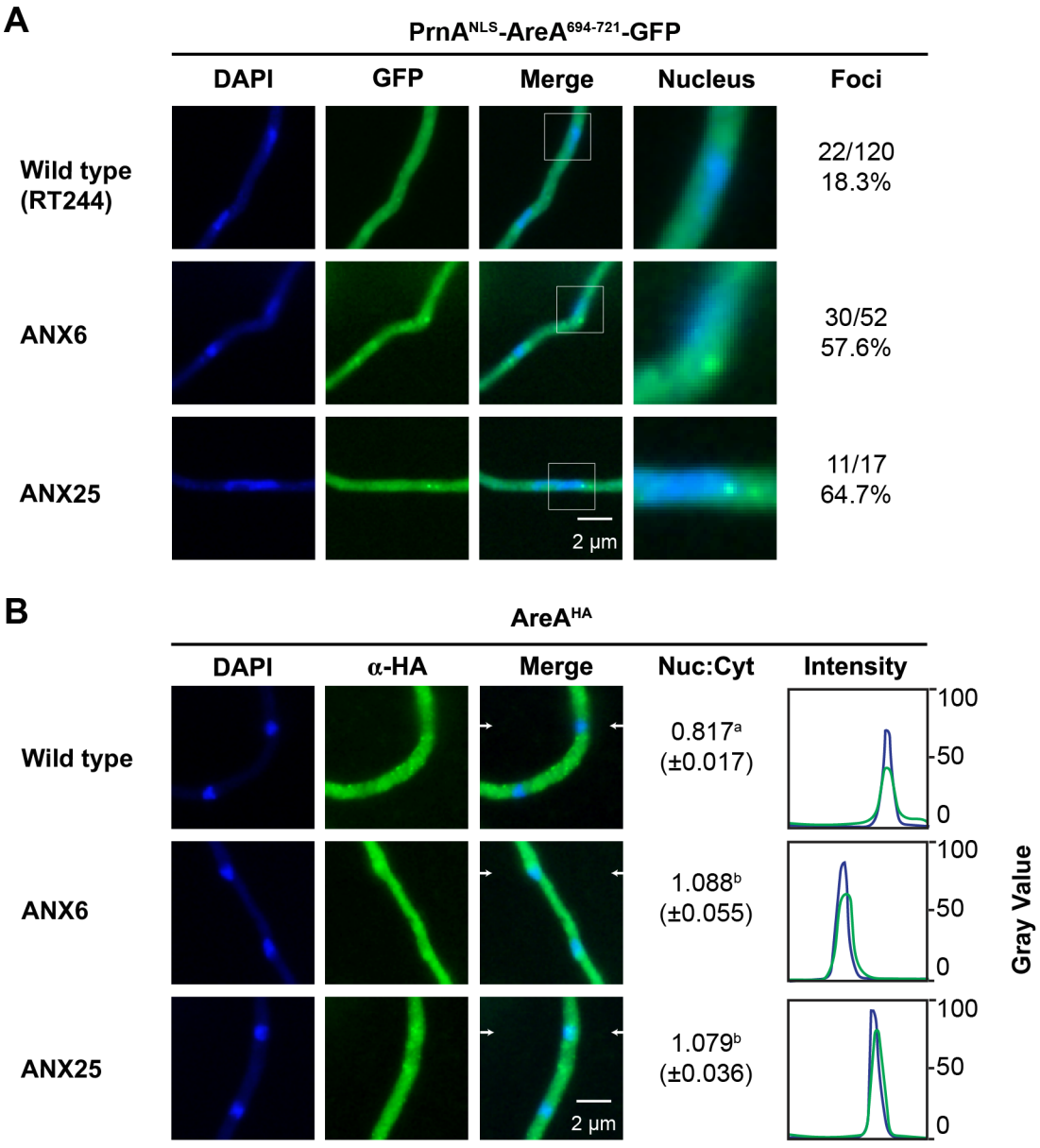

Figure 6.14 Effects of ANX6 and ANX25 on nuclear export.

Table 6.4 Haploidization mapping of ANX6.

Chr.[a]	Marker	Segregation in Repulsion	Repulsion
I	*yA1*	17/35	43%
I	*biA1*	17/35	43%
II	*AcrA1*	13/35	37%
III	*galA1*	35/35	100%
IV[b,c]	*pyroA4*	–	–
V	*facA303*	20/35	57%
VI	*sB3*	12/35	34%
VII[c]	*nicB3*	0/35	0%
VIII	*riboB2*	23/35	65%
Chr.[a]	**Marker**	**Pro utilizing progeny**	**Co-segregation**
VII[d]	*A.f.pyroA*	13/35	37%

[a] Chromosome
[b] Could not score due to homozygous *pyroA4* on chromosome IV
[c] *A.f pyroA* at *prnA* was selected to isolate $prnA^{NLS}$-$areA^{694-621}$-*gfp* haploids
[d] ANX mutations on chromosome VII will co-segregate with *A.f.pyroA*

Table 6.5 Sequence changes in the classical mutants *niiA4*, *pyrG89,* and *riboB2*.

Mutant	Nucleotide Change	Amino Acid Change	Wild type and altered protein sequence	Effect
niiA4	ΔG2254	Gly-652-Gln	649-VPGGEITADKLI 649-VPEVKSQPTS*	Frameshift
pyrG89	G511A	Gly-151-Asp	148-QRGLL 148-QRDLL	Missense
riboB2	ΔC856	Arg-286-Val	284-YLRQEGRGI 284-YLVKKAEV*	Frameshift

6.4.4.iii Identification and characterization of the ANX25 causative mutation.

As described previously in Chapter 5.4.2, whole genome sequencing is a powerful tool for identifying novel mutations. To identify the potential causative mutation(s) in ANX25 next generation sequencing was carried out on genomic DNA of ANX25 and the mutagenesis parent RT244. Reads were mapped to the *A. nidulans* FGSC_A4 reference genome using Burrows-Wheeler Alignment which generated 4 fold or better coverage for >97.6% of the genome. From our whole genome sequencing described here and in Chapter 5 we were also able to identify the probable causative mutations in the classical *pyrG89*, *niiA4* and *riboB2* mutants, which have not previously been reported (Table 6.5).

As 4-NQO induces single nucleotide substitutions, Free Bayes Variant analysis (McKenna *et al.* 2010) was used to identify potential causative mutations. ANX25 contained 70 mutations that were absent in the wild type parent, consistent with 4-NQO inducing an average of approximately 105 mutations per genome (Downes *et al.* 2014a). 69 of the variants were nucleotide substitutions and the remaining one variant was a single nucleotide deletion. Mapping of the mutations showed 43/70 occurred in transcribed regions and 34 in protein coding sequence. These 34 mutations were assessed for potential effect on the transcribed proteins: 8/34 mutations were silent, 25/34 mutations caused missense substitutions and 1/43 mutations caused a nonsense substitution resulting in a 532 amino acid truncation of a 1,243 amino acid protein (Table 6.6). Therefore, whole genome sequencing identified 26 mutations potentially affecting protein function and conferring the ANX25 proline utilization phenotype. As mapping data was unavailable for ANX25, the 26 mutations were examined for the effect on the protein (i.e substitution or truncation) and predicted function of the protein. From this analysis the most likely candidate causative mutation is in AN2086/*nup159* as this gene encodes an essential nuclear pore protein (Osmani *et al.* 2006a). Furthermore, in yeast Nup159 is known to interact with the CRM1 exportin (Floer and Blobel 1999; Jensen *et al.* 2000). The mutation in *nup159* is a C to A transversion at nucleotide +2,955 resulting in a proline to glutamine substitution (CCA to CAA) at residue 953 (Figure 6.15). This proline is conserved in 17/20 *Aspergillus* orthologs in AspGD, the exceptions being *Aspergillus sydowii* (Gln), *Aspergillus versicolor* (Gln) and *Aspergillus glaucus* (Leu). Interestingly it is also part of a Serine/Threonine-Proline motif that is conserved and repeated at least 12 times throughout the 20 orthologs (Figure 6.15; data not shown). Serine/Threonine-Proline motifs are often the target of

phosphorylation by proline-directed kinases (SUZUKI 1989; VULLIET *et al.* 1989; NIGG 1991; MITCHELL AND TOLLERVEY 2000b) and phosphorylation events at these sites can regulate protein function (eg. SCHUTKOWSKI *et al.* 1998). To determine whether the *nup159*^{P953Q} mutation is sufficient to confer nuclear localization of PrnA^{NLS}-AreA$^{694-621}$-Gfp the *nup159* locus, excluding the start codon, with 1,434 bp upstream and 1,965 bp downstream of the DNA sequence change was amplified from ANX25 and transformed into RT244 selecting for proline utilization as a result of double cross over integration at *nup159*, however no proline utilizing transformants have been recovered from two separate transformations.

Table 6.6 Effects of ANX25 mutations in coding regions.

Gene	cDNA Base Change	Protein Change	Effect	Function
AN0304	C49A	Arg-17-Arg	Silent	Cellular response to stress
AN0450	G297T	Cys-297-Ser	Missense	tRNA binding activity
AN0494/*cbhB*	G406A	Asp-136-Asn	Missense	Cellulose 1,4-beta-cellobiosidase
AN1101	G813A	Thr-271-Thr	Silent	Unknown function
AN1309	G218A	Arg-73-Lys	Missense	Predicted GTPase activity
AN1623	C545A	Thr-182-Ile	Missense	Predicted oxidoreductase
AN2086/*nup159*	C2858T	Pro-953-Gln	Missense	Nuclear pore complex protein
AN2195	C936C	Ser-312-Ser	Silent	Predicted zinc ion binding activity
AN2300/*atrD*	G3339A	Pro-1113-Pro	Silent	ATP-binding cassette transporter
AN2695	C424A	Arg-142-Ser	Missense	Protein of unknown function
AN3117	G3355A	Gly-1119-Ser	Missense	Copper-exporting ATPase activity
AN3184	G841C	Gly-281-Arg	Missense	Putative aldose 1-epimerase
AN3228/*pfkE*	G489C	Val-163-Val	Silent	Predicted prenyltransferase
AN3306	C176T	Ser-59-Leu	Missense	Protein of unknown function
AN3321	G709A	Ala-237-Thr	Missense	Aspartic-type endopeptidase
AN4481	G775C	Gly-259-Arg	Missense	Secondary metabolite biosynthesis
AN4493/*rpdA*	G141A	Met-47-Ile	Missense	Histone deacetylase
AN4817	G1029A	Val-343-Val	Silent	Role in transmembrane transport
AN4859/*pmaA*	G494A	Gly-165-Asp	Missense	Plasma membrane ATPase
AN5620	G1513C	Asp-505-His	Missense	DNA-directed DNA polymerase
AN5908/*tpiB*	G456A	Met-152-Ile	Missense	Triose-phosphate isomerase
AN6007	G2369T	Gly-790-Val	Missense	ATP-dependent helicase activity
AN6156	G493A	Ala-165-Thr	Missense	Predicted DNA binding
AN6248	G241A	Asp-81-Asn	Missense	Adenyl-nucleotide exchange
AN6434/*CYP672A1*	G1056A	Pro-352-Pro	Silent	Putative cytochrome P450
AN6551	G4090A	Ala-1364-Thr	Missense	Predicted ATP binding activity
AN7118	G628A	Gly-22-Arg	Missense	Predicted DNA binding
AN7391	C1416T	Leu-472-Leu	Silent	Unknown function
AN8859	G7C	Gly-3-Arg	Missense	Aspartate kinase
AN9063	C2131T	Glu-711-Stop	Nonsense	Unknown function
AN9263	C400A	Pro-134-Thr	Missense	Unknown function
AN9267	C662A	Ser-221-Tyr	Missense	Unknown function
AN9278	C1421G	Ser-474-Cys	Missense	Predicted oxidoreductase activity
AN11207	G658A	Asp-220-Asn	Missense	Predicted oxidoreductase activity

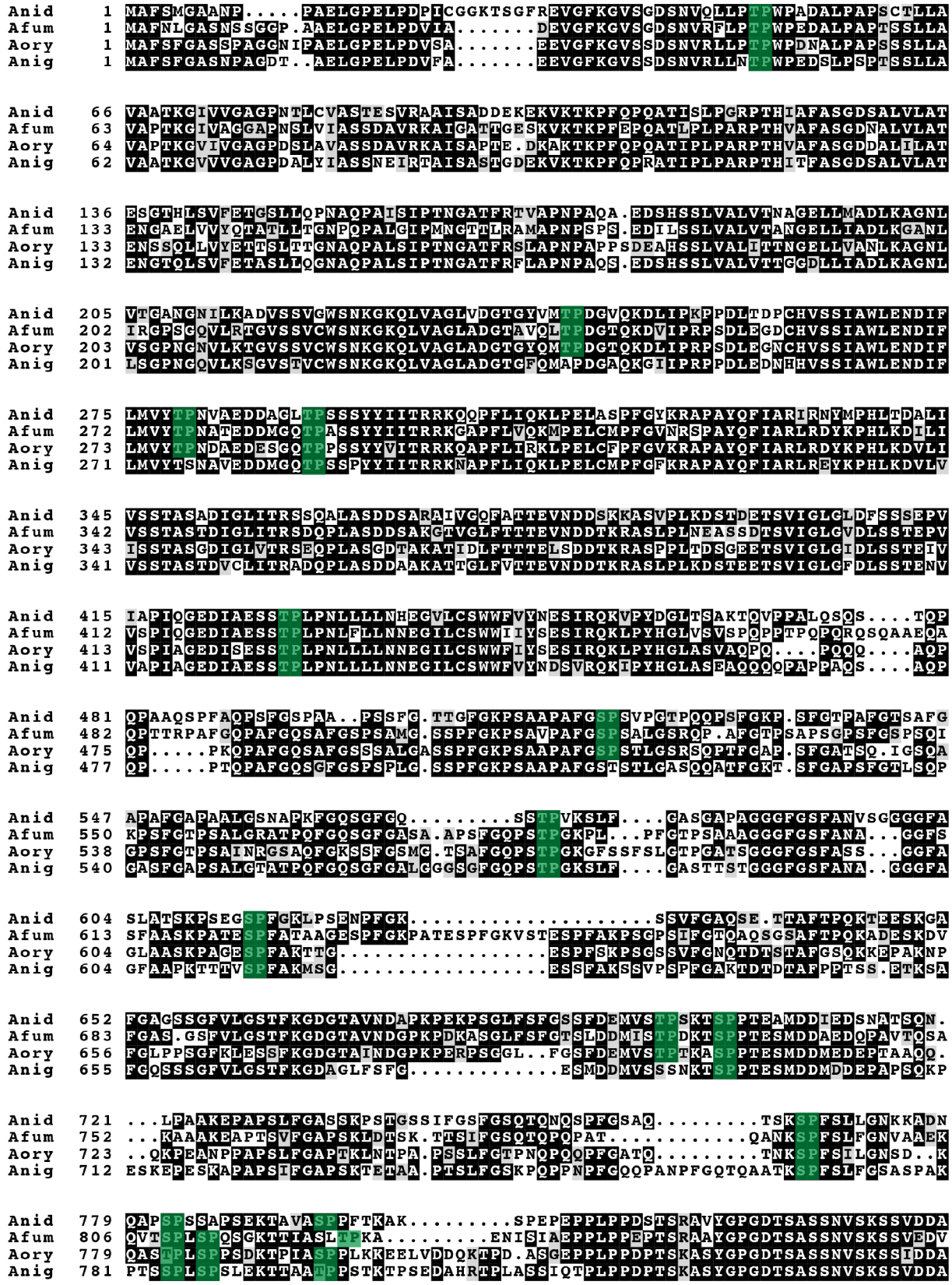

Figure 6.15 Alignment of Nup159 with homologs from Aspergilli.

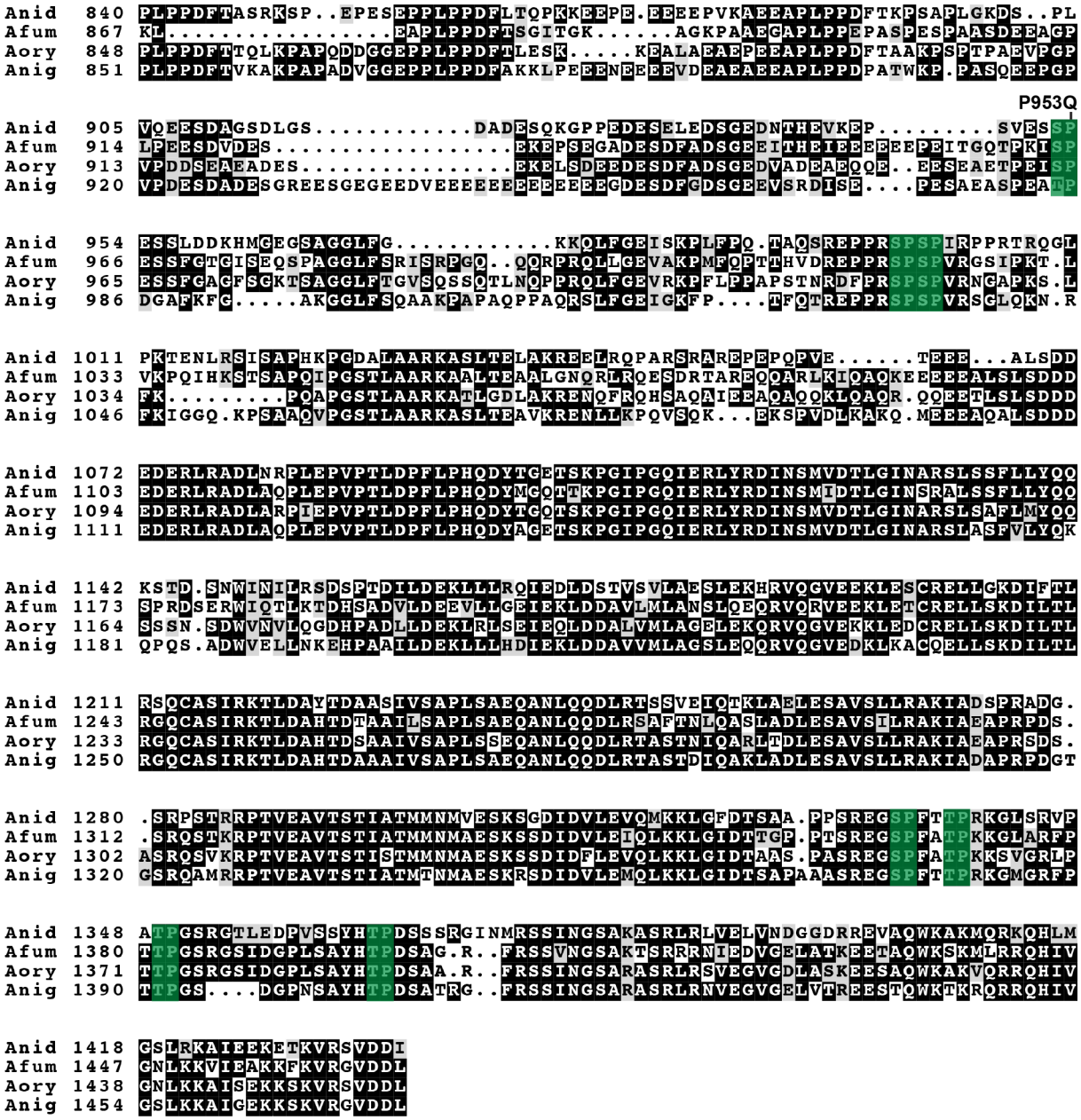

Figure 6.15 Alignment of Nup159 with homologs from Aspergilli.

Clustal Omega protein alignment of *A. nidulans* Nup159 (Anid) with orthologs from *A. fumigatus* (Afum), *A. oryzae* (Aory) and, *A. niger* (Anig). The predicted ANX25 mutation at residue 953 is marked. 15 conserved and six partially conserved Ser/Thr-Pro residue pairs, which may be the target of proline-directed kinases, are highlighted in green.

6.5 Discussion

6.5.1 The AreA nuclear export signal.

The GATA transcription factor AreA accumulates in the nucleus in response to nitrogen starvation, and CrmA rapidly exports nuclear AreA in response to nitrogen nutrients or carbon starvation (TODD *et al.* 2005). Sequence analysis identified a single AreA CRM1-type nuclear export signal C-terminal of the zinc finger DNA-binding domain at residues 703-712 (TODD *et al.* 2005). By fusing this nuclear export sequence to the constitutively nuclear PrnA protein (POKORSKA *et al.* 2000) we were able to identify a functional NES. Deletion of the sequence encoding these residues in the native protein context expressed from *gpdA*(p)*areA*$^{HA.\Delta 703\text{-}712}$ resulted in constitutive nuclear localization during nitrogen sufficiency (i.e. growth on ammonium), during carbon starvation and during combined carbon and nitrogen starvation, conditions where AreA is primarily cytoplasmic. Furthermore, during nitrogen limitation (i.e. growth on nitrate or proline) AreA$^{HA.\Delta 703\text{-}712}$ showed nuclear accumulation, conditions where wild type AreA is equally distributed between the nucleus and the cytoplasm. Therefore these residues are required for nuclear export of AreA under a range of conditions.

The AreA NES is highly conserved in fungal homologs and animal orthologs suggesting that these proteins may also be exported from the nucleus or may shuttle between the nucleus and cytoplasm. In humans GATA-4 is exported following modification by glycogen synthase kinase 3β (MORISCO *et al.* 2001) and GATA-6 is exported from the nucleus in response to the presence of anisomycin, which inhibits protein synthesis (USHIJIMA AND MAEDA 2012). In *F. fujikuroi* regulated nuclear accumulation of AreA in response to nitrogen starvation has been demonstrated (MICHIELSE *et al.* 2014). However, in *Gibberella zeae* AreA accumulates in the nucleus during both nitrogen starvation and growth on nitrate and is also present in the nucleus during growth on rich media (MIN *et al.* 2012), suggesting nuclear export of *G. zeae* AreA is not regulated, or at least regulated differently to *A. nidulans* AreA, despite having complete sequence identity with *A. nidulans* AreA residues 670 to 722, which contains the NES (data not shown). Interestingly, mutation of the final two hydrophobic residues in the AreA NES, Leu-710 and Leu-712, either separately or together, had no effect on AreA^{HA} localization (R.B. Todd unpublished). Mutation of these residues often results in loss of nuclear export (e.g. FISCHER *et al.* 1995; WEN *et al.* 1995; STOMMEL *et al.* 1999; HENDERSON AND ELEFTHERIOU 2000), however

the CRM1-type NES in mammalian huntintin can function when one but not two of the five hydrophobic residues are lost (MAIURI *et al.* 2013). Nine of the fourteen residues between AreA 699 and 712 are hydrophobic; therefore it is possible that the seven remaining hydrophobic residues in this region form a functional NES in the mutant AreA$^{HA.L710A.L712A}$.

We characterized the AreA NES (703-712) by mutational analysis. A serendipitious mutation identified a key histidine residue within the AreA NES, His-704, which is required for regulated AreA nucleo-cytoplasmic distribution. This residue could be critical for interaction of AreA with the nuclear exportin CrmA, or it may be modified to regulate interaction with CrmA and thereby nuclear export. For several CRM1-type NESs post-translational modification is a key step in regulated nuclear export, e.g. GATA-6 in mammals and ZO-2 in zebrafish (GONZALEZ-MARISCAL *et al.* 2006; USHIJIMA AND MAEDA 2012). Protein histidines may be modified by either phosphorylation or methylation (BOYER *et al.* 1962; ASATOOR AND ARMSTRONG 1967; JOHNSON *et al.* 1967), therefore we explore in Chapter 7 whether modification of His-704 is the mechanism through which *A. nidulans* regulates AreA nuclear export.

6.5.2 A second AreA nuclear export signal?

Deletion of the AreA NES region conferred nuclear accumulation. However, AreA$^{HA.\Delta703-712}$ showed lower levels of nuclear accumulation, calculated as the ratio of fluorescence between the nucleus and the cytoplasm, during growth on ammonium than during nitrogen starvation. The nuclear to cytoplasmic ratio of AreA$^{HA.\Delta703-712}$ during growth on ammonium was also lower than for wild type AreA^{HA} during nitrogen starvation. If AreA residues 703-712 form the sole nuclear export signal we would expect AreA$^{HA.\Delta703-712}$ to accumulate in the nucleus and to show an equivalent level of nuclear accumulation regardless of growth condition. The lower nuclear accumulation of AreA$^{HA.\Delta703-712}$ on ammonium than AreA^{HA} after nitrogen starvation may be due to differential transcription, differential protein stability, lack of cell cycle arrest, a second nuclear export signal, or unmasking of regulated nuclear import in the nuclear export signal mutant. Differential transcription is the least likely possibility as both *areA*^{HA} and *areA*$^{HA.\Delta703-712}$ are expressed from the constitutive *gpdA* promoter specifically to avoid different transcription levels. Differential protein stability might cause these effects if AreA$^{HA.\Delta703-712}$ is less stable than

AreA^{HA} in the nucleus but more stable in the cytoplasm during growth on ammonium. This would result in a higher level of cytoplasmic AreA and a lower level of nuclear AreA, and as a result a lower nuclear to cytoplasmic fluorescence ratio. The lower nuclear levels of AreA$^{HA.\Delta 703-712}$ during nitrogen sufficiency than of AreA^{HA} during nitrogen starvation, despite being predicted to accumulate for the entire growth period instead of only after a shift to nitrogen starvation, may be explained by loss of AreA$^{HA.\Delta 703-712}$ nuclear accumulation during the closed mitosis when partial disassembly of the nuclear pore complex occurs and many nuclear proteins are dispersed to the cytoplasm (DE SOUZA *et al.* 2004; DE SOUZA *et al.* 2006). Although the effects of nutrients on the cell cycle have not been studied in *A. nidulans,* the lack of nuclear division and hyphal extension during nitrogen starvation suggest that nitrogen starvation triggers cell cycle arrest (R.B. Todd, pers. commun.). But why then is there not strong nuclear accumulation of AreA$^{HA.\Delta 703-712}$ in carbon-starved mycelia in the presence of ammonium despite likely cell cycle arrest? AreA may contain a second nuclear export signal. The ValidNES database of NES-containing proteins (http://validness.ym.edu.tw/PROTEIN.php) lists 36 out of 221 proteins with multiple nuclear export signals, including the NES rich pericentrin in humans, which has five NESs (LIU *et al.* 2010). NESs in the same protein can have an equal functions and mutation of either has a similar effect, e.g. in *D. melanogaster* SimA (ROMERO *et al.* 2008), they can also have unequal effects where one NES is stronger than the other as with the two NESs in carbohydrate responsive binding protein (ChREBP) in rat hepatocytes (FUKASAWA *et al.* 2010), or they may respond to different signals, as is the case for the redox-sensitive and redox-insensitive NESs of Nsf2 (LI *et al.* 2005; LI *et al.* 2006). Using ValidNES software we found three additional predicted CRM1-type NESs in AreA. A variant lacking all three additional putative NESs, AreA$^{HA.\Delta 60-423}$, shows increased nuclear localization, though not nuclear accumulation during nitrogen sufficiency. This mutant protein is more stable in extracts than the wild type protein (G.Y. Busot, C.C. Hunter, and R.B. Todd, unpublished data). Therefore one or more of these three putative NESs may be functional but are considerably weaker than the characterized NES at residues 703-712.

6.5.3 Conservation of NESs near transcription factor DNA binding domains

CRM1-type nuclear export signals have a range of physiological effects from regulating the response of transcription to nitrogen starvation and hypoxia (TODD *et al.* 2005; ROMERO *et al.* 2008) to excluding actin from the nucleus where it is harmful (WADA *et al.* 1998). The AreA NES is C-terminal of the four Zn^{2+} coordinating cysteines that form the DNA binding motif and overlaps with several DNA-contact residues. Alignment of this region of AreA with fungal homologs and animal orthologs shows it is highly conserved and more conserved than the flanking regions. The DNA binding motifs of proteins tend to be highly conserved. The strong conservation of GATA transcription factor NESs as functional NESs are observed throughout transcription factors, in N-terminal regions, e.g. Williams-Beuren syndrome critical region gene 14 (*Wbscr14*) in mammals (MERLA *et al.* 2004), C-terminal regions, e.g. NF-E2-related factor (Nrf2) in mammals (LI *et al.* 2005), as well as away from the DNA binding domain, e.g. NirA in *A. nidulans* (BERNREITER *et al.* 2007). NESs have been observed within and adjacent to DNA binding domains from an array of transcription factor families including in the nuclear receptor C4-zinc fingers, Signal Transducers and Activators of Transcription DNA-binding domains, Z-DNA binding domain, basic helix-loop-helix domains, the E2F family DNA-binding domain (MCBRIDE *et al.* 2000; BLACK *et al.* 2001; GAUBATZ *et al.* 2001; ROMERO *et al.* 2008), and now the GATA zinc finger of AreA.

6.5.4 Screening for AreA nuclear export regulatory proteins.

We aimed to elucidate the regulatory events that underlie AreA nuclear export and nuclear accumulation using a genetic suppressor screen for mutants affected in nuclear export via the AreA NES. We used a PrnA-AreA^{NES}-GFP fusion strain in which the fusion protein is exported from the nucleus conferring loss of proline utilization to screen for mutants following 4-NQO mutagenesis by selection for growth on proline. We established using a pilot screen that this strategy successfully identifies mutants affected in the fusion gene or in novel genes unlinked to the fusion construct or *crmA*. The eight mutations that mapped to the fusion gene were truncation mutations and unfortunately did not identify any important nuclear export signal residues. We also expected to identify genes that encode proteins that regulate the AreA-CrmA interaction and machinery required for AreA nuclear export. We isolated two novel mutants unlinked to the fusion construct or *crmA* that have decreased nuclear export of both PrnA-AreA^{NES}-GFP and of AreA^{HA}. We have characterized one of these mutants, ANX25, and the mutagenesis parent by whole genome sequencing and found 70 mutations unique to the mutant.

A putative ANX25 causative mutation lies in an essential nuclear pore protein encoding gene *nup159* (OSMANI *et al.* 2006b). Homologs of *nup159* are also essential in *S. cerevisiae* and *S. pombe*, though not in *C. elegans* (CRONSHAW *et al.* 2002; GALY *et al.* 2003; CHEN *et al.* 2004). The isolation of a mutant of *nup159* highlights the power of mutagenesis and genetic screening to identify essential genes involved in biological processes. To show that *nup159*^{P953Q} is the causative mutation it will need to either be reconstructed in isolation from the other 69 sequence changes in ANX25 or complemented with wild type *nup159*. Nup159 is a FG (phenylalanine-glycine) nucleoporin, which lines the center of the nuclear pore complex, primarily on the cytoplasmic side (ALBER *et al.* 2007), and in *A. nidulans* Nup159 disperses from the nuclear pore complex during mitosis (DE SOUZA *et al.* 2004). In *S. cerevisiae* Nup159 interacts with the CRM1 exportin and RanGTP to facilitate the release of cargo into the cytoplasm (FLOER AND BLOBEL 1999; JENSEN *et al.* 2000) and mutants of Nup159 show defects in mRNA export (HODGE *et al.* 1999). Therefore the effect of the *nup159*^{P953Q} mutation on AreA nuclear export may result from reduced CrmA cargo unloading and would therefore be expected to affect regulated export of additional proteins as well as mRNA export.

Work is ongoing to characterize the causative mutation in ANX6. Haploidization mapped ANX6 to chromosome three. As *nup159* is on chromosome seven, the ANX6 and ANX25

mutations likely affect different genes. For identification of ANX25 we used a direct sequencing approach, however analysis of the 4-NQO mutagenic spectrum shows mutants contain an average of 100 sequence changes which can hamper the identification of the causative mutation (DOWNES *et al.* 2014a). A bulked segregant approach, where the genomes of several progeny with and without the phenotype of interest are sequenced and compared, can directly identify the putative causative mutation unique to the affected progeny (TAN *et al.* 2014). This simpler approach could be easily incorporated into the *prnA-areA*^{NES}*-gfp* genetic screen as crossing is already used to determine whether mutations are in the fusion gene, *crmA* or a novel gene.

We characterized the mutagenic spectrum of the chemical mutagen 4-NQO using data generated from our first round of screening after 4-NQO mutagenesis and from a genetic screen carried out using 4-NQO mutagenesis to identify organelle transport defective mutants (TAN *et al.* 2014). Our analysis showed that with the right dose of 4-NQO to treat conidia we could feasibly generate and screen through every possible substitution in the *A. nidulans* genome (DOWNES *et al.* 2014a). In our first round of mutagenesis we used a 3% survival rate on ~10^8 spores to generate mutants. Our modeling predicts that with this dose of 4-NQO we would need to mutagenize ~$2x10^9$ conidia to generate a mutation in every nucleotide. As we have a strong selectable phenotype, proline utilization, the next round of mutagenesis and screening should be carried out with a lower dose of 4-NQO. For example a 4-NQO dose resulting in a 50% survival rate of $4x10^7$ conidia is predicted to cause a mutation in every A:T base pair, and every possible substitution of every G:C base pair, i.e. mutation to C:G, A:T, and T:A. Using a lower kill percentage will recover more mutants which can be screened with our strong selectable phenotype, this approach is therefore more likely to identify the genes which are required for regulated AreA nuclear export as the mutations will not be lost in the killed conidia.

6.6 Future Directions

Our analysis of AreA nuclear export suggests there may be additional weak nuclear export signal(s) that respond to ammonium, and we have identified three candidate motifs by *in silico* analysis. To test our hypothesis several experiments could be carried out. The first experiment will be to determine whether nuclear accumulated AreA$^{HA.\Delta 703\text{-}712}$ is rapidly exported from the nucleus following addition of ammonium to nitrogen starved cells. As the export of AreA is extremely rapid and export can be observed within 5 minutes (TODD *et al.* 2005) the potential effects of differential expression, differential stability and cell cycle arrest should be removed. Secondly the putative NESs could be fused individually to a constitutively nuclear protein such as *stuA* or *prnA* (SUELMANN *et al.* 1997; POKORSKA *et al.* 2000) to determine whether they confer nuclear export. Finally, deletion of each of the putative NESs in combination with the confirmed NES in AreA^{HA} could be examined to determine whether combinations confer different levels of nuclear to cytoplasmic AreA, particularly during carbon starvation in the presence of ammonium.

The regulatory signals that result in AreA nuclear export remain to be characterized. It is not known what molecule signals export, what the sensor protein is and what other proteins are required to transduce the signal to AreA. We generated a mutant, ANX6, which is defective in nuclear export of PrnA-AreA^{NES}-GFP and AreA^{HA}, and the causative mutation is yet to be determined. Whole genome sequencing of ANX6, as with ANX25, could be used to identify the causative mutation. However, our analysis of 4-NQO mutants indicates that there are likely between 71 and 240 mutations in mutants derived from 4-NQO chemical mutagenesis. Therefore, it is likely a better strategy to sequence pooled genomic DNA of progeny for bulked segregant analysis to pinpoint the mutation. Bulked segregant whole genome sequencing is a powerful way to identify the causative mutation (TAN *et al.* 2014). Further mutagenesis to scale up the genetic screen, with a more informed approach based on our 4-NQO mutagenic spectrum analysis, followed by screening for mutants with suppression of the *prnA-areA*^{NES}*-gfp* proline non-utilizing phenotype is also likely to identify additional genes that are required for regulated AreA nuclear export.

The ANX25 strain, which we isolated from our pilot genetic screen contains the *nup159*^{P953Q} mutation, and numerous other mutations. It is important to identify the causative mutation, which can be done by either reconstructing the mutation in the RT244 strain used for

mutagenesis or complementing the mutation in ANX25 and testing whether proline utilization is lost. ANX25 also secretes a red pigment into the media. This red pigment may be an uncharacterized secondary metabolite. It will be of great interest to determine what this red pigment is, and if it is a secondary metabolite whether its production is due to defective nuclear export or one of the other mutations in this ANX25 strain.

[*Tabula rasa.*]

Chapter 7 - Exploration of protein histidine modification as a mechanism for regulated AreA nuclear export

7.1 Abstract

The *Aspergillus nidulans* GATA transcription factor AreA shows regulated sub-cellular distribution. During nitrogen sufficiency AreA is primarily cytoplasmic, but during nitrogen nutrient starvation AreA accumulates in the nucleus. Mutational analysis of the CRM1-type nuclear export sequence of AreA identified a highly conserved histidine residue, His-704, as being required for regulated nuclear export. Histidine residues may be modified by either phosphorylation or methylation. Using a histidine non-modifiable His-704-Ala AreA variant, we show that this nuclear export sequence mutation confers constitutive nuclear localization on AreA. Phosphorylation of His-704 could be carried out by the only *A. nidulans* nucleoside diphosphate kinase SwoH. As *swoH* is an essential gene, we examined the effect of a *swoH1* temperature sensitive mutant, a newly generated *swoH*$^{+}$/*swoH*Δ heterozygous diploid and two phosphorylation mimics *areA*^{H704D} and *areA*^{H704E} on AreA localization. Both of the *swoH* mutants showed wild type distribution of AreA during growth on ammonium and during nitrogen starvation, however the two phosphorylation mimics failed to induce nuclear export. Therefore, histidine phosphorylation is unlikely to regulate AreA nuclear export. Methylation of His-704 would be carried out by a protein histidine methyltransferase. We have identified the putative *A. nidulans* protein histidine methyltransferase encoded by AN1445 (*phmA*) by sequence comparison to HPM1 from *Saccharomyces cerevisiae.* Deletion of *phmA*Δ conferred pleiotropic effects including reduced growth rate and increased production of sexual fruiting bodies, but no effects on AreA nucleocytoplasmic distribution were observed. A methylation mimic AreA^{H704F} also failed to induce nuclear export. Therefore we conclude that modification of His-704 by either phosphorylation or methylation is unlikely to be the signal mediating regulated AreA nuclear export. All of the point mutations in H704 conferred nuclear localization on ammonium. Therefore we predict His-704 is required for efficient interaction with the CrmA exportin..

7.2 Introduction

The *Aspergillus nidulans* GATA transcription factor AreA shows regulated sub-cellular distribution. During nitrogen sufficiency AreA is primarily cytoplasmic, but during nitrogen nutrient starvation AreA accumulates in the nucleus (TODD *et al.* 2005). Regulated AreA subcellular distribution is mediated by the CRM-1 type exportin CrmA (TODD *et al.* 2005). Analysis of AreA identified at least one CRM-1 type nuclear export sequence (NES) required for regulated nuclear export (Chapter 6). One means by which nuclear export may be regulated is via post-translational modification. For example phosphorylation of mammalian GATA-6 by the c-Jun kinase pathway promotes nuclear export (USHIJIMA AND MAEDA 2012). Similarly, during recovery from reactive oxygen species stress mammalian SRB2 is exported from the nucleus following reduction of a disulfide bond (PAPP *et al.* 2006). We showed that the highly conserved His-704 residue within the AreA NES is required for regulated nuclear export (see Chapter 6.4.3). Therefore we investigated whether modification of AreA His-704 provides the molecular mechanism for regulated AreA nuclear export. Protein histidine residues can be modified by either phosphorylation or methylation (BOYER *et al.* 1962; ASATOOR AND ARMSTRONG 1967; JOHNSON *et al.* 1967). Under this model unmodified AreA would accumulate in the nucleus during nitrogen starvation. The addition of a nitrogen nutrient would trigger a signaling cascade, culminating in the modification of AreA His-704. This modification could promote interaction with the CrmA exportin and lead to rapid nuclear export (Figure 6.1). Modification of a protein histidine can occur on either nitrogen atom in the side chain (Figure 6.1) and can result from either reversible phosphorylation by nucleoside diphosphate kinases (NDPK) or methylation by protein histidine methyltransferases (WEBB *et al.* 2010; KEE AND MUIR 2012).

Protein histidine modifications have been poorly studied compared with covalent modifications of other residues, but protein histine phosphorylation is better studied than protein histidine methylation (reviewed in ATTWOOD *et al.* 2007; KEE AND MUIR 2012). NDPK encoding genes have been characterized in several fungi, including *Saccharomyces cerevisiae* (*YNK1*), *Schizosaccharomyces pombe* (*NDK1*), and *Neurospora crassa* (*ndk-1*). In all three fungi loss-of-function mutants are viable (FUKUCHI *et al.* 1993; IZUMIYA AND YAMAMOTO 1995; LEE *et al.* 2006). *A. nidulans* has only one NDPK encoding gene, *swoH*, which was identified in a genetic screen for mutants with polarity maintenance defects (MOMANY *et al.* 1999). The *swoH1* mutant

identified in their screen is a temperature sensitive mutant, which forms swollen autolytic cells and has reduced conidiation at restrictive temperatures (MOMANY *et al.* 1999). Analysis of NDPK activity in *swoH1* strains showed reduced function at both permissive (25ºC) and restrictive (42ºC) temperatures (LIN *et al.* 2003). Attempts to isolate haploid knockout *swoH* strains were unsuccessful; therefore it is thought that *swoH* is essential in *A. nidulans* (LIN *et al.* 2003). Compared with NDPKs, protein histidine methyltransferases are poorly understood in eukaryotes and only a single gene has been characterized, *HPM1* in *S. cerevisiae* (WEBB *et al.* 2010). Hpm1p methylates Rpl3p, which is a ribosomal 60S subunit protein (WEBB *et al.* 2010). A recent study of methylation in yeast identified several other proteins containing methylhistidines (Table 7.1), including the ribosomal 30S protein (WANG *et al.* 2015). Methylhistidines have also been reported in actin and myosin from skeletal muscle (ASATOOR AND ARMSTRONG 1967; JOHNSON *et al.* 1967), and the migration-inhibitory-factor-related protein from mouse spleen (RAFTERY *et al.* 1996), however there are no reports of methylhistidines in transcription factors.

To examine the possible effects of His-704 phosphorylation on AreA we examined the effects of *swoH1* and a heterozygous *swoH*$^{+}$/*swoH*Δ diploid and found that neither mutant alters AreA nuclear accumulation. We also identified and deleted the putative *A. nidulans* protein histidine methyltransferase gene AN1445 (*phmA*), and showed that it also does not affect AreA nuclear export. Protein histidine modification mimics of AreA for phosphorylation (*areA*$^{HA.H704D}$, *areA*$^{HA.H704E}$) and methylation (*areA*$^{HA.H704F}$) did not inhibit nuclear accumulation, but instead conferred increased nuclear localization during growth on ammonium. Therefore modification of His-704 may not be a signal for nuclear export.

Table 7.1 Protein histidine methylation events in *S. cerevisiae.*

Protein	Residue	Protein Description
Rad17[a]	mH54	DNA damage checkpoint protein
Rpl3[b]	mH243	Ribosomal 60S subunit protein L3
Rps1B[a]	mH101	Ribosomal 40S subunit protein 10
Tef1[a]	mH26, mH388	Translation elongation factor EF-1 alpha

[a] Wang *et al*. (2015)
[b] Webb *et al*. (2010)

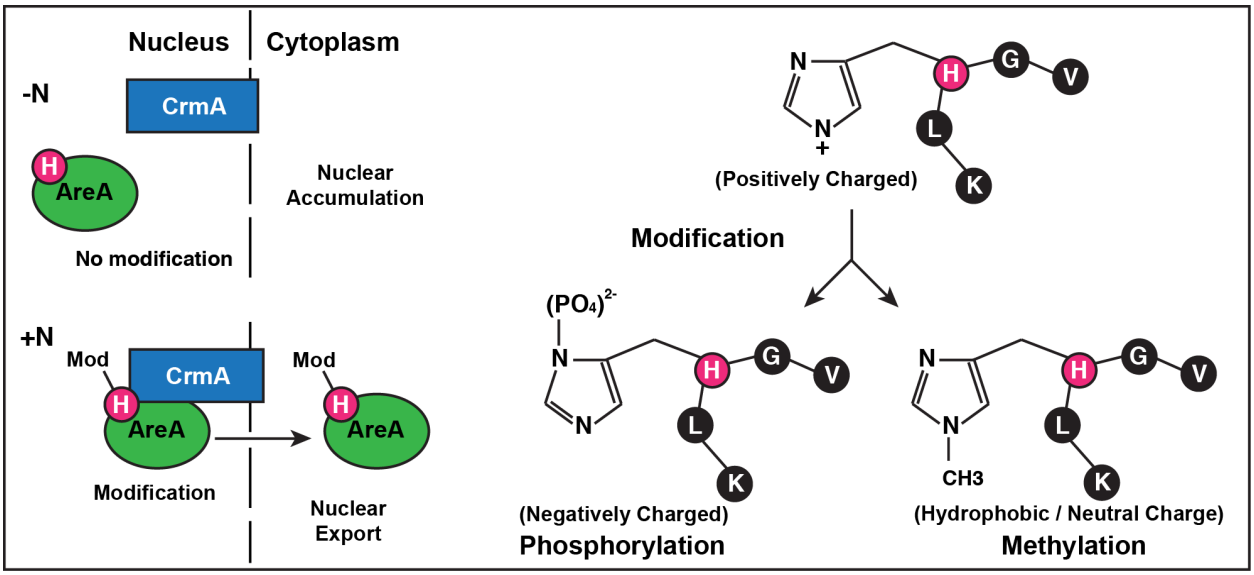

Figure 7.1 Model for regulated AreA nuclear accumulation by His-704 modification.

During nitrogen starvation (-N) His-704 of the AreA nuclear export signal is not modified and AreA accumulates in the nucleus. The addition of a nitrogen nutrient (+N) leads to modification of His-704 by either phosphorylation or methylation. Modification of the AreA NES leads to interaction with the CrmA exportin and loss of nuclear accumulation.

7.3 Materials & Method

7.3.1 Strain construction

A full list of strains and genotypes used in this chapter can be found in Table 2.1-3. Relevant genotypes of strains are listed here. The *fmdS-lacZ* reporter was introduced into a strain containing *gpdA*(p)*areA*$^{HA.H704A}$ by crossing RT51 (*gpdA*(p)*areA*$^{HA.H704A}$) with MH12326 (*pyroA4 fmdS-lacZ*) to construct RT153. The *swoH1* mutation in RT14 was crossed to MH11050 (*areA*^{HA}Δ *fmdS-lacZ*) to generate an *areA*Δ *swoH1 fmdS-lacZ* strain (RT18). RT18 was crossed to MH9926 (*gpdA*(p)*areA*^{HA} *fmdS-lacZ*) to generate RT20 (*swoH1 gpdA*(p)*areA*^{HA} *fmdS-lacZ*). The phosphatase deletion set was kindly provided by Stephen Osmani (Ohio State University). The AN8216::*A.f.pyrG* (*swoH*Δ) (Δ -103 to +951 bp) knockout construct was sourced from the Fungal Genetics Stock Center (McCluskey *et al.* 2010) and transformed into RT52 (*gpdA*(p)*areA*^{HA} *pyrG89 nkuA*Δ) and transformants selected by pyrimidine prototrophy. Single integration of the knockout construct by double crossover homologous recombination at the *swoH* locus was confirmed by Southern blot analysis using *Kpn*I (wild type: 4.8 kb ; Δ: 4.1 kb), *Xho*I (wild type: 2.2 kb ; Δ: 3.4 kb) and *Hind*III (wild type: 2.2 & 2.7 kb ; Δ: 2.9 kb) using the wildtype *swoH* 1.7 kb band (-667 to +1,020 bp) from amplification with swoH_fwd (5'-GGATGAGCCTTTGGCGGCGA-3') and swoH_rev (5'-ACGCCGTGGTTTGCGAGGAC -3') as probe. The wild type *swoH* and *swoH*Δ were amplificatied by PCR from genomic DNA with swoH_fwd and swoH_rev. Kendra Siebert (Kansas State University) generated the *xylP*(p)::*swoH* strain by transforming pKS6 into MH11131 (*gpdA*(p)*areA*^{HA} *pyroA4 nkuA*Δ) and selecting for single copy integration and pyridoxine prototrophy. The AN1445::*A.f.pyrG* (*phmA*Δ) (Δ -2 to +1,355 bp) knockout construct was sourced from the Fungal Genetics Stock Center (McCluskey *et al.* 2010) and transformed into RT52 (*gpdA*(p)*areA*^{HA} *pyrG89 nkuA*Δ) and transformants selected for pyrimidine prototrophy. Single intergration of the knockout construct by double crossover homologous recombination at the *phmA* locus was confirmed by Southern blot analysis using *Kpn*I (wild type: 5.1 kb; Δ: 4.3 kb) and *Cla*I (wild type: 3.8 & 6.7 kb; Δ: 10.9 kb). Histidine modification mimic strains containing *gpdA*(p)*areA*$^{HA.H704D}$ (RT317), *gpdA*(p)*areA*$^{HA.H704E}$ (RT315), and *gpdA*(p)*areA*$^{HA.H704F}$ (RT316) were constructed by Cameron Hunter (Kansas State University) by two-step gene replacement.

7.4 Results

7.4.1 Characterization of an AreA Histidine 704 non-modifiable mutant

The AreA histidine 704 residue could potentially be modified by phosphorylation or methylation. As alanine residues cannot be modified by either phosphorylation or methylation a *gpdA*(p)*areA*$^{HA.H704A}$ mutant, representing a His-704 non-modifiable variant of the AreA NES, was constructed (C.C. Hunter, K.S. Siebert, and R.B. Todd, unpublished). Strains containing *gpdA*(p)*areA*$^{HA.H704A}$ were unable to utilize alternative nitrogen sources (Figure 7.2A) and had reduced expression of the AreA regulated *fmdS-lacZ* reporter gene (Figure 7.2B). This contrasted with the His-704-Asn mutant, *gpdA*(p)*areA*$^{HA.H704N}$, which was not defective for either nitrogen utilization or *fmdS-lacZ* expression (Figure 7.2A; Chapter 6). His-704 is a DNA contact residue (STARICH *et al.* 1998) and the difference in phenotype between His-704-Ala and His-704-Asn is likely due to asparagine being a polar residue, which may be more similar to the generally uncharged histidine than an aliphatic alanine residue. AreA$^{HA.H704A}$ showed higher levels of nuclear distribution during growth on ammonium than wild type (Figure 7.2C). We further examined AreA$^{HA.H704A}$ localization after growth on the alternative nitrogen sources alanine and proline, and during carbon starvation. In all conditions AreA$^{HA.H704A}$ nuclear localization was increased compared with the wild type control (Figure 7.3). Therefore AreA His-704 is important for nucleo-cytoplasmic distribution in response to nitrogen nutrients or carbon starvation and therefore is a candidate target for protein histidine modification.

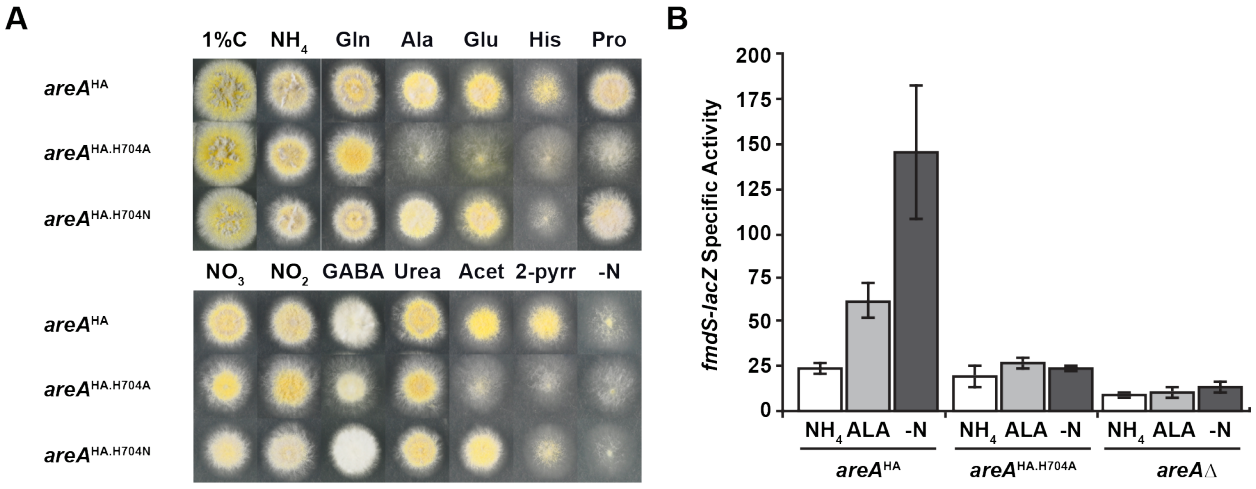

Figure 7.2 Non-modifiable AreA$^{HA.H704A}$ is required for function.

A) Growth of *areA*^{HA} (MH10897), *areA*$^{HA.H704A}$ (RT163), and, *areA*$^{HA.H704N}$ (RT104) on solid supplemented ANM with 10 mM ammonium (NH_4), glutamine (Gln), alanine (Ala), glutamate (Glu), histidine (His), proline (Pro), nitrate (NO_3), nitrite (NO_2), ɣ-aminobutyric acid (GABA), urea, acetamide (Acet), 2-pyrrolidinone (2-pyrr), and nitrogen free media (-N) at 37ºC for 2 days. **B)** Expression of the *fmdS-lacZ* reporter in *gpdA*(p)*areA*^{HA} (RT10897), *gpdA*(p)*areA*$^{HA.H704A}$ (RT153), and *areA*Δ (RT10967) after 16 hours growth in ANM supplemented with 10 mM ammonium tartrate before transfer to supplemented ANM with 10 mM ammonium (NH_4), alanine (Ala) or nitrogen starvation (-N) at 37ºC for 4 hours.

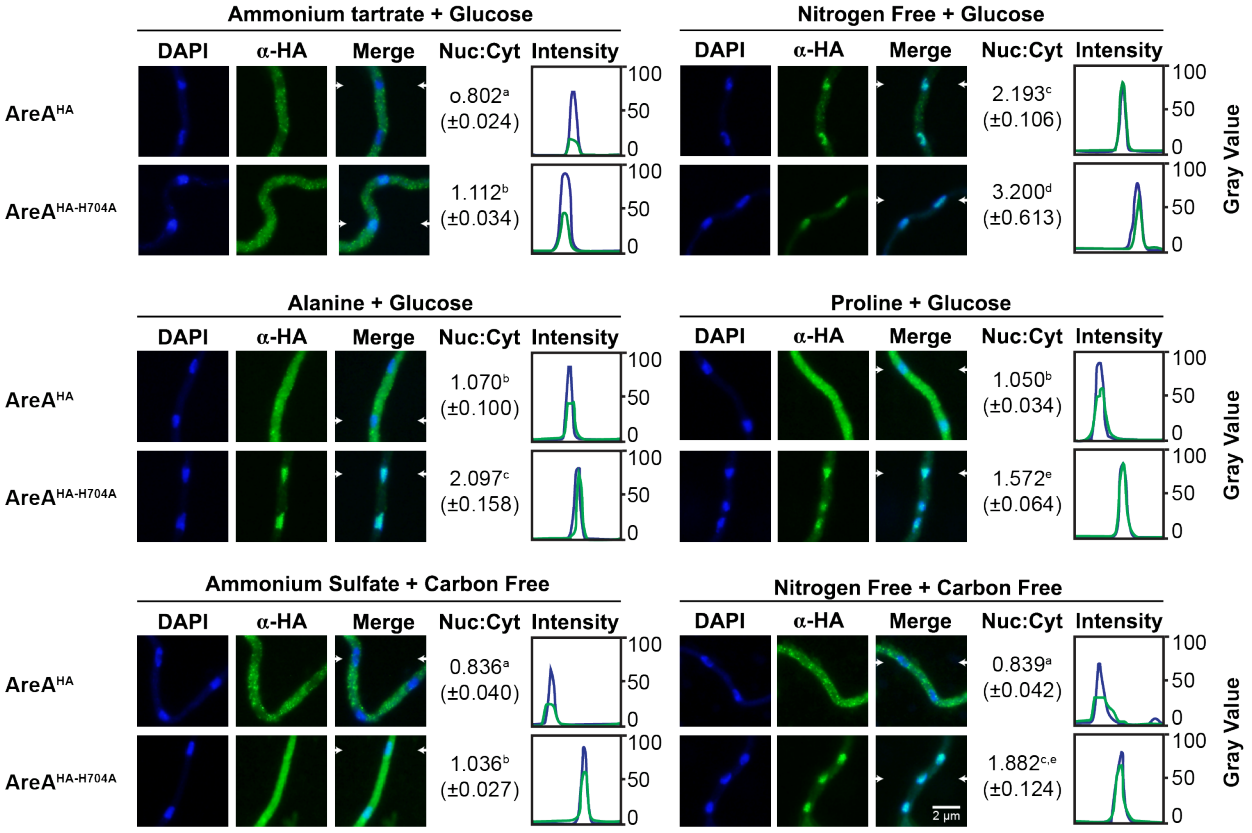

Figure 7.3 AreA$^{HA.H704A}$ is nuclear under all tested conditions.

The subcellular distribution of AreA^{HA} (RT9949) and AreA$^{HA.H704A}$ (RT268) after growth at 25ºC in supplemented liquid ANM containing 10 mM ammonium for 14 hours and transferred to supplemented ANM containing 10 mM ammonium tartrate, alanine, proline or no nitrogen source (nitrogen free), or supplemented carbon free media containing 10 mM ammonium sulfate or no nitrogen source (nitrogen free) for 4 hours. DAPI stains DNA and marks the location of nuclei. AreA^{HA} (α-HA) was visualized by UV fluorescence microscopy following immunostaining with α-HA (3F10) and Alexa Fluor-488-conjugated goat anti-rat antibodies. Nuclear to Cytoplasmic fluorescence ratio (Nuc : Cyt) was calculated from the mean α-HA fluorescence ratio of 13 nuclei and adjacent cytoplasm. SEM is shown. Superscript lowercase letters indicate significantly different groups using the two-tailed Student's t-test ($p < 0.05$). Arrowheads show transects used to generate a fluorescence intensity plots for DAPI (blue) and α-HA (green).

7.4.2 SwoH: A protein histidine nucleotide diphosphate kinase

7.4.2.i Analysis of the temperature sensitive swoH1 mutant.

The temperature sensitive *swoH1* mutant was isolated from a genetic screen for polarity defects (MOMANY *et al.* 1999). The *swoH1* temperature sensitive mutant shows growth defects at the restrictive temperature of 42ºC due to a Val-83-Phe substitution in the active site pocket (LIN *et al.* 2003). The *swoH1* mutant has less than 25% of wild type NDPK function at both permissive (25ºC) and restrictive (42ºC) temperatures (LIN *et al.* 2003); as a result, any effects of *swoH1* on AreA may conceivably be seen at either the permissive or restrictive temperature. We therefore tested the effects of *swoH1* on a range of nitrogen sources at 25ºC, 37ºC, and 42ºC (Figure 7.4). *swoH1* showed no specific defects for any nitrogen source at the permissive temperature and showed weak growth at the restrictive temperature, with the exception of glutamine. Interestingly clearing of milk occurred in the *swoH1* mutant at 42ºC, and therefore there is no effect on production and secretion of extracellular proteases. At the intermediate temperature *swoH1* showed reduced growth on some nitrogen sources (e.g. nitrate, nitrite, and 2-pyrrolidinone) but strong growth on others (e.g. ammonium and glutamine), suggesting a role in nitrogen utilization or its regulation (Figure 7.4). To determine whether gene expression of AreA target genes is regulated by *swoH1* we assayed expression of *fmdS-lacZ* on a range of nitrogen nutrients and during nitrogen starvation at both the permissive temperature and following a shift to the restrictive temperature (Figure 7.5A). Only during nitrogen starvation at the restrictive temperature did expression differ from wild type, where expression of *fmdS-lacZ* was increased in the *swoH1* mutant. By assaying a *swoH1 areA*Δ double mutant it was determined that the effect of *swoH1* on *fmdS-lacZ* was dependent on the presence of AreA (Figure 7.5B). We also performed immunofluorescence microscopy to determine the subcellular distribution of $AreA^{HA}$ in the *swoH1* mutant. Germlings were grown at both the permissive and restrictive temperatures, however the temperature sensitive defects of *swoH1* resulted in poor growth and immunostaining at 42ºC (data not shown). At 25ºC there was no significant difference between $AreA^{HA}$ nucleo-cytoplasmic distribution in wild type and *swoH1* during either nitrogen sufficiency or nitrogen starvation (Figure 7.6). To further explore the effects of *swoH1* on AreA nuclear export we generated a cross of the proline non-utilizing strain containing the *prnA-areA*^{NES}*-gfp* construct (Chapter 6) and a *swoH1* strain to test for suppression of AreA NES activity by the *swoH1*

mutation. Strains containing *prnA-areA*^{NES}*-gfp* are unable to utilize proline as a carbon source (Chapter 6.4.2). If *swoH1* were involved in regulated AreA nuclear export we would expect 75% proline utilizing progeny rather than 50% proline utilizing progeny if *swoH1* has no effect. Growth testing of 46 progeny showed that 22 were able to grow on proline as a carbon source, and thus no effect of *swoH1* on nuclear export of PrnA-AreA^{NES}-GFP (Tables 7.2 & 7.2).

Table 7.2 Cross of *swoH1* to *prnA-areA*^{NES}*-gfp* $H_0$1: *swoH1* does suppress export.

RT18[a]**:** *yA1 chaA1 pyroA*$^{+}$ *pabaA1 swoH1 gpdA*(p)*areA*Δ *fmdS-lacZ* X **RT244**[b]**:** *biA1 prnA-areA*^{NES}*-gfp-A.f.pyro gpdA*(p)*areA*^{HA} *pyroA4 fmdS-lacZ crmA*^{1525C}*-pyrG*$^{+}$ *pyrG89*					
	$H_0$1: *swoH1* supresses *prnA-areA*^{NES}*-gfp* export				
Genotype	**Exp.**	**Obs.**	**χ^2 (d.f = 1)**	**P**	**Reject or Retain H_0**
pyroA^{-}	25%	11/46	0.029	0.8648	Retain
swoH1	50%	21/46	0.348	0.5553	Retain
prnA^{+}	75%	22/46	18.11	<0.0001	Reject
prnA^{+}, *swoH1*	50%	9/46	17.043	<0.0001	Reject

[a]*swoH1* was scored at 42ºC on 1% complete media
[b]*prnA-areA*^{NES}*-gfp-A.f.pyro* was scored at 30ºC with proline as a carbon source

Table 7.3 Cross of *swoH1* to *prnA-areA*^{NES}*-gfp* $H_0$2: *swoH1* does not suppress export.

RT18[a]**:** *yA1 chaA1 pyroA*$^{+}$ *pabaA1 swoH1 gpdA*(p)*areA*Δ *fmdS-lacZ* X **RT244**[b]**:** *biA1 prnA-areA*^{NES}*-gfp-A.f.pyro gpdA*(p)*areA*^{HA} *pyroA4 fmdS-lacZ crmA*^{1525C}*-pyrG*$^{+}$ *pyrG89*					
	$H_0$2: *swoH1* does not supress *prnA-areA*^{NES}*-gfp* export				
Genotype	**Exp.**	**Obs.**	**χ^2 (d.f = 1)**	**P**	**Reject or Retain H_0**
pyroA^{-}	25%	11/46	0.029	0.8648	Retain
swoH1	50%	21/46	0.348	0.5553	Retain
prnA^{+}	50%	22/46	0.087	0.7681	Retain
prnA^{+}, *swoH1*	25%	9/46	0.725	0.3946	Retain

[a]*swoH1* was scored at 42ºC on 1% complete media
[b]*prnA-areA*^{NES}*-gfp-A.f.pyro* was scored at 30ºC with proline as a carbon source

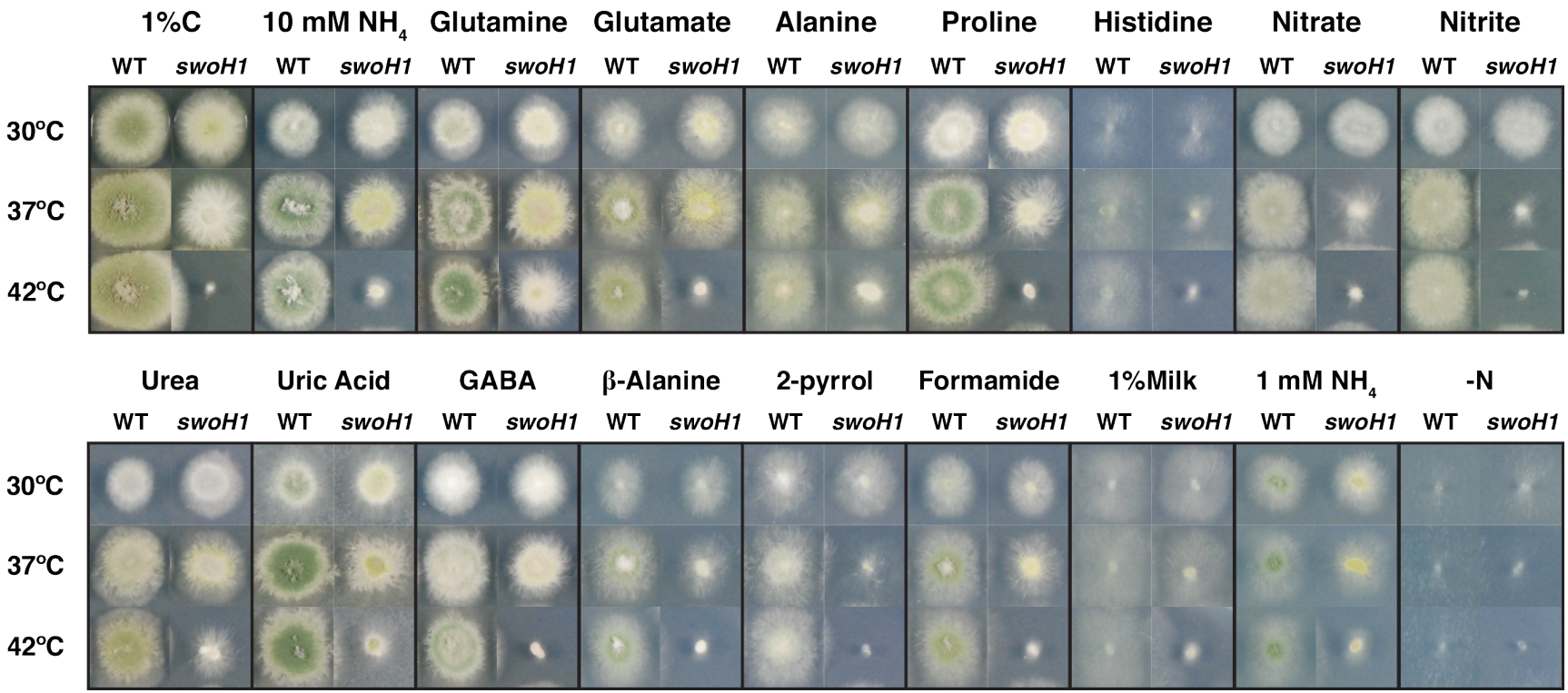

Figure 7.4 Nitrogen nutrient affects *swoH1* mutant growth at 37°C.

Growth of wild type (MH1) and *swoH1* (RT14) on solid ANM supplemented with 10 mM of various nitrogen sources unless stated. NH_4: ammonium tartrate, GABA: ɣ-aminobutyric acid, 2-pyroll: 2-pyrrolidinone, -N: nitrogen free media

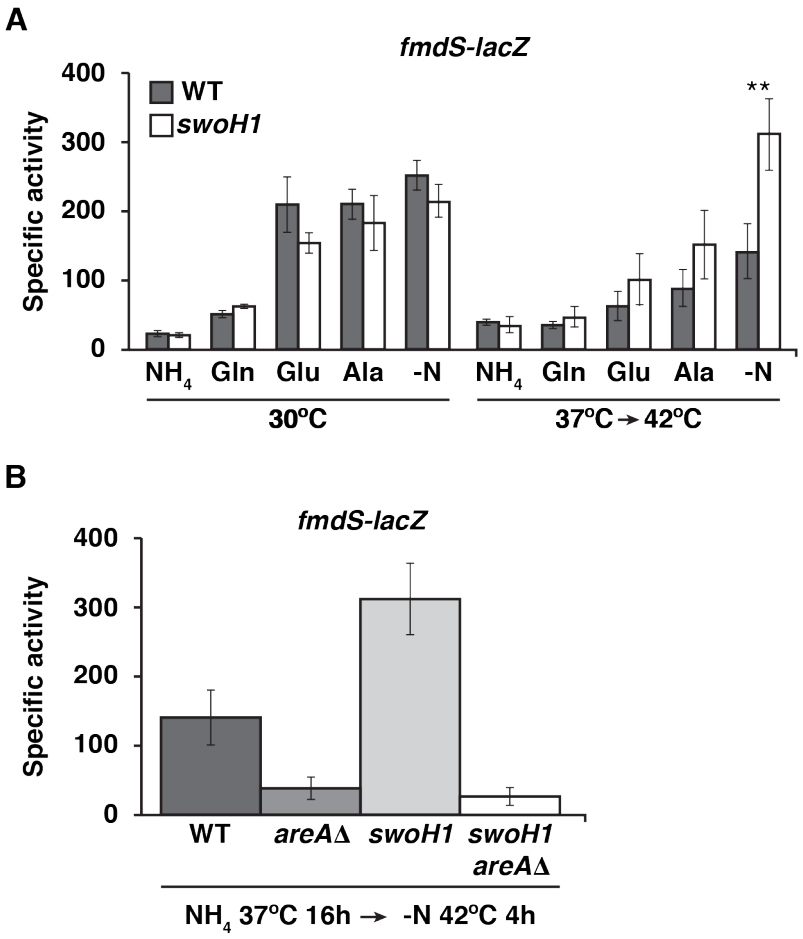

Figure 7.5 SwoH regulates AreA target gene activation during nitrogen starvation.

Expression of the *fmdS-lacZ* reporter in wild type (RT19), *swoH1* (RT20), *areA*Δ (RT11050) and, *areA*Δ *swoH1* (RT18) strains after 16 hours growth in supplemented liquid ANM with 10 mM ammonium tartrate before transfer to supplemented ANM with 10 mM ammonium (NH_4), glutamine (Gln), glutamate (Glu), and alanine (Ala) **(A)** or during nitrogen starvation (-N) for a further 4 hours **(A and B)**, indicated temperature shifts occurred simultaneously with the media transfer.

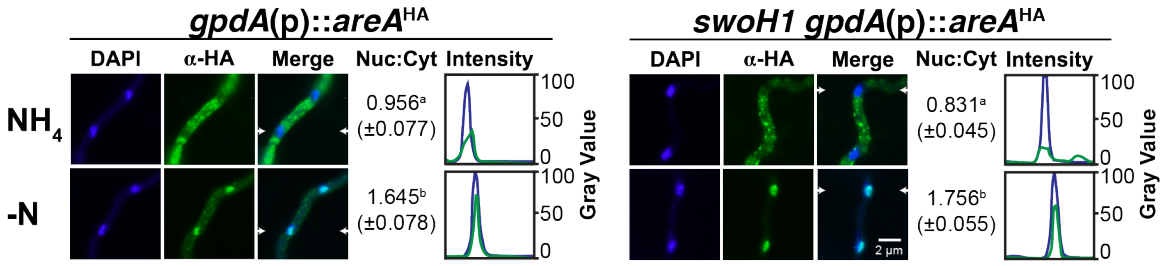

Figure 7.6 SwoH does not regulates AreA^{HA} nuclear export.

The subcellular distribution of AreA^{HA} in wild type (MH9949) and *swoH1* (RT20) after growth at 25ºC in supplemented liquid ANM containing 10 mM ammonium for 14 hours and transferred to supplemented ANM containing 10 mM ammonium (NH_4) or no nitrogen source (-N) for 4 hours. DAPI stains DNA and marks the location of nuclei. AreA^{HA} (α-HA) was visualized by UV fluorescence microscopy following immunostaining with α-HA (3F10) and Alexa Fluor-488-conjugated goat anti-rat antibodies. Nuclear to Cytoplasmic fluorescence ratio (Nuc : Cyt) was calculated from the mean α-HA fluorescence ratio of 13 nuclei and adjacent cytoplasm. SEM is shown. Superscript lowercase letters indicate significantly different groups using the two-tailed Student's t-test ($p < 0.05$). Arrowheads show transects used to generate a fluorescence intensity plots for DAPI (blue) and α-HA (green).

7.4.2.ii Inducible overexpression of swoH.

The increased expression of *fmdS-lacZ* conferred by the *swoH1* reduced-function mutant during nitrogen starvation may indicate a role for SwoH in repressing AreA activation. Overexpression of AreB or NmrA, both of which repress AreA dependent transcriptional activation, has been shown to repress growth on various nitrogen nutrients (WONG *et al.* 2007; WONG *et al.* 2009). To overexpress *swoH* Kendra Siebert (Kansas State University) generated a construct in which the *swoH* coding region was expressed from the xylose inducible *xylP* promoter (ZADRA *et al.* 2000; K.S. Siebert and R.B. Todd unpublished). No observable difference in nitrogen utilization was observed in strains containing *xylP*(p)::*swoH* compared with wild type when grown on xylose with a range of preferred and alternative nitrogen nutrients (Figure 7.7). Therefore, unlike NmrA and AreB, SwoH overexpression does not repress AreA.

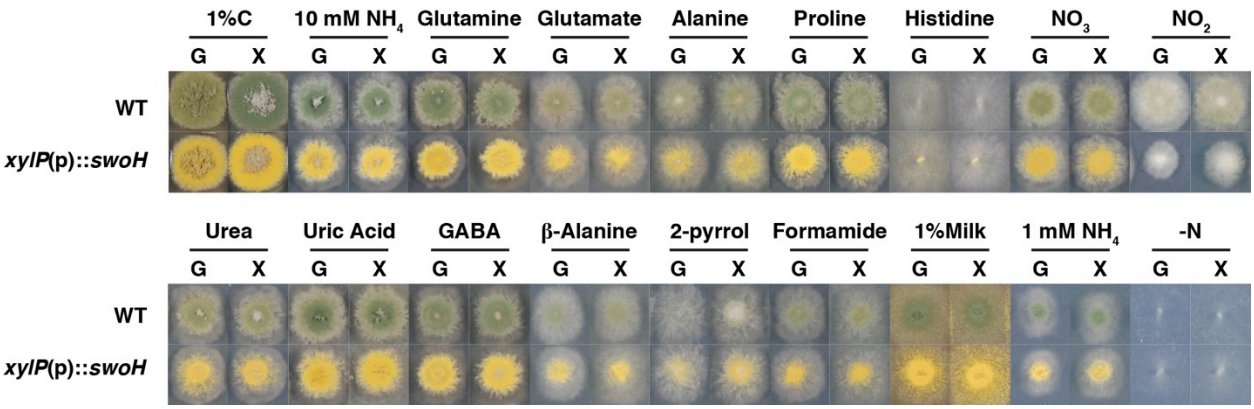

Figure 7.7 SwoH overexpression does not repress nitrogen utilization

Growth of wild type (MH1) and *xylP*(p)::*swoH1* (RT21) on 1% complete media and supplemented solid carbon free media with either 1% (w/v) glucose (G) or xylose (X) as the carbon source and 10 mM of nitrogen sources unless stated. Ammonium tartrate (NH_4), nitrate (NO_3), nitrite (NO_2), ɣ-aminobutyric acid (GABA), 2-pyrrolidinone (2-pyrrol), and nitrogen free (-N).

7.4.2.iii Generation and characterization of a **swoHΔ** *mutant.*

Previous attempts to isolate a haploid *swoH* knockout mutant were unsuccessful and it was concluded that *swoH* is likely an essential gene (LIN *et al.* 2003). However, protoplast recovery and haploidization by Lin and colleagues was carried out on nitrate at 37ºC. Given that our *swoH1* growth tests showed poor growth under these conditions and stronger growth on ammonium and glutamine at 37ºC we attempted to isolate a knockout mutant using an AN8216/*swoH*Δ *A.f.pyrG*$^{+}$ knockout cassette from the Fungal Genetics Stock Center (Figure 7.8A). A single transformant was isolated after selection for uridine and uracil prototrophy with ammonium as the nitrogen source. This mutant displayed sporadic, sectoring growth and was suspected to be a [*swoH*$^{+}$ + *swoH*Δ] heterokaryon (Figure 7.8B). Several attempts at heterokaryon resecue (OSMANI *et al.* 2006b) failed to isolate a *pyrG*$^{+}$ strain, although numerous *pyrG*$^{-}$ (*swoH*$^{+}$) colonies were isolated. Southern blot analysis of the heterokaryon confirmed the presence of both wild type and *swoH*Δ bands (Figure 7.8C). Surprisingly, after some passaging the heterokaryon formed a stable colony with pale conidia (Figure 7.8B), a trait suggestive of diploidization. PCR amplification confirmed the presence of both the wild type *swoH* locus and the *swoH*Δ mutation in the stable colony (Figure 7.8D). Diploids can be distinguished from haploids by measuring the conidia diameter, as diploid conidia are larger due to the increased DNA content (PONTECORVO *et al.* 1953). Comparison of conidia from the parent, the sectoring heterokaryon, the new stable colony and a control diploid showed that a *swoH*$^{+}$/*swoH*Δ heterozygous diploid had formed (Figure 7.8E,F). This diploid is homozygous at all loci except *swoH*. Several attempts to generate haploids following benlate-induced haploidization were carried out, however as with heterokaryon rescue, only *pyrG*$^{-}$ (*swoH*$^{+}$) colonies were isolated. As such it is likely the conclusion of (LIN *et al.* 2003) was indeed correct and *swoH* is an essential gene. The *swoH*$^{+}$/*swoH*Δ diploid presented the opportunity to assess whether *swoH*Δ affected AreA localization by testing for haploinsufficient effects. Microscopy of AreA^{HA} in the *swoH*$^{+}$/*swoH*Δ strain and a control diploid showed no observable effect on regulated nuclear export during nitrogen sufficiency and nitrogen starvation (Figure 7.9).

Figure 7.8 Generation of *swoH*$^{+}$/*swoH*Δ diploid.

A) Knockout cassette for *swoH* from the Fungal Genetics Stock Center was used to generate a s*woH*Δ mutant **B)** Sectoring growth morphology of a *pyrG*$^{+}$ transformant identified as being heterokaryotic developed into a stable pale colony identified as being diploid **C)** Southern blot of the [*swoH*$^{+}$ + *swoH*Δ] heterokaryon probed with a 1.7 kb fragment of wild type *swoH* (-0.7 to +1 kb). *Kpn*I cuts wild type *swoH* at -2.8 kb and +2.0 kb relative to the ATG to generate a 4.8 kb fragment. *A.f. pyrG* contains a *Kpn*I site at +1.3 kb and generates 1.3 kb, 4.1 kb fragments upon digestion, the larger of which contains sufficient wild type sequence to generate a detectable band. **D)** PCR Amplification of the *swoH* locus from genomic DNA of the [*swoH*$^{+}$ + *swoH*Δ] heterokaryon and the *swoH*$^{+}$/*swoH*Δ diploid (RT174). Replacement of 1.0 kb of *swoH* with 1.7 kp of *A.f.pyrG* results in an increased band side in the *swoH*Δ. **E-F)** Strain ploidy was determined by microscopy and diameter measurement of conidia from wild type haploid (RT52), heterokaryon [*swoH*$^{+}$ + *swoH*Δ], diploid *swoH*$^{+}$/*swoH*Δ and wild type diploid (MH11167). Error bars depict standard deviation. Lower case letter indicate significantly different groups using the two-tailed Student's t-test, $p < 0.05$, n=25.

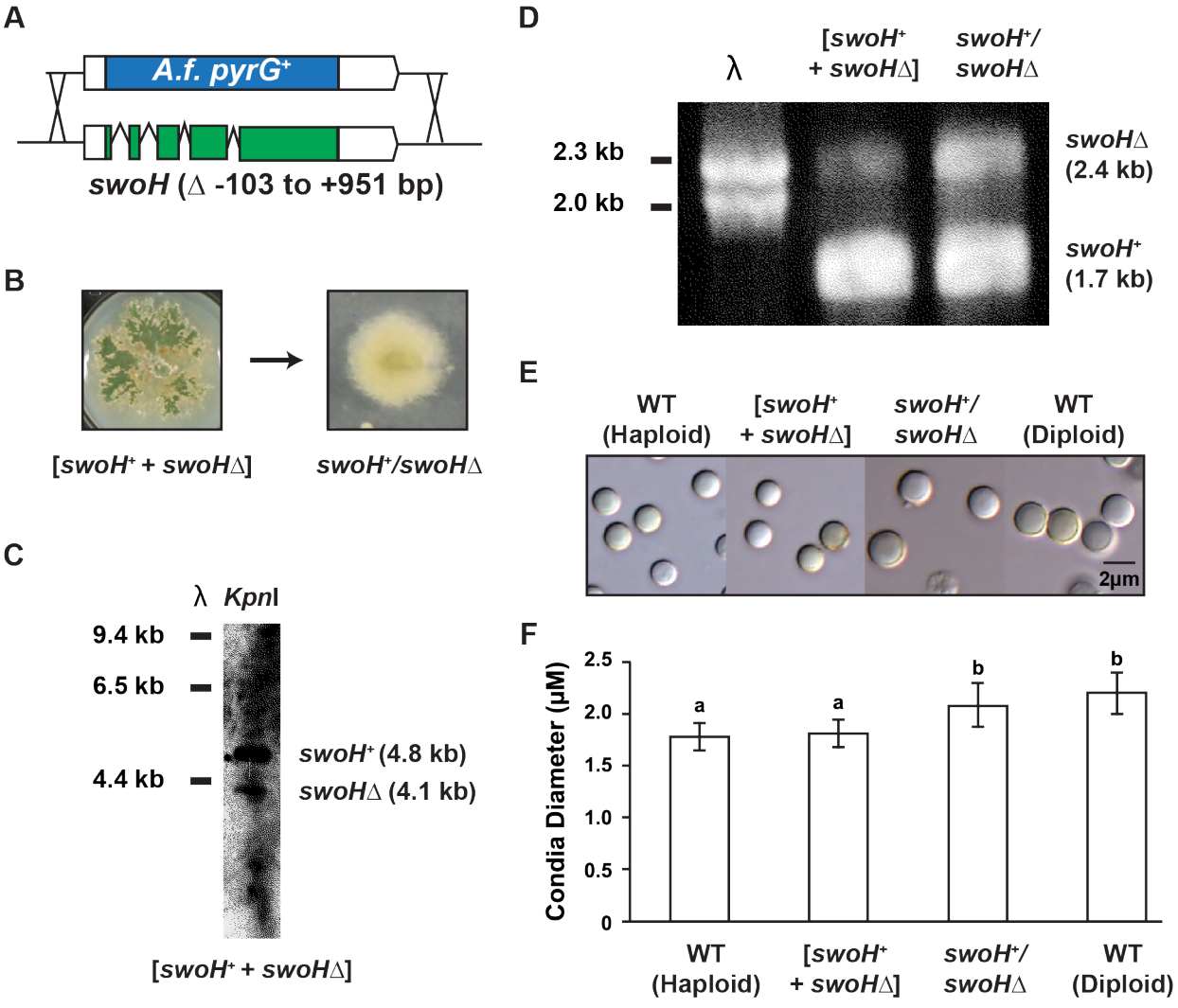

Figure 7.8 Generation of *swoH*$^+$/*swoH*Δ diploid.

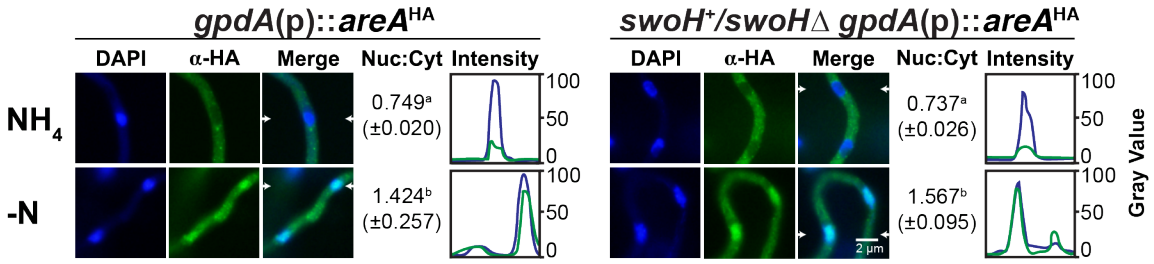

Figure 7.9 The *swoH*$^{+}$/*swoH*Δ diploid has wild type AreA^{HA} subcellular distribution.

The subcellular distribution of AreA^{HA} in wild type (MH11167) and *swoH*$^{+}$/*swoH*Δ (RT174) diploid strains after growth at 25ºC in supplemented liquid ANM containing 10 mM ammonium for 14 hours and transferred to supplemented ANM containing 10 mM ammonium (NH_4) or no nitrogen source (-N) for 4 hours. DAPI stains DNA and marks the location of nuclei. AreA^{HA} (α-HA) was visualized by UV fluorescence microscopy following immunostaining with α-HA (3F10) and Alexa Fluor-488-conjugated goat anti-rat antibodies. Nuclear to Cytoplasmic fluorescence ratio (Nuc : Cyt) was calculated from the mean α-HA fluorescence ratio of 13 nuclei and adjacent cytoplasm. SEM is shown. Superscript lowercase letters indicate significantly different groups using the two-tailed Student's t-test ($p < 0.05$). Arrowheads show transects used to generate a fluorescence intensity plots for DAPI (blue) and α-HA (green).

7.4.3 Screening of the Phosphatase knockout set

If reversible phosphorylation of AreA regulates nuclear export, it is expected that a phosphatase, or multiple phosphatases, would be involved in protein modification. *A. nidulans* contains 30 phosphatase-encoding genes, six of which are essential and 24 are non-essential, however five of these non-essential genes confer major growth defects when mutated (SON AND OSMANI 2009; ZHONG *et al.* 2014). Conditional expression strains, under the control of the *alc* promoter, were generated for the essential genes and genes with major growth defects (SON AND OSMANI 2009). We obtained these strains to screen for effects on nitrogen utilization. We examined the phosphatase mutant sets for their ability to utilize a range of nitrogen nutrients on glucose as a carbon source (Figure 7.10). None of the strains expressing essential genes from the *alc* promoter grew in the absence of ethanol-induced expression on any nitrogen nutrient (data not shown). Several of the strains within the deletion set, were generated in a *wA3 nirA14* background and consequently were unable to utilize nitrate or nitrite, and this is unrelated to the phosphatase mutation (SON AND OSMANI 2009). The strain lacking AN1467, which is the predicted ortholog of *S. cerevisiae* PTC7, was unable to utilize glutamate, glutamine, alanine, nitrate or formamide as a nitrogen nutrient but grew well on 10 mM ammonium and other nitrogen nutrients such as proline and urea suggesting some involvement in nitrogen utilization. The *sitA*Δ mutant was able to utilize all nitrogen nutrients when they were supplied at 10 mM but was unable to use ammonium at low concentrations, suggesting SitA may be required for AreA activation during nitrogen limitation or starvation.

Figure 7.10 Nitrogen utilization screen of non-essential phosphatase gene deletion mutants. The non-essential phosphatase deletion set was grown for 2 days at 37ºC on supplemented solid ANM containing 10 mM of various nitrogen sources (unless stated). NH_4: ammonium tartrate, NO_3: nitrate, NO_2: nitrite, GABA: ɣ-aminobutyric acid. White wild type (MH11556; *wA3*) and green wild type (MH1) were used as controls. For characterized *A. nidulans* genes the name is given in parenthesis (lower case italics), and the predicted *S. cerevisiae* ortholog is given for uncharacterized genes (upper case). AspGD does not have a predicted *S. cerevisiae* ortholog for AN10138. Target residues are as stated on AspGD (www.aspergillusgenome.org).

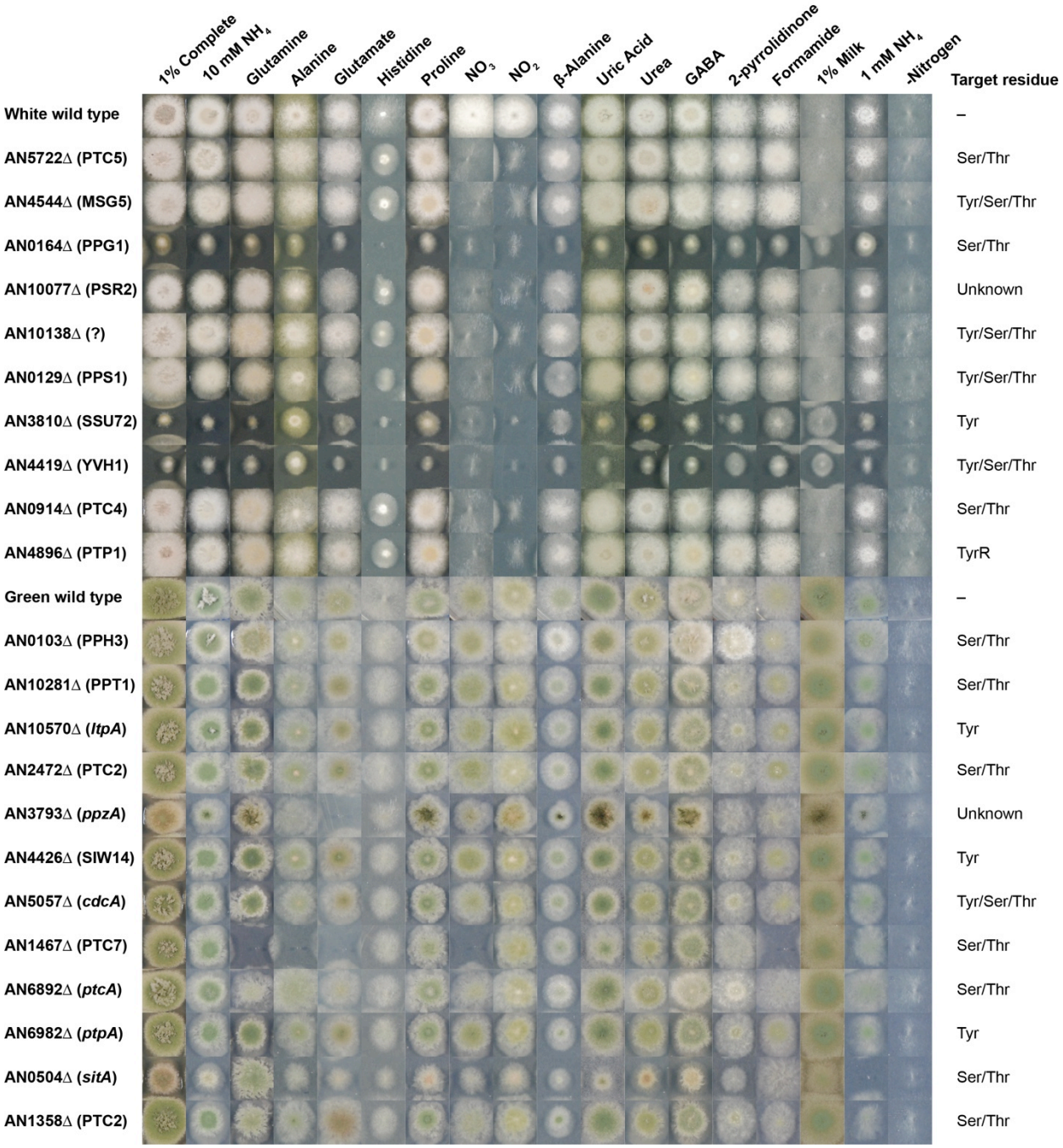

Figure 7.10 Nitrogen utilization screen of non-essential phosphatase gene deletion mutants.

7.4.4 PhmA: A protein histidine methyltransferase

Protein histidine residues may be methylated by protein histidine methyltransferases (WEBB *et al.* 2010). These enzymes are poorly studied; only one protein histidine methyltransferase, HPM1 in *S. cerevisiae*, has been characterized in Eukaryotes (WEBB *et al.* 2010). By blastp of the *A. nidulans* genome we identified a single HPM1 ortholog, AN1445, which we named *phmA* for ***p***rotein ***h***istidine ***m***ethyltransferase. Alignment of HPM1 and PhmA show poor overall conservation and only 28% identity (Figure 7.11). We constructed a *phmA*Δ mutant by transformation of an AN1445/*phmA*Δ *A.f.pyrG*$^{+}$ knockout construct, sourced from FGSC, into RT52 (*gpdA*(p)*areA*^{HA} *pyrG89 nkuA*Δ) followed by selection for pyrimidine prototrophy (Figure 7.12A). Two independent transformants were selected and each was confirmed by Southern blot to have a single homologous integration at the AN1445 locus (data not shown). *phmA*Δ resulted in pleiotropic growth defects including reduced growth rate, delayed germination and a preference for producing sexual cleistothecia rather than asexual conidia (Figure 7.12B-E). As *phmA* is a putative methyltransferase we considered it might be defective in methionine biosynthesis, however supplementation with either cysteine or methionine had no effect on growth (Figure 7.12C). Osmotic stabilization of the solid growth media with 1M sucrose or 1M sorbitol restored conidiation and indicates a possible role for PhmA in osmo-regulation of the sexual to asexual balance (Figure 7.12C). Osmotic stabilization did not improve the overall growth rate (Figure 7.12D). To determine if PhmA is involved in nitrogen utilization we screened *phmA*Δ for growth on various nitrogen sources on both osmotic-stabilized and non-stabilized media (Figure 7.13). *phmA*Δ grew as well on alternative nitrogen sources as on preferred nitrogen sources. *phmA*Δ did not show susceptibility to the toxic nitrogen analogs thiourea and chlorate during growth on ammonium, indicating *phmA*Δ does not confer AreA derepression (Figure 7.13).

To determine if PhmA is involved in regulated AreA nuclear export immunofluorescence microscopy was carried out on a strain expressing AreA^{HA}. Due to the slow growth of *phmA*Δ the wild type control was set up later to germinate at approximately the same time as the *phmA*Δ strain. In this way both strains were transferred to fresh media with either ammonium or nitrogen starvation conditions at a similar growth stage for an identical 4 hours. In the presence of ammonium and during nitrogen starvation localization of AreA^{HA} in the *phmA*Δ mutant resembled that of wild type (Figure 7.14). Furthermore there was no significant difference

between the ratios of nuclear to cytoplasmic fluorescence when *phmA*Δ was compared with wild type. Therefore it appears that PhmA does not regulate AreA nuclear export.

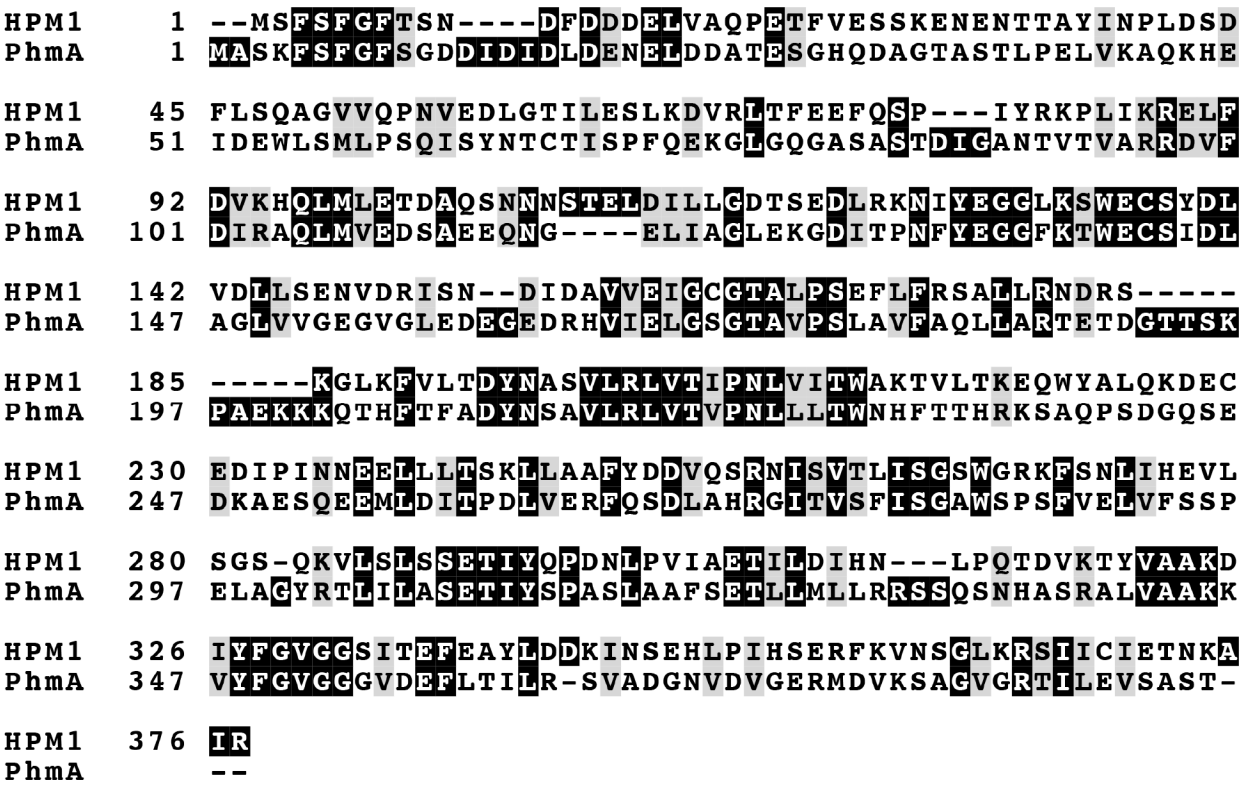

Figure 7.11 Alignment of the protein histidine methyltransferases PhmA and HPM1

Protein sequences for *S. cerevisiae* HPM1 and *A. nidulans* PhmA were downloaded from SGD (www.yeastgenome.org) and AspGD (www.aspergillusgenome.org) respectively. Sequences were aligned in Clustal Omega using default settings and shaded in Boxshade (http://www.ch.embnet.org/software/BOX_form.html) with 50% identity (black) and 50% similarity (gray).

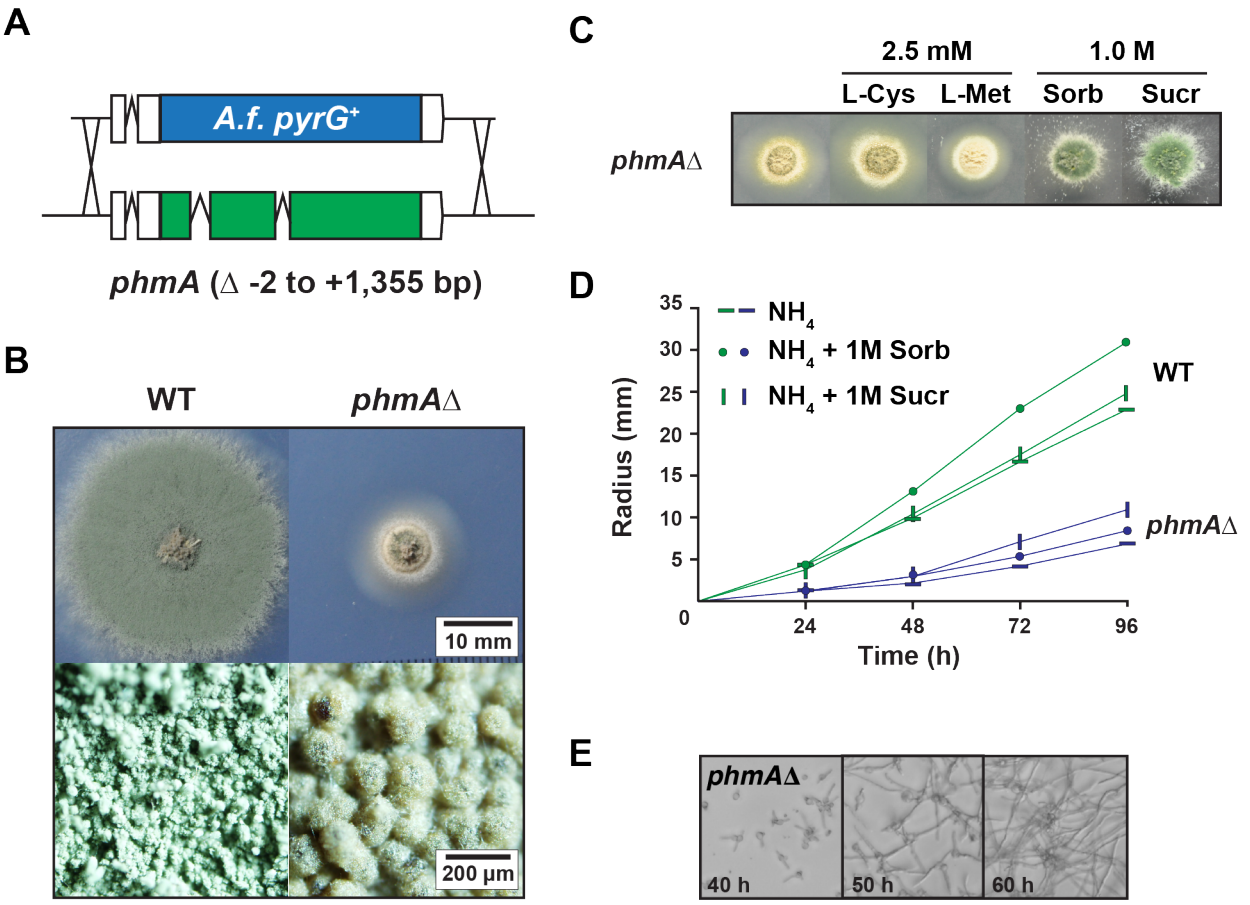

Figure 7.12 *phmA*Δ is pleiotropic and affects sexual development.

A) The knockout cassette for *phmA* from the Fungal Genetics Stock Center was used to generate a *phmA*Δ mutant **B)** Colony morphology of wild type (MH1) and *phmA*Δ (RT263) grown on supplemented solid ANM media containing 10 mM ammonium. **C)** *phmA*Δ grown on supplemented solid ANM media containing 10 mM ammonium with cysteine (L-Cys), methionine (L-met), sorbitol (Sorb), and sucrose (Sucr) at the indicated concentrations. **D)** Growth rate of wild type (MH1) and and *phmA*Δ (RT263) grown on supplemented solid ANM media containing 10 mM ammonium (NH_4) with sorbitol (Sorb), and sucrose (Sucr). **E)** Microscopy of *phmA*Δ (RT263) germlings grown in supplemented liquid ANM media containing 10 mM ammonium.

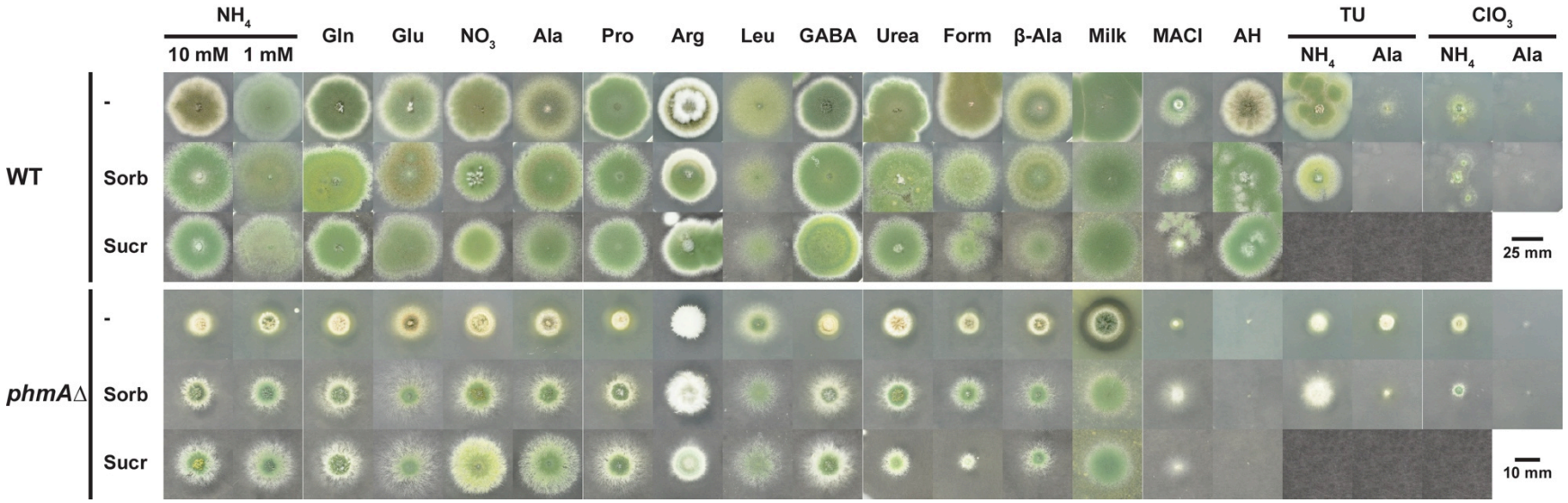

Figure 7.13 Screen of *phm*Δ for nitrogen utilization effects.

Wild type (MH1) and *phmA*Δ (RT263) were grown for 4 days at 37ºC on supplemented solid ANM containing 10 mM (unless stated) of ammonium (NH_4), glutamine (Gln), glutamate (Glu), nitrate (NO_3), alanine (Ala), proline (Pro), arginine (Arg), leucine (Leu), ɣ-aminobutyric acid (GABA), urea, formamide (Form), β-alanine (β -Ala), and 2 % Milk. For toxic nitrogen analog tests 200 mM methyl ammonium chloride (MACl), 0.3 mM aspartate hydroxamate (AH), 10 mM thiourea (TU) and 5 mM chlorate (ClO_3) were provided in addition to 10 mM alanine (Ala). 200 mM chlorate (ClO_3) and 10 mM thiourea (TU) were provided in addition to 5 mM ammonium (NH_4).

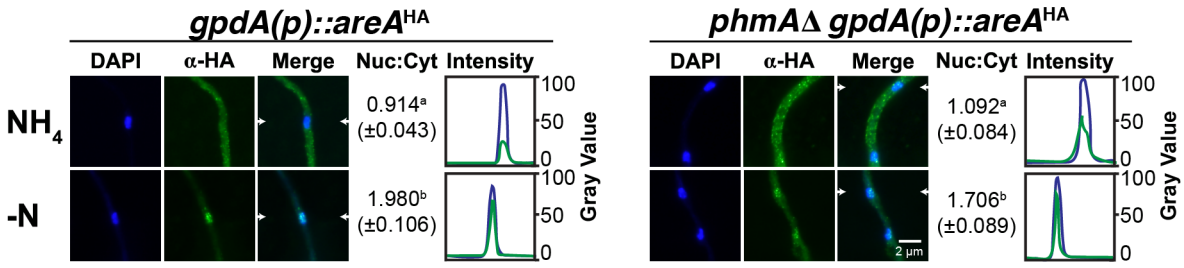

Figure 7.14 *phmA*Δ does not affect AreA^{HA} localization.

The subcellular distribution of AreA^{HA} in wild type (MH9949) and *phmA*Δ (RT263) strains after growth at 25ºC in supplemented liquid ANM containing 10 mM ammonium for 14 hours and transferred to supplemented ANM containing 10 mM ammonium (NH_4) or no nitrogen source (-N) for 4 hours. Nuclei are visualized by DAPI staining. AreA^{HA} (α-HA) was visualized by UV fluorescence microscopy following immunostaining with α-HA (3F10) and Alexa Fluor-488-conjugated goat anti-rat antibodies. Nuclear to Cytoplasmic fluorescence ratio (Nuc : Cyt) was calculated from the mean α-HA fluorescence ratio of 13 nuclei and adjacent cytoplasm. SEM is shown. Superscript lowercase letters indicate significantly different groups using the two-tailed Student's t-test ($p < 0.05$). Arrowheads show transects used to generate a fluorescence intensity plots for DAPI (blue) and α-HA (green).

7.4.5 Modification mimic mutant analysis of AreA

Protein modifications may be mimicked by certain amino acid substitutions (DAVIS 2004). Our proposed model of regulated AreA nuclear export involves the modification His-704 by either phosphorylation or methylation. Because of their negative charge, aspartate and glutamate residues are used to mimic phosphorylation (DAVIS 2004). Similarly a bulky-hydrophobic phenylalanine residue may be used to mimic methylation. Therefore two AreA His-704 phosphorylation mimics, expressing $AreA^{HA.H704D}$ and $AreA^{HA.H704E}$, as well as an His-704 methylation mimic, expressing $AreA^{HA.H704F}$, were constructed by two-step gene replacement at the *areA* locus (C.C. Hunter, K.S. Siebert, and R.B. Todd unpublished). We tested these mimics for growth on a range of nitrogen nutrients. All three mutants grew like wild type on the preferred nitrogen nutrients ammonium and glutamine as well as on urea and nitrate (Figure 7.15A). However, like $areA^{HA.H704A}$ they showed reduced growth on many alternative nitrogen nutrients consistent with reduced AreA function as a result of mutation of the His-704 DNA-contact residue (STARICH *et al.* 1998). Immunofluorescence microscopy showed that all three His-704 modification mimics accumulated in the nucleus during nitrogen starvation and did not confer nuclear export (Figure 7.15B). Furthermore the three modification mimics showed increased nuclear localization during nitrogen sufficiency, indicating they impaired AreA nuclear export (Figure 7.15B). As the modification mimics do not confer nuclear export it is likely that our model of His-704 being the target of a nuclear export signal is incorrect; instead, it is likely that His-704 is required for efficient interaction with the hydrophobic binding pocket of CrmA, and that any change to this residue reduces the affinity of that interaction.

Figure 7.15 AreA His-704 modification mimics confer reduced nuclear export.

A) Growth of *gpdA*(p)*areA*^{HA} (MH10897), *gpdA*(p)*areA*$^{HA.H704D}$ (RT317), *gpdA*(p)*areA*$^{HA.H704E}$ (RT315), and *gpdA*(p)*areA*$^{HA.H704F}$ (RT316) on solid ANM supplemented with 10 mM each ammonium (NH_4), glutamine (Gln), alanine (Ala), glutamate (Glu), histidine (His), isoleucine (Ile), proline (Pro), valine (Val) nitrate (NO_3), nitrite (NO_2), ɣ-aminobutyric acid (GABA), urea, acetamide (Acet), 2-pyrrolidinone (2-pyrr), 2% milk and nitrogen starvation media (-N) at 37ºC for 2 days. **B)** The subcellular distribution of AreA^{HA} (MH9949), AreA$^{HA.H704D}$ (RT317), AreA$^{HA.H704E}$ (RT315), and AreA$^{HA.H704F}$ (RT316) after growth at 25ºC in supplemented liquid ANM containing 10 mM ammonium for 14 hours and transferred to supplemented ANM containing 10 mM ammonium (NH_4) or no nitrogen source (-N) for 4 hours. DAPI stains the nuclei. AreA^{HA} (α-HA) was visualized by UV fluorescence microscopy following immunostaining with α-HA (3F10) and Alexa Fluor-488-conjugated goat anti-rat antibodies. Nuclear to Cytoplasmic fluorescence ratio (Nuc : Cyt) was calculated from the mean α-HA fluorescence ratio of 13 nuclei and adjacent cytoplasm. SEM is shown. Superscript lowercase letters indicate significantly different groups using the two-tailed Student's t-test ($p < 0.05$). Arrowheads show transects used to generate a fluorescence intensity plots for DAPI (blue) and α-HA (green).

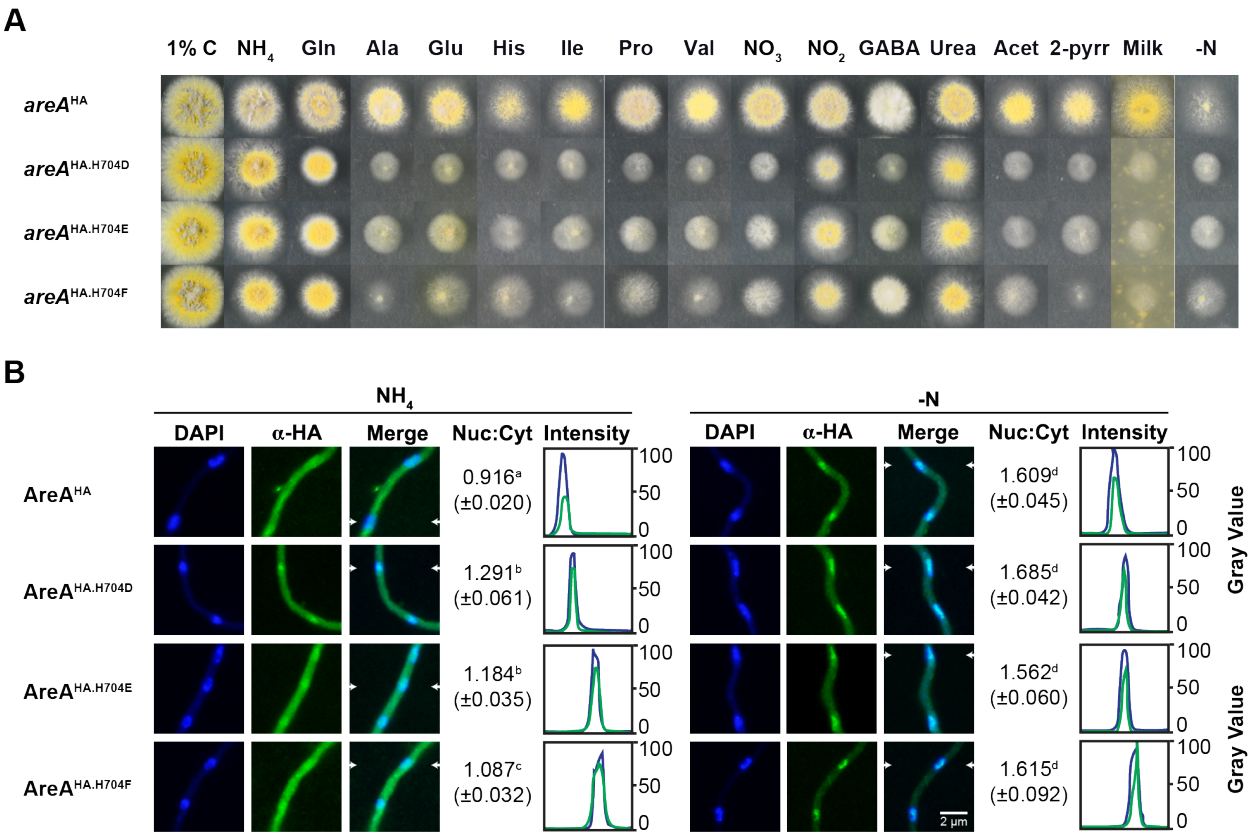

Figure 7.15 AreA His-704 modification mimics confer reduced nuclear export.

7.5 Discussion

Regulated nuclear export of many proteins, including AreA in *A. nidulans*, is dependent on interaction between an inherent nuclear export signal (NES) and the CRM1-type nuclear exportin (TODD *et al.* 2005; NGUYEN *et al.* 2012). We showed that histidine 704, which lies within the AreA NES, is required for regulated nuclear export (Chapter 6.4.3), and because of this finding we formulated a model whereby modification of His-704 was the signal that triggered nuclear export of AreA in response to the presence of a nitrogen nutrient (Figure 7.1). Mutation of His-704 to the non-modifiable residue alanine resulted in constitutive nuclear localization of $AreA^{HA}$ and was consistent with the hypothesis that modification conferred nuclear export. Therefore we examined genes encoding enzymes predicted to modify histidines and generated His-704 modification mimics.

7.5.1 Histidine 704 modification is not the nuclear export signal.

To determine whether His-704 modification was the trigger for regulated nuclear export of AreA we took both candidate gene and site-specific mutagenesis approaches. We identified two genes in *A. nidulans* that might be responsible for modification of a protein histidine residue the NDPK SwoH, which was previously characterized (LIN *et al.* 2003), and the protein histidine methyltransferase PhmA, which we have characterized in this work. We showed that *swoH* is an essential gene. Therefore our analysis was carried out in a temperature sensitive mutant and a heterozygous $swoH^{+}/swoH\Delta$ diploid, which are known and predicted to have reduced NDPK activity than wild type, respectively (LIN *et al.* 2003; this study). Neither of these strains altered the nucleo-cytoplasmic distribution of $AreA^{HA}$ during either nitrogen sufficiency or nitrogen starvation. As both strains retain NDPK activity we cannot categorically rule out regulation of AreA nucleo-cytoplasmic distribution by SwoH. We isolated a deletion mutant of *phmA*Δ. Analysis of $AreA^{HA}$ localization in the *phmA*Δ mutant showed wild type nucleo-cytoplasmic distribution during nitrogen sufficiency and nuclear accumulation during nitrogen starvation. As there is only one predicted protein histidine methyltransferase in *A. nidulans* we can conclude that PhmA, and as a result protein histidine modification, is not required for AreA nuclear export or nuclear accumulation.

In addition to studying mutants lacking putative protein histidine modifying enzymes we also generated $AreA^{HA}$ variants that carried either a His-704 phosphorylation or a methylation

mimic. None of these mutations was consistent with our hyposthesis that they would confer nuclear export during nitrogen starvation. Conversely we observed that, like AreA$^{HA.H704A}$, they accumulated in the nucleus during nitrogen sufficiency. We have now studied five different histidine 704 substitutions: asparagine (polar), alanine (hydrophobic), glutamine (negatively charge), aspartate (negatively charged), and phenylalanine (hydrophobic). The weakest effect on AreA nuclear distribution was seen in His-704-Asn, which conferred nuclear localization but not nuclear accumulation during nitrogen sufficiency. The His-704-Asn is the least drastic change in sidechain charge. Interaction of NESs with the CRM1 exportin cargo-binding site is affected by both the hydrophobic residues and the flanking protein sequence (GUTTLER *et al.* 2010). Based on our observations with His-704 mutations, we predict that the positive charge of His-704 is required for efficient interaction with the CrmA exportin in *A. nidulans* during nitrogen sufficiency.

7.5.2 Alternative mechanisms that may regulate AreA nuclear export.

We found no effect on regulated AreA^{HA} nucleo-cytoplasmic distribution in either the *phmA*Δ or *swoH1* mutants indicating that neither of these proteins is likely to be required for nuclear accumulation or nuclear export. Therefore the mechanism by which regulated subcellular distribution of AreA is achieved remains to be elucidated. Experiments in other systems have shown that a diverse array of signals can confer regulated nucleocytoplasmic distribution of proteins including enzyme facilitated protein modification, environmental condition derived protein modification, and protein-protein interactions (Figure 7.16). The zebrafish ZO-2 protein contains four functional and co-operative NESs, however substitution of a single serine residue for glutamine in a putative PKC phosphorylation site within one of the NESs, to generate a phosphorylation mimic, is sufficient to confer CRM1 dependent nuclear export (JARAMILLO *et al.* 2004; GONZALEZ-MARISCAL *et al.* 2006) and sumoylation is required for TEL nuclear export (WOOD *et al.* 2003). Similarly the mammalian the c-Jun kinase is required for GATA-6 nuclear export (USHIJIMA AND MAEDA 2012). Interestingly the predicted site of phosphorylation in GATA-6 does not lie within the predicted nuclear export singal but is N-terminal (USHIJIMA AND MAEDA 2012), suggesting that sequences outside of the predicted GATA-6 NES may be involved in regulated nuclear export. In both of the above examples the modified protein is exported. In contrast for mammalian STE20-like kinase (MST), phosphorylation results in

nuclear accumulation (LEE *et al.* 2001). The modification of a threonine residue, which lays outside of the NES, in MST is predicted to confer conformational change that exposes the NLS and masks the NES (LEE *et al.* 2001). Masking of the SRB2 NES in HeLa cells is also thought to be responsible for blocking nuclear export, however in this case, masking results from direct sensing of redox state and the formation of a disulfide bond (PAPP *et al.* 2006). Similarly redox dependent modification of a cysteine within one of the two Nrf2 NESs results in nuclear accumulation in HeLa calls (LI *et al.* 2005; LI *et al.* 2006). Masking of the NES can occur via protein-protein interaction, for example dimerization of Survivin, and tetramerization of p53 in mammalian cells blocks recognition of an NES by CRM1 and results in decreased nuclear export (STOMMEL *et al.* 1999; ENGELSMA *et al.* 2007). Finally interaction with organic molecules or effectors can regulate export, such as with Bach1 export following binding of heme (SUZUKI *et al.* 2004). AreA interacts with several other proteins including NmrA, TamA and NirA, however other interactors are possible (SMALL *et al.* 1999; LAMB *et al.* 2004; BERGER *et al.* 2006; KOTAKA *et al.* 2008). Therefore protein-protein interaction may be the regulatory mechanism facilitating AreA nuclear accumulation. NmrA was proposed to regulate AreA nuclear localization (LAMB *et al.* 2004), however *nmrA* is not required for nuclear accumulation or nuclear export (TODD *et al.* 2005). AreA is expected to interact with TamA during nitrogen sufficiency (SMALL *et al.* 1999; DOWNES *et al.* 2014b), suggesting interaction with TamA is not the import-export switch. Therefore if interaction with another protein is the export regulatory mechanism then it is likely with an unknown protein. Post-translational modification may be the signal for either nuclear export or nuclear accumulation. Phosphorylation and sumoylation have been considered as possible modifications (K.H. Wong, M.A. Davis, M.J. Hynes, and R.B Todd, unpublished data). AreA is highly modified by phosphorylation (WONG 2007). However, the S711 and T714 phosphorylation mimic mutants affecting the AreA NES or immediately adjacent sequences, respectively do not perturb AreA nucleocytoplasmic distribution. Although deletion of the *sumO* gene prevents nuclear accumulation, this is likely indirect as the non-sumoylatable K713R mutant shows wild type nuclear accumulation (K.H. Wong, M.A. Davis, M.J Hynes, and R.B. Todd, unpublished data). Further experimentation will be required to determine which of these mechanisms is responsible.

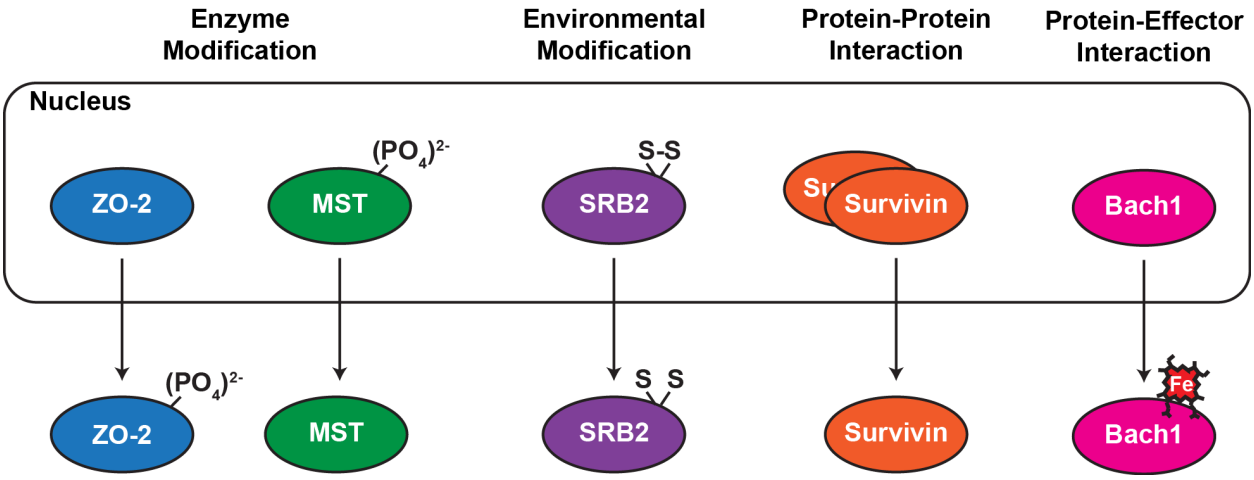

Figure 7.16 Characterized mechanisms that regulated nuclear export

A diverse range of signals have been characterized as regulating CRM1 exportin dependent nuclear export including modification by kinases and phosphatases, oxidative stress induced disulfide bonds, dimerization and interaction with effectors such as heme.

7.5.3 Regulation of sexual development by phmA.

The true wild type *A. nidulans* preferentially produces sexual fruiting bodies, cleistothecia, which contain ascospores, when grown in the dark. Exposure to red light results in a developmental switch to producing asexual conidiospores (MOONEY AND YAGER 1990). Loss-of-function point mutations of *veA* lead to the production of conidia in either light or dark conditions (KAFER 1965; KIM *et al.* 2002). Because of the benefits of primarily working with asexual spores much of the research in *A. nidulans* is carried out in a *veA1* point mutation background, which is considered "wild type" (KAFER 1965). We constructed the *phmA*Δ mutant in a *veA1* background and were surprised to discover that it suppressed the *veA1* mutation and generated primarily cleistothecia. VeA is light responsive, during growth in the dark it is primarily cytoplasmic and exposure to red light induces nuclear localization of the protein (STINNETT *et al.* 2007). The *veA1* mutant results from mutation of the ATG start codon to ATT, this mutation results in translation starting at the second ATG and an N-terminally truncated VeA protein that does not accumulate in the nucleus in response to light (KIM *et al.* 2002; STINNETT *et al.* 2007; BAYRAM *et al.* 2008). Suppression of the *veA1* mutant by *phmA*Δ suggests that the putative protein histidine methyltransferase is potentially involved in regulating the sexual-asexual developmental switch. Another methyltransferase, LaeA, is also involved in sexual development; *laeA*Δ is insensitive to light and produces cleistothecia under both light and dark conditions (SARIKAYA BAYRAM *et al.* 2010). Furthermore the putative LaeA-like methyltransferase LlmF interacts with VeA and negatively regulates sexual development (PALMER *et al.* 2013). As *phmA*Δ suppresses the effects of the *veA1* mutation it will be of great interest to determine the effects of *phmA*Δ in *veA*$^{+}$, *laeA*Δ, and *llmF*Δ backgrounds. We were able to repair the *phmA*Δ developmental defect by osmotically stabilizing the growth media. In addition to light, the sexual-asexual switch is also controlled by stress, pheromones, and the oxygen to carbon dioxide ratio (reviewed in BAYRAM AND BRAUS 2012). Therefore PhmA may be involved in developmental signaling independently of VeA and LaeA.

7.6 Future Directions

The purpose of this chapter was to determine whether or not a reversible protein histidine modification results in regulated AreA nucleocytoplasmic distribution. Our evidence suggests that this is not the case. However, histidine-704 is clearly required for nuclear export. One possibility is that this residue is required for interaction with the CrmA exportin. Yeast two-hybrid experiments of the wild type and mutant variants of AreA NES with the CrmA exportin may be able to determine whether this is the case. The sidechain or charge of His-704 at physiological pH may be important for interaction with the CrmA cargo-binding site. We have not made a substitution to a positively charged amino acid. The effect of a histidine-704-substitution to arginine or lysine will allow the importance of charge at this site in the NES for nuclear export to be assessed.

It is possible that AreA is modified at a residue other than His-704, that multiple modifications are involved, or that AreA interacts with an unknown protein and this leads to nuclear export. These possibilities can be addressed in a scaled up genetic screen using the *prnA-areA*^{NES}*-gfp* construct described in Chpater 6. This screen should identify both genes encoding AreA export regulatory proteins and residues within the NES that are essential for export. One limitation of this screen is that the region of AreA within the construct is limited to ten amino acids upstream and downstream of the NES, therefore residues outside of this region that may impact nuclear export will not be identified in this screen. To address this a biochemical approach may also be taken; AreA is rapidly exported from the nucleus after nuclear accumulation when a nitrogen nutrient is added. Immunoprecipitation of AreA^{HA} from extracts prepared minutes after the addition of the nitrogen nutrient could be followed by Mass Spectroscopy analysis to identify interacting proteins or protein modifications that are not observed during AreA nuclear accumulation.

Despite not having an effect on regulated AreA^{HA} nuclear export, the *phmA*Δ mutant showed an interesting sexual phenotype – the preference for sexual over asexual reproduction. Our analysis was carried out in the *veA1* background, which confers preferential conidiation in light and dark growth conditions. The supression of this phenotype by *phmA* is extremely interesting and needs to be further explored. Possible experiments include generating a *phmA*Δ

strain in a *veA*$^{+}$ background and combining the mutation with other mutants in genes that encode VeA interacting proteins, such as *velB*, *velC, llmF* and *laeA*.

References

Abreu, C., M. Sanguinetti, S. Amillis and A. Ramon, (2010) UreA, the major urea/H+ symporter in *Aspergillus nidulans*. Fungal Genet Biol 47**:** 1023-1033.

Adachi, Y., and M. Yanagida, (1989) Higher order chromosome structure is affected by cold-sensitive mutations in a *Schizosaccharomyces pombe* gene *crm1*$^{+}$ which encodes a 115-kD protein preferentially localized in the nucleus and its periphery. J Cell Biol 108**:** 1195-1207.

Alber, F., S. Dokudovskaya, L. M. Veenhoff, W. Zhang, J. Kipper, D. Devos, A. Suprapto, O. Karni-Schmidt, R. Williams, B. T. Chait *et al.*, (2007) The molecular architecture of the nuclear pore complex. Nature 450**:** 695-701.

Albert, T. K., M. Lemaire, N. L. van Berkum, R. Gentz, M. A. Collart and H. T. Timmers, (2000) Isolation and characterization of human orthologs of yeast CCR4-NOT complex subunits. Nucleic Acids Res 28**:** 809-817.

Allen, B. L., and D. J. Taatjes, (2015) The Mediator complex: a central integrator of transcription. Nat Rev Mol Cell Biol 16**:** 155-166.

Amar, N., F. Messenguy, M. El Bakkoury and E. Dubois, (2000) ArgRII, a component of the ArgR-Mcm1 complex involved in the control of arginine metabolism in *Saccharomyces cerevisiae*, is the sensor of arginine. Mol Cell Biol 20**:** 2087-2097.

Andersen, M. R., J. B. Nielsen, A. Klitgaard, L. M. Petersen, M. Zachariasen, T. J. Hansen, L. H. Blicher, C. H. Gotfredsen, T. O. Larsen, K. F. Nielsen *et al.*, (2013) Accurate prediction of secondary metabolite gene clusters in filamentous fungi. Proc Natl Acad Sci USA 110**:** E99-107.

Andreadis, A., Y. P. Hsu, M. Hermodson, G. Kohlhaw and P. Schimmel, (1984) Yeast *LEU2*. Repression of mRNA levels by leucine and primary structure of the gene product. J Biol Chem 259**:** 8059-8062.

Andrianopoulos, A., and M. J. Hynes, (1988) Cloning and analysis of the positively acting regulatory gene *amdR* from *Aspergillus nidulans*. Mol Cell Biol 8**:** 3532-3541.

Andrianopoulos, A., and M. J. Hynes, (1990) Sequence and functional analysis of the positively acting regulatory gene *amdR* from *Aspergillus nidulans*. Mol Cell Biol 10**:** 3194-3203.

Andrianopoulos, A., S. Kourambas, J. A. Sharp, M. A. Davis and M. J. Hynes, (1998) Characterization of the *Aspergillus nidulans nmrA* gene involved in nitrogen metabolite repression. J Bacteriol 180**:** 1973-1977.

Appleyard, M. V., J. Sloan, G. J. Kana'n, I. S. Heck, J. R. Kinghorn and S. E. Unkles, (1998) The *Aspergillus nidulans cnxF* gene and its involvement in molybdopterin biosynthesis. Molecular characterization and analysis of in vivo generated mutants. J Biol Chem 273**:** 14869-14876.

Arnaud, M. B., G. C. Cerqueira, D. O. Inglis, M. S. Skrzypek, J. Binkley, M. C. Chibucos, J. Crabtree, C. Howarth, J. Orvis, P. Shah *et al.*, (2012) The *Aspergillus* Genome Database (AspGD): recent developments in comprehensive multispecies curation, comparative genomics and community resources. Nucleic Acids Res 40**:** D653-659.

Arnold, K., L. Bordoli, J. Kopp and T. Schwede, (2006) The SWISS-MODEL workspace: a web-based environment for protein structure homology modelling. Bioinformatics 22**:** 195-201.

Arst, H. N., Jr., and D. J. Cove, (1973) Nitrogen metabolite repression in *Aspergillus nidulans*. Mol Gen Genet 126**:** 111-141.

Arst, H. N., Jr., and D. W. MacDonald, (1973) A mutant of *Aspergillus nidulans* lacking NADP-linked glutamate dehydrogenase. Mol Gen Genet 122**:** 261-265.

Arst, H. N., Jr., and C. R. Bailey, (1980) Genetic evidence for a second asparaginase in *Aspergillus nidulans*. J Gen Microbiol 121**:** 243-247.

Asatoor, A. M., and M. D. Armstrong, (1967) 3-methylhistidine, a component of actin. Biochem Biophys Res Commun 26**:** 168-174.

Attwood, P. V., M. J. Piggott, X. L. Zu and P. G. Besant, (2007) Focus on phosphohistidine. Amino Acids 32**:** 145-156.

Bahn, Y. S., C. Xue, A. Idnurm, J. C. Rutherford, J. Heitman and M. E. Cardenas, (2007) Sensing the environment: lessons from fungi. Nat Rev Microbiol 5**:** 57-69.

Bai, Y. L., and G. B. Kohlhaw, (1991) Manipulation of the 'zinc cluster' region of transcriptional activator LEU3 by site-directed mutagenesis. Nucleic Acids Res 19**:** 5991-5997.

Baichwal, V. R., T. S. Cunningham, P. R. Gatzek and G. B. Kohlhaw, (1983) Leucine biosynthesis in yeast : Identification of two genes (*LEU4*, *LEU5*) that affect α-Isopropylmalate synthase activity and evidence that *LEU1* and *LEU2* gene expression is controlled by α-Isopropylmalate and the product of a regulatory gene. Curr Genet 7**:** 369-377.

Baker, C. R., V. Hanson-Smith and A. D. Johnson, (2013) Following gene duplication, paralog interference constrains transcriptional circuit evolution. Science 342**:** 104-108.

Bal, J., E. M. Kajtaniak and N. J. Pieniążek, (1977) 4-Nitroquinoline-1-oxide: A good mutagen for *Aspergillus nidulans*. Mutation Research 56**:** 153-156.

Barry, S. M., and G. L. Challis, (2009) Recent advances in siderophore biosynthesis. Curr Opin Chem Biol 13**:** 205-215.

Bassett, E. J., M. S. Keith, G. J. Armelagos, D. L. Martin and A. R. Villanueva, (1980) Tetracycline-labeled human bone from ancient Sudanese Nubia (A.D. 350). Science 209**:** 1532-1534.

Baumgartner, U., B. Hamilton, M. Piskacek, H. Ruis and H. Rottensteiner, (1999) Functional analysis of the Zn(II)2Cys6 transcription factors Oaf1p and Pip2p. Different roles in fatty acid induction of beta-oxidation in *Saccharomyces cerevisiae*. J Biol Chem 274**:** 22208-22216.

Bayram, O., S. Krappmann, M. Ni, J. W. Bok, K. Helmstaedt, O. Valerius, S. Braus-Stromeyer, N. J. Kwon, N. P. Keller, J. H. Yu *et al.*, (2008) VelB/VeA/LaeA complex coordinates light signal with fungal development and secondary metabolism. Science 320**:** 1504-1506.

Bayram, O., and G. H. Braus, (2012) Coordination of secondary metabolism and development in fungi: the velvet family of regulatory proteins. FEMS Microbiol Rev 36**:** 1-24.

Beck, T., and M. N. Hall, (1999) The TOR signalling pathway controls nuclear localization of nutrient-regulated transcription factors. Nature 402**:** 689-692.

Berger, H., R. Pachlinger, I. Morozov, S. Goller, F. Narendja, M. Caddick and J. Strauss, (2006) The GATA factor AreA regulates localization and *in vivo* binding site occupancy of the nitrate activator NirA. Mol Microbiol 59**:** 433-446.

Berger, H., A. Basheer, S. Bock, Y. Reyes-Dominguez, T. Dalik, F. Altmann and J. Strauss, (2008) Dissecting individual steps of nitrogen transcription factor cooperation in the *Aspergillus nidulans* nitrate cluster. Mol Microbiol 69**:** 1385-1398.

Bergmann, S., J. Schumann, K. Scherlach, C. Lange, A. A. Brakhage and C. Hertweck, (2007) Genomics-driven discovery of PKS-NRPS hybrid metabolites from *Aspergillus nidulans*. Nat Chem Biol 3**:** 213-217.

Bergmann, S., A. N. Funk, K. Scherlach, V. Schroeckh, E. Shelest, U. Horn, C. Hertweck and A. A. Brakhage, (2010) Activation of a silent fungal polyketide biosynthesis pathway through regulatory cross talk with a cryptic nonribosomal peptide synthetase gene cluster. Appl Environ Microbiol 76**:** 8143-8149.

Beri, R. K., H. Whittington, C. F. Roberts and A. R. Hawkins, (1987) Isolation and characterization of the positively acting regulatory gene *qutA* from *Aspergillus nidulans*. Nucleic Acids Res 15**:** 7991-8001.

Bernreiter, A., A. Ramon, J. Fernandez-Martinez, H. Berger, L. Araujo-Bazan, E. A. Espeso, R. Pachlinger, A. Gallmetzer, I. Anderl, C. Scazzocchio *et al.*, (2007) Nuclear export of the transcription factor NirA is a regulatory checkpoint for nitrate induction in *Aspergillus nidulans*. Mol Cell Biol 27**:** 791-802.

Bertram, P. G., J. H. Choi, J. Carvalho, W. Ai, C. Zeng, T. F. Chan and X. F. Zheng, (2000) Tripartite regulation of Gln3p by TOR, Ure2p, and phosphatases. J Biol Chem 275**:** 35727-35733.

Bi, Y. M., Y. Zhang, T. Signorelli, R. Zhao, T. Zhu and S. Rothstein, (2005) Genetic analysis of *Arabidopsis* GATA transcription factor gene family reveals a nitrate-inducible member important for chlorophyll synthesis and glucose sensitivity. Plant J 44**:** 680-692.

Biasini, M., S. Bienert, A. Waterhouse, K. Arnold, G. Studer, T. Schmidt, F. Kiefer, T. G. Cassarino, M. Bertoni, L. Bordoli *et al.*, (2014) SWISS-MODEL: modelling protein tertiary and quaternary structure using evolutionary information. Nucleic Acids Res 42**:** W252-258.

Bielska, E., M. Schuster, Y. Roger, A. Berepiki, D. M. Soanes, N. J. Talbot and G. Steinberg, (2014) Hook is an adapter that coordinates kinesin-3 and dynein cargo attachment on early endosomes. J Cell Biol 204**:** 989-1007.

Black, B. E., J. M. Holaska, F. Rastinejad and B. M. Paschal, (2001) DNA binding domains in diverse nuclear receptors function as nuclear export signals. Curr Biol 11**:** 1749-1758.

Blankenberg, D., A. Gordon, G. Von Kuster, N. Coraor, J. Taylor, A. Nekrutenko and The Galaxy Team, (2010a) Manipulation of FASTQ data with Galaxy. Bioinformatics 26**:** 1783-1785.

Blankenberg, D., G. Von Kuster, N. Coraor, G. Ananda, R. Lazarus, M. Mangan, A. Nekrutenko and J. Taylor, (2010b) Galaxy: a web-based genome analysis tool for experimentalists. Curr Protoc Mol Biol 89:19.10.1-19.10.21.

Blankenberg, D., G. Von Kuster, E. Bouvier, D. Baker, E. Afgan, N. Stoler, The Galaxy Team, J. Taylor and A. Nekrutenko, (2014) Dissemination of scientific software with Galaxy ToolShed. Genome Biol 15**:** 403.

Boeck, R., S. Tarun, Jr., M. Rieger, J. A. Deardorff, S. Muller-Auer and A. B. Sachs, (1996) The yeast Pan2 protein is required for poly(A)-binding protein-stimulated poly(A)-nuclease activity. J Biol Chem 271**:** 432-438.

Bok, J. W., Y. M. Chiang, E. Szewczyk, Y. Reyes-Dominguez, A. D. Davidson, J. F. Sanchez, H. C. Lo, K. Watanabe, J. Strauss, B. R. Oakley *et al.*, (2009) Chromatin-level regulation of biosynthetic gene clusters. Nat Chem Biol 5**:** 462-464.

Bolton, M. D., B. P. Thomma and B. D. Nelson, (2006) *Sclerotinia sclerotiorum* (Lib.) de Bary: biology and molecular traits of a cosmopolitan pathogen. Mol Plant Pathol 7**:** 1-16.

Borneman, A. R., M. J. Hynes and A. Andrianopoulos, (2001) An *STE12* homolog from the asexual, dimorphic fungus *Penicillium marneffei* complements the defect in sexual development of an *Aspergillus nidulans steA* mutant. Genetics 157**:** 1003-1014.

Bouhired, S., M. Weber, A. Kempf-Sontag, N. P. Keller and D. Hoffmeister, (2007) Accurate prediction of the *Aspergillus nidulans* terrequinone gene cluster boundaries using the transcriptional regulator LaeA. Fungal Genet Biol 44**:** 1134-1145.

Boyer, P. D., M. Deluca, K. E. Ebner, D. E. Hultquist and J. B. Peter, (1962) Identification of phosphohistidine in digests from a probable intermediate of oxidative phosphorylation. J Biol Chem 237**:** PC3306-PC3308.

Brakhage, A. A., and V. Schroeckh, (2011) Fungal secondary metabolites - strategies to activate silent gene clusters. Fungal Genet Biol 48**:** 15-22.

Bricmont, P. A., J. R. Daugherty and T. G. Cooper, (1991) The *DAL81* gene product is required for induced expression of two differently regulated nitrogen catabolic genes in *Saccharomyces cerevisiae*. Mol Cell Biol 11**:** 1161-1166.

Brisco, P. R., and G. B. Kohlhaw, (1990) Regulation of yeast *LEU2*. Total deletion of regulatory gene *LEU3* unmasks GCN4-dependent basal level expression of *LEU2*. J Biol Chem 265**:** 11667-11675.

Bromann, K., M. Toivari, K. Viljanen, A. Vuoristo, L. Ruohonen and T. Nakari-Setala, (2012) Identification and characterization of a novel diterpene gene cluster in *Aspergillus nidulans*. PLoS One 7**:** e35450.

Brown, C. E., S. Z. Tarun, Jr., R. Boeck and A. B. Sachs, (1996) *PAN3* encodes a subunit of the Pab1p-dependent poly(A) nuclease in *Saccharomyces cerevisiae*. Mol Cell Biol 16**:** 5744-5753.

Brown, S. J., P. J. Kellett and S. J. Lippard, (1993) Ixr1, a yeast protein that binds to platinated DNA and confers sensitivity to cisplatin. Science 261**:** 603-605.

Brownlee, A. G., and H. N. Arst, Jr., (1983) Nitrate uptake in *Aspergillus nidulans* and involvement of the third gene of the nitrate assimilation gene cluster. J Bacteriol 155**:** 1138-1146.

Burger, G., J. Strauss, C. Scazzocchio and B. F. Lang, (1991a) *nirA*, the pathway-specific regulatory gene of nitrate assimilation in *Aspergillus nidulans*, encodes a putative GAL4-type zinc finger protein and contains four introns in highly conserved regions. Mol Cell Biol 11**:** 5746-5755.

Burger, G., J. Tilburn and C. Scazzocchio, (1991b) Molecular cloning and functional characterization of the pathway-specific regulatory gene *nirA*, which controls nitrate assimilation in *Aspergillus nidulans*. Mol Cell Biol 11**:** 795-802.

Butler, J. S., (2002) The yin and yang of the exosome. Trends Cell Biol 12**:** 90-96.

Caddick, M., (2004) *Nitrogen Regulation in Mycelial Fungi*. R. Brambl, and G.A Marzluf (Eds.) The Mycota III Biochemistry and Molecular Biology, Springer-Verlag, Berlin Heidelberg, pp349-367.

Canovas, D., A. T. Marcos, A. Gacek, M. S. Ramos, G. Gutierrez, Y. Reyes-Dominguez and J. Strauss, (2014) The histone acetyltransferase GcnE (*GCN5*) plays a central role in the regulation of *Aspergillus* asexual development. Genetics 197**:** 1175-1189.

Cardillo, S. B., C. E. Levi, M. Bermudez Moretti and S. Correa Garcia, (2012) Interplay between the transcription factors acting on the GATA- and GABA-responsive elements of *Saccharomyces cerevisiae UGA* promoters. Microbiology 158**:** 925-935.

Carlson, J. M., A. Chakravarty, C. E. DeZiel and R. H. Gross, (2007) SCOPE: a web server for practical *de novo* motif discovery. Nucleic Acids Res 35**:** W259-264.

Carlson, M., (1997) Genetics of transcriptional regulation in yeast: connections to the RNA polymerase II CTD. Annu Rev Cell Dev Biol 13**:** 1-23.

Carvalho, J., P. G. Bertram, S. R. Wente and X. F. Zheng, (2001) Phosphorylation regulates the interaction between Gln3p and the nuclear import factor Srp1p. J Biol Chem 276**:** 25359-25365.

Carvalho, J., and X. F. Zheng, (2003) Domains of Gln3p interacting with karyopherins, Ure2p, and the target of rapamycin protein. J Biol Chem 278**:** 16878-16886.

Casalone, E., C. Barberio, D. Cavalieri and M. Polsinelli, (2000) Identification by functional analysis of the gene encoding α-isopropylmalate synthase II (*LEU9*) in *Saccharomyces cerevisiae*. Yeast 16**:** 539-545.

Cazelle, B., A. Pokorska, E. Hull, P. M. Green, G. Stanway and C. Scazzocchio, (1998) Sequence, exon-intron organization, transcription and mutational analysis of *prnA*, the gene encoding the transcriptional activator of the *prn* gene cluster in *Aspergillus nidulans*. Mol Microbiol 28**:** 355-370.

Cerqueira, G. C., M. B. Arnaud, D. O. Inglis, M. S. Skrzypek, G. Binkley, M. Simison, S. R. Miyasato, J. Binkley, J. Orvis, P. Shah *et al.*, (2014) The *Aspergillus* Genome Database: multispecies curation and incorporation of RNA-Seq data to improve structural gene annotations. Nucleic Acids Res 42**:** D705-710.

Chakravarty, A., J. M. Carlson, R. S. Khetani, C. E. DeZiel and R. H. Gross, (2007a) SPACER: identification of cis-regulatory elements with non-contiguous critical residues. Bioinformatics 23**:** 1029-1031.

Chakravarty, A., J. M. Carlson, R. S. Khetani and R. H. Gross, (2007b) A novel ensemble learning method for de novo computational identification of DNA binding sites. BMC Bioinformatics 8**:** 249.

Chandrasekaran, C., and E. Betrán, (2008) Origins of new genes and pseudogenes. Nature Education 1**:** 181.

Chang, L. F., T. S. Cunningham, P. R. Gatzek, W. J. Chen and G. B. Kohlhaw, (1984) Cloning and characterization of yeast Leu4, one of two genes responsible for α-isopropylmalate synthesis. Genetics 108**:** 91-106.

Chang, L. F., P. R. Gatzek and G. B. Kohlhaw, (1985) Total deletion of yeast *LEU4*: further evidence for a second α-isopropylmalate synthase and evidence for tight *LEU4-MET4* linkage. Gene 33**:** 333-339.

Charron, F., and M. Nemer, (1999) GATA transcription factors and cardiac development. Semin Cell Dev Biol 10**:** 85-91.

Chen, X. Q., X. Du, J. Liu, M. K. Balasubramanian and D. Balasundaram, (2004) Identification of genes encoding putative nucleoporins and transport factors in the fission yeast *Schizosaccharomyces pombe*: a deletion analysis. Yeast 21**:** 495-509.

Cherry, J. M., E. L. Hong, C. Amundsen, R. Balakrishnan, G. Binkley, E. T. Chan, K. R. Christie, M. C. Costanzo, S. S. Dwight, S. R. Engel *et al.*, (2012) *Saccharomyces* Genome Database: the genomics resource of budding yeast. Nucleic Acids Res 40**:** D700-705.

Chiang, Y. M., K. H. Lee, J. F. Sanchez, N. P. Keller and C. C. Wang, (2009a) Unlocking fungal cryptic natural products. Nat Prod Commun 4**:** 1505-1510.

Chiang, Y. M., E. Szewczyk, A. D. Davidson, N. Keller, B. R. Oakley and C. C. Wang, (2009b) A gene cluster containing two fungal polyketide synthases encodes the biosynthetic pathway for a polyketide, asperfuranone, in *Aspergillus nidulans*. J Am Chem Soc 131**:** 2965-2970.

Christensen, U., B. S. Gruben, S. Madrid, H. Mulder, I. Nikolaev and R. P. de Vries, (2011) Unique regulatory mechanism for D-galactose utilization in *Aspergillus nidulans*. Appl Environ Microbiol 77**:** 7084-7087.

Claros, M. G., and P. Vincens, (1996) Computational method to predict mitochondrially imported proteins and their yargeting sequences. European Journal of Biochemistry 241**:** 779-786.

Clutterbuck, A. J., (1973) Gene symbols in *Aspergillus nidulans*. Genet Res 21**:** 291-296.

Coffman, J.A., R. Rai, D.M. Loprete, T. Cunningham, V. Svetlov and T.G. Cooper (1997) Cross regulation of four GATA factors the control nitrogen catabolic gene expression in *Saccharomyces cerevisiae*. J Bacteriol 179: 3416-3429

Conlan, R. S., N. Gounalaki, P. Hatzis and D. Tzamarias, (1999) The Tup1-Cyc8 protein complex can shift from a transcriptional co-repressor to a transcriptional co-activator. J Biol Chem 274**:** 205-210.

Conlon, H., I. Zadra, H. Haas, H. N. Arst, Jr., M. G. Jones and M. X. Caddick, (2001) The *Aspergillus nidulans* GATA transcription factor gene *areB* encodes at least three proteins and features three classes of mutation. Mol Microbiol 40**:** 361-375.

Coradetti, S. T., J. P. Craig, Y. Xiong, T. Shock, C. Tian and N. L. Glass, (2012) Conserved and essential transcription factors for cellulase gene expression in ascomycete fungi. Proc Natl Acad Sci USA 109**:** 7397-7402.

Cove, D. J., (1966) The induction and repression of nitrate reductase in the fungus *Aspergillus nidulans*. Biochim Biophys Acta 113**:** 51-56.

Cove, D. J., (1976) Chlorate toxicity in *Aspergillus nidulans*: The selection and characterization of chlorate resistant mutants. Heredity 36: 191-203.

Cronshaw, J. M., A. N. Krutchinsky, W. Zhang, B. T. Chait and M. J. Matunis, (2002) Proteomic analysis of the mammalian nuclear pore complex. J Cell Biol 158**:** 915-927.

Crooks, G. E., G. Hon, J. M. Chandonia and S. E. Brenner, (2004) WebLogo: a sequence logo generator. Genome Res 14**:** 1188-1190.

Cubero, B., D. Gomez and C. Scazzocchio, (2000) Metabolite repression and inducer exclusion in the proline utilization gene cluster of *Aspergillus nidulans*. J Bacteriol 182**:** 233-235.

David, H., G. Hofmann, A. P. Oliveira, H. Jarmer and J. Nielsen, (2006) Metabolic network driven analysis of genome-wide transcription data from *Aspergillus nidulans*. Genome Biol 7**:** R108.

Davis, B. G., (2004) Biochemistry. Mimicking posttranslational modifications of proteins. Science 303**:** 480-482.

Davis, M. A., C. S. Cobbett and M. J. Hynes, (1988) An *amdS-lacZ* fusion for studying gene regulation in *Aspergillus*. Gene 63**:** 199-212.

Davis, M. A., A. J. Small, S. Kourambas and M. J. Hynes, (1996) The *tamA* gene of *Aspergillus nidulans* contains a putative zinc cluster motif which is not required for gene function. J Bacteriol 178**:** 3406-3409.

De Souza, C. P., A. H. Osmani, S. B. Hashmi and S. A. Osmani, (2004) Partial nuclear pore complex disassembly during closed mitosis in *Aspergillus nidulans*. Curr Biol 14**:** 1973-1984.

De Souza, C. P., S. B. Hashmi, K. P. Horn and S. A. Osmani, (2006) A point mutation in the *Aspergillus nidulans sonB*^{Nup98} nuclear pore complex gene causes conditional DNA damage sensitivity. Genetics 174**:** 1881-1893.

DePristo, M. A., E. Banks, R. Poplin, K. V. Garimella, J. R. Maguire, C. Hartl, A. A. Philippakis, G. del Angel, M. A. Rivas, M. Hanna *et al.*, (2011) A framework for variation discovery and genotyping using next-generation DNA sequencing data. Nat Genet 43**:** 491-498.

Diaz-Sanchez, V., J. Avalos and M. C. Limon, (2012) Identification and regulation of *fusA*, the polyketide synthase gene responsible for fusarin production in *Fusarium fujikuroi*. Appl Environ Microbiol 78**:** 7258-7266.

Dickinson, J. R., and V. Norte, (1993) A study of branched-chain amino acid aminotransferase and isolation of mutations affecting the catabolism of branched-chain amino acids in *Saccharomyces cerevisiae*. FEBS Lett 326**:** 29-32.

Divon, H. H., and R. Fluhr, (2007) Nutrition acquisition strategies during fungal infection of plants. FEMS Microbiol Lett 266**:** 65-74.

Do, E., G. Hu, M. Caza, D. Oliveira, J. W. Kronstad and W. H. Jung, (2015) Leu1 plays a role in iron metabolism and is required for virulence in *Cryptococcus neoformans*. Fungal Genet Biol 75**:** 11-19.

Downes, D. J., M. A. Davis, S. D. Kreutzberger, B. L. Taig and R. B. Todd, (2013) Regulation of the NADP-glutamate dehydrogenase gene *gdhA* in *Aspergillus nidulans* by the Zn(II)2Cys6 transcription factor LeuB. Microbiology 159**:** 2467-2480.

Downes, D. J., M. Chonofsky, K. Tan, B. T. Pfannenstiel, S. L. Reck-Peterson and R. B. Todd, (2014a) Characterization of the mutagenic spectrum of 4-nitroquinoline 1-oxide (4-NQO) in *Aspergillus nidulans* by whole genome sequencing. G3 (Bethesda) 4**:** 2483-2492.

Downes, D. J., M. A. Davis, K. H. Wong, S. D. Kreutzberger, M. J. Hynes and R. B. Todd, (2014b) Dual DNA binding and coactivator functions of *Aspergillus nidulans* TamA, a Zn(II)2Cys6 transcription factor. Mol Microbiol 92**:** 1198-1211.

Dowzer, C. E., and J. M. Kelly, (1991) Analysis of the *creA* gene, a regulator of carbon catabolite repression in *Aspergillus nidulans*. Mol Cell Biol 11**:** 5701-5709.

Drainas, C., and J. A. Pateman, (1977) L-Asparaginase activity in the fungus *Aspergillus nidulans*. Biochem Soc Trans 5**:** 259-261.

Dyer, P. S., and C. M. O'Gorman, (2012) Sexual development and cryptic sexuality in fungi: insights from *Aspergillus species*. FEMS Microbiol Rev 36**:** 165-192.

Dynan, W. S., and R. Tjian, (1985) Control of eukaryotic messenger RNA synthesis by sequence-specific DNA-binding proteins. Nature 316**:** 774-778.

Dzikowska, A., M. Kacprzak, R. Tomecki, M. Koper, C. Scazzocchio and P. Weglenski, (2003) Specific induction and carbon/nitrogen repression of arginine catabolism gene of *Aspergillus nidulans* – functional *in vivo* analysis of the *otaA* promoter. Fungal Genet Biol 38**:** 175-186.

Eden, A., G. Simchen and N. Benvenisty, (1996) Two yeast homologs of *ECA39*, a target for c-Myc regulation, code for cytosolic and mitochondrial branched-chain amino acid aminotransferases. J Biol Chem 271**:** 20242-20245.

Eden, A., and N. Benvenisty, (1998) Characterization of a branched-chain amino-acid aminotransferase from *Schizosaccharomyces pombe*. Yeast 14**:** 189-194.

ElBerry, H. M., M. L. Majumdar, T. S. Cunningham, R. A. Sumrada and T. G. Cooper, (1993) Regulation of the urea active transporter gene (*DUR3*) in *Saccharomyces cerevisiae*. J Bacteriol 175**:** 4688-4698.

Elble, R., and B. K. Tye, (1991) Both activation and repression of a-mating-type-specific genes in yeast require transcription factor Mcm1. Proc Natl Acad Sci USA 88**:** 10966-10970.

Emanuelsson, O., H. Nielsen, S. Brunak and G. von Heijne, (2000) Predicting subcellular localization of proteins based on their N-terminal amino acid sequence. J Mol Biol 300**:** 1005-1016.

Empel, J., I. Sitkiewicz, A. Andrukiewicz, K. Lasocki, P. Borsuk and P. Weglenski, (2001) *arcA*, the regulatory gene for the arginine catabolic pathway in *Aspergillus nidulans*. Mol Genet Genomics 266**:** 591-597.

Engelsma, D., J. A. Rodriguez, A. Fish, G. Giaccone and M. Fornerod, (2007) Homodimerization antagonizes nuclear export of survivin. Traffic 8**:** 1495-1502.

Felenbok, B., D. Sequeval, M. Mathieu, S. Sibley, D. I. Gwynne and R. W. Davies, (1988) The ethanol regulon in *Aspergillus nidulans*: characterization and sequence of the positive regulatory gene *alcR*. Gene 73**:** 385-396.

Feng, B., and G. A. Marzluf, (1998) Interaction between major nitrogen regulatory protein NIT2 and pathway-specific regulatory factor NIT4 is required for their synergistic activation of gene expression in *Neurospora crassa*. Mol Cell Biol 18**:** 3983-3990.

Feng, G. H., and T. J. Leonard, (1998) Culture conditions control expression of the genes for aflatoxin and sterigmatocystin biosynthesis in *Aspergillus parasiticus* and *A. nidulans*. Appl Environ Microbiol 64**:** 2275-2277.

Fidel, S., J. H. Doonan and N. R. Morris, (1988) *Aspergillus nidulans* contains a single actin gene which has unique intron locations and encodes a gamma-actin. Gene 70**:** 283-293.

Finn, R. D., A. Bateman, J. Clements, P. Coggill, R. Y. Eberhardt, S. R. Eddy, A. Heger, K. Hetherington, L. Holm, J. Mistry *et al.*, (2014) Pfam: the protein families database. Nucleic Acids Res 42**:** D222-230.

Fischer, U., J. Huber, W. C. Boelens, I. W. Mattaj and R. Luhrmann, (1995) The HIV-1 Rev activation domain is a nuclear export signal that accesses an export pathway used by specific cellular RNAs. Cell 82**:** 475-483.

Fisher, M. C., D. A. Henk, C. J. Briggs, J. S. Brownstein, L. C. Madoff, S. L. McCraw and S. J. Gurr, (2012) Emerging fungal threats to animal, plant and ecosystem health. Nature 484**:** 186-194.

Fleming, A., (1929) On the antibacterial action of cultures of a *Penicillium*, with special reference to their use in the isolation of *B. influenzæ*. Br J Exp Pathol 10**:** 226-236.

Floer, M., and G. Blobel, (1999) Putative reaction intermediates in Crm1-mediated nuclear protein export. J Biol Chem 274**:** 16279-16286.

Fornerod, M., M. Ohno, M. Yoshida and I. W. Mattaj, (1997a) CRM1 is an export receptor for leucine-rich nuclear export signals. Cell 90**:** 1051-1060.

Fornerod, M., J. van Deursen, S. van Baal, A. Reynolds, D. Davis, K. G. Murti, J. Fransen and G. Grosveld, (1997b) The human homologue of yeast CRM1 is in a dynamic subcomplex with CAN/Nup214 and a novel nuclear pore component Nup88. EMBO J 16**:** 807-816.

Fraser, J. A., M. A. Davis and M. J. Hynes, (2001) The formamidase gene of *Aspergillus nidulans*: regulation by nitrogen metabolite repression and transcriptional interference by an overlapping upstream gene. Genetics 157**:** 119-131.

Friden, P., and P. Schimmel, (1988) *LEU3* of *Saccharomyces cerevisiae* activates multiple genes for branched-chain amino acid biosynthesis by binding to a common decanucleotide core sequence. Mol Cell Biol 8**:** 2690-2697.

Froeliger, E. H., and B. E. Carpenter, (1996) *NUT1*, a major nitrogen regulatory gene in *Magnaporthe grisea*, is dispensable for pathogenicity. Mol Gen Genet 251**:** 647-656.

Fu, S. C., K. Imai and P. Horton, (2011) Prediction of leucine-rich nuclear export signal containing proteins with NESsential. Nucleic Acids Res 39**:** e111.

Fu, S. C., H. C. Huang, P. Horton and H. F. Juan, (2013) ValidNESs: a database of validated leucine-rich nuclear export signals. Nucleic Acids Res 41**:** D338-343.

Fu, Y. H., J. L. Young and G. A. Marzluf, (1988) Molecular cloning and characterization of a negative-acting nitrogen regulatory gene of *Neurospora crassa*. Mol Gen Genet 214**:** 74-79.

Fu, Y. H., and G. A. Marzluf, (1990) *nit-2*, the major nitrogen regulatory gene of *Neurospora crassa*, encodes a protein with a putative zinc finger DNA-binding domain. Mol Cell Biol 10**:** 1056-1065.

Fukasawa, M., Q. Ge, R. M. Wynn, S. Ishii and K. Uyeda, (2010) Coordinate regulation/localization of the carbohydrate responsive binding protein (ChREBP) by two nuclear export signal sites: discovery of a new leucine-rich nuclear export signal site. Biochem Biophys Res Commun 391**:** 1166-1169.

Fukuchi, T., J. Nikawa, N. Kimura and K. Watanabe, (1993) Isolation, overexpression and disruption of a *Saccharomyces cerevisiae YNK* gene encoding nucleoside diphosphate kinase. Gene 129**:** 141-146.

Fukuda, M., S. Asano, T. Nakamura, M. Adachi, M. Yoshida, M. Yanagida and E. Nishida, (1997) CRM1 is responsible for intracellular transport mediated by the nuclear export signal. Nature 390**:** 308-311.

Fung, H. Y., and Y. M. Chook, (2014) Atomic basis of CRM1-cargo recognition, release and inhibition. Semin Cancer Biol 27**:** 52-61.

Funke, T., H. Han, M. L. Healy-Fried, M. Fischer and E. Schönbrunn, (2006) Molecular basis for the herbicide resistance of Roundup Ready crops. Proc Natl Acad Sci USA 103**:** 13010-13015.

Furey, T. S., (2012) ChIP-seq and beyond: new and improved methodologies to detect and characterize protein-DNA interactions. Nat Rev Genet 13**:** 840-852.

Gacek, A., and J. Strauss, (2012) The chromatin code of fungal secondary metabolite gene clusters. Appl Microbiol Biotechnol 95**:** 1389-1404.

Galagan, J. E., S. E. Calvo, C. Cuomo, L.-J. Ma, J. R. Wortman, S. Batzoglou, S.-I. Lee, M. Basturkmen, C. C. Spevak, J. Clutterbuck *et al.*, (2005a) Sequencing of *Aspergillus nidulans* and comparative analysis with *A. fumigatus* and *A. oryzae*. Nature 438**:** 1105-1115.

Galagan, J. E., M. R. Henn, L. J. Ma, C. A. Cuomo and B. Birren, (2005b) Genomics of the fungal kingdom: insights into eukaryotic biology. Genome Res 15**:** 1620-1631.

Galy, V., I. W. Mattaj and P. Askjaer, (2003) *Caenorhabditis elegans* nucleoporins Nup93 and Nup205 determine the limit of nuclear pore complex size exclusion *in vivo*. Mol Biol Cell 14**:** 5104-5115.

Gamsjaeger, R., C. K. Liew, F. E. Loughlin, M. Crossley and J. P. Mackay, (2007) Sticky fingers: zinc-fingers as protein-recognition motifs. Trends Biochem Sci 32**:** 63-70.

Garcia, I., R. Gonzalez, D. Gomez and C. Scazzocchio, (2004) Chromatin rearrangements in the *prnD-prnB* bidirectional promoter: dependence on transcription factors. Eukaryot Cell 3**:** 144-156.

Gardner, K. H., T. Pan, S. Narula, E. Rivera and J. E. Coleman, (1991) Structure of the binuclear metal-binding site in the GAL4 transcription factor. Biochemistry 30**:** 11292-11302.

Garrett, R. H., and D. J. Cove, (1976) Formation of NADPH-nitrate reductase activity in vitro from *Aspergillus nidulans niaD* and *cnx* mutants. Mol Gen Genet 149**:** 179-186.

Garrison, E., and G. Marth, (2012) Haplotype-based variant detection from short-read sequencing. Http://Arxiv.Org/Abs/1207.3907.

Gaubatz, S., J. A. Lees, G. J. Lindeman and D. M. Livingston, (2001) E2F4 is exported from the nucleus in a CRM1-dependent manner. Mol Cell Biol 21**:** 1384-1392.

Georgianna, D. R., and G. A. Payne, (2009) Genetic regulation of aflatoxin biosynthesis: from gene to genome. Fungal Genet Biol 46**:** 113-125.

Gerke, J., O. Bayram, K. Feussner, M. Landesfeind, E. Shelest, I. Feussner and G. H. Braus, (2012) Breaking the silence: protein stabilization uncovers silenced biosynthetic gene clusters in the fungus *Aspergillus nidulans.* Appl Environ Microbiol 78**:** 8234-8244.

Giardine, B., C. Riemer, R. C. Hardison, R. Burhans, L. Elnitski, P. Shah, Y. Zhang, D. Blankenberg, I. Albert, J. Taylor *et al.*, (2005) Galaxy: a platform for interactive large-scale genome analysis. Genome Res 15**:** 1451-1455.

Goecks, J., A. Nekrutenko, J. Taylor and The Galaxy Team, (2010) Galaxy: a comprehensive approach for supporting accessible, reproducible, and transparent computational research in the life sciences. Genome Biol 11**:** R86.

Goff, L., C. Trapnell and D. Kelley, (2013) cummeRbund: Analysis, exploration, manipulation, and visualization of Cufflinks high-throughput sequencing data. R package version 2.8.2.

Gomez, D., I. Garcia, C. Scazzocchio and B. Cubero, (2003) Multiple GATA sites: protein binding and physiological relevance for the regulation of the proline transporter gene of *Aspergillus nidulans*. Mol Microbiol 50**:** 277-289.

Gonzalez-Mariscal, L., A. Ponce, L. Alarcon and B. E. Jaramillo, (2006) The tight junction protein ZO-2 has several functional nuclear export signals. Exp Cell Res 312**:** 3323-3335.

Gough, J. A., and N. E. Murray, (1983) Sequence diversity among related genes for recognition of specific targets in DNA molecules. J Mol Biol 166**:** 1-19.

Grundlinger, M., S. Yasmin, B. E. Lechner, S. Geley, M. Schrettl, M. Hynes and H. Haas, (2013) Fungal siderophore biosynthesis is partially localized in peroxisomes. Mol Microbiol 88**:** 862-875.

Guex, N., M. C. Peitsch and T. Schwede, (2009) Automated comparative protein structure modeling with SWISS-MODEL and Swiss-PdbViewer: A historical perspective. ELECTROPHORESIS 30**:** S162-S173.

Guglielmi, B., N. L. van Berkum, B. Klapholz, T. Bijma, M. Boube, C. Boschiero, H. M. Bourbon, F. C. Holstege and M. Werner, (2004) A high resolution protein interaction map of the yeast Mediator complex. Nucleic Acids Res 32**:** 5379-5391.

Guttler, T., T. Madl, P. Neumann, D. Deichsel, L. Corsini, T. Monecke, R. Ficner, M. Sattler and D. Gorlich, (2010) NES consensus redefined by structures of PKI-type and Rev-type nuclear export signals bound to CRM1. Nat Struct Mol Biol 17**:** 1367-1376.

Haas, H., and G. A. Marzluf, (1995) NRE, the major nitrogen regulatory protein of *Penicillium chrysogenum*, binds specifically to elements in the intergenic promoter regions of nitrate assimilation and penicillin biosynthetic gene clusters. Curr Genet 28**:** 177-183.

Haas, H., I. Zadra, G. Stoffler and K. Angermayr, (1999) The *Aspergillus nidulans* GATA factor SreA is involved in regulation of siderophore biosynthesis and control of iron uptake. J Biol Chem 274**:** 4613-4619.

Han, K. H., K. Y. Han, J. H. Yu, K. S. Chae, K. Y. Jahng and D. M. Han, (2001a) The *nsdD* gene encodes a putative GATA-type transcription factor necessary for sexual development of *Aspergillus nidulans*. Mol Microbiol 41**:** 299-309.

Han, S. J., J. S. Lee, J. S. Kang and Y. J. Kim, (2001b) Med9/Cse2 and Gal11 modules are required for transcriptional repression of distinct group of genes. J Biol Chem 276**:** 37020-37026.

Heck, I. S., J. D. Schrag, J. Sloan, L. J. Millar, G. Kanan, J. R. Kinghorn and S. E. Unkles, (2002) Mutational analysis of the gephyrin-related molybdenum cofactor biosynthetic gene *cnxE* from the lower eukaryote *Aspergillus nidulans*. Genetics 161**:** 623-632.

Hellauer, K., M. H. Rochon and B. Turcotte, (1996) A novel DNA binding motif for yeast zinc cluster proteins: the Leu3p and Pdr3p transcriptional activators recognize everted repeats. Mol Cell Biol 16**:** 6096-6102.

Henderson, B. R., and A. Eleftheriou, (2000) A comparison of the activity, sequence specificity, and CRM1-dependence of different nuclear export signals. Exp Cell Res 256**:** 213-224.

Hidalgo, P., A. Z. Ansari, P. Schmidt, B. Hare, N. Simkovich, S. Farrell, E. J. Shin, M. Ptashne and G. Wagner, (2001) Recruitment of the transcriptional machinery through GAL11P: structure and interactions of the GAL4 dimerization domain. Genes Dev 15**:** 1007-1020.

Hinnebusch, A. G., and K. Natarajan, (2002) Gcn4p, a master regulator of gene expression, is controlled at multiple levels by diverse signals of starvation and stress. Eukaryot Cell 1**:** 22-32.

Hodge, C. A., H. V. Colot, P. Stafford and C. N. Cole, (1999) Rat8p/Dbp5p is a shuttling transport factor that interacts with Rat7p/Nup159p and Gle1p and suppresses the mRNA export defect of *xpo1-1* cells. EMBO J 18**:** 5778-5788.

Horst, R. J., C. Zeh, A. Saur, S. Sonnewald, U. Sonnewald and L. M. Voll, (2012) The *Ustilago maydis* Nit2 homolog regulates nitrogen utilization and is required for efficient induction of filamentous growth. Eukaryot Cell 11**:** 368-380.

Horton, P., K. J. Park, T. Obayashi, N. Fujita, H. Harada, C. J. Adams-Collier and K. Nakai, (2007) WoLF PSORT: protein localization predictor. Nucleic Acids Res 35**:** W585-587.

Hortschansky, P., M. Eisendle, Q. Al-Abdallah, A. D. Schmidt, S. Bergmann, M. Thon, O. Kniemeyer, B. Abt, B. Seeber, E. R. Werner *et al.*, (2007) Interaction of HapX with the CCAAT-binding complex--a novel mechanism of gene regulation by iron. EMBO J 26**:** 3157-3168.

Hu, Y., T. G. Cooper and G. B. Kohlhaw, (1995) The *Saccharomyces cerevisiae* Leu3 protein activates expression of *GDH1*, a key gene in nitrogen assimilation. Mol Cell Biol 15**:** 52-57.

Hull, E. P., P. M. Green, H. N. Arst, Jr. and C. Scazzocchio, (1989) Cloning and physical characterization of the L-proline catabolism gene cluster of *Aspergillus nidulans*. Mol Microbiol 3**:** 553-559.

Hunter, C. C., K. S. Siebert, D. J. Downes, K. H. Wong, S. D. Kreutzberger, J. A. Fraser, D. F. Clarke, M. J. Hynes, M. A. Davis and R. B. Todd, (2014) Multiple nuclear localization signals mediate nuclear localization of the GATA transcription factor AreA. Eukaryot Cell 13**:** 527-538.

Hynes, M. J., (1975) Studies on the role of the *areA* gene in the regulation of nitrogen catabolism in *Aspergillus nidulans*. Aust J Biol Sci 28**:** 301-313.

Hynes, M. J., and J. M. Kelly, (1977) Pleiotropic mutants of *Aspergillus nidulans* altered in carbon metabolism. Mol Gen Genet 150**:** 193-204.

Hynes, M. J., (1980) A mutation, adjacent to gene *amdS*, defining the site of action of positive-control gene *amdR* in *Aspergillus nidulans*. J Bacteriol 142**:** 400-406.

Hynes, M.J., O.W. Draht and M.A. Davis (2002) Regulation of the *acuF* gene, encoding phosphoenolpyruvate carboxykinase in the filamentous fungus *Aspergillus nidulans*. J Bacteriol 184: 183-190.

Hynes, M. J., S. L. Murray, A. Duncan, G. S. Khew and M. A. Davis, (2006) Regulatory genes controlling fatty acid catabolism and peroxisomal functions in the filamentous fungus *Aspergillus nidulans*. Eukaryot Cell 5**:** 794-805.

Hynes, M. J., E. Szewczyk, S. L. Murray, Y. Suzuki, M. A. Davis and H. M. Sealy-Lewis, (2007) Transcriptional control of gluconeogenesis in *Aspergillus nidulans*. Genetics 176**:** 139-150.

Inglis, D. O., J. Binkley, M. S. Skrzypek, M. B. Arnaud, G. C. Cerqueira, P. Shah, F. Wymore, J. R. Wortman and G. Sherlock, (2013) Comprehensive annotation of secondary metabolite biosynthetic genes and gene clusters of *Aspergillus nidulans*, *A. fumigatus*, *A. niger* and *A. oryzae*. BMC Microbiol 13**:** 91.

Izumiya, H., and M. Yamamoto, (1995) Cloning and functional analysis of the *ndk1* gene encoding nucleoside-diphosphate kinase in *Schizosaccharomyces pombe*. J Biol Chem 270**:** 27859-27864.

Janner, F., F. Flury and U. Leupold, (1979) Reversion of nonsense mutants induced by 4-nitroquinoline-1-oxide in *Schizosaccharomyces pombe*. Mutat Res 63**:** 11-19.

Jaramillo, B. E., A. Ponce, J. Moreno, A. Betanzos, M. Huerta, E. Lopez-Bayghen and L. Gonzalez-Mariscal, (2004) Characterization of the tight junction protein ZO-2 localized at the nucleus of epithelial cells. Exp Cell Res 297**:** 247-258.

Jedidi, I., F. Zhang, H. Qiu, S. J. Stahl, I. Palmer, J. D. Kaufman, P. S. Nadaud, S. Mukherjee, P. T. Wingfield, C. P. Jaroniec *et al.*, (2010) Activator Gcn4 employs multiple segments of Med15/Gal11, including the KIX domain, to recruit mediator to target genes in vivo. J Biol Chem 285**:** 2438-2455.

Jensen, T. H., M. Neville, J. C. Rain, T. McCarthy, P. Legrain and M. Rosbash, (2000) Identification of novel *Saccharomyces cerevisiae* proteins with nuclear export activity: cell cycle-regulated transcription factor Ace2p shows cell cycle-independent nucleocytoplasmic shuttling. Mol Cell Biol 20**:** 8047-8058.

Johnson, P., C. I. Harris and S. V. Perry, (1967) 3-methylhistidine in actin and other muscle proteins. Biochem J 105**:** 361-370.

Johnston, M., and J. Dover, (1987) Mutations that inactivate a yeast transcriptional regulatory protein cluster in an evolutionarily conserved DNA binding domain. Proc Natl Acad Sci USA 84**:** 2401-2405.

Johnstone, I. L., P. C. McCabe, P. Greaves, S. J. Gurr, G. E. Cole, M. A. Brow, S. E. Unkles, A. J. Clutterbuck, J. R. Kinghorn and M. A. Innis, (1990) Isolation and characterisation of the *crnA-niiA-niaD* gene cluster for nitrate assimilation in *Aspergillus nidulans*. Gene 90**:** 181-192.

Jones, S. A., H. N. Arst, Jr. and D. W. Macdonald, (1981) Gene roles in the *prn* cluster of *Aspergillus nidulans*. Curr Genet 3**:** 49-56.

Kaessmann, H., (2010) Origins, evolution, and phenotypic impact of new genes. Genome Res 20**:** 1313-1326.

Kafer, E., (1965) Origins of translocations in *Aspergillus nidulans*. Genetics 52**:** 217-232.

Kageyama, R., T. Ohtsuka and T. Kobayashi, (2007) The Hes gene family: repressors and oscillators that orchestrate embryogenesis. Development 134**:** 1243-1251.

Kassouf, M. T., H. Chagraoui, P. Vyas and C. Porcher, (2008) Differential use of SCL/TAL-1 DNA-binding domain in developmental hematopoiesis. Blood 112**:** 1056-1067.

Kassouf, M. T., J. R. Hughes, S. Taylor, S. J. McGowan, S. Soneji, A. L. Green, P. Vyas and C. Porcher, (2010) Genome-wide identification of TAL1's functional targets: insights into its mechanisms of action in primary erythroid cells. Genome Res 20**:** 1064-1083.

Katz, M. E., and M. J. Hynes, (1989) Isolation and analysis of the acetate regulatory gene, *facB*, from *Aspergillus nidulans*. Mol Cell Biol 9**:** 5696-5701.

Ke, Y., X. Wang, M. Feng, C. Wei, Z. Jiang, L. Jin and D. Lu, (2002) Analysis of mutation sites of BRCA1 gene in Chinese patients with breast cancer. Zhonghua Yi Xue Yi Chuan Xue Za Zhi 19**:** 383-385.

Kee, J. M., and T. W. Muir, (2012) Chasing phosphohistidine, an elusive sibling in the phosphoamino acid family. ACS Chem Biol 7**:** 44-51.

Keller, N. P., G. Turner and J. W. Bennett, (2005) Fungal secondary metabolism - from biochemistry to genomics. Nat Rev Microbiol 3**:** 937-947.

Kelly, D. E., N. Krasevec, J. Mullins and D. R. Nelson, (2009) The CYPome (Cytochrome P450 complement) of *Aspergillus nidulans*. Fungal Genet Biol 46 Suppl 1**:** S53-61.

Kerppola, T. K., and T. Curran, (1991) DNA bending by Fos and Jun: the flexible hinge model. Science 254**:** 1210-1214.

Kidder, B. L., G. Hu and K. Zhao, (2011) ChIP-Seq: technical considerations for obtaining high-quality data. Nat Immunol 12**:** 918-922.

Kiefer, F., K. Arnold, M. Künzli, L. Bordoli and T. Schwede, (2009) The SWISS-MODEL Repository and associated resources. Nucleic Acids Res 37**:** D387-D392.

Kim, D., G. Pertea, C. Trapnell, H. Pimentel, R. Kelley and S. L. Salzberg, (2013) TopHat2: accurate alignment of transcriptomes in the presence of insertions, deletions and gene fusions. Genome Biol 14**:** R36.

Kim, H., K. Han, K. Kim, D. Han, K. Jahng and K. Chae, (2002) The *veA* gene activates sexual development in *Aspergillus nidulans*. Fungal Genet Biol 37**:** 72-80.

Kim, H., and C. P. Woloshuk, (2008) Role of AREA, a regulator of nitrogen metabolism, during colonization of maize kernels and fumonisin biosynthesis in *Fusarium verticillioides*. Fungal Genet Biol 45**:** 947-953.

Kinghorn, J. R., and J. A. Pateman, (1973) NAD and NADP L-glutamate dehydrogenase activity and ammonium regulation in *Aspergillus nidulans*. J Gen Microbiol 78**:** 39-46.

Kinghorn, J. R., and J. A. Pateman, (1975a) Studies of partially repressed mutants at the *tamA* and *areA* loci in *Aspergillus nidulans*. Mol Gen Genet 140**:** 137-147.

Kinghorn, J. R., and J. A. Pateman, (1975b) The structural gene for NADP L-glutamate dehydrogenase in *Aspergillus nidulans*. J Gen Microbiol 86**:** 294-300.

Kingsbury, J. M., Z. Yang, T. M. Ganous, G. M. Cox and J. H. McCusker, (2004) Novel chimeric spermidine synthase-saccharopine dehydrogenase gene (SPE3-LYS9) in the human pathogen *Cryptococcus neoformans*. Eukaryot Cell 3**:** 752-763.

Kingsbury, J. M., and J. H. McCusker, (2010) Cytocidal amino acid starvation of *Saccharomyces cerevisiae* and *Candida albicans* acetolactate synthase (*ilv2*Δ) mutants is influenced by the carbon source and rapamycin. Microbiology 156**:** 929-939.

Kispal, G., H. Steiner, D. A. Court, B. Rolinski and R. Lill, (1996) Mitochondrial and cytosolic branched-chain amino acid transaminases from yeast, homologs of the *myc* oncogene-regulated Eca39 protein. J Biol Chem 271**:** 24458-24464.

Kohlhaw, G. B., (2003) Leucine biosynthesis in fungi: entering metabolism through the back door. Microbiol Mol Biol Rev 67**:** 1-15, table of contents.

Kolar, M., K. Holzmann, G. Weber, E. Leitner and H. Schwab, (1991) Molecular characterization and functional analysis in *Aspergillus nidulans* of the 5'-region of the *Penicillium chrysogenum* isopenicillin N synthetase gene. J Biotechnol 17**:** 67-80.

Kosman, D. J., (2003) Molecular mechanisms of iron uptake in fungi. Mol Microbiol 47**:** 1185-1197.

Kosugi, S., M. Hasebe, M. Tomita and H. Yanagawa, (2008) Nuclear export signal consensus sequences defined using a localization-based yeast selection system. Traffic 9**:** 2053-2062.

Kotaka, M., C. Johnson, H. K. Lamb, A. R. Hawkins, J. Ren and D. K. Stammers, (2008) Structural analysis of the recognition of the negative regulator NmrA and DNA by the zinc finger from the GATA-type transcription factor AreA. J Mol Biol 381**:** 373-382.

Krol, K., I. Y. Morozov, M. G. Jones, T. Wyszomirski, P. Weglenski, A. Dzikowska and M. X. Caddick, (2013) RrmA regulates the stability of specific transcripts in response to both nitrogen source and oxidative stress. Mol Microbiol 89**:** 975-988.

Kudla, B., M. X. Caddick, T. Langdon, N. M. Martinez-Rossi, C. F. Bennett, S. Sibley, R. W. Davies and H. N. Arst, Jr., (1990) The regulatory gene *areA* mediating nitrogen metabolite repression in *Aspergillus nidulans*. Mutations affecting specificity of gene activation alter a loop residue of a putative zinc finger. EMBO J 9**:** 1355-1364.

Kudo, N., N. Matsumori, H. Taoka, D. Fujiwara, E. P. Schreiner, B. Wolff, M. Yoshida and S. Horinouchi, (1999) Leptomycin B inactivates CRM1/exportin 1 by covalent modification at a cysteine residue in the central conserved region. Proc Natl Acad Sci USA 96**:** 9112-9117.

la Cour, T., L. Kiemer, A. Molgaard, R. Gupta, K. Skriver and S. Brunak, (2004) Analysis and prediction of leucine-rich nuclear export signals. Protein Eng Des Sel 17**:** 527-536.

Lamb, H. K., K. Leslie, A. L. Dodds, M. Nutley, A. Cooper, C. Johnson, P. Thompson, D. K. Stammers and A. R. Hawkins, (2003) The negative transcriptional regulator NmrA discriminates between oxidized and reduced dinucleotides. J Biol Chem 278**:** 32107-32114.

Lamb, H. K., J. Ren, A. Park, C. Johnson, K. Leslie, S. Cocklin, P. Thompson, C. Mee, A. Cooper, D. K. Stammers *et al.*, (2004) Modulation of the ligand binding properties of the transcription repressor NmrA by GATA-containing DNA and site-directed mutagenesis. Protein Sci 13**:** 3127-3138.

Langdon, T., A. Sheerins, A. Ravagnani, M. Gielkens, M. X. Caddick and H. N. Arst, Jr., (1995) Mutational analysis reveals dispensability of the N-terminal region of the *Aspergillus* transcription factor mediating nitrogen metabolite repression. Mol Microbiol 17**:** 877-888.

Larkin, M. A., G. Blackshields, N. P. Brown, R. Chenna, P. A. McGettigan, H. McWilliam, F. Valentin, I. M. Wallace, A. Wilm, R. Lopez *et al.*, (2007) Clustal W and Clustal X version 2.0. Bioinformatics 23**:** 2947-2948.

Larson, J. R., E. M. Facemyer, K. F. Shen, L. Ukil and S. A. Osmani, (2014) Insights into dynamic mitotic chromatin organization through the NIMA kinase suppressor SonC, a chromatin-associated protein involved in the DNA damage response. Genetics 196**:** 177-195.

Lee, B., Y. Yoshida and K. Hasunuma, (2006) Photomorphogenetic characteristics are severely affected in nucleoside diphosphate kinase-1 (*ndk-1*)-disrupted mutants in *Neurospora crassa*. Mol Genet Genomics 275**:** 9-17.

Lee, B. Y., S. Y. Han, H. G. Choi, J. H. Kim, K. H. Han and D. M. Han, (2005) Screening of growth- or development-related genes by using genomic library with inducible promoter in *Aspergillus nidulans*. J Microbiol 43**:** 523-528.

Lee, J. I., Y. M. Yu, Y. M. Rho, B. C. Park, J. H. Choi, H. M. Park and P. J. Maeng, (2005) Differential expression of the *chsE* gene encoding a chitin synthase of *Aspergillus nidulans* in response to developmental status and growth conditions. FEMS Microbiol Lett 249**:** 121-129.

Lee, K. K., T. Ohyama, N. Yajima, S. Tsubuki and S. Yonehara, (2001) MST, a physiological caspase substrate, highly sensitizes apoptosis both upstream and downstream of caspase activation. J Biol Chem 276**:** 19276-19285.

Lee, S. B., and J. W. Taylor, (1990) Isolation of DNA from fungal mycelia and single spores., pp. 282-287 in *PCR protocols: a guide to methods and applications.*, edited by M. A. Innis, J. J. Gelfand, J. J. Sninsky and T. J. White. Academic Press, San Diego, USA.

Li, H., and R. Durbin, (2009) Fast and accurate short read alignment with Burrows-Wheeler transform. Bioinformatics 25**:** 1754-1760.

Li, H., B. Handsaker, A. Wysoker, T. Fennell, J. Ruan, N. Homer, G. Marth, G. Abecasis, R. Durbin and S. Genome Project Data Processing, (2009) The Sequence Alignment/Map format and SAMtools. Bioinformatics 25**:** 2078-2079.

Li, W., M. R. Jain, C. Chen, X. Yue, V. Hebbar, R. Zhou and A. N. Kong, (2005) Nrf2 Possesses a redox-insensitive nuclear export signal overlapping with the leucine zipper motif. J Biol Chem 280**:** 28430-28438.

Li, W., S. W. Yu and A. N. Kong, (2006) Nrf2 possesses a redox-sensitive nuclear exporting signal in the Neh5 transactivation domain. J Biol Chem 281**:** 27251-27263.

Lin, H., L. Li, X. Jia, D. M. Ward and J. Kaplan, (2011) Genetic and biochemical analysis of high iron toxicity in yeast: iron toxicity is due to the accumulation of cytosolic iron and occurs under both aerobic and anaerobic conditions. J Biol Chem 286**:** 3851-3862.

Lin, X., C. Momany and M. Momany, (2003) SwoHp, a nucleoside diphosphate kinase, is essential in *Aspergillus nidulans*. Eukaryot Cell 2**:** 1169-1177.

Liu, X., C-K. Lee, J.A. Granek, N.D. Clarke and J.D. Lieb, (2006) Whole-genome comparison of Leu3 binding *in vitro* and *in vivo* reveals the importance of nucleosome occupancy in target site selection. Genome Res 16: 1517-1528.

Liu, Q., J. Yu, X. Zhuo, Q. Jiang and C. Zhang, (2010) Pericentrin contains five NESs and an NLS essential for its nucleocytoplasmic trafficking during the cell cycle. Cell Res 20**:** 948-962.

Lowry, J. A., and W. R. Atchley, (2000) Molecular evolution of the GATA family of transcription factors: conservation within the DNA-binding domain. J Mol Evol 50**:** 103-115.

MacCabe, A. P., M. B. Riach, S. E. Unkles and J. R. Kinghorn, (1990) The *Aspergillus nidulans npeA* locus consists of three contiguous genes required for penicillin biosynthesis. EMBO J 9**:** 279-287.

MacCabe, A. P., H. van Liempt, H. Palissa, S. E. Unkles, M. B. Riach, E. Pfeifer, H. von Dohren and J. R. Kinghorn, (1991) Delta-(L-alpha-aminoadipyl)-L-cysteinyl-D-valine synthetase from *Aspergillus nidulans*. Molecular characterization of the *acvA* gene encoding the first enzyme of the penicillin biosynthetic pathway. J Biol Chem 266**:** 12646-12654.

MacDonald, D. W., H. N. Arst, Jr. and D. J. Cove, (1974) The threonine dehydratase structural gene in *Aspergillus nidulans*. Biochim Biophys Acta 362**:** 60-65.

Macheda, M. L., M. J. Hynes and M. A. Davis, (1999) The *Aspergillus nidulans gltA* gene encoding glutamate synthase is required for ammonium assimilation in the absence of NADP-glutamate dehydrogenase. Curr Genet 34**:** 467-471.

Mackay, E. M., and J. A. Pateman, (1982) The regulation of urease activity in *Aspergillus nidulans*. Biochem Genet 20**:** 763-776.

MacPherson, S., M. Larochelle and B. Turcotte, (2006) A fungal family of transcriptional regulators: the zinc cluster proteins. Microbiol Mol Biol Rev 70**:** 583-604.

Maiuri, T., T. Woloshansky, J. Xia and R. Truant, (2013) The huntingtin N17 domain is a multifunctional CRM1 and Ran-dependent nuclear and cilial export signal. Hum Mol Genet 22**:** 1383-1394.

Makita, T., Y. Katsuyama, S. Tani, H. Suzuki, N. Kato, R. B. Todd, M. J. Hynes, N. Tsukagoshi, M. Kato and T. Kobayashi, (2009) Inducer-dependent nuclear localization of a Zn(II)2Cys6 transcriptional activator, AmyR, in *Aspergillus nidulans*. Biosci Biotechnol Biochem 73**:** 391-399.

Malik, S., and R. G. Roeder, (2010) The metazoan Mediator co-activator complex as an integrative hub for transcriptional regulation. Nat Rev Genet 11**:** 761-772.

Mamane, Y., K. Hellauer, M. H. Rochon and B. Turcotte, (1998) A linker region of the yeast zinc cluster protein Leu3p specifies binding to everted repeat DNA. J Biol Chem 273**:** 18556-18561.

Mamnun, Y. M., R. Pandjaitan, Y. Mahe, A. Delahodde and K. Kuchler, (2002) The yeast zinc finger regulators Pdr1p and Pdr3p control pleiotropic drug resistance (PDR) as homo- and heterodimers in vivo. Mol Microbiol 46**:** 1429-1440.

Marchler-Bauer, A., M. K. Derbyshire, N. R. Gonzales, S. Lu, F. Chitsaz, L. Y. Geer, R. C. Geer, J. He, M. Gwadz, D. I. Hurwitz *et al.*, (2015) CDD: NCBI's conserved domain database. Nucleic Acids Res 43**:** D222-226.

Margelis, S., C. D'Souza, A. J. Small, M. J. Hynes, T. H. Adams and M. A. Davis, (2001) Role of glutamine synthetase in nitrogen metabolite repression in *Aspergillus nidulans*. J Bacteriol 183**:** 5826-5833.

Markina-Inarrairaegui, A., O. Etxebeste, E. Herrero-Garcia, L. Araujo-Bazan, J. Fernandez-Martinez, J. A. Flores, S. A. Osmani and E. A. Espeso, (2011) Nuclear transporters in a multinucleated organism: functional and localization analyses in *Aspergillus nidulans*. Mol Biol Cell 22**:** 3874-3886.

Marzluf, G. A., (1997) Genetic regulation of nitrogen metabolism in the fungi. Microbiol Mol Biol Rev 61**:** 17-32.

Matthews, J. M., and M. Sunde, (2002) Zinc fingers--folds for many occasions. IUBMB Life 54**:** 351-355.

May, G. S., M. L. Tsang, H. Smith, S. Fidel and N. R. Morris, (1987) *Aspergillus nidulans* beta-tubulin genes are unusually divergent. Gene 55**:** 231-243.

McBride, K. M., C. McDonald and N. C. Reich, (2000) Nuclear export signal located within the DNA-binding domain of the STAT1 transcription factor. EMBO J 19**:** 6196-6206.

McCluskey, K., A. Wiest and M. Plamann, (2010) The Fungal Genetics Stock Center: a repository for 50 years of fungal genetics research. J Biosci 35**:** 119-126.

McCluskey, K., A. E. Wiest, I. V. Grigoriev, A. Lipzen, J. Martin, W. Schackwitz and S. E. Baker, (2011) Rediscovery by Whole Genome Sequencing: Classical Mutations and Genome Polymorphisms in *Neurospora crassa*. G3 (Bethesda) 1**:** 303-316.

McCully, K. S., and E. Forbes, (1965) The use of p-fluorophenylalanine with 'master strains' of *Aspergillus nidulans* for assigning genes to linkage groups. Genet Res 6**:** 352-359.

McKenna, A., M. Hanna, E. Banks, A. Sivachenko, K. Cibulskis, A. Kernytsky, K. Garimella, D. Altshuler, S. Gabriel, M. Daly *et al.*, (2010) The Genome Analysis Toolkit: a MapReduce framework for analyzing next-generation DNA sequencing data. Genome Res 20**:** 1297-1303.

Merla, G., C. Howald, S. E. Antonarakis and A. Reymond, (2004) The subcellular localization of the ChoRE-binding protein, encoded by the Williams-Beuren syndrome critical region gene 14, is regulated by 14-3-3. Hum Mol Genet 13**:** 1505-1514.

Michielse, C. B., A. Pfannmuller, M. Macios, P. Rengers, A. Dzikowska and B. Tudzynski, (2014) The interplay between the GATA transcription factors AreA, the global nitrogen regulator and AreB in *Fusarium fujikuroi*. Mol Microbiol 91**:** 472-493.

Miethke, M., and M. A. Marahiel, (2007) Siderophore-based iron acquisition and pathogen control. Microbiol Mol Biol Rev 71**:** 413-451.

Mihlan, M., V. Homann, T. W. Liu and B. Tudzynski, (2003) AREA directly mediates nitrogen regulation of gibberellin biosynthesis in *Gibberella fujikuroi*, but its activity is not affected by NMR. Mol Microbiol 47**:** 975-991.

Miley, G. R., D. Fantz, D. Glossip, X. Lu, R. M. Saito, R. E. Palmer, T. Inoue, S. Van Den Heuvel, P. W. Sternberg and K. Kornfeld, (2004) Identification of residues of the *Caenorhabditis elegans* LIN-1 ETS domain that are necessary for DNA binding and regulation of vulval cell fates. Genetics 167**:** 1697-1709.

Miller, L. M., H. A. Hess, D. B. Doroquez and N. M. Andrews, (2000) Null mutations in the *lin-31* gene indicate two functions during *Caenorhabditis elegans* vulval development. Genetics 156**:** 1595-1602.

Min, K., Y. Shin, H. Son, J. Lee, J. C. Kim, G. J. Choi and Y. W. Lee, (2012) Functional analyses of the nitrogen regulatory gene *areA* in *Gibberella zeae*. FEMS Microbiol Lett 334**:** 66-73.

Mitchell, P., and D. Tollervey, (2000a) mRNA stability in eukaryotes. Curr Opin Genet Dev 10**:** 193-198.

Mitchell, P., and D. Tollervey, (2000b) Musing on the structural organization of the exosome complex. Nat Struct Biol 7**:** 843-846.

Momany, M., P. J. Westfall and G. Abramowsky, (1999) *Aspergillus nidulans swo* mutants show defects in polarity establishment, polarity maintenance and hyphal morphogenesis. Genetics 151**:** 557-567.

Monahan, B. J., J. A. Fraser, M. J. Hynes and M. A. Davis, (2002a) Isolation and characterization of two ammonium permease genes, *meaA* and *mepA*, from *Aspergillus nidulans*. Eukaryot Cell 1**:** 85-94.

Monahan, B. J., S. E. Unkles, I. T. Tsing, J. R. Kinghorn, M. J. Hynes and M. A. Davis, (2002b) Mutation and functional analysis of the *Aspergillus nidulans* ammonium permease MeaA and evidence for interaction with itself and MepA. Fungal Genet Biol 36**:** 35-46.

Monahan, B. J., M. C. Askin, M. J. Hynes and M. A. Davis, (2006) Differential expression of *Aspergillus nidulans* ammonium permease genes is regulated by GATA transcription factor AreA. Eukaryot Cell 5**:** 226-237.

Mooney, J. L., and L. N. Yager, (1990) Light is required for conidiation in *Aspergillus nidulans*. Genes Dev 4**:** 1473-1482.

Morisco, C., K. Seta, S. E. Hardt, Y. Lee, S. F. Vatner and J. Sadoshima, (2001) Glycogen synthase kinase 3beta regulates GATA4 in cardiac myocytes. J Biol Chem 276**:** 28586-28597.

Morozov, I. Y., M. G. Martinez, M. G. Jones and M. X. Caddick, (2000) A defined sequence within the 3' UTR of the *areA* transcript is sufficient to mediate nitrogen metabolite signalling via accelerated deadenylation. Mol Microbiol 37**:** 1248-1257.

Morozov, I. Y., M. Galbis-Martinez, M. G. Jones and M. X. Caddick, (2001) Characterization of nitrogen metabolite signalling in *Aspergillus* via the regulated degradation of *areA* mRNA. Mol Microbiol 42**:** 269-277.

Morozov, I. Y., M. G. Jones, A. A. Razak, D. J. Rigden and M. X. Caddick, (2010) CUCU modification of mRNA promotes decapping and transcript degradation in *Aspergillus nidulans*. Mol Cell Biol 30**:** 460-469.

Morozov, I. Y., M. G. Jones, D. G. Spiller, D. J. Rigden, C. Dattenbock, R. Novotny, J. Strauss and M. X. Caddick, (2010) Distinct roles for Caf1, Ccr4, Edc3 and CutA in the co-ordination of transcript deadenylation, decapping and P-body formation in *Aspergillus nidulans*. Mol Microbiol 76**:** 503-516.

Muro-Pastor, M. I., R. Gonzalez, J. Strauss, F. Narendja and C. Scazzocchio, (1999) The GATA factor AreA is essential for chromatin remodelling in a eukaryotic bidirectional promoter. EMBO J 18**:** 1584-1597.

Muro-Pastor, M. I., J. Strauss, A. Ramon and C. Scazzocchio, (2004) A paradoxical mutant GATA factor. Eukaryot Cell 3**:** 393-405.

Nakai, K., and P. Horton, (1999) PSORT: a program for detecting sorting signals in proteins and predicting their subcellular localization. Trends Biochem Sci 24**:** 34-36.

Nakai, K., and P. Horton, (2007) Computational prediction of subcellular localization. Methods Mol Biol 390**:** 429-466.

Narendja, F., S. P. Goller, M. Wolschek and J. Strauss, (2002) Nitrate and the GATA factor AreA are necessary for in vivo binding of NirA, the pathway-specific transcriptional activator of *Aspergillus nidulans*. Mol Microbiol 44**:** 573-583.

Nayak, T., E. Szewczyk, C. E. Oakley, A. Osmani, L. Ukil, S. L. Murray, M. J. Hynes, S. A. Osmani and B. R. Oakley, (2006) A versatile and efficient gene-targeting system for *Aspergillus nidulans*. Genetics 172**:** 1557-1566.

Neville, M., F. Stutz, L. Lee, L. I. Davis and M. Rosbash, (1997) The importin-beta family member Crm1p bridges the interaction between Rev and the nuclear pore complex during nuclear export. Curr Biol 7**:** 767-775.

Neville, M., and M. Rosbash, (1999) The NES-Crm1p export pathway is not a major mRNA export route in *Saccharomyces cerevisiae*. EMBO J 18**:** 3746-3756.

Nguyen, K. T., M. P. Holloway and R. A. Altura, (2012) The CRM1 nuclear export protein in normal development and disease. Int J Biochem Mol Biol 3**:** 137-151.

Nichane, M., X. Ren, J. Souopgui and E. J. Bellefroid, (2008) Hairy2 functions through both DNA-binding and non DNA-binding mechanisms at the neural plate border in *Xenopus*. Dev Biol 322**:** 368-380.

Niehaus, E. M., K. Kleigrewe, P. Wiemann, L. Studt, C. M. Sieber, L. R. Connolly, M. Freitag, U. Guldener, B. Tudzynski and H. U. Humpf, (2013) Genetic manipulation of the *Fusarium fujikuroi* fusarin gene cluster yields insight into the complex regulation and fusarin biosynthetic pathway. Chem Biol 20**:** 1055-1066.

Niehaus, E. M., S. Janevska, K. W. von Bargen, C. M. Sieber, H. Harrer, H. U. Humpf and B. Tudzynski, (2014) Apicidin F: characterization and genetic manipulation of a new secondary metabolite gene cluster in the rice pathogen *Fusarium fujikuroi*. PLoS One 9**:** e103336.

Niehaus, E. M., K. W. von Bargen, J. J. Espino, A. Pfannmuller, H. U. Humpf and B. Tudzynski, (2014) Characterization of the fusaric acid gene cluster in *Fusarium fujikuroi*. Appl Microbiol Biotechnol 98**:** 1749-1762.

Nielsen, H., J. Engelbrecht, S. Brunak and G. von Heijne, (1997) Identification of prokaryotic and eukaryotic signal peptides and prediction of their cleavage sites. Protein Engineering 10**:** 1-6.

Nigg, E. A., (1991) The substrates of the cdc2 kinase. Semin Cell Biol 2**:** 261-270.

Nigg, E. A., (1997) Nucleocytoplasmic transport: signals, mechanisms and regulation. Nature 386**:** 779-787.

Nitsche, B. M., J. Crabtree, G. C. Cerqueira, V. Meyer, A. F. Ram and J. R. Wortman, (2011) New resources for functional analysis of omics data for the genus *Aspergillus*. BMC Genomics 12**:** 486.

Nogi, Y., and T. Fukasawa, (1980) A novel mutation that affects utilization of galactose in *Saccharomyces cerevisiae*. Curr Genet 2**:** 115-120.

Nowrousian, M., I. Teichert, S. Masloff and U. Kuck, (2012) Whole-Genome Sequencing of *Sordaria macrospora* Mutants Identifies Developmental Genes. G3 2**:** 261-270.

Oberegger, H., M. Schoeser, I. Zadra, M. Schrettl, W. Parson and H. Haas, (2002) Regulation of *freA*, *acoA*, *lysF*, and *cycA* expression by iron availability in *Aspergillus nidulans*. Appl Environ Microbiol 68**:** 5769-5772.

Oliver, J. D., S. J. Kaye, D. Tuckwell, A. E. Johns, D. A. Macdonald, J. Livermore, P. A. Warn, M. Birch and M. J. Bromley, (2012) The *Aspergillus fumigatus* dihydroxyacid dehydratase Ilv3A/IlvC is required for full virulence. PLoS One 7**:** e43559.

Olszewska, A., K. Krol, P. Weglenski and A. Dzikowska, (2007) Arginine catabolism in *Aspergillus nidulans* is regulated by the *rrmA* gene coding for the RNA-binding protein. Fungal Genet Biol 44**:** 1285-1297.

Oppermann, U., C. Filling, M. Hult, N. Shafqat, X. Wu, M. Lindh, J. Shafqat, E. Nordling, Y. Kallberg, B. Persson *et al.*, (2003) Short-chain dehydrogenases/reductases (SDR): the 2002 update. Chem Biol Interact 143-144**:** 247-253.

Osherov, N., J. Mathew and G. S. May, (2000) Polarity-defective mutants of *Aspergillus nidulans*. Fungal Genet Biol 31**:** 181-188.

Osmani, A. H., J. Davies, H. L. Liu, A. Nile and S. A. Osmani, (2006a) Systematic deletion and mitotic localization of the nuclear pore complex proteins of *Aspergillus nidulans*. Mol Biol Cell 17**:** 4946-4961.

Osmani, A. H., B. R. Oakley and S. A. Osmani, (2006b) Identification and analysis of essential *Aspergillus nidulans* genes using the heterokaryon rescue technique. Nat Protoc 1**:** 2517-2526.

Palmer, J. M., J. M. Theisen, R. M. Duran, W. S. Grayburn, A. M. Calvo and N. P. Keller, (2013) Secondary metabolism and development is mediated by LlmF control of VeA subcellular localization in *Aspergillus nidulans*. PLoS Genet 9**:** e1003193.

Pan, H., B. Feng and G. A. Marzluf, (1997) Two distinct protein-protein interactions between the NIT2 and NMR regulatory proteins are required to establish nitrogen metabolite repression in *Neurospora crassa*. Mol Microbiol 26**:** 721-729.

Pan, T., and J. E. Coleman, (1989) Structure and function of the Zn(II) binding site within the DNA-binding domain of the GAL4 transcription factor. Proc Natl Acad Sci USA 86**:** 3145-3149.

Pan, T., and J. E. Coleman, (1991) Sequential assignments of the 1H NMR resonances of Zn(II)2 and 113Cd(II)2 derivatives of the DNA-binding domain of the GAL4 transcription factor reveal a novel structural motif for specific DNA recognition. Biochemistry 30**:** 4212-4222.

Papp, L. V., J. Lu, F. Striebel, D. Kennedy, A. Holmgren and K. K. Khanna, (2006) The redox state of SECIS binding protein 2 controls its localization and selenocysteine incorporation function. Mol Cell Biol 26**:** 4895-4910.

Pardo, E., and M. Orejas, (2014) The *Aspergillus nidulans* Zn(II)2Cys6 transcription factor AN5673/RhaR mediates L-rhamnose utilization and the production of α-L-rhamnosidases. Microb Cell Fact 13**:** 161.

Parker, D., K. Ferreri, T. Nakajima, V. J. LaMorte, R. Evans, S. C. Koerber, C. Hoeger and M. R. Montminy, (1996) Phosphorylation of CREB at Ser-133 induces complex formation with CREB-binding protein via a direct mechanism. Mol Cell Biol 16**:** 694-703.

Pateman, J. A., D. J. Cove, B. M. Rever and D. B. Roberts, (1964) A common co-factor for nitrate reductase and xanthine dehydrogenase which also regulates the synthesis of nitrate reductase. Nature 201**:** 58-60.

Pateman, J. A., B. M. Rever and D. J. Cove, (1967) Genetic and biochemical studies of nitrate reduction in *Aspergillus nidulans*. Biochem J 104**:** 103-111.

Pateman, J. A., (1969) Regulation of synthesis of glutamate dehydrogenase and glutamine synthetase in micro-organisms. Biochem J 115**:** 769-775.

Pellier, A. L., R. Lauge, C. Veneault-Fourrey and T. Langin, (2003) CLNR1, the AREA/NIT2-like global nitrogen regulator of the plant fungal pathogen *Colletotrichum lindemuthianum* is required for the infection cycle. Mol Microbiol 48**:** 639-655.

Perez-Garcia, A., S. S. Snoeijers, M. H. Joosten, T. Goosen and P. J. De Wit, (2001) Expression of the Avirulence gene Avr9 of the fungal tomato pathogen *Cladosporium fulvum* is regulated by the global nitrogen response factor NRF1. Mol Plant Microbe Interact 14**:** 316-325.

Pfaffl, M. W., (2001) A new mathematical model for relative quantification in real-time RT-PCR. Nucleic Acids Res 29**:** e45.

Piskacek, M., A. Vasku, R. Hajek and A. Knight, (2015) Shared structural features of the 9aaTAD family in complex with CBP. Mol Biosyst 11**:** 844-851.

Piskacek, S., M. Gregor, M. Nemethova, M. Grabner, P. Kovarik and M. Piskacek, (2007) Nine-amino-acid transactivation domain: establishment and prediction utilities. Genomics 89**:** 756-768.

Platt, A., T. Langdon, H. N. Arst, Jr., D. Kirk, D. Tollervey, J. M. Sanchez and M. X. Caddick, (1996a) Nitrogen metabolite signalling involves the C-terminus and the GATA domain of the *Aspergillus* transcription factor AreA and the 3' untranslated region of its mRNA. EMBO J 15**:** 2791-2801.

Platt, A., A. Ravagnani, H. Arst, Jr., D. Kirk, T. Langdon and M. X. Caddick, (1996b) Mutational analysis of the C-terminal region of AREA, the transcription factor mediating nitrogen metabolite repression in Aspergillus nidulans. Mol Gen Genet 250**:** 106-114.

Pokorska, A., C. Drevet and C. Scazzocchio, (2000) The analysis of the transcriptional activator PrnA reveals a tripartite nuclear localisation sequence. J Mol Biol 298**:** 585-596.

Polotnianka, R., B. J. Monahan, M. J. Hynes and M. A. Davis, (2004) TamA interacts with LeuB, the homologue of *Saccharomyces cerevisiae* Leu3p, to regulate *gdhA* expression in *Aspergillus nidulans*. Mol Genet Genomics 272**:** 452-459.

Pomraning, K. R., K. M. Smith and M. Freitag, (2011) Bulk segregant analysis followed by high-throughput sequencing reveals the *Neurospora* cell cycle gene, *ndc-1*, to be allelic with the gene for ornithine decarboxylase, *spe-1*. Eukaryot Cell 10**:** 724-733.

Pontecorvo, G., J. A. Roper, L. M. Hemmons, K. D. Macdonald and A. W. Bufton, (1953) The genetics of *Aspergillus nidulans*. Adv Genet 5**:** 141-238.

Poss, Z. C., C. C. Ebmeier and D. J. Taatjes, (2013) The Mediator complex and transcription regulation. Crit Rev Biochem Mol Biol 48**:** 575-608.

Prakash, L., and F. Sherman, (1973) Mutagenic specificity: reversion of iso-1-cytochrome *c* mutants of yeast. J Mol Biol 79**:** 65-82.

Prakash, L., J. W. Stewart and F. Sherman, (1974) Specific induction of transitions and transversions of GC base pairs by 4-nitroquinoline-1-oxide in iso-1-cytochrome *c* mutants of yeast. J Mol Biol 85**:** 51-56.

Quinlan, A. R., and I. M. Hall, (2010) BEDTools: a flexible suite of utilities for comparing genomic features. Bioinformatics 26**:** 841-842.

Raftery, M. J., C. A. Harrison, P. Alewood, A. Jones and C. L. Geczy, (1996) Isolation of the murine S100 protein MRP14 (14 kDa migration-inhibitory-factor-related protein) from activated spleen cells: characterization of post-translational modifications and zinc binding. Biochem J 316**:** 285-293.

Ramon, D., L. Carramolino, C. Patino, F. Sanchez and M. A. Penalva, (1987) Cloning and characterization of the isopenicillin N synthetase gene mediating the formation of the beta-lactam ring in *Aspergillus nidulans*. Gene 57**:** 171-181.

Ravagnani, A., L. Gorfinkiel, T. Langdon, G. Diallinas, E. Adjadj, S. Demais, D. Gorton, H. N. Arst, Jr. and C. Scazzocchio, (1997) Subtle hydrophobic interactions between the seventh residue of the zinc finger loop and the first base of an HGATAR sequence determine promoter-specific recognition by the *Aspergillus nidulans* GATA factor AreA. EMBO J 16**:** 3974-3986.

Reade, J. P., and A. H. Cobb, (2002) New, quick tests for herbicide resistance in black-grass (*Alopecurus myosuroides* Huds) based on increased glutathione S-transferase activity and abundance. Pest Manag Sci 58**:** 26-32.

Reece, R. J., and M. Ptashne, (1993) Determinants of binding-site specificity among yeast C6 zinc cluster proteins. Science 261**:** 909-911.

Retief, J. D., (2000) Phylogenetic analysis using PHYLIP. Methods Mol Biol 132**:** 243-258.

Reyes-Dominguez, Y., F. Narendja, H. Berger, A. Gallmetzer, R. Fernandez-Martin, I. Garcia, C. Scazzocchio and J. Strauss, (2008) Nucleosome positioning and histone H3 acetylation are independent processes in the *Aspergillus nidulans prnD-prnB* bidirectional promoter. Eukaryot Cell 7**:** 656-663.

Romero, N. M., M. Irisarri, P. Roth, A. Cauerhff, C. Samakovlis and P. Wappner, (2008) Regulation of the *Drosophila* hypoxia-inducible factor alpha Sima by CRM1-dependent nuclear export. Mol Cell Biol 28**:** 3410-3423.

Rosenbaum, E., M. O. Hoque, Y. Cohen, M. Zahurak, M. A. Eisenberger, J. I. Epstein, A. W. Partin and D. Sidransky, (2005) Promoter hypermethylation as an independent prognostic factor for relapse in patients with prostate cancer following radical prostatectomy. Clin Cancer Res 11**:** 8321-8325.

Rosenkranz, H. S., and L. A. Poirier, (1979) Evaluation of the mutagenicity and DNA-modifying activity of carcinogens and noncarcinogens in microbial systems. J Natl Cancer Inst 62**:** 873-891.

Rottensteiner, H., A. J. Kal, B. Hamilton, H. Ruis and H. F. Tabak, (1997) A heterodimer of the Zn(II)2Cys6 transcription factors Pip2p and Oaf1p controls induction of genes encoding peroxisomal proteins in *Saccharomyces cerevisiae*. Eur J Biochem 247**:** 776-783.

Salazar, M., W. Vongsangnak, G. Panagiotou, M. R. Andersen and J. Nielsen, (2009) Uncovering transcriptional regulation of glycerol metabolism in Aspergilli through genome-wide gene expression data analysis. Mol Genet Genomics 282**:** 571-586.

Sambrook, J., E. F. Fritsch and T. Maniatis, (1989) *Molecular Cloning*. Cold Spring Harbour Laboratory Press, Cold Spring Harbour, NY.

Sambrook, J., and D. W. Russell, (2001) *Molecular Cloning: A Laboratory Manual*. Cold Spring Harbour Laboratory Press, Cold Spring Harbor, NY.

Sanguinetti, M., S. Amillis, S. Pantano, C. Scazzocchio and A. Ramon, (2014) Modelling and mutational analysis of *Aspergillus nidulans* UreA, a member of the subfamily of urea/H(+) transporters in fungi and plants. Open Biol 4**:** 140070.

Sarikaya Bayram, O., O. Bayram, O. Valerius, H. S. Park, S. Irniger, J. Gerke, M. Ni, K. H. Han, J. H. Yu and G. H. Braus, (2010) LaeA control of velvet family regulatory proteins for light-dependent development and fungal cell-type specificity. PLoS Genet 6**:** e1001226.

Scherlach, K., A. Sarkar, V. Schroeckh, H. M. Dahse, M. Roth, A. A. Brakhage, U. Horn and C. Hertweck, (2011) Two induced fungal polyketide pathways converge into antiproliferative spiroanthrones. Chembiochem 12**:** 1836-1839.

Schinko, T., H. Berger, W. Lee, A. Gallmetzer, K. Pirker, R. Pachlinger, I. Buchner, T. Reichenauer, U. Guldener and J. Strauss, (2010) Transcriptome analysis of nitrate assimilation in *Aspergillus nidulans* reveals connections to nitric oxide metabolism. Mol Microbiol 78**:** 720-738.

Schmittgen, T. D., and K. J. Livak, (2008) Analyzing real-time PCR data by the comparative C(T) method. Nat Protoc 3**:** 1101-1108.

Schneider, T. D., and R. M. Stephens, (1990) Sequence logos: a new way to display consensus sequences. Nucleic Acids Res 18**:** 6097-6100.

Schroeckh, V., K. Scherlach, H. W. Nutzmann, E. Shelest, W. Schmidt-Heck, J. Schuemann, K. Martin, C. Hertweck and A. A. Brakhage, (2009) Intimate bacterial-fungal interaction triggers biosynthesis of archetypal polyketides in *Aspergillus nidulans*. Proc Natl Acad Sci USA 106**:** 14558-14563.

Schutkowski, M., A. Bernhardt, X. Z. Zhou, M. Shen, U. Reimer, J. U. Rahfeld, K. P. Lu and G. Fischer, (1998) Role of phosphorylation in determining the backbone dynamics of the serine/threonine-proline motif and Pin1 substrate recognition. Biochemistry 37**:** 5566-5575.

Sellick, C. A., and R. J. Reece, (2005) Eukaryotic transcription factors as direct nutrient sensors. Trends Biochem Sci 30**:** 405-412.

Seo, J. A., Y. Guan and J. H. Yu, (2003) Suppressor mutations bypass the requirement of *fluG* for asexual sporulation and sterigmatocystin production in *Aspergillus nidulans*. Genetics 165**:** 1083-1093.

Shaaban, M., J. M. Palmer, W. A. El-Naggar, M. A. El-Sokkary, S. E. Habib el and N. P. Keller, (2010) Involvement of transposon-like elements in penicillin gene cluster regulation. Fungal Genet Biol 47**:** 423-432.

Shimizu, M., T. Fujii, S. Masuo and N. Takaya, (2010) Mechanism of *de novo* branched-chain amino acid synthesis as an alternative electron sink in hypoxic *Aspergillus nidulans* cells. Appl Environ Microbiol 76**:** 1507-1515.

Sibthorp, C., H. Wu, G. Cowley, P. W. Wong, P. Palaima, I. Y. Morozov, G. D. Weedall and M. X. Caddick, (2013) Transcriptome analysis of the filamentous fungus *Aspergillus nidulans* directed to the global identification of promoters. BMC Genomics 14**:** 847.

Sievers, F., A. Wilm, D. Dineen, T. J. Gibson, K. Karplus, W. Li, R. Lopez, H. McWilliam, M. Remmert, J. Soding *et al.*, (2011) Fast, scalable generation of high-quality protein multiple sequence alignments using Clustal Omega. Mol Syst Biol 7**:** 539.

Skala, J., E. Capieaux, E. Balzi, W. N. Chen and A. Goffeau, (1991) Complete sequence of the *Saccharomyces cerevisiae LEU1* gene encoding isopropylmalate isomerase. Yeast 7**:** 281-285.

Small, A. J., M. J. Hynes and M. A. Davis, (1999) The TamA protein fused to a DNA-binding domain can recruit AreA, the major nitrogen regulatory protein, to activate gene expression in *Aspergillus nidulans*. Genetics 153**:** 95-105.

Small, A. J., R. B. Todd, M. C. Zanker, S. Delimitrou, M. J. Hynes and M. A. Davis, (2001) Functional analysis of TamA, a coactivator of nitrogen-regulated gene expression in *Aspergillus nidulans*. Mol Genet Genomics 265**:** 636-646.

Small, I., N. Peeters, F. Legeai and C. Lurin, (2004) Predotar: A tool for rapidly screening proteomes for N-terminal targeting sequences. Proteomics 4**:** 1581-1590.

Snoeijers, S. S., A. Pérez-García, J. M.H.A.J. and P. J. G. M. De Wit, (2000) The Effect of Nitrogen on Disease Development and Gene Expression in Bacterial and Fungal Plant Pathogens. Eur J Plant Pathol 106**:** 493-506.

Son, S., and S. A. Osmani, (2009) Analysis of all protein phosphatase genes in *Aspergillus nidulans* identifies a new mitotic regulator, *fcp1*. Eukaryot Cell 8**:** 573-585.

Sophianopoulou, V., and C. Scazzocchio, (1989) The proline transport protein of *Aspergillus nidulans* is very similar to amino acid transporters of *Saccharomyces cerevisiae*. Mol Microbiol 3**:** 705-714.

Stammers, D. K., J. Ren, K. Leslie, C. E. Nichols, H. K. Lamb, S. Cocklin, A. Dodds and A. R. Hawkins, (2001) The structure of the negative transcriptional regulator NmrA reveals a structural superfamily which includes the short-chain dehydrogenase/reductases. EMBO J 20**:** 6619-6626.

Starich, M. R., M. Wikstrom, H. N. Arst, Jr., G. M. Clore and A. M. Gronenborn, (1998) The solution structure of a fungal AreA protein-DNA complex: an alternative binding mode for the basic carboxyl tail of GATA factors. J Mol Biol 277**:** 605-620.

Stinnett, S. M., E. A. Espeso, L. Cobeno, L. Araujo-Bazan and A. M. Calvo, (2007) *Aspergillus nidulans* VeA subcellular localization is dependent on the importin alpha carrier and on light. Mol Microbiol 63**:** 242-255.

Stommel, J. M., N. D. Marchenko, G. S. Jimenez, U. M. Moll, T. J. Hope and G. M. Wahl, (1999) A leucine-rich nuclear export signal in the p53 tetramerization domain: regulation of subcellular localization and p53 activity by NES masking. EMBO J 18**:** 1660-1672.

Suarez, T., N. Oestreicher, J. Kelly, G. Ong, T. Sankarsingh and C. Scazzocchio, (1991) The *uaY* positive control gene of *Aspergillus nidulans*: fine structure, isolation of constitutive mutants and reversion patterns. Mol Gen Genet 230**:** 359-368.

Suarez, T., M. V. de Queiroz, N. Oestreicher and C. Scazzocchio, (1995) The sequence and binding specificity of UaY, the specific regulator of the purine utilization pathway in *Aspergillus nidulans*, suggest an evolutionary relationship with the Ppr1 protein of *Saccharomyces cerevisiae*. EMBO J 14**:** 1453-1467.

Suelmann, R., N. Sievers and R. Fischer, (1997) Nuclear traffic in fungal hyphae: in vivo study of nuclear migration and positioning in *Aspergillus nidulans*. Mol Microbiol 25**:** 757-769.

Suetsugu, S., and T. Takenawa, (2003) Translocation of N-WASP by nuclear localization and export signals into the nucleus modulates expression of HSP90. J Biol Chem 278**:** 42515-42523.

Suzuki, H., S. Tashiro, S. Hira, J. Sun, C. Yamazaki, Y. Zenke, M. Ikeda-Saito, M. Yoshida and K. Igarashi, (2004) Heme regulates gene expression by triggering Crm1-dependent nuclear export of Bach1. EMBO J 23**:** 2544-2553.

Suzuki, M., (1989) SPXX, a frequent sequence motif in gene regulatory proteins. J Mol Biol 207**:** 61-84.

Suzuki, Y., S. L. Murray, K. H. Wong, M. A. Davis and M. J. Hynes, (2012) Reprogramming of carbon metabolism by the transcriptional activators AcuK and AcuM in *Aspergillus nidulans*. Mol Microbiol 84**:** 942-964.

Takahashi, S., K. Kontani, Y. Araki and T. Katada, (2007) Caf1 regulates translocation of ribonucleotide reductase by releasing nucleoplasmic Spd1-Suc22 assembly. Nucleic Acids Res 35**:** 1187-1197.

Tamayo, E. N., A. Villanueva, A. A. Hasper, L. H. de Graaff, D. Ramon and M. Orejas, (2008) CreA mediates repression of the regulatory gene *xlnR* which controls the production of xylanolytic enzymes in *Aspergillus nidulans*. Fungal Genet Biol 45**:** 984-993.

Tan, K., A. J. Roberts, M. Chonofsky, M. J. Egan and S. L. Reck-Peterson, (2014) A microscopy-based screen employing multiplex genome sequencing identifies cargo-specific requirements for dynein velocity. Mol Biol Cell 25**:** 669-678.

Tani, S., Y. Katsuyama, T. Hayashi, H. Suzuki, M. Kato, K. Gomi, T. Kobayashi and N. Tsukagoshi, (2001) Characterization of the *amyR* gene encoding a transcriptional activator for the amylase genes in *Aspergillus nidulans*. Curr Genet 39**:** 10-15.

Thakur, J. K., H. Arthanari, F. Yang, S. J. Pan, X. Fan, J. Breger, D. P. Frueh, K. Gulshan, D. K. Li, E. Mylonakis *et al.*, (2008) A nuclear receptor-like pathway regulating multidrug resistance in fungi. Nature 452**:** 604-609.

Thakur, J. K., H. Arthanari, F. Yang, K. H. Chau, G. Wagner and A. M. Naar, (2009) Mediator subunit Gal11p/MED15 is required for fatty acid-dependent gene activation by yeast transcription factor Oaf1p. J Biol Chem 284**:** 4422-4428.

Tjian, R., (1978) The binding site on SV40 DNA for a T antigen-related protein. Cell 13**:** 165-179.

Tobin, M. B., M. D. Fleming, P. L. Skatrud and J. R. Miller, (1990) Molecular characterization of the acyl-coenzyme A:isopenicillin N acyltransferase gene (*penDE*) from *Penicillium chrysogenum* and *Aspergillus nidulans* and activity of recombinant enzyme in Escherichia coli. J Bacteriol 172**:** 5908-5914.

Toda, T., M. Shimanuki, Y. Saka, H. Yamano, Y. Adachi, M. Shirakawa, Y. Kyogoku and M. Yanagida, (1992) Fission yeast *pap1*-dependent transcription is negatively regulated by an essential nuclear protein, *crm1*. Mol Cell Biol 12**:** 5474-5484.

Todd, R. B., and A. Andrianopoulos, (1997) Evolution of a fungal regulatory gene family: the Zn(II)2Cys6 binuclear cluster DNA binding motif. Fungal Genet Biol 21**:** 388-405.

Todd, R. B., R. L. Murphy, H. M. Martin, J. A. Sharp, M. A. Davis, M. E. Katz and M. J. Hynes, (1997) The acetate regulatory gene *facB* of *Aspergillus nidulans* encodes a Zn(II)2Cys6 transcriptional activator. Mol Gen Genet 254**:** 495-504.

Todd, R. B., A. Andrianopoulos, M. A. Davis and M. J. Hynes, (1998) FacB, the *Aspergillus nidulans* activator of acetate utilization genes, binds dissimilar DNA sequences. EMBO J 17**:** 2042-2054.

Todd, R. B., J. A. Fraser, K. H. Wong, M. A. Davis and M. J. Hynes, (2005) Nuclear accumulation of the GATA factor AreA in response to complete nitrogen starvation by regulation of nuclear export. Eukaryot Cell 4**:** 1646-1653.

Todd, R. B., M. A. Davis and M. J. Hynes, (2007a) Genetic manipulation of *Aspergillus nidulans*: heterokaryons and diploids for dominance, complementation and haploidization analyses. Nat Protoc 2**:** 822-830.

Todd, R. B., M. A. Davis and M. J. Hynes, (2007b) Genetic manipulation of *Aspergillus nidulans*: meiotic progeny for genetic analysis and strain construction. Nat Protoc 2**:** 811-821.

Todd, R. B., M. Zhou, R. A. Ohm, H. A. Leeggangers, L. Visser and R. P. de Vries, (2014) Prevalence of transcription factors in ascomycete and basidiomycete fungi. BMC Genomics 15**:** 214.

Toh-e, A., P. Guerry-Kopecko and R. B. Wickner, (1980) A stable plasmid carrying the yeast Leu2 gene and containing only yeast deoxyribonucleic acid. J Bacteriol 141**:** 413-416.

Trapnell, C., D. G. Hendrickson, M. Sauvageau, L. Goff, J. L. Rinn and L. Pachter, (2013) Differential analysis of gene regulation at transcript resolution with RNA-seq. Nat Biotechnol 31**:** 46-53.

Traven, A., B. Jelicic and M. Sopta, (2006) Yeast Gal4: a transcriptional paradigm revisited. EMBO Rep 7**:** 496-499.

Tribus, M., J. Galehr, P. Trojer, G. Brosch, P. Loidl, F. Marx, H. Haas and S. Graessle, (2005) HdaA, a major class 2 histone deacetylase of *Aspergillus nidulans*, affects growth under conditions of oxidative stress. Eukaryot Cell 4**:** 1736-1745.

Trzcinska-Danielewicz, J., T. Ishikawa, A. Micialkiewicz and J. Fronk, (2008) Yeast transcription factor Oaf1 forms homodimer and induces some oleate-responsive genes in absence of Pip2. Biochem Biophys Res Commun 374**:** 763-766.

Tsong, A. E., B. B. Tuch, H. Li and A. D. Johnson, (2006) Evolution of alternative transcriptional circuits with identical logic. Nature 443**:** 415-420.

Tucker, M., M. A. Valencia-Sanchez, R. R. Staples, J. Chen, C. L. Denis and R. Parker, (2001) The transcription factor associated Ccr4 and Caf1 proteins are components of the major cytoplasmic mRNA deadenylase in *Saccharomyces cerevisiae*. Cell 104**:** 377-386.

Tudzynski, B., and K. Holter, (1998) Gibberellin biosynthetic pathway in *Gibberella fujikuroi*: evidence for a gene cluster. Fungal Genet Biol 25**:** 157-170.

Tudzynski, B., H. Kawaide and Y. Kamiya, (1998) Gibberellin biosynthesis in *Gibberella fujikuroi*: cloning and characterization of the copalyl diphosphate synthase gene. Curr Genet 34**:** 234-240.

Tudzynski, B., (2014) Nitrogen regulation of fungal secondary metabolism in fungi. Front Microbiol 5**:** 656.

Unkles, S. E., K. L. Hawker, C. Grieve, E. I. Campbell, P. Montague and J. R. Kinghorn, (1991) *crnA* encodes a nitrate transporter in *Aspergillus nidulans*. Proc Natl Acad Sci USA 88**:** 204-208.

Unkles, S. E., J. Smith, G. J. Kanan, L. J. Millar, I. S. Heck, D. H. Boxer and J. R. Kinghorn, (1997) The *Aspergillus nidulans cnxABC* locus is a single gene encoding two catalytic domains required for synthesis of precursor Z, an intermediate in molybdenum cofactor biosynthesis. J Biol Chem 272**:** 28381-28390.

Unkles, S. E., D. Zhou, M. Y. Siddiqi, J. R. Kinghorn and A. D. Glass, (2001) Apparent genetic redundancy facilitates ecological plasticity for nitrate transport. EMBO J 20**:** 6246-6255.

Ushijima, H., and M. Maeda, (2012) cAMP-dependent proteolysis of GATA-6 is linked to JNK-signaling pathway. Biochem Biophys Res Commun 423**:** 679-683.

Van der Auwera, G. A., M. O. Carneiro, C. Hartl, R. Poplin, G. Del Angel, A. Levy-Moonshine, T. Jordan, K. Shakir, D. Roazen, J. Thibault *et al.*, (2013) From FastQ data to high confidence variant calls: the Genome Analysis Toolkit best practices pipeline. Curr Protoc Bioinformatics 11**:** 11 10 11-11 10 33.

Velasco, J. A., J. Cansado, M. C. Pena, T. Kawakami, J. Laborda and V. Notario, (1993) Cloning of the dihydroxyacid dehydratase-encoding gene (*ILV3*) from *Saccharomyces cerevisiae*. Gene 137**:** 179-185.

Vienken, K., M. Scherer and R. Fischer, (2005) The Zn(II)2Cys6 putative *Aspergillus nidulans* transcription factor repressor of sexual development inhibits sexual development under low-carbon conditions and in submersed culture. Genetics 169**:** 619-630.

Vienken, K., and R. Fischer, (2006) The Zn(II)2Cys6 putative transcription factor NosA controls fruiting body formation in *Aspergillus nidulans*. Mol Microbiol 61**:** 544-554.

von Dohren, H., (2009) A survey of nonribosomal peptide synthetase (NRPS) genes in *Aspergillus nidulans*. Fungal Genet Biol 46 Suppl 1**:** S45-52.

Vulliet, P. R., F. L. Hall, J. P. Mitchell and D. G. Hardie, (1989) Identification of a novel proline-directed serine/threonine protein kinase in rat pheochromocytoma. J Biol Chem 264**:** 16292-16298.

Wada, A., M. Fukuda, M. Mishima and E. Nishida, (1998) Nuclear export of actin: a novel mechanism regulating the subcellular localization of a major cytoskeletal protein. EMBO J 17**:** 1635-1641.

Wada, M., S. Nakamori and H. Takagi, (2003) Serine racemase homologue of *Saccharomyces cerevisiae* has L-threo-3-hydroxyaspartate dehydratase activity. FEMS Microbiol Lett 225**:** 189-193.

Wagner, D., A. Schmeinck, M. Mos, I. Y. Morozov, M. X. Caddick and B. Tudzynski, (2010) The bZIP transcription factor MeaB mediates nitrogen metabolite repression at specific loci. Eukaryot Cell 9**:** 1588-1601.

Wang, K., Y. J. Zhou, H. Liu, K. Cheng, J. Mao, F. Wang, W. Liu, M. Ye, Z. K. Zhao and H. Zou, (2015) Proteomic analysis of protein methylation in the yeast *Saccharomyces cerevisiae*. J Proteomics 114**:** 226-233.

Wang, Y., W. Li, Y. Siddiqi, V. F. Symington, J. R. Kinghorn, S. E. Unkles and A. D. Glass, (2008) Nitrite transport is mediated by the nitrite-specific high-affinity NitA transporter and by nitrate transporters NrtA, NrtB in *Aspergillus nidulans*. Fungal Genet Biol 45**:** 94-102.

Wapinski, I., A. Pfeffer, N. Friedman and A. Regev, (2007) Natural history and evolutionary principles of gene duplication in fungi. Nature 449**:** 54-61.

Webb, K. J., C. I. Zurita-Lopez, Q. Al-Hadid, A. Laganowsky, B. D. Young, R. S. Lipson, P. Souda, K. F. Faull, J. P. Whitelegge and S. G. Clarke, (2010) A novel 3-methylhistidine modification of yeast ribosomal protein Rpl3 is dependent upon the YIL110W methyltransferase. J Biol Chem 285**:** 37598-37606.

Weiss, M. J., and S. H. Orkin, (1995) GATA transcription factors: key regulators of hematopoiesis. Exp Hematol 23**:** 99-107.

Wen, W., J. L. Meinkoth, R. Y. Tsien and S. S. Taylor, (1995) Identification of a signal for rapid export of proteins from the nucleus. Cell 82**:** 463-473.

Wiemann, P., A. Willmann, M. Straeten, K. Kleigrewe, M. Beyer, H. U. Humpf and B. Tudzynski, (2009) Biosynthesis of the red pigment bikaverin in *Fusarium fujikuroi*: genes, their function and regulation. Mol Microbiol 72**:** 931-946.

Williams, B. A., S. Sillaots, A. Tsang and R. Storms, (1996) Isolation by genetic complementation of two differentially expressed genes for β-isopropylmalate dehydrogenase from *Aspergillus niger*. Curr Genet 30**:** 305-311.

Wilson, R. A., R. P. Gibson, C. F. Quispe, J. A. Littlechild and N. J. Talbot, (2010) An NADPH-dependent genetic switch regulates plant infection by the rice blast fungus. Proc Natl Acad Sci USA 107**:** 21902-21907.

Wolfger, H., Y. Mahe, A. Parle-McDermott, A. Delahodde and K. Kuchler, (1997) The yeast ATP binding cassette (ABC) protein genes *PDR10* and *PDR15* are novel targets for the Pdr1 and Pdr3 transcriptional regulators. FEBS Lett 418**:** 269-274.

Wong, K. H., (2007) Regulation of Nitrogen Metabolite repression in *Aspergillus nidulans:* Transcriptional and Post-transcriptional controls of *areA* and *nmrA*, PhD Thesis p. 236 in *Department of Genetics*. The University of Melbourne, Melbourne, Victoria, Australia.

Wong, K. H., M. J. Hynes, R. B. Todd and M. A. Davis, (2007) Transcriptional control of *nmrA* by the bZIP transcription factor MeaB reveals a new level of nitrogen regulation in *Aspergillus nidulans*. Mol Microbiol 66**:** 534-551.

Wong, K. H., M. J. Hynes and M. A. Davis, (2008) Recent advances in nitrogen regulation: a comparison between *Saccharomyces cerevisiae* and filamentous fungi. Eukaryot Cell 7**:** 917-925.

Wong, K. H., M. J. Hynes, R. B. Todd and M. A. Davis, (2009) Deletion and overexpression of the *Aspergillus nidulans* GATA factor AreB reveals unexpected pleiotropy. Microbiology 155**:** 3868-3880.

Wood, L. D., B. J. Irvin, G. Nucifora, K. S. Luce and S. W. Hiebert, (2003) Small ubiquitin-like modifier conjugation regulates nuclear export of TEL, a putative tumor suppressor. Proc Natl Acad Sci USA 100**:** 3257-3262.

Wood, T. M., and S. I. McCrae, (1996) Arabinoxylan-degrading enzyme system of the fungus *Aspergillus awamori*: purification and properties of an alpha-L-arabinofuranosidase. Appl Microbiol Biotechnol 45**:** 538-545.

Woudstra, E. C., C. Gilbert, J. Fellows, L. Jansen, J. Brouwer, H. Erdjument-Bromage, P. Tempst and J. Q. Svejstrup, (2002) A Rad26-Def1 complex coordinates repair and RNA pol II proteolysis in response to DNA damage. Nature 415**:** 929-933.

Xia, J., D. H. Lee, J. Taylor, M. Vandelft and R. Truant, (2003) Huntingtin contains a highly conserved nuclear export signal. Hum Mol Genet 12**:** 1393-1403.

Xiao, X., Y. H. Fu and G. A. Marzluf, (1995) The negative-acting NMR regulatory protein of *Neurospora crassa* binds to and inhibits the DNA-binding activity of the positive-acting nitrogen regulatory protein NIT2. Biochemistry 34**:** 8861-8868.

Xu, J., X. Wang, L. Hu, J. Xia, Z. Wu, N. Xu, B. Dai and B. Wu, (2015) A novel ionic liquid-tolerant *Fusarium oxysporum* BN secreting ionic liquid-stable cellulase: Consolidated bioprocessing of pretreated lignocellulose containing residual ionic liquid. Bioresour Technol 181**:** 18-25.

Yan, T., D. Yoo, T. Z. Berardini, L. A. Mueller, D. C. Weems, S. Weng, J. M. Cherry and S. Y. Rhee, (2005) PatMatch: a program for finding patterns in peptide and nucleotide sequences. Nucleic Acids Res 33**:** W262-266.

Yang, F., B. W. Vought, J. S. Satterlee, A. K. Walker, Z. Y. Jim Sun, J. L. Watts, R. DeBeaumont, R. M. Saito, S. G. Hyberts, S. Yang *et al.*, (2006) An ARC/Mediator subunit required for SREBP control of cholesterol and lipid homeostasis. Nature 442**:** 700-704.

Yao, X., X. Wang and X. Xiang, (2014) FHIP and FTS proteins are critical for dynein-mediated transport of early endosomes in *Aspergillus*. Mol Biol Cell 25**:** 2181-2189.

Yeung, N., M. S. Cline, A. Kuchinsky, M. E. Smoot and G. D. Bader, (2008) Exploring biological networks with Cytoscape software. Curr Protoc Bioinformatics 23:8.13:8.13.1-8.13.20.

Yu, J. H., R. A. Butchko, M. Fernandes, N. P. Keller, T. J. Leonard and T. H. Adams, (1996) Conservation of structure and function of the aflatoxin regulatory gene *aflR* from *Aspergillus nidulans* and *A. flavus*. Curr Genet 29**:** 549-555.

Yuan, G. F., Y. H. Fu and G. A. Marzluf, (1991) *nit-4*, a pathway-specific regulatory gene of *Neurospora crassa*, encodes a protein with a putative binuclear zinc DNA-binding domain. Mol Cell Biol 11**:** 5735-5745.

Yue, D., N. Maizels and A. M. Weiner, (1996) CCA-adding enzymes and poly(A) polymerases are all members of the same nucleotidyltransferase superfamily: characterization of the CCA-adding enzyme from the archaeal hyperthermophile *Sulfolobus shibatae*. RNA 2**:** 895-908.

Zadra, I., B. Abt, W. Parson and H. Haas, (2000) *xylP* promoter-based expression system and its use for antisense downregulation of the *Penicillium chrysogenum* nitrogen regulator NRE. Appl Environ Microbiol 66**:** 4810-4816.

Zenke, F.T., R. Engels, V. Vollenbroich, J. Meyer, C.P. Hollenberg and K.D. Breunig, (1996) Activation of Gal4p by galactose-dependent interaction of galactokinase and Gal80p. Science 272: 1662-1665

Zhang, J., R. Qiu, H. N. Arst, Jr., M. A. Penalva and X. Xiang, (2014) HookA is a novel dynein-early endosome linker critical for cargo movement *in vivo*. J Cell Biol 204**:** 1009-1026.

Zhang, Y., T. Liu, C. A. Meyer, J. Eeckhoute, D. S. Johnson, B. E. Bernstein, C. Nusbaum, R. M. Myers, M. Brown, W. Li *et al.*, (2008) Model-based analysis of ChIP-Seq (MACS). Genome Biol 9**:** R137.

Zhao, M., X. Yang, Y. Fu, H. Wang, Y. Ning, J. Yan, Y. G. Chen and G. Wang, (2013) Mediator MED15 modulates transforming growth factor beta (TGFbeta)/Smad signaling and breast cancer cell metastasis. J Mol Cell Biol 5**:** 57-60.

Zhao, X., S. L. Hume, C. Johnson, P. Thompson, J. Huang, J. Gray, H. K. Lamb and A. R. Hawkins, (2010) The transcription repressor NmrA is subject to proteolysis by three *Aspergillus nidulans* proteases. Protein Sci 19**:** 1405-1419.

Zheng, X., X. Dai, Y. Zhao, Q. Chen, F. Lu, D. Yao, Q. Yu, X. Liu, C. Zhang, X. Gu *et al.*, (2007) Restructuring of the dinucleotide-binding fold in an NADP(H) sensor protein. Proc Natl Acad Sci USA 104**:** 8809-8814.

Zhong, G. W., P. Jiang, W. R. Qiao, Y. W. Zhang, W. F. Wei and L. Lu, (2014) Protein phosphatase 2A (PP2A) regulatory subunits ParA and PabA orchestrate septation and conidiation and are essential for PP2A activity in *Aspergillus nidulans*. Eukaryot Cell 13**:** 1494-1506.

Zhou, Z., and S. J. Elledge, (1992) Isolation of *crt* mutants constitutive for transcription of the DNA damage inducible gene *RNR3* in *Saccharomyces cerevisiae*. Genetics 131**:** 851-866.

[This page is not blank.]

Appendix A - Downes *et al*. (2013)

Research conducted as part of this dissertation for Chapter 3 "Leucine Biosynthesis" has been published in Downes D.J., M.A. Davis, S.D. Kreutzberger, B.L. Taig and R.B Todd (2013) Regulation of the NADP-glutamate dehydrogenase gene *gdhA* in *Aspergillus nidulans* by the Zn(II)2Cys6 transcription factor LeuB. *Microbiology* **159 (12):** 2467-2480 (doi:10.1099/mic.0.071514-0). My contribution to this work while at Kansas State University was the experimental design, real-time reverse-transcriptase PCR analysis, construction of 19 *A. nidulans* strains by crossing and transformation, *lacZ* expression assays, bioinformatics analyses, and writing the manuscript. The full article is included in this appendix.

Microbiology (2013), **159**, 2467–2480 **DOI** 10.1099/mic.0.071514-0

Regulation of the NADP-glutamate dehydrogenase gene *gdhA* in *Aspergillus nidulans* by the Zn(II)2Cys6 transcription factor LeuB

Damien J. Downes,[1,2] Meryl A. Davis,[2] Sara D. Kreutzberger,[2]† Brendan L. Taig[2] and Richard B. Todd[1,2]

Correspondence
Richard B. Todd
rbtodd@k-state.edu

[1]Department of Plant Pathology, Kansas State University, 4024 Throckmorton Plant Sciences Center, Manhattan, KS 66506, USA

[2]Department of Genetics, University of Melbourne, Parkville, VIC 3010, Australia

NADP-dependent glutamate dehydrogenase (NADP-GDH) is a key enzyme in the assimilation of alternative nitrogen nutrient sources through ammonium in fungi. In *Aspergillus nidulans*, NADP-GDH is encoded by *gdhA*. Several transcription factors are known to regulate *gdhA* expression, including AreA, the major transcription activator of nitrogen metabolic genes, and TamA, a co-activator of AreA. TamA also interacts with LeuB, the regulator of leucine biosynthesis. We have investigated the effects of leucine biosynthesis on *gdhA* regulation, and found that leucine regulates the levels of NADP-GDH activity and *gdhA* expression. We show, using mutants with perturbed levels of α-isopropylmalate (α-IPM), that this leucine biosynthesis intermediate affects *gdhA* regulation. Leucine regulation of *gdhA* requires a functional LeuB with an intact Zn(II)2Cys6 DNA-binding domain. By analysing the prevalence of putative LeuB DNA-binding sites in promoters of *gdhA* orthologues we predict broad conservation of leucine regulation of NADP-GDH expression within ascomycetes except in the fusaria and fission yeasts. Using promoter mutations in *gdhA–lacZ* reporter genes we identified two sites of action for LeuB within the *A. nidulans gdhA* promoter. These two sites lack sequence identity, with one site conforming to the predicted LeuB DNA-binding site consensus motif, whereas the second site is a novel regulatory sequence element conserved in *Aspergillus gdhA* promoters. These data suggest that LeuB regulates NADP-GDH expression in response to leucine levels, which may act as an important sensor of nitrogen availability.

Received 18 July 2013
Accepted 10 September 2013

INTRODUCTION

Ammonium is the preferred nitrogen source for many micro-organisms and its assimilation requires the activity of NADP-dependent glutamate dehydrogenase (NADP-GDH). NADP-GDH catalyses the synthesis of glutamate from 2-oxoglutarate, an intermediate of the Krebs cycle, and ammonium sourced from either the external environment or internally via metabolism. In *Aspergillus nidulans* and *Neurospora crassa*, NADP-GDH is encoded by a single gene, *gdhA* and *am*, respectively (Arst & MacDonald, 1973; Gurr *et al.*, 1986; Hawkins *et al.*, 1989; Kinghorn & Pateman, 1973, 1975; Kinnaird & Fincham, 1983). In contrast, *Saccharomyces cerevisiae* has two NADP-GDH genes, *GDH1* and *GDH3*, which are active under different growth conditions (Avendaño *et al.*, 1997; DeLuna *et al.*, 2001). Mutants of *gdhA*, *am* or *GDH1*/*GDH3* lacking NADP-GDH function have reduced growth on ammonium compared with WT strains (Arst & MacDonald, 1973; Avendaño *et al.*, 1997; Fincham, 1988; Fincham & Baron, 1977; Fincham *et al.*, 2000; Kinghorn & Pateman, 1973). In *A. nidulans*, *gdhA* mutants are leaky as the assimilation of nitrogen through ammonium occurs by the non-preferred route of glutamine synthetase and glutamate synthetase (Arst *et al.*, 1975; Kinghorn & Pateman, 1976; Macheda *et al.*, 1999; Margelis *et al.*, 2001). *gdhA* mutants also show derepression of several alternative nitrogen assimilation pathways (Hynes, 1974; Kinghorn & Pateman, 1973; Pateman *et al.*, 1973). As NADP-GDH is the primary assimilation route for nitrogen sources via ammonium, draws substrates from the tricarboxylic acid cycle and is required for correct regulation of alternative nitrogen assimilation genes, its synthesis is highly regulated, particularly in response to different nitrogen sources.

In *A. nidulans*, *gdhA* mRNA is highly expressed during growth on ammonium and glutamine, whereas strains

†Present address: Rand Farm Supplies, Lot 5/Kindra St, Rand, NSW 2642, Australia.

Abbreviations: α-IPM, α-isopropylmalate; β-IPM, β-isopropylmalate; NADP-GDH, NADP-dependent glutamate dehydrogenase.

grown on glutamate have lower levels of *gdhA* mRNA expression (Hawkins *et al.*, 1989). This pattern of regulation by these nitrogen sources is also observed for NADP-GDH activity (Pateman, 1969), and is conserved in *Aspergillus awamori* and *Botrytis cinerea* (Cardoza *et al.*, 1998; Santos *et al.*, 2001). Additionally, Caddick *et al.* (2006) found that different nitrogen regimes do not regulate stability of the *gdhA* mRNA transcript. Therefore, differences in *gdhA* expression are likely due to transcriptional regulation. Several transcription factors are known to regulate NADP-GDH expression. In *N. crassa*, *am* is regulated by the CCAAT-binding factor AAB (Chen & Kinsey, 1994; Chen *et al.*, 1998; Frederick & Kinsey, 1990a, b), as well as the global nitrogen utilization GATA transcription factor NIT2 (Dantzig *et al.*, 1979). Likewise, *S. cerevisiae* requires the homologues of these transcription factors, HAP2/3/4/5 and Gln3p, respectively, for full expression of *GDH1* and *GDH3* (Dang *et al.*, 1996; Daugherty *et al.*, 1993; Hernández *et al.*, 2011; Riego *et al.*, 2002). *GDH1* and *GDH3* encode isomers that arose during whole-genome duplication and they are differentially expressed dependent upon the carbon sources available in a mechanism involving chromatin remodelling by Swi/SNF and Gcn5p (Avendaño *et al.*, 2005; DeLuna *et al.*, 2001). *GDH1* is also regulated by the amino acid starvation pathway transcription regulator Gcn4p (Hinnebusch, 1988; Riego *et al.*, 2002) and the leucine biosynthesis pathway transcription regulator Leu3p (Hu *et al.*, 1995). *A. nidulans gdhA* is regulated by the CCAAT-binding complex AnCF (Papagiannopoulos *et al.*, 1996; M. A. Davis unpublished data) and the global nitrogen regulator AreA (Christensen *et al.*, 1998). AreA is itself highly regulated by multiple mechanisms, including autogenous regulation and differential transcript stability (Caddick *et al.*, 2006; Langdon *et al.*, 1995; Morozov *et al.*, 2000, 2001, 2010; Platt *et al.*, 1996), regulated nuclear export (Todd *et al.*, 2005), and interactions with the co-repressor NmrA (Andrianopoulos *et al.*, 1998; Kotaka *et al.*, 2008; Lamb *et al.*, 2004) and a co-activator TamA (Davis *et al.*, 1996; Small *et al.*, 1999, 2001). These mechanisms combine to minimize AreA activation of most nitrogen catabolic target genes during growth on ammonium (reviewed by Wong *et al.*, 2008). However, the regulation of certain genes for ammonium uptake and assimilation, such as *meaA* (Monahan *et al.*, 2006) and *gdhA*, is markedly different than the regulation of AreA-regulated catabolic genes. High-level expression of *gdhA* requires AreA for activation during growth on ammonium (Christensen *et al.*, 1998; Polotnianka *et al.*, 2004). It was hypothesized that additional *gdhA* promoter-specific proteins may assist activation. Investigation of the co-activator TamA, which interacts with the extreme C-terminus of AreA, revealed that *tamA*Δ has a more severe effect than *areA*Δ on NADP-GDH levels, suggesting that TamA has a role in *gdhA* regulation in addition to its role as a co-activator of AreA (Polotnianka *et al.*, 2004; Small *et al.*, 1999). A yeast two-hybrid screen for proteins that interact with TamA identified LeuB, the homologue of *S. cerevisiae* Leu3p, which regulates the synthesis of leucine (Polotnianka *et al.*, 2004).

S. cerevisiae Leu3p acts as a dual activator/repressor and has DNA-binding sites in the promoters of several genes in the branched-chain amino acid biosynthesis pathway, including *BAT1*, *LEU1*, *LEU2*, *LEU4*, *ILV2* and *ILV5* (Friden & Schimmel, 1988; Hellauer *et al.*, 1996; Kohlhaw, 2003). Leu3p transcriptional activation function requires α-isopropylmalate (α-IPM), the product of α-IPM synthetase encoded by *LEU4* and *LEU9* (Baichwal *et al.*, 1983; Casalone *et al.*, 2000; Chang *et al.*, 1984, 1985). High cellular leucine levels inhibit α-IPM synthetase activity, reducing α-IPM abundance and converting Leu3p to a repressor (Sze *et al.*, 1992). LeuB and Leu3p are required for WT levels of expression of NADP-GDH from *gdhA* and *GDH1*, respectively (Hu *et al.*, 1995; Polotnianka *et al.*, 2004). In this paper, we characterize the effects of loss of α-IPM synthetase or α-IPM isomerase activity on *gdhA* expression in *A. nidulans*, and provide evidence that changes in α-IPM levels regulate NADP-GDH gene expression. We identify conserved putative LeuB/Leu3p sites in *gdhA* orthologues in certain phylogenetic groups within the Ascomycota. We also determine that the activity of LeuB as a transcriptional regulator requires a functional Zn(II)2Cys6 DNA-binding domain for activation of *gdhA* expression through two promoter elements, only one of which conforms to the known Leu3p consensus DNA-binding motif.

METHODS

***A. nidulans* strains, media and growth conditions.** *A. nidulans* strains used in this study are listed in Table 1 using annotation described by Clutterbuck (1974). *A. nidulans* growth conditions and media were as described by Cove (1966), with pH adjusted to 6.5. *Aspergillus* nitrogen-free minimal medium (ANM), appropriately supplemented for auxotrophies, contained 1 % (w/v) glucose as the carbon source and nitrogen sources at a final concentration of 10 mM. Genetic analysis was performed as described by Clutterbuck (1974) and Todd *et al.* (2007).

Transformation and enzyme assays. *A. nidulans* protoplasts were prepared according to Yelton *et al.* (1984), with omission of β-glucuronidase and replacement of Novozyme 234 by Lysing Enzymes (Sigma), and transformation was carried out as described by Andrianopoulos & Hynes (1988), except with 10–30 min PEG treatments and omission of the wash to remove PEG prior to plating. β-Galactosidase and NADP-GDH assays were performed as described by Davis *et al.* (1988) and Pateman (1969), respectively, using soluble protein extracts from mycelia grown for 16 h at 37 °C. β-Galactosidase specific activity is expressed as $A_{420\ nm} \times 10^3$ per minute per milligram of soluble protein. One unit of NADP-GDH specific activity is defined as 1 nmol NADP reduced per minute per milligram of soluble protein. Protein concentrations were calculated according to Bradford (1976) using the Bio-Rad Protein Assay reagent (Bio-Rad) following the manufacturer's instructions.

Molecular techniques. *Escherichia coli* strains used in this study were Top 10 (Invitrogen) and NM522 (Promega). Standard DNA manipulation methods were as described by Sambrook & Russell (2001). *Ex Taq* (TaKaRa) or Phusion (Finnzymes) DNA polymerases

Table 1. *A. nidulans* strains used in this study

Strain	Genotype
MH1	*biA1*
MH11036	*pyroA4 nkuA*Δ::*argB riboB2*
MH11094	*amdS–lacZ pyroA4 nkuA*Δ::*Bar niiA4*
MH11879	*wA1 pyroA4*
MH12101	*A.f.pyroA–gdhA*(–753 bp) *–lacZ@amdS pyroA4 nkuA*Δ::*Bar niiA4*
MH12106	*A.f.pyroA–gdhA*(−487 to −368)–*gpdA*p_{mini}–*lacZ@amdS pyroA4 nkuA*::*Bar niiA4*
MH12179	*leuB*Δ::*riboB A.f.pyroA–gdhA*(−487 to −368)–*gpdA*p_{mini}–*lacZ@amdS pyroA4 niiA4*
MH12181	*biA1 leuB*Δ::*riboB A.f.pyroA–gdhA*(−753 bp)–*lacZ@amdS pyroA4 niiA4*
MH12609	*yA1 pabaA1 leuB*Δ::*riboB pyroA4 nkuA*Δ::*Bar niiA4*
MH12620	*pabaA1 leuB*^{C69A}–*A.f.pyroA pyroA4 nkuA*Δ::*Bar riboB2 niiA4*
RT93	*pabaA1 leuB*^{C69A}–*A.f.pyroA A.f.pyroA–gdhA*(−753 bp)–*lacZ@amdS pyroA4 nkuA*Δ::*Bar riboB2 niiA4*
RT152	*A.f.pyroA–gdhA*(−753 bp Δ–431 to −422)–*lacZ@amdS pyroA4 nkuA*Δ::*Bar niiA4*
RT155	*A.f.pyroA–gdhA*(−753 bp Δ–501 to −492)–*lacZ@amdS pyroA4 nkuA*Δ::*Bar niiA4*
RT156	*A.f.pyroA–gdhA*(−753 bp Δ–250 to −241)–*lacZ@amdS pyroA4 nkuA*Δ::*Bar niiA4*
RT157	*A.f.pyroA–gdhA*(−753 bp Δ–501 to −492, Δ–250 to −241)–*lacZ@amdS pyroA4 nkuA*Δ::*Bar niiA4*
RT182	*biA1 luA1 A.f.pyroA–gdhA*(−753 bp)–*lacZ@amdS niiA4*
RT195	*biA1 leuB*Δ::*riboB A.f.pyroA–gdhA*(−753 bp Δ–431 to −422)–*lacZ@amdS pyroA4 nkuA*Δ::*Bar niiA4*
RT198	*biA1 leuB*Δ::*riboB, A.f.pyroA–gdhA*(−753 bp Δ–501 to −492)–*lacZ@amdS pyroA4 nkuA*Δ::*Bar niiA4*
RT201	*biA1 leuB*Δ::*riboB A.f.pyroA–gdhA*(−753 bp Δ–250 to −241)–*lacZ@amdS pyroA4 nkuA*Δ::*Bar niiA4*
RT204	*biA1 leuB*Δ::*riboB A.f.pyroA–gdhA*(−753 bp Δ–501 to −492, Δ–250 to −241)–*lacZ@amdS pyroA4 nkuA*Δ::*Bar niiA4*
RT219	*pyroA4 nkuA*Δ::*argB riboB2 leuC*Δ::*A.f.pyro*
RT220	*A.f.pyroA–gdhA*(−753 bp)–*lacZ@amdS pyroA4 nkuA*Δ::*argB riboB2 leuC*Δ::*A.f.pyro niiA4*
RT349	*A.f.pyroA–gdhA*(−753 bp Δ–501 to −492, Δ–431 to −422, Δ–250 to −241)–*lacZ@amdS pyroA4 nkuA*Δ::*Bar niiA4*
RT350	*biA1 leuB*Δ::*riboB A.f.pyroA–gdhA*(−753 bp Δ–501 to −492, Δ–431 to −422, Δ–250 to −241)–*lacZ@amdS pyroA4 nkuA*Δ::*Bar*
RT352	*A.f.pyroA–gdhA*(−753 bp Δ–501 to −241)–*lacZ@amdS pyroA4 nkuA*Δ::*Bar niiA4*
RT353	*biA1 leuB*Δ::*riboB A.f.pyroA–gdhA*(−753 bp Δ–501 to −241)–*lacZ@amdS pyroA4 nkuA*Δ::*Bar niiA4*
RT356	*A.f.pyroA–gdhA*(−240 bp)–*lacZ@amdS pyroA4 nkuA*Δ::*Bar niiA4*
RT357	*biA1 leuB*Δ::*riboB A.f.pyroA–gdhA*(−240 bp)–*lacZ@amdS pyroA4 nkuA*Δ::*Bar*
RT373	*biA1 acuJ*p_{mini}–*lacZ@argB nkuA*Δ::*Bar pyroA4 tamA*Δ
RT374	*biA1 acuJ*p_{mini}–*lacZ@argB nkuA*Δ::*Bar leuB*Δ::*riboB pyroA4 tamA*Δ

were used for PCR. Restriction enzymes (Promega) were used following the manufacturer's instructions. Plasmid DNA was prepared using the Wizard Plus SVMinipreps DNA Purification System (Promega) and genomic DNA was isolated according to Lee & Taylor (1990). Applied Genetic Diagnostics (University of Melbourne, Australia) or Kansas State University DNA Sequencing and Genotyping Facility (Kansas, USA) carried out DNA sequencing. For Southern analysis, DNA was transferred from gels to Hybond-N+ membranes (GE Healthcare) using 0.4 M NaOH. Probes were made either by random hexanucleotide priming with [α-^{32}P]dATP (Bresatec) and the Klenow fragment of DNA polymerase I (Promega) or the DIG High Prime DNA Labelling and Detection Starter Kit II (Roche) following the manufacturer's instructions.

Deletion of AN0840 (*leuC*). A 3.3 kb genomic DNA fragment containing AN0840 (*leuC*) (−975 to +2302) was amplified from MH1 using primers leuCfwd (5′-CCACCTTCCACTAAGTTGAA-3′) and leuCrev (5′-ATTATATTGGCGGGTGAGCA-3′), and cloned into pGEM-T-easy (Promega) to create pBT7168. The *Bam*HI–*Nru*I fragment of pSM6358 containing the *A. fumigatus pyroA* (*A.f.pyroA*) selectable marker was cloned into the *Bgl*II and *Stu*I sites of *leuC* in pBT7168 replacing bases –92 to +1986 and creating plasmid pDD7537. The deletion cassette was amplified with leuCfwd and leuCrev, and transformed into MH11036 (*pyroA4 nkuA*Δ *riboB2*). Transformants were selected for pyridoxine prototrophy, tested for leucine auxotrophy and single-copy gene replacement of *leuC* confirmed by Southern analysis. Segregation was confirmed by crossing to MH11879 (*wA1 pyroA4*). Complementation of the *leuC*Δ mutant was performed by gene-targeting WT *leuC* (pBT7168) to *leuC*Δ 5′ flanking sequences by single crossover in RT219 (*pyroA4 nkuA*Δ *leuC*Δ *riboB2*). Leucine prototrophs were directly selected. Integration of *leuC*$^+$ was confirmed by Southern blot.

Construction of a *leuB*^{C69A} mutant. pRP5390 (Polotnianka *et al.*, 2004) was digested with *Stu*I/*Eco*RV and self-ligated to produce pBT6962. Inverse PCR of pBT6962 using leuBzfinv1 (5′-Phos-GACGGACGCTTCCCGCT-3′; mutation underlined) and leuBzdinv2 (5′-Phos-CATGGATCCTGGACAACATC-3′) and subsequent ligation mutated TG to GC in pBT7164. The *Sna*BI–*Spe*I fragment was ligated into *Sma*I/*Spe*I-cut pSM6363 containing *A.f.pyroA* to create pDD7536. pDD7536 was transformed into MH12609 (*yA1 pabaA1 leuB*Δ *pyroA4 nkuA*Δ *niiA4*) and transformants were selected for pyridoxine prototrophy. Single-copy integrants targeted to the 5′ flank of the *leuB*Δ were confirmed by Southern analysis.

Construction of *gdhA* reporter fusions. *gdhA* promoter fragments were amplified by PCR from MH1 genomic DNA using the gdhA5Xho (5′-CCGCTCGAGGCATATACAGCAGCGGCAC-3′) forward primer with the gdhA2BglII (5′-GAAGATCTGGAAGGTTAGACATTTTTGCG-3′) reverse primer. PCR products digested with *Xho*I and *Bgl*II were ligated into *Xho*I/*Bam*HI-cut pYS7225, a plasmid containing a 3′ truncated *gpdA*p_{mini}–*lacZ* fusion from pAN5-mini

lacking the 3′ 370 codons of *lacZ* (Punt *et al.*, 1995) and *A.f.pyroA* from pSM6363 (M. J. Hynes, M. A. Davis and S. Murray unpublished). Ligation into *Xho*I/*Bam*HI sites replaced the *gpdA* sequence creating translational fusion of *gdhA–lacZ* in pSL6976. The −487 to −368 bp *gdhA* promoter fragment was amplified with gdhAfwdXho2 (5′-CCGCTCGAGGCTTCCGCCCAGAGATAA-3′) and gdhArevPst1 (5′-AACTGCAGAGGAACCATAGGATCGGAA-3′). The *Xho*I/*Pst*I-digested PCR product was cloned into pYS7225 creating pSL6973, containing the *gdhA* promoter fragment in the *gpdA*p_{mini}–*lacZ* reporter. These plasmids were transformed into MH11094 (*amdS–lacZ pyroA4 nkuA*Δ *niiA4*) and targeted to *amdS–lacZ* to generate full-length *gdhA–lacZ* fusions by homologous recombination (Nayak *et al.*, 2006). Transformants were selected for pyridoxine prototrophy and single-copy integrants were confirmed by Southern analysis.

Mutation of the *gdhA* promoter. Inverse PCR mutagenesis of pDD149 containing the *Xho*I–*Hin*dIII *gdhA* promoter fragment from pSL6976 in pBluescriptSK+ (Stratagene) was performed by amplification with leu1delfwd (5′-Phos-GTGGGCTTCCGCCCAGAGATAA-3′) and leu1delrev (5′-Phos-AATCCGGGACATTCTCGTGAC-3′) to delete bases −501 to −492, leu2delfwd (5′-Phos-CAGTATACTCATTCGCCGGCC-3′) and leu2delrev (5′-Phos-AATCCGGGACATTCTCGTGAC-3′) to delete bases −250 to −241, condelfwd (5′-Phos-CCTTGCTAGTATTAGCTTTGTGC-3′) and condelrev (5′-Phos-GGGTGTTAGTCGAACGTTTA-3′) to delete bases −431 to −422, leu2delfwd and leu1delrev to delete bases −501 to −241, and leu2delfwd and sk+xhorev (5′-Phos-CTCGAGGGGGGGCCC-3′) to create a 5′ truncation at −240 bp. Self-ligation of PCR products produced pDD134, pDD135, pDD130, pDD205 and pDD208, respectively. pDD134 was further amplified with leu2delfwd and leu2delrev, and ligated to create pDD136; subsequent amplification with condelfwd and condelrev produced pDD204. The mutated *Xho*I–*Hin*dIII promoter fragments were cloned into *Xho*I/*Hin*dIII-cut pSL6976, replacing the WT *gdhA* promoter, to make pDD137 (Δ–501 to −492), pDD138 (Δ–250 to −241), pDD131 (Δ–431 to −422), pDD207 (Δ–501 to −241), pDD210 (−240 bp), pDD139 (Δ–501 to −492, Δ–250 to −241) and pDD206 (Δ–501 to −492, Δ–431 to −422, Δ–250 to −241). These plasmids were gene-targeted in single copy in MH11094 as above.

DNA-binding site alignments. The 1.0 kb *gdhA* upstream sequences from *Aspergillus clavatus*, *A. nidulans*, *Aspergillus niger*, *Aspergillus oryzae*, *Aspergillus flavus*, *Aspergillus fumigatus*, *Aspergillus terreus* and *Neosartorya fischeri* (also known as *Aspergillus fischeri*) were obtained from the Broad Institute database (http://www.broadinstitute.org/annotation/genome/aspergillus_group). The 1.0 kb upstream sequences of *LEU1*, *LEU2*, *LEU4*, *ILV2* and *ILV5* were sourced from the *Saccharomyces* Genome Database, SGD (www.yeastgenome.org) (Cherry *et al.*, 2012). The 1.0 kb upstream sequences of *luA*, *leuC*, AN0912, AN4956 and AN2525 were sourced from the *Aspergillus* Genome Database, AspGD (www.aspgd.org) (Arnaud *et al.*, 2012). Putative DNA-binding sites and flanking nucleotides were identified through manual searches for $CCGN_4CGG$ consensus sites and manually aligned. Consensus motifs of aligned sequences were generated using WebLogo (www.weblogo.berkley.edu) (Crooks *et al.*, 2004; Schneider & Stephens, 1990).

DNA and protein sequences and phylogenetic analyses. Gene identification and primary analysis were performed using AspGD and SGD (Arnaud *et al.*, 2012; Cherry *et al.*, 2012). *In silico* manipulation of DNA and protein sequences was carried out in Geneious version 5.3.5 created by Biomatters (http://www.geneious.com). Alignments, unless otherwise stated, were performed using CLUSTALW2 (Larkin *et al.*, 2007) and shaded using MacBoxshade 2.15E (M. D. Baron) with default settings. For phylogenetic analysis of ascomycete NADP-GDH promoters, genes were identified by BLASTP using full-length *A. nidulans* GdhA and *S. cerevisiae* Gdh1p, and the Broad Institute Fungal Genomes Initiative FGI: Fungal Genomes Protein database (http://www.broadinstitute.org/annotation/genome/FGI_Blast/Blast.html, 15 April 2013). The NADP-GDH protein sequences identified were used to construct an unrooted neighbour-joining phylogenetic tree in Geneious using the default settings.

RESULTS

Leucine inhibits *gdhA* expression

In *S. cerevisiae*, the LeuB orthologue, Leu3p, is activated by α-IPM, a leucine biosynthesis intermediate produced when cellular levels of leucine are low. High cellular leucine levels deplete α-IPM and cause Leu3p to function as a repressor (reviewed by Kohlhaw, 2003). To determine the effects of leucine availability on *gdhA* regulation in *A. nidulans* we examined the effects of exogenous leucine on levels of the native NADP-GDH enzyme and a *gdhA–lacZ* reporter gene. We gene-targeted in single copy a reporter construct containing a translational fusion of −753 bp of the *gdhA* promoter to *lacZ*. Like the native *gdhA* transcript and NADP-GDH enzyme (Hawkins *et al.*, 1989; Pateman, 1969), the *gdhA–lacZ* reporter gene was highly expressed during growth in the presence of ammonium or glutamine and had reduced levels of expression during growth on glutamate (Fig. 1a). Consistent with previous reports of NADP-GDH enzyme activity (Pateman, 1969), over the 5–20 mM range the effect of nitrogen source rather than the effect of nitrogen concentration was the main determinant of *gdhA–lacZ* levels. Both the *gdhA–lacZ* reporter (Fig. 1b) and NADP-GDH encoded by the WT gene (Table 2) showed lower levels of activity in the presence of 2 mM leucine than in its absence, consistent with conservation of the mechanism of leucine metabolic control of NADP-GDH expression between *A. nidulans* and yeast. No negative effect on levels of the *gdhA–lacZ* reporter resulted from addition of the other two branched-chain amino acids, isoleucine and valine, or by tyrosine (Fig. 1b).

α-IPM levels modulate *gdhA* expression

During leucine biosynthesis, α-IPM produced by α-IPM synthetase is converted by α-IPM isomerase to β-isopropylmalate (β-IPM). In *A. nidulans*, α-IPM isomerase is encoded by *luA* and the loss-of-function mutant *luA1* is a leucine auxotroph (Polotnianka *et al.*, 2004). However, the gene for α-IPM synthetase has not been characterized. *S. cerevisiae* α-IPM synthetase is encoded by two genes, *LEU4* and *LEU9* (Casalone *et al.*, 2000; Chang *et al.*, 1984, 1985). BLASTP searches of the *A. nidulans* non-redundant protein sequence database with Leu4p and Leu9p identified a single protein encoded by AN0840, which we named *leuC*. BLASTN and TBLASTN searches of the *A. nidulans* genome sequence indicated that AN0840 is unique. Alignment of Leu4p, Leu9p and LeuC protein sequences revealed strong conservation throughout the protein, including the leucine feedback regulatory R-region (Cavalieri *et al.*, 1999) (Fig. 1c), consistent with the three α-IPM synthetases sharing the

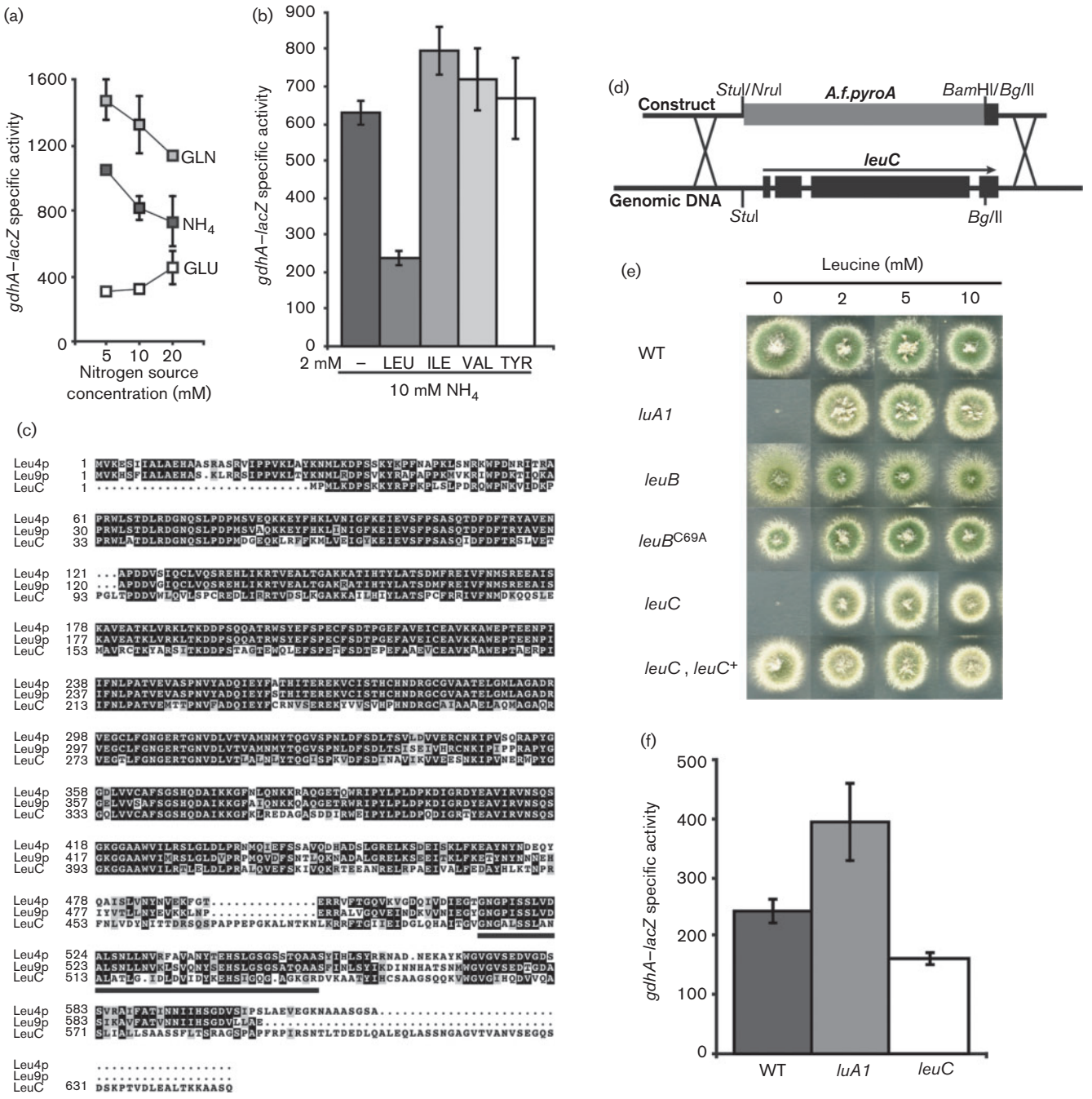

Fig. 1. Leucine biosynthesis regulates *gdhA–lacZ*. (a) LacZ enzyme activity was assayed for the *gdhA–lacZ* reporter strain, with 753 bp of the *gdhA* promoter fused to *lacZ*, grown on 1 % glucose-minimal media (ANM) supplemented with 5, 10 or 20 mM ammonium tartrate (NH_4), glutamate (GLU) or glutamine (GLN), and (b) grown on ANM with 10 mM ammonium tartrate in the presence or absence of 2 mM leucine (LEU), isoleucine (ILE), valine (VAL) or tyrosine (TYR) for 16 h at 37 °C. (c) Alignment of α-IPM synthetases from *S. cerevisiae* and *A. nidulans*. The protein sequences for *S. cerevisiae* Leu4p (YNL104C), Leu9p (YOR108W) and *A. nidulans* LeuC (AN0840) were aligned using CLUSTALW2 and shaded using MacBoxshade. The R-region in Leu4p, which is required for leucine feedback regulation (Cavalieri *et al.*, 1999), is underlined. (d) *leuC* (AN0840) was deleted by gene replacement with an *A.f.pyroA* cassette. Black boxes, *leuC* exons; horizontal lines, *leuC* flanking DNA or introns; grey box, selectable marker. The direction of *leuC* transcription is indicated by an arrow. (e) *luA1*, *leuB*Δ, *leuB*^{C69A} and *leuC*Δ leucine biosynthesis mutants as well as complemented *leuC*Δ (*leuC*Δ, *leuC*$^{+}$) and WT strains were grown for 2 days on 10 mM ammonium tartrate in the presence of 0, 2, 5 and 10 mM leucine. (f) A WT strain and leucine biosynthesis mutants *luA1* and *leuC*Δ were assayed for expression of the *gdhA–lacZ* reporter after 16 h growth in ANM supplemented with 10 mM ammonium tartrate and 2 mM leucine at 37 °C. For assays in (a), (b) and (f) soluble protein extracts were prepared from mycelia and measured for β-galactosidase specific activity. Error bars, SEM ($n \geqslant 3$).

Table 2. Leucine biosynthesis regulates NADP-GDH activity

Genotype	NADP-GDH enzyme activity*	
	NH_4	NH_4 + 2 mM leucine
WT	118.4 (±7.88)	62.35 (±8.48)
*leuB*Δ	42.84 (±3.38)	ND
leuB^{C69A}	66.83 (±4.71)	ND
luA1	ND	142.1 (±16.43)

*NADP-GDH enzyme specific activity was assayed for soluble protein extracts of mycelia grown in 1% glucose-minimal media supplemented with 10 mM ammonium tartrate (NH_4) for 16 h at 37 °C in the presence or absence of 2 mM leucine. SEM is given in parentheses ($n \geqslant 3$). ND, Not determined.

same common ancestor (Larson & Idnurm, 2010). LeuC has a C-terminal extension absent in both Leu4p and Leu9p. We cloned the *leuC* gene using PCR primers designed to the genome sequence and deleted *leuC* by homologous gene replacement with the *A.f.pyroA* selectable marker (Fig. 1d). The *leuC*Δ mutant is a strict leucine auxotroph, indicating that *leuC* is the only significant α-IPM synthetase-encoding gene in *A. nidulans* (Fig. 1e). In an outcross, leucine auxotrophy segregated as a single gene with reduced viability of *leuC*Δ progeny and co-segregated with the *A.f.pyroA* selectable marker (data not shown). Complementation of *leuC*Δ with WT *leuC* restored leucine prototrophy (Fig. 1e).

The *luA1* α-IPM isomerase mutant, predicted to have higher levels of α-IPM due to inability to convert α-IPM to β-IPM, showed higher levels of *gdhA–lacZ* expression (Fig. 1f) and NADP-GDH enzyme specific activity (Table 2) than the WT strain. Conversely, the *leuC*Δ α-IPM synthetase mutant, unable to synthesize α-IPM, had lower levels of *gdhA–lacZ* expression than WT (Fig. 1f). Overall, the genetic data indicate that the levels of α-IPM influence the levels of activation of *gdhA* expression.

LeuB DNA-binding domain is required for function

To determine the contribution of LeuB to *gdhA* expression we measured NADP-GDH enzyme activity and *gdhA–lacZ* reporter levels in a *leuB*Δ mutant. NADP-GDH enzyme activity (Table 2) and *gdhA–lacZ* reporter levels (Fig. 2a) were reduced in a *leuB*Δ mutant compared with WT during growth on ammonium. Unlike in WT, there was no negative effect of leucine addition in a *leuB*Δ mutant. Therefore, inhibition of *gdhA–lacZ* expression by leucine is LeuB dependent. To avoid any potential complications due to effects of *leuB*Δ on general protein synthesis and amino acid starvation, *leuB* mutant strains were supplemented with 2 mM leucine for subsequent *gdhA–lacZ* experiments.

To determine whether LeuB contributes to *gdhA* expression as a DNA-binding protein, we assessed the effect of

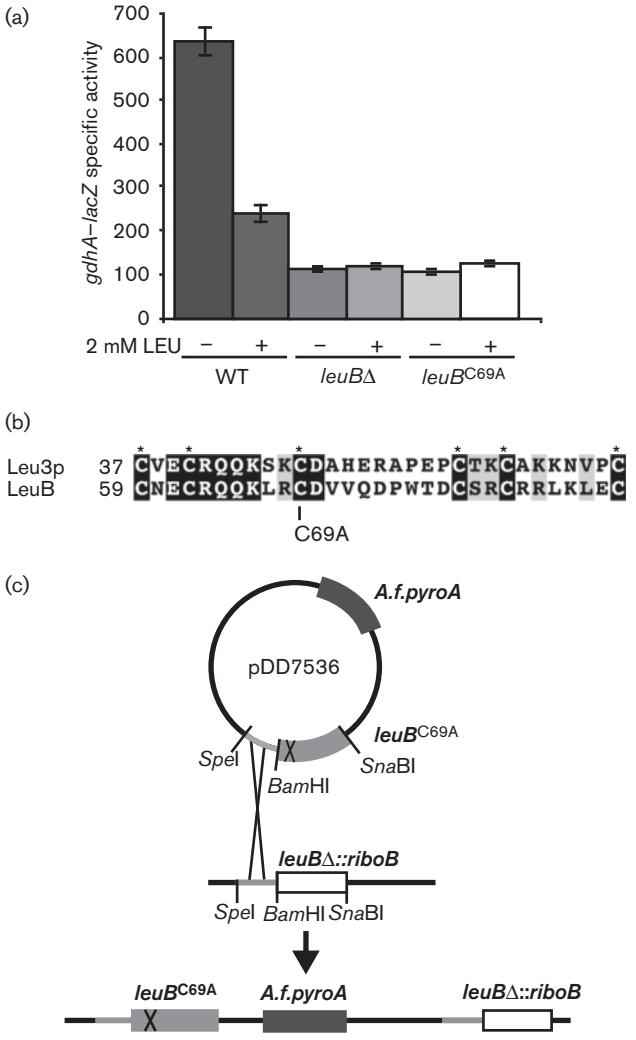

Fig. 2. LeuB requires a functional zinc cluster for activation of *gdhA–lacZ* expression. (a) WT, *leuB*Δ and *leuB*^{C69A} strains containing the *gdhA–lacZ* reporter were grown for 16 h in appropriately supplemented 1% glucose-minimal medium in the presence of 10 mM ammonium tartrate with or without 2 mM leucine (LEU). Soluble protein extracts were prepared from mycelia and assayed for β-galactosidase specific activity. Error bars, SEM ($n \geqslant 3$). (b) Alignment of zinc cluster regions from Leu3p and LeuB with six conserved cysteines (*). The codon encoding the third cysteine of *leuB* was mutated to produce C69A. (c) Single crossover between pDD7536 and the 5′ region of *leuB*Δ::*riboB* created a full-length copy of *leuB*^{C69A} under the control of the native promoter.

specifically altering the LeuB zinc cluster DNA-binding motif while retaining the remainder of the protein. Mutation of the third cysteine codon of the Leu3p zinc cluster confers loss of function (Bai & Kohlhaw, 1991). We mutated the equivalent codon to an alanine codon to generate *leuB*^{C69A} (Fig. 2b). The mutant gene was targeted in single copy at *leuB* in a *leuB*Δ mutant (Fig. 2c). The

leuB^{C69A} transformant, like *leuB*Δ, is a leaky leucine auxotroph (Fig. 1e). Furthermore, the level of reduction of *gdhA–lacZ* activity was equivalent for *leuB*Δ and *leuB*^{C69A} strains (Fig. 2a). Mutation of the LeuB DNA-binding domain also reduced NADP-GDH enzyme activity expressed from the WT promoter (Table 2). Therefore, although currently it is not possible to preclude other effects of this mutation such as those on protein stability or protein folding, the most likely explanation is that the DNA-binding domain of LeuB is required for WT regulation of both leucine biosynthesis and *gdhA* expression.

Identification of predicted LeuB DNA-binding sites in the *gdhA* promoter

Zn(II)2Cys6 proteins usually bind DNA as dimers. The amino acid sequence between the final cysteine residue of the zinc binuclear cluster and the first heptad repeat of the coiled-coils together with the DNA sequence of the target site are thought to determine DNA-binding site specificity (Liang *et al.*, 1996; Marmorstein *et al.*, 1992; Noël & Turcotte, 1998; Reece & Ptashne, 1993). Alignment of the linker–heptad regions of Leu3p and LeuB showed conservation of both the linker length and hydrophobic residues at the 1 and 4 positions of three heptads (Fig. 3a). Therefore, like Leu3p, LeuB is predicted to bind everted CCG triplet repeats separated by a 4 nt spacer, $CCGN_4CGG$ (Hellauer *et al.*, 1996; Mamane *et al.*, 1998). We compared the promoter sequences of five *A. nidulans* leucine biosynthesis pathway genes with *S. cerevisiae* homologues that are directly regulated by Leu3p binding. The 1.0 kb sequences upstream of the ATG start codons of *luA* (*LEU1*), AN0912 (*LEU2*), *leuC* (*LEU4*), AN4956 (*ILV2*) and AN2525 (*ILV5*) contain multiple direct, inverted and everted CCG/CGG triplet repeat pairs; however, the only spacing between triplets found in all five promoters was 4 bp (data not shown), consistent with LeuB recognizing DNA-binding sites conforming to a $CCGN_4CGG$ consensus. Interestingly, the N_4 spacer region of putative LeuB DNA-binding sites shows less conservation than that for Leu3p (Fig. 3b). In *S. cerevisiae*, Leu3p recognizes the same consensus motif in the *GDH1* promoter as that found in leucine biosynthesis gene promoters (Hellauer *et al.*, 1996). We also identified two putative LeuB DNA-binding sites, CCGCAAGCGG and CCGACTCCGG at −501 to −492 and −250 to −241 bp, respectively, upstream of the *gdhA* start codon (Fig. 3c). We searched the promoters of *gdhA* genes from seven closely related *Aspergillus* species for $CCGN_4CGG$ sites. In all of these species, a proximal site was found within 300 bp of the *gdhA* start codon, and in three species (*A. fumigatus*, *A. terreus* and *N. fischeri*) a second distal site was also identified between 780 and 470 bp upstream of the start codon. Alignment of the distal sites and proximal sites from each species shows absolute conservation of the proximal binding site, whereas the distal binding site has conserved triplets but less conservation of the spacer region (Fig. 3d).

Putative LeuB binding sites are present in NADP-GDH gene promoters in many ascomycetes

Regulation of NADP-GDH expression by leucine biosynthesis has only been reported in *A. nidulans* (Polotnianka *et al.*, 2004; this work) and *S. cerevisiae* (Hu *et al.*, 1995). We were interested to what extent this mechanism may operate throughout the Ascomycota. By BLASTP analysis of sequenced genomes available from the Broad Institute searched with the protein sequences of Gdh1p and GdhA, we identified 44 NADP-GDH-encoding genes from ascomycetes. These 44 genes represent 21 unique genera and 38 unique species. Our analysis included multiple sequenced isolates of *Candida albicans* (two), *Histoplasma capsulatum* (three) and *Paracoccidioides brasiliensis* (three) for within-species comparison. *S. cerevisiae* was the only species with multiple NADP-GDH-encoding genes. No putative Leu3p/LeuB sites ($CCGN_4CGG$) were found 1.0 kb upstream of 18 *gdhA* orthologues, 16 NADP-GDH gene promoters contained a single putative LeuB binding site and 10 of the promoters contained two predicted LeuB sites (Fig. 4). None of the promoters contained more than two putative LeuB/Leu3p DNA-binding sites. Interestingly, two of the *P. brasiliensis* isolates had one putative binding site, whereas the third isolate had two putative LeuB/Leu3p binding sites. Fungi that lacked putative LeuB/Leu3p DNA-binding sites upstream of the NADP-GDH gene were generally clustered into closely related genera (Fig. 4), suggesting those clades may have lost direct leucine regulation of *gdhA* orthologues. LeuB/Leu3p DNA-binding sites upstream of *gdhA* were found in all *Aspergillus* species analysed, in *N. crassa* and *H. capsulatum* as well as in some *Candida* species, but were not found in either the fission yeasts or the fusaria.

LeuB activates *gdhA* expression via the proximal consensus LeuB DNA-binding site

To determine whether LeuB acts via either or both of the two putative LeuB DNA-binding sites in the *A. nidulans* *gdhA* promoter we deleted both sites separately and in combination from the *gdhA–lacZ* reporter gene (Fig. 5a). Deletion of the highly conserved proximal site, −250 to −241, resulted in strongly reduced β-galactosidase levels. Therefore, the proximal site likely mediates LeuB activation. However, deletion of the distal site, −501 to −492, caused an increase in expression of *gdhA–lacZ* compared with the WT promoter. When both predicted LeuB DNA-binding sites were removed from the *gdhA–lacZ* promoter expression was higher than when the proximal site alone was deleted, indicating that the negative effect of deleting the proximal site was countered by removal of the distal site. We measured expression of the *gdhA–lacZ* reporter genes lacking either or both LeuB DNA-binding sites in the *leuB*Δ mutant. Two key observations inform our understanding of *gdhA* regulation. First, all three mutated reporter genes, including

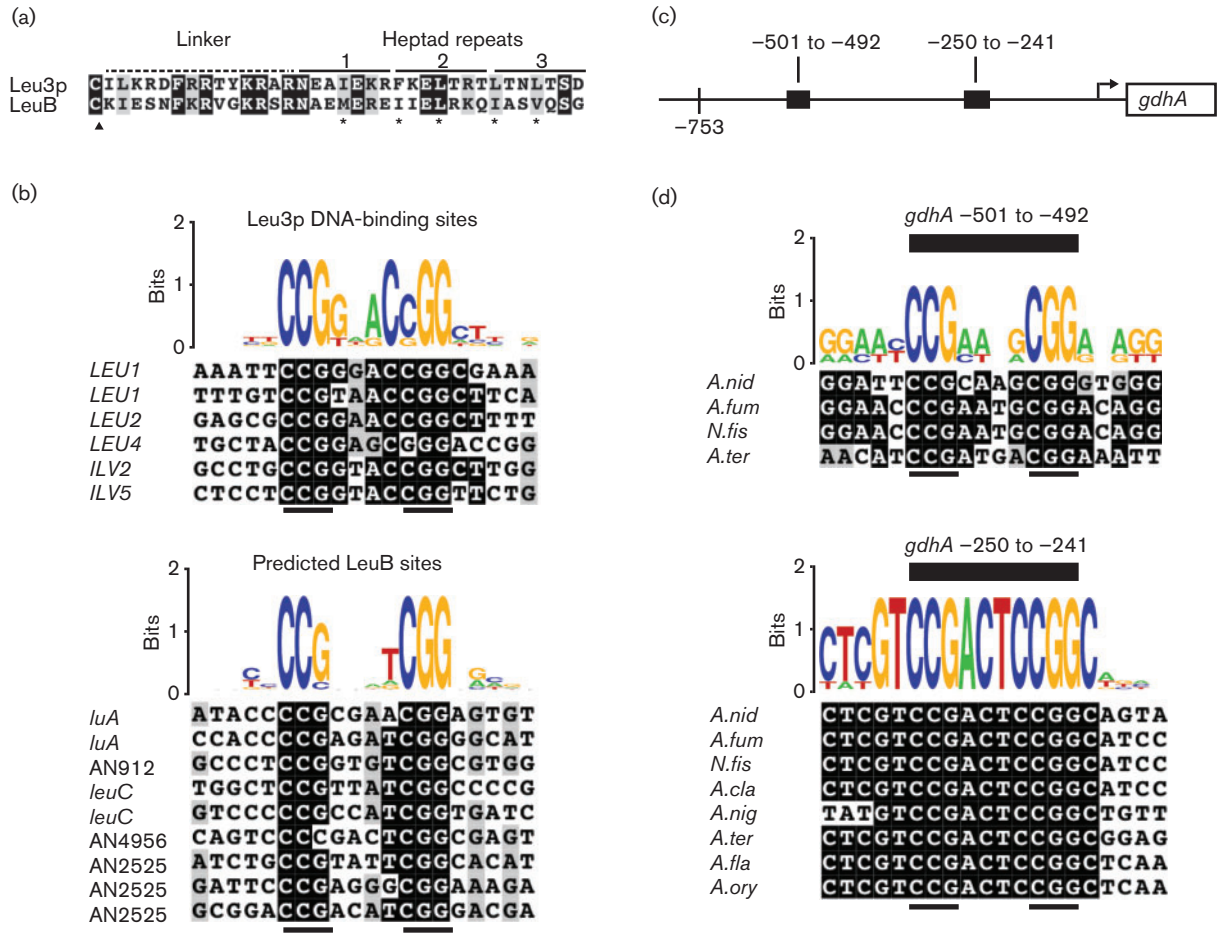

Fig. 3. Identification of LeuB binding sites in the *gdhA* promoter. (a) Alignment of the final cysteine (▲) of the zinc binuclear cluster, linker region (dotted line) and first three heptad repeats (solid lines) of Leu3p and LeuB with conservation of hydrophobic residues (*) at positions 1 and 4. (b) $CCGN_4CGG$ sequences with flanking nucleotides were identified in the −1.0 kb region of known and predicted leucine biosynthesis genes from *S. cerevisiae* and *A. nidulans*, and manually aligned within species. Alignments were used to generate WebLogo consensus motifs for Leu3p and LeuB. *LEU1*, *luA*, *leuC* and AN2525 each contain multiple putative $CCGN_4CGG$ DNA-binding sites. (c) The promoter region 753 bp upstream of the *A. nidulans gdhA* ATG contains two putative LeuB $CCGN_4CGG$ consensus DNA-binding sites (black boxes). (d) Alignment of proximal and distal LeuB consensus DNA-binding sites in the *gdhA* promoter from *A. nidulans* (A.nid), *A. fumigatus* (A.fum), *N. fischeri* (N.fis), *A. clavatus* (A.cla), *A. niger* (A.nig), *A. terreus* (A.ter), *A. flavus* (A.fla) and *A. oryzae* (A.ory). Everted CCG/CGG repeats are underlined. For (b) and (d) units measure bits of information proportional to sequence conservation.

the reporter lacking both LeuB sites, showed leucine inhibition via WT LeuB and reduced expression in the *leuB*Δ mutant, indicating that *leuB*Δ and deletion of the LeuB DNA-binding sites are additive (Fig. 5a). Therefore, LeuB contributes to activation of *gdhA* expression independently of the consensus LeuB DNA-binding sites, either via regulation of another transcription factor that activates *gdhA* expression or by LeuB DNA binding at a non-consensus regulatory element. Second, *gdhA–lacZ* levels were lower in the *leuB*Δ strain in the absence of the proximal site than when it remained intact, suggesting that an unknown positive factor activates *gdhA* expression via the proximal site or an overlapping sequence in the absence of LeuB.

LeuB acts via a non-consensus site in the *gdhA* promoter

To determine the location of the additional non-consensus LeuB site of action within the *gdhA* promoter we created a −240 bp *gdhA–lacZ* 5′ truncated fusion containing the shortest *gdhA* promoter that retains the TATA-box. The −240 bp *gdhA–lacZ* reporter gene supported low basal levels of expression, but was not affected by the addition of leucine or by *leuB*Δ (Fig. 5a). Therefore, LeuB acts within the −753 to −241 bp region upstream of *gdhA*. We next constructed a variant of the −753 bp *gdhA–lacZ* reporter lacking both LeuB consensus motifs and the intervening region (Δ–501 to −241 bp *gdhA–lacZ*). Like the −240 bp

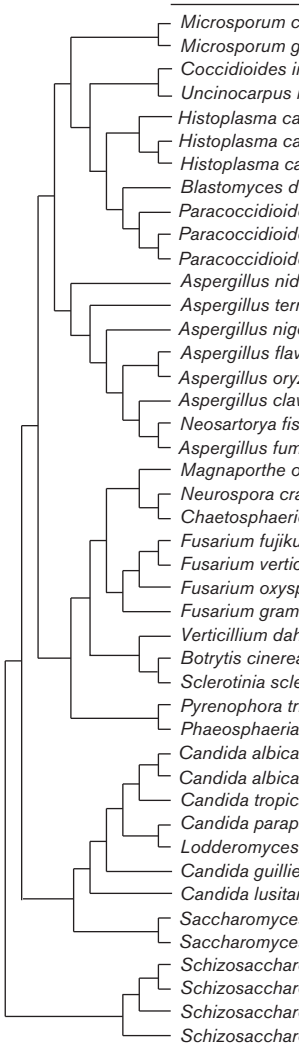

Species	Locus	LeuB/Leu3p consensus sites			
		Location	Sequence	Location	Sequence
Microsporum canis	MCYG_01308.2	–	–	–	–
Microsporum gypseum	MYGY_01849.2	−740 to −731	CCGTTATCGG	–	–
Coccidioides immitis	CIRG_08037	–	–	–	–
Uncinocarpus reesii	UREG_06801.1	–	–	–	–
Histoplasma capsulatum (G186AR)	HCBG_02281.2	−801 to −792	CCGGTCGCGG	–	–
Histoplasma capsulatum (H143)	HCDG_01555.2	−794 to −785	CCGGTCTCGG	–	–
Histoplasma capsulatum (H88)	HCEG_01414.2	−795 to −786	CCGGTCTCGG	–	–
Blastomyces dermatitidis	BDDG_09854.2	−638 to −629	CCGTTCCCGG	−999 to −990	CCGTCATCGG
Paracoccidioides brasiliensis (Pb01)	PAAG_07689.1	−627 to −618	CCGTTTCCGG	–	–
Paracoccidioides brasiliensis (Pb03)	PABG_04154.1	−638 to −629	CCGTTTCCGG	−984 to −975	CCGTCATCGG
Paracoccidioides brasiliensis (Pb18)	PADG_04516.1	−638 to −629	CCGTTTCCGG	−978 to −969	CCGTCATCGG
Aspergillus nidulans†	ANID_04376.1	−250 to −241	CCGGACTCGG	−501 to −492	CCGCAAGCGG
Aspergillus terreus†	ATEG_05563.1	−151 to −142	CCGGACTCGG	−780 to −771	CCGATGACGG
Aspergillus niger†	An04g00990	−251 to −242	CCGGACTCGG	–	–
Aspergillus flavus†	AFL2G_04738.2	−263 to −254	CCGGACTCGG	–	–
Aspergillus oryzae†	AO090023000923	−263 to −254	CCGGACTCGG	–	–
Aspergillus clavatus†	ACLA_045900	−306 to −297	CCGGACTCGG	–	–
Neosartorya fischeri†	NFIA_109570	−229 to −220	CCGGACTCGG	−479 to −470	CCGAATGCGG
Aspergillus fumigatus†	Afu4g06620	−232 to −223	CCGGACTCGG	−483 to −474	CCGAATGCGG
Magnaporthe oryzae	MGG_08074.7	−627 to −618	CCGAGAACGG	–	–
Neurospora crassa	NCU01195.7	−631 to −622	CCGACCTCGG	–	–
Chaetosphaeridium globosum	CHGG_07713.1	–	–	–	–
Fusarium fujikuroi	AJ315471	–	–	–	–
Fusarium verticillioides	FVEG_07988.3	–	–	–	–
Fusarium oxysporum	FOXG_01626.2	–	–	–	–
Fusarium graminearum	FGSG_07174.3	–	–	–	–
Verticillium dahliae	VDAG_08339.1	–	–	–	–
Botrytis cinerea	BC1G_13490.1	−536 to −527	CCGATCACGG	−775 to −766	CCGTTGTCGG
Sclerotinia sclerotiorum	SS1G_09120	−537 to −528	CCGATCACGG	−771 to −762	CCGTTGTCGG
Pyrenophora tritici-repentis	PTRG_04082.1	−173 to −164	CCGCCAGCGG	−468 to −459	CCGACTTCGG
Phaeosphaeria nodorum	SNOG_05229	−385 to −376	CCGTGAGCGG	–	–
Candida albicans (sc5314)	orf19.4716	–	–	–	–
Candida albicans (WO-1)	CAWG_03213.1	–	–	–	–
Candida tropicalis	CTRG_04035.3	−514 to −505	CCGGAAGCGG	–	–
Candida parapsilosis	CPAG_05384	–	–	–	–
Lodderomyces elongisporus	LELG_04591.1	–	–	–	–
Candida guilliermondii	PGUG_03895	−141 to −132	CCGGTAGCGG	–	–
Candida lusitaniae	CLUG_04306.1	−323 to −314	CCGATATCGG	–	–
Saccharomyces cerevisiae_GDH1	YOR375C	−404 to −395	CCGGAACCGG	–	–
Saccharomyces cerevisiae_GDH3	YAL062W	–	–	–	–
Schizosaccharomyces octosporus	SCOG_04027	–	–	–	–
Schizosaccharomyces cryophilus	SPOG_04767.1	–	–	–	–
Schizosaccharomyces pombe	SPCC622.12c	–	–	–	–
Schizosaccharomyces japonicus	SJAG_03266.5	–	–	–	–

Fig. 4. LeuB/Leu3p DNA-binding sites are present in NADP-GDH gene promoters within the Ascomycota. BLASTP was used to identify 44 NADP-GDH-encoding genes from ascomycetes. The 1.0 kb sequence upstream of the first ATG was searched for the presence of predicted LeuB/Leu3p CCGN$_4$CGG DNA-binding sites. Promoter sequences were sourced from the Broad Institute Fungal Genome Initiative or for *F. fujikuroi* from GenBank. Cladogram showing evolutionary relationship of NADP-GDH orthologues constructed using protein sequences for each represented NADP-GDH gene. Branches represent relationships between orthologues, but not evolutionary distance. The CCGAACTTCGG conserved element is only present in *Aspergillus* species *gdhA* promoters (†).

reporter, neither addition of leucine nor *leuB*Δ reduced expression of the Δ–501 to −241 bp *gdhA–lacZ* reporter (Fig. 5a), localizing the additional LeuB site of action between the two LeuB consensus sites. To confirm the additional site of action for LeuB we inserted *gdhA* promoter sequences from the region between the consensus sites, −487 to −368, into the minimal promoter of the *gpdA*p$_{mini}$*–lacZ* reporter gene (Punt *et al.*, 1995) to create *gdhA*p$_{mini}$*–lacZ*. We assayed this reporter in WT and the *leuB*Δ mutant, and found that either the addition of leucine or *leuB*Δ conferred reduced reporter gene expression (Fig. 5b). Assays of a control *gpdA*p$_{mini}$*–lacZ* reporter containing a fragment of the *acuJ* promoter (Hynes *et al.*, 2006) showed no negative effect of leucine or *leuB*Δ (Fig. 5c). Therefore, LeuB activation of the *gdhA* promoter is mediated, in part, independently of LeuB consensus DNA-binding sites through the −487 to −368 bp region.

In a separate study, we have identified a positive-acting promoter element CCGAACTTCGG located at −432 to −422 bp upstream of the *gdhA* ATG conserved within

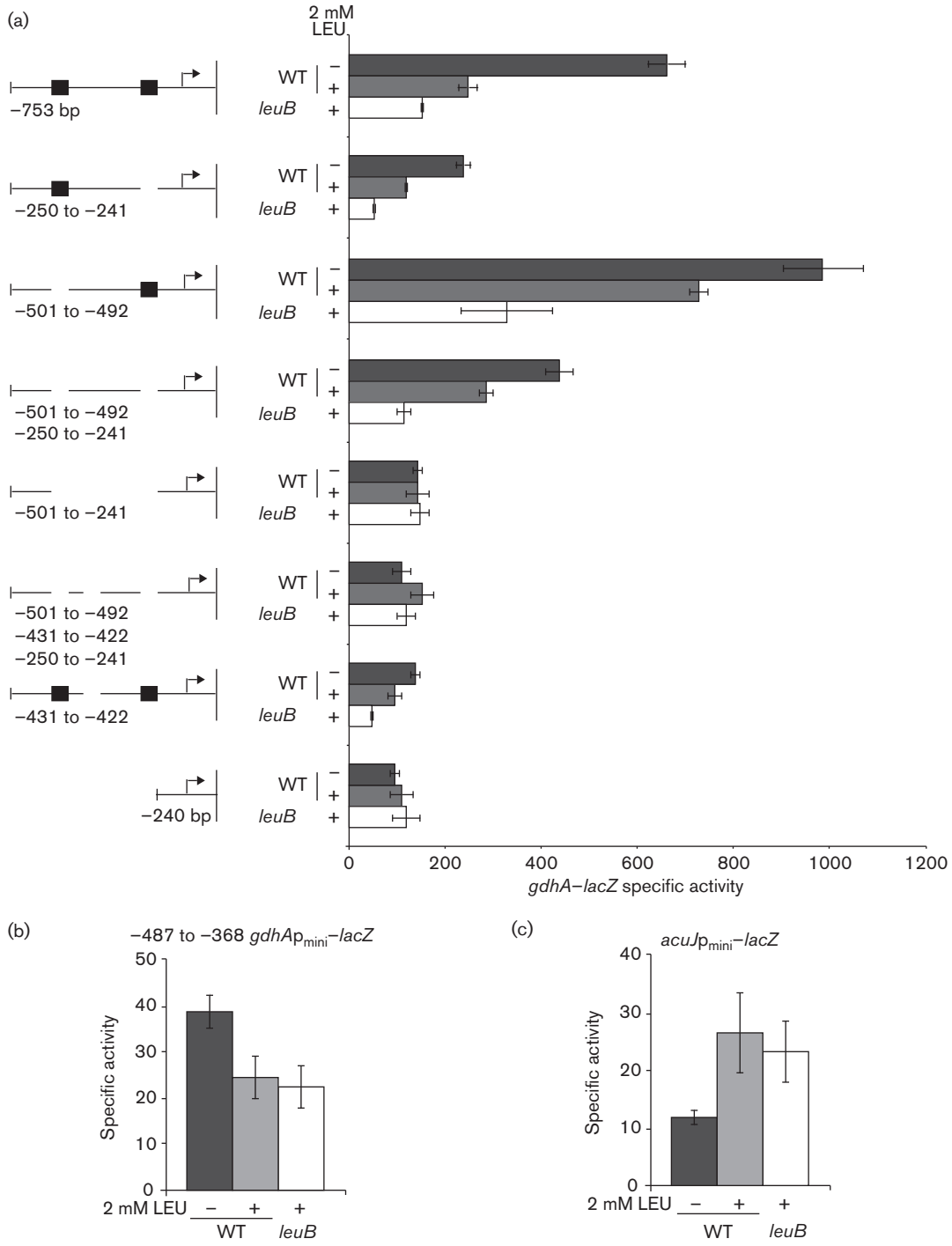

Fig. 5. LeuB regulates *gdhA* through two conserved sites. (a) *gdhA–lacZ* reporters containing deletions of putative LeuB regulatory elements, (b) the *gpdA*p_{mini}*–lacZ* reporter containing the −487 to −368 region of the *gdhA* promoter, and (c) the *gpdA*p_{mini}*–lacZ* reporter containing a fragment of the *acuJ* promoter were assayed in WT and *leuB*Δ strains grown in supplemented 1 % glucose-minimal medium containing 10 mM ammonium tartrate for 16 h at 37 °C with or without 2 mM leucine (LEU). Soluble protein extracts were prepared from mycelia and assayed for β-galactosidase specific activity. Error bars, SEM ($n \geqslant 3$).

Aspergillus species *gdhA* promoters (D. J. Downes, M. A. Davis, K. H. Wong, S. D. Kreutzberger, M. J. Hynes & R. B. Todd, in preparation). This element contains a $CCGN_5CGG$ motif similar to the LeuB consensus motif, varying only by 1 nt within the spacer. We deleted 10 nt of this element (Δ–431 to −422) from the −753 bp reporter

lacking both predicted LeuB consensus sites. This triple-site deletion reporter was unaffected by either addition of leucine or *leuB*Δ (Fig. 5a), indicating that LeuB does not act at sites other than those deleted in this construct and that this conserved element is a LeuB site of action. A −753 bp *gdhA–lacZ* reporter lacking only the conserved element but retaining the proximal and distal LeuB consensus sites was reduced in a *leuB*Δ strain compared with WT (Fig. 5a), consistent with LeuB activation via the proximal LeuB consensus site. Therefore, the full LeuB activation of *gdhA* expression occurs via both the proximal consensus site and the non-consensus element. We searched the promoters of the 44 ascomycete NADP-GDH-encoding genes analysed above and found the CCGAACTTCGG element conserved only within *Aspergillus* species (Fig. 4).

DISCUSSION

NADP-GDH functions as a key enzyme in nitrogen assimilation and draws a substrate directly from the tricarboxylic acid cycle, intricately involving NADP-GDH in core carbon and nitrogen metabolism. *gdhA* expression therefore responds to metabolites sourced from the environment and through cellular processes via metabolic flux. Indeed, *gdhA* displays differential expression in response to ammonium, glutamate or glutamine and responds to nitrate (Pateman, 1969; Schinko *et al.*, 2010). We have now shown that *gdhA* is regulated by leucine biosynthesis intermediates via the LeuB transcription factor. Therefore, regulation of *gdhA* expression is a potential response to metabolic flux. Leucine, despite comprising a significant proportion of the protein-incorporated amino acids in *Aspergillus* species, is one of the least-abundant free amino acids, representing <1 % of the amino acid pool (Berger *et al.*, 2008; Stokes & Gunness, 1946). Inherently low levels of free leucine likely make it a sensitive sensor for general depletion of amino acids and may signal a need for greater levels of glutamate synthesis to replenish amino acid levels. Branched-chain amino acid biosynthesis requires glutamate as the amine donor in the final transamination step for the production of isoleucine, valine and leucine. In *S. cerevisiae*, leucine biosynthesis genes are regulated by Leu3p binding to a well-defined $CCGN_4CGG$ binding site (reviewed by Kohlhaw 2003). We have shown that the equivalent structural gene promoters in *A. nidulans* share a similar consensus binding site, as does the *A. nidulans gdhA* promoter. Furthermore, we have shown by perturbing α-IPM levels both physiologically with the addition of exogenous leucine and genetically by disrupting either α-IPM synthetase or α-IPM isomerase, that the activity of LeuB, like Leu3p, responds to α-IPM levels (Hu *et al.*, 1995). Additionally, leucine inhibition of *gdhA* expression is directly mediated by LeuB, which requires a functional DNA-binding domain for *gdhA* regulation. Similarly, *S. cerevisiae GDH1* is directly regulated by Leu3p via UAS binding sites in an α-IPM-dependent manner (Hu *et al.*, 1995). Regulation of NADP-GDH by leucine biosynthesis is therefore conserved between *A. nidulans* and *S. cerevisiae*. We determined the extent to which leucine biosynthesis regulation of NADP-GDH may be conserved throughout the Ascomycota by analysis of 5′ *gdhA* homologues for LeuB/Leu3p consensus DNA-binding sites. Interestingly, numerous species have consensus $CCGN_4CGG$ binding site motifs in their NADP-GDH gene promoters, suggesting widespread conservation of LeuB/Leu3p regulation. Some species lack $CCGN_4CGG$ consensus sites as well as the non-canonical LeuB target site we found 5′ of *A. nidulans gdhA*, suggesting alternative regulatory mechanisms. For these species nitrogen may be preferentially incorporated via glutamine synthetase and glutamate synthetase, as is the case in some ectomycorrhizal fungi (Morel *et al.*, 2006). In *F. fujikuroi*, a species lacking a LeuB/Leu3p site in the NADP-GDH promoter, GS plays both functional and regulatory roles in nitrogen metabolism (Teichert *et al.*, 2004).

Our analysis of LeuB consensus sites in the *A. nidulans gdhA* promoter provided several new insights into the regulatory mechanisms underlying *gdhA* expression. Based on our finding that LeuB played a positive role in regulating *gdhA* expression and that the LeuB zinc finger was essential for this activation, we initially predicted that both sites would mediate this regulation. Deletion of the proximal site was consistent with this, resulting in significantly reduced *gdhA* expression and indicating that LeuB activation of *gdhA* occurs in part via the highly conserved proximal site. However, deletion of this site alone did not abolish the action of LeuB, suggesting that additional sequences were involved. Deletion of the distal site did not influence the contribution of LeuB, but rather led to an increase in expression. In addition to acting at the proximal LeuB site, we found that LeuB also acts via a novel site of action, which does not conform to the Leu3p DNA-binding site consensus. This novel element is conserved within *Aspergillus* species and, like the LeuB/Leu3p consensus motif, contains everted CCG triplets, although the triplets are separated by a 5 bp spacer ($CCGN_5CGG$). For Zn(II)2Cys6 transcription factors, spacer length is a key factor determining DNA-binding specificity, based in part on recognition by the linker region (MacPherson *et al.*, 2006; Schjerling & Holmberg, 1996; Todd & Andrianopoulos, 1997). *In vitro* DNA binding of Leu3p is lost if the length of the spacer region is altered (Hellauer *et al.*, 1996), thus it is unlikely that LeuB binds this site as a homodimer. One possibility is that LeuB may indirectly exert its effect by activating expression of another transcription factor, which binds this site. Leu3p is known to bind to the promoters of several other transcription factors (Tang *et al.*, 2006). Alternatively, LeuB may bind this site directly as a heterodimer with another Zn(II)2Cys6 transcription factor, as seen for *A. nidulans* AcuK and AcuM (Suzuki *et al.*, 2012), and *S. cerevisiae* Oaf1p and Pip2p (Rottensteiner *et al.*, 1997; Trzcinska-Danielewicz *et al.*, 2008) or Pdr1p and Pdr3p (Mamnun *et al.*, 2002; Wolfger *et al.*, 1997). This novel site mediates a

significant contribution to *gdhA* expression. Therefore, the combined action of LeuB via the proximal consensus site and the conserved element, possibly by heterodimerization with or regulation of an unknown factor, may be a means by which cells utilize leucine levels to sense changes in nitrogen metabolic flux and respond by altering levels of the key nitrogen assimilation enzyme NADP-GDH.

ACKNOWLEDGEMENTS

This work was supported by the Australian Research Council's Discovery Projects funding scheme (project no. DP0558002), Kansas NSF EPSCoR First Award EPS-0903806, the Kansas State University Plant Biotechnology Center and the Johnson Center for Basic Cancer Research. We acknowledge the expert technical assistance of K. Nguyen, K. S. Siebert, C. C. Hunter and B. T. Pfannenstiel. We thank K. H. Wong for comments. Contribution no. 14-008-J from the Kansas Agricultural Experiment Station.

REFERENCES

Andrianopoulos, A. & Hynes, M. J. (1988). Cloning and analysis of the positively acting regulatory gene *amdR* from *Aspergillus nidulans*. *Mol Cell Biol* **8**, 3532–3541.

Andrianopoulos, A., Kourambas, S., Sharp, J. A., Davis, M. A. & Hynes, M. J. (1998). Characterization of the *Aspergillus nidulans nmrA* gene involved in nitrogen metabolite repression. *J Bacteriol* **180**, 1973–1977.

Arnaud, M. B., Cerqueira, G. C., Inglis, D. O., Skrzypek, M. S., Binkley, J., Chibucos, M. C., Crabtree, J., Howarth, C., Orvis, J. & other authors (2012). The *Aspergillus* Genome Database (AspGD): recent developments in comprehensive multispecies curation, comparative genomics and community resources. *Nucleic Acids Res* **40** (Database issue), D653–D659.

Arst, H. N., Jr & MacDonald, D. W. (1973). A mutant of *Asperigillus nidulans* lacking NADP-linked glutamate dehydrogenase. *Mol Gen Genet* **122**, 261–265.

Arst, H. N., Jr, Parbtani, A. A. & Cove, D. J. (1975). A mutant of *Aspergillus nidulans* defective in NAD-linked glutamate dehydrogenase. *Mol Gen Genet* **138**, 164–171.

Avendaño, A., Deluna, A., Olivera, H., Valenzuela, L. & Gonzalez, A. (1997). *GDH3* encodes a glutamate dehydrogenase isozyme, a previously unrecognized route for glutamate biosynthesis in *Saccharomyces cerevisiae*. *J Bacteriol* **179**, 5594–5597.

Avendaño, A., Riego, L., DeLuna, A., Aranda, C., Romero, G., Ishida, C., Vázquez-Acevedo, M., Rodarte, B., Recillas-Targa, F. & other authors (2005). Swi/SNF-GCN5-dependent chromatin remodelling determines induced expression of *GDH3*, one of the paralogous genes responsible for ammonium assimilation and glutamate biosynthesis in *Saccharomyces cerevisiae*. *Mol Microbiol* **57**, 291–305.

Bai, Y. L. & Kohlhaw, G. B. (1991). Manipulation of the 'zinc cluster' region of transcriptional activator LEU3 by site-directed mutagenesis. *Nucleic Acids Res* **19**, 5991–5997.

Baichwal, V. R., Cunningham, T. S., Gatzek, P. R. & Kohlhaw, G. B. (1983). Leucine biosynthesis in yeast. *Curr Genet* **7**, 369–377.

Berger, H., Basheer, A., Böck, S., Reyes-Dominguez, Y., Dalik, T., Altmann, F. & Strauss, J. (2008). Dissecting individual steps of nitrogen transcription factor cooperation in the *Aspergillus nidulans* nitrate cluster. *Mol Microbiol* **69**, 1385–1398.

Bradford, M. M. (1976). A rapid and sensitive method for the quantitation of microgram quantities of protein utilizing the principle of protein-dye binding. *Anal Biochem* **72**, 248–254.

Caddick, M. X., Jones, M. G., van Tonder, J. M., Le Cordier, H., Narendja, F., Strauss, J. & Morozov, I. Y. (2006). Opposing signals differentially regulate transcript stability in *Aspergillus nidulans*. *Mol Microbiol* **62**, 509–519.

Cardoza, R. E., Moralejo, F. J., Gutiérrez, S., Casqueiro, J., Fierro, F. & Martín, J. F. (1998). Characterization and nitrogen-source regulation at the transcriptional level of the *gdhA* gene of *Aspergillus awamori* encoding an NADP-dependent glutamate dehydrogenase. *Curr Genet* **34**, 50–59.

Casalone, E., Barberio, C., Cavalieri, D. & Polsinelli, M. (2000). Identification by functional analysis of the gene encoding α-isopropylmalate synthase II (*LEU9*) in *Saccharomyces cerevisiae*. *Yeast* **16**, 539–545.

Cavalieri, D., Casalone, E., Bendoni, B., Fia, G., Polsinelli, M. & Barberio, C. (1999). Trifluoroleucine resistance and regulation of alpha-isopropyl malate synthase in *Saccharomyces cerevisiae*. *Mol Gen Genet* **261**, 152–160.

Chang, L. F., Cunningham, T. S., Gatzek, P. R., Chen, W. J. & Kohlhaw, G. B. (1984). Cloning and characterization of yeast Leu4, one of two genes responsible for alpha-isopropylmalate synthesis. *Genetics* **108**, 91–106.

Chang, L. F., Gatzek, P. R. & Kohlhaw, G. B. (1985). Total deletion of yeast *LEU4*: further evidence for a second alpha-isopropylmalate synthase and evidence for tight *LEU4-MET4* linkage. *Gene* **33**, 333–339.

Chen, H. & Kinsey, J. A. (1994). Sequential gel mobility shift scanning of 5′ upstream sequences of the *Neurospora crassa am* (GDH) gene. *Mol Gen Genet* **242**, 399–403.

Chen, H., Crabb, J. W. & Kinsey, J. A. (1998). The *Neurospora aab-1* gene encodes a CCAAT binding protein homologous to yeast *HAP5*. *Genetics* **148**, 123–130.

Cherry, J. M., Hong, E. L., Amundsen, C., Balakrishnan, R., Binkley, G., Chan, E. T., Christie, K. R., Costanzo, M. C., Dwight, S. S. & other authors (2012). Saccharomyces Genome Database: the genomics resource of budding yeast. *Nucleic Acids Res* **40** (Database issue), D700–D705.

Christensen, T., Hynes, M. J. & Davis, M. A. (1998). Role of the regulatory gene *areA* of *Aspergillus oryzae* in nitrogen metabolism. *Appl Environ Microbiol* **64**, 3232–3237.

Clutterbuck, A. J. (1974). *Aspergillus nidulans* genetics. In *Handbook of Genetics*, vol. 1, pp. 447–510. Edited by R. C. King. New York: Plenum Press.

Cove, D. J. (1966). The induction and repression of nitrate reductase in the fungus *Aspergillus nidulans*. *Biochim Biophys Acta* **113**, 51–56.

Crooks, G. E., Hon, G., Chandonia, J. M. & Brenner, S. E. (2004). WebLogo: a sequence logo generator. *Genome Res* **14**, 1188–1190.

Dang, V. D., Bohn, C., Bolotin-Fukuhara, M. & Daignan-Fornier, B. (1996). The CCAAT box-binding factor stimulates ammonium assimilation in *Saccharomyces cerevisiae*, defining a new cross-pathway regulation between nitrogen and carbon metabolisms. *J Bacteriol* **178**, 1842–1849.

Dantzig, A. H., Wiegmann, F. L., Jr & Nason, A. (1979). Regulation of glutamate dehydrogenases in *nit-2* and *am* mutants of *Neurospora crassa*. *J Bacteriol* **137**, 1333–1339.

Daugherty, J. R., Rai, R., el Berry, H. M. & Cooper, T. G. (1993). Regulatory circuit for responses of nitrogen catabolic gene expression to the GLN3 and DAL80 proteins and nitrogen catabolite repression in *Saccharomyces cerevisiae*. *J Bacteriol* **175**, 64–73.

Davis, M. A., Cobbett, C. S. & Hynes, M. J. (1988). An *amdS-lacZ* fusion for studying gene regulation in *Aspergillus*. *Gene* **63**, 199–212.

Davis, M. A., Small, A. J., Kourambas, S. & Hynes, M. J. (1996). The *tamA* gene of *Aspergillus nidulans* contains a putative zinc cluster motif which is not required for gene function. *J Bacteriol* **178**, 3406–3409.

DeLuna, A., Avendano, A., Riego, L. & Gonzalez, A. (2001). NADP-glutamate dehydrogenase isoenzymes of *Saccharomyces cerevisiae*. Purification, kinetic properties, and physiological roles. *J Biol Chem* **276**, 43775–43783.

Fincham, J. R. (1988). The *Neurospora am* gene and allelic complementation. *Bioessays* **9**, 169–172.

Fincham, J. R. & Baron, A. J. (1977). The molecular basis of an osmotically reparable mutant of *Neurospora crassa* producing unstable glutamate dehydrogenase. *J Mol Biol* **110**, 627–642.

Fincham, J. R., Kinsey, J. A., Fuentes, A. M., Cummings, N. J. & Connerton, I. F. (2000). The *Neurospora am* gene and NADP-specific glutamate dehydrogenase: mutational sequence changes and functional effects – more mutants and a summary. *Genet Res* **76**, 1–10.

Frederick, G. D. & Kinsey, J. A. (1990a). Nucleotide sequence and nuclear protein binding of the two regulatory sequences upstream of the *am* (GDH) gene in *Neurospora*. *Mol Gen Genet* **221**, 148–154.

Frederick, G. D. & Kinsey, J. A. (1990b). Distant upstream regulatory sequences control the level of expression of the *am* (GDH) locus of *Neurospora crassa*. *Curr Genet* **18**, 53–58.

Friden, P. & Schimmel, P. (1988). LEU3 of *Saccharomyces cerevisiae* activates multiple genes for branched-chain amino acid biosynthesis by binding to a common decanucleotide core sequence. *Mol Cell Biol* **8**, 2690–2697.

Gurr, S. J., Hawkins, A. R., Drainas, C. & Kinghorn, J. R. (1986). Isolation and identification of the *Aspergillus nidulans gdhA* gene encoding NADP-linked glutamate dehydrogenase. *Curr Genet* **10**, 761–766.

Hawkins, A. R., Gurr, S. J., Montague, P. & Kinghorn, J. R. (1989). Nucleotide sequence and regulation of expression of the *Aspergillus nidulans gdhA* gene encoding NADP dependent glutamate dehydrogenase. *Mol Gen Genet* **218**, 105–111.

Hellauer, K., Rochon, M. H. & Turcotte, B. (1996). A novel DNA binding motif for yeast zinc cluster proteins: the Leu3p and Pdr3p transcriptional activators recognize everted repeats. *Mol Cell Biol* **16**, 6096–6102.

Hernández, H., Aranda, C., López, G., Riego, L. & González, A. (2011). Hap2-3-5-Gln3 determine transcriptional activation of *GDH1* and *ASN1* under repressive nitrogen conditions in the yeast *Saccharomyces cerevisiae*. *Microbiology* **157**, 879–889.

Hinnebusch, A. G. (1988). Mechanisms of gene regulation in the general control of amino acid biosynthesis in *Saccharomyces cerevisiae*. *Microbiol Rev* **52**, 248–273.

Hu, Y., Cooper, T. G. & Kohlhaw, G. B. (1995). The *Saccharomyces cerevisiae* Leu3 protein activates expression of *GDH1*, a key gene in nitrogen assimilation. *Mol Cell Biol* **15**, 52–57.

Hynes, M. J. (1974). Effects of ammonium, L-glutamate, and L-glutamine on nitrogen catabolism in *Aspergillus nidulans*. *J Bacteriol* **120**, 1116–1123.

Hynes, M. J., Murray, S. L., Duncan, A., Khew, G. S. & Davis, M. A. (2006). Regulatory genes controlling fatty acid catabolism and peroxisomal functions in the filamentous fungus *Aspergillus nidulans*. *Eukaryot Cell* **5**, 794–805.

Kinghorn, J. R. & Pateman, J. A. (1973). NAD and NADP L-glutamate dehydrogenase activity and ammonium regulation in *Aspergillus nidulans*. *J Gen Microbiol* **78**, 39–46.

Kinghorn, J. R. & Pateman, J. A. (1975). The structural gene for NADP L-glutamate dehydrogenase in *Aspergillus nidulans*. *J Gen Microbiol* **86**, 294–300.

Kinghorn, J. R. & Pateman, J. A. (1976). Mutants of *Aspergillus nidulans* lacking nicotinamide adenine dinucleotide-specific glutamate dehydrogenase. *J Bacteriol* **125**, 42–47.

Kinnaird, J. H. & Fincham, J. R. (1983). The complete nucleotide sequence of the *Neurospora crassa am* (NADP-specific glutamate dehydrogenase) gene. *Gene* **26**, 253–260.

Kohlhaw, G. B. (2003). Leucine biosynthesis in fungi: entering metabolism through the back door. *Microbiol Mol Biol Rev* **67**, 1–15.

Kotaka, M., Johnson, C., Lamb, H. K., Hawkins, A. R., Ren, J. & Stammers, D. K. (2008). Structural analysis of the recognition of the negative regulator NmrA and DNA by the zinc finger from the GATA-type transcription factor AreA. *J Mol Biol* **381**, 373–382.

Lamb, H. K., Ren, J., Park, A., Johnson, C., Leslie, K., Cocklin, S., Thompson, P., Mee, C., Cooper, A. & other authors (2004). Modulation of the ligand binding properties of the transcription repressor NmrA by GATA-containing DNA and site-directed mutagenesis. *Protein Sci* **13**, 3127–3138.

Langdon, T., Sheerins, A., Ravagnani, A., Gielkens, M., Caddik, M. X. & Arst, H. N., Jr (1995). Mutational analysis reveals dispensability of the N-terminal region of the *Aspergillus* transcription factor mediating nitrogen metabolite repression. *Mol Microbiol* **17**, 877–888.

Larkin, M. A., Blackshields, G., Brown, N. P., Chenna, R., McGettigan, P. A., McWilliam, H., Valentin, F., Wallace, I. M., Wilm, A. & other authors (2007). Clustal W and Clustal X version 2.0. *Bioinformatics* **23**, 2947–2948.

Larson, E. M. & Idnurm, A. (2010). Two origins for the gene encoding alpha-isopropylmalate synthase in fungi. *PLoS ONE* **5**, e11605.

Lee, S. B. & Taylor, J. W. (1990). Isolation of DNA from fungal mycelia and single spores. In *PCR Protocols: A Guide to Methods and Applications*, pp. 282–287. Edited by M. A. Innis, D. H. Gelfand, J. S. Sninsky & T. J. White. San Diego, CA: Academic Press.

Liang, S. D., Marmorstein, R., Harrison, S. C. & Ptashne, M. (1996). DNA sequence preferences of GAL4 and PPR1: how a subset of Zn2 Cys6 binuclear cluster proteins recognizes DNA. *Mol Cell Biol* **16**, 3773–3780.

Macheda, M. L., Hynes, M. J. & Davis, M. A. (1999). The *Aspergillus nidulans gltA* gene encoding glutamate synthase is required for ammonium assimilation in the absence of NADP-glutamate dehydrogenase. *Curr Genet* **34**, 467–471.

MacPherson, S., Larochelle, M. & Turcotte, B. (2006). A fungal family of transcriptional regulators: the zinc cluster proteins. *Microbiol Mol Biol Rev* **70**, 583–604.

Mamane, Y., Hellauer, K., Rochon, M. H. & Turcotte, B. (1998). A linker region of the yeast zinc cluster protein Leu3p specifies binding to everted repeat DNA. *J Biol Chem* **273**, 18556–18561.

Mamnun, Y. M., Pandjaitan, R., Mahé, Y., Delahodde, A. & Kuchler, K. (2002). The yeast zinc finger regulators Pdr1p and Pdr3p control pleiotropic drug resistance (PDR) as homo- and heterodimers in vivo. *Mol Microbiol* **46**, 1429–1440.

Margelis, S., D'Souza, C., Small, A. J., Hynes, M. J., Adams, T. H. & Davis, M. A. (2001). Role of glutamine synthetase in nitrogen metabolite repression in *Aspergillus nidulans*. *J Bacteriol* **183**, 5826–5833.

Marmorstein, R., Carey, M., Ptashne, M. & Harrison, S. C. (1992). DNA recognition by GAL4: structure of a protein-DNA complex. *Nature* **356**, 408–414.

Monahan, B. J., Askin, M. C., Hynes, M. J. & Davis, M. A. (2006). Differential expression of *Aspergillus nidulans* ammonium permease genes is regulated by GATA transcription factor AreA. *Eukaryot Cell* **5**, 226–237.

Morel, M., Buée, M., Chalot, M. & Brun, A. (2006). NADP-dependent glutamate dehydrogenase: a dispensable function in ectomycorrhizal fungi. *New Phytol* **169**, 179–190.

Morozov, I. Y., Martinez, M. G., Jones, M. G. & Caddick, M. X. (2000). A defined sequence within the 3′ UTR of the *areA* transcript is sufficient to mediate nitrogen metabolite signalling via accelerated deadenylation. *Mol Microbiol* **37**, 1248–1257.

Morozov, I. Y., Galbis-Martinez, M., Jones, M. G. & Caddick, M. X. (2001). Characterization of nitrogen metabolite signalling in *Aspergillus* via the regulated degradation of *areA* mRNA. *Mol Microbiol* **42**, 269–277.

Morozov, I. Y., Jones, M. G., Razak, A. A., Rigden, D. J. & Caddick, M. X. (2010). CUCU modification of mRNA promotes decapping and transcript degradation in *Aspergillus nidulans*. *Mol Cell Biol* **30**, 460–469.

Nayak, T., Szewczyk, E., Oakley, C. E., Osmani, A., Ukil, L., Murray, S. L., Hynes, M. J., Osmani, S. A. & Oakley, B. R. (2006). A versatile and efficient gene-targeting system for *Aspergillus nidulans*. *Genetics* **172**, 1557–1566.

Noël, J. & Turcotte, B. (1998). Zinc cluster proteins Leu3p and Uga3p recognize highly related but distinct DNA targets. *J Biol Chem* **273**, 17463–17468.

Papagiannopoulos, P., Andrianopoulos, A., Sharp, J. A., Davis, M. A. & Hynes, M. J. (1996). The *hapC* gene of *Aspergillus nidulans* is involved in the expression of CCAAT-containing promoters. *Mol Gen Genet* **251**, 412–421.

Pateman, J. A. (1969). Regulation of synthesis of glutamate dehydrogenase and glutamine synthetase in micro-organisms. *Biochem J* **115**, 769–775.

Pateman, J. A., Kinghorn, J. R., Dunn, E. & Forbes, E. (1973). Ammonium regulation in *Aspergillus nidulans*. *J Bacteriol* **114**, 943–950.

Platt, A., Langdon, T., Arst, H. N., Jr, Kirk, D., Tollervey, D., Sanchez, J. M. & Caddick, M. X. (1996). Nitrogen metabolite signalling involves the C-terminus and the GATA domain of the Aspergillus transcription factor AREA and the 3′ untranslated region of its mRNA. *EMBO J* **15**, 2791–2801.

Polotnianka, R., Monahan, B. J., Hynes, M. J. & Davis, M. A. (2004). TamA interacts with LeuB, the homologue of *Saccharomyces cerevisiae* Leu3p, to regulate *gdhA* expression in *Aspergillus nidulans*. *Mol Genet Genomics* **272**, 452–459.

Punt, P. J., Kuyvenhoven, A. & van den Hondel, C. A. (1995). A mini-promoter *lacZ* gene fusion for the analysis of fungal transcription control sequences. *Gene* **158**, 119–123.

Reece, R. J. & Ptashne, M. (1993). Determinants of binding-site specificity among yeast C6 zinc cluster proteins. *Science* **261**, 909–911.

Riego, L., Avendaño, A., DeLuna, A., Rodríguez, E. & González, A. (2002). *GDH1* expression is regulated by GLN3, GCN4, and HAP4 under respiratory growth. *Biochem Biophys Res Commun* **293**, 79–85.

Rottensteiner, H., Kal, A. J., Hamilton, B., Ruis, H. & Tabak, H. F. (1997). A heterodimer of the Zn2Cys6 transcription factors Pip2p and Oaf1p controls induction of genes encoding peroxisomal proteins in *Saccharomyces cerevisiae*. *Eur J Biochem* **247**, 776–783.

Sambrook, J. & Russell, D. W. (2001). *Molecular Cloning: A Laboratory Manual*, 3rd edn. Cold Spring Harbor, NY: Cold Spring Harbor Laboratory Press.

Santos, M., Rebordinos, L., Gutiérrez, S., Cardoza, R. E., Martín, J. F. & Cantoral, J. M. (2001). Characterization of the *gdhA* gene from the phytopathogen *Botrytis cinerea*. *Fungal Genet Biol* **34**, 193–206.

Schinko, T., Berger, H., Lee, W., Gallmetzer, A., Pirker, K., Pachlinger, R., Buchner, I., Reichenauer, T., Güldener, U. & Strauss, J. (2010). Transcriptome analysis of nitrate assimilation in *Aspergillus nidulans* reveals connections to nitric oxide metabolism. *Mol Microbiol* **78**, 720–738.

Schjerling, P. & Holmberg, S. (1996). Comparative amino acid sequence analysis of the C6 zinc cluster family of transcriptional regulators. *Nucleic Acids Res* **24**, 4599–4607.

Schneider, T. D. & Stephens, R. M. (1990). Sequence logos: a new way to display consensus sequences. *Nucleic Acids Res* **18**, 6097–6100.

Small, A. J., Hynes, M. J. & Davis, M. A. (1999). The TamA protein fused to a DNA-binding domain can recruit AreA, the major nitrogen regulatory protein, to activate gene expression in *Aspergillus nidulans*. *Genetics* **153**, 95–105.

Small, A. J., Todd, R. B., Zanker, M. C., Delimitrou, S., Hynes, M. J. & Davis, M. A. (2001). Functional analysis of TamA, a coactivator of nitrogen-regulated gene expression in *Aspergillus nidulans*. *Mol Genet Genomics* **265**, 636–646.

Stokes, J. L. & Gunness, M. (1946). The amino acid composition of microorganisms. *J Bacteriol* **52**, 195–207.

Suzuki, Y., Murray, S. L., Wong, K. H., Davis, M. A. & Hynes, M. J. (2012). Reprogramming of carbon metabolism by the transcriptional activators AcuK and AcuM in *Aspergillus nidulans*. *Mol Microbiol* **84**, 942–964.

Sze, J. Y., Woontner, M., Jaehning, J. A. & Kohlhaw, G. B. (1992). In vitro transcriptional activation by a metabolic intermediate: activation by Leu3 depends on alpha-isopropylmalate. *Science* **258**, 1143–1145.

Tang, L., Liu, X. & Clarke, N. D. (2006). Inferring direct regulatory targets from expression and genome location analyses: a comparison of transcription factor deletion and overexpression. *BMC Genomics* **7**, 215.

Teichert, S., Schönig, B., Richter, S. & Tudzynski, B. (2004). Deletion of the *Gibberella fujikuroi* glutamine synthetase gene has significant impact on transcriptional control of primary and secondary metabolism. *Mol Microbiol* **53**, 1661–1675.

Todd, R. B. & Andrianopoulos, A. (1997). Evolution of a fungal regulatory gene family: the Zn(II)2Cys6 binuclear cluster DNA binding motif. *Fungal Genet Biol* **21**, 388–405.

Todd, R. B., Fraser, J. A., Wong, K. H., Davis, M. A. & Hynes, M. J. (2005). Nuclear accumulation of the GATA factor AreA in response to complete nitrogen starvation by regulation of nuclear export. *Eukaryot Cell* **4**, 1646–1653.

Todd, R. B., Davis, M. A. & Hynes, M. J. (2007). Genetic manipulation of *Aspergillus nidulans*: meiotic progeny for genetic analysis and strain construction. *Nat Protoc* **2**, 811–821.

Trzcinska-Danielewicz, J., Ishikawa, T., Miciałkiewicz, A. & Fronk, J. (2008). Yeast transcription factor Oaf1 forms homodimer and induces some oleate-responsive genes in absence of Pip2. *Biochem Biophys Res Commun* **374**, 763–766.

Wolfger, H., Mahé, Y., Parle-McDermott, A., Delahodde, A. & Kuchler, K. (1997). The yeast ATP binding cassette (ABC) protein genes PDR10 and PDR15 are novel targets for the Pdr1 and Pdr3 transcriptional regulators. *FEBS Lett* **418**, 269–274.

Wong, K. H., Hynes, M. J. & Davis, M. A. (2008). Recent advances in nitrogen regulation: a comparison between *Saccharomyces cerevisiae* and filamentous fungi. *Eukaryot Cell* **7**, 917–925.

Yelton, M. M., Hamer, J. E. & Timberlake, W. E. (1984). Transformation of *Aspergillus nidulans* by using a *trpC* plasmid. *Proc Natl Acad Sci U S A* **81**, 1470–1474.

Edited by: N. Keller

[Cette page a été laissée vierge intentionnellement]

Appendix B - Downes *et al.* (2014b)

Research conducted as part of this dissertation for Chapter 4 “Dual function transcription factors” has been published in Downes D.J., M.A. Davis, K.H. Wong, S.D Kreutzberger, M.J. Hynes, & R.B. Todd (2014) Dual DNA-binding and coactivator functions of *Aspergillus nidulans* TamA, a Zn(II)2Cys6 transcription factor. *Molecular Microbiology* **92(6):** 1198-1211. (DOI: 10.1111/mmi.12620). My contribution to this work while at Kansas State University was the experimental design, real-time reverse-transcriptase PCR analysis, construction of 20 *A. nidulans* strains by crossing and transformation, *lacZ* expression assay, electrophoretic mobility shift assays, protein purification, preparation of samples for ChIP, bioinformatics analyses, and writing the manuscript. The full article and supplementary is included in this appendix.

Molecular Microbiology (2014) 92(6), 1198–1211 ■
doi:10.1111/mmi.12620
First published online 7 May 2014

Dual DNA binding and coactivator functions of *Aspergillus nidulans* TamA, a Zn(II)2Cys6 transcription factor

Damien J. Downes,[1,2] Meryl A. Davis,[2] Koon Ho Wong,[3,4] Sara D. Kreutzberger,[2†] Michael J. Hynes[2] and Richard B. Todd[1,2*]

[1]*Department of Plant Pathology, Kansas State University, 4024 Throckmorton Plant Sciences Center, Manhattan, KS 66506, USA.*

[2]*Department of Genetics, The University of Melbourne, Parkville, Vic. 3010, Australia.*

[3]*Department of Biological Chemistry & Molecular Pharmacology, Harvard Medical School, 240 Longwood Ave, Room C2-325, Boston, MA 02115, USA.*

[4]*Faculty of Health Sciences, University of Macau, Macau SAR, China.*

Summary

Transcription factors containing DNA binding domains generally regulate transcription by direct interaction with DNA. For most transcription factors, including the fungal Zn(II)2Cys6 zinc binuclear cluster transcription factors, the DNA binding motif is essential for function. However, *Aspergillus nidulans* TamA and the related *Saccharomyces cerevisiae* Dal81p protein contain Zn(II)2Cys6 motifs shown to be dispensable for function. TamA acts at several promoters as a coactivator of the global nitrogen GATA transcription factor AreA. We now show that TamA is the major transcriptional activator of *gdhA*, encoding the key nitrogen metabolism enzyme NADP-glutamate dehydrogenase. Moreover, activation of *gdhA* by TamA occurs primarily by a mechanism requiring the TamA DNA binding motif. We show that the TamA DNA binding motif is required for DNA binding of FLAG-epitope-tagged TamA to the *gdhA* promoter. We identify a conserved promoter element required for TamA activation, and show that TamA and AreA are reciprocally required for full binding at the *gdhA* promoter under conditions where AreA is inactive at most promoters but active at *gdhA*. Therefore TamA has dual functions as a DNA-binding transcription factor and a non-DNA-binding coactivator. Dual DNA-binding and coactivator functions provide an additional level of combinatorial control to mediate gene-specific expression.

Accepted 14 April, 2014. *For correspondence. E-mail rbtodd@k-state.edu; Tel. (+1) 785 532 0692; Fax (+1) 785 532 5692. †Present address: Rand Farm Supplies, Lot 5/Kindra St, Rand, NSW 2642, Australia.

Introduction

Transcription factors regulate gene expression in response to environmental stimuli to control cellular processes either by direct DNA binding to promoters of target genes or by protein–protein interactions with other transcription factors. The *Saccharomyces cerevisiae* galactose utilization system provides examples of both types of transcription factor. Structural genes are activated directly by DNA binding of Gal4p to upstream regulatory sequences and the Gal80p non-DNA binding repressor binds Gal4p to repress target genes (reviewed in Traven *et al.*, 2006). The presence of a DNA binding motif is generally sufficient to characterize a transcription factor as DNA binding. In eukaryotes many classes of DNA binding transcription factors regulate gene expression, including several zinc coordinating families such as C2H2 and GATA zinc finger proteins (Todd and Andrianopoulos, 1997). The Zn(II)2Cys6 zinc binuclear cluster or Gal4p family is unique to fungi where it is the most prevalent transcription factor class (MacPherson *et al.*, 2006; Todd *et al.*, 2014). The six cysteines of the zinc binuclear cluster coordinate two zinc(II) ions, with the first and fourth cysteines acting as bridging ligands coordinating both ions (Gardner *et al.*, 1991; Pan and Coleman, 1991). Zinc(II) binding is required for the correct secondary structure and for DNA binding (Pan and Coleman, 1989; 1991). Missense substitution of single cysteine residues within the Zn(II)2Cys6 motif of *S. cerevisiae* Gal4p and Leu3p, *Neurospora crassa* Nit4, and *Aspergillus nidulans* FacB abolishes DNA binding (Johnston and Dover, 1987; Bai and Kohlhaw, 1991; Yuan *et al.*, 1991; Todd *et al.*, 1998). DNA binding specificity of the Zn(II)2Cys6 family members is usually mediated by recognition of distinct combinations of repeated, inverted or everted CCG trinucleotide repeats (Todd and Andrianopoulos, 1997; MacPherson *et al.*, 2006) and for most transcription factors in this class it is assumed or known that the DNA binding motif is essential for function.

A. nidulans TamA represents an unusual class of Zn(II)2Cys6 regulatory proteins in which mutation of the DNA binding domain does not confer loss of function

(Davis *et al*., 1996). Originally identified in genetic screens for simultaneous resistance to toxic nitrogen source analogues, *tamA* mutants have reduced levels of the key nitrogen assimilatory enzyme NADP-dependent glutamate dehydrogenase (NADP-GDH) activity and elevated intracellular ammonium levels (Kinghorn and Pateman, 1975a; Arst *et al*., 1982). Mutation of the critical fourth zinc-coordinating cysteine (Cys90) of the TamA N-terminal Zn(II)2Cys6 motif did not prevent complementation of either the methylammonium resistance or reduced growth on ammonium or acetamide phenotypes of the *tamA24* loss-of-function mutant (Davis *et al*., 1996). Furthermore, constructs carrying an in-frame deletion of the TamA Zn(II)2Cys6 motif complemented the methylammonium resistance and growth phenotypes of the *tamA* deletion mutant (Small *et al*., 1999; 2001). Therefore, DNA binding was considered dispensable for function. The related *S. cerevisiae* Dal81p protein also contains a dispensable Zn(II)2Cys6 motif (Bricmont *et al*., 1991; Cardillo *et al*., 2012). TamA was shown to activate the acetamidase-encoding *amdS* gene, as *amdS–lacZ* reporter gene expression was reduced in the *tamA*Δ mutant (Small *et al*., 1999; 2001). Using yeast two-hybrid assays TamA was shown to interact with the C-terminus of the major nitrogen transcription regulator AreA (Small *et al*., 1999; 2001). When TamA sequences lacking the Zn(II)2Cys6 motif are tethered to the promoter by fusion to heterologous DNA binding domains, TamA activates gene expression in an AreA-dependent manner requiring an intact AreA C-terminus, indicating that TamA recruits AreA to activate gene expression (Small *et al*., 1999; 2001). Therefore, TamA was found to act as a coactivator of AreA rather than as a direct DNA binding transcription factor. However, studies of the nitrogen assimilation gene *gdhA*, which encodes NADP-GDH (Gurr *et al*., 1986; Hawkins *et al*., 1989), showed *tamA*Δ had a more severe effect on expression than *areA*Δ, suggesting additional roles (Polotnianka *et al*., 2004).

Mutants in *A. nidulans gdhA*, *N. crassa am* and *S. cerevisiae GDH1* lacking NADP-GDH have reduced growth compared with wild type when ammonium is the sole nitrogen source (Arst and MacDonald, 1973; Kinghorn and Pateman, 1973; 1975b; Fincham and Baron, 1977; Fincham, 1988; Avendano *et al*., 1997; Fincham *et al*., 2000; DeLuna *et al*., 2001). These genes are controlled by several conserved regulatory mechanisms. *am* and *GDH1* are regulated by the global nitrogen GATA factor NIT2/Gln3p, respectively, and the CCAAT-binding factor (Dantzig *et al*., 1979; Frederick and Kinsey, 1990a,b; Daugherty *et al*., 1993; Chen and Kinsey, 1994; Chen *et al*., 1998; Riego *et al*., 2002). *GDH1* is also regulated by the branched-chain amino acid biosynthesis regulator Leu3p (Hu *et al*., 1995) and the amino acid starvation regulator Gcn4p (Riego *et al*., 2002). In *A. nidulans*, *gdhA* expression is regulated at the transcriptional level (Pateman, 1969; Hawkins *et al*., 1989; Caddick *et al*., 2006; Downes *et al*., 2013) by the branched amino acid biosynthesis regulator LeuB (Polotnianka *et al*., 2004; Downes *et al*., 2013) and the global nitrogen regulator AreA (Christensen *et al*., 1998).

AreA regulates genes required for utilization of alternative nitrogen nutrient sources (Arst and Cove, 1973; Hynes, 1975; Wilson and Arst, 1998). During nitrogen sufficient growth (ammonium or glutamine), AreA activation of nitrogen catabolic genes is generally minimized by *areA* mRNA instability (Platt *et al*., 1996a; Morozov *et al*., 2000; 2001; Caddick *et al*., 2006) and protein–protein interaction with NmrA (Andrianopoulos *et al*., 1998; Lamb *et al*., 2004; Kotaka *et al*., 2008). However, AreA remains active at the promoters of the ammonium permease *meaA* (Monahan *et al*., 2006) and *gdhA* genes (Christensen *et al*., 1998; Polotnianka *et al*., 2004), likely facilitated by promoter-specific elements. At the *gdhA* promoter the contribution of TamA to expression is greater than that of AreA, implicating TamA as the major determinant of *gdhA* expression (Polotnianka *et al*., 2004). Herein we show that regulation of *gdhA* by TamA is achieved by both DNA-binding and non-DNA-binding mechanisms. We show that full expression of *gdhA* requires a functional Zn(II)2Cys6 motif and we identify a conserved element in *Aspergillus gdhA* promoters that serves as the site of action for TamA. We demonstrate for the first time that TamA is a DNA-binding transcription factor, and we show that the TamA Zn(II)2Cys6 motif is required for binding to the *gdhA* promoter. Furthermore, TamA promoter occupancy is affected by the nitrogen source, and binding correlates with *gdhA* expression levels. We also show that TamA and AreA are reciprocally required for binding to the *gdhA* promoter. We conclude that TamA has dual DNA-binding activator and DNA-binding-independent coactivator functions that are dictated by promoter context.

Results

TamA has dual DNA binding and non-DNA binding roles

The TamA Zn(II)2Cys6 DNA-binding motif is poorly conserved compared with other regions of the protein in TamA orthologues in the Ascomycetes, but the six zinc-coordinating cysteines of the Zn(II)2Cys6 motif are retained suggesting functional relevance (Figs S1 and S2). The dispensability of the TamA DNA-binding motif for complementation of *tamA24* mutant phenotypes was demonstrated using ectopically integrated, multicopy *tamA*^{C90L} constructs carrying a non-conservative substitution (Davis *et al*., 1996). The C90L substitution affects the fourth zinc-coordinating cysteine and, like equivalent mutations [e.g. FacB (Todd *et al*., 1998, reviewed in Todd and

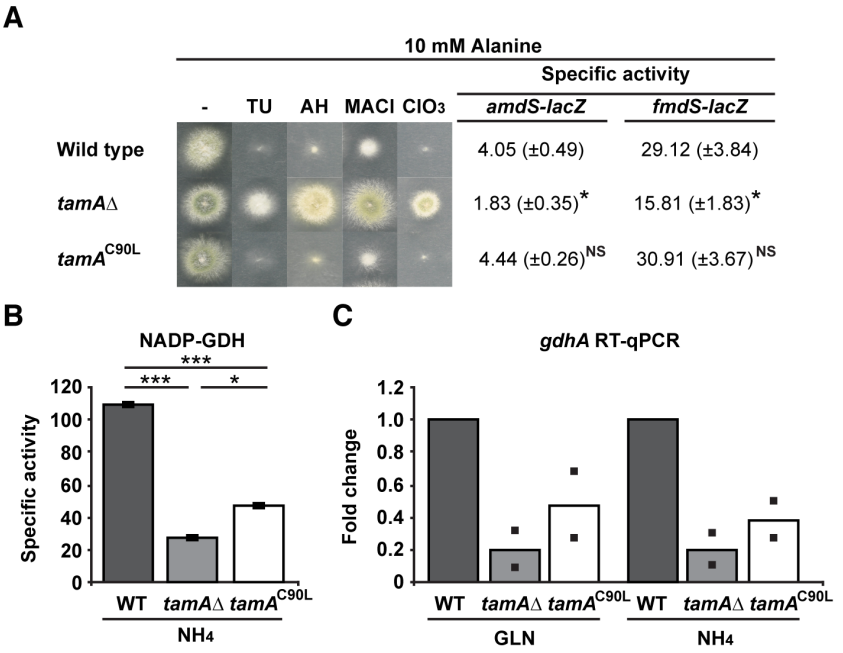

Fig. 1. The TamA Zn(II)2Cys6 motif is required for *gdhA* expression.
A. Wild type (MH1) and *tamA* variants (MH8694 and MH11808) were grown for 2 days on alanine ANM with 10 mM thiourea (TU), 0.3 mM L-aspartate–hydroxamate (AH), 200 mM methylammonium chloride (MACl), or 5 mM chlorate (ClO_3). LacZ specific activity was assayed for soluble protein extracts of mycelia from *amdS–lacZ* strains (MH11556, RT162 and RT171) and *fmdS–lacZ* strains (MH12326, RT163 and RT172) grown in alanine ANM for 16 h at 37°C. SEM is in parenthesis ($n \geq 3$).
B. NADP-GDH enzyme activity was measured in soluble extracts from wild type (MH12101), *tamA*Δ (MH12174) and $tamA^{C90L}$ (MH12597) mycelia grown in ammonium tartrate ANM for 16 h. Error bars depict SEM ($n \geq 3$).
C. *gdhA* transcript levels in RNA isolated from wild type (MH1), *tamA*Δ (RT162) and $tamA^{C90L}$ (RT171) strains grown for 16 h in glutamine or ammonium tartrate ANM were measured using RT-qPCR. Mean fold change (bars) of two biological replicates (squares) are shown. Transcript levels were normalized to *benA*.
For A and B, statistical significance is indicated as $P < 0.05$ (*), $P < 0.01$ (**), $P < 0.001$ (***), or not significant (NS).

Andrianopoulos, 1997)], is predicted to abolish zinc coordination and DNA-binding capacity. We determined the effect of specifically disrupting this motif in TamA by targeting a single copy of the $tamA^{C90L}$ mutant gene to the *tamA*Δ locus using homologous recombination. The targeted single copy $tamA^{C90L}$ strain was sensitive to methylammonium and showed full expression of the nitrogen-regulated *amdS–lacZ* reporter gene after nitrogen limitation (alanine) (Fig. 1A), consistent with previous data for ectopically integrated $tamA^{C90L}$ (Davis *et al*., 1996). Next we tested the $tamA^{C90L}$ strain for sensitivity to thiourea, aspartate–hydroxamate and chlorate. Like wild type strains and contrasting with the resistance phenotypes of the *tamA*Δ strain, $tamA^{C90L}$ was sensitive to all three toxic nitrogen analogues (Fig. 1A). We also measured expression of another nitrogen-regulated gene *fmdS* (Fraser *et al*., 2001) following nitrogen limitation using the *fmdS–lacZ* reporter gene and found that *tamA*Δ but not $tamA^{C90L}$ affected expression (Fig. 1A). Therefore TamA regulates *amdS*, *fmdS*, and resistance to four toxic nitrogen analogues in a DNA-binding independent manner, consistent with TamA action as a coactivator.

As TamA is a major activator of *gdhA* expression (Polotnianka *et al*., 2004), we determined the role of the TamA DNA-binding motif at this promoter. In contrast to the effects on *amdS* and *fmdS* expression, assays of NADP-GDH activity (Fig. 1B) and real-time reverse-transcriptase PCR (Fig. 1C) during nitrogen sufficiency (ammonium or glutamine) revealed reduced *gdhA* expression in both the *tamA*Δ and $tamA^{C90L}$ mutants. Therefore the TamA DNA-binding motif functions in *gdhA* regulation, and TamA uses both DNA-binding-dependent and DNA-binding-independent mechanisms to regulate its target genes. Interestingly the reduction of *gdhA* expression was significantly greater in *tamA*Δ than the $tamA^{C90L}$ strain (Fig. 1B), indicating TamA may employ both mechanisms at the *gdhA* promoter.

Identification of regulatory regions in the gdhA promoter

To identify key regulatory regions of the *gdhA* promoter we constructed *gdhA–lacZ* translational fusion reporter genes containing truncations 1994, 753 and 307 bp upstream of the start codon (Fig. 2A). We assayed each reporter gene after growth on glutamine, glutamate or ammonium, and in an *areA*Δ mutant after growth on ammonium (Fig. 2B). Like the native *gdhA* gene (Pateman, 1969; Hawkins *et al*., 1989), the −1994 and −753 bp *gdhA–lacZ* reporter genes were highly expressed on ammonium or glutamine and expression was reduced after growth on glutamate. In contrast, the −307 bp *gdhA–lacZ* fusion showed similar low levels of expression on all three nitrogen sources, suggesting the −307 to −1 bp region does not mediate nitrogen regulation. *areA*Δ conferred reduced expression of the −1994 and −753 bp *gdhA–lacZ* reporters but not the −307 bp *gdhA–lacZ* reporter (Fig. 2B), consistent with the distribution of AreA HGATAR binding sites (Fig. 2A) (Ravagnani *et al*., 1997).

To identify the site(s) of TamA action we measured the effects of *tamA*Δ and $tamA^{C90L}$ on *gdhA–lacZ* expression

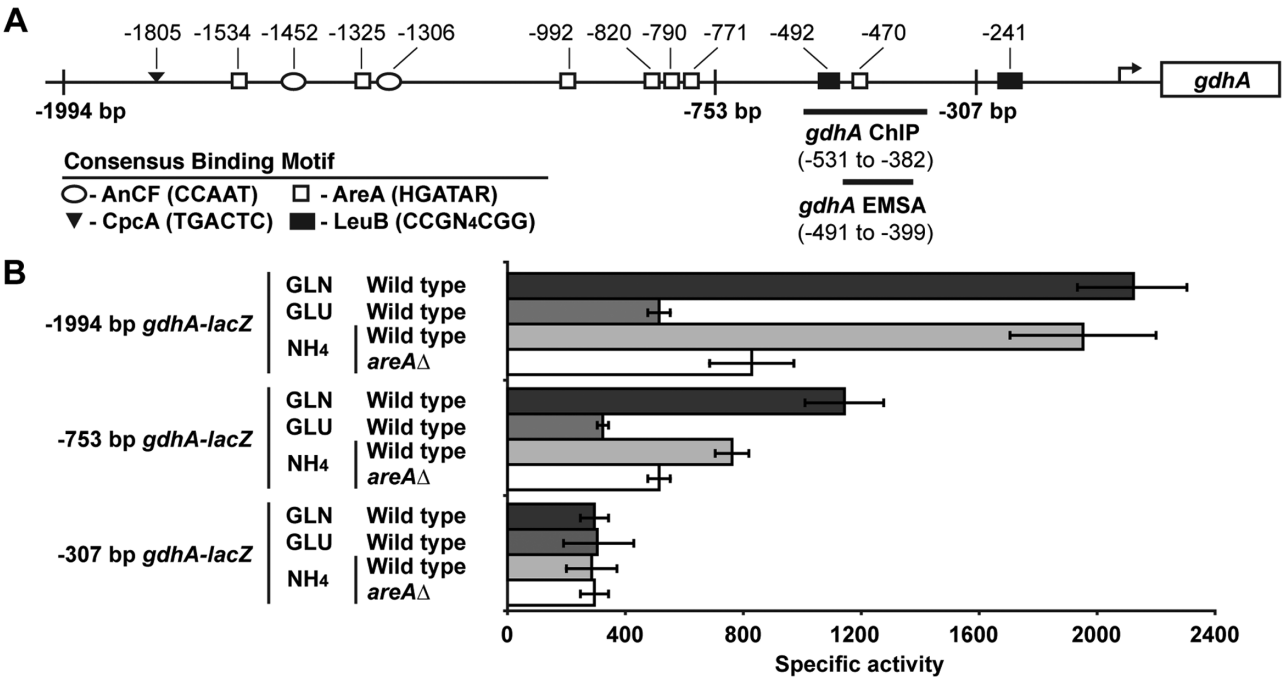

Fig. 2. Regulatory regions in the *gdhA* promoter.
A. The *gdhA* promoter contains putative DNA binding sites for the transcription factors AnCF (van Heeswijck and Hynes, 1991), AreA (Ravagnani *et al*., 1997), CpcA (Hoffmann *et al*., 2001) and LeuB (Downes *et al*., 2013).
B. β-Galactosidase levels expressed from *gdhA–lacZ* reporter genes were assayed from soluble cell extracts of wild type (RT151, MH12101 and MH12102) and *areA*Δ (RT158, MH12168 and MH12265) mycelia grown on glutamine (GLN), glutamate (GLU) or ammonium tartrate (NH_4) ANM for 16 h at 37°C. Strains carried either 1994, 753 or 307 bp of the *gdhA* promoter fused to *lacZ*. Error bars depict SEM ($n \geq 3$).

after growth on ammonium (Fig. 3A), or glutamine (Fig. S3A). Both *tamA*Δ and *tamA*^{C90L} conferred reduced expression of the –1994 and –753 bp *gdhA–lacZ* reporters, but not the –307 bp *gdhA–lacZ* reporter indicating that TamA contribution to *gdhA* expression requires sequences 5′ of –307 bp. Moreover, *tamA*Δ conferred a greater reduction than the *areA*Δ on –1994 and –753 bp reporter gene expression (compare Fig. 3A and Fig. 2B), consistent with TamA regulating expression via DNA binding rather than only as a coactivator of AreA. The expression level for the –753 bp *gdhA–lacZ* reporter was equally affected in *tamA*^{C90L} and *tamA*Δ strains. Therefore, the DNA binding motif is essential for TamA action between –753 and –308 bp in the *gdhA* promoter. However, *tamA*Δ had a significantly more severe effect than *tamA*^{C90L} on the –1994 bp *gdhA–lacZ* reporter (Fig. 3A) and NADP-GDH activity (Fig. 1A), suggesting that TamA also functions further upstream of –753 bp independent of its DNA binding domain.

Identification of a conserved site that conforms to a zinc cluster DNA binding site

TamA function is conserved between *A. nidulans* and *Aspergillus oryzae* (Small *et al*., 2001). Although conservation of the TamA Zn(II)2Cys6 motif is poor across the Ascomycetes (Fig. S2A), this motif is highly conserved within the Eurotiales (Aspergilli and Penicillia). Phylogenetic analyses of the Zn(II)2Cys6 motif compared with the region C-terminal to the zinc cluster revealed differences in the clustering of TamA orthologues (Fig. S2B and C), consistent with lower selection pressures on the Zn(II)2Cys6 motif than on other functional regions. To identify a putative TamA DNA binding site we used SCOPE computational promoter analysis (Carlson *et al*., 2007) to find overrepresented motifs in the 1.0 kb upstream of *gdhA* orthologues from *A. nidulans* and seven other Aspergilli. Seven putative regulatory motifs were identified in the *A. nidulans gdhA* promoter, however only three lie within the TamA region of action, –753 to –308 bp. Of these three motifs, the sequence that occurred most significantly in the query group was BCCGAASTTCGG (Table S1), which corresponds to –433 to –422 in *A. nidulans gdhA*. Within this 12 bp sequence lies an 11 bp palindrome containing everted CCG repeats, characteristic of some zinc binuclear cluster DNA binding sites (Todd and Andrianopoulos, 1997), flanking a central conserved five base-pair spacer. The other two motifs do not contain elements typical of binding sites for Zn(II)2Cys6 proteins. Alignment of the identified sequence and its flanking sequences among all eight

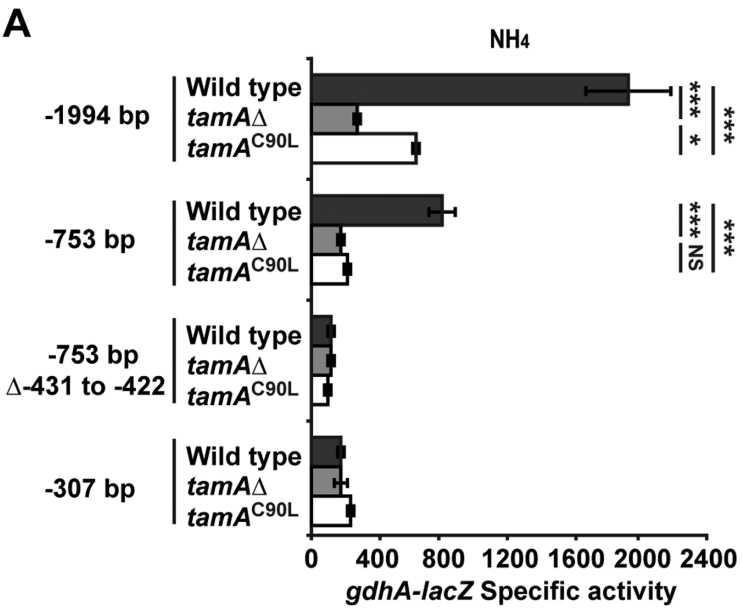

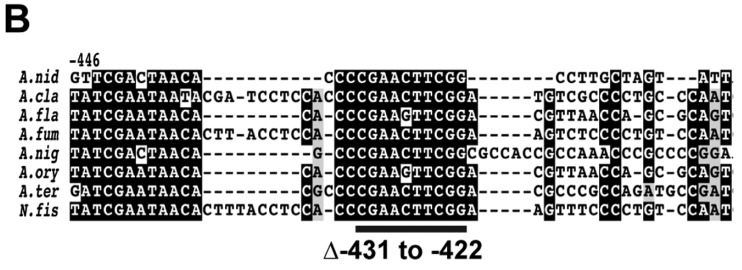

Fig. 3. TamA requires DNA binding function in the –753 to –308 bp region of *gdhA*.
A. β-Galactosidase activity of soluble protein extracts from wild type (RT151, MH12101, RT152 and MH12102), *tamA*Δ (RT165, MH12174, RT194 and MH12175) and *tamA*^{C90L} (RT218, MH12597, RT246, and MH12614) strains containing either the –1994, –753, mutated –753 or –307 bp *gdhA–lacZ* reporter genes, respectively, grown in ammonium tartrate ANM. Error bars depict SEM ($n \geq 3$). Statistical significance is indicated, where carried out, as $P < 0.05$ (*), $P < 0.001$ (***), or not significant (NS).
B. ClustalX2 alignment of the –534 to –382 bp region of the *A. nidulans* (A.nid) *gdhA* promoter with the equivalent region from *gdhA* orthologue promoters of *Aspergillus niger* (A.nig), *A. oryzae* (A.ory), *Aspergillus flavus* (A.fla), *Neosartorya fischeri* (N.fis), *Aspergillus fumigatus* (A.fum), and *Aspergillus clavatus* (A.cla) revealed a conserved CCCGAASTTCGG sequence. Black shading represents > 75% identity.

species revealed strong conservation (Fig. 3B). This conserved sequence is also present in the promoters of *gdhA* homologues from several other Ascomycetes, including *Penicillium chrysogenum* and *Phaeosphearia nododorum* (Fig. S2D).

TamA acts via the conserved CCCGAACTTCGG gdhA promoter element

We deleted nucleotides –431 to –422 of the predicted TamA target site in the –753 bp *gdhA–lacZ* reporter construct. This mutated promoter conferred reduced *gdhA–lacZ* levels, indicating that the conserved element is required for wild type levels of *gdhA* expression (Fig. 3A). Importantly, expression of the mutated *gdhA–lacZ* reporter was unchanged in both *tamA*Δ and *tamA*^{C90L} backgrounds. Therefore, this conserved sequence is required for TamA Zn(II)2Cys6 motif-dependent activation of *gdhA* and likely represents the TamA DNA binding site.

To determine whether TamA physically interacts with this region, we C-terminally FLAG epitope-tagged wild type TamA (TamA^{FLAG}) by single copy integration at the *tamA* locus (Fig. S4A), and the TamA^{C90L} Zn(II)2Cys6 mutant protein (TamA$^{C90L\text{-}FLAG}$) expressed from 1.4 kb of the *tamA* promoter in a single ectopic copy (Fig. S4B). Expression of functional tagged proteins was confirmed by Western blot (Fig. S4C), sensitivity to toxic nitrogen analogues (Fig. S4D) and expression of the –753 bp *gdhA–lacZ* reporter (Fig. S4E). Chromatin-immunoprecipitation (ChIP) analysis was conducted on the promoters of *gdhA* and *amdS*, and the constitutively expressed β-tubulin gene *benA* (Jung and Oakley, 1990). TamA^{FLAG} binding, but no binding of TamA$^{C90L\text{-}FLAG}$, was detected after growth on glutamine or ammonium only at the *gdhA* promoter (Fig. 4A), indicating that the Zn(II)2Cys6 motif was required for binding and suggesting a direct TamA-DNA interaction. To confirm this interaction we performed electrophoretic mobility shift assay (EMSA) on the –491 to –399 bp region of the *gdhA* promoter using immunoprecipitated TamA^{FLAG} and TamA$^{C90L\text{-}FLAG}$. We detected a single retarded band in binding reactions containing the wild type TamA protein but no shift was seen for the TamA^{C90L} mutant protein (Fig. 4B). Therefore, we propose that TamA binds the conserved CCGAACTTCGG sequence within the *gdhA* promoter. The absence of binding by the TamA$^{C90L\text{-}FLAG}$ protein to the *gdhA* promoter in both ChIP and EMSA experiments provides strong evidence that mutation of the fourth zinc-coordinating

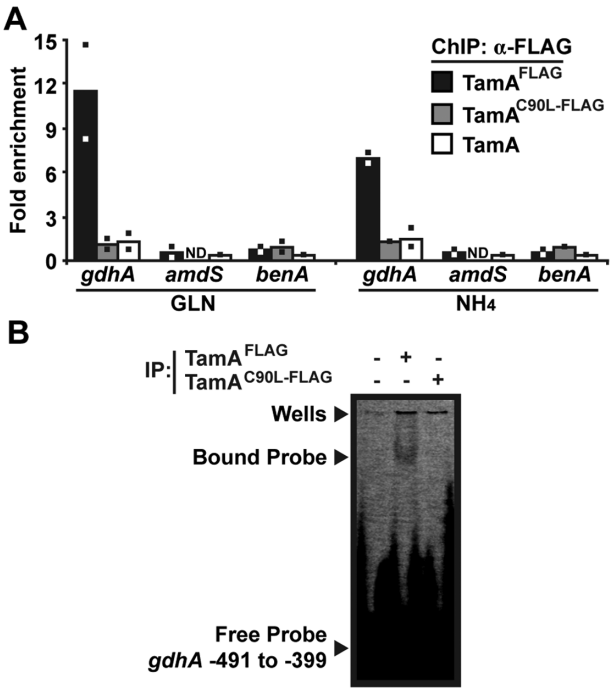

Fig. 4. TamA binds the *gdhA* upstream region.
A. α-FLAG-ChIP of *gdhA*, *amdS* and *benA* from TamA^{FLAG} (RT322), TamA$^{C90L\text{-}FLAG}$ (RT376) and wild type TamA (MH1) strains grown in glutamine (GLN) or ammonium tartrate (NH_4) ANM for 16 h. Mean fold enrichment (bars) of two biological replicates (squares) are shown. Results were normalized to the *gdhA* coding region.
B. Electrophoretic mobility shift assay of the –491 bp to –399 bp *gdhA* promoter region with immunoprecipitated TamA^{FLAG} (RT322) and TamA$^{C90L\text{-}FLAG}$ (RT376) proteins.

cysteine of TamA abolishes DNA binding function. To identify additional putative TamA DNA-binding targets we searched the 1.0 kb flanks and coding regions of all genes in *A. nidulans*, *A. oryzae*, *Aspergillus niger* and *Aspergillus fumigatus* for the conserved sequence (Table 1). Only two other genes in the *A. nidulans* genome have an exact matching sequence in their promoters. Across the genomes of the three other *Aspergillus* species only 12 genes contain a promoter sequence absolutely conserved with the TamA DNA binding site. Furthermore, *gdhA* is the only orthologous gene with a predicted TamA DNA binding site represented in more than one species, suggesting that the site in the *gdhA* promoter may be the only functional site, and that there are likely few direct TamA DNA-binding targets other than *gdhA*.

TamA DNA binding at gdhA is regulated by nitrogen source

Our ChIP analysis of TamA DNA binding revealed a difference in DNA binding levels at *gdhA* after growth on ammonium or glutamine. To further investigate the effects of nitrogen source on TamA DNA binding we performed ChIP after growth on the alternative nitrogen sources nitrate, alanine or glutamate. TamA promoter occupancy was lowest on glutamate, intermediate on ammonium or alanine, and highest on glutamine or nitrate (Fig. 5A). To determine if DNA binding levels were indicative of *gdhA* expression levels we assayed the –1994 and –753 bp *gdhA–lacZ* reporter strains grown on ammonium, glutamine, glutamate or alanine, and the –1994 bp *gdhA–lacZ* reporter strain grown on nitrate (Figs 5B and S3B). The levels of GdhA–LacZ activity correlated strongly with TamA DNA binding levels, and expression was reduced in the *tamA*Δ mutant. Therefore, regulation of TamA levels or TamA binding at the *gdhA* promoter may control *gdhA* levels in response to changes in nitrogen conditions.

TamA and AreA binding at gdhA is cooperative

We determined whether TamA binding at 5′ *gdhA* requires AreA. TamA^{FLAG} binding was severely reduced in the *areA*Δ mutant (Fig. 6A). Therefore, TamA DNA binding at the *gdhA* promoter is dependent upon both a functional Zn(II)2Cys6 motif and AreA. Assays of the –753 bp *gdhA–lacZ* reporter gene in an *areA217* mutant, which harbours a point mutation in the DNA-binding domain and lacks AreA DNA binding capacity (Platt *et al*., 1996b), showed similarly reduced levels as *areA*Δ indicating that DNA binding is required for AreA function in this region of the *gdhA* promoter (Fig. 6B). To determine whether TamA is required for AreA binding, we performed ChIP of AreA^{HA} (Todd *et al*., 2005) at the *gdhA* promoter in wild type and *tamA*Δ strains. AreA binding was observed after growth on ammonium or glutamine, and was severely reduced in the *tamA*Δ mutant (Fig. 6C), suggesting that TamA may recruit AreA to *gdhA* or stabilize AreA binding at the *gdhA* promoter. This raises the possibility that *gdhA* activation by AreA requires the TamA DNA binding site. Assays of the –753 bp *gdhA–lacZ* reporter lacking bases –431 to –422 revealed no additive effect of *areA*Δ (Fig. 6B). Therefore, TamA and AreA show cooperative DNA binding to regulate *gdhA*.

Discussion

DNA binding is generally considered essential for function of transcription factors bearing a DNA binding domain. However, TamA and Dal81p are unusual Zn(II)2Cys6 transcription factors that act as non-DNA-binding coactivators that recruit additional transcription factors (Bricmont *et al*., 1991; Davis *et al*., 1996; Muro-Pastor *et al*., 1999; Small *et al*., 1999; 2001; Sylvain *et al*., 2011; Cardillo *et al*., 2012). While previous evidence suggested that the Zn(II)2Cys6 motifs are dispensable for function, both proteins retain the six cysteine residues of the zinc binuclear cluster. This study has revealed that full expression of *gdhA*

Table 1. Putative TamA DNA binding targets identified using PatMatch[a].

Species	Downstream gene	Matching pattern	Matching positions		Description
			Begin	End	
Aspergillus nidulans	AN0149/*mdpF*	CCCGAAGTTCGG	–745	–734	Putative zinc-dependent hydrolase; member of the monodictyphenone (mdp) secondary metabolite biosynthesis gene cluster
	AN1403	CCGAAGTTCGG	–246	–236	Orthologue(s) have porphobilinogen synthase activity, role in haem biosynthetic process and cytosol, nucleus localization
	AN4376/*gdhA*	CCCGAACTTCGG	–433	–422	NADP-linked glutamate dehydrogenase
Aspergillus fumigatus	Afu2g10300	CCCGAAGTTCGG	–622	–610	40S ribosomal protein S17
	Afu2g16610	CCGAACTTCGG	–386	–376	Predicted oxidoreductase activity and role in oxidation-reduction process
	Afu2g16620	CCGAAGTTCGG	–564	–554	Has domain(s) with predicted ATP binding, protein tyrosine kinase activity
	Afu4g06620/*gdhA*	CCCGAACTTCGG	–393	–382	Glutamate dehydrogenase
	Afu5g07290	CCGAACTTCGG	–112	–102	Has domain(s) with predicted FMN binding, iron ion binding, oxidoreductase activity and role in oxidation-reduction process
	Afu8g00680	CCGAACTTCGG	–397	–387	Orthologue of *A. nidulans* AN8444/*celA*; similarity to cellulose synthase; predicted role in beta-glucan synthesis
Aspergillus niger	An04g00990/*gdhA*	CCCGAACTTCGG	–441	–430	NADP-dependent glutamate dehydrogenase
	An04g02610	CCCGAACTTCGG	–201	–190	Succinate-semialdehyde dehydrogenase [NAD(P)+]
	An11g02620	CCGAAGTTCGG	–516	–506	Alanine transaminase
	An14g03210	CCGAAGTTCGG	–117	–107	Orthologue of *A. nidulans* AN2893/*fhdA* putative forkhead-associated domain protein
	An14g03220	CCGAACTTCGG	–139	–129	Has domain(s) with predicted heat shock protein binding activity
Aspergillus oryzae	AO090023000923/*gdhA*	CCCGAAGTTCGG	–414	–403	Glutamate dehydrogenase

a. PatMatch (http://www.aspergillusgenome.org/cgi-bin/PATMATCH/nph-patmatch).

encoding NADP-GDH, a key ammonium assimilation enzyme in most fungi, is dependent upon a functional TamA DNA binding motif. Therefore, the DNA-binding domain of TamA is not dispensable for *gdhA* regulation. Moreover, TamA is a dual function transcription factor with both DNA-binding activator and coactivator roles. We showed that TamA binds via its Zn(II)2Cys6 domain to the *gdhA* promoter, and that TamA DNA binding and AreA DNA binding are interdependent. As TamA nuclear localization is not dependent on AreA (Small *et al.*, 2001), this effect is likely at the level of cooperative binding. Cooperative DNA binding is known for AreA with the nitrate utilization pathway-specific Zn(II)2Cys6 activator NirA (Narendja *et al.*, 2002; Berger *et al.*, 2006), and for the *N. crassa* AreA and NirA orthologues (Feng and Marzluf, 1998). We also showed that TamA promoter occupancy at *gdhA* is affected by the nitrogen source, and this correlates with the level of *gdhA–lacZ* expression. This suggests that TamA DNA binding, or the combined interdependent DNA binding of TamA and AreA, is the primary determinant of *gdhA* expression levels in response to nitrogen source. We defined the TamA site of action in the *gdhA* promoter as a conserved 12 bp sequence containing two potential Zn(II)2Cys6 binding motifs; a canonical $CCGN_5CGG$ site and a non-canonical $CCCN_6CCG$ site. The first motif is consistent with consensus Zn(II)2Cys6 recognition sites containing two CCG triplets and is the more probable recognition motif, however variation in triplet sequence is known (Todd *et al.*, 1998; Badis *et al.*, 2008). We have recently shown that LeuB regulates *gdhA* in response to leucine levels via two sites of action, one of which corresponds to the TamA site (Downes *et al.*, 2013). This site does not conform to a LeuB consensus DNA binding site and therefore the action of LeuB via this sequence may be indirect. The significance and mechanism of LeuB action via the same site as TamA in the *gdhA* promoter is being studied. The occurrence of the TamA target sequence in the *A. nidulans* genome is low suggesting few other direct targets, if any. We predict that, based on the dispensability of the TamA DNA binding motif for activation of *amdS–lacZ* and *fmdS–lacZ*, TamA will act as a coactivator via indirect binding to some additional AreA sites in the genome. However, it is possible that TamA may also regulate additional genes via different DNA-binding partners and divergent DNA binding sites, and therefore ChIP-seq will be needed to identify all TamA binding sites in the genome.

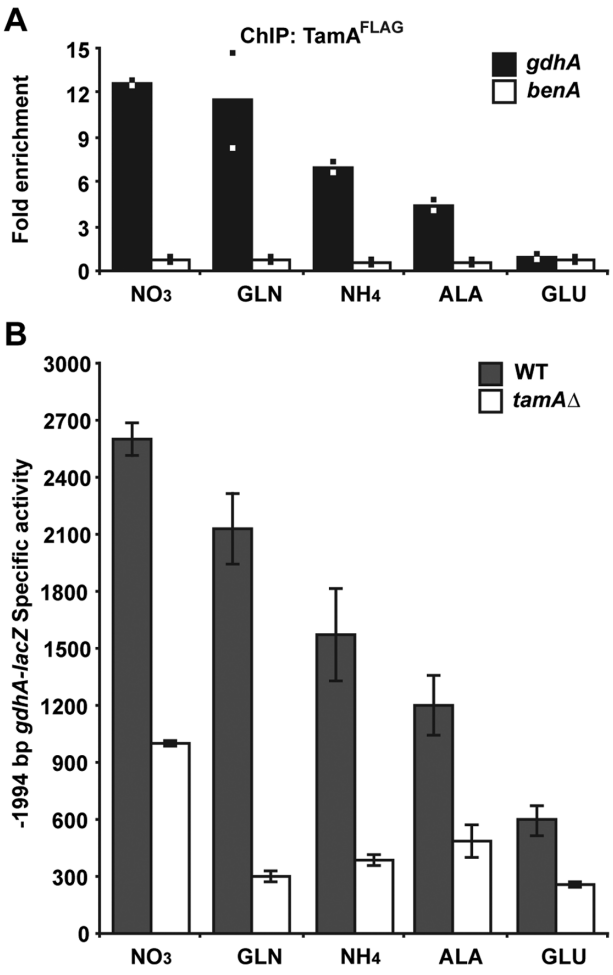

Fig. 5. TamA promoter occupancy is regulated by nitrogen source.
A. α-FLAG-ChIP of *gdhA* and *benA* from the TamA^{FLAG} strain (RT322) grown in nitrate (NO_3), glutamine (GLN), ammonium tartrate (NH_4), alanine (ALA), or glutamate (GLU) ANM for 16 h. Mean fold enrichment (bars) of two biological replicates (squares) are shown. Results were normalized to the *gdhA* coding region.
B. β-Galactosidase activity of soluble protein extracts from wild type (RT151, or for nitrate RT399) and *tamA*Δ (RT165, or for nitrate RT400) strains containing either the −1994 bp *gdhA–lacZ* reporter gene grown in nitrate (NO_3), glutamine (GLN), ammonium tartrate (NH_4), alanine (ALA) or glutamate (GLU) ANM for 16 h. Error bars depict SEM ($n \geq 3$).

TamA orthologues exhibit unusually low conservation of the DNA-binding motif, which is usually the most conserved region of Zn(II)2Cys6 transcription factors (Todd and Andrianopoulos, 1997; MacPherson *et al*., 2006). Greater conservation of regions outside of the TamA DNA-binding motif is observed, including but not limited to the Middle Homology Region found in many Zn(II)2Cys6 proteins. This suggests that non-DNA-binding functions, such as protein–protein interactions with the transcription machinery or signalling responses, are more highly conserved in TamA orthologues than DNA-binding functions. TamA interacts with the DNA-binding transcription factors LeuB and AreA and acts as a coactivator of AreA at the *amdS* promoter (Small *et al*., 1999; Polotnianka *et al*., 2004). Our data suggests that TamA also acts as a coactivator at the *fmdS* promoter and the promoters of genes conferring sensitivity to several toxic nitrogen analogues. The weak activity of TamA^{C90L} upstream of −753 bp of *gdhA* indicates potential coactivator function at this promoter as well. The coactivator functions of TamA at *gdhA* likely occur via protein–protein interactions with AreA as there are multiple AreA (HGATAR) sites in the promoter, however other interactors are also possible. The low level conservation of the DNA-binding motif is consistent with few DNA binding targets allowing co-evolution of cognate DNA binding motifs and DNA binding sites, and suggests that TamA orthologues beyond the Aspergilli and Penicillia may recognize different DNA binding site targets in different species. The TamA-related yeast protein Dal81p, which has a dispensable Zn(II)2Cys6 motif and acts as a non-DNA binding coactivator (Bricmont *et al*., 1991; Cardillo *et al*., 2012), requires interaction with the DNA-binding transcription factors Uga3p, Dal82p or Stp1p/Stp2p for activation of target genes (Scott *et al*., 2000; Boban and Ljungdahl, 2007; Sylvain *et al*., 2011; Cardillo *et al*., 2012) and no direct DNA binding has been reported. Genome-wide binding analysis has identified putative target genes for Dal81p including *GDH1* (Harbison *et al*., 2004), but it is unknown whether this is via direct DNA binding and no role for Dal81p in regulation of *GDH1* has been reported. Bioinformatics analyses identified putative regulatory elements targeted by Dal81p (Harbison *et al*., 2004; MacIsaac *et al*., 2006); however, the two Dal81p target sequences found are dissimilar to the TamA target site we identified. One of these Dal81p sites likely represents UAS_{GABA} (Talibi *et al*., 1995; Cardillo *et al*., 2012). Dal81p was shown by ChIP to interact with the *S. cerevisiae UGA1*, *UGA2* and *UGA4* promoters, after induction by GABA (Cardillo *et al*., 2010; 2012). However, the Zn(II)2Cys6 motif of Dal81p is dispensable for activation of these targets, suggesting indirect binding of UAS_{GABA} through Uga3p (Sylvain *et al*., 2011; Cardillo *et al*., 2012). Based on our findings for TamA, Dal81p may also have dual activation roles, however due to the divergence in DNA binding motif it is unlikely that DNA binding sites are conserved.

The paradigm for function of transcription factors containing DNA-binding motifs, including Zn(II)2Cys6 members, is regulation of a specific subset of genes by direct DNA binding (MacPherson *et al*., 2006). TamA does not conform to this model because it regulates genes in multiple pathways using DNA binding-dependent and DNA binding-independent mechanisms. Dual DNA-binding and coactivator function likely allows for differential regulation of targets through unrelated DNA binding motifs, and may contribute to transcription network plasticity and promoter

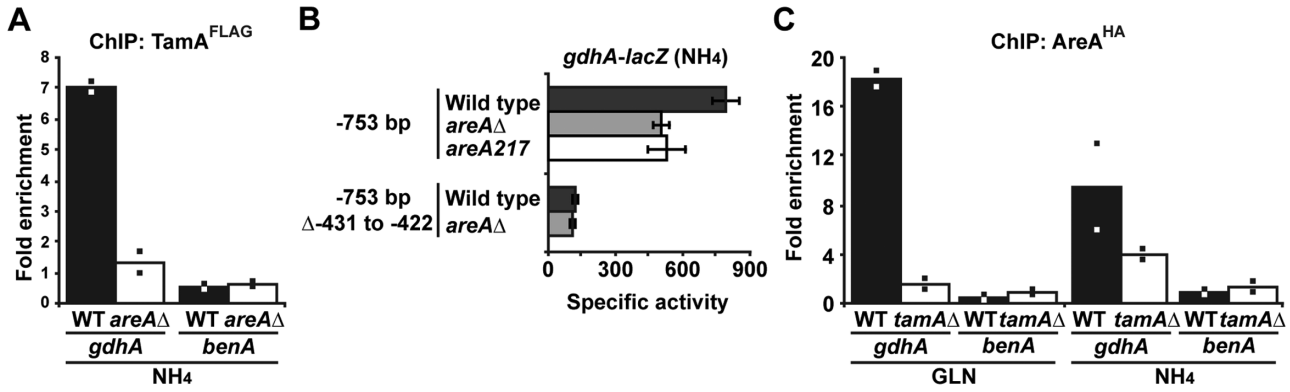

Fig. 6. AreA and TamA are reciprocally required for binding of the *gdhA* promoter.
A. α-FLAG ChIP of *gdhA* in TamA^{FLAG} strains lacking (RT322) or carrying (RT323) *areA*Δ from mycelia grown for 16 h in ammonium tartrate (NH_4) ANM. Mean fold enrichment (bars) of two biological replicates (squares) are shown. Results were normalized to the *gdhA* coding region.
B. β-Galactosidase activity of soluble protein extracts from wild type (MH12101 and RT152), *areA*Δ (MH12168 and RT379) or *areA217* (MH12582) strains containing either the −753 or mutated −753 bp *gdhA–lacZ* reporter genes grown in ammonium ANM for 16 h. Error bars depict SEM ($n \geq 3$).
C. α-HA ChIP of *gdhA* in AreA^{HA} strains lacking (MH9949) or carrying (RT277) *tamA*Δ from mycelia grown for 16 h in ammonium tartrate (NH_4) or glutamine (GLN) ANM. Mean fold enrichment (bars) of two biological replicates (squares) are shown. Results were normalized to the *gdhA* coding region.

evolution (Li and Johnson, 2010). Dual function basic Helix-Loop-Helix transcription factors, which act by DNA-binding or non-DNA-binding modes depending on cell-type, have been reported for the Hairy repressors in *Drosophila*, *Xenopus* and zebrafish (Kageyama *et al*., 2007; Nichane *et al*., 2008) and mouse SCL/TAL-1 (Kassouf *et al*., 2008). The finding that TamA cooperatively binds with AreA at the promoter of a key nitrogen assimilation gene while acting as an AreA coactivator at other sites in the same cell-type, may indicate an unrecognized mechanism of dual DNA-binding and non-DNA-binding action, according to promoter context, for transcription factors to facilitate combinatorial control of gene networks.

Experimental procedures

A. nidulans *strains, media, growth conditions, transformation and enzyme assays*

A. nidulans strains used are listed (Table 2). *A. nidulans* growth conditions and media were as described (Cove, 1966), adjusted to pH 6.5. *Aspergillus* nitrogen-free minimal media (ANM), supplemented for auxotrophies, contained 1% (w/v) glucose and nitrogen sources added to a final concentration of 10 mM. *A. nidulans* transformation and genetic analysis were performed as described (Todd *et al*., 2007; Downes *et al*., 2013). β-Galactosidase and NADP-GDH assays were performed as described (Pateman, 1969; Davis *et al*., 1988) using soluble protein extracts from mycelia grown for 16 h at 37°C. β-Galactosidase specific activity is expressed as $A_{420} \times 10^3$ min^{-1} mg^{-1} of soluble protein. One unit of NADP-GDH activity is defined as 1 nmol of NADP reduced min^{-1} mg^{-1} of soluble protein. Protein determinations used Bio-Rad Protein Assay reagent (Bio-Rad). Statistical significance was tested using an unequal variance two-sample *t*-test.

Molecular techniques

Standard molecular techniques (Sambrook and Russell, 2001) were used unless specified. *Escherichia coli* Top 10 (Invitrogen) and NM522 (Promega) strains were used. Ex Taq (TaKaRa) or Phusion (Finnzymes) DNA polymerases were used for PCR. Restriction enzymes (Promega) were used following the manufacturer's instructions. Plasmid DNA was prepared using Wizard Plus SVMinipreps DNA Purification System (Promega) and genomic DNA was isolated as described (Lee and Taylor, 1990). Applied Genetic Diagnostics (University of Melbourne, Australia) or Kansas State University DNA Sequencing and Genotyping Facility (Kansas, USA) conducted DNA sequencing. For Southern analysis, DNA transfer to Hybond N + membranes (GE Healthcare) used 0.4 M NaOH. Probes were made either by random hexanucleotide priming with [α-^{32}P]-dATP (Bresatec) and the Klenow fragment of DNA polymerase I (Promega) or DIG High Prime DNA Labeling and Detection Starter Kit II (Roche) following the manufacturer's instructions. RNA was isolated from strains grown in liquid culture for 16 h by grinding under liquid nitrogen, phenol-chloroform-isoamylalcohol extraction and lithium chloride precipitation (Sambrook and Russell, 2001). Oligonucleotides used are listed (Table S2). For quantitative real-time reverse-transcriptase PCR (RT-qPCR), RNA was quantified in a Nanodrop1000 and quality was assessed by agarose separation. RNA from two biological replicates was treated with RQ1 DNase (Promega) and cDNA made using the Reverse Transcriptase System (Promega). qPCR in a MyiQ thermocycler (Bio-Rad) used iTAQ™ Universal SYBR® Green Supermix (Bio-Rad) and were analysed with iQ5 v2.1 (Bio-Rad). *gdhA* (+360 to +508 bp) and *benA* (+1354 to +1486 bp) were amplified with gdhAqPCR-F/R and

Table 2. *A. nidulans* strains used in this work.

Strain	Genotype
MH1	*biA1*
MH8694	*biA1 tamAΔ riboB2*
MH9949	*biA1 gpdA*(p)*–areA*^{HA} *amdS–lacZ*
MH11036	*pyroA4 nkuAΔ::argB riboB2*
MH11094	*amdS–lacZ pyroA4 nkuAΔ niiA4*
MH11401	*pabaA1 areA102 nkuAΔ::argB tamAΔ niiA4 riboB2*
MH11556	*wA1 amdS–lacZ pyroA4*
MH11808	*pabaA1 nkuAΔ::argB tamA*^{C90L} *riboB2*
MH12101	*A.f.pyroA–gdhA*(–753 bp)*–lacZ@amdS pyroA4 nkuAΔ::Bar niiA4*
MH12102	*A.f.pyroA–gdhA*(–307 bp)*–lacZ@amdS pyroA4 nkuAΔ::Bar niiA4*
MH12168	*areAΔ A.f.pyroA–gdhA*(–753 bp)*–lacZ@amdS pyroA4 nkuAΔ::Bar niiA4*
MH12174	*biA1 A.f.pyroA–gdhA*(–753 bp)*–lacZ@amdS pyroA4 nkuAΔ::Bar tamAΔ niiA4*
MH12175	*biA1 A.f.pyroA–gdhA*(–307 bp)*–lacZ@amdS pyroA4 nkuAΔ::Bar tamAΔ niiA4*
MH12265	*areAΔ A.f.pyroA–gdhA*(–307 bp)*–lacZ@amdS pyroA4 nkuAΔ::Bar niiA4*
MH12326	*yA1 pabaA1 fmdS–lacZ pyroA4 nkuAΔ riboB2*
MH12582	*yA1 areA217 A.f.pyroA–gdhA*(–753 bp)*–lacZ@amdS pyroA4 nkuAΔ::Bar riboB2*
MH12597	*A.f.pyroA–gdhA*(–753 bp)*–lacZ@amdS pyroA4 nkuAΔ::Bar tamA*^{C90L} *riboB2*
MH12614	*A.f.pyroA–gdhA*(–307 bp)*–lacZ@amdS pyroA4 nkuAΔ::Bar tamA*^{C90L} *niiA4 riboB2*
RT151	*A.f.pyroA–gdhA*(–1994 bp)*–lacZ@amdS pyroA4 nkuAΔ::Bar niiA4*
RT152	*A.f.pyroA–gdhA*(–753 bp Δ–431 to –422)*–lacZ@amdS pyroA4 nkuAΔ::Bar niiA4*
RT158	*areAΔ A.f.pyroA–gdhA*(–1994 bp)*–lacZ@amdS pyroA4 nkuAΔ::Bar niiA4 riboB2*
RT162	*biA1 amdS–lacZ pyroA4 tamAΔ riboB2*
RT163	*biA1 fmdS–lacZ nkuAΔ tamAΔ riboB2*
RT165	*A.f.pyroA–gdhA*(–1994 bp)*–lacZ@amdS pyroA4 nkuAΔ::Bar tamAΔ niiA4*
RT171	*biA1 amdS–lacZ pyroA4 nkuAΔ tamA*^{C90L} *riboB2*
RT172	*pabaA1 fmdS–lacZ nkuAΔ tamA*^{C90L} *riboB2*
RT194	*biA1 A.f.pyroA–gdhA*(–753 bp Δ–431 to –422)*–lacZ@amdS pyroA4 nkuAΔ::Bar tamAΔ*
RT218	*pabaA1 A.f.pyroA–gdhA*(–1994 bp)*–lacZ@amdS pyroA4 nkuAΔ::Bar tamA*^{C90L} *niiA4*
RT246	*biA1 pabaA1 A.f.pyroA–gdhA*(–753 bp Δ–431 to –422)*–lacZ@amdS pyroA4 nkuAΔ::Bar tamA*^{C90L} *riboB2*
RT277	*biA1 gpdA*(p)*–areA*^{HA} *fmdS–lacZ tamAΔ niiA4*
RT299	*pyroA4 nkuAΔ::argB tamA*^{FLAG}*–A.f.pyroA riboB2*
RT322	*biA1 pyroA4 nkuAΔ::argB tamA*^{FLAG}*–A.f.pyroA riboB2*
RT323	*biA1 areAΔ pyroA4 nkuAΔ::argB tamA*^{FLAG}*–A.f.pyroA riboB2*
RT376	*biA1 A.f.riboB–tamA*$^{C90L–FLAG}$*@fmdS–lacZ nkuAΔ::Bar tamAΔ riboB2*
RT377	*A.f.pyroA–gdhA*(–753 bp)*–lacZ@amdS pyroA4 nkuAΔ::Bar tamA*^{FLAG}*–A.f.pyroA*
RT379	*areAΔ A.f.pyroA–gdhA*(–753 bp Δ–431 to –422)*–lacZ@amdS pyroA4 niiA4 riboB2*
RT399	*A.f.pyroA–gdhA*(–1994 bp)*–lacZ@amdS pyroA4 nkuAΔ::Bar riboB2*
RT400	*A.f.pyroA–gdhA*(–1994 bp)*–lacZ@amdS pyroA4 nkuAΔ::Bar tamAΔ*

benAqPCR-F/R, which have efficiencies of 109.0% and 100.7% respectively at $T_a = 55.9°C$. Fold change was calculated using the $\Delta\Delta C_T$ efficiency correction method (Pfaffl, 2001; Schmittgen and Livak, 2008).

Reporter gene and strain construction

Construction of *gdhA* reporter genes and strains used the strategy described previously (Downes *et al.*, 2013). Fragments of the *gdhA* promoter were amplified by PCR from MH1 genomic DNA using the forward primers gdhA1XhoI-F, gdhA5XhoI-F or gdhA8XhoI-F with gdhA2BglII-R. PCR products were digested with XhoI and BglII and ligated into XhoI/BamHI cut pYS7225 (Downes *et al.*, 2013) to create pSL6974 (–1994 bp), pSL6976 (–753 bp) and pSL6977 (–307 bp) respectively, containing translational fusions of *gdhA–lacZ*. Plasmids were transformed into MH11094 (*amdS–lacZ pyroA4 nkuAΔ niiA4*) and targeted to *amdS–lacZ* by homologous recombination (Nayak *et al.*, 2006; Suzuki *et al.*, 2012). Construction of wild type and mutated –753 bp *gdhA–lacZ* has previously been reported (Downes *et al.*, 2013). Transformants were selected for pyridoxine prototrophy and single copy integrants confirmed by Southern analysis.

Construction of tamA^{C90L}*, tamA*^{FLAG} *and tamA*$^{C90L\text{-}FLAG}$

The full *tamA*^{C90L} gene was subcloned from pXBBPstSal-18 (Davis *et al.*, 1996) by digestion with BamHI and ligation into pSM6392 containing the *A. fumigatus riboB* selectable marker to create pSL6679. pSL6679 was targeted to *tamA* flanking sequences by single crossover in the *tamA* deletion strain MH11401 (*nkuAΔ tamAΔ riboB2*), to produce a single copy insertion of the *tamA*^{C90L} gene. For TamA epitope-tagging, the 3′ coding region (+1219 to +2217) of *tamA* was amplified using tamAFLAG-F and tamAFLAG-R containing the FLAG-epitope encoding sequence. The PCR product was digested with SacI and cloned into SacI-digested p6363 to create pDD188 (3′ *tamA*^{FLAG}), which was transformed into MH11036 (*pyroA4 nkuAΔ riboB2*) by single crossover at *tamA* producing a single copy full-length tagged gene. pSL6679 was digested with SacI/BamHI to delete the 3′ *tamA* coding sequence to create pDD209. 3′ *tamA*^{FLAG} was excised from

pDD188 by SacI digest and ligated into SacI cut pDD209 to create pDD211 (*tamA*$^{C90L\text{-}FLAG}$) containing a tagged full-length copy of the C90L mutant *tamA* and 1.4 kb 5′ sequence. pDD211 was targeted to the *fmdS–lacZ* locus of RT163 (*fmdS–lacZ nkuA*Δ *tamA*Δ *riboB2*) in single copy. Strains transformed with *tamA* variants were selected for riboflavin prototrophy. Single copy integration was confirmed by Southern analysis.

In silico *analyses*

DNA sequence analysis was done in Geneious version 5.3.5 created by Biomatters (http://www.geneious.com). Alignments were done using ClustalW2 (Larkin *et al*., 2007) and shaded in MacBoxshade 2.15E (M.D. Baron). 1.0 kb *gdhA* upstream sequences from *Aspergillus clavatus*, *A. nidulans*, *A. niger*, *A. oryzae*, *Aspergillus flavus*, *A. fumigatus*, *Aspergillus terreus* and *Neosartorya fischeri* were obtained from the Broad Institute database (http://www.broadinstitute.org/annotation/genome/aspergillus_group). SCOPE analysis was conducted as described (Carlson *et al*., 2007). Unrooted phylogenetic trees were constructed in Geneious using protein sequences identified from NCBI by BLASTp with Dal81p and TamA. PatMatch analysis (http://www.aspergillusgenome.org/cgi-bin/PATMATCH/nph-patmatch) used either CCCGAAS TTCGG or CCGAASTTCGG to search open reading frame DNA plus genomic sequences 1000 bp upstream and downstream.

Chromatin immunoprecipitation (ChIP) and electrophoretic mobility shift assay (EMSA)

Mycelia were grown for 16 h, fixed in 1% formaldehyde for 20 m then quenched with 0.6 M glycine. ChIP was performed for two biological replicates as previously described (Suzuki *et al*., 2012) using 2 μg of either anti-FLAG (M2, Sigma) or anti-HA (F7, Santa Cruz Biotechnology). Quantitative real-time PCR was performed for *gdhA* –531 to –382 (gdhApro-F/R), *gdhA* +310 to +407 (gdhAcod-F/R), *amdS* –213 to –125 (amdSpro-F/R), and *benA* –224 to –125 (benApro-F/R). EMSA probe (–491 to –399 bp *gdhA*) was amplified using leuB1del-F and Infrared Dye IRD700-labelled IRgdhAprobe-R (IDT) from pDD149 (Downes *et al*., 2013). EMSA was carried out in native 4% polyacrylamide gels as previously described (Todd *et al*., 1998) with 6 ng of probe, 1 μg poly d(I-C) and 6 μg immunoprecipitated TamA^{FLAG} or TamA$^{C90L\text{-}FLAG}$. Infrared fluorescence images (700 nm) were captured directly from the EMSA gel using Odyssey Image Studio Software and the Odyssey Fc (LI-COR).

Protein purification and Western blots and column immunoprecipitation

TamA^{FLAG} and TamA$^{C90L\text{-}FLAG}$ were extracted from 2.0 g of mycelia, grown for 16 h in ANM supplemented with 10 mM ammonium tartrate, by homogenization in 10 ml extraction buffer (50 mM Tris-HCl pH8, 137 mM NaCl, 2.7 mM KCl, 1.0 mM $MgCl_2$ and 1× Amresco protease inhibitor cocktail) using FastPrep-24 (MP Bio) at 6.5 m/s 5 times for 20 s with 5 m cooling periods. Mycelial debris was removed by two 4°C centrifugations at 16 100 *g* for 10 m and 2 m. Tagged proteins were purified using FLAG Immunoprecipitation Kit (Sigma) by 3× peptide elution. For Western blot, proteins were separated by 12% SDS-PAGE, transferred to PVDF membranes by electroblot, detected using monoclonal 1:15 000 M2 anti-FLAG (Sigma) and 1:10 000 anti-mouse/rabbit-IgG-POD (Roche) antibodies, and development with the BM Chemiluminescence Western blotting kit (Roche). Images were captured using Odyssey Image Studio Software and the Odyssey Fc (LI-COR).

Acknowledgements

We thank A. Andrianopoulos for assistance with bioinformatics, G.Y. Busot for assistance with protein manipulation, and acknowledge expert technical assistance of C.C. Hunter, and B.T. Pfannenstiel. This work was supported by the Australian Research Council's *Discovery Project* funding scheme Project Number DP0558002, Kansas NSF EPSCoR First Award EPS-0903806, The Kansas State University Plant Biotechnology Center, and the Johnson Center for Basic Cancer Research. Contribution No. 14-065-J from the Kansas Agricultural Experiment Station. The authors have no conflict of interest to declare.

References

Andrianopoulos, A., Kourambas, S., Sharp, J.A., Davis, M.A., and Hynes, M.J. (1998) Characterization of the *Aspergillus nidulans nmrA* gene involved in nitrogen metabolite repression. *J Bacteriol* **180:** 1973–1977.

Arst, H.N., Brownlee, A.G., and Cousen, S.A. (1982) Nitrogen metabolite repression in *Aspergillus nidulans* – a farewell to *tamA*? *Curr Genet* **6:** 245–257.

Arst, H.N., Jr, and Cove, D.J. (1973) Nitrogen metabolite repression in *Aspergillus nidulans*. *Mol Gen Genet* **126:** 111–141.

Arst, H.N., Jr, and MacDonald, D.W. (1973) A mutant of *Aspergillus nidulans* lacking NADP-linked glutamate dehydrogenase. *Mol Gen Genet* **122:** 261–265.

Avendano, A., Deluna, A., Olivera, H., Valenzuela, L., and Gonzalez, A. (1997) *GDH3* encodes a glutamate dehydrogenase isozyme, a previously unrecognized route for glutamate biosynthesis in *Saccharomyces cerevisiae*. *J Bacteriol* **179:** 5594–5597.

Badis, G., Chan, E.T., van Bakel, H., Pena-Castillo, L., Tillo, D., Tsui, K., *et al*. (2008) A library of yeast transcription factor motifs reveals a widespread function for Rsc3 in targeting nucleosome exclusion at promoters. *Mol Cell* **32:** 878–887.

Bai, Y.L., and Kohlhaw, G.B. (1991) Manipulation of the 'zinc cluster' region of transcriptional activator LEU3 by site-directed mutagenesis. *Nucleic Acids Res* **19:** 5991–5997.

Berger, H., Pachlinger, R., Morozov, I., Goller, S., Narendja, F., Caddick, M., and Strauss, J. (2006) The GATA factor AreA regulates localization and *in vivo* binding site occupancy of the nitrate activator NirA. *Mol Microbiol* **59:** 433–446.

Boban, M., and Ljungdahl, P.O. (2007) Dal81 enhances Stp1-

and Stp2-dependent transcription necessitating negative modulation by inner nuclear membrane protein Asi1 in *Saccharomyces cerevisiae*. *Genetics* **176:** 2087–2097.
Bricmont, P.A., Daugherty, J.R., and Cooper, T.G. (1991) The *DAL81* gene product is required for induced expression of two differently regulated nitrogen catabolic genes in *Saccharomyces cerevisiae*. *Mol Cell Biol* **11:** 1161–1166.
Caddick, M.X., Jones, M.G., van Tonder, J.M., Le Cordier, H., Narendja, F., Strauss, J., and Morozov, I.Y. (2006) Opposing signals differentially regulate transcript stability in *Aspergillus nidulans*. *Mol Microbiol* **62:** 509–519.
Cardillo, S.B., Bermudez Moretti, M., and Correa Garcia, S. (2010) Uga3 and Uga35/Dal81 transcription factors regulate *UGA4* transcription in response to gamma-aminobutyric acid and leucine. *Eukaryot Cell* **9:** 1262–1271.
Cardillo, S.B., Levi, C.E., Bermudez Moretti, M., and Correa Garcia, S. (2012) Interplay between the transcription factors acting on the GATA- and GABA-responsive elements of *Saccharomyces cerevisiae* UGA promoters. *Microbiology* **158:** 925–935.
Carlson, J.M., Chakravarty, A., DeZiel, C.E., and Gross, R.H. (2007) SCOPE: a web server for practical de novo motif discovery. *Nucleic Acids Res* **35:** W259–W264.
Chen, H., and Kinsey, J.A. (1994) Sequential gel mobility shift scanning of 5′ upstream sequences of the *Neurospora crassa am* (GDH) gene. *Mol Gen Genet* **242:** 399–403.
Chen, H., Crabb, J.W., and Kinsey, J.A. (1998) The Neurospora *aab-1* gene encodes a CCAAT binding protein homologous to yeast *HAP5*. *Genetics* **148:** 123–130.
Christensen, T., Hynes, M.J., and Davis, M.A. (1998) Role of the regulatory gene *areA* of *Aspergillus oryzae* in nitrogen metabolism. *Appl Environ Microbiol* **64:** 3232–3237.
Cove, D.J. (1966) The induction and repression of nitrate reductase in the fungus *Aspergillus nidulans*. *Biochim Biophys Acta* **113:** 51–56.
Dantzig, A.H., Wiegmann, F.L., Jr, and Nason, A. (1979) Regulation of glutamate dehydrogenases in *nit-2* and *am* mutants of *Neurospora crassa*. *J Bacteriol* **137:** 1333–1339.
Daugherty, J.R., Rai, R., el Berry, H.M., and Cooper, T.G. (1993) Regulatory circuit for responses of nitrogen catabolic gene expression to the GLN3 and DAL80 proteins and nitrogen catabolite repression in *Saccharomyces cerevisiae*. *J Bacteriol* **175:** 64–73.
Davis, M.A., Cobbett, C.S., and Hynes, M.J. (1988) An *amdS–lacZ* fusion for studying gene regulation in *Aspergillus*. *Gene* **63:** 199–212.
Davis, M.A., Small, A.J., Kourambas, S., and Hynes, M.J. (1996) The *tamA* gene of *Aspergillus nidulans* contains a putative zinc cluster motif which is not required for gene function. *J Bacteriol* **178:** 3406–3409.
DeLuna, A., Avendano, A., Riego, L., and Gonzalez, A. (2001) NADP-glutamate dehydrogenase isoenzymes of *Saccharomyces cerevisiae*. Purification, kinetic properties, and physiological roles. *J Biol Chem* **276:** 43775–43783.
Downes, D.J., Davis, M.A., Kreutzberger, S.D., Taig, B.L., and Todd, R.B. (2013) Regulation of the NADP-glutamate dehydrogenase gene *gdhA* in *Aspergillus nidulans* by the Zn(II)2Cys6 transcription factor LeuB. *Microbiology* **159:** 2467–2480.
Feng, B., and Marzluf, G.A. (1998) Interaction between major nitrogen regulatory protein NIT2 and pathway-specific regulatory factor NIT4 is required for their synergistic activation of gene expression in *Neurospora crassa*. *Mol Cell Biol* **18:** 3983–3990.
Fincham, J.R. (1988) The Neurospora *am* gene and allelic complementation. *Bioessays* **9:** 169–172.
Fincham, J.R., and Baron, A.J. (1977) The molecular basis of an osmotically reparable mutant of *Neurospora crassa* producing unstable glutamate dehydrogenase. *J Mol Biol* **110:** 627–642.
Fincham, J.R., Kinsey, J.A., Fuentes, A.M., Cummings, N.J., and Connerton, I.F. (2000) The Neurospora *am* gene and NADP-specific glutamate dehydrogenase: mutational sequence changes and functional effects–more mutants and a summary. *Genet Res* **76:** 1–10.
Fraser, J.A., Davis, M.A., and Hynes, M.J. (2001) The formamidase gene of *Aspergillus nidulans*: regulation by nitrogen metabolite repression and transcriptional interference by an overlapping upstream gene. *Genetics* **157:** 119–131.
Frederick, G.D., and Kinsey, J.A. (1990a) Distant upstream regulatory sequences control the level of expression of the *am* (GDH) locus of *Neurospora crassa*. *Curr Genet* **18:** 53–58.
Frederick, G.D., and Kinsey, J.A. (1990b) Nucleotide sequence and nuclear protein binding of the two regulatory sequences upstream of the *am* (GDH) gene in Neurospora. *Mol Gen Genet* **221:** 148–154.
Gardner, K.H., Pan, T., Narula, S., Rivera, E., and Coleman, J.E. (1991) Structure of the binuclear metal-binding site in the GAL4 transcription factor. *Biochemistry* **30:** 11292–11302.
Gurr, S.J., Hawkins, A.R., Drainas, C., and Kinghorn, J.R. (1986) Isolation and identification of the *Aspergillus nidulans gdhA* gene encoding NADP-linked glutamate dehydrogenase. *Curr Genet* **10:** 761–766.
Harbison, C.T., Gordon, D.B., Lee, T.I., Rinaldi, N.J., Macisaac, K.D., Danford, T.W., *et al.* (2004) Transcriptional regulatory code of a eukaryotic genome. *Nature* **431:** 99–104.
Hawkins, A.R., Gurr, S.J., Montague, P., and Kinghorn, J.R. (1989) Nucleotide sequence and regulation of expression of the *Aspergillus nidulans gdhA* gene encoding NADP dependent glutamate dehydrogenase. *Mol Gen Genet* **218:** 105–111.
van Heeswijck, R., and Hynes, M.J. (1991) The *amdR* product and a CCAAT-binding factor bind to adjacent, possibly overlapping DNA sequences in the promoter region of the *Aspergillus nidulans amdS* gene. *Nucleic Acids Res* **19:** 2655–2660.
Hoffmann, B., Valerius, O., Andermann, M., and Braus, G.H. (2001) Transcriptional autoregulation and inhibition of mRNA translation of amino acid regulator gene *cpcA* of filamentous fungus *Aspergillus nidulans*. *Mol Biol Cell* **12:** 2846–2857.
Hu, Y., Cooper, T.G., and Kohlhaw, G.B. (1995) The *Saccharomyces cerevisiae* Leu3 protein activates expression of *GDH1*, a key gene in nitrogen assimilation. *Mol Cell Biol* **15:** 52–57.
Hynes, M.J. (1975) Studies on the role of the *areA* gene in the

regulation of nitrogen catabolism in *Aspergillus nidulans*. *Aust J Biol Sci* **28:** 301–313.
Johnston, M., and Dover, J. (1987) Mutations that inactivate a yeast transcriptional regulatory protein cluster in an evolutionarily conserved DNA binding domain. *Proc Natl Acad Sci USA* **84:** 2401–2405.
Jung, M.K., and Oakley, B.R. (1990) Identification of an amino acid substitution in the *benA*, beta-tubulin gene of *Aspergillus nidulans* that confers thiabendazole resistance and benomyl supersensitivity. *Cell Motil Cytoskeleton* **17:** 87–94.
Kageyama, R., Ohtsuka, T., and Kobayashi, T. (2007) The Hes gene family: repressors and oscillators that orchestrate embryogenesis. *Development* **134:** 1243–1251.
Kassouf, M.T., Chagraoui, H., Vyas, P., and Porcher, C. (2008) Differential use of SCL/TAL-1 DNA-binding domain in developmental hematopoiesis. *Blood* **112:** 1056–1067.
Kinghorn, J.R., and Pateman, J.A. (1973) NAD and NADP L-glutamate dehydrogenase activity and ammonium regulation in *Aspergillus nidulans*. *J Gen Microbiol* **78:** 39–46.
Kinghorn, J.R., and Pateman, J.A. (1975a) Studies of partially repressed mutants at the *tamA* and *areA* loci in *Aspergillus nidulans*. *Mol Gen Genet* **140:** 137–147.
Kinghorn, J.R., and Pateman, J.A. (1975b) The structural gene for NADP L-glutamate dehydrogenase in *Aspergillus nidulans*. *J Gen Microbiol* **86:** 294–300.
Kotaka, M., Johnson, C., Lamb, H.K., Hawkins, A.R., Ren, J., and Stammers, D.K. (2008) Structural analysis of the recognition of the negative regulator NmrA and DNA by the zinc finger from the GATA-type transcription factor AreA. *J Mol Biol* **381:** 373–382.
Lamb, H.K., Ren, J., Park, A., Johnson, C., Leslie, K., Cocklin, S., *et al*. (2004) Modulation of the ligand binding properties of the transcription repressor NmrA by GATA-containing DNA and site-directed mutagenesis. *Protein Sci* **13:** 3127–3138.
Larkin, M.A., Blackshields, G., Brown, N.P., Chenna, R., McGettigan, P.A., McWilliam, H., *et al*. (2007) Clustal W and Clustal X version 2.0. *Bioinformatics* **23:** 2947–2948.
Lee, S.B., and Taylor, J.W. (1990) Isolation of DNA from fungal mycelia and single spores. In *PCR Protocols: A Guide to Methods and Applications*. Innis, M.A., Gelfand, D.H., Sninsky, J.S., and White, T.J. (eds). San Diego: Academic Press, pp. 282–287.
Li, H., and Johnson, A.D. (2010) Evolution of transcription networks–lessons from yeasts. *Curr Biol* **20:** R746–R753.
MacIsaac, K.D., Wang, T., Gordon, D.B., Gifford, D.K., Stormo, G.D., and Fraenkel, E. (2006) An improved map of conserved regulatory sites for *Saccharomyces cerevisiae*. *BMC Bioinformatics* **7:** 113.
MacPherson, S., Larochelle, M., and Turcotte, B. (2006) A fungal family of transcriptional regulators: the zinc cluster proteins. *Microbiol Mol Biol Rev* **70:** 583–604.
Monahan, B.J., Askin, M.C., Hynes, M.J., and Davis, M.A. (2006) Differential expression of *Aspergillus nidulans* ammonium permease genes is regulated by GATA transcription factor AreA. *Eukaryot Cell* **5:** 226–237.
Morozov, I.Y., Martinez, M.G., Jones, M.G., and Caddick, M.X. (2000) A defined sequence within the 3′ UTR of the *areA* transcript is sufficient to mediate nitrogen metabolite signalling via accelerated deadenylation. *Mol Microbiol* **37:** 1248–1257.
Morozov, I.Y., Galbis-Martinez, M., Jones, M.G., and Caddick, M.X. (2001) Characterization of nitrogen metabolite signalling in *Aspergillus* via the regulated degradation of *areA* mRNA. *Mol Microbiol* **42:** 269–277.
Muro-Pastor, M.I., Gonzalez, R., Strauss, J., Narendja, F., and Scazzocchio, C. (1999) The GATA factor AreA is essential for chromatin remodelling in a eukaryotic bidirectional promoter. *EMBO J* **18:** 1584–1597.
Narendja, F., Goller, S.P., Wolschek, M., and Strauss, J. (2002) Nitrate and the GATA factor AreA are necessary for *in vivo* binding of NirA, the pathway-specific transcriptional activator of *Aspergillus nidulans*. *Mol Microbiol* **44:** 573–583.
Nayak, T., Szewczyk, E., Oakley, C.E., Osmani, A., Ukil, L., Murray, S.L., *et al*. (2006) A versatile and efficient gene-targeting system for *Aspergillus nidulans*. *Genetics* **172:** 1557–1566.
Nichane, M., Ren, X., Souopgui, J., and Bellefroid, E.J. (2008) Hairy2 functions through both DNA-binding and non DNA-binding mechanisms at the neural plate border in Xenopus. *Dev Biol* **322:** 368–380.
Pan, T., and Coleman, J.E. (1989) Structure and function of the Zn(II) binding site within the DNA-binding domain of the GAL4 transcription factor. *Proc Natl Acad Sci USA* **86:** 3145–3149.
Pan, T., and Coleman, J.E. (1991) Sequential assignments of the 1H NMR resonances of Zn(II)2 and 113Cd(II)2 derivatives of the DNA-binding domain of the GAL4 transcription factor reveal a novel structural motif for specific DNA recognition. *Biochemistry* **30:** 4212–4222.
Pateman, J.A. (1969) Regulation of synthesis of glutamate dehydrogenase and glutamine synthetase in microorganisms. *Biochem J* **115:** 769–775.
Pfaffl, M.W. (2001) A new mathematical model for relative quantification in real-time RT-PCR. *Nucleic Acids Res* **29:** e45.
Platt, A., Langdon, T., Arst, H.N., Jr, Kirk, D., Tollervey, D., Sanchez, J.M., and Caddick, M.X. (1996a) Nitrogen metabolite signalling involves the C-terminus and the GATA domain of the *Aspergillus* transcription factor AREA and the 3′ untranslated region of its mRNA. *EMBO J* **15:** 2791–2801.
Platt, A., Ravagnani, A., Arst, H., Jr, Kirk, D., Langdon, T., and Caddick, M.X. (1996b) Mutational analysis of the C-terminal region of AREA, the transcription factor mediating nitrogen metabolite repression in *Aspergillus nidulans*. *Mol Gen Genet* **250:** 106–114.
Polotnianka, R., Monahan, B.J., Hynes, M.J., and Davis, M.A. (2004) TamA interacts with LeuB, the homologue of *Saccharomyces cerevisiae* Leu3p, to regulate *gdhA* expression in *Aspergillus nidulans*. *Mol Genet Genomics* **272:** 452–459.
Ravagnani, A., Gorfinkiel, L., Langdon, T., Diallinas, G., Adjadj, E., Demais, S., *et al*. (1997) Subtle hydrophobic interactions between the seventh residue of the zinc finger loop and the first base of an HGATAR sequence determine promoter-specific recognition by the *Aspergillus nidulans* GATA factor AreA. *EMBO J* **16:** 3974–3986.
Riego, L., Avendano, A., DeLuna, A., Rodriguez, E., and

Gonzalez, A. (2002) *GDH1* expression is regulated by GLN3, GCN4, and HAP4 under respiratory growth. *Biochem Biophys Res Commun* **293:** 79–85.
Sambrook, J., and Russell, D.W. (2001) *Molecular Cloning: A Laboratory Manual*. Cold Spring Harbor, NY: Cold Spring Harbor Laboratory Press.
Schmittgen, T.D., and Livak, K.J. (2008) Analyzing real-time PCR data by the comparative C(T) method. *Nat Protoc* **3:** 1101–1108.
Scott, S., Abul-Hamd, A.T., and Cooper, T.G. (2000) Roles of the Dal82p domains in allophanate/oxalurate-dependent gene expression in *Saccharomyces cerevisiae*. *J Biol Chem* **275:** 30886–30893.
Small, A.J., Hynes, M.J., and Davis, M.A. (1999) The TamA protein fused to a DNA-binding domain can recruit AreA, the major nitrogen regulatory protein, to activate gene expression in *Aspergillus nidulans*. *Genetics* **153:** 95–105.
Small, A.J., Todd, R.B., Zanker, M.C., Delimitrou, S., Hynes, M.J., and Davis, M.A. (2001) Functional analysis of TamA, a coactivator of nitrogen-regulated gene expression in *Aspergillus nidulans*. *Mol Genet Genomics* **265:** 636–646.
Suzuki, Y., Murray, S.L., Wong, K.H., Davis, M.A., and Hynes, M.J. (2012) Reprogramming of carbon metabolism by the transcriptional activators AcuK and AcuM in *Aspergillus nidulans*. *Mol Microbiol* **84:** 942–964.
Sylvain, M.A., Liang, X.B., Hellauer, K., and Turcotte, B. (2011) Yeast zinc cluster proteins Dal81 and Uga3 cooperate by targeting common coactivators for transcriptional activation of gamma-aminobutyrate responsive genes. *Genetics* **188:** 523–534.
Talibi, D., Grenson, M., and Andre, B. (1995) Cis- and trans-acting elements determining induction of the genes of the gamma-aminobutyrate (GABA) utilization pathway in *Saccharomyces cerevisiae*. *Nucleic Acids Res* **23:** 550–557.
Todd, R.B., and Andrianopoulos, A. (1997) Evolution of a fungal regulatory gene family: the Zn(II)2Cys6 binuclear cluster DNA binding motif. *Fungal Genet Biol* **21:** 388–405.
Todd, R.B., Andrianopoulos, A., Davis, M.A., and Hynes, M.J. (1998) FacB, the *Aspergillus nidulans* activator of acetate utilization genes, binds dissimilar DNA sequences. *EMBO J* **17:** 2042–2054.
Todd, R.B., Fraser, J.A., Wong, K.H., Davis, M.A., and Hynes, M.J. (2005) Nuclear accumulation of the GATA factor AreA in response to complete nitrogen starvation by regulation of nuclear export. *Eukaryot Cell* **4:** 1646–1653.
Todd, R.B., Davis, M.A., and Hynes, M.J. (2007) Genetic manipulation of *Aspergillus nidulans*: meiotic progeny for genetic analysis and strain construction. *Nat Protoc* **2:** 811–821.
Todd, R.B., Zhou, M., Ohm, R.A., Leeggangers, H.A.C.F., Visser, L., and de Vries, R.P. (2014) Prevalence of transcription factors in ascomycete and basidiomycete fungi. *BMC Genomics* **15:** 214.
Traven, A., Jelicic, B., and Sopta, M. (2006) Yeast Gal4: a transcriptional paradigm revisited. *EMBO Rep* **7:** 496–499.
Wilson, R.A., and Arst, H.N., Jr (1998) Mutational analysis of AREA, a transcriptional activator mediating nitrogen metabolite repression in *Aspergillus nidulans* and a member of the 'streetwise' GATA family of transcription factors. *Microbiol Mol Biol Rev* **62:** 586–596.
Yuan, G.F., Fu, Y.H., and Marzluf, G.A. (1991) *nit-4*, a pathway-specific regulatory gene of *Neurospora crassa*, encodes a protein with a putative binuclear zinc DNA-binding domain. *Mol Cell Biol* **11:** 5735–5745.

Supporting information

Additional supporting information may be found in the online version of this article at the publisher's web-site.

Supporting Information.

Dual DNA Binding and Coactivator Functions of *Aspergillus nidulans* TamA, a Zn(II)2Cys6 Transcription Factor.

Damien J. Downes, Meryl A. Davis, Koon Ho Wong, Sara D. Kreutzberger, Michael J. Hynes, and Richard B. Todd.

Fig. S1. Alignment of TamA orthologs.

ClustalW2 alignment of *A. nidulans* TamA with orthologs from *Magnaporthe oryzae, Fusarium fujikuroi, Neurospora crassa, A. oryzae, Penicillium chrysogenum, Podospora anserina, Yarrowia lipolytica, Candida albicans, S. cerevisiae* and *Schizosaccharoymces pombe*. The six cysteines (*) in the Zn(II)2Cys6 DNA binding motif (red box), the fungal middle homology region (green box) and putative nuclear localization signals (yellow boxes) are indicated.

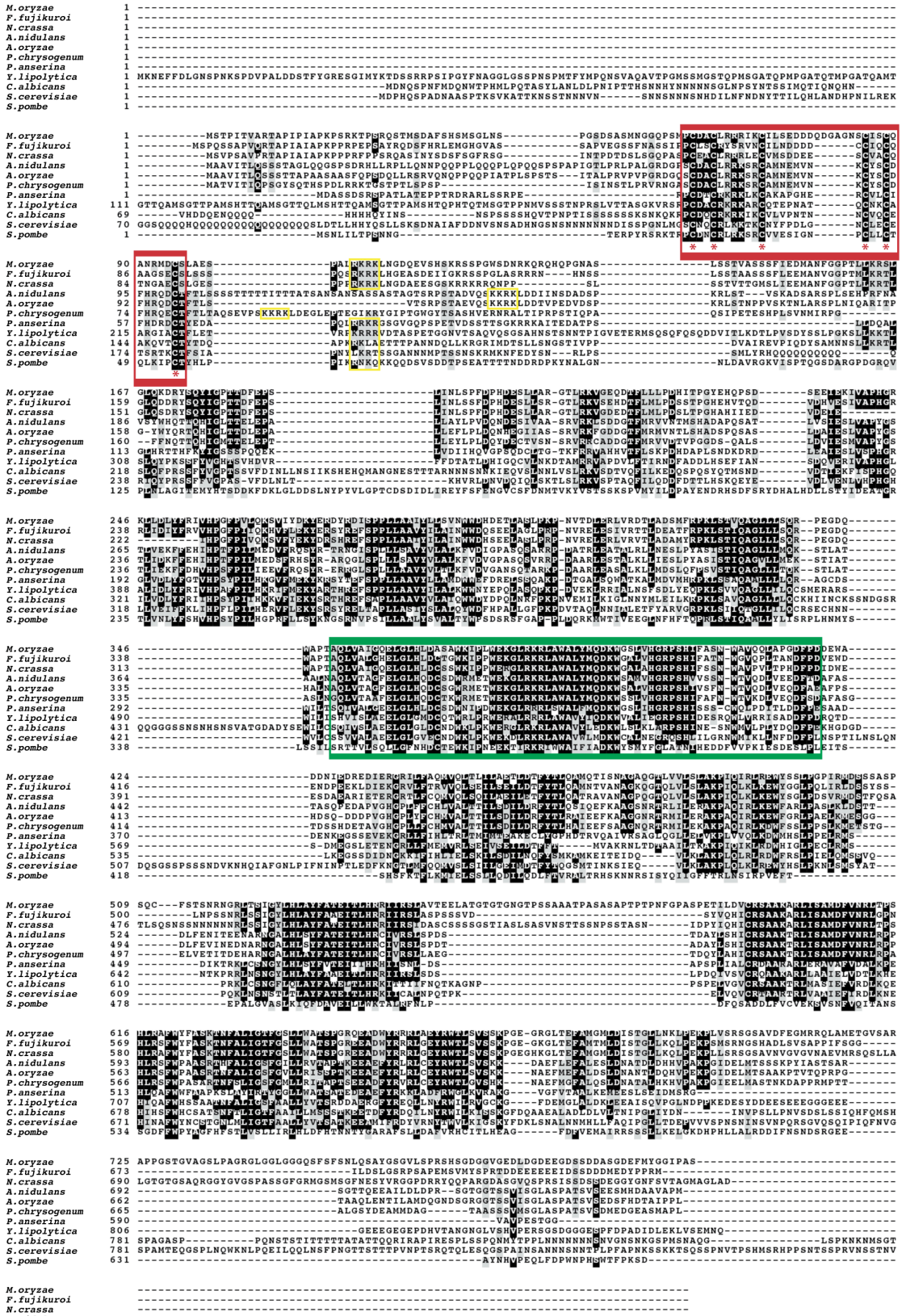
M.oryzae
F.fujikuroi
N.crassa
A.nidulans
A.oryzae
P.chrysogenum
P.anserina
Y.lipolytica
C.albicans
S.cerevisiae
S.pombe

Fig. S2. Phylogenetic analysis of TamA and prevalence of putative TamA DNA binding sites in *gdhA* orthologs.

A. Alignment of the DNA binding motif of TamA/Dal81p orthologs from *A. nidulans, A. oryzae, P. chrysogenum, Penicillium marneffei, Coccidioidies immitis, Phaeorsphearia nododorum, S. pombe, Y. lipolytica, C. albicans, Candida guilliermondii, P. anserina, S. cerevisiae, F. fujikuroi, Verticillium dahliae*, *N. crassa* and *M. oryzae*. Conserved cysteines are marked (*).

B. Phylogenetic analysis of the region aligned in (A).

C. Phylogenetic analysis of the protein sequence following the final cysteine of the DNA binding motif including the middle homology region and C-terminus.

D. Identification of putative TamA binding sites in the 1.0 kb promoter region of *gdhA* homologs. Location is relative to the ATG start codon, and nearest HGATAR is upstream (-) or downstream (+) relative to the putative TamA site.

A

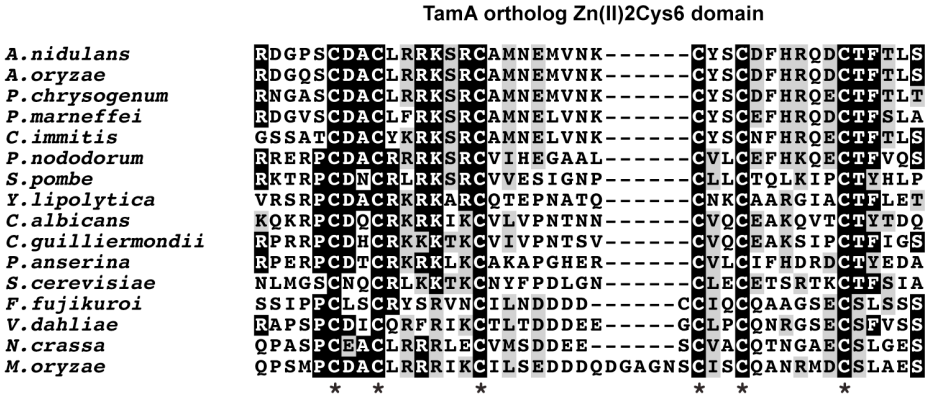

B

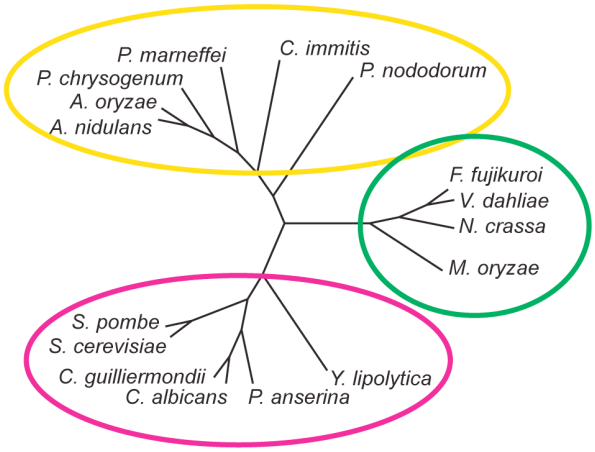

C

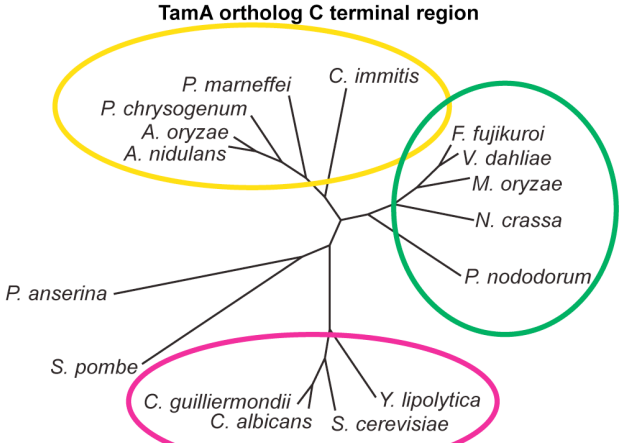

D

Putative TamA CCGN$_5$CGG Binding sites in -1.0 kb of *gdhA* homologs

Species	Sequence	Location	Nearest HGATAR	Zn(II)2Cys6 Clade	C terminus Clade
A. nidulans	CCGAACTTCGG	-432 to -422 bp	-37 bp		
A. oryzae	CCGAAGTTCGG	-413 to -403 bp	-41 bp		
P. chrysogenum	CCGAACTTCGG	-356 to -346 bp	-14 bp		
P. marneffei	ND	-	-		
C. immitis	ND	-	-		
P. nododorum	CCGACCATCGG	-472 to -462 bp	+150 bp		
F. fujikuroi	Absent	-	-		
V. dahliae	CCGACTGGCGG	-245 to -235 bp	-367 bp		
N. crassa	Absent	-	-		
M. oryzae	Absent	-	-		
Y. lipolytica	Absent	-	-		
P. anserina	Absent	-	-		
C. guilliermondii	CCGGGGCTCGG	-430 to -420 bp	-109 bp		
C. albicans	Absent	-	-		
S. cerevisiae	Absent	-	-		
S. pombe	CCGTTGCACGG	-662 to -665 bp	-1 bp		

Fig. S3. Effect of *tamA* mutations on *gdhA-lacZ* expression during growth on glutamine.

A. Wild type (RT151, MH12101, and MH12102), *tamA*Δ (RT165, MH12174, and MH12175) and *tamA*^{C90L} (RT218, MH12597, and MH12614) strains containing either the -1994, -753 or -307 bp *gdhA-lacZ* reporter genes, respectively, were assayed for β-galactosidase specific activity after 16 h growth in glutamine ANM media. Error bars depict SEM (n≥3).

B. β-galactosidase activity of soluble protein extracts from wild type (MH12101) and *tamA*Δ (MH12174) strains containing the -753 bp *gdhA-lacZ* reporter gene grown in glutamine (GLN), ammonium tartrate (NH_4), alanine (ALA) or glutamate (GLU) ANM for 16 h. Error bars depict SEM (n≥3).

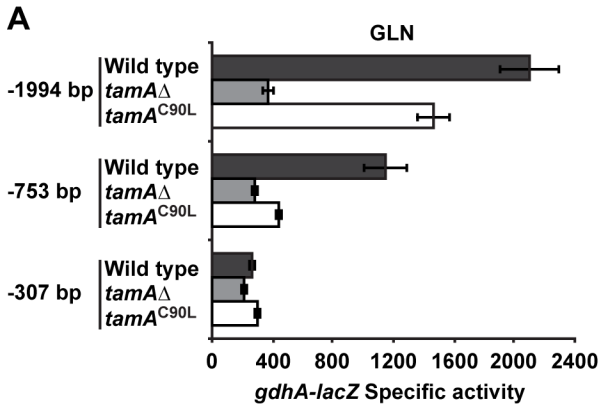

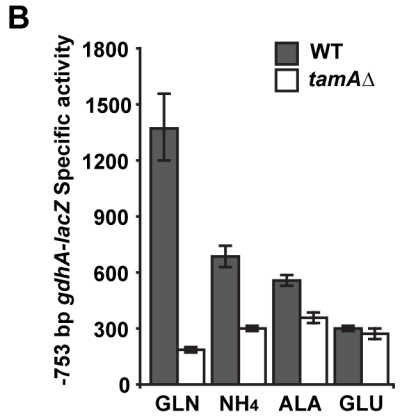

Fig. S4. Epitope tagging strategy for TamA.

A. Construction of *tamA*^{FLAG} was by replacement of the 3' coding region of native *tamA* with a FLAG-tagged variant in single copy.

B. A full copy *tamA*$^{C90L\text{-}FLAG}$ under the control of 1.4 kb *tamA* promoter region was targeted to the *fmdS-lacZ* locus in single copy in a *tamA*Δ strain.

C. Expression of TamA^{FLAG} (RT322) and TamA$^{C90L\text{-}FLAG}$ (RT376) in strains grown for 16 h in 10 mM ammonium tartrate ANM was confirmed by Western blot.

D. Strains expressing either TamA (Wild type, MH1), TamA^{FLAG} (RT299) or TamA$^{C90L\text{-}FLAG}$ (RT376) were grown on 10 mM alanine ANM in the presence of toxic nitrogen analogs thiourea (TU), aspartate hydroxamate (AH), methylammonium chloride (MACl) and chlorate (ClO_3).

E. Wild type (MH12101) and *tamA*^{FLAG} (RT377) strains containing the -753 bp *gdhA-lacZ* reporter were assayed for β-galactosidase specific activity after 16 h growth in 10 mM ammonium tartrate ANM. Error bars depict SEM ($n \geq 3$).

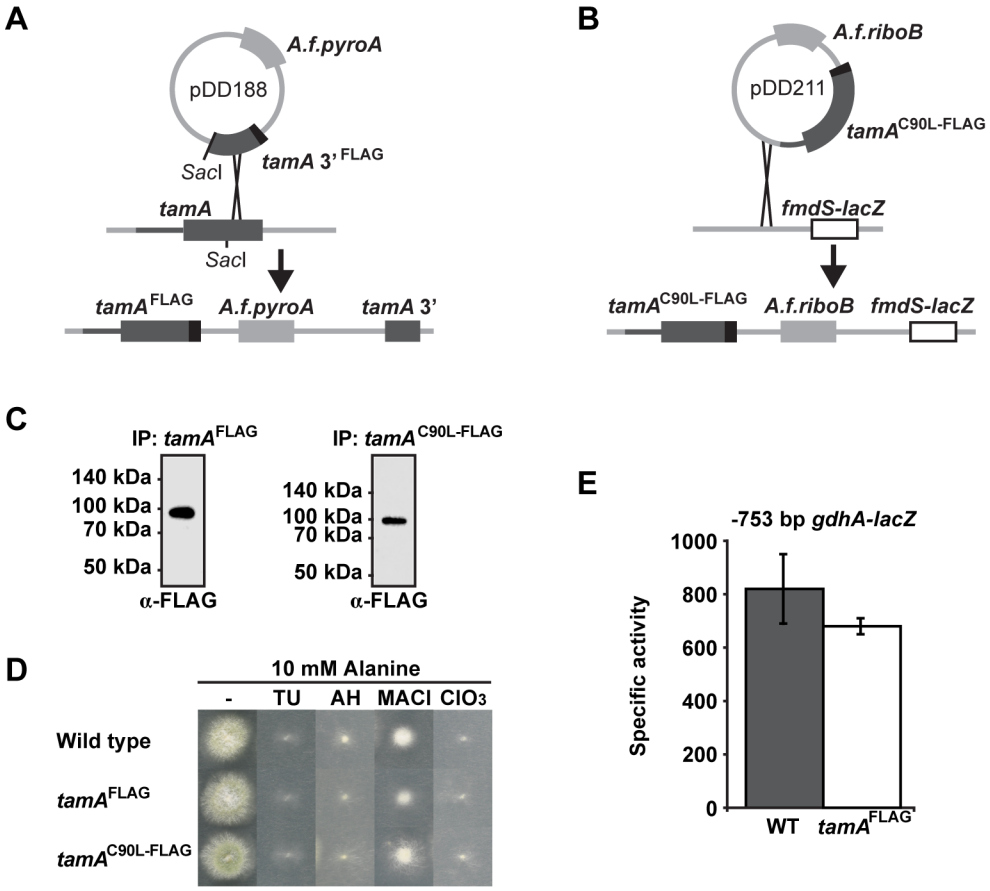
A
A.f.pyroA
pDD188
SacI
tamA 3' FLAG
tamA
SacI
tamA FLAG
A.f.pyroA
tamA 3'
B
A.f.riboB
pDD211
tamA C90L-FLAG
fmdS-lacZ
tamA C90L-FLAG
A.f.riboB
fmdS-lacZ
C
IP: tamA FLAG
140 kDa
100 kDa
70 kDa
50 kDa
α-FLAG
IP: tamA C90L-FLAG
140 kDa
100 kDa
70 kDa
50 kDa
α-FLAG
D
10 mM Alanine
-
TU
AH
MACl
ClO3
Wild type
tamA FLAG
tamA C90L-FLAG
E
-753 bp gdhA-lacZ
Specific activity
1000
800
600
400
200
0
WT
tamA FLAG

Table S1. SCOPE analysis of eight Aspergillus NADP-GDH promoters.

SCOPE-Identified Consensus Sequence	Sig Score[a]	Position(s) in *gdhA* promoter[b]	Sequence(s) in *A. nidulans*
YSYCSKMC	122.8	-918 to -911	CGCCGTCC
		-770 to -763	CCCCCGCC
		-256 to -249	TCTCGTCC
		-253 to -246	CGTCCGAC
		-227 to -220	CGCCGGCC
		-221 to -214	CCTCCGCC
		-209 to -202	CGCCGTCC
		-206 to -199	CGTCCGCC
BCCGAASTTCGG	122.2	-433 to -422	CCCGAACTTCGG
TCGYCVBHCTCCG	100.7	-254 to -242	TCGTCCGACTCCG
		-228 to -216	TCGCCGGCCTCCG
GCGGRDHBYCGCC	83.7	Absent	
ATCNVATAA	55.4	Absent	
ATRATAAYAA	54.4	Absent	
ATKTCCCGGA	44.5	-513 to -504	ATGTCCCGGA
CCTCC	44.4	-935 to -931	CCTCC
		-656 to -652	CCTCC
		-393 to -389	CCTCC
		-370 to -366	CCTCC
		-282 to -278	CCTCC
		-221 to -217	CCTCC
TCTTC	43.4	-785 to -781	TCTTC
		-259 to -255	TCTTC
		-74 to -70	TCTTC
CTTATC	39.1	-996 to -991	CTTATC
		-974 to -469	CTTATC
		-124 to -119	CTTATC
		-29 to -24	CTTATC

[a] Sig score measures over-representation of a particular motif as the -log2 of the expected number of motifs of the given length and degeneracy in the 1 kb promoter of NADP-GDH genes in eight Aspergilli when compared against the 1 kb region of all genes from *A. nidulans*.

[b] Position relative to the *A. nidulans gdhA* ATG.

Table S2. Oligonucleotides used in this study.

Primer use and name	Sequence (5' → 3')
Oligonucleotides for *tamA*^{FLAG} tagging	
tamAFLAG-F	CCGCTGGGTTTGAGCTCGGGC
tamAFLAG-R	TTTGAGCTCTTACTTGTCGTCGTCGTCCTTGTAGTCCATCGGA GCAACAGCCGC
Oligonucleotides for *gdhA-lacZ* construction	
gdhA1XhoI-F	CCGCTC-GAGTGAGGATTGAAGGATTGAGGG
gdhA5XhoI-F	CCGCTCGAGGCATATACAGCAGCGGCAC
gdhA8XhoI-F	CCGCTCGAGCGACTTTCCCGCCAGATTTT
gdhA2BglII-R	GAAGATCTGGAAGGTTAGACATTTTTGCG
condel-F	Phos-CCTTGCTAGTATTAGCTTTGTGC
condel-R	Phos-GGGTGTTAGTCGAACGTTTA
Oligonucleotides for RT-qPCR	
gdhAqPCR-F	AATGCTCTCACAGGACTAA
gdhAqPCR-R	GGTACAGAAGCGACGAAT
benAqPCR-F	CCTGCTCCGCTATCTTCC
benAqPCR-R	GACTGGTTCTTGCTCTGGAT
Oligonucleotides for qChIP	
gdhApro-F	TTACCTAATGTCACGAGAATGTC
gdhApro-R	CGGAAAGGGAGGGCTAAG
gdhAcod-F	CCGTCAACCTTTCTATCCT
gdhAcod-R	GGCAAACATCCAATGAAGT
amdSpro-F	CTTTCCTTGGCCCGTAAA
amdSpro-R	ATGGTGTTGATAAGAGACTAAT
benApro-F	TACGGGCGATCCACTTAGTT
benApro-R	ACAGGAGCGAGATCAGGAGA
Oligonucleotides for EMSA	
leuB1del-F	Phos-GTGGGCTTCCGCCCAGAGATAA
IRgdhAprobe-R	Infrared Dye IRD700-TTGCACAAAGCTAATACTAGCAAGGCCG

Appendix C - ValidNESs analysis of GATA factors

GATA factors from the Animal, Plant and Fungal kingdoms were assessed for the presence of CRM1-type NESs using ValidNES prediction software. Results are reported in Table C.1. The predicted NESs from plant GATA factors and AreA paralogs were mapped onto proteins to determine distribution throughout the protein (Figure C.1 and Figure C.2).

Table C.1 ValidNESs analysis of Animal, Plant and Fungal GATA Factors

Protein	Accession Number	Protein Level Probability[1]	Coordinates	Motif	Motif Probability[2]
Kingdom Animalia					
Homo sapiens					
GATA1	P15976	0.29	291 to 297	VNRPLTM	0.27
			367 to 372	LGPVVL	0.23
GATA2	P23769	0.09	382 to 388	VNRPLTM	0.26
GATA3	P23771	0.32	350 to 356	INRPLTM	0.32
			184 to 190	LKYQVPL	0.29
GATA4	P43694	0.64	400 to 405	LSALKL	0.52
			399 to 405	VLSALKL	0.34
			304 to 310	VPRPLAM	0.25
			1 to 7	MYQSLAM	0.15
GATA5	Q9BWX5	0.23	276 to 282	VPRPLAM	0.37
GATA6	Q92908	0.41	477 to 483	VPRPLAM	0.38
Danio rerio					
GATA-1	AAI24484	0.11	325 to 331	VNRPLTM	0.22
			224 to 230	LRNKMRL	0.15
GATA-2	AAH53131	0.28	358 to 364	VNRPLTM	0.27
			205 to 211	LRGSLAM	0.22
GATA-3	Q91428	0.28	343 to 349	INRPLTM	0.32
			39 to 45	LAEDVDV	0.16
GATA-4	AAF15275	0.21	254 to 260	VPRPLAM	0.19
GATA-5	CAB43400	0.42	274 to 280	VPRPLAM	0.39
GATA-6	AAH677110	0.25	384 to 390	VPRPLAM	0.26
			59 to 65	LHSYVHF	0.25
			453 to 458	VGQVDV	0.16
			452 to 458	LVGQVDV	0.15
Drosophila melanogaster					
Serpent	P52172	0.11		No motif >0.15	
Pannier	Q9VEZ8	0.41	258 to 264	LKPSLSL	0.36
			207 to 213	VNRPLAM	0.30
Grain	P91623	0.14	354 to 360	VNRPLTM	0.42
Caenorhabditis elegans					
EGL-18	Q9BIM5	0.14	299 to 305	VRRPIEM	0.20
EGL-27	Q09228	0.43	823 to 829	LQQAVML	0.23
ELT-1	P28515	0.31	73 to 78	FSGMDM	0.35
			410 to 415	MKNLNL	0.31
			305 to 311	VERPITM	0.17
			151 to 157	VQSSVPI	0.16
ELT-2	Q10566	0.30	105 to 111	LYSGIPV	0.32
ELT-3	Q21128	0.42	87 to 92	IFELNL	0.34
			85 to 90	FNIFEL	0.16
ELT-6	CCD71628	0.32	168 to 174	MMNLLNL	0.17
ELT-7	AAC17756	0.53	176 to 182	VKRPLSL	0.64
END-1	O44353	0.56	86 to 92	MFGSLDM	0.60
			87 to 92	FGSLDM	0.52
END-3	Q9XUW7	0.08		No motif >0.15	
MED-1	Q9GSP3	0.00		No classical motif	
MED-2	AAK93857	0.00		No classical motif	

[1] NESsential score at the protein level indicates how likely the given protein contains a NES

[2] NESsential score of each putative site indicates the probability to be a functional NES

Table C.1 ValidNESs analysis of Animal, Plant and Fungal GATA Factors (continued).

Protein	Accession Number	Protein Level Probability[1]	Coordinates	Motif	Motif Probability[2]
		Xenopus laevis			
GATA-1	AAA49722	0.28	267 to 273	VNRPLTM	0.56
			60 to 65	LQPFTL	0.16
GATA-2	AAA49723	0.10	354 to 360	VNRPLTM	0.27
GATA-3	AAA49724	0.22	343 to 349	INRPLTM	0.52
			396 to 401	LSHIPF	0.18
GATA-4	NP_001085355	0.23	273 to 279	VPRPLAM	0.29
			322 to 327	MRPIKI	0.17
GATA-5	NP_001079831	0.34	271 to 277	VPRPLAM	0.36
		Kingdom Plantae			
		Arabidopsis thaliana			
GATA-1	Q8LAU9	0.76	10 to 15	LLNFSV	0.68
			7 to 13	MDDLLNF	0.63
GATA-2	AAD32831	0.14	14 to 20	IDDLLDF	0.15
GATA-3	Q8L4M6	0.14	45 to 51	VECFLDF	0.24
GATA-4	O49743	0.20	63 to 69	FTHDLCV	0.18
GATA-5	Q9FH57	0.48	10 to 16	VRKEMAL	0.23
			43 to 49	VDDLLDL	0.23
GATA-6	Q9SD38	0.36	30 to 36	VDDLLDF	0.21
			303 to 308	VQTVQV	0.17
GATA-7	O65515	0.39	8 to 13	LGDFSV	0.30
			224 to 229	VLELRL	0.18
			13 to 19	VDDLLDL	0.16
BME3	Q9SV30	0.29		No motif >0.15	
GATA-9	O82632	0.62	20 to 26	VDDLLDF	0.35
			4 to 10	IAPELFL	0.19
GATA-10	Q8VZP4	0.40	121 to 126	LTPVSV	0.33
GATA-11	Q6DBP8	0.55	25 to 31	LINHLDV	0.84
			26 to 31	INHLDV	0.63
			120 to 125	LSPVSV	0.32
GATA-12	P69781	0.41	98 to 103	VHKLEL	0.65
			67 to 73	FSGDLCI	0.23
			16 to 21	VDDLLV	0.19
GATA-13	Q9SKN8	0.50	1 to 7	MNNDLWL	0.26
			251 to 256	IIYMRM	0.20
GATA-14	Q9M1U2	0.13	15 to 20	MQKIPI	0.24
GATA-15	Q8LG10	0.43	109 to 115	LGREVMM	0.35
			136 to 141	VLLMAL	0.18
GATA-16	Q9FJ10	0.61	101 to 106	LMDLGI	0.41
GATA-17	Q9LIB5	0.48	143 to 149	VSKFLDL	0.24
MNP	Q8LC79	0.43	277 to 283	LSWRLNV	0.41
			67 to 73	VDCTLSL	0.31
GATA-19	Q6QPM2	0.22	193 to 199	LSWRLNV	0.42
			177 to 182	VDDVRV	0.24
			206 to 211	VHDFTM	0.17
			205 to 211	LVHDFTM	0.17
GATA-20	Q9ZPX20	0.17	38 to 44	VDCTLSL	0.15

[1] NESsential score at the protein level indicates how likely the given protein contains a NES

[2] NESsential score of each putative site indicates the probability to be a functional NES

Table C.1 ValidNESs analysis of Animal, Plant and Fungal GATA Factors (continued).

Protein	Accession Number	Protein Level Probability[1]	Coordinates	Motif	Motif Probability[2]
		Arabidopsis thaliana			
GNC	Q5HZ36	0.79	286 to 291	VQQLPL	0.56
			386 to 391	VLLMAL	0.22
			57 to 63	LSSYLPF	0.21
			5 to 11	FHYSIDL	0.21
CGA1	Q9SZI6	0.43	271 to 277	ILSPLPL	0.64
			272 to 277	LSPLPL	0.37
			58 to 63	LSYFPF	0.37
			340 to 345	ILLMAL	0.36
GATA-23	Q8LC59	0.62	108 to 113	LCLLLL	0.29
ZML1	Q8GXL7	0.31		No motif >0.15	
TIFY1	Q9LRH6	0.24		No motif >0.15	
GATA-26	Q8W4H1	0.59	197 to 202	MSMVSV	0.34
			326 to 332	LPHSLRM	0.25
			490 to 495	LLLLDL	0.21
GATA-27	Q5PP38	0.28	253 to 259	LLCSIDL	0.20
			254 to 259	LCSIDL	0.17
ZML2	Q8H1G0	0.59	103 to 108	VQAVLL	0.44
GATA-29	Q9LT45	0.57	7 to 13	LTLKLGL	0.19
		Kingdom Fungi			
		Phylum Ascomycota			
		Aspergillus nidulans			
AreB	AAG49352	0.58	215 to 220	VSELDL	0.33
			296 to 302	LAKRMKL	0.25
LreA	CBF82714	0.21	646 to 652	LIAHLRF	0.19
LreB	XP_661211	0.60	211 to 216	LENVRL	0.96
			315 to 320	LNDVEL	0.55
			64 to 90	VHDLLL	0.32
			320 to 326	LLTGLHF	0.18
			413 to 419	VCGCVHI	0.15
NsdD	XP_660756	0.23	320 to 326	VEEMLNI	0.17
SreA	XP_657780	0.00		No classical motif	
		Saccharomyces cerevisiae			
Dal80p	P26343	0.43	229 to 234	ISELEL	0.95
Gat2p	P40209	0.35		No motif >0.15	
Gat3p	AAS56856	0.16		No motif >0.15	
Gat4p	AAS56173	0.39	18 to 24	VPVQLLL	0.53
			83 to 88	FRKLIL	0.32
			82 to 88	FFRKLIL	0.31
Gzf3p	P42944	0.38	511 to 516	INELEL	0.87
		Candida albicans			
Ash1p	EAK98090	0.32	146 to 152	IVPTVSL	0.48
			147 to 152	VPTVSL	0.46
Gzf3p	EAK69759	0.31	545 to 550	ISELEL	0.59
			583 to 588	VMNLQI	0.44
			308 to 314	ITSPLLL	0.28
			580 to 586	LDEVMNL	0.16

[1] NESsential score at the protein level indicates how likely the given protein contains a NES
[2] NESsential score of each putative site indicates the probability to be a functional NES

Table C.1 ValidNESs analysis of Animal, Plant and Fungal GATA Factors (continued).

Species	Protein & Accession Number	Protein Level Probability[1]	Coordinates	Motif	Motif Probability[2]
		Candida albicans			
Sfu1p	EAL04857	0.21	471 to 422	LPSIQL	0.22
			399 to 405	LRAPIHI	0.19
orf19.1150	EAK93929	0.44	405 to 411	FQTDFSL	0.44
			399 to 404	LLNMMNI	0.42
			74 to 79	LDIFKM	0.26
			396 to 402	IDKLLNM	0.24
		Neurospora crassa			
Asd-4	ESA43052	0.77	373 to 377	LDELEV	0.78
Sre	XP_961978	0.46	266 to 271	ITALHV	0.41
			101 to 106	VATLGL	0.17
Sub-1	ESA42507	0.08		No motif >0.15	
WC-1	Q01371	0.19	594 to 599	LKGLFL	0.33
WC-2	P78714	0.44	71 to 77	MSMSLDV	0.74
			274 to 280	FCQAVFM	0.16
		Schizosaccharomyces pombe			
Ams2p	NP_588400	0.36	220 to 225	VEELEL	0.30
			411 to 416	FAQLEL	0.28
			652 to 658	FSLELGL	0.23
			673 to 678	MTDLVM	0.20
			9 to 14	VTSLPL	0.19
			121 to 127	FIVEFGI	0.18
			672 to 678	LMTDLVM	0.17
			140 to 146	LQNSFEV	0.16
			334 to 340	IEEQLTL	0.16
			131 to 137	IEIKLRF	0.15
Fep1p	NP_592936	0.32	420 to 426	VGESVCL	0.18
Sfh1	NP_588001	0.15		No motif >0.15	
SPCC1393	NP_587966	0.55	537 to 543	LDNSVIV	0.45
			303 to 309	MDASLKL	0.26
			489 to 495	LSKSVTM	0.23
		Phylum Basidiomycota			
		***Cryptococcus neoformans var grubii* H99**			
ASD-4	AFR92329	0.48	608 to 613	MMHLTL	0.56
			1206 to 1212	VVRPLSL	0.29
			1207 to 1212	VRPLSL	0.15
WC-2	AFR95399	0.58	271 to 277	LEEELGM	0.79
			251 to 257	LEAFLDV	0.37
			254 to 259	FLDVKL	0.17
CNAG_00035	AFR92174	0.02		No motif >0.15	
CNAG_01551	AFR97756	0.59	383 to 388	LVHMKL	0.52
CNAG_01708	AFR97911	0.63	37 to 43	LAESLVL	0.71
			866 to 872	VGFEMPV	0.19
			693 to 698	VQLLNL	0.19
			728 to 734	MKGVMTL	0.17
CNAG_01841	AFR98036	0.02		No motif >0.15	
CNAG_01883	AFR98080	0.11	286 to 292	FTSPITL	0.22

[1] NESsential score at the protein level indicates how likely the given protein contains a NES

[2] NESsential score of each putative site indicates the probability to be a functional NES

Table C.1 ValidNESs analysis of Animal, Plant and Fungal GATA Factors (continued).

Protein	Accession Number	Protein Level Probability[1]	Coordinates	Motif	Motif Probability[2]
***Cryptococcus neoformans var grubii* H99**					
CNAG_03401	AFR96624	0.29	427 to 432	LASLGM	0.31
			266 to 272	MMKHVDM	0.21
CNAG_04263	AFR96993	0.69	368 to 373	VKELEV	0.85
			1 to 6	MDHLVL	0.54
			319 to 324	VEALQV	0.37
			638 to 644	VWRKLVL	0.21
			264 to 269	MERIIM	0.18
CNAG_04864	AFR97352	0.42	756 to 762	VENKMAL	0.37
			923 to 928	MSGVPL	0.30
CNAG_05153	AFR94418	0.34	175 to 181	IDISLGL	0.31
			10 to 15	IHQLPV	0.24
			673 to 678	VEGFSM	0.20
			179 to 185	LGLNMGL	0.16
CNAG_06762	AFR93038	0.71	201 to 206	LTQLKM	0.84
			252 to 258	LSPHIHL	0.43
			208 to 214	LDEIICL	0.22
Ustilago maydis					
URB-1	XP_757197	0.62	808 to 814	LRDELLF	0.89
UM_00706	XP_756853	0.51	220 to 226	LVLPFQL	0.62
			928 to 934	MRFILPL	0.34
			1150 to 1155	LLDLPM	0.33
			973 to 979	IEPELKL	0.29
			334 to 339	VLPLSL	0.21
			1138 to 1143	VAEFLV	0.20
			1155 to 1160	MEEIKI	0.18
			226 to 231	LPFVDV	0.17
UM_00895	XP_757042	0.22	466 to 472	LAQGVSI	0.25
			505 to 510	IESVLI	0.19
UM_02664	XP_758811	0.39	626 to 632	LIADMDL	0.64
			627 to 632	IADMDL	0.29
			613 to 618	FLELKL	0.22
			373 to 379	VEELLDF	0.15
UM_03708	XP_759855	0.94	221 to 226	LADLGL	0.87
			809 to 815	FSTGVPM	0.38
			194 to 200	LNHHIDL	0.30
UM_04076	XP_760223	0.8	133 to 139	LARRLDL	0.76
UM_05518	XP_761665	0.65	594 to 600	LRAELNL	0.75
			372 to 377	IGRLSL	0.66
			105 to 111	LTTSIDL	0.42
			298 to 303	LDNMAL	0.40
			255 to 261	LDSLLYV	0.29
			687 to 692	LDQLAI	0.23
UM_05577	XP_761724	0.22	861 to 867	IEMDMWL	0.22
UM_05773	XP_761920	0.27	221 to 226	LTSSLSM	0.31
			192 to 197	IANFSV	0.16

[1] NESsential score at the protein level indicates how likely the given protein contains a NES

[2] NESsential score of each putative site indicates the probability to be a functional NES

Table C.1 ValidNESs analysis of Animal, Plant and Fungal GATA Factors (continued).

Protein	Accession Number	Protein Level Probability[1]	Coordinates	Motif	Motif Probability[2]
		Ustilago maydis			
UM_04252	XP_760399	0.46	286 to 291	LRRLHL	0.42
			313 to 318	ITDLLL	0.39
			896 to 901	MMAMTL	0.39
			209 to 215	FDPLLLI	0.28
			1630 to 1636	VVRPLSL	0.28
			190 to 196	LLVTFRL	0.24
			76 to 82	VGVGVGV	0.23
			318 to 324	LHSSLSL	0.23
			191 to 196	LVTFRL	0.22
			1631 to 1636	VRPLSL	0.22
			212 to 217	LLLILF	0.22
			7 to 12	FGSIAL	0.20
			10 to 16	IALVVGV	0.18
			188 to 194	VLLLVTF	0.18
			1 to 7	MITRLKF	0.16
			326 to 332	LSLSLSL	0.15
			189 to 194	LLLVTF	0.15

[1] NESsential score at the protein level indicates how likely the given protein contains a NES
[2] NESsential score of each putative site indicates the probability to be a functional NES

Figure C.1 Distribution of ValidNESs predicted motifs in Planta

ValidNESs predicted NES motifs for animal GATA factors were mapped onto the respective protein. Motifs adjacent to a DNA binding motif (bolded) were used to generate consensus motifs. Units are bits of information proportional to sequence conservation

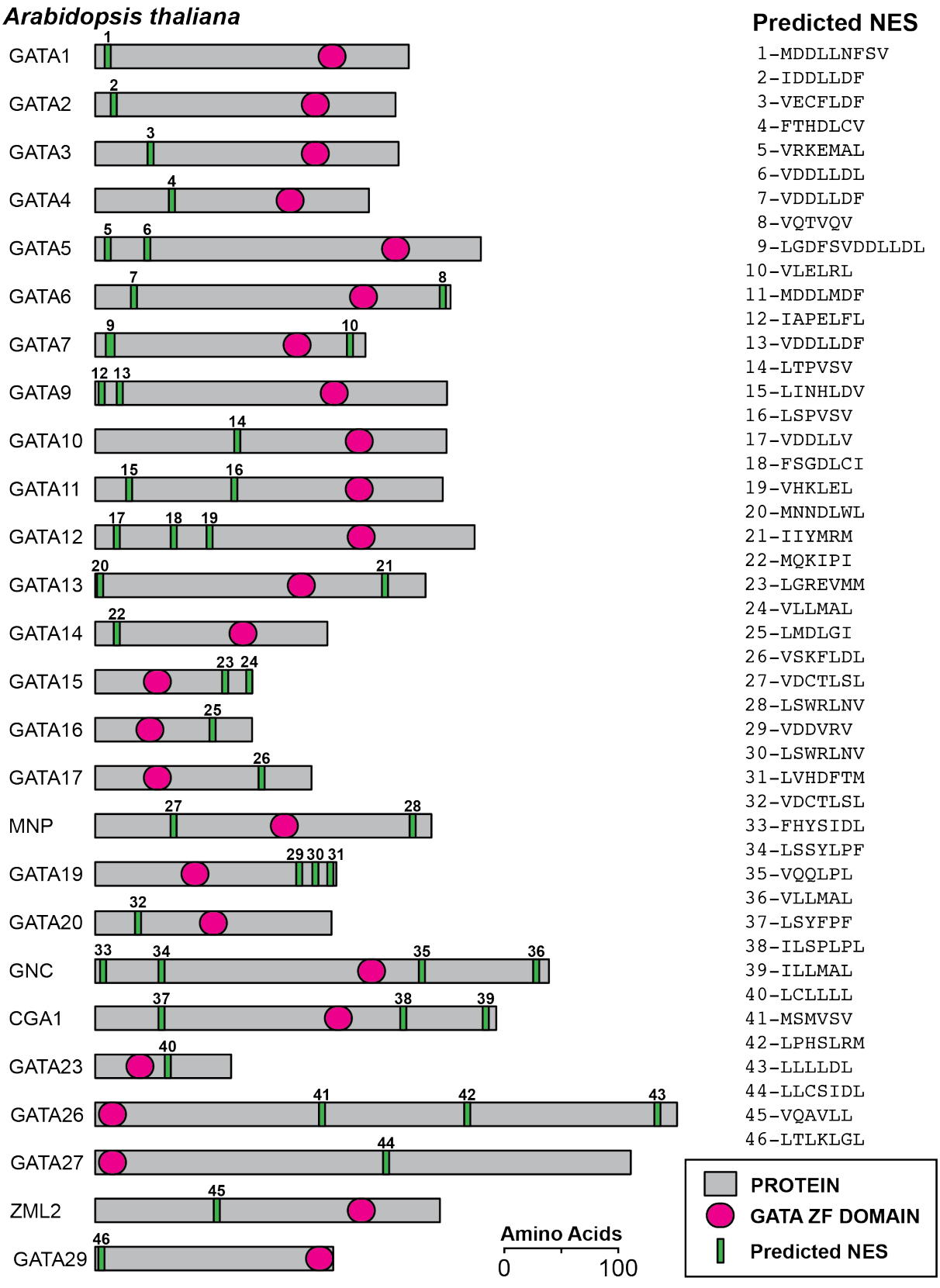

Figure C.1 Distribution of ValidNESs predicted motifs in Planta

Figure C.2 Distribution of ValidNESs predicted motifs in Ascomycota AreA paralogs

ValidNESs predicted NES motifs for animal GATA factors were mapped onto the respective protein. Motifs adjacent to a DNA binding motif (bolded) were used to generate consensus motifs. Units are bits of information proportional to sequence conservation

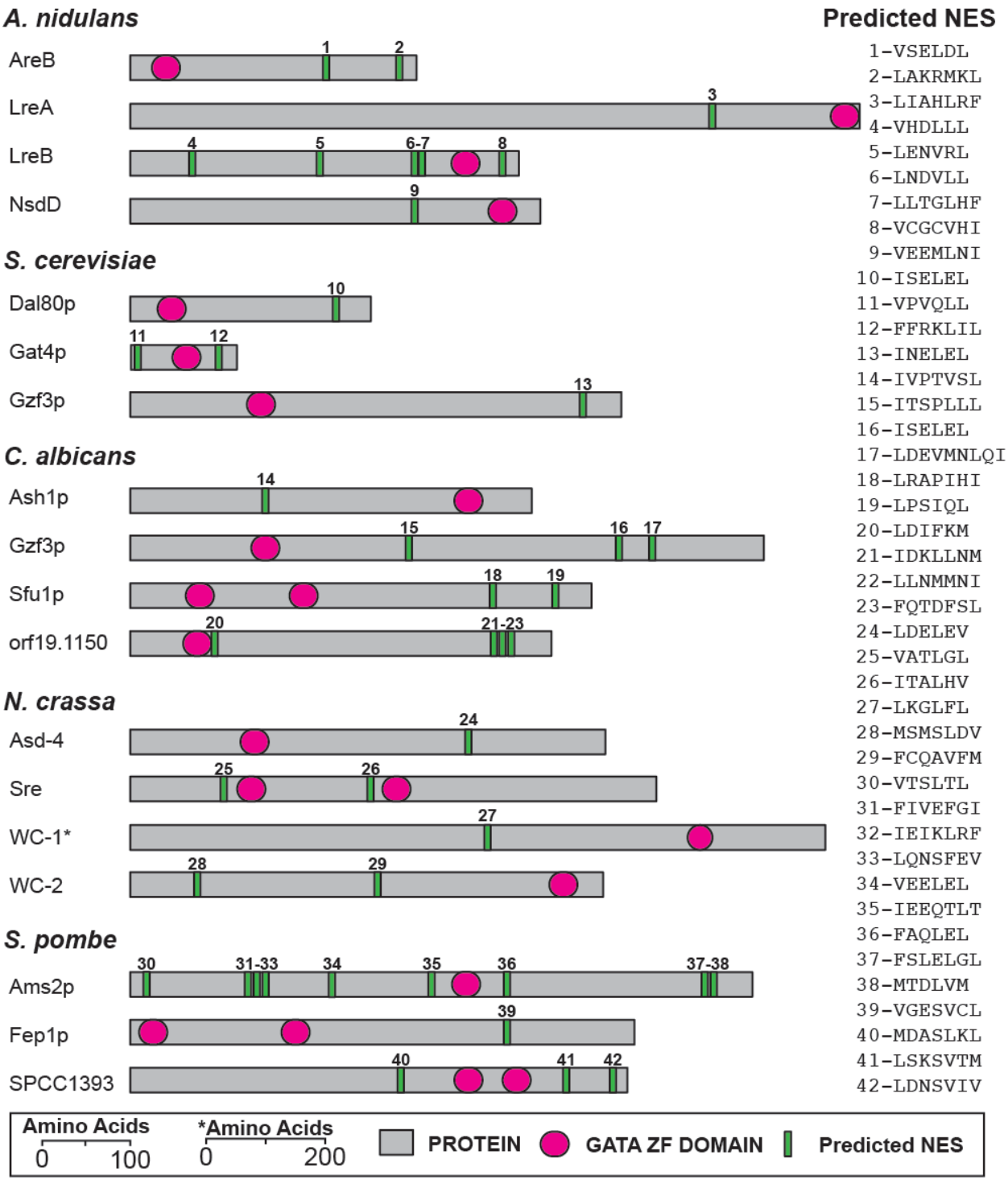

Figure C.2 Distribution of ValidNESs predicted motifs in Ascomycota AreA paralogs

[Diese seite wurde bewusst frei gelassen.]

Downes *et al*. (2014a)

Research conducted as part of this dissertation for Chapter 6 "The AreA Nuclear Export Signal" has been published in Downes D.J., M. Chonofsky, K. Tan, B.T. Pfannenstiel, S. L. Reck-Peterson & R.B. Todd (2014) Characterization of the Mutagenic Spectrum of 4-Nitroquinoline 1-Oxide (4-NQO) in *Aspergillus nidulans* by Whole Genome Sequencing. *G3 (Bethseda)* **4 (12):** 2483-2492. (doi: 10.1534/g3.114.014712). My contribution to this work while at Kansas State University was the experimental design, construction of 11 *A. nidulans* strains by transformation and mutagenesis, genome sequencing of three strains, variant analysis, statistical and modeling analysis, and writing the manuscript. The full article is included in this appendix. Supplementary data can be accessed online.

Characterization of the Mutagenic Spectrum of 4-Nitroquinoline 1-Oxide (4-NQO) in *Aspergillus nidulans* by Whole Genome Sequencing

Damien J. Downes,* Mark Chonofsky,† Kaeling Tan,†,‡ Brandon T. Pfannenstiel,*,[1] Samara L. Reck-Peterson,† and Richard B. Todd*,[2]

*Department of Plant Pathology, Kansas State University, Manhattan, Kansas 66506, †Department of Cell Biology, Harvard Medical School, Boston, Massachusetts 02115, and ‡Faculty of Health Sciences, University of Macau, Taipa, Macau SAR, China

ABSTRACT 4-Nitroquinoline 1-oxide (4-NQO) is a highly carcinogenic chemical that induces mutations in bacteria, fungi, and animals through the formation of bulky purine adducts. 4-NQO has been used as a mutagen for genetic screens and in both the study of DNA damage and DNA repair. In the model eukaryote *Aspergillus nidulans*, 4-NQO–based genetic screens have been used to study diverse processes, including gene regulation, mitosis, metabolism, organelle transport, and septation. Early work during the 1970s using bacterial and yeast mutation tester strains concluded that 4-NQO was a guanine-specific mutagen. However, these strains were limited in their ability to determine full mutagenic potential, as they could not identify mutations at multiple sites, unlinked suppressor mutations, or G:C to C:G transversions. We have now used a whole genome resequencing approach with mutant strains generated from two independent genetic screens to determine the full mutagenic spectrum of 4-NQO in *A. nidulans*. Analysis of 3994 mutations from 38 mutant strains reveals that 4-NQO induces substitutions in both guanine and adenine residues, although with a 19-fold preference for guanine. We found no association between mutation load and mutagen dose and observed no sequence bias in the residues flanking the mutated purine base. The mutations were distributed randomly throughout most of the genome. Our data provide new evidence that 4-NQO can potentially target all base pairs. Furthermore, we predict that current practices for 4-NQO–induced mutagenesis are sufficient to reach gene saturation for genetic screens with feasible identification of causative mutations via whole genome resequencing.

KEYWORDS
filamentous fungi
genetic screen
chemical mutagenesis
4-nitroquinoline 1-oxide
whole genome sequencing

doi: 10.1534/g3.114.014712
Manuscript received September 29, 2014; accepted for publication October 25, 2014; published Early Online October 27, 2014.

Supporting information is available online at http://www.g3journal.org/lookup/suppl/doi:10.1534/g3.114.014712/-/DC1
Sequence data from this article have been deposited with the NCBI Sequence Read Archive under the accession number SRP047490.
[1]Present address: Department of Medical Microbiology and Immunology, University of Wisconsin, Madison, WI 53706.
[2]Corresponding author: Department of Plant Pathology, Kansas State University, 4024 Throckmorton Plant Sciences Center, Manhattan, KS 66506. E-mail: rbtodd@k-state.edu

4-Nitroquinoline 1-oxide (4-NQO) is a highly carcinogenic chemical that causes mutations in bacteria, fungi, and animals. 4-NQO has been used widely in the study of DNA damage and DNA repair and to generate mutants for genetic screens. 4-NQO induces mutagenesis after metabolic conversion to 4-hydroxyaminoquinolone 1-oxide (4-HAQO) (Miller 1970), which forms stable bulky adducts on purines (Tada and Tada 1976). Based on *in vitro* studies as well as in *Escherichia coli* and animal cells, 4-HAQO forms the majority of adducts (~50%) on the second nitrogen (N2) of guanine (Tada and Tada 1971; Galiegue-Zouitina *et al.* 1986; Bailleul *et al.* 1989). However, carbon eight (C8) guanine adducts (Bailleul *et al.* 1981; Galiègue-Zouitina *et al.* 1984; Tada *et al.* 1984) and nitrogen six (N6) adenine adducts (Galiegue-Zouitina *et al.* 1985, 1986) also occur at a lower frequency, ~30% and ~10%, respectively (Bailleul *et al.* 1989). Additional lesions were thought to be caused by production of reactive oxygen species (Kohda *et al.* 1986). In *E. coli* and mammalian cells, 4-HAQO adducts are repaired by the

nucleotide excision repair pathway (Ikenaga *et al.* 1975a,b, 1977; Ikenaga and Kakunaga 1977), and in *E. coli* the error prone DNA polymerase IV (Pol IV) is the likely cause of sequence changes (Williams *et al.* 2010). Early work to characterize the mutagenic effects of 4-NQO in the yeasts *Saccharomyces cerevisiae* and *Schizosaccharomyces pombe*, as well as in the bacteria *Salmonella typhimurium* and *E. coli*, relied upon reversion of characterized auxotrophic tester strains, as DNA sequencing technology was not yet readily available (Prakash *et al.* 1974; Janner *et al.* 1979; Rosenkranz and Poirier 1979). These experiments identified the changes induced by 4-NQO as G:C to A:T transitions, G:C to T:A transversions, and frameshifts (Prakash *et al.* 1974; Janner *et al.* 1979; Rosenkranz and Poirier 1979). However, differences in frequency and mutation type varied between species and with 4-NQO concentration (Rosenkranz and Poirier 1979). Studies relying on reversion tester strains are limited by their inability to detect or determine multiple mutations in the same target gene as well as unlinked suppressor mutations, and the lack of strains to specifically detect G:C to C:G transversions (Prakash and Sherman 1973). In addition, these strains were not informative as to how flanking sequence affects mutagenic potential. Furthermore, auxotrophic reversion tester strains may show mutational bias due to functional constraints. Therefore, the full 4-NQO mutagenic spectrum, including type and relative frequency of induced mutations as well as the effect of flanking sequence, remains to be determined.

The genetic model filamentous fungus *Aspergillus nidulans* has been invaluable for advances in understanding a variety of eukaryotic cellular processes, including cell-cycle progression, development, response to DNA damage and pH changes, gene regulation, and metabolism (Clutterbuck 1969; Arst and Cove 1973; Morris 1975; Oakley and Oakley 1989; Harris *et al.* 1994; Goldman and Kafer 2004; Penalva *et al.* 2008; Wong *et al.* 2008). Many of these advances have been made using genetic screens. The versatility of *A. nidulans* for genetic analysis is due to several amenable characteristics, including stable haploid and diploid life stages as well as asexual and sexual reproduction (Pontecorvo *et al.* 1953). Heterozygous diploid strains, constructed via the parasexual cycle, can be used for analysis of dominance or complementation and to map novel mutations to a chromosome by haploidization (Todd *et al.* 2007a). Mutations can then be mapped more finely by classical genetic mapping via the sexual cycle (Todd *et al.* 2007b). Furthermore, the well-developed DNA-mediated transformation system, with homologous gene targeting and multiple selectable markers, enables construction of strains for mutational analysis and selection of mutants in genetic screens, and reconstruction of identified candidate mutations to identify the causative mutation associated with the mutant phenotype (Nayak *et al.* 2006). *A. nidulans* has been used extensively in genetic screens for mutants generated by a variety of chemical and physical mutagens, including *N*-methyl-*N*′-nitro-*N*-nitrosoguanidine (MNNG) (Clutterbuck 1969; Hynes and Pateman 1970a,b; Arst and Cove 1973; Osman *et al.* 1993), nitrous acid (Apirion 1965; Clutterbuck 1969), diethyl sulfate (Clutterbuck 1969), ultraviolet (UV) light (Pontecorvo *et al.* 1953; Clutterbuck 1969; Axelrod *et al.* 1973; Morris 1975; Osman *et al.* 1993), and X-rays (Pontecorvo *et al.* 1953). However, many genetic screens in *A. nidulans* use 4-NQO (Harris *et al.* 1994; Wu *et al.* 1998; Pokorska *et al.* 2000; Conlon *et al.* 2001; Heck *et al.* 2002; Kinghorn *et al.* 2005; Cecchetto *et al.* 2012; Larson *et al.* 2014; Tan *et al.* 2014) because it is safer and more stable than MNNG and it is thought to produce primarily single base-pair substitutions, which can generate both loss-of-function and altered function mutants. These altered function mutants are important for identifying essential genes in which larger mutations would be lethal. The utility and application of 4-NQO as a mutagen in genetic screens highlight the importance of understanding the full consequences of 4-NQO mutagenesis.

To fully characterize the mutagenic potential of any chemical, analysis of mutations that are unbiased by the selection method or gene function is required. A genomics approach, rather than sampling a single gene target by reversion of auxotrophies, overcomes limitations imposed by functional constraints, as mutations in noncoding regions and mutations unrelated to the selection and independent of function also can be detected. Whole genome sequencing has been used to identify the effects of ethyl methanesulfonate, ethylnitrosourea, and UV light in several eukaryotes, including *Arabidopsis thaliana* (Uchida *et al.* 2011), *Danio rerio* (Voz *et al.* 2012), *Caenorhabditis elegans* (Flibotte *et al.* 2010), and the apicomplexan parasite *Toxoplasma gondii* (Farrell *et al.* 2014). Recent advances in sequencing technology have permitted rapid and affordable resequencing of fungal genomes, and this has enabled identification of causative mutations in mutants generated in genetic screens (McCluskey *et al.* 2011; Pomraning *et al.* 2011; Nowrousian *et al.* 2012; Bielska *et al.* 2014; Tan *et al.* 2014; Yao *et al.* 2014; Zhang *et al.* 2014). In this work, we have used a genome resequencing approach to fully characterize the 4-NQO mutagenic spectrum at a whole genome level using almost 4000 4-NQO−induced mutations arising from independent genetic screens (Tan *et al.* 2014; this study). 4-NQO causes all possible base-pair substitutions with a 19-fold preference for guanine over adenine residues.

MATERIALS AND METHODS

A. nidulans strains, media, growth conditions

A. nidulans strains RT244 (*biA1 pyrG89 gpdA*(p)*areA*^{HA} *fmdS-lacZ pyroA4 nkuA*Δ*::Bar* [*prnA::areA*^{NES}*::gfp::AfpyroA*] *crmA*^{T525C}*::pyrG*) and RPA520 (*yA::*[*gpdA*(p)mCherry::FLAG::PTS1*::Afpyro*] *pabaA1 pyrG89* [TagGFP2*::rabA::AfpyrG*] *pyroA4 nkuA*Δ*::argB* [HH1::TagBFP*::Afribo*]) were used for mutagenesis. Mutant strains generated from RPA520 were outcrossed to RPA478 (*pyrG89* [TagGFP2*::rabA::AfpyrG*] *pyroA4 nkuA*Δ*::argB* [HH1::TagBFP*::Afribo*] *riboB2*) or RPA496 (*pyrG89* [TagGFP2*::rabA::AfpyrG*] *pyroA4 nkuA*Δ*::argB* [HH1::TagBFP*::Afribo*]). *A. nidulans* growth conditions and media adjusted to pH 6.5 were as described (Cove 1966). *Aspergillus* nitrogen-free minimal media containing 1% w/v glucose and nitrogen sources (ammonium tartrate, sodium nitrate, or L-proline) added to a final concentration of 10 mM (Cove 1966), or rich yeast and glucose media (Szewczyk *et al.* 2006), supplemented for auxotrophies, were used for growth.

Mutagenesis and sequencing

Mutagenesis using 4-NQO (Sigma-Aldrich) was carried out primarily as described (Holt and May 1996; Tan *et al.* 2014). In summary, ~10^7 or ~10^8 conidia, suspended in phosphate buffer (0.1 M potassium phosphate pH 7.0, 0.01% Tween 80) and quantified using a hemocytometer, were exposed to 0.24−4.0 μg mL^{-1} 4-NQO at 37° for 30 min. 4-NQO was quenched with an equal volume of 0.5 M sodium thiosulfate and washed twice in phosphate buffer. Strains were recovered from 50%, 10%, and 3% survival treatments (0.24 μg mL^{-1} 4-NQO per 10^7 spores, 0.45 μg mL^{-1} 4-NQO per 10^7 spores, and 4.0 μg mL^{-1} 4-NQO per 10^8 spores, respectively) after 2−4 days' growth on either yeast and glucose media or supplemented *Aspergillus* nitrogen-free minimal media containing 10 mM L-proline and tested for mutant phenotypes. Proline-using mutant phenotypes in strains derived from RT244 were mapped by meiotic crossing to RT250 (*yA1 pabaA1 pyrG89 gpdA*(p)*areA*^{HA} *fmdS-lacZ prn-309*). Genomic DNA was isolated as described (Lee and Taylor 1990). The genomes of RT244 and a derivative mutant strain were sequenced by the Genome Sequencing Facility (Kansas University Medical Center, Kansas City, Kansas) on an Illumina HiSEQ 2500 platform using single-end 50-bp reads. The

genomes of RPA478, RPA496, RPA520, and bulked segregrant progeny of derivative mutant strains were sequenced by single-end, whole genome sequencing on the Illumina Genome Analyzer HiSeq 2000 platform, generating sequence reads ~50 base pairs in length (Tan *et al.* 2014). For mutant strains from RT244 showing tight linkage of the causative mutation and *prnA*, the mutations were identified by amplification of the *prnA*::*areA*^{NES}::*gfp* regions with prn3′-F (5′-TCACGGCTATTCCGTGCTTTGA-3′) and gfp5′-R (5′-ACGCT GAACTTGTGGCCGTTA-3′) using Ex Taq (TaKaRa) and sequencing at Kansas State University DNA Sequencing and Genotyping Facility.

In silico analysis

In silico analysis used the Galaxy platform (galaxyproject.org) (Blankenberg *et al.* 2010b) and Broad Genome Analysis Toolkit (GATK; broadinstitute.org/gatk) (McKenna *et al.* 2010). FASTA files were converted to FASTQ format using FASTQ Groomer (Blankenberg *et al.* 2010a). Sequence quality was determined using FastQC (Li and Durbin 2009) (bioinformatics.babraham.ac.uk/projects/fastqc/). Nucleotide sequence reads were aligned using Burrows-Wheeler Alignment for Illumina with default settings to the *A. nidulans* FGSC_A4 genome (Version S10) downloaded from AspGD (Cerqueira *et al.* 2014). Genome coverage was determined using BEDTools (Quinlan and Hall 2010). Sequence coverage was lacking or not aligned for the centromeres, the ribosomal rRNA repeats, and mitochondrial sequences. Variants were identified using FreeBayes (Garrison and Marth 2012) with default settings except for report polymorphism probability (−P: 0.01), ploidy (−p: 1), minimum observations (−F: 0.5), and minimum coverage (−!: 4) or using GATK (Depristo *et al.* 2011) with default settings except for quality score >50 (−stand_call_conf: 50.0, −stand_emit_conf: 10.0) and down sampling to 50 fold coverage (−dcov: 50.0). Variants unique to mutant strains were identified using Select Variants (Depristo *et al.* 2011). Aligned sequence reads from wild-type strains were manually inspected to confirm the absence of all identified unique variants. Box plots were generated using JMP 11 (SAS), outliers in boxplots are points lying 1.5 × interquartile range (third quartile to first quartile) above the third quartile or below the first quartile. The Student's *t*-test and simple χ^2 test were computed in Excel (Microsoft Office). SAS 9.4 (SAS) was used for exponential quantile-quantile plots (CAPABILITY procedure: QQplot / exponential, σ = est, θ = est), Kolmogorov-Smirnov tests (UNIVARIATE procedure with histogram & exponential settings), and categorical χ^2 tests (FREQ and GENMOD procedures). Consensus motifs of mutated sites were generated using WebLogo (Crooks *et al.* 2004) (weblogo.berkeley.edu). *A. nidulans* sequence annotation of transcribed and intergenic regions, and gene function descriptions were obtained from AspGD (Cerqueira *et al.* 2014), and descriptions of yeast orthologs were obtained from SGD (Cherry *et al.* 2012).

Prediction of saturation

We derived the following random sampling with replacement equation that can be adjusted to calculate the probability of a specific mutation of every nucleotide (nucleotide saturation) or every possible substitution at every nucleotide (substitution saturation):

$$P_{S(X)} = \left(1 - \left(1 - f.b^{-1}\right)^{m.s.(1-k)}\right)^{b}$$

The standard equation for probability of a specific event (**X**) given multiple random samples with replacement is $P_{(X)} = 1 - (1 - N^{-1})^{n}$, where $\mathbf{N^{-1}}$ is the probability of the specific event given a single sample was taken, and **n** is the number of samples taken. For our equation, N^{-1} is replaced with the relative frequency with which a specific mutation arises (**f**) divided by the total number of base pairs at which it could have arisen (**b**). The number of samples is the mean number of mutations arising per spore (**m**), multiplied by the number of treated spores (**s**), multiplied by the number of surviving spores (**1 − k**), where k is the proportion kill, *i.e.*, for a mutation at a single base-pair $P_{S(X)} = 1\text{-}(1\text{-}f.b^{-1})^{m.s.(1-k)}$. To determine the probability of a mutation at every possible base pair, where the likelihood of mutating any base pair is equivalent due to random mutagenesis, the probability of a single event is raised to the power of the number of base pairs (**b**), giving the final equation $\mathbf{P_{S(X)}}$ for the probability of saturation of a specific mutation (**X**). The following values were used: $P_{S(G\rightarrow H)}$ f = 0.95, $P_{S(G\rightarrow A)}$ f = 0.53, $P_{S(G\rightarrow T)}$ f = 0.276, $P_{S(G\rightarrow C)}$ f = 0.14, $P_{S(A\rightarrow B)}$ f = 0.05, $P_{S(A\rightarrow C)}$ f = 0.01, $P_{S(A\rightarrow G)}$ f = 0.03, $P_{S(A\rightarrow T)}$ f = 0 0.01), b = 15241995.5 using a 50% GC content in *A. nidulans* (Galagan *et al.* 2005), m = 105, s is variable and k = 0.5 (50% kill) or 0.9 (90% kill).

The probability of nucleotide saturation of both guanine and adenine is therefore:

$$P_{S(G\rightarrow H \text{ and } A\rightarrow B)} = P_{S(G\rightarrow H)} \times P_{S(A\rightarrow B)}$$

And the probability of substitution saturation of both guanine and adenine is as follows:

$$P_{S(G\rightarrow A,T,C \text{ and } A\rightarrow C,G,T)} = P_{S(G\rightarrow A)} \times P_{S(G\rightarrow T)} \times P_{S(G\rightarrow C)} \times P_{S(A\rightarrow C)} \times P_{S(A\rightarrow G)} \times P_{S(A\rightarrow T)}$$

RESULTS AND DISCUSSION

4-NQO mutations are distributed across the genome

To determine the effects of 4-NQO mutagenesis on *A. nidulans* DNA, we used whole genome sequence data from two independent genetic screens. The first mutagenesis involved direct selection for reversion of a proline nonutilization phenotype conferred by fusion of a nuclear export signal to the transcription factor PrnA (D. J. Downes and R. B. Todd, unpublished data). Mutant strains were generated with a dose of 4-NQO resulting in 97% kill. We isolated nine mutant strains from this screen by direct selection for proline utilization. For eight mutant strains, the causative mutations mapped to the *prnA* locus, whereas for the ninth mutant strain the proline utilization phenotype was unlinked to *prnA*. Mutations in *prnA* were identified by sequencing polymerase chain reaction products (Table 1). The strain containing the unlinked mutation and the mutagenesis parent were used for whole genome sequencing. The second mutagenesis was for a microscopy-based screen for defective organelle transport on rich media (Tan *et al.* 2014). Conidia were treated with doses of 4-NQO conferring 50% or 90% kill. Mutant strains of interest were identified by visual screening for mislocalization of fluorescently labeled nuclei, endosomes and peroxisomes (Tan *et al.* 2014). To identify all lesions induced in this screen bulked segregant progeny of 40 mutant strains, 17 from 50% kill, and 23 from 90% kill, the mutagenesis parent and the outcross parents were sequenced. Reads from both screens were mapped to the *A. nidulans* FGSC_A4 reference genome (Galagan *et al.* 2005), providing sufficient coverage high quality variant calling in all regions excluding centromeres and the nucleolar organizing region ribosomal DNA repeats on Chromosome V (Brody *et al.* 1991; Clutterbuck and Farman 2008). Although our mutant strains were selected or chosen for specific phenotypes and therefore bias may occur for the causative mutation, most of the mutations arising throughout the genome will be random mutations unrelated to the observed phenotypes. Therefore, these mutations represent a data set of 4-NQO−derived sequence changes that are

Table 1 4-NQO mutations selected by phenotype at specific loci in *A. nidulans*

Target(s)	Reference	% Kill[a]	Number and type of mutation							
			G → A	G → C	G → T	A → C	A → G	A → T	+N[b]	ΔN[c]
areA	Al Taho *et al.* 1984; Kudla *et al.* 1990	99.9			1					
areB	Conlon *et al.* 2001	–	1		1					
cnxE	Heck *et al.* 2002	–	5		3			1		1
hypA	Harris *et al.* 1994; Kaminskyj and Hamer 1998; Shi *et al.* 2004	70	2							
hypB	Kaminskyj and Hamer 1998; Yang *et al.* 2008	–		1						
kinA, nudA,F,K	Tan *et al.* 2014	50, 90	1	1	5					
meaA	Monahan *et al.* 2002	–	9	1	2		1		1	2
nimA	Wu *et al.* 1998	80–95		1						
nimA, sonA-C	Larson *et al.* 2014	—	21	9	4					
nrtA	Kinghorn *et al.* 2005	—	7	5	5					
prnA	Pokorska *et al.* 2000	—	28							
prnA-areA^{NES}*-gfp*	This study	97			6					2
sepH	Harris *et al.* 1994; Bruno *et al.* 2001	70		1						
swoA	Harris *et al.* 1994; Momany *et al.* 1999; Shaw and Momany 2002	70			1					
swoC	Harris *et al.* 1994; Momany *et al.* 1999; Lin and Momany 2003	70			1					
swoF	Harris *et al.* 1994; Momany *et al.* 1999; Shaw *et al.* 2002	70			1					
swoH	Harris *et al.* 1994; Momany *et al.* 1999; Lin *et al.* 2003	70			1					
uaY	Oestreicher and Scazzocchio 2009	>99	17	8	12			2	1	1
uaY	Cecchetto *et al.* 2012	90		16	1	2		3		
Total			91	43	44	2	1	6	2	6

4-NQO, 4-nitroquinoline 1-oxide.
[a] –, not reported.
[b] +N, insertion.
[c] ΔN, deletion.

neither biased by selection nor constrained by function. In total we identified almost 7000 mutations in the 41 mutant strains that were absent in the parents. However, ~42% of these mutations were in just three strains. These three mutant strains each carried a substitution or nonsense mutation in at least one DNA repair gene (Supporting Information, File S1). These genes either lacked mutations in the 38 mutant strains with a lower mutation load, or in three cases carried only silent mutations or conservative substitutions. As the mutations arising in the three high mutation load strains may be due to defective DNA repair, rather than resulting directly from 4-NQO–induced mutagenesis, they were excluded from further analysis. Of the remaining 3994 4-NQO–induced mutations distributed across the genomes of 38 mutant strains, 3993 were single-nucleotide substitutions and one was a ΔG:C single base-pair deletion (File S2). The total number of mutations per strain ranged from 23 to 240; however, there was no significant difference in the mutation load arising from different 4-NQO doses and kill percentages (Figure 1). Therefore, we pooled the data for mutants isolated following different mutagen doses for subsequent analyses. The lack of a dose effect on the number of observed mutations per strain in our dataset seems somewhat counterintuitive. It is possible that this could result from the sample size of our data, or our inability to determine the number of mutations in the unrecovered strains killed or selected against.

To determine whether the effects of 4-NQO are biased toward particular regions of the genome or occur randomly, we classified each of the 3994 mutations as affecting either predicted transcribed regions (5′ untranslated region, coding, intron and 3′ untranslated region sequences) or intergenic regions (all other sequences). We found 2724 mutations within predicted transcribed regions and 1270 mutations in intergenic regions, consistent with relative genome content for each class. The mutations mapped to all regions of the genome, excluding mitochondrial DNA, the centromeres, and ribosomal repeats, where low coverage limited single-nucleotide polymorphism (SNP) calling (Figure 2A). The observed number of mutations per chromosome was not significantly different from that expected, calculated based on DNA content under random distribution ($\chi^2 = 4.7$, *d.f.* = 7, $P = 0.695$) (Figure 2A). The distances between randomly occurring mutations are

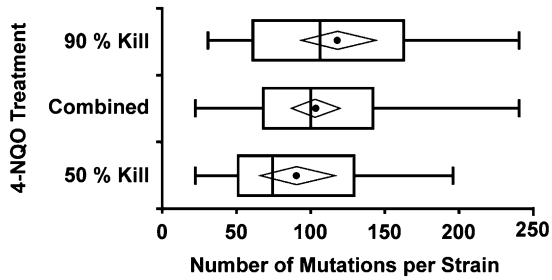

Figure 1 Number of point mutations per strain is not dose-dependent. Distribution of the number of mutations per strain resulting from 50% kill (N = 17; 0.24 μg mL^{-1} 4-NQO per 10^7 spores) and 90% kill (N = 20; 0.45 μg mL^{-1} 4-NQO per 10^7 spores) as well as combined data (N = 38). There was no significant difference between the number of mutations induced by 50% kill compared with 90% kill using unpaired unequal distribution Student's *t*-test. The combined data includes the single mutant from 97% kill (4.0 μg mL^{-1} 4-NQO per 10^8 spores) with 70 mutations. Boxplots show minimum and maximum (whiskers), median (dividing line), mean (circle), and 95% confidence interval of mean (diamond).

expected to follow an exponential distribution with a rate of λ, where λ^{-1} is the mean distance between mutations (Sun *et al.* 2006; Farrell *et al.* 2014). The majority of the mutations were 3−11 kbp apart with a mean spacing of 7461 bp (Figure 2B). An exponential quantile-quantile plot comparing the observed distances between mutations in the whole genome against the expected exponential distribution shows a close match with the theoretical distribution (Figure 2C). However, a one-sample Kolmogorov-Smirnov goodness-of-fit test has a *P*-value < 0.01 (N = 3977, mean = 7,461.44, D = 0.0247) suggesting the observed data differ significantly from the expected trend. To determine whether this was consistent across the genome, we constructed quantile-quantile plots for each of the eight chromosomes (Figure 2D). Like the whole genome data, the observed distribution for each chromosome follows the exponential line closely. For all chromosomes except Chromosome II, the Kolmogorov-Smirnov test statistically supports an exponential distribution. Therefore, the majority of 4-NQO−generated mutations

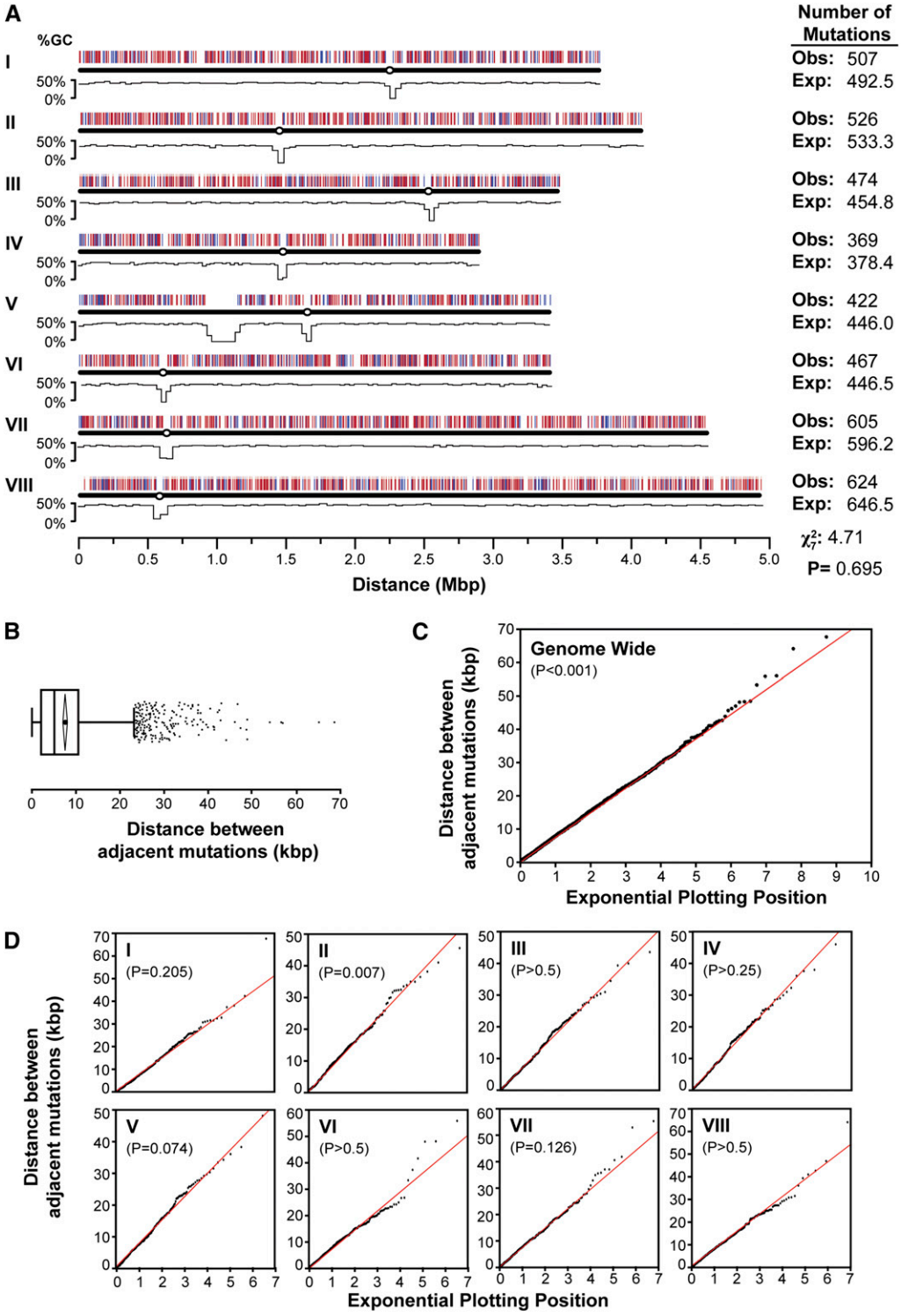

Figure 2 4-NQO mutations are randomly distributed across the genome. (A) *A. nidulans* chromosome map showing locations of 3994 mutations arising from 4-NQO mutagenesis and %GC content (Galagan *et al.* 2005). Mutations within genes (transcribed regions) are red and those outside genes are blue. Centromeres are marked as circles. Expected (Exp.) number of mutations per chromosome was calculated by dividing 3994 by the proportion of genome content in each chromosome. Obs., observed. (B) Boxplot of distance between mutations showing minimum and maximum values within 1.5 × interquartile range of the box (whiskers), median (dividing line), mean (circle), 95% confidence interval of mean (diamond), and outliers (squares). (C−D) Exponential quantile-quantile plot of distances between mutations compared with theoretical exponential distribution (red line) where λ^{-1} = mean. *P*-value shown for Kolmogorov-Smirnov test D statistic. N is the number of distances between mutations. Distances between mutations flanking centromeres and the ribosomal repeats were excluded. Genome (N = 3977, mean = 7461.44, D = 0.0247), I (N = 505, mean = 7332.67, D = 0.0388), II (N = 524, mean = 7610.55, D = 0.0584), III (N = 472, mean = 7226.80, D = 0.0297), IV (N = 367, mean = 7717.14, D = 0.0375), V (N = 419, mean = 7411.85, D = 0.0529), VI (N = 465, mean = 7167.69, D = 0.0251), VII (N = 603, mean = 7397.4, D = 0.0389), VIII (N = 622, mean = 7782.67, D = 0.0201).

conform to the expected exponential distribution and are randomly distributed. We observed 71 mutations in very close proximity (<10 bp) to another mutation in the same mutant (File S3). These mutations may have arisen either independently from multiple bulky adducts or from a single adduct and an additional repair-based error. Because these two events cannot be distinguished and these mutations comprise <2% of the total data pool, they are considered individual events for all further analyses.

4-NQO confers all six possible transitions and transversions

4-NQO was previously reported to induce transitions or transversions of guanine residues and frameshifts in bacteria and yeasts (Prakash *et al.* 1974; Janner *et al.* 1979; Rosenkranz and Poirier 1979). However, adducts of adenine are also formed and therefore adenine is a possible target (Galiègue-Zouitina *et al.* 1984, 1985; Bailleul *et al.* 1989; Menichini *et al.* 1989). Of the 3994 mutations identified from our screens, 3799 (95.12%) resulted from mutation of a guanine and only 195 (4.88%) from mutation of an adenine, consistent with the preference for guanine adduct formation (Figure 3, A and B). For SNPs of both guanine and adenine transition mutations were more frequent than transversions, with 56.27% (2137/3798) transitions for guanine (χ^2 = 59.65, *d.f.* = 1, $P < 0.0001$) and 55.90% (109/195) transitions for adenine (χ^2 = 2.71, *d.f.* = 1, $P = 0.099$). The most common mutation was G:C to A:T. Conversion of G:C to T:A, or conversion of G:C to C:G occurred at intermediate frequencies (Figure 3A). Mutation of A:T was rare (<5%) and in some individual mutant strains was not detected, but all three possible substitutions were observed in the complete data set (Figure 3B). To ensure the low frequency of adenine mutations was consistent with chemical mutagenesis rather than spontaneous mutation, we estimated the predicted level of spontaneous changes. Although studies of spontaneous mutation rate have been carried out in *A. nidulans*, they provide rates only for specific loci and not the whole genome (Lilly 1965; Alderson and Hartley 1969; Babudri and Morpurgo 1990; Baracho and Baracho 2003). Spontaneous mutation rates are very similar in *Aspergillus* spp., *Neurospora crassa*, and *S. cerevisiae* (Drake *et al.* 1998). Using an estimate of 0.0034 mutations per replication (Drake *et al.* 1998) with 30 days active growth between mutagenesis and sequencing and 1 hr per nuclear division (Bainbridge 1976), we predict an average of 2.5 spontaneous mutations may have arisen per strain. Similarly, calculations using sequence length and number of generations based on two whole genome studies in *S. cerevisiae* (Lynch *et al.* 2008; Zhu *et al.* 2014) predict just 3.5 spontaneous mutations per strain. By distributing the number of predicted spontaneous mutations across the six possible changes at the ratio described in the whole genome studies (Lynch *et al.* 2008; Zhu *et al.* 2014), we found all three types of A:T substitutions were more frequent than the expected spontaneous mutation level (Figure 3B). Therefore 4-NQO mutagenesis can cause all possible single-nucleotide substitutions. In previous 4-NQO mutagenesis studies using tester strains, mutations of adenine were reported as either absent (Prakash *et al.* 1974) or low-frequency events (~7%) and were only significantly different to nonmutagenized control strains in three of six experiments (Janner *et al.* 1979). We found only one occurrence of a deletion and no insertions. This low indel frequency suggests that this mutation may have arisen spontaneously. Therefore, we found no evidence for 4-NQO−induced frameshift mutations.

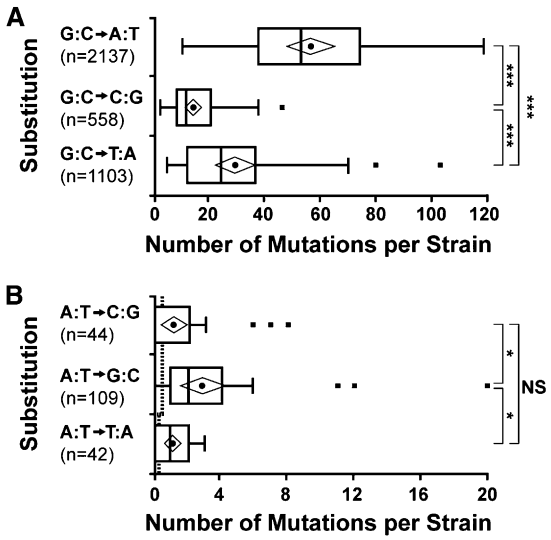

Figure 3 4-NQO induces all six possible base pair substitutions. Distribution of the number of substitutions affecting guanine-cytosine (A) and adenine-thymine (B) base pairs per mutant. Note the different scales on the x-axis for A and B. The dashed line in B shows the predicted number of spontaneous mutations per individual. Boxplots show minimum and maximum values within 1.5 × interquartile range of the box (whiskers), median (dividing line), mean (circle), 95% confidence interval of mean (diamond), and outliers (squares). Using unpaired unequal distribution Student's *t*-test: NS, not significantly different, $^{*}P < 0.05$ and $^{***}P < 0.001$.

4-NQO−induced mutations are not influenced by nucleotide flanking sequence

For some mutagens, such as UV light and methyl-nitroso urea, the sequence context can influence the outcome of mutagenesis (Kurowska *et al.* 2012; Setlow *et al.* 1963). We analyzed the adjacent sequence for each of the six mutation types using the 10 upstream and 10 downstream nucleotides of all 3993 SNPs (Figure S1). For all six substitutions, there was no consensus outside of the affected residue, suggesting that only the adenine or guanine is required for efficient adduct formation. Therefore, 4-NQO can potentially target any nucleotide pair within the *A. nidulans* genome.

Phenotype-associated 4-NQO mutation spectrum frequencies differ from nonbiased whole genome data

Although mutant strains arising from the screens in this work were selected for specific restoration of proline utilization or defective organelle transport phenotypes, we expect only one or a few of the mutations identified by whole genome sequencing of each mutant strain to contribute to the selected phenotype as causative mutations (Nowrousian *et al.* 2012; Tan *et al.* 2014). Although mutations at some loci will be constrained by function due to their requirement for growth or viability under the selection conditions, normal morphology, or ability to cross for genetic analysis, for example, the majority of mutations are expected to be unrelated to the selection. 4-NQO has been used in many mutagenic screens since being reported as a good mutagen for producing both loss-of-function and altered function mutants in *A. nidulans* (Bal *et al.* 1977). We collated data from the literature and from this study for genetic screens in which mutants were selected for a diverse range of phenotypes and where sequence data were reported or the exact mutation associated with the selected phenotype could be inferred (Table 1). To compare our whole genome mutation frequencies with phenotype-selected mutation frequencies, we used a one-way frequency table with χ^2 analysis. The distribution of mutation types for the two data sets was significantly different (χ^2 = 22.50, *d.f.* = 5, $P = 0.0004$). Interestingly, G:C to C:G and A:T to T:A transversions were significantly more common, whereas

G:C to A:T and A:T to G:C transitions were less common in the phenotype-selected data compared with the whole genome data set (Figure 4). These differences may be accounted for by the functional constraints of the selection of these mutations. For 24 amino acid codons (those encoding Phe, Leu Tyr, His, Gln, Asn, Lys, Asp, Glu, Cys, Ser, Arg) a transition in the third base position results in a synonymous change unlikely to alter the phenotype, whereas a transversion causes a nonsynonymous change. To test this hypothesis, we performed one-way frequency analysis on the number of transitions and transversions in the two data sets ($\chi^2 = 3.60$, *d.f.* = 1, $P = 0.057$). Although not significantly different by the conventional 95% confidence level, this test raises the possibility that functional constraints in the selection of mutants could be an important parameter. Therefore, the rates and types of mutations identified by whole genome sequencing of mutants likely approximate the true mutagenic spectrum for survivors of 4-NQO mutagenesis in *A. nidulans*, whereas the historical data are impacted by the constraints of phenotypic selection at the specific loci studied.

Prediction of 4-NQO screen saturation

The purpose of a genetic screen is to identify genes contributing to a particular phenotype. Generally, a screen that has identified every gene associated with a pathway or phenotype is considered a saturation screen, as was most elegantly demonstrated in the seminal *Drosophila melanogaster* developmental screen carried out by Nüsslein-Volhard and Wieschaus (1980). Even though estimating the number of possible genes involved in the pathway or phenotype is difficult, several methods, which use gamma or Poisson distributions, have been used to predict gene saturation (Pollock and Larkin 2004). Our whole genome characterization of 4-NQO mutagenesis identified both the mean number and relative frequencies of nucleotide substitutions and therefore allows prediction of the probability of saturation by using a random sampling with replacement equation (see the section *Materials and Methods*). Our approach calculates the number of spores required to mutate every nucleotide (nucleotide saturation), which is an overestimate of the number of spores required to reach gene saturation. Using our equation, we calculate 2×10^7 or 1×10^8 spores with a kill of 50% and 90%, respectively, are sufficient to isolate a mutation in every A:T and G:C pair and in effect reach nucleotide saturation (Figure 5A).

How many spores would need to be used to isolate every possible mutation at every possible site? Using the same equation, we determined the number of spores required to generate every possible substitution at every nucleotide (substitution saturation). Interestingly, only 4×10^7 spores are required with a 50% kill to reach substitution saturation for guanine, and only 15 times as many spores (6×10^8) are required to reach substitution saturation of both guanine and adenine (Figure 5B). Using a 90% kill, substitution saturation of guanine can be achieved with 2×10^8 spores; however, 4×10^9 spores are required to saturate adenines. Current 4-NQO mutagenesis protocols in *A. nidulans* use between 10^7 and 10^8 spores, and therefore easily reach nucleotide saturation or even substitution saturation. Many laboratories use alternative physical or chemical mutagenesis methods for *A. nidulans*, including UV light and MNNG. It will be interesting to use the approach we used here to do a comparative study of the outcomes and efficacy of these mutagens.

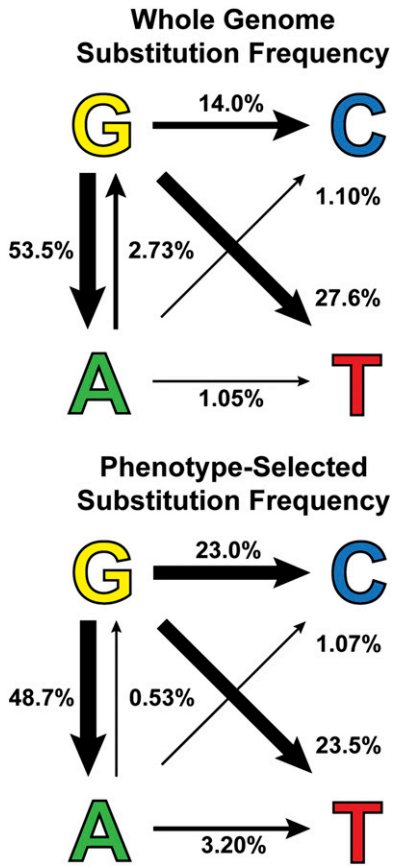

Figure 4 4-NQO affects primarily guanine nucleotides. Relative frequency (percent) of nucleotide substitutions identified by whole genome sequencing of random mutations and in phenotype-selected changes from published screens and this study (Table 1). Weighted arrows indicate change from wild type to mutant nucleotide.

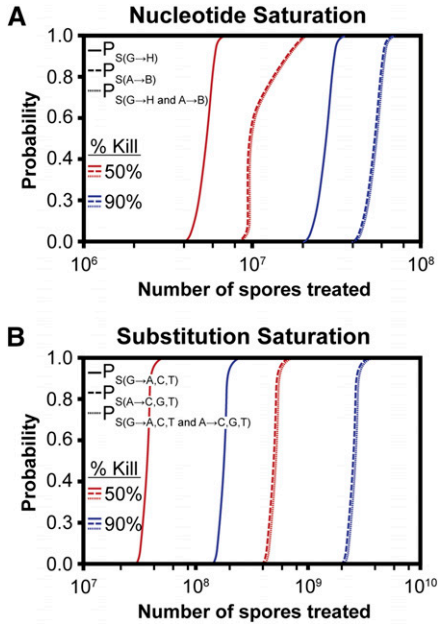

Figure 5 Number of spores required for screen saturation. (A) Probability of mutating every G:C (solid), A:T (dashed), and every nucleotide (dotted) in the *A. nidulans* genome at least once (nucleotide saturation) with 4-NQO doses causing 50% (red), and 90% kill (blue) were calculated using a random sampling with replacement equation. Note, $P_{S(G\rightarrow H \text{ and } A\rightarrow B)} = P_{S(A\rightarrow B)}$ as for this number of treated spores $P_{S(G\rightarrow H)} = 1$. (B) The same equation was used to calculate the number of spores required to generate every possible substitution at every nucleotide (substitution saturation) under the same conditions. Note, $P_{S(G\rightarrow A,C,T \text{ and } A\rightarrow C,G,T)} = P_{S(A\rightarrow C,G,T)}$ as for this number of treated spores $P_{S(G\rightarrow A,C,T)} = 1$.

Mutant screens in *A. nidulans* to characterize diverse cellular processes, including metabolism, mitosis, and organelle transport have used the highly carcinogenic chemical mutagen 4-NQO to induce sequence changes. Using a whole genome approach, we have characterized the mutagenic spectrum of 4-NQO and determined that its effects are distributed across the genome in a manner unbiased by sequence other than a preference for guanine over adenine at a ratio of 19:1. Interestingly, 4-NQO dose did not impact the number of mutations caused within a single surviving strain for 50% and 90% kill percentages. Therefore, future screens and kill percentages can be designed to suit whether selection or manual screening is required to identify a trait of interest. The number of mutations ranged between 23 and 240 per mutant. Importantly for *A. nidulans* mutant screens, this is a manageable number of candidate mutations to test for causation of the selected phenotype when combined with the power of haploidization and/or meiotic mapping, or with bulk segregant analysis. Additionally, we have shown that all six possible sequence transitions and transversions are induced by 4-NQO adduct repair, making it possible to conduct saturation screens with this chemical. We conclude that current practices using 4-NQO mutagenesis are sufficient to reach gene saturation in genetic screens. Therefore, our findings provide genome-wide evidence for the assertion of Bal *et al.*, (Bal *et al.* 1977) that "4-NQO is a good mutagen for *A. nidulans*."

ACKNOWLEDGMENTS

We greatly appreciate the expert assistance of Andrew Princep, Bethany Grabow, and Tim Todd with statistical and probability analyses; technical assistance of Ian Hollyer; and technical advice of Koon Ho Wong. This work was supported by a Kansas NSF EPSCoR First Award EPS-0903806 (R.B.T.), a K-INBRE Scholarship funded by National Institute for General Medical Sciences award P20GM103418 (B.T.P.), a Kansas State University (KSU) Integrated Genomics Facility Competitive Seed Grant (R.B.T.), the KSU Plant Biotechnology Center (R.B.T.), the KSU Johnson Center for Basic Cancer Research (R.B.T., B.T.P.), and a National Institutes of Health New Innovator award OD004268 (S.L.R.-P.). Publication of this article was funded in part by the KSU Open Access Publishing Fund. This is contribution number 15-090-J from the Kansas Agricultural Experiment Station.

LITERATURE CITED

Al Taho, N. M., H. M. Sealy-Lewis, and C. Scazzocchio, 1984 Suppressible alleles in a wide domain regulatory gene in *Aspergillus nidulans*. Curr. Genet. 8: 245–251.

Alderson, T., and M. J. Hartley, 1969 Specificity for spontaneous and induced forward mutation at several gene loci in *Aspergillus nidulans*. Mutat. Res. 8: 255–264.

Apirion, D., 1965 The two-way selection of mutants and revertants in respect of acetate utilization and resistance to fluoro-acetate in *Aspergillus nidulans*. Genet. Res. 6: 317–329.

Arst, H. N., Jr, and D. J. Cove, 1973 Nitrogen metabolite repression in *Aspergillus nidulans*. Mol. Gen. Genet. 126: 111–141.

Axelrod, D. E., M. Gealt, and M. Pastushok, 1973 Gene control of developmental competence in *Aspergillus nidulans*. Dev. Biol. 34: 9–15.

Babudri, N., and G. Morpurgo, 1990 Frequency of spontaneous and induced recessive mutations in a diploid strain of *Aspergillus nidulans*. Mutat. Res. 230: 187–195.

Bailleul, B., S. Galiegue, and M. H. Loucheux-Lefebvre, 1981 Adducts from the reaction of O,O'-diacetyl or O-acetyl derivatives of the carcinogen 4-hydroxyaminoquinoline 1-oxide with purine nucleosides. Cancer Res. 41: 4559–4565.

Bailleul, B., P. Daubersies, S. Galiègue-Zouitina, and M. H. Loucheux-Lefebvre, 1989 Molecular basis of 4-nitroquinoline 1-oxide carcinogenesis. Jpn. J. Cancer Res. 80: 691–697.

Bainbridge, B. W., 1976 Estimation of the generation time and peripheral growth zone of *Aspergillus nidulans* and *Alternaria solani* hyphae from radial growth rates and ranges in apical cell length. J. Gen. Microbiol. 97: 125–127.

Bal, J., E. M. Kajtaniak, and N. J. Pieniążek, 1977 4-Nitroquinoline-1-oxide: a good mutagen for *Aspergillus nidulans*. Mutat. Res. 56: 153–156.

Baracho, M. S., and I. R. Baracho, 2003 An analysis of the spontaneous mutation rate measurement in filamentous fungi. Genet. Mol. Biol. 26: 83–87.

Bielska, E., M. Schuster, Y. Roger, A. Berepiki, D. M. Soanes *et al.*, 2014 Hook is an adapter that coordinates kinesin-3 and dynein cargo attachment on early endosomes. J. Cell Biol. 204: 989–1007.

Blankenberg, D., A. Gordon, G. Von Kuster, N. Coraor, J. Taylor *et al.*, 2010a Manipulation of FASTQ data with Galaxy. Bioinformatics 26: 1783–1785.

Blankenberg, D., G. Von Kuster, N. Coraor, G. Ananda, R. Lazarus *et al.*, 2010b Galaxy: a web-based genome analysis tool for experimentalists. Curr. Protoc. Mol. Biol. Chapter 19: Unit 19.10.1–21.

Brody, H., J. Griffith, A. J. Cuticchia, J. Arnold, and W. E. Timberlake, 1991 Chromosome-specific recombinant DNA libraries from the fungus *Aspergillus nidulans*. Nucleic Acids Res. 19: 3105–3109.

Bruno, K. S., J. L. Morrell, J. E. Hamer, and C. J. Staiger, 2001 SepH, a Cdc7p orthologue from *Aspergillus nidulans*, functions upstream of actin ring formation during cytokinesis. Mol. Microbiol. 42: 3–12.

Cecchetto, G., M. Richero, N. Oestreicher, M. I. Muro-Pastor, S. Pantano *et al.*, 2012 Mutations in the basic loop of the Zn binuclear cluster of the UaY transcriptional activator suppress mutations in the dimerisation domain. Fungal Genet. Biol. 49: 731–743.

Cerqueira, G. C., M. B. Arnaud, D. O. Inglis, M. S. Skrzypek, G. Binkley *et al.*, 2014 The *Aspergillus* Genome Database: multispecies curation and incorporation of RNA-Seq data to improve structural gene annotations. Nucleic Acids Res. 42(Database issue): D705–D710.

Cherry, J. M., E. L. Hong, C. Amundsen, R. Balakrishnan, G. Binkley *et al.*, 2012 *Saccharomyces* Genome Database: the genomics resource of budding yeast. Nucleic Acids Res. 40(Database issue): D700–D705.

Clutterbuck, A. J., 1969 A mutational analysis of conidial development in *Aspergillus nidulans*. Genetics 63(2): 317–327.

Clutterbuck, A. J., and M. L. Farman, 2008 *Aspergillus nidulans*: linkage map and genome sequence: closing gaps and adding telomeres, pp. 57–73 in *The Aspergilli: Genomics, Medical Aspects, Biotechnology, and Research Methods*, edited by G. H. Goldman, and S. A. Osmani. CRC Press, Boca Raton, FL.

Conlon, H., I. Zadra, and H. Haas, H. N. Arst, Jr, M. G. Jones *et al.*, 2001 The *Aspergillus nidulans* GATA transcription factor gene *areB* encodes at least three proteins and features three classes of mutation. Mol. Microbiol. 40: 361–375.

Cove, D. J., 1966 The induction and repression of nitrate reductase in the fungus *Aspergillus nidulans*. Biochim. Biophys. Acta 113: 51–56.

Crooks, G. E., G. Hon, J. M. Chandonia, and S. E. Brenner, 2004 WebLogo: a sequence logo generator. Genome Res. 14: 1188–1190.

DePristo, M. A., E. Banks, R. Poplin, K. V. Garimella, J. R. Maguire *et al.*, 2011 A framework for variation discovery and genotyping using next-generation DNA sequencing data. Nat. Genet. 43: 491–498.

Drake, J. W., B. Charlesworth, D. Charlesworth, and J. F. Crow, 1998 Rates of spontaneous mutation. Genetics 148: 1667–1686.

Farrell, A., B. I. Coleman, B. Benenati, K. M. Brown, I. J. Blader *et al.*, 2014 Whole genome profiling of spontaneous and chemically induced mutations in *Toxoplasma gondii*. BMC Genomics 15: 354.

Flibotte, S., M. L. Edgley, I. Chaudhry, J. Taylor, S. E. Neil *et al.*, 2010 Whole-genome profiling of mutagenesis in *Caenorhabditis elegans*. Genetics 185: 431–441.

Galagan, J. E., S. E. Calvo, C. Cuomo, L. J. Ma, J. R. Wortman *et al.*, 2005 Sequencing of *Aspergillus nidulans* and comparative analysis with *A. fumigatus* and *A. oryzae*. Nature 438: 1105–1115.

Galiègue-Zouitina, S., B. Bailleul, and M. H. Loucheux-Lefebvre, 1984 Guanyl-C8-arylamination of DNA by the ultimate carcinogen of 4-nitroquinoline-1-oxide: a spectrophotometric titration. Anal. Biochem. 138: 454–457.

Galiègue-Zouitina, S., B. Bailleul, and M. H. Loucheux-Lefebvre, 1985 Adducts from *in vivo* action of the carcinogen 4-hydroxyaminoquinoline 1-oxide in rats and from *in vitro* reaction of 4-acetoxyaminoquinoline 1-oxide with DNA and polynucleotides. Cancer Res. 45: 520–525.

Galiègue-Zouitina, S., B. Bailleul, Y. M. Ginot, B. Perly, P. Vigny *et al.*, 1986 N2-guanyl and N6-adenyl arylation of chicken erythrocyte DNA by the ultimate carcinogen of 4-nitroquinoline 1-oxide. Cancer Res. 46: 1858–1863.

Garrison, E., and G. Marth, 2012 Haplotype-based variant detection from short-read sequencing. Available at: http://arxiv.org/abs/1207.3907. Accessed November 4, 2014.

Goldman, G. H., and E. Kafer, 2004 *Aspergillus nidulans* as a model system to characterize the DNA damage response in eukaryotes. Fungal Genet. Biol. 41: 428–442.

Harris, S. D., J. L. Morrell, and J. E. Hamer, 1994 Identification and characterization of *Aspergillus nidulans* mutants defective in cytokinesis. Genetics 136: 517–532.

Heck, I. S., J. D. Schrag, J. Sloan, L. J. Millar, G. Kanan *et al.*, 2002 Mutational analysis of the gephyrin-related molybdenum cofactor biosynthetic gene *cnxE* from the lower eukaryote *Aspergillus nidulans*. Genetics 161: 623–632.

Holt, C. L., and G. S. May, 1996 An extragenic suppressor of the mitosis-defective *bimD6* mutation of *Aspergillus nidulans* codes for a chromosome scaffold protein. Genetics 142: 777–787.

Hynes, M. J., and J. A. Pateman, 1970a The genetic analysis of regulation of amidase synthesis in *Aspergillus nidulans*. I. Mutants able to utilize acrylamide. Mol. Gen. Genet. 108: 97–106.

Hynes, M. J., and J. A. Pateman, 1970b The genetic analysis of regulation of amidase synthesis in *Aspergillus nidulans*. II. Mutants resistant to fluoroacetamide. Mol. Gen. Genet. 108: 107–116.

Ikenaga, M., H. Ichikawa-Ryo, and S. Kondo, 1975a The major cause of inactivation and mutation by 4-nitroquinoline 1-oixde in *Escherichia coli*: excisable 4NQO-purine adducts. J. Mol. Biol. 92: 341–356.

Ikenaga, M., Y. Ishii, M. Tada, T. Kakunaga, and H. Takebe, 1975b Excision-repair of 4-nitroquinolin-1-oxide damage responsible for killing, mutation, and cancer. Basic Life Sci. 5B: 763–771.

Ikenaga, M., and T. Kakunaga, 1977 Excision of 4-nitroquinoline 1-oxide damage and transformed in mouse cells. Cancer Res. 37: 3672–3678.

Ikenaga, M., H. Takebe, and Y. Ishii, 1977 Excision repair of DNA base damage in human cells treated with the chemical carcinogen 4-nitroquinoline 1-oxide. Mutat. Res. 43: 415–427.

Janner, F., F. Flury, and U. Leupold, 1979 Reversion of nonsense mutants induced by 4-nitroquinoline-1-oxide in *Schizosaccharomyces pombe*. Mutat. Res. 63: 11–19.

Kaminskyj, S. G., and J. E. Hamer, 1998 *hyp* loci control cell pattern formation in the vegetative mycelium of *Aspergillus nidulans*. Genetics 148: 669–680.

Kinghorn, J. R., J. Sloan, G. J. Kana'n, E. R. Dasilva, D. A. Rouch *et al.*, 2005 Missense mutations that inactivate the *Aspergillus nidulans nrtA* gene encoding a high-affinity nitrate transporter. Genetics 169: 1369–1377.

Kohda, K., M. Tada, H. Kasai, S. Nishimura, and Y. Kawazoe, 1986 Formation of 8-hydroxyguanine residues in cellular DNA exposed to the carcinogen 4-nitroquinoline 1-oxide. Biochem. Biophys. Res. Commun. 139: 626–632.

Kudla, B., M. X. Caddick, T. Langdon, N. M. Martinez-Rossi, C. F. Bennett *et al.*, 1990 The regulatory gene *areA* mediating nitrogen metabolite repression in *Aspergillus nidulans*. Mutations affecting specificity of gene activation alter a loop residue of a putative zinc finger. EMBO J. 9: 1355–1364.

Kurowska, M., A. Labocha-Pawlowska, D. Gnizda, M. Maluszynski, and I. Szarejko, 2012 Molecular analysis of point mutations in a barley genome exposed to MNU and gamma rays. Mutat. Res. 738–739: 52–70.

Larson, J. R., E. M. Facemyer, K. F. Shen, L. Ukil, and S. A. Osmani, 2014 Insights into dynamic mitotic chromatin organization through the NimA kinase suppressor SonC, a chromatin-associated protein involved in the DNA damage response. Genetics 196: 177–195.

Lee, S. B., and J. W. Taylor, 1990 Isolation of DNA from fungal mycelia and single spores, pp. 282–287 in *PCR Protocols: A guide to Methods and Applications*, edited by M. A. Innis, D. H. Gelfand, J. S. Sninsky, and T. J. White. Academic Press, San Diego, CA.

Li, H., and R. Durbin, 2009 Fast and accurate short read alignment with Burrows-Wheeler transform. Bioinformatics 25: 1754–1760.

Lilly, J. L., 1965 An investigation of the suitability of the suppressors of *meth1* in *Aspergillus nidulans* for the study of induced and spontaneous mutation. Mutat. Res. 2: 192–195.

Lin, X., and M. Momany, 2003 The *Aspergillus nidulans swoC1* mutant shows defects in growth and development. Genetics 165: 543–554.

Lin, X., C. Momany, and M. Momany, 2003 SwoHp, a nucleoside diphosphate kinase, is essential in *Aspergillus nidulans*. Eukaryot. Cell 2: 1169–1177.

Lynch, M., W. Sung, K. Morris, N. Coffey, C. R. Landry *et al.*, 2008 A genome-wide view of the spectrum of spontaneous mutations in yeast. Proc. Natl Acad. Sci. USA 105: 9272–9277.

McCluskey, K., A. E. Wiest, I. V. Grigoriev, A. Lipzen, J. Martin *et al.*, 2011 Rediscovery by whole genome sequencing: classical mutations and genome polymorphisms in *Neurospora crassa*. G3 (Bethesda) 1: 303–316.

McKenna, A., M. Hanna, E. Banks, A. Sivachenko, K. Cibulskis *et al.*, 2010 The Genome Analysis Toolkit: a MapReduce framework for analyzing next-generation DNA sequencing data. Genome Res. 20: 1297–1303.

Menichini, P., G. Fronza, S. Tornaletti, S. Galiègue-Zouitina, B. Bailleul *et al.*, 1989 In vitro DNA modification by the ultimate carcinogen of 4-nitroquinoline-1-oxide: influence of superhelicity. Carcinogenesis 10: 1589–1593.

Miller, J. A., 1970 Carcinogenesis by chemicals: an overview—G. H. A. Clowes memorial lecture. Cancer Res. 30: 559–576.

Momany, M., P. J. Westfall, and G. Abramowsky, 1999 *Aspergillus nidulans swo* mutants show defects in polarity establishment, polarity maintenance and hyphal morphogenesis. Genetics 151: 557–567.

Monahan, B. J., S. E. Unkles, I. T. Tsing, J. R. Kinghorn, M. J. Hynes *et al.*, 2002 Mutation and functional analysis of the *Aspergillus nidulans* ammonium permease MeaA and evidence for interaction with itself and MepA. Fungal Genet. Biol. 36: 35–46.

Morris, N. R., 1975 Mitotic mutants of *Aspergillus nidulans*. Genet. Res. 26: 237–254.

Nayak, T., E. Szewczyk, C. E. Oakley, A. Osmani, L. Ukil *et al.*, 2006 A versatile and efficient gene-targeting system for *Aspergillus nidulans*. Genetics 172: 1557–1566.

Nowrousian, M., I. Teichert, S. Masloff, and U. Kuck, 2012 Whole-genome sequencing of *Sordaria macrospora* mutants identifies developmental genes. G3 (Bethesda) 2: 261–270.

Nüsslein-Volhard, C., and E. Wieschaus, 1980 Mutations affecting segment number and polarity in *Drosophila*. Nature 287: 795–801.

Oakley, C. E., and B. R. Oakley, 1989 Identification of gamma-tubulin, a new member of the tubulin superfamily encoded by *mipA* gene of *Aspergillus nidulans*. Nature 338: 662–664.

Oestreicher, N., and C. Scazzocchio, 2009 Phenotypes of mutations in the 5′-UTR of a limiting transcription factor in *Aspergillus nidulans* can be accounted for by translational inhibition and leaky scanning. Genetics 181: 1261–1272.

Osman, F., B. Tomsett, and P. Strike, 1993 The isolation of mutagen-sensitive nuv mutants of *Aspergillus nidulans* and their effects on mitotic recombination. Genetics 134: 445–454.

Penalva, M. A., J. Tilburn, and E. Bignell, and H. N. Arst, Jr., 2008 Ambient pH gene regulation in fungi: making connections. Trends Microbiol. 16: 291–300.

Pokorska, A., C. Drevet, and C. Scazzocchio, 2000 The analysis of the transcriptional activator PrnA reveals a tripartite nuclear localisation sequence. J. Mol. Biol. 298: 585–596.

Pollock, D. D., and J. C. Larkin, 2004 Estimating the degree of saturation in mutant screens. Genetics 168: 489–502.

Pomraning, K. R., K. M. Smith, and M. Freitag, 2011 Bulk segregant analysis followed by high-throughput sequencing reveals the Neurospora cell cycle gene, *ndc-1*, to be allelic with the gene for ornithine decarboxylase, *spe-1*. Eukaryot. Cell 10: 724–733.

Pontecorvo, G., J. A. Roper, L. M. Hemmons, K. D. Macdonald, and A. W. Bufton, 1953 The genetics of *Aspergillus nidulans*. Adv. Genet. 5: 141–238.
Prakash, L., and F. Sherman, 1973 Mutagenic specificity: reversion of iso-1-cytochrome *c* mutants of yeast. J. Mol. Biol. 79: 65–82.
Prakash, L., J. W. Stewart, and F. Sherman, 1974 Specific induction of transitions and transversions of GC base pairs by 4-nitroquinoline-1-oxide in iso-1-cytochrome *c* mutants of yeast. J. Mol. Biol. 85: 51–56.
Quinlan, A. R., and I. M. Hall, 2010 BEDTools: a flexible suite of utilities for comparing genomic features. Bioinformatics 26: 841–842.
Rosenkranz, H. S., and L. A. Poirier, 1979 Evaluation of the mutagenicity and DNA-modifying activity of carcinogens and noncarcinogens in microbial systems. J. Natl Cancer Inst. 62: 873–891.
Setlow, R. B., P. A. Swenson, and W. L. Carrier, 1963 Thymine dimers and inhibition of DNA synthesis by ultraviolet irradiation of cells. Science 142: 1464–1466.
Shaw, B. D., and M. Momany, 2002 *Aspergillus nidulans* polarity mutant *swoA* is complemented by protein O-mannosyltransferase *pmtA*. Fungal Genet. Biol. 37: 263–270.
Shaw, B. D., C. Momany, and M. Momany, 2002 *Aspergillus nidulans swoF* encodes an N-myristoyl transferase. Eukaryot. Cell 1: 241–248.
Shi, X., Y. Sha, and S. Kaminskyj, 2004 *Aspergillus nidulans hypA* regulates morphogenesis through the secretion pathway. Fungal Genet. Biol. 41: 75–88.
Sun, Y. V., A. M. Levin, E. Boerwinkle, H. Robertson, and S. L. Kardia, 2006 A scan statistic for identifying chromosomal patterns of SNP association. Genet. Epidemiol. 30: 627–635.
Szewczyk, E., T. Nayak, C. E. Oakley, H. Edgerton, Y. Xiong *et al.*, 2006 Fusion PCR and gene targeting in *Aspergillus nidulans*. Nat. Protoc. 1: 3111–3120.
Tada, M., and M. Tada, 1971 Interaction of a carcinogen, 4-nitroquinoline-1-oxide, with nucleic acids: chemical degradation of the adducts. Chem. Biol. Interact. 3: 225–229.
Tada, M., and M. Tada, 1976 Main binding sites of the carcinogen, 4-nitroquinoline 1-oxide in nucleic acids. Biochim. Biophys. Acta 454: 558–566.
Tada, M., K. H. Kohda, and Y. Kawazoe, 1984 Biomimetic preparation and structure determination of QGI, one of the quinoline-DNA base adducts formed in cells treated with 4-nitroquinoline 1-oxide. Gann 75: 976–985.
Tan, K., A. J. Roberts, M. Chonofsky, M. J. Egan, and S. L. Reck-Peterson, 2014 A microscopy-based screen employing multiplex genome sequencing identifies cargo-specific requirements for dynein velocity. Mol. Biol. Cell 25: 669–678.
Todd, R. B., M. A. Davis, and M. J. Hynes, 2007a Genetic manipulation of *Aspergillus nidulans*: heterokaryons and diploids for dominance, complementation and haploidization analyses. Nat. Protoc. 2: 822–830.
Todd, R. B., M. A. Davis, and M. J. Hynes, 2007b Genetic manipulation of *Aspergillus nidulans*: meiotic progeny for genetic analysis and strain construction. Nat. Protoc. 2: 811–821.
Uchida, N., T. Sakamoto, T. Kurata, and M. Tasaka, 2011 Identification of EMS-induced causal mutations in a non-reference *Arabidopsis thaliana* accession by whole genome sequencing. Plant Cell Physiol. 52: 716–722.
Voz, M. L., W. Coppieters, I. Manfroid, A. Baudhuin, V. Von Berg *et al.*, 2012 Fast homozygosity mapping and identification of a zebrafish ENU-induced mutation by whole-genome sequencing. PLoS ONE 7: e34671.
Williams, A. B., K. M. Hetrick, and P. L. Foster, 2010 Interplay of DNA repair, homologous recombination, and DNA polymerases in resistance to the DNA damaging agent 4-nitroquinoline-1-oxide in *Escherichia coli*. DNA Repair (Amst.) 9: 1090–1097.
Wong, K. H., M. J. Hynes, and M. A. Davis, 2008 Recent advances in nitrogen regulation: a comparison between *Saccharomyces cerevisiae* and filamentous fungi. Eukaryot. Cell 7: 917–925.
Wu, L., S. A. Osmani, and P. M. Mirabito, 1998 A role for NIMA in the nuclear localization of cyclin B in *Aspergillus nidulans*. J. Cell Biol. 141: 1575–1587.
Yang, Y., A. M. El-Ganiny, G. E. Bray, D. A. Sanders, and S. G. Kaminskyj, 2008 *Aspergillus nidulans hypB* encodes a Sec7-domain protein important for hyphal morphogenesis. Fungal Genet. Biol. 45: 749–759.
Yao, X., X. Wang, and X. Xiang, 2014 FHIP and FTS proteins are critical for dynein-mediated transport of early endosomes in Aspergillus. Mol. Biol. Cell 25: 2181–2189.
Zhang, J., R. Qiu, H. N. Arst, Jr, M. A. Penalva, and X. Xiang, 2014 HookA is a novel dynein-early endosome linker critical for cargo movement in vivo. J. Cell Biol. 204: 1009–1026.
Zhu, Y. O., M. L. Siegal, D. W. Hall, and D. A. Petrov, 2014 Precise estimates of mutation rate and spectrum in yeast. Proc. Natl Acad. Sci. USA 111: E2310–E2318.

Communicating editor: A. Rokas

"The trouble with having an open mind, of course,
is that people will insist on coming along and trying to put things in it"
– Sir Terry Pratchett (Diggers)